

Archipelago Model Compound Synthesis by Rhodium-catalyzed Annulations of Island-tethered  
Alkynes with Aromatic Substrates

by

Yaowei Guo

A thesis submitted in partial fulfillment of the requirements for the degree of

Doctor of Philosophy

Department of Chemistry  
University of Alberta

© Yaowei Guo, 2022

## Abstract

Asphaltenes are the most complex constituents in bitumen. They are distinguished from other components in bitumen by high density, high viscosity and a strong tendency to form aggregates in solutions. Asphaltene aggregates may precipitate as a result of small environmental changes, which is problematic for industrial production processes, thus restricting the bitumen resources as an alternative to conventional petroleum. To maximize bitumen resources, studies of asphaltene structures and aggregation behavior were conducted by many petroleum scientists.

By applying several newly developed analytical techniques, different asphaltene structural models have been proposed, one of which is called “archipelago model”. This model describes asphaltenes as multiple polycyclic aromatic hydrocarbon islands linked together by alkyl chain bridges, and attributes asphaltene aggregation to different types of intramolecular and intermolecular associations. Results from many analytical techniques suggest the presence of archipelago structures in asphaltenes, but they have never been fully characterized from asphaltenes so far.

Recent years, a new way to study asphaltenes has been developed, by using synthetic model compounds bearing archipelago structures to imitate asphaltenes. However, due to some factors such as low synthetic yields, low molecular weights, and lack of heteroatoms, these model compounds cannot imitate authentic asphaltenes well, which limits the scope of asphaltene studies.

This dissertation describes an efficient approach to prepare a new library of archipelago model compounds that have high molecular weights, high structural complexity and variable heteroatom inclusion. At first, neutral model compounds were prepared by rhodium-catalyzed

annulations of island-tethered alkynes with aryl-boron derivatives. The obtained model compounds all exhibit archipelago structures. Some of them incorporate sulfur, which has rarely been reported previously. These model compounds have compositions that differ from each other but are comparable to authentic asphaltenes, making them reasonable asphaltene models. The solution molecular and supramolecular structures of one model compound were determined by applying  $^1\text{H}$ -Diffusion ordered NMR spectroscopy ( $^1\text{H}$ -DOSY). This is the first time that  $^1\text{H}$ -DOSY has been used to characterize a synthetic asphaltene model compound.

Subsequently, nitrogen cation-embedded archipelago compounds were synthesized by rhodium-catalyzed annulations of island-tethered alkynes with nitrogen-containing arenes, which creates a new category of archipelago model compounds that have never been reported. These cationic nitrogen compounds have obviously different features than related neutral model compounds. They are good materials for studying the influence of supramolecular interactions in asphaltene aggregation.

All synthesized archipelago model compounds were characterized by  $^1\text{H}$  and  $^{13}\text{C}\{^1\text{H}\}$  NMR spectroscopies, high-resolution mass spectrometry and elemental analysis to confirm structures and purities. Overall, efficient methodologies were successfully developed to provide archipelago model compounds that can better represent native asphaltenes than previously reported.

## Preface

Chapter 1 of this thesis includes a brief overview of asphaltene chemistry development, asphaltene model compound synthesis, recent alkyne annulation methodologies, as well as extended reaction scope studies of alkyne annulation reactions. My former colleague, Mark Aloisio, assisted me in synthesizing the starting material, 2-iodonaphthalene, and in purifying the reagents and solvents for reactions in this chapter.

Chapter 2 of this thesis describes the preparation of aromatic island-tethered dialkyl alkynes. The synthesis of starting material 9-(4-chlorobutyl)phenanthrene was designed and conducted by a former group member, Colin Diner, and by my colleague, David E. Scott. Meanwhile, Mark Aloisio also assisted me in synthesizing the starting material, 4-(4-chlorobutyl)dibenzothiophene for alkyne preparation.

Chapters 3 and 4 contain the synthetic details of archipelago model compounds and corresponding solution behavior study of one archipelago model compound. These two chapters are entirely based on my original work, in which I was the reaction designer and experimentalist.

Chapter 5 provides the summary and future perspectives of this thesis work. My colleague Munashe Chizema is conducting the synthesis of carboxyl-containing porphyrin structures and benzoquinolizinium cationic-porphyrin anionic dimers at present. I hope to perform the supramolecular characterizations of desired cationic-anionic dimer compounds soon.

None of the results in this thesis have as yet been published. One manuscript is in progress and will be submitted shortly to a journal that is yet to be determined. A second manuscript will describe the cationic compounds and include AFM imaging and supramolecular analysis. I will be a co-author of some manuscripts that come from studies being carried out by petroleum



chemists and engineers.

## Acknowledgements

I would like to first thank my supervisor, Prof. Jeffery M. Stryker. My research work at University of Alberta was conducted under Jeff's meticulous guidance. During the research, Jeff touched me deeply with his profound academic knowledge and rigorous scientific attitude. He always encouraged me to try more and not be afraid to fail, and trusted that I can find the right answer, which makes me learned much practical experience from these attempts. Whenever I encounter difficulties, Jeff often tried to stimulate my innovative thinking and gave valuable suggestions, which benefits me a lot. As my program is coming to an end, I realize how much Jeff influenced me and improved me.

I would like to thank my PhD examination committee for reading my thesis and attending my defense. Prof. Rik Tykwinski and Prof. Eric Rivard provided me a lot of advice, which makes me better understand and familiarize myself with the academic background of my field. That helps me to see more clearly what I want to pursue. I also appreciate Prof. Clive, West and Lundgren for their input during my candidacy exam.

During my research work at Department of Chemistry, the staff in the analytical facilities are always helpful. Thank you to Ryan McKay, Mark Miskolzie, and Nupur Dabral for your help with NMR spectroscopy. Thank you to Wayne Moffat and Jennifer Jones for elemental analysis, UV-Vis and fluorescence spectroscopy. Thank you to Randy Whittal from mass spectrometry facility. I also want to thank Andrew Yeung, Michael Barteski from chemistry stores, Jason Dibbs from the glass shop, Ryan Lewis from shipping and receiving, and Anita Weiler, Lin Ferguson, Laura Pham for their administrative help.

Being a teaching assistant was a fun experience in my PhD career at University of Alberta. I was happy to work with a fantastic lab director, Dr. Hayley Wan. I got a great exercise and met many studious and friendly students during this experience.

I also received much assistance from other members in our lab during my experimental works. I would like to thank all past and present members in Stryker group, especially Dr. Robin Hamilton, Dr. David Scott, Dr. Orain Brown, Dr. Asama Vorapattanapong and Mark Aloisio. I really enjoy the relaxed and active research atmosphere when working with them.

At last, I would also like to express my thanks to my family and my friends. The past few years have been a difficult time for all of us. Without their tremendous spiritual support, I would not have persevered to where I am today.

## Table of Contents

|  |           |
|--|-----------|
| <b>1. Development of Asphaltene Model Compounds Synthesis.....</b>               | <b>1</b>  |
| 1.1 Asphaltene extraction and analysis .....                                     | 1         |
| 1.1.1 Bitumen and asphaltenes as natural resources .....                         | 1         |
| 1.1.2 Chemical composition of asphaltenes.....                                   | 3         |
| 1.2 Asphaltene structural models .....   | 6         |
| 1.2.1 Continental asphaltene model .....   | 6         |
| 1.2.2 Evidence for the presence of archipelago compounds in asphaltenes .....    | 8         |
| 1.3 Methodologies for preparing archipelago model compounds .....                | 12        |
| 1.3.1 Traditional archipelago model compounds.....                               | 12        |
| 1.3.2 Advanced synthetic approaches to archipelago model compounds.....          | 14        |
| 1.4 Transition metal-catalyzed alkyne annulation reactions .....                 | 17        |
| 1.4.1 Transition metal-catalyzed [2+2+2] alkyne annulation reactions.....        | 17        |
| 1.4.2 Transition metal-catalyzed [4+2] alkyne annulation reactions .....         | 28        |
| 1.4.3 Conclusions.....   | 38        |
| 1.4.4 Applications of alkyne annulations to archipelago compound synthesis ..... | 39        |
| Research Objectives. ....  | 41        |
| Results and Discussions.....   | 41        |
| 1.5 Probing the preliminary scope studies of alkyne annulations .....            | 41        |
| 1.5.1 Rhodium-catalyzed annulations of 1-naphthylboronic acid with alkynes.....  | 42        |
| 1.5.2 Cobalt-catalyzed annulations of 2-iodonaphthalene with alkynes.....        | 44        |
| Experimental Section.....  | 48        |
| <b>2. Synthetic Approaches to Island-tethered Dialkyl Alkynes.....</b>           | <b>53</b> |
| 2.1 Traditional methodologies for preparing dialkyl alkynes .....                | 54        |
| 2.2 Modern methodologies for preparing dialkyl alkynes .....                     | 55        |
| 2.2.1 Limiting issues in cross-coupling reactions.....                           | 55        |

|       |   |    |
|-------|---|----|
| 2.2.2 | Palladium-catalyzed Sonogashira coupling of terminal alkynes and alkyl halides using <i>N</i> -heterocyclic carbene ligands ..... | 59 |
| 2.2.3 | Palladium-catalyzed oxidative cross-coupling of alkynes and alkylzinc reagents .....  | 61 |
| 2.2.4 | Copper-catalyzed cross-coupling of alkyl Grignard reagents and alkynyl halides .....  | 63 |
| 2.2.5 | First-row transition metal-catalyzed cross-couplings of alkyl halides and alkynyl Grignard reagents .....                         | 65 |
| 2.2.6 | Molybdenum- or tungsten-catalyzed alkyne metathesis.....  | 69 |
|       | Results and Discussions.....  | 75 |
| 2.3   | Synthesis of phenanthrene-tethered dialkyl alkyne.....  | 75 |
| 2.4   | Synthesis of dibenzothiophene-tethered dialkyl alkyne.....  | 78 |
| 2.5   | Synthesis of the tetraethylphenanthrene-tethered dialkyl alkyne.....  | 82 |
|       | Conclusion.....   | 87 |
|       | Experimental Section.....   | 87 |

### **3. Archipelago Compounds Synthesis by Rhodium-catalyzed Aryl-boron/Alkyne Annulation .....103**

|       |  |     |
|-------|--|-----|
| 3.1   | The synthesis of archipelago compounds by rhodium-catalyzed [4+2] annulations of 2-biphenylboronic acid with alkynes.....          | 104 |
| 3.2   | Optimization of the rhodium-catalyzed [2+2+2] annulations of aryl-boron derivatives with alkynes.....                              | 106 |
| 3.2.1 | Annulations of 2-naphthylboronic acid with dialkyl alkynes.....  | 106 |
| 3.2.2 | Preparation of aryl pinacol boronates .....  | 109 |
| 3.3   | The synthesis of archipelago compounds by rhodium-catalyzed [2+2+2] annulations of aryl pinacol boronates with alkynes.....        | 111 |
| 3.4   | Chemical compositions of synthetic archipelago model compounds .....   | 115 |
| 3.5   | Studies on the second order <sup>1</sup> H NMR signals of archipelago model compounds.....   | 119 |
| 3.6   | Characterization of an archipelago model compound by <sup>1</sup> H-Diffusion-Ordered NMR Spectroscopy ( <sup>1</sup> H-DOSY)..... | 124 |
| 3.6.1 | Introduction to the <sup>1</sup> H-DOSY technique.....   | 124 |
| 3.6.2 | Characterization of an archipelago model compound by <sup>1</sup> H-DOSY .....   | 126 |

|   |            |
|---|------------|
| Conclusion .....  | 135        |
| Experimental Section.....   | 136        |
| <b>4. Synthesis of Cationic Nitrogen-containing Archipelago<br/>Compounds by Rhodium-catalyzed Arene/Alkyne Annulations ...</b> | <b>153</b> |
| 4.1 Synthetic approaches to cationic nitrogen-embedded PAHs .....   | 153        |
| 4.1.1 Synthetic approaches to quinolinium and isoquinolinium motifs.....  | 154        |
| 4.1.2 Synthetic approaches to quinolizinium and benzoquinolizinium motifs .....   | 156        |
| Results and Discussions.....  | 162        |
| 4.2 The synthesis of archipelago compounds by [4+2] annulations of 2-phenylpyridine<br>with alkynes .....                       | 162        |
| 4.3 The synthesis of archipelago compounds by [4+2] annulations of <i>N</i> -phenylpyridinium<br>triflate with alkynes .....    | 164        |
| 4.3.1 Annulations of <i>N</i> -phenylpyridinium triflate with 5-decyne.....   | 166        |
| 4.3.2 Annulations of <i>N</i> -phenylpyridinium triflate with island-tethered alkynes .....                                     | 172        |
| Conclusion .....  | 178        |
| Experimental Section.....   | 179        |
| <b>5. Conclusions and Future Perspectives .....</b>   | <b>191</b> |
| 5.1 Project summary.....  | 191        |
| 5.2 Unresolved issues and future objectives .....   | 192        |
| 5.2.1 Archipelago compounds from triethylpyrene islands .....   | 192        |
| 5.2.2 Archipelago compounds containing oxygen functional groups.....  | 193        |
| 5.2.3 Biomarker anion-containing archipelago compounds .....  | 196        |
| <b>Bibliography.....</b>  | <b>199</b> |
| <b>Appendix 1: <sup>1</sup>H and <sup>13</sup>C{<sup>1</sup>H} NMR Spectra .....</b>  | <b>211</b> |
| <b>Appendix 2: <sup>1</sup>H-<sup>1</sup>H COSY, HSQC, and HMBC Spectra.....</b>  | <b>281</b> |
| <b>Appendix 3: UV-Vis and Fluorescence Spectra .....</b>  | <b>284</b> |

## List of Tables

|   |     |
|---|-----|
| <b>Table 3-1.</b> Synthesis of archipelago compounds by [4+2] annulations of 2-biphenylboronic acid with alkynes. ....  | 104 |
| <b>Table 3-2.</b> Theoretical and experimental elemental composition of compound <b>263</b> . ....  | 105 |
| <b>Table 3-3.</b> Synthesis of five-island archipelago compounds by rhodium-catalyzed [2+2+2] annulations of aryl pinacol boronates with alkynes. ....                    | 111 |
| <b>Table 3-4.</b> Compositional analyses of synthetic archipelago compounds. ....   | 115 |
| <b>Table 3-5.</b> Diffusion coefficients and relative diffusion coefficients as a function of compound <b>278</b> concentration in CD <sub>2</sub> Cl <sub>2</sub> . .... | 127 |

## List of Figures

|   |     |
|---|-----|
| <b>Figure 1-1.</b> SARA analysis of bitumen.....  | 2   |
| <b>Figure 1-2.</b> Elemental compositions for petroleum asphaltenes.....  | 4   |
| <b>Figure 1-3.</b> Examples of possible nickel- and vanadyl-porphyrins characterized from bitumen. .  | 6   |
| <b>Figure 1-4.</b> Assigned structures of four actual molecules in an asphaltene sample based on AFM measurements by Schuler and co-workers.....    | 8   |
| <b>Figure 1-5.</b> A schematic diagram of supramolecular archipelago model. ....  | 10  |
| <b>Figure 1-6.</b> An actual archipelago-type molecule in coal-derived asphaltenes observed by Schuler and co-workers using AFM. ....               | 11  |
| <b>Figure 1-7.</b> Commercially available dipyrenyl alkanes as archipelago model compounds.....   | 12  |
| <b>Figure 1-8.</b> Some other examples of [3+2], [4+2] or [5+2] alkyne annulation reactions. ....   | 38  |
| <b>Figure 2-1.</b> Representative examples of diaryl alkyne and dialkyl alkyne. ....  | 53  |
| <b>Figure 2-2.</b> Two best alkyne metathesis catalysts from Tamm and co-workers' optimization studies. ....  | 74  |
| <b>Figure 2-3.</b> An alkyne metathesis catalyst prepared by Fürstner and co-workers. ....  | 75  |
| <b>Figure 3-1.</b> Detailed <sup>1</sup> H NMR spectrum of archipelago compound <b>277</b> and signal assignments in 3.5–2.5 ppm region. ....       | 120 |
| <b>Figure 3-2.</b> Detailed <sup>1</sup> H NMR spectrum of archipelago compound <b>277</b> and signal assignments in 2.2–1.6 ppm region. ....       | 122 |
| <b>Figure 3-3.</b> Detailed <sup>1</sup> H NMR spectra of archipelago compound <b>277</b> at (a) room temperature, (b) 100 °C, and (c) –80 °C. .... | 123 |
| <b>Figure 3-4.</b> <sup>1</sup> H-DOSY NMR spectrum of archipelago model compound <b>278</b> in CD <sub>2</sub> Cl <sub>2</sub> .....               | 125 |
| <b>Figure 3-5.</b> Diffusion coefficients of compound <b>278</b> as a function of <b>278</b> concentration. ....                                    | 128 |



|  |     |
|--|-----|
| <b>Figure 3-6.</b> Diffusion coefficients of dichloromethane as a function of <b>278</b> concentration. .... | 128 |
| <b>Figure 3-7.</b> Relative diffusion coefficients as a function of <b>278</b> concentration. ....           | 129 |
| <b>Figure 4-1.</b> Examples for cationic nitrogen-embedded PAHs. ....  | 153 |
| <b>Figure 4-2.</b> List of all cationic nitrogen-containing compounds prepared in chapter 4. ....            | 179 |
| <b>Figure 5-1.</b> Triethyl-substituted bromopyrene prepared by Diner <i>et al.</i> ....                     | 192 |
| <b>Figure 5-2.</b> Expected archipelago model compounds from triethylpyrene island. ....                     | 193 |
| <b>Figure 5-3.</b> Target structures of carboxyl-containing porphyrin synthesis. ....                        | 197 |

## List of Schemes

|   |    |
|---|----|
| <b>Scheme 1-1.</b> Traditional synthetic approaches to obtain archipelago compounds.....  | 14 |
| <b>Scheme 1-2.</b> Archipelago compounds synthesis by nickel-catalyzed Kumada coupling. ....  | 15 |
| <b>Scheme 1-3.</b> [2+2+2] Alkyne annulation and [4+2] alkyne annulation reactions.....   | 17 |
| <b>Scheme 1-4.</b> Some examples of [2+2+2] annulation reactions. ....  | 18 |
| <b>Scheme 1-5.</b> Synthesis of octa-substituted anthracene by annulations of 1,2,4,5-tetraiodobenzene with zirconacyclopentadienes. .... | 19 |
| <b>Scheme 1-6.</b> Rhodium-catalyzed [2+2+2] annulations of aryl boronic acids with alkynes and proposed mechanism.....                   | 22 |
| <b>Scheme 1-7.</b> Cobalt-catalyzed [2+2+2] annulations of aryl iodides with alkynes and proposed mechanism. ....                         | 24 |
| <b>Scheme 1-8.</b> Other examples of [2+2+2] alkyne annulation reactions. ....  | 27 |
| <b>Scheme 1-9.</b> Rhodium-catalyzed [4+2] annulations of the 2-biphenylboronic acid <b>75</b> with alkynes. ....                         | 29 |
| <b>Scheme 1-10.</b> Rhodium-catalyzed [4+2] annulations of 2-phenylpyridine derivatives with alkynes and proposed mechanism.....          | 32 |
| <b>Scheme 1-11.</b> Cobalt-catalyzed [4+2] annulations of 2-phenylpyridine with alkynes and proposed mechanism.....                       | 34 |
| <b>Scheme 1-12.</b> Rhodium-catalyzed [4+2] single/double annulations of <i>N</i> -phenylpyridinium triflate with alkynes.....            | 35 |
| <b>Scheme 1-13.</b> Proposed mechanism for rhodium-catalyzed [4+2] annulation of <i>N</i> -phenylpyridinium triflate with alkynes. ....   | 37 |
| <b>Scheme 1-14.</b> Synthesis of archipelago compounds by alkyne annulations. ....  | 40 |

|   |    |
|---|----|
| <b>Scheme 1-15.</b> Rhodium-catalyzed annulation of 1-naphthylboronic acid with 5-decyne.....   | 42 |
| <b>Scheme 1-16.</b> Transmetallation and alkyne insertion steps for rhodium-catalyzed annulation of alkynes with (a)1-naphthylboronic acid and (b) 2-naphthylboronic acid. .... | 44 |
| <b>Scheme 1-17.</b> Electrophilic aromatic substitution process for the formation of (a) anthracene product and (b) phenanthrene product. ....                                  | 46 |
| <b>Scheme 2-1.</b> Dialkyl alkyne preparation by deprotonation/ $S_N2$ substitution pathway.....  | 54 |
| <b>Scheme 2-2.</b> Mechanism of typical Sonogashira couplings. ....   | 56 |
| <b>Scheme 2-3.</b> $\beta$ -Hydride elimination pathway for Sonogashira couplings. ....   | 58 |
| <b>Scheme 2-4.</b> Proposed mechanism of copper-catalyzed cross-coupling of alkyl Grignard reagents with alkynyl bromides.....  | 64 |
| <b>Scheme 2-5.</b> Proposed mechanism for nickel-catalyzed alkyl-alkynyl cross-coupling. ....   | 67 |
| <b>Scheme 2-6.</b> Proposed mechanism for iron-catalyzed alkyl-alkynyl cross-coupling.....  | 69 |
| <b>Scheme 2-7.</b> Alkyne metathesis by Schrock-type alkylidyne catalyst via metallacyclobutadiene intermediates. ....  | 70 |
| <b>Scheme 2-8.</b> Metathesis mechanism of a terminal methylated alkyne involving a Schrock-type catalyst. ....   | 71 |
| <b>Scheme 2-9.</b> DMC formation and terminal alkyne polymerization involving a Schrock-type catalyst. ....   | 72 |
| <b>Scheme 2-10.</b> Synthesis of the phenanthrene-tethered dialkyl alkyne. ....   | 77 |
| <b>Scheme 2-11.</b> Synthesis of phenanthrene-tethered dialkyl alkyne by copper-catalyzed cross-coupling.....   | 78 |
| <b>Scheme 2-12.</b> Synthesis of DBT-tethered dialkyl alkyne. ....  | 80 |

|  |     |
|--|-----|
| <b>Scheme 2-13.</b> Synthesis of the unsymmetrical alkyne by <i>n</i> -BuLi deprotonation/S <sub>N</sub> 2 substitution.   | 82  |
| <b>Scheme 2-14.</b> Attempts to synthesize the TEP-tethered alkyne by <i>n</i> -BuLi deprotonation/S <sub>N</sub> 2 substitution.  | 84  |
| <b>Scheme 2-15.</b> Synthesis of the TEP-tethered dialkyl alkyne by Kumada coupling.   | 86  |
| <b>Scheme 3-1.</b> Miura's [4+2] and [2+2+2] annulations of aryl-boron derivatives with alkynes.   | 103 |
| <b>Scheme 3-2.</b> Annulations of pinacol boronate with island-tethered alkynes.   | 109 |
| <b>Scheme 3-3.</b> Preparation of aryl pinacol boronates from aryl boronic acids.  | 110 |
| <b>Scheme 3-4.</b> Preparation of aryl pinacol boronates from aryl Grignard reagents.  | 110 |
| <b>Scheme 4-1.</b> Direct syntheses of quinolinium motifs.   | 155 |
| <b>Scheme 4-2.</b> Synthesis of isoquinolinium salts by [4+2] alkyne annulation reactions.   | 156 |
| <b>Scheme 4-3.</b> Syntheses of quinolizinium motifs.  | 158 |
| <b>Scheme 4-4.</b> Synthesis of benzo[ <i>a</i> ]quinolinium motifs via three RCM routes by Cuadro and co-workers.   | 159 |
| <b>Scheme 4-5.</b> Synthetic approaches to benzo[ <i>c</i> ]quinolizinium motifs.  | 161 |
| <b>Scheme 4-6.</b> Rhodium-catalyzed [4+2] annulations of 2-phenylpyridine with island-tethered alkynes.   | 163 |
| <b>Scheme 4-7.</b> Proposed syntheses of (a) symmetrical five-island archipelago compounds and (b) unsymmetrical archipelago compounds by rhodium-catalyzed [4+2] annulations of <i>N</i> -phenylpyridinium triflate with island-tethered alkynes. | 165 |
| <b>Scheme 4-8.</b> Rhodium-catalyzed (a) double and (b) single [4+2] annulation of <i>N</i> -phenylpyridinium triflate with 5-decyne.  | 166 |

|  |     |
|--|-----|
| <b>Scheme 4-9.</b> Formation of the five-membered rhodacycle in (a) the first [4+2] annulation and (b) the second [4+2] annulation.....  | 167 |
| <b>Scheme 4-10.</b> A plausible Wang's annulation mechanism including the carbene intermediate.....  | 171 |
| <b>Scheme 4-11.</b> Carbene generation and alkyne insertion steps for annulation using benzo[ <i>a</i> ]quinolizinium salt <b>85d</b> . ....   | 172 |
| <b>Scheme 4-12.</b> Synthesis of archipelago compounds by rhodium-catalyzed [4+2] annulations of DBT-tethered alkyne with (a) <i>N</i> -phenylpyridinium triflate and (b) benzo[ <i>c</i> ]quinolizinium compound <b>366</b> .....           | 173 |
| <b>Scheme 4-13.</b> Synthesis of archipelago compounds by rhodium-catalyzed [4+2] annulations of phenanthrene-tethered alkyne with (a) <i>N</i> -phenylpyridinium triflate and (b) benzo[ <i>c</i> ]quinolizinium compound <b>366</b> . .... | 176 |
| <b>Scheme 4-14.</b> An alternative route for synthesizing the unsymmetrical compound <b>382</b> . ....   | 178 |
| <b>Scheme 5-1.</b> Possible synthetic routes for archipelago compounds with alcohol or carboxyl groups.....  | 195 |
| <b>Scheme 5-2.</b> Possible synthetic route for archipelago compounds with phenol groups. ....   | 196 |

## List of Equations

|   |    |
|---|----|
| <b>Equation 1-1.</b> Archipelago compounds synthesized by MCR.....  | 16 |
| <b>Equation 1-2.</b> Pd-catalyzed [2+2+2] annulations of <i>o</i> -diiodoarenes with alkynes.....                           | 20 |
| <b>Equation 1-3.</b> Rhodium-catalyzed [2+2+2] annulations of non-functionalized arenes with alkynes. ....                  | 25 |
| <b>Equation 1-4.</b> Other [4+2] annulations of 2-fuctionalized biphenyl with alkynes to obtain phenanthrene products. .... | 30 |
| <b>Equation 1-5.</b> Cobalt-catalyzed annulation of 2-iodonaphthalene with 3-hexyne. ....                                   | 45 |
| <b>Equation 1-6.</b> Cobalt-catalyzed annulation of 1-iodonaphthalene with 3-hexyne. ....                                   | 47 |
| <b>Equation 1-7.</b> Cobalt-catalyzed annulations of 2-iodonaphthalene with 3-hexyne or 5-decyne. ....                      | 47 |
| <b>Equation 2-1.</b> Effect of ligands on a Sonogashira coupling of an alkyl bromide with a terminal alkyne. ....           | 59 |
| <b>Equation 2-2.</b> Representative examples of Sonogashira coupling using alkyl halides. ....                              | 60 |
| <b>Equation 2-3.</b> Sonogashira coupling of bromocycloheptane with 1-octyne.....   | 61 |
| <b>Equation 2-4.</b> Palladium-catalyzed oxidative cross-coupling of terminal alkynes with alkylzinc reagents. ....         | 62 |
| <b>Equation 2-5.</b> Copper-catalyzed cross-coupling of alkyl Grignard reagents with alkynyl bromides.....                  | 63 |
| <b>Equation 2-6.</b> Nickel-catalyzed cross-coupling of alkyl halides with alkynyl Grignard reagents. ....                  | 66 |
| <b>Equation 2-7.</b> Iron-catalyzed cross-coupling of alkyl halides with alkynyl Grignard reagents. .                       | 68 |
| <b>Equation 2-8.</b> Tungsten-catalyzed metathesis of 1-heptyne. ....   | 72 |

|   |     |
|---|-----|
| <b>Equation 2-9.</b> Molybdenum-catalyzed terminal alkyne metathesis.....   | 73  |
| <b>Equation 2-10.</b> Synthesis of 9-(4-chlorobutyl)phenanthrene by cobalt-catalyzed Kumada coupling.....   | 75  |
| <b>Equation 2-11.</b> Synthesis of 4-(4-chlorobutyl)dibenzothiophene by deprotonation/S <sub>N</sub> 2 substitution.....  | 79  |
| <b>Equation 2-12.</b> Synthesis of DBT-tethered dialkyl alkyne by nickel-catalyzed cross-coupling.  | 81  |
| <b>Equation 2-13.</b> Synthesis of DBT-tethered dialkyl alkyne by iron-catalyzed cross-coupling. ...  | 81  |
| <b>Equation 2-14.</b> Synthesis of the brominated TEP.....  | 83  |
| <b>Equation 2-15.</b> Synthesis of TEP-tethered dialkyl alkyne by nickel-catalyzed cross-coupling..   | 85  |
| <b>Equation 3-1.</b> Attempt to synthesize [2+2+2] annulation product by 2-biphenylboronic acid and 5-decyne. ....  | 106 |
| <b>Equation 3-2.</b> Aerobic annulation of 2-naphthylboronic acid with 5-decyne. ....   | 106 |
| <b>Equation 3-3.</b> Anaerobic annulation of 2-naphthylboronic acid with 5-decyne.....  | 107 |
| <b>Equation 3-4.</b> Annulation of 2-naphthylboronic acid with phenanthrene-tethered alkyne. ....   | 108 |
| <b>Equation 3-5.</b> A large-scale synthesis of a DBT-tethered archipelago model compound.....  | 113 |
| <b>Equation 3-6.</b> Attempt to synthesize a triphenylene-type adduct by annulation of 4,4,5,5-tetramethyl-2-(phenanthren-9-yl)-1,3,2-dioxaborolane with 5-decyne. .... | 114 |
| <b>Equation 3-7.</b> Attempt to synthesize a nine-island archipelago compound by annulation of 1,4-benzenediboronic acid bis(pinacol) ester with alkyne. ....           | 115 |
| <b>Equation 4-1.</b> Quinolinium salt preparation by reaction of quinoline with alkyl halide. ....  | 154 |
| <b>Equation 4-2.</b> Synthesis of benzo[ <i>a</i> ]quinolizinium motif by platinum-catalyzed intramolecular cyclization. ....   | 160 |
| <b>Equation 4-3.</b> Rhodium-catalyzed [4+2] annulation of 2-phenylpyridine with 5-decyne.....  | 163 |

|  |     |
|--|-----|
| <b>Equation 4-4.</b> Cobalt-catalyzed [4+2] annulation of 2-phenylpyridine with 5-decyne. ....   | 164 |
| <b>Equation 4-5.</b> Attempt of [4+2] annulation using benzo[ <i>a</i> ]quinolizinium compound <b>85d</b> and 5-decyne. ....   | 170 |
| <b>Equation 4-6.</b> Synthesis of an archipelago compound by rhodium-catalyzed single [4+2] annulation of DBT-tethered alkyne with <i>N</i> -phenylpyridinium triflate. .... | 175 |
| <b>Equation 5-1.</b> Ion exchanges of cationic nitrogen-embedded archipelago compounds with carboxyl-containing porphyrin structures. ....                                   | 198 |



## List of Abbreviations

|                   |   |
|-------------------|---|
| Ac                | Acetyl  |
| acac              | Acetylacetonyl  |
| Ac <sub>2</sub> O | Acetic anhydride  |
| AFM               | Atomic force microscopy   |
| Ar                | Aromatic  |
| bpy               | 2,2'-Bipyridine   |
| br                | Broad   |
| Bu                | Butyl   |
| <i>n</i> -Bu      | Normal butyl  |
| <i>t</i> -Bu      | Tertiary butyl  |
| calcd             | Calculated  |
| cat               | Catalyst  |
| Cbz               | Carbazole   |
| cm                | Centimeter  |
| cod               | 1,5-Cyclooctadiene  |
| COSY              | Correlation spectroscopy  |
| Cp                | Cyclopentadienide   |
| Cp*               | 1,2,3,4,5-Pentamethylcyclopentadienide  |
| Cy                | Cyclohexyl  |
| d                 | Doublet   |
| Da                | Dalton  |
| dba               | Dibenzylideneacetone  |
| DBT               | Dibenzothiophene  |
| DCE               | 1,2-Dichloroethane  |
| DCIB              | 1,2-Dichloroisobutane   |
| DCM               | Dichloromethane   |
| DCTB              | <i>trans</i> -2-[3-(4- <i>tert</i> -Butylphenyl)-2-methyl-2-propenylidene]malononitrile |

|                   |   |
|-------------------|---|
| dd                | Doublet of doublets   |
| DIC               | <i>N, N'</i> -Diisopropylcarbodiimide                       |
| DMC               | Deprotiometallacycle  |
| DMEDA             | <i>N, N'</i> -Dimethylethylenediamine                       |
| DMF               | <i>N, N</i> -Dimethylformamide                              |
| DMI               | 1,3-Dimethyl-2-imidazolidinone                              |
| DMPU              | 1,3-Dimethyl-3,4,5,6-tetrahydro-2( <i>1H</i> )-pyrimidinone |
| DMSO              | Dimethyl sulfoxide  |
| DNA               | Deoxyribonucleic acid                                       |
| DOSY              | Diffusion ordered spectroscopy                              |
| dppe              | Ethylenebis(diphenylphosphine)                              |
| dtbpy             | 4,4'-Di- <i>tert</i> -butyl-2,2'-bipyridyl                  |
| EA                | Elemental analysis  |
| EI                | Electron ionization   |
| en                | Ethylenediamine   |
| equiv             | Equivalents   |
| ESI               | Electrospray ionization                                     |
| Et                | Ethyl   |
| Et <sub>2</sub> O | Diethyl ether   |
| EtOAc             | Ethyl acetate   |
| EtOH              | Ethanol   |
| FT-ICR            | Fourier-transform ion cyclotron resonance                   |
| FT-IR             | Fourier-transform infrared                                  |
| G                 | Gauss   |
| g                 | Gram  |
| h                 | Hour  |
| HBpin             | Pinacolborane   |
| HMBC              | Heteronuclear multiple bond correlation                     |
| HOBt              | 1-Hydroxybenzotriazole                                      |

|        |   |
|--------|---|
| HOTf   | Trifluoromethanesulfonic acid   |
| HRMS   | High-resolution mass spectrometry   |
| HSQC   | Heteronuclear single quantum coherence  |
| Hz     | Hertz   |
| IBiox7 | Dispiro[cycloheptane-1,3'(2' <i>H</i> )-imidazo[5,1- <i>b</i> :4,3- <i>b'</i> ]bisoxazol[4]ium-7'(8' <i>H</i> ),1''-cycloheptane] |
| K      | Degrees Kelvin  |
| LDA    | Lithium diisopropylamide  |
| M      | Molar   |
| m      | Multiplet   |
| MALDI  | Matrix-assisted laser desorption/ionization   |
| Me     | Methyl  |
| MeCN   | Acetonitrile  |
| MeOH   | Methanol  |
| Mes    | Mesityl   |
| mg     | Milligram   |
| MHz    | Megahertz   |
| min    | Minute  |
| mL     | Milliliter  |
| mM     | Millimolar  |
| mm     | Millimeter  |
| mmol   | Millimole   |
| mol    | Mole  |
| MPa    | Megapascal  |
| MS     | Mass spectrometry   |
| ms     | Millisecond   |
| NBS    | <i>N</i> -Bromosuccinimide  |
| NFSI   | <i>N</i> -Fluorobenzenesulfonimide  |
| NHC    | <i>N</i> -heterocyclic carbene  |
| nm     | Nanometer   |

|                      |   |
|----------------------|---|
| NMP                  | 1-Methyl-2-pyrrolidone                          |
| NMR                  | Nuclear magnetic resonance                      |
| OAc                  | Acetoxy   |
| OTf                  | Triflate  |
| O-TMEDA              | Bis[2-( <i>N,N</i> -dimethylamino)ethyl] ether  |
| PAH                  | Polycyclic aromatic hydrocarbon                 |
| Ph                   | Phenyl  |
| PhCl                 | Chlorobenzene                                   |
| Phen                 | Phenanthrene                                    |
| pin                  | Pinacolato                                      |
| ppm                  | Parts per million                               |
| Pr                   | Propyl  |
| <i>n</i> -Pr         | Normal propyl                                   |
| <i>i</i> -Pr         | Isopropyl                                       |
| psi                  | Pound-force per square inch                     |
| q                    | Quartet   |
| quint                | Quintet   |
| RCM                  | Ring-closing metathesis                         |
| <i>R<sub>f</sub></i> | Retention factor                                |
| rt                   | Room temperature                                |
| s                    | Singlet   |
| SANS                 | Small angle neutron scattering                  |
| SPhos                | 2-Dicyclohexylphosphino-2',6'-dimethoxybiphenyl |
| t                    | Triplet   |
| TBAB                 | Tetrabutylammonium bromide                      |
| TBAI                 | Tetrabutylammonium iodide                       |
| TBS                  | <i>Tert</i> -Butyldimethylsilyl                 |
| td                   | Triplet of doublets                             |
| TEP                  | 1,2,3,4-Tetraethylphenanthrene                  |

|       |   |
|-------|---|
| THF   | Tetrahydrofuran                                 |
| TLC   | Thin layer chromatography                       |
| TMEDA | <i>N, N, N', N'</i> -Tetramethylethylenediamine |
| UV    | Ultraviolet                                     |
| Å     | Angstrom  |
| °C    | Degrees Celsius                                 |
| μL    | Microliter                                      |

# **1. Development of Asphaltene Model Compounds Synthesis**

Petroleum is a fundamental raw material that is linked to almost all areas of chemical industry. Light crude oil, or conventional petroleum, is in great demand in daily life and production. It is common knowledge that fossil fuels, including petroleum, coal, and natural gas, are non-renewable resources and their reserves will certainly decrease over time. The high demand for light crude oil reflects the fact that it will deplete in the near future. Meanwhile, heavy crude oil and bitumen have not been fully exploited and utilized, offering a significant resource for scientists seeking alternatives for petroleum refining. Bitumen is an extremely complex mixture containing numerous types of organic components.<sup>1</sup> Asphaltene, as a part of bitumen, raises quite a lot of undesired characteristics during industrial production.<sup>2</sup> Therefore, research into the nature of asphaltene constituents is necessary before the bitumen resources can be used as an alternative energy source to petroleum.

## **1.1 Asphaltene extraction and analysis**

### **1.1.1 Bitumen and asphaltenes as natural resources**

Bitumen is defined as the part of crude oil which has a viscosity higher than  $10^5 \text{ mPa}\cdot\text{s}$ .<sup>3</sup> It is a natural resource that is widely distributed around the world.<sup>1,4</sup> As one of the largest deposits in the world, the bitumen reserves in Alberta are estimated to be 1.7 trillion barrels,<sup>5</sup> which is mainly located in Athabasca, Peace River, Cold Lake, and Lloydminster.<sup>5,6</sup> The physical properties of bitumen are quite different from those of conventional light oil. Bitumen has a density greater than that of water ( $1000 \text{ kg/m}^3$ ).<sup>3</sup> Bitumen also has low mobility and high viscosity, making its production and pipelining difficult.<sup>7,8</sup> The addition of a suitable solvent is necessary to reduce the viscosity of bitumen.<sup>1</sup>

The solvent addition method allows the separation of different components in bitumen. Bitumen can be divided into two major categories based on solubility: maltenes and asphaltenes. Maltenes are the components that are soluble in *n*-alkanes (e.g., *n*-pentane or *n*-heptane). In contrast, asphaltenes are the components that are soluble in toluene but insoluble in *n*-alkanes.<sup>9</sup> Maltenes can also be divided into three subclasses: saturates, aromatics and resins, based on the polarity of each fraction. This simple analysis scheme for bitumen is called “SARA analysis” (Figure 1-1).<sup>1,10,11</sup>

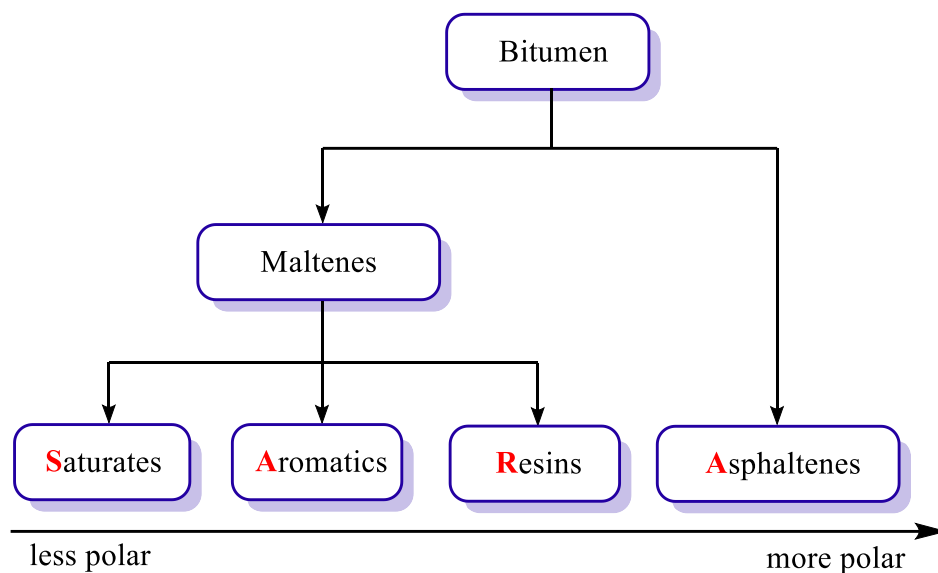


**Figure 1-1.** SARA analysis of bitumen.

Among the above four components, the asphaltene fraction is the heaviest and most complex part in terms of chemical composition.<sup>12</sup> Asphaltene appears as a friable, infusible solid.<sup>9</sup> The molecules in asphaltene usually exist as aggregates when dissolved in solvents, which makes them tend to precipitate.<sup>1</sup> Asphaltene aggregates may precipitate as a result of small environmental changes during production, transportation or processing.<sup>2, 13 - 16</sup> Precipitated asphaltenes can cause a series of problems, such as the clogging of pipelines,<sup>17</sup> deactivation of

catalysts,<sup>18</sup> reduced storage capacity,<sup>19</sup> and the fouling of equipment.<sup>20</sup> So, asphaltenes are regarded as the most problematic part of bitumen in oil upgrading.<sup>1,9</sup> In addition, the precipitation of asphaltenes always traps valuable maltenes in the aggregates,<sup>21</sup> leading to loss of maltene materials. To maximize bitumen resources and avoid the side effects caused by asphaltene precipitation, petroleum scientists are eager to understand asphaltene's structure and aggregation behavior.

Due to the high degree of complexity in chemical composition and aggregation behavior, none of the current analysis techniques are able to provide exact structures of the constituents of asphaltene.<sup>22</sup> Only partial information can be acquired from existing techniques, which determine the rough structural motifs of asphaltenes as described in section 1.2.

It should be noted that, besides petroleum, asphaltenes can also be extracted from raw coal.<sup>23</sup> The chemical composition and structures of coal-derived asphaltenes are different than petroleum-derived asphaltenes; e.g., coal-derived asphaltenes usually have lower molecular weights, more hydroxyl and pyrrolic groups, and more and longer alkyl chains.<sup>23,24</sup> In this dissertation, asphaltenes refer specifically to petroleum-derived asphaltenes.

### **1.1.2 Chemical composition of asphaltenes**

Elemental analysis is the oldest and simplest mean of chemical characterization of petroleum.<sup>6</sup> Understanding the chemical composition of asphaltenes is important because chemical composition can afford some useful information for structural determination. Asphaltene samples from different origins or sources have varied chemical compositions and the solvents used for precipitation also affect the asphaltene composition.<sup>6</sup> Figure 1-2 shows approximate



mean values of CHNOS compositions for asphaltenes from various sources (precipitated by *n*-pentane).<sup>6</sup>

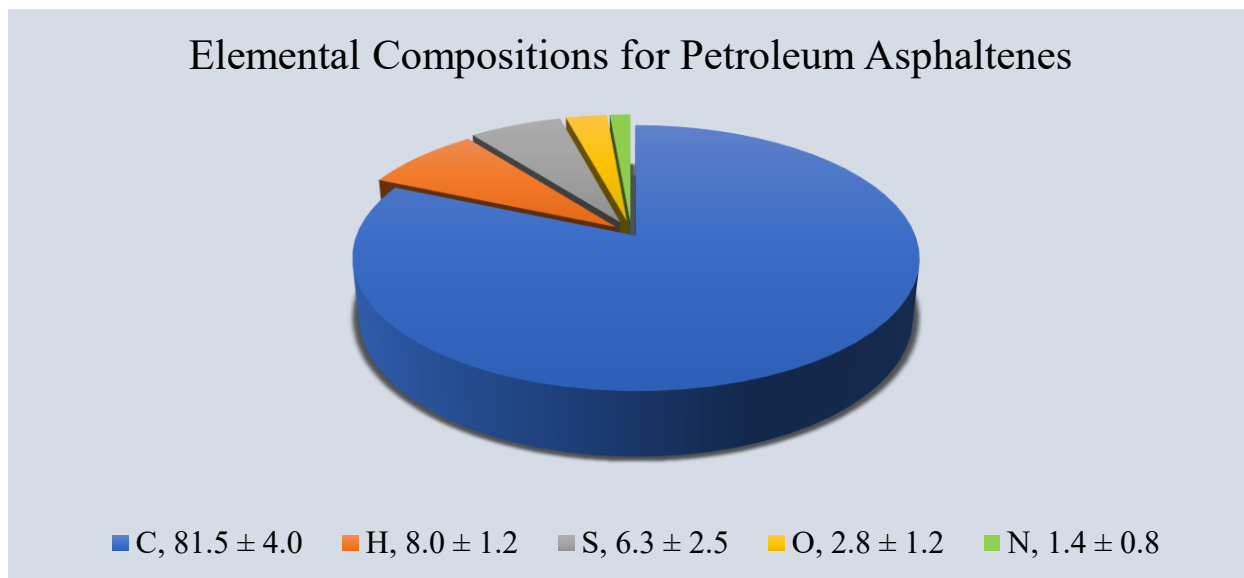


**Figure 1-2.** Elemental compositions for petroleum asphaltenes.<sup>6</sup>

More detailed information of asphaltene composition is listed below:

1. *Molecular weight.* Because of the aggregation behavior, the molecular weights of asphaltenes vary a lot by different techniques used.<sup>25,26</sup> Now, it is commonly agreed that the range is 200-1500 Da while the average value is 500-800 Da.<sup>27-29</sup>

2. *Carbon and hydrogen.* Asphaltene samples, regardless of their origins and sources, usually have similar hydrogen-to-carbon ratios (H/C ratio) of 1.0 to 1.2.<sup>6</sup> The H/C ratio of asphaltene is much lower than the average H/C ratio of bitumen (1.4 to 1.6),<sup>6</sup> due to the presence of more polycyclic aromatic hydrocarbon (PAH) systems in asphaltenes than other components in bitumen.<sup>22</sup>

3. *Nitrogen*. The nitrogen content of all asphaltene samples is basically the same, within the range of 0.9-1.8%, which is higher than the nitrogen content in maltenes.<sup>6</sup> Nitrogen atoms are mainly found in aromatic heterocycles.<sup>30</sup> Fused-ring pyrrole derivatives are the most significant nitrogen source followed by polycyclic pyridines, including quinolines, benzoquinolines and tetracyclic analogues.<sup>22, 31-33</sup>

4. *Sulfur*. Sulfur is the most abundant heteroatom by weight in most asphaltene samples but the content varies widely in samples from different origins – Alberta asphaltene contains more than 7% sulfur, while Utah asphaltene contains less than 1%.<sup>6,31</sup> The sulfur content in asphaltene is always higher than that of its bituminous source.<sup>6</sup> Sulfur atoms are mainly found in polycyclic aromatic heterocycles (e.g., benzothiophenes, dibenzothiophenes, naphthobenzothiophenes) as well as sulfides.<sup>30,31</sup>

5. *Oxygen*. The oxygen content of asphaltene is frequently reported by the mass difference between CHNS contents and the sample.<sup>6</sup> Oxygen content also varies considerably for some asphaltene samples due to exposure to atmospheric oxygen.<sup>6</sup> Oxygen atoms are mostly found in many functional groups (e.g., carboxylic acids, alcohols, ketones), mostly on alkyl sidechains.<sup>30,31,34</sup>

6. *Trace metals*. Asphaltene contains more than twenty metal elements. The concentrations of all trace metals are higher in asphaltenes than in maltenes.<sup>6</sup> V, Ni and Fe are the trace metals with highest concentrations in asphaltenes.<sup>6</sup> Among them, Ni and V are usually found to coordinate to biomarkers such as porphyrins (Figure 1-3).<sup>30,35</sup>

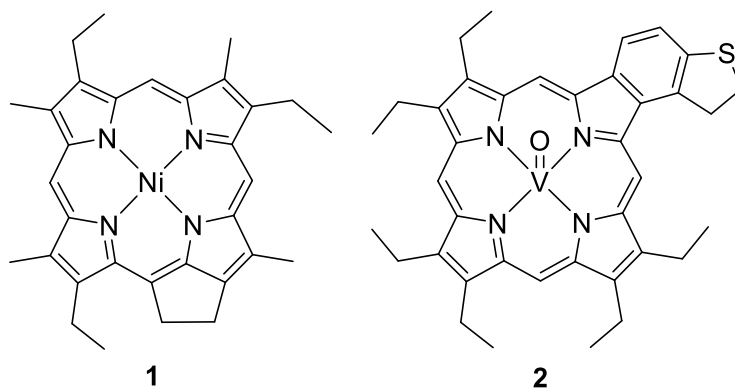


**Figure 1-3.** Examples of possible nickel- and vanadyl-porphyrins characterized from bitumen.<sup>36,37</sup>

## 1.2 Asphaltene structural models

### 1.2.1 Continental asphaltene model

Due to the chemical complexity of asphaltenes, petroleum chemists have attempted to separate it into subfractions that can be characterized easily.<sup>38,39</sup> Several techniques have also been employed to study asphaltenes, including vapor phase osmometry (VPO) and mass spectrometry for measuring molecular composition,<sup>28,38,40-45</sup> small angle neutron scattering (SANS) for determining intermolecular interactions and asphaltene aggregation,<sup>38,39,46</sup> isothermal titration calorimetry (ITC) for investigating asphaltene association,<sup>47-49</sup> fluorescence depolarization (FD) for measuring asphaltene molecular size,<sup>25,50</sup> near-infrared spectroscopy (NIR) for characterizing asphaltene aggregation,<sup>51,52</sup> infrared spectroscopy (IR) for assessing hydrogen bonds,<sup>53,54</sup> UV-vis spectroscopy for analyzing PAH systems,<sup>55</sup> and NMR spectroscopy for studying asphaltene diffusion in solvents.<sup>56,57</sup>

Based on the analytical results, Yen and co-workers first proposed an asphaltene model structure in 1961.<sup>58</sup> This model, known as the “Yen model”, describes the structure of asphaltene as a

PAH core with long, functionalized alkyl chains attached to the periphery. Later, Mullins and co-workers proposed a modified version of the Yen model. They pointed out that asphaltene PAH molecules can form nanoaggregates with aggregation numbers  $\sim 6$ , and the nanoaggregates constitute into clusters with aggregation numbers  $\sim 8$ .<sup>12, 59-61</sup> This modified Yen model is known as the “Yen-Mullins model”. Because of its structural characteristics, the Yen-Mullins model is also called the “island model” or the “continental model”.

In recent years, atomic force microscopy (AFM) has become a powerful tool to image individual molecules and provide structural information.<sup>62</sup> Schuler and co-workers have adapted AFM to visualize single molecules in petroleum asphaltene samples from different resources.<sup>24,63</sup> They observed great structural diversities in all asphaltene samples, but most molecules possess a large PAH core with indeterminate peripheral alkyl substituents (Figure 1-4).<sup>63</sup> Their findings are in accordance with the continental model.

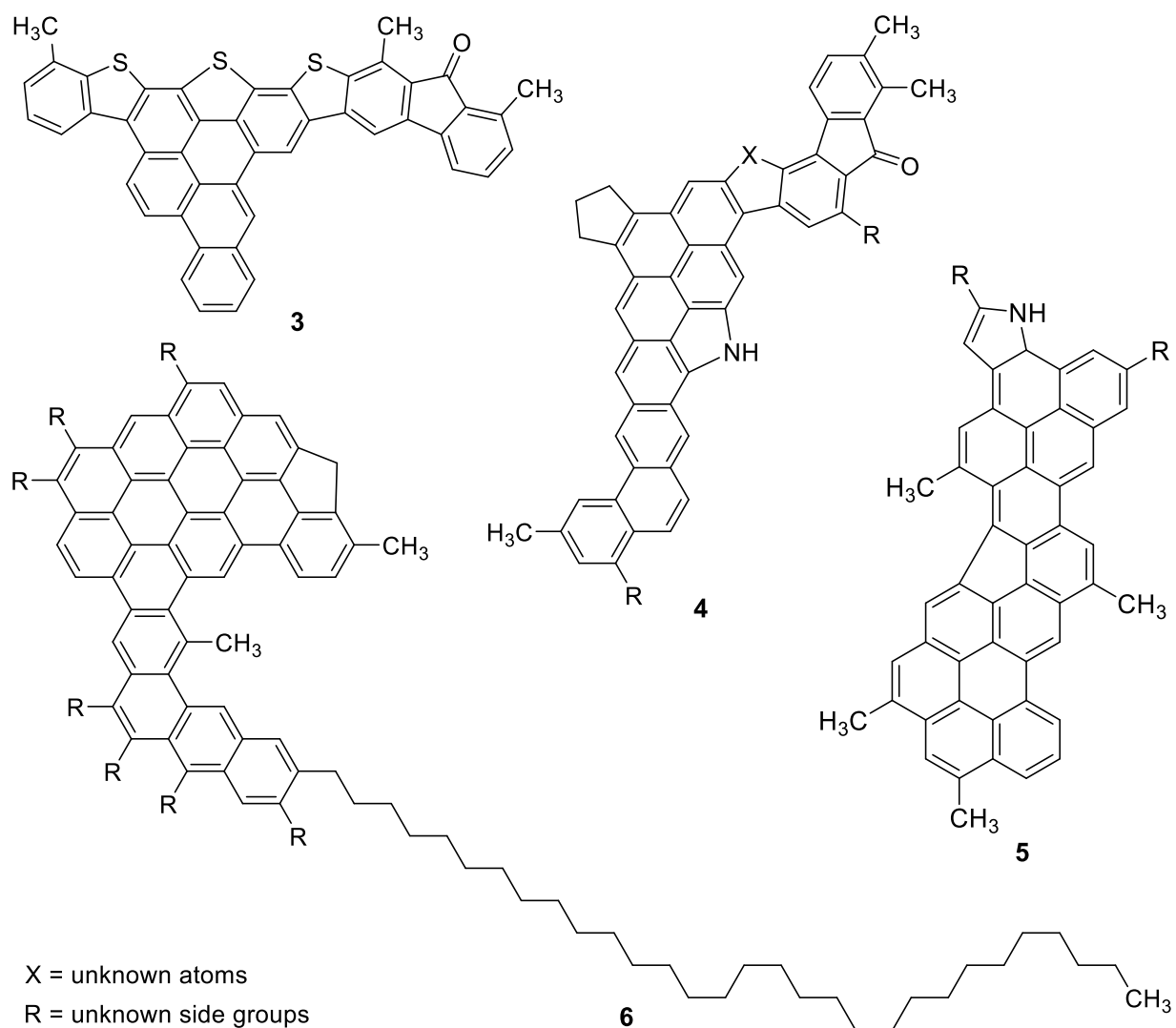


**Figure 1-4.** Assigned structures of four actual molecules in an asphaltene sample based on AFM measurements by Schuler and co-workers.<sup>63</sup>

### 1.2.2 Evidence for the presence of archipelago compounds in asphaltenes

Although the continental model is supported by a variety of experimental results, it fails to explain many properties observed in asphaltenes. For example, the continental model attributes asphaltene aggregation to electrostatic and/or van der Waals forces through parallel and perpendicular stacking of the large planar aromatics ( $\pi$ - $\pi$  stacking).<sup>61,64</sup> However, Gray and co-

workers studied continental model compounds and found that  $\pi$ - $\pi$  stacking is too weak to account for asphaltene aggregation in dilute solution or at elevated temperatures.<sup>65</sup> Also, they found that their synthetic continental model compounds do not adhere to silica like native asphaltenes.<sup>66</sup> Other experimental results, including solvent entrapment tests by SANS<sup>67</sup> and thermal cracking,<sup>68,69</sup> also indicate that the continental model alone cannot be used to well represent asphaltenes.

Therefore, another asphaltene structural model was proposed to explain the deficiencies of the continental model. This model, known as the “archipelago model”, describes asphaltene structures as multiple smaller PAH cores (usually 1-4 rings) linked together by alkyl chains.<sup>70,71</sup> Later, Gray and co-workers proposed a supramolecular archipelago model (Figure 1-5).<sup>66</sup> This model attributes asphaltene aggregation to several types of intramolecular and intermolecular associations, including acid-base interactions, hydrogen bonding,  $\pi$ - $\pi$  stacking and coordination to transition metal ions.<sup>66</sup>

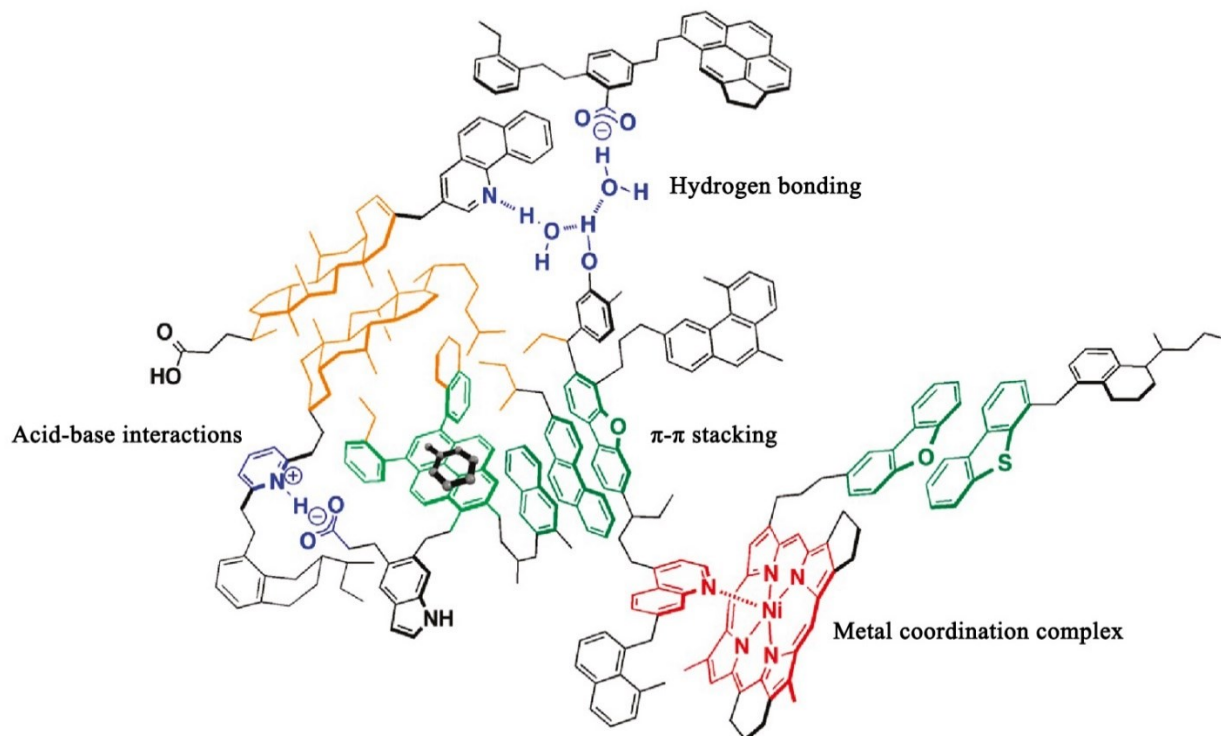


**Figure 1-5.** A schematic diagram of supramolecular archipelago model (“Supramolecular assembly model for aggregation of petroleum asphaltenes,” *Energy Fuels* **2011**, 25, 3125–3134. Adapted with permission from authors. Copyright 2012 American Chemical Society).<sup>66</sup>

More recently, Rodgers and co-workers employed high-resolution FT-ICR-MS to investigate asphaltene molecular composition.<sup>72-74</sup> They determined that continental and archipelago motifs coexist in asphaltene samples, and the ratio is sample dependent (e.g., Wyoming deposit asphaltenes are continental dominant while Athabasca bitumen asphaltenes are archipelago dominant).<sup>74</sup> They also suggested that extensive cleaning of the asphaltene sample is necessary for FT-ICR-MS to provide accurate results.<sup>72</sup> Continental compounds show a much greater efficiency of ionization than archipelago compounds, which could be a reason that previous MS results always pointed to the dominance of continental structures in asphaltenes.<sup>72</sup>

However, the current AFM measurements of asphaltenes rarely provide archipelago-type structures. Among all the samples observed by Schuler and co-workers', molecule **7** is the only archipelago-type structure they found in a coal-derived asphaltene sample, but two islands in **7** are separated by only one C(Ar)-C(Ar) bond (Figure 1-6).<sup>24</sup> Planar molecules are more easily recognized by AFM than non-planar ones,<sup>75</sup> which may be a reason for the dominance of continental structures in asphaltene AFM images. Although recent studies have demonstrated that AFM could detect simple synthetic archipelago model compounds,<sup>75,76</sup> up to now, there are no reports proving the existence of a large number of archipelago compounds in asphaltenes from AFM measurements.

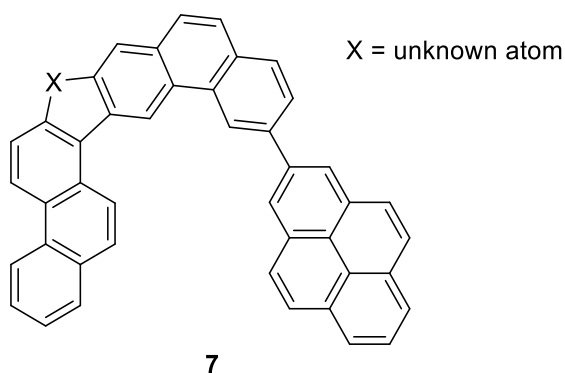


**Figure 1-6.** An actual archipelago-type molecule in coal-derived asphaltenes observed by Schuler and co-workers using AFM.<sup>24</sup>

Therefore, an alternative way to study archipelago compounds was developed, by using synthetic model compounds with known archipelago-type structures to imitate authentic asphaltenes and to establish characterization methods and properties. Several research groups have been devoted to this area. The results of their studies are discussed next.



### 1.3 Methodologies for preparing archipelago model compounds

#### 1.3.1 Traditional archipelago model compounds

Synthetic archipelago compounds have been widely adopted to study asphaltenes using many analytical techniques. For example, Sabbah and co-workers compared laser desorption/laser ionization mass spectra of synthetic archipelago compounds with asphaltenes, to investigate asphaltene structural characteristics.<sup>44,77</sup> Gray and co-workers carried out pyrolysis experiments at 365-420 °C with archipelago model compounds to reveal the chemical mechanism for the formation of asphaltenes in the natural environment.<sup>78</sup> Alshareef and co-workers studied the asphaltene coke formation with archipelago model compounds.<sup>79</sup> Schuler and co-workers tested the possibility of characterizing aliphatic moieties in asphaltenes from AFM using archipelago model compounds.<sup>75</sup>

However, archipelago compounds are rarely commercially available. Dipyrrenyl alkanes **8** are a series of commercial archipelago compounds frequently used in asphaltene studies (Figure 1-7).<sup>75,76,80</sup> These compounds possess only two unsubstituted pyrene islands and an axis of symmetry, which cannot be considered good models for the extremely complicated asphaltenes.

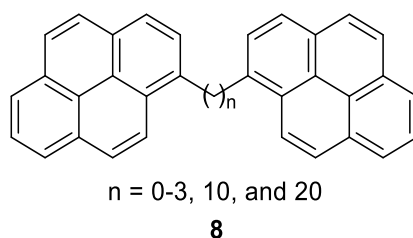
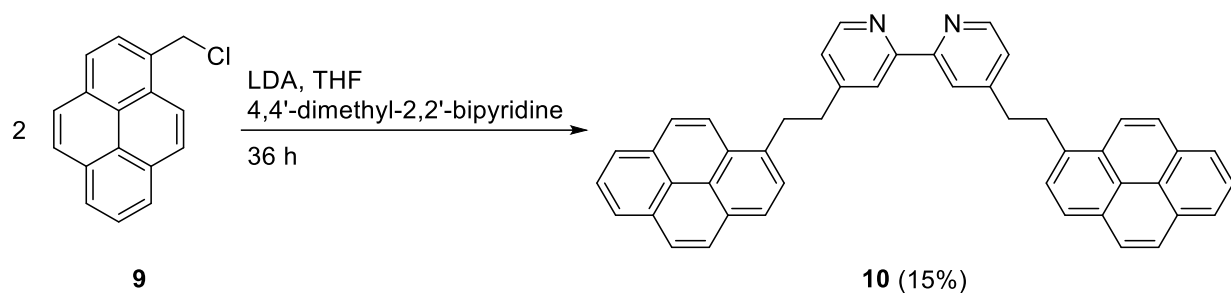


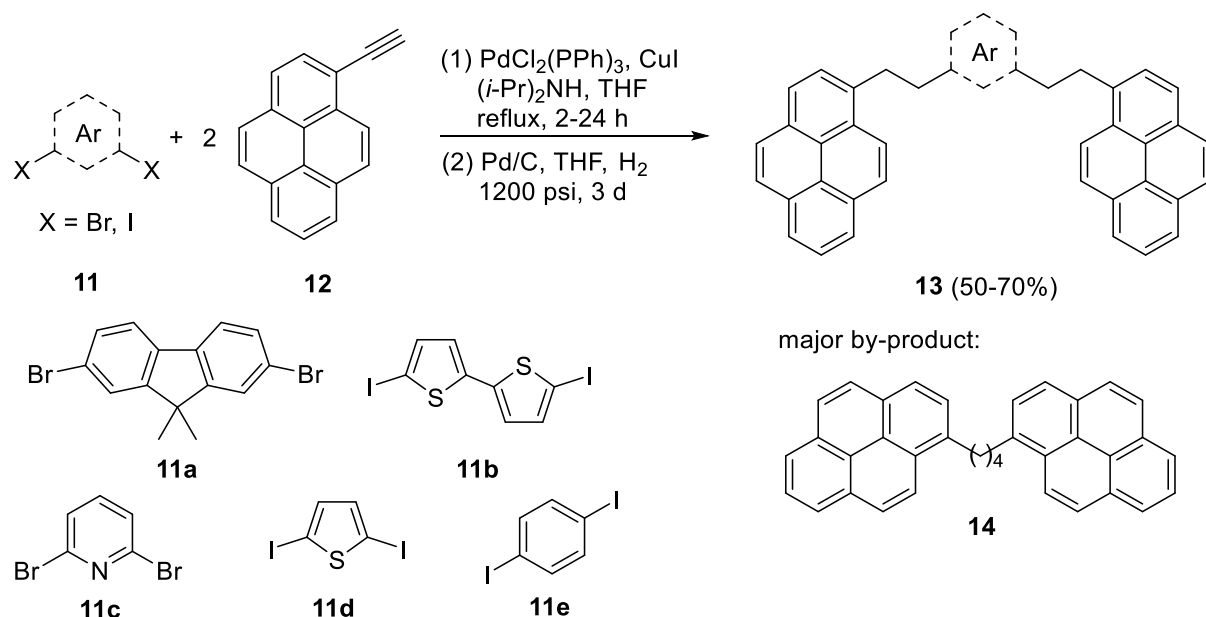
**Figure 1-7.** Commercially available dipyrrenyl alkanes as archipelago model compounds.

To acquire archipelago compounds with more than two simple islands, synthetic approaches must be utilized (Scheme 1-1). In 2008, Fenniri and co-workers prepared a bipyridine-based archipelago compound **10** using benzylic deprotonation and subsequent alkylation, but the yield was only 15% (Scheme 1-1a).<sup>81</sup> Later in 2010, Sabbah and co-workers synthesized a variety of archipelago compounds **13** by Sonogashira coupling of 1-ethynylpyrene **12** with dihalo aromatic substrates **11** followed by hydrogenation (Scheme 1-1b).<sup>44</sup> The yields were moderate because of the significant formation of side product **14** in all reactions, which results from the homocoupling/hydrogenation of **12**. In addition, none of the reported products from this synthetic approach has more than three PAH cores, which limits the research of archipelago compounds with high molecular weights. Advanced synthetic methodologies must be developed to obtain archipelago compounds with higher molecular weights and structural complexity.

(a) Benzylic deprotonation/alkylation (Fenniri, 2008):



(b) Sonogashira coupling followed by hydrogenation (Sabbah, 2010):

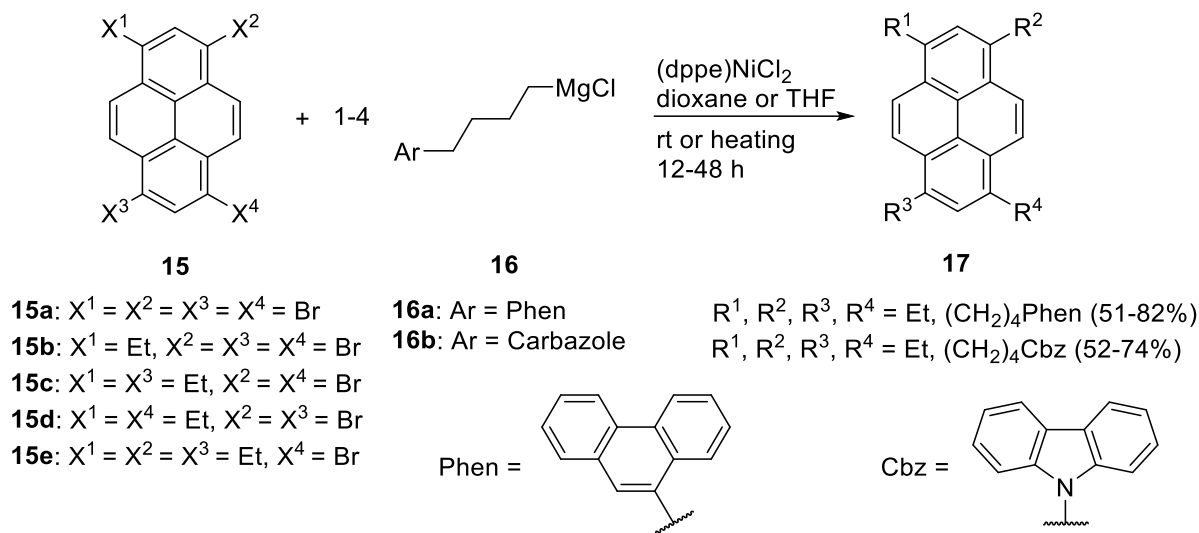


**Scheme 1-1.** Traditional synthetic approaches to obtain archipelago compounds.<sup>44,81</sup>

### 1.3.2 Advanced synthetic approaches to archipelago model compounds

In 2015, Stryker and co-workers reported a methodology for preparing a new library of archipelago compounds **17** with up to five islands (Scheme 1-2).<sup>82</sup> The Grignard reagents of alkylated phenanthrene or carbazole **16** undergo nickel-catalyzed Kumada couplings with mono- to tetra- bromo-substituted pyrenes **15**, generating archipelago compounds **17** with two to five islands. The products can be obtained in moderate to good yields at gram-scale without

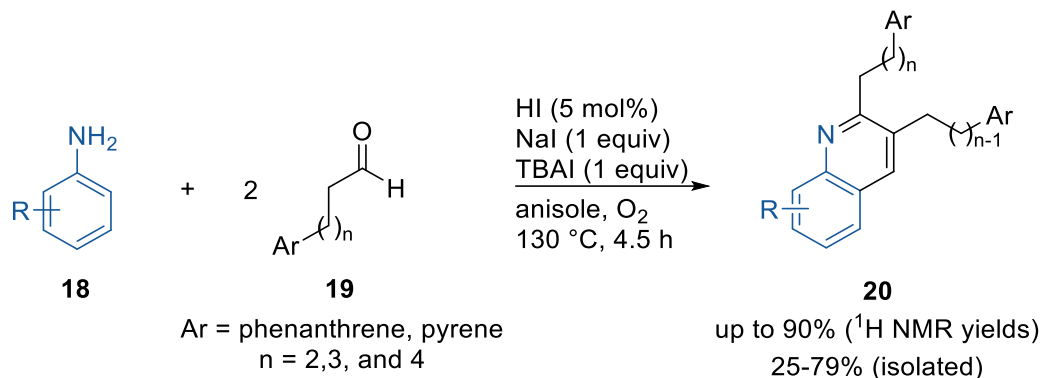
chromatographic purification, which demonstrates an attractive application to asphaltene studies.<sup>83,84</sup>



**Scheme 1-2.** Archipelago compounds synthesis by nickel-catalyzed Kumada coupling.<sup>82</sup>

Although the synthesis of high molecular weight archipelago compounds was achieved, compounds **17** are symmetrical in structure and cannot appropriately imitate the highly complex authentic asphaltenes. Also, the compounds do not contain basic nitrogen or sulfur atoms as are found in asphaltenes. Therefore, Stryker and co-workers continued to work on the preparation of archipelago compounds and provided a new approach using a multicomponent cyclocondensation reaction (MCR) to prepare unsymmetrical structures **20** (Equation 1-1).<sup>85</sup> Reactions of aniline derivatives **18** and island-tethered aldehydes **19** yielded a variety of three-island archipelago products **20** containing basic nitrogen atoms, which makes these compounds characteristic models of asphaltenes. Unfortunately, although <sup>1</sup>H NMR spectroscopy indicated efficient conversions of the starting materials to products, self-aggregation issues restricted the isolation of some products and the purified yields were just moderate. In addition, attempts to

use bi-directional anilines to make five-island archipelago compounds were not successful. Model compounds are limited to three islands in this synthetic strategy.<sup>22</sup>



**Equation 1-1.** Archipelago compounds synthesized by MCR.<sup>85</sup>

Besides the model compounds with PAH cores, biomarker-containing archipelago compounds were also designed, including compounds with embedded steroids<sup>86,87</sup> or porphyrins.<sup>88-90</sup> More recently, a literature review by Scott *et al.*, provides a detailed summary of the archipelago model compounds that have been synthesized so far.<sup>91</sup>

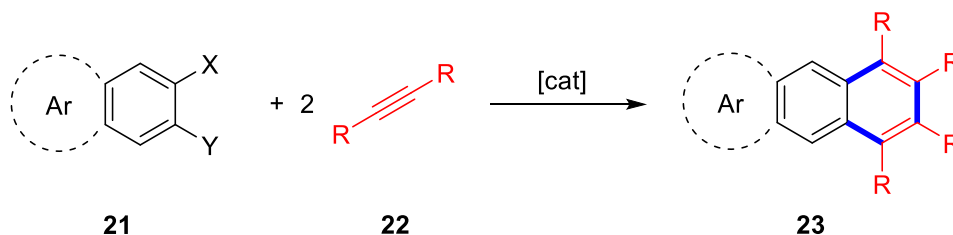
At present, the scope of archipelago compound synthesis is still limited by many factors, including molecular weights, reaction scale, and heteroatom inclusion. Thus, novel synthetic strategies must be developed to overcome the difficulties and allow us to make “real” archipelago model compounds. Many transition metal-catalyzed alkyne annulation reactions reported in recent years provide useful methods for synthesizing new-types of archipelago compounds, as discussed in detail next.

## 1.4 Transition metal-catalyzed alkyne annulation reactions

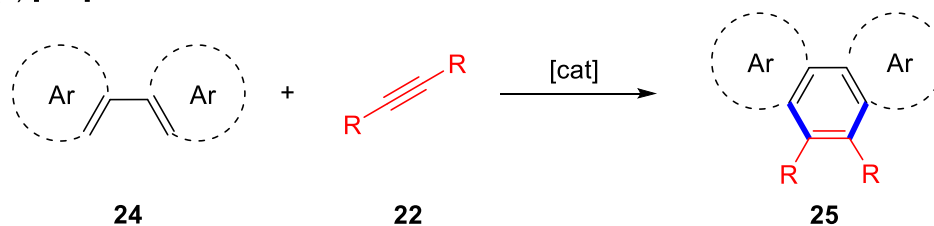
Alkyne annulation reaction is a type of cross-coupling reaction between aromatic substrates and alkynes. Typically, these reactions require a transition metal complex as the catalyst (e.g., Rh, Pd, and Co). Alkyne annulation reactions are powerful tools for making compounds containing large polycyclic arenes, which show attractive semiconducting<sup>92-95</sup> and photochemical properties.<sup>96-98</sup> Therefore, research into alkyne annulation reactions has been popular in recent years.

The alkyne annulation reactions can be divided into two main categories: [2+2+2] annulation reactions and [4+2] annulation reactions (Scheme 1-3).

(a) [2+2+2] annulation reactions



(b) [4+2] annulation reactions

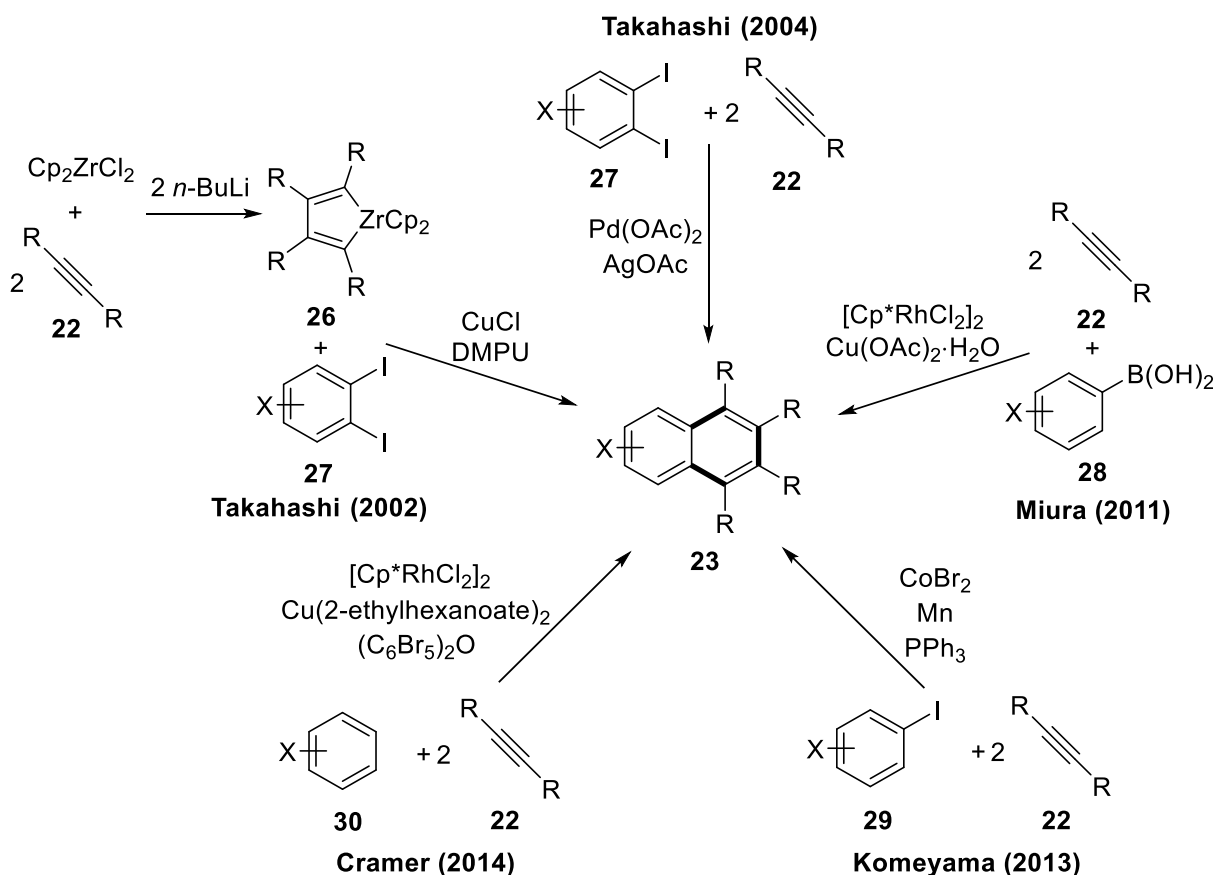


**Scheme 1-3.** [2+2+2] Alkyne annulation and [4+2] alkyne annulation reactions.

### 1.4.1 Transition metal-catalyzed [2+2+2] alkyne annulation reactions

[2+2+2] annulation is an effective methodology to make polycyclic arenes with multiple substituents. In a [2+2+2] annulation reaction, one molecule of aromatic substrate **21** couples

with two molecules of alkyne **22** to produce a tetra-substituted ring-expanded arene **23** (Scheme 1-3). Some examples of [2+2+2] annulations are summarized in Scheme 1-4 and discussed briefly below.

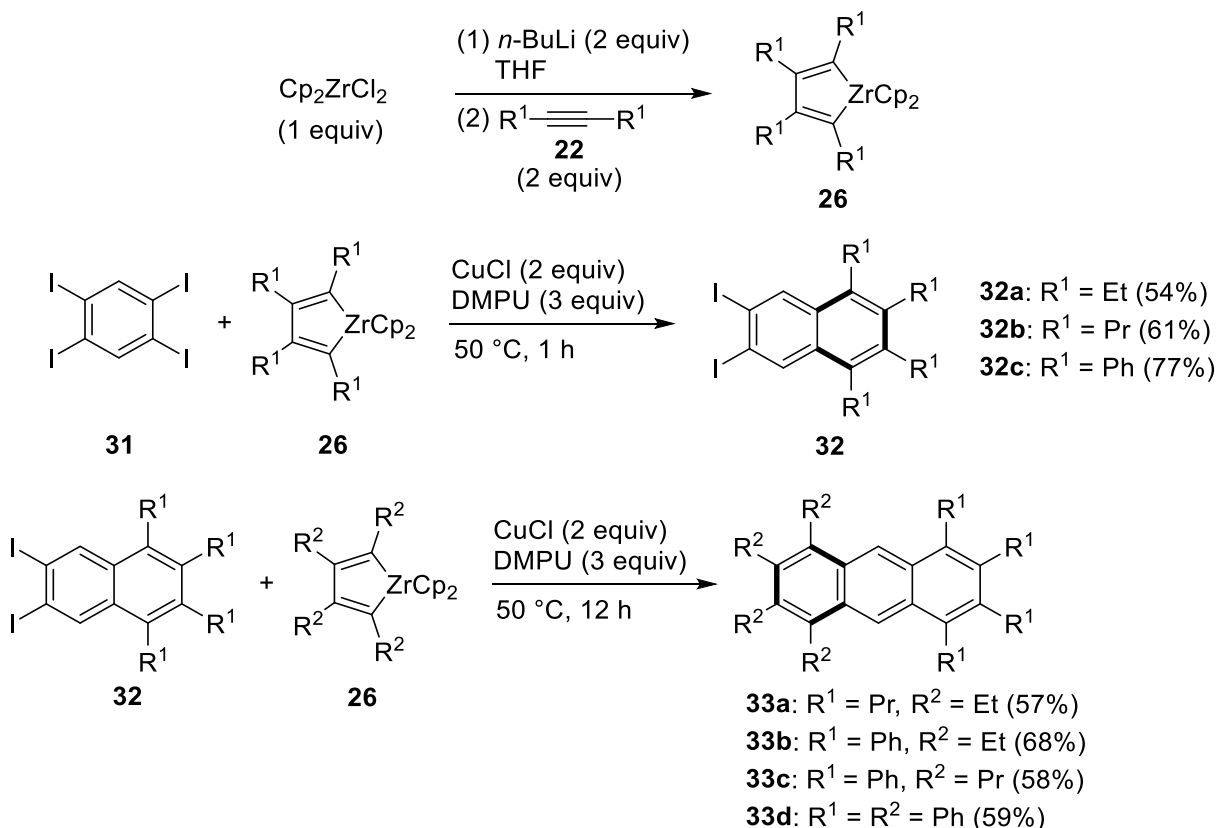


**Scheme 1-4.** Some examples of [2+2+2] annulation reactions.<sup>99-103</sup>

### 1. Copper-catalyzed annulations of *o*-diiodoarenes with zirconacyclopentadienes

A pioneering study of [2+2+2] annulation was reported by Takahashi and co-workers in 2002 (Scheme 1-5).<sup>99</sup> This annulation proceeds in two steps. The *o*-diiodoarene (**31** and **32**) couples with zirconacyclopentadienes **26**, which are prepared from  $\text{Cp}_2\text{ZrCl}_2$ ,  $n\text{-BuLi}$  and two alkynes, to provide a ring extended arene product (**32** and **33**). Takahashi and co-workers synthesized

different octa-substituted anthracene adducts **33a-d** by using 1,2,4,5-tetraiodobenzene **31** and different alkynes as the starting substrates.



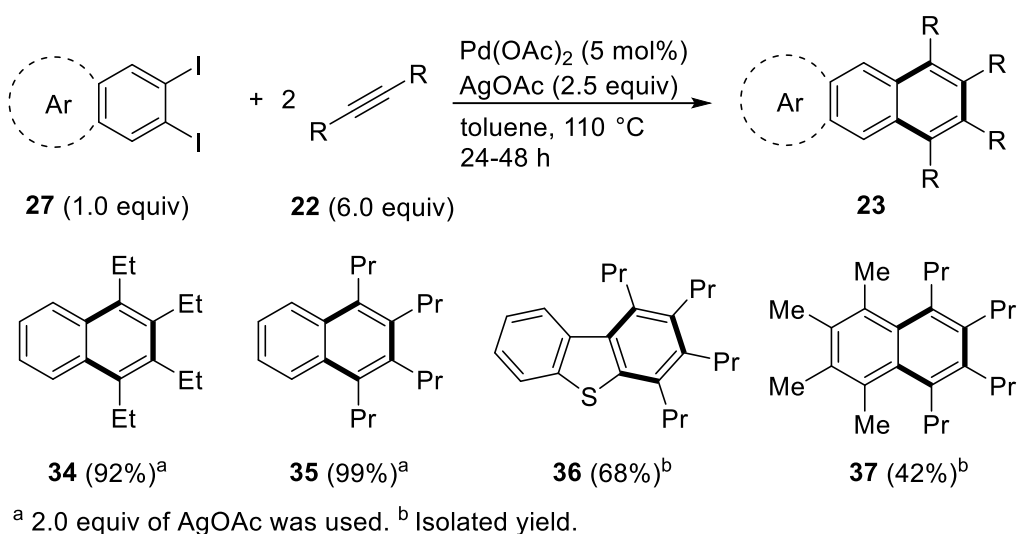
**Scheme 1-5.** Synthesis of octa-substituted anthracene by annulations of 1,2,4,5-tetraiodobenzene with zirconacyclopentadienes.<sup>99</sup>

## 2. Palladium-catalyzed annulations of *o*-diiodoarenes with alkynes

Takahashi and co-workers described another [2+2+2] annulation in 2004 to avoid using stoichiometric amounts of the zirconium reagent and  $\text{CuCl}$  (Equation 1-2).<sup>100</sup> In this reaction, an *o*-diiodoarene **27** couples with alkynes to give a [2+2+2] adduct **23** in the presence of  $\text{Pd}(\text{OAc})_2$  catalyst and silver acetate oxidant. The authors did not investigate the mechanism further. Although this one-step annulation makes the synthesis of ring-expanded arene more convenient,



it suffers largely from the lack of commercial availability of *o*-diiodoarene substrates. Moreover, the addition of 6 equivalents of alkyne means that 4 equivalents of alkyne are wasted during the reaction. To be practical, new alkyne annulation strategies have been introduced to improve the efficiency.



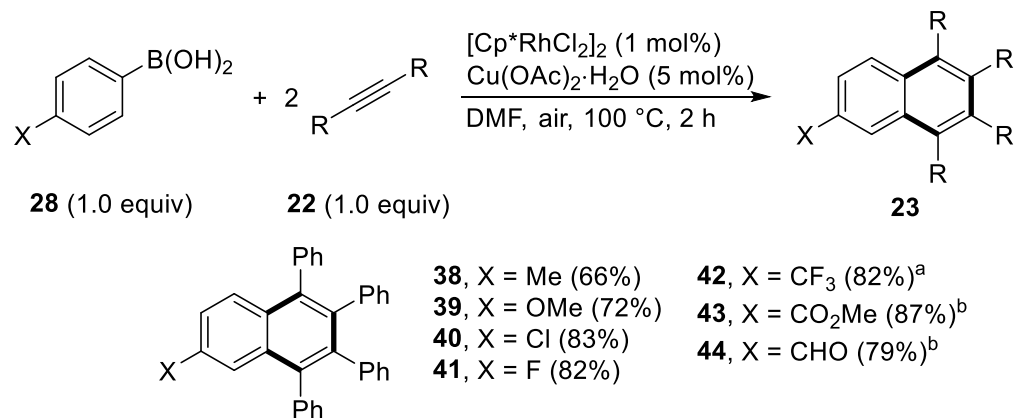
**Equation 1-2.** Pd-catalyzed [2+2+2] annulations of *o*-diiodoarenes with alkynes.<sup>100</sup>

### 3. Rhodium-catalyzed annulations of aryl boronic acids with alkynes

In 2011, Miura and co-workers reported a [2+2+2] annulation reaction to overcome the difficulties in using *o*-diiodoarenes (Scheme 1-6).<sup>101</sup> The annulations of aryl boronic acids **28** with alkynes provide ring extension products **23** in the presence of  $[\text{Cp}^*\text{RhCl}_2]_2$  catalyst and  $\text{Cu(OAc)}_2 \cdot \text{H}_2\text{O}$  oxidant. Studies of the reaction scope showed that this annulation tolerates functional groups on the aryl boronic acids.

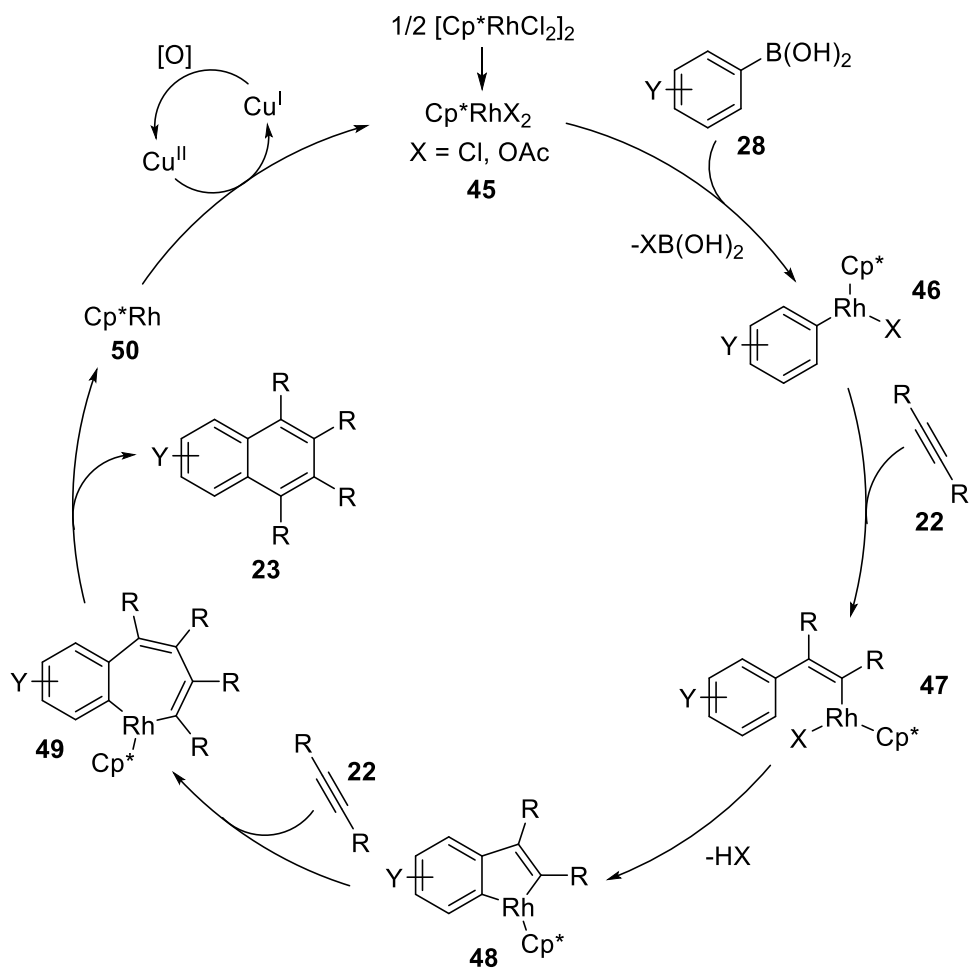
Miura and co-workers proposed a mechanism for this process. Initially,  $[\text{Cp}^*\text{RhCl}_2]_2$  dissociates to monomer  $\text{Cp}^*\text{RhX}_2$  ( $\text{X} = \text{Cl}$  or  $\text{OAc}$ ) **45**. Transmetalation of **45** to the aryl boronic acid **28** generates intermediate **46**. Then, the alkyne coordination and subsequent insertion give

intermediate **47**. An *ortho* C-H activation produces five-membered rhodacycle **48**. Insertion of a second alkyne forms seven-membered intermediate **49**. Subsequent reductive elimination yields the annulation product. Finally, the Cp\*Rh species is oxidized by Cu<sup>II</sup>, releasing the active catalyst and completing the catalytic cycle.



<sup>a</sup> Cu(OCOCF<sub>3</sub>)<sub>2</sub>·nH<sub>2</sub>O (5 mol%) replaces Cu(OAc)<sub>2</sub>·H<sub>2</sub>O.

<sup>b</sup> AgOCOCF<sub>3</sub> (1 equiv) replaces Cu(OAc)<sub>2</sub>·H<sub>2</sub>O under N<sub>2</sub>.

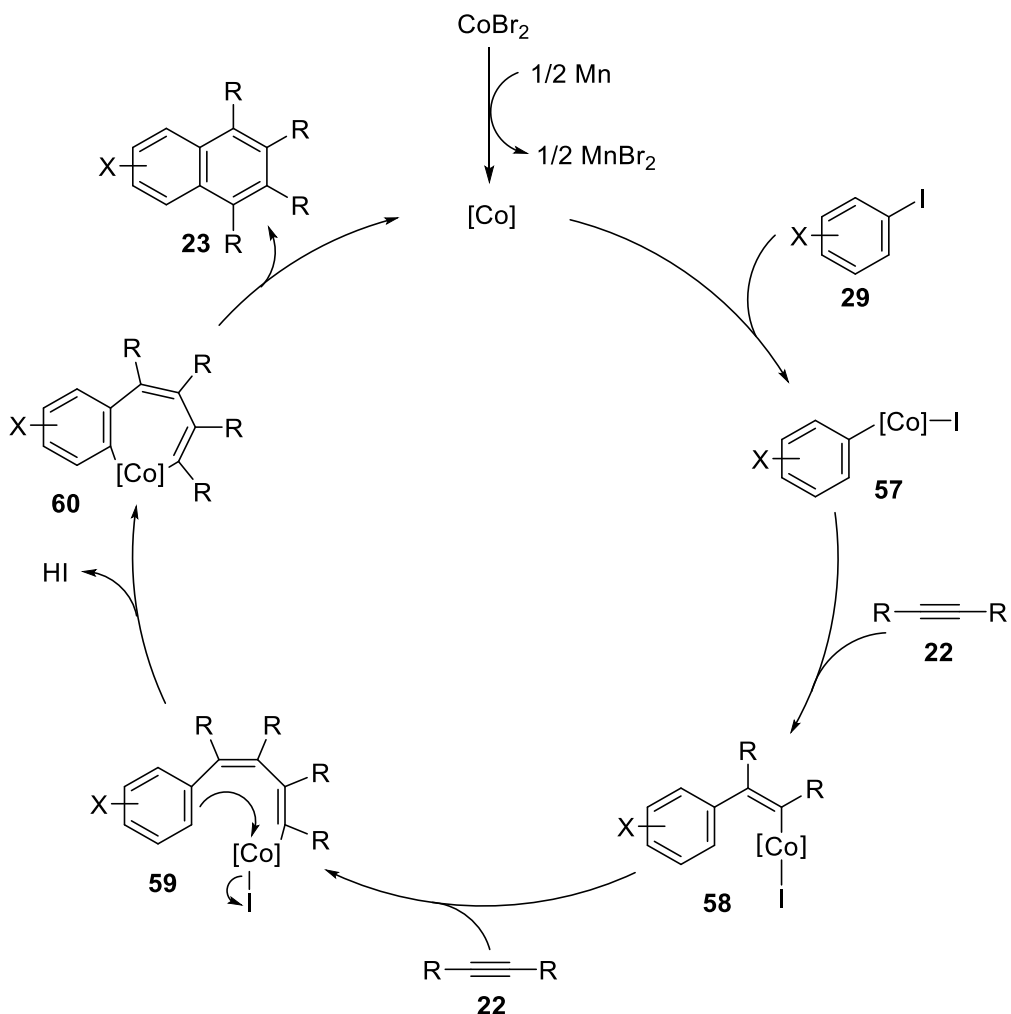
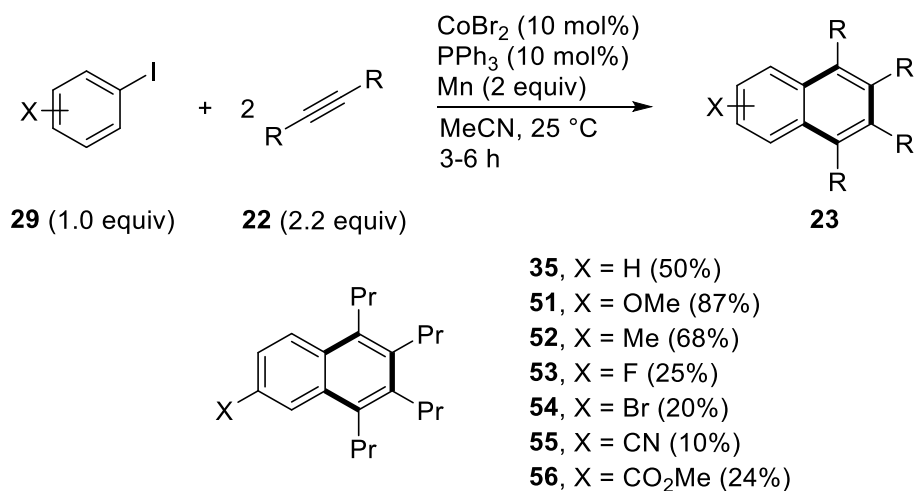


**Scheme 1-6.** Rhodium-catalyzed [2+2+2] annulations of aryl boronic acids with alkynes and proposed mechanism.<sup>101</sup>

#### 4. Cobalt-catalyzed annulations of aryl iodides with alkynes

In 2013, Komeyama and co-workers reported a less-expensive [2+2+2] annulation method using aryl iodides **29** and alkynes (Scheme 1-7).<sup>102</sup> The reaction requires CoBr<sub>2</sub> as the catalyst and stoichiometric manganese metal as the reductant. This annulation method is efficient for electron-rich arenes (e.g., **51** and **52**). However, for electron-poor arenes, the reaction yields are typically low (e.g., **53-56**).

Komeyama and co-workers proposed a mechanism to explain the outcomes of this reaction. The CoBr<sub>2</sub> pre-catalyst is reduced by Mn and coordinates PPh<sub>3</sub> to generate a low valent cobalt species abbreviated as [Co]. This active catalyst is oxidized by aryl iodides to give intermediate **57**. Then, alkyne coordination and insertion afford intermediate **59** via **58**. The next step involves an electrophilic aromatic substitution of **59**, which provides a seven-membered intermediate **60**. The reductive elimination of **60** produces the annulation product and regenerates the active Co(I) catalyst. The involvement of an electrophilic aromatic substitution step is the reason why electron-rich arenes give higher yields than electron-poor arenes. Beside this cobalt-catalyzed annulation, electrophilic aromatic substitution was also proposed as a part of the mechanism in some palladium-catalyzed annulations of alkynes with aryl iodides.<sup>104,105</sup>

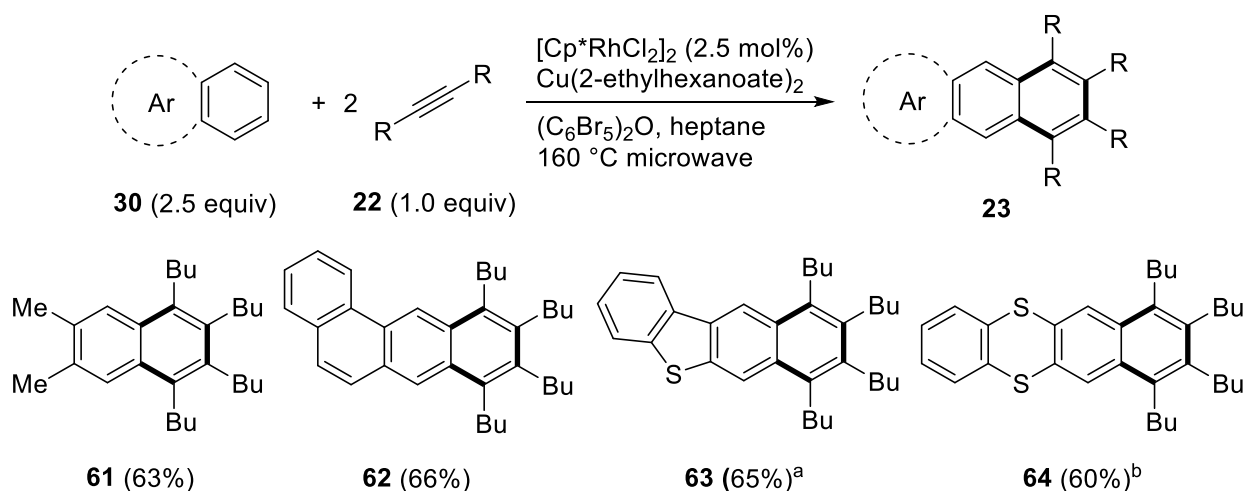


**Scheme 1-7.** Cobalt-catalyzed [2+2+2] annulations of aryl iodides with alkynes and proposed mechanism.<sup>102</sup>

## 5. Rhodium-catalyzed annulations of non-functionalized arenes with alkynes

In 2014, Cramer and co-workers reported a new alkyne annulation method using a completely non-functionalized arene **30** and  $[\text{Cp}^*\text{RhCl}_2]_2$  catalyst, under microwave irradiation (Equation 1-3).<sup>103</sup> Because the aromatic substrates are non-functionalized and easily available, this annulation reaction can be applied to many complex arenes, such as *o*-dimethyl benzene, phenanthrene, dibenzothiophene and thianthrene, to generate annulation products **61-64**.

Some weaknesses, however, restrict the efficiency of this methodology. For example, 2.5 equivalents of the arene are required. Also, for some aromatic substrates, mixtures of isomeric products are obtained (e.g., **63** and **64**). The proposed mechanism for this methodology is similar to the mechanism proposed for Miura's annulation (Scheme 1-6).<sup>101</sup> The only difference is that the aryl-rhodium intermediate **46** is generated by C-H activation of arene **30** with the electrophilic catalyst  $\text{Cp}^*\text{RhX}_2$  ( $\text{X} = \text{Cl}, \text{OAc}$ ) directly instead of transmetallation of boronic acids with  $\text{Cp}^*\text{RhX}_2$  species.



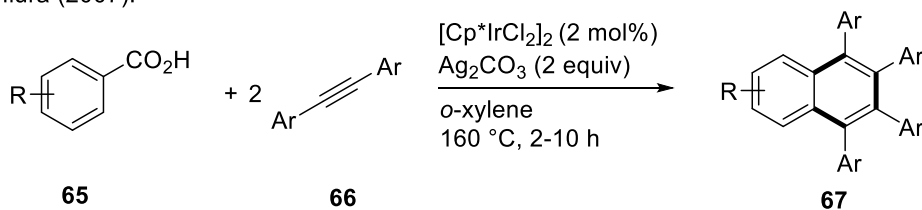
<sup>a</sup> 3.7:1 linear/angular isomer, combined yield. <sup>b</sup> 3:1 linear/angular isomer, combined yield.

**Equation 1-3.** Rhodium-catalyzed [2+2+2] annulations of non-functionalized arenes with alkynes.<sup>103</sup>

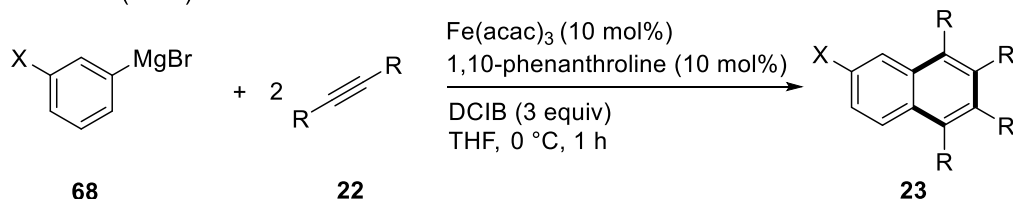
## 6. Other [2+2+2] alkyne annulation examples

Other examples of [2+2+2] annulations are summarized below. Aryl carboxylic acids (**65**, **69**),<sup>106-108</sup> aryl magnesium bromides (**68**),<sup>109</sup> indoles (**71**) and indolines (**73**)<sup>98</sup> are used as substrates for alkyne coupling, yielding tetra-substituted arenes as products (Scheme 1-8).

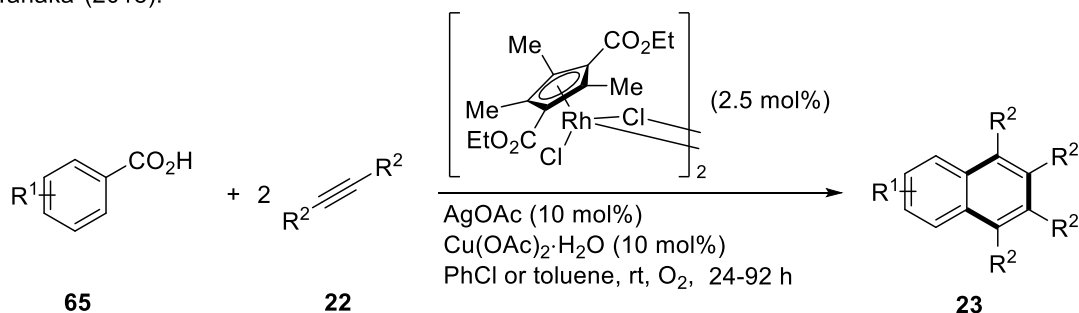
Miura (2007):



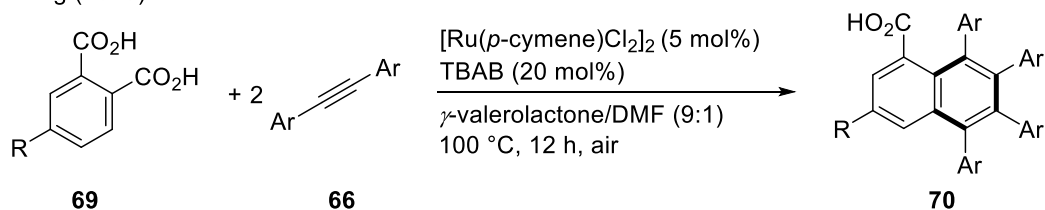
Nakamura (2012):



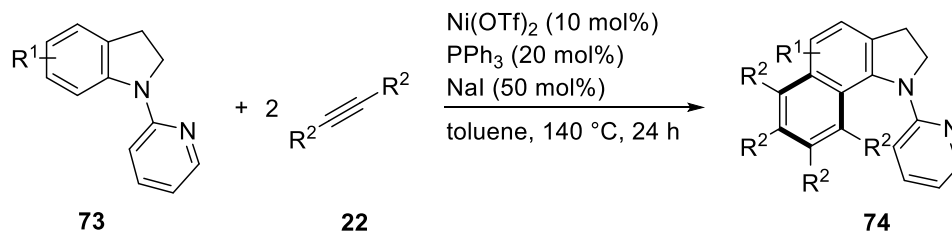
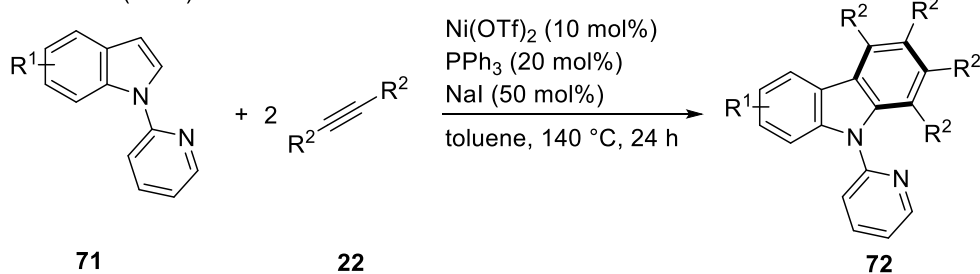
Tanaka (2018):



Zheng (2019):



Ravikumar (2021):



**Scheme 1-8.** Other examples of [2+2+2] alkyne annulation reactions.<sup>98,106-109</sup>



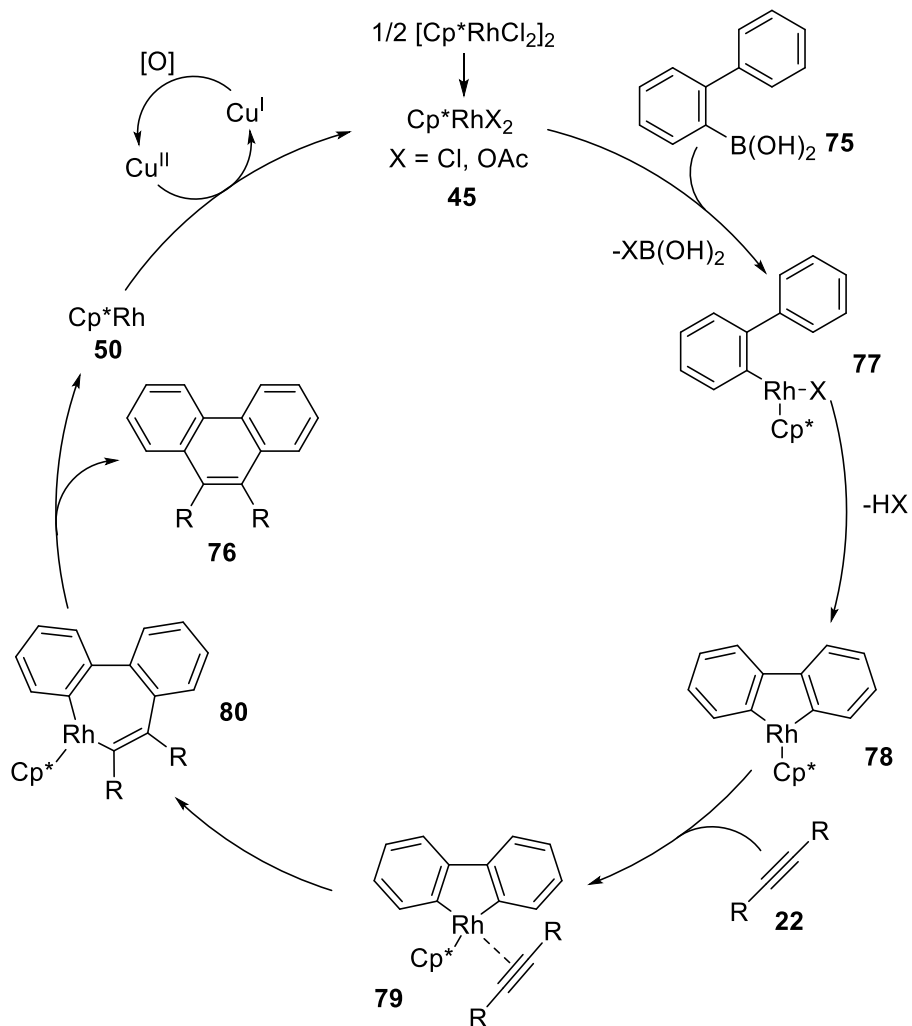
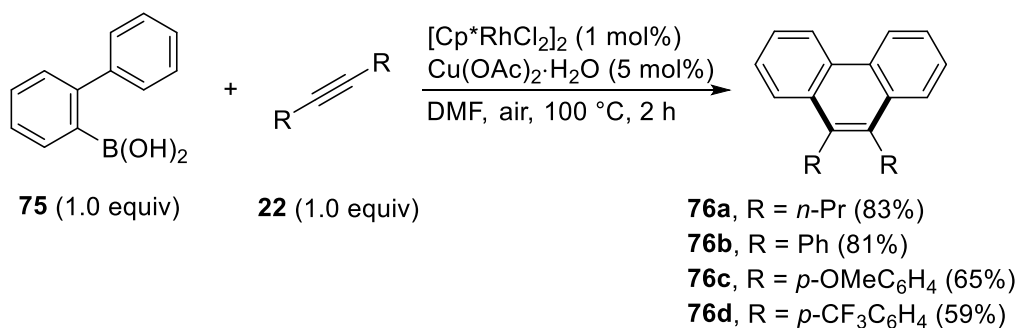
### 1.4.2 Transition metal-catalyzed [4+2] alkyne annulation reactions

Similar to [2+2+2] annulations, [4+2] annulations are also effective methodologies for the synthesis of polycyclic arenes. In contrast to [2+2+2] annulations, one molecule of aromatic substrate **24** couples with one molecule of alkyne **22** to produce a di-substituted polycyclic arene **25** in [4+2] annulations (Scheme 1-3). Thus, the [4+2] annulation product molecular weight is usually lower than similar [2+2+2] adducts. Research into [4+2] annulations is popular because products usually can be obtained in excellent yields and reactions tolerate a range of functional groups. Some examples of [4+2] annulation reactions are briefly discussed below.

#### 1. Rhodium-catalyzed annulations of 2-biphenylboronic acid with alkynes

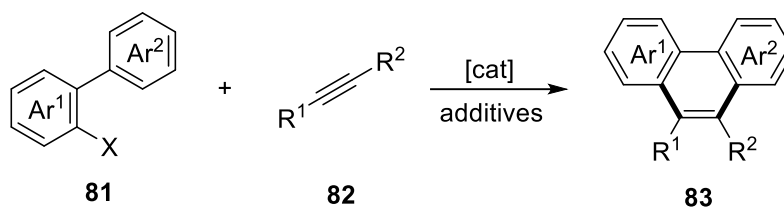
After the report of [2+2+2] annulations of aryl boronic acids with alkynes, Miura and co-workers subsequently demonstrated that the same reaction conditions can be adapted to [4+2] annulations of 2-biphenylboronic acid **75** with alkynes (Scheme 1-9).<sup>110</sup> The proposed mechanism for this process is similar to the [2+2+2] annulation (Scheme 1-6). In this case, the [4+2] annulation products **76** are obtained because the five-membered rhodacycle intermediate **78** forms after the initial transmetallation step. Deuterium-labeling experiments suggested that the formation of **78** is fast and irreversible. In the subsequent step, the alkyne coordinates to rhodium in **78** and inserts to the Rh-C bond to generate intermediate **80** via **79**. In turn, **80** undergoes reductive elimination to provide the phenanthrene-type product **76**.

Miura and co-workers did not observe any eight-membered-ring [2+2+2] annulation product. Because the nine-membered rhodacycle is unfavorably strained, it is less likely to insert the second alkyne molecule to the Rh-C bond in **80** in preference to reductive elimination.



**Scheme 1-9.** Rhodium-catalyzed [4+2] annulations of 2-biphenylboronic acid **75** with alkynes.<sup>110</sup>

Besides Miura's [4+2] annulations of 2-biphenylboronic acid with alkynes, 9,10-disubstituted phenanthrene compounds were also synthesized by other [4+2] annulation strategies (Equation 1-4)<sup>105,111-115</sup> using various 2-funcionalized biphenyl and different catalysts.



**Larock** (1997): X = I. Pd(OAc)<sub>2</sub>, NaOAc, LiCl, DMF, 100 °C.

**Glorius** (2010): X = COOH. Pd(OAc)<sub>2</sub>, acridine, Ag<sub>2</sub>CO<sub>3</sub>, DMF, 140 °C.

**Nakamura** (2011): X = MgBr. Fe(acac)<sub>3</sub>, dtbpy, 1,2-dichloroisobutane, THF, rt.

**Miura** (2014): X = OCl. [IrCl(cod)]<sub>2</sub>, P(*t*-Bu)<sub>3</sub>, *o*-xylene, 160 °C.

**Yoshikai** (2017): X = MgBr·LiCl. CrCl<sub>2</sub>, bpy, THF, 80 °C.

**Knochel** (2019): X = Br. *n*-Bu<sub>2</sub>LaCl·4LiCl, FeCl<sub>3</sub>, THF, -50 °C to rt.

**Equation 1-4.** Other [4+2] annulations of 2-funcionalized biphenyl with alkynes to obtain phenanthrene products.<sup>105,111-115</sup>

## 2. Rhodium-catalyzed annulations of 2-phenylpyridine with alkynes

In 2013, Huang and co-workers reported a [4+2] alkyne annulation using 2-phenylpyridine derivatives **84** to produce benzo[*a*]quinolizinium triflate motifs **85** (Scheme 1-10).<sup>116</sup> (For more information about common cationic nitrogen-embedded PAHs, see chapter 4). Molecular oxygen can be used as the oxidant to replace the metal salts, so this methodology is more environmentally benign and has greater atomic economy. The reaction scope indicates that most nitrogen-containing substrates couple with alkynes to afford cycloadducts in good to excellent yields.

Huang and co-workers proposed a mechanism, supported by X-ray crystallography and high-resolution mass spectrometric results. The nitrogen atom in starting substrate **86** coordinates to rhodium and the *ortho* C-H bond activation gives intermediate **87**. Alkyne coordination and insertion into the Rh-C bond generates intermediate **89** via **88**. The reductive elimination provides intermediate **90**, in which rhodium binds to the benzo[*a*]quinolizinium moiety through  $\eta^4$ -coordination. Subsequent oxidization of **90** by O<sub>2</sub> releases the product **85** and regenerates the active catalyst.

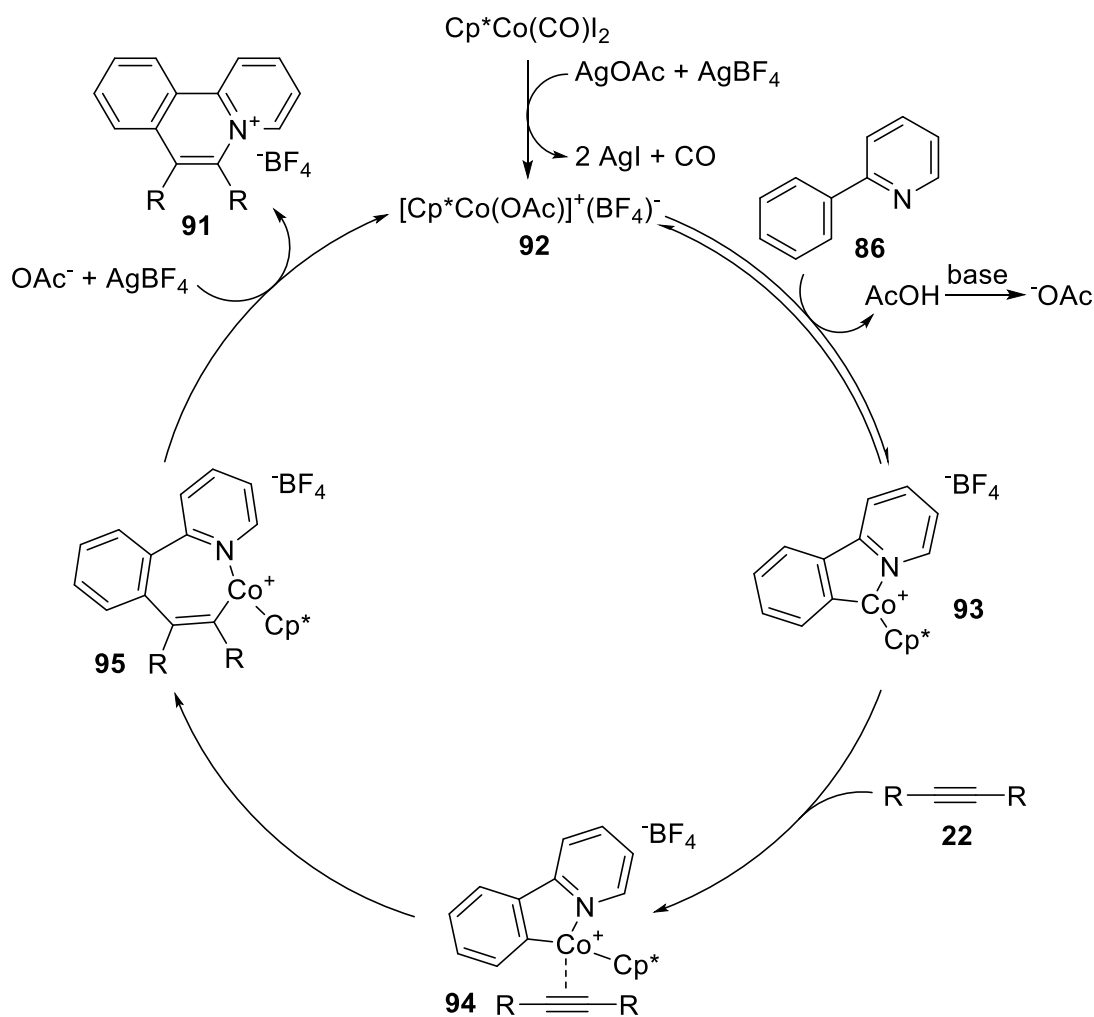
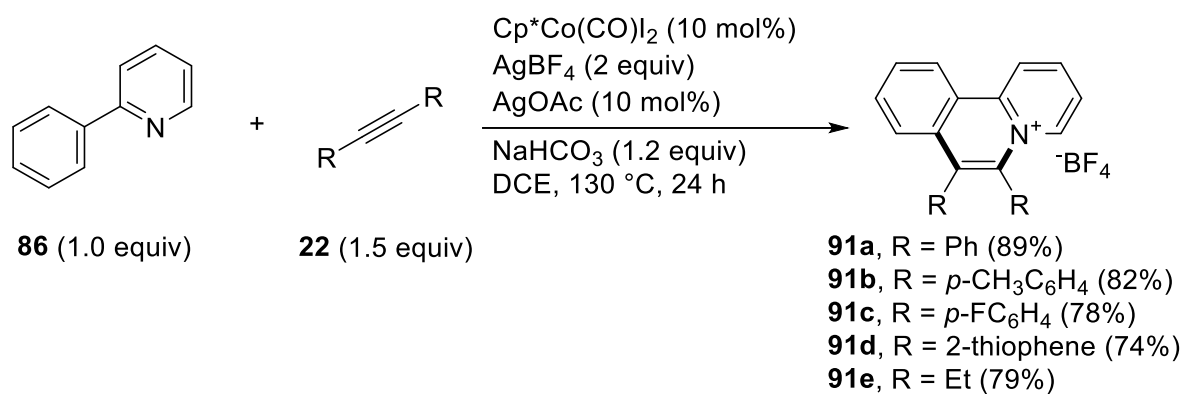


### 3. Cobalt-catalyzed annulations of 2-phenylpyridine with alkynes

Another [4+2] annulation method was developed by Cheng and co-workers using cobalt catalysis,<sup>117</sup> in which the product structures are similar to Huang's annulation. 2-Phenylpyridine **86** couples with alkynes to yield the annulation adducts **91** in the presence of Cp\*Co(CO)I<sub>2</sub> as the pre-catalyst (Scheme 1-11).

Cheng and co-workers proposed a mechanism for this type of reaction. Silver salts AgOAc and AgBF<sub>4</sub> remove the I<sup>-</sup> from the pre-catalyst and generate the active catalyst **92**. The nitrogen in 2-phenylpyridine **86** coordinates to the cobalt center and **93** is formed by an *ortho* C-H activation process. Deuterium-labeling experiments suggested that this C-H activation process is reversible and likely to be rate-determining. To get reasonable yields, NaHCO<sub>3</sub> is required to neutralize the acetic acid produced from the C-H activation. Subsequent alkyne coordination and insertion give intermediate **95** via **94**. Reductive elimination delivers the benzo[*a*]quinolizinium product **91**. The Cp\*Co fragment is oxidized by AgBF<sub>4</sub> and acetate additives to regenerate the active catalyst.

In addition to the above methodologies reported by Huang and Cheng, the benzo[*a*]quinolizinium skeletons have also been accessed under different reactions conditions, using cobalt, rhodium or iridium catalysts, as reported by Jones (Rh and Ir),<sup>118</sup> Cheng (Rh)<sup>119</sup> and Wang (Co and Ir).<sup>120</sup>

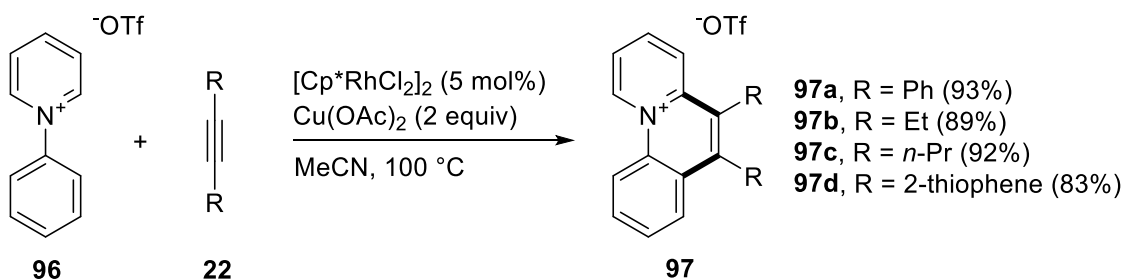


**Scheme 1-11.** Cobalt-catalyzed [4+2] annulations of 2-phenylpyridine with alkynes and proposed mechanism.<sup>117</sup>

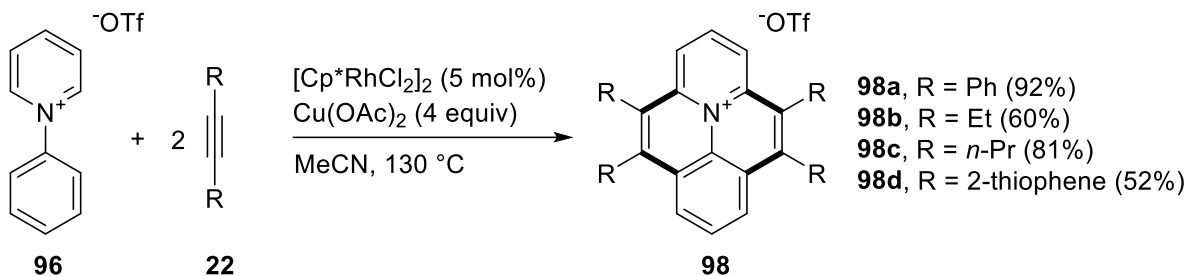
#### 4. Rhodium-catalyzed annulations of *N*-phenylpyridinium triflate with alkynes

In 2016, Wang and co-workers reported a very effective rhodium-catalyzed [4+2] annulation of alkynes with *N*-phenylpyridinium triflate **96**.<sup>121</sup> This 1:1 annulation process produces benzo[*c*]quinolizinium cations **97** at 100 °C (Scheme 1-12a). If another equivalent of alkyne and oxidant are added, the 2:1 coupling product **98** is obtained at 130 °C (Scheme 1-12b). The isolated benzo[*c*]quinolizinium product **97a** can also serve as the starting material to prepare 2:1 adducts **98a** and **99** (Scheme 1-12c).

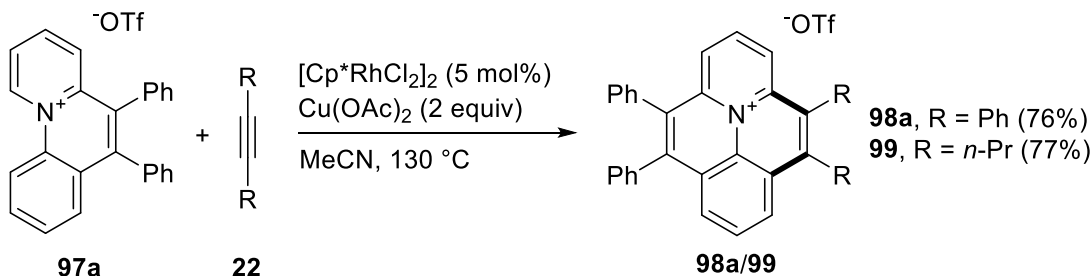
(a) Rh-catalyzed single [4+2] annulation of *N*-phenylpyridinium triflate with alkynes:



(b) Rh-catalyzed double [4+2] annulation of *N*-phenylpyridinium triflate with alkynes:



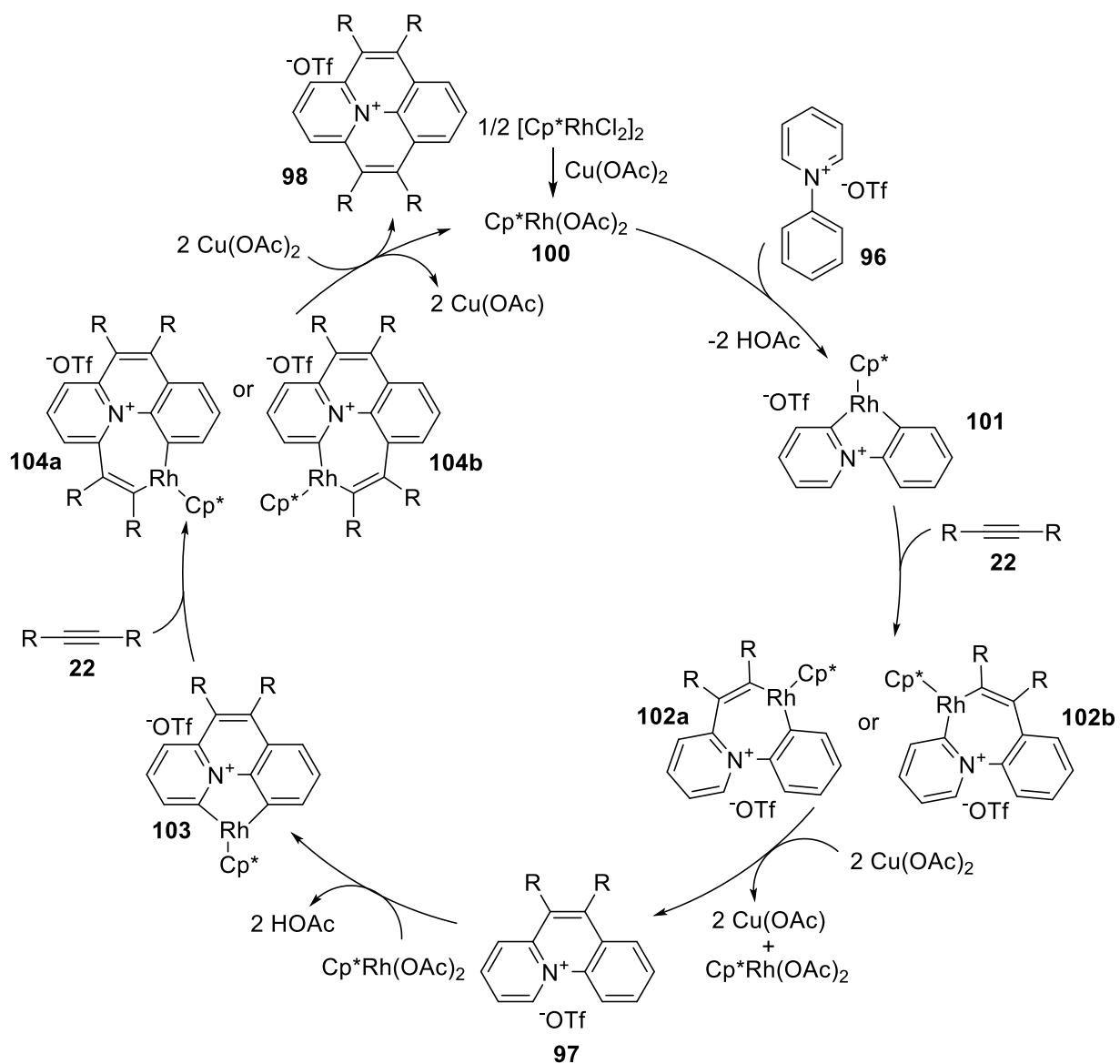
(c) Rh-catalyzed [4+2] annulation of benzo[*c*]quinolizinium product **97a** with alkynes:



**Scheme 1-12.** Rhodium-catalyzed [4+2] single/double annulations of *N*-phenylpyridinium triflate with alkynes.<sup>121</sup>



The authors proposed a plausible mechanism for this process (Scheme 1-13). Unlike the above methodologies by Huang and Cheng, the pyridinium nitrogen in **96** does not have a lone pair and cannot coordinate to rhodium. Thus, the authors assumed that the formation of a pyridine-based carbene ligand is likely to trigger the initial C-H activation and produce rhodacycles **101** and **103**, according to some reports about pyridine-based carbene-metal complexes.<sup>122 - 124</sup> However, attempts to isolate this carbene intermediate were unsuccessful. The alkyne insertion and reductive elimination steps are similar to other [4+2] annulations. For a plausible mechanism involving the carbene intermediate, see Scheme 4-10.



**Scheme 1-13.** Proposed mechanism for rhodium-catalyzed [4+2] annulation of *N*-phenylpyridinium triflate with alkynes.<sup>121</sup>

## 5. Other alkyne annulation examples

Besides the examples listed above, other [4+2] annulations allow the use of aromatic substrates with more diverse functional groups and heteroatoms. Similar to [4+2] annulation, some [3+2] or [5+2] alkyne annulation examples were also reported, producing five-membered or seven-

membered cycloadducts, respectively. Selected examples of these annulation products are summarized in Figure 1-8.<sup>125-134</sup>

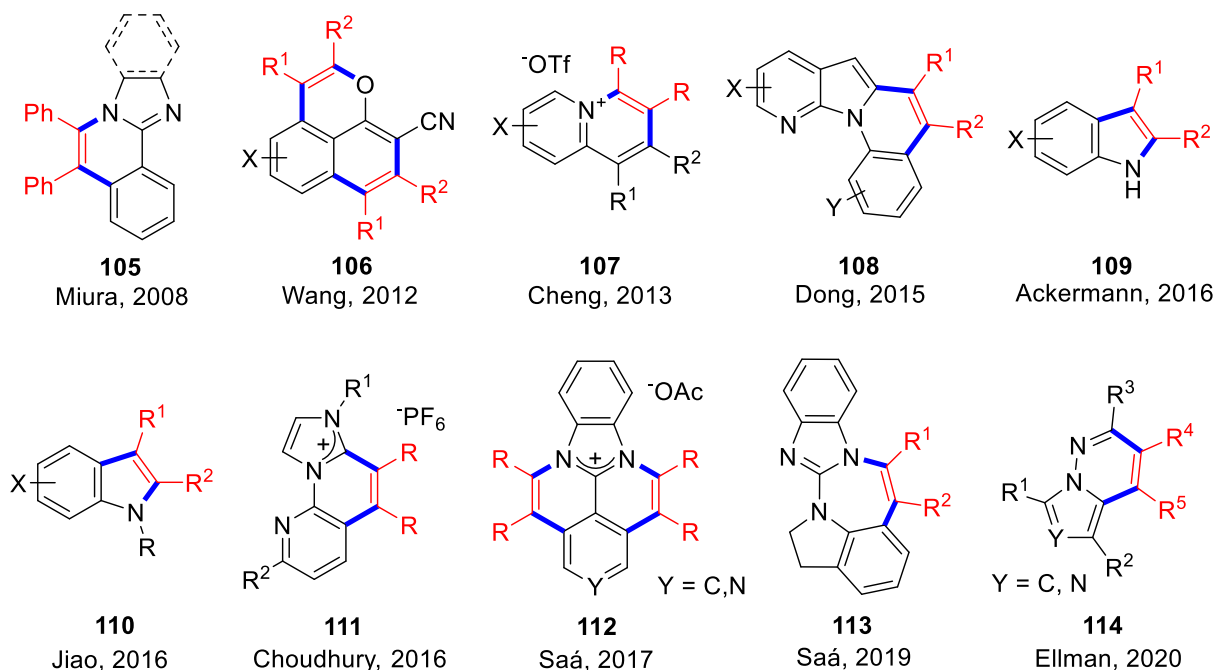


**Figure 1-8.** Some other examples of [3+2], [4+2] or [5+2] alkyne annulation reactions.

### 1.4.3 Conclusions

From all alkyne annulation examples presented above, I can tentatively draw some conclusions about the similarities and differences among those reactions.

**Catalyst.** Rhodium is the most frequently used transition metal and [Cp\*RhCl<sub>2</sub>]<sub>2</sub> is the most common pre-catalyst for alkyne annulations. Rhodium catalysis usually proceeds via an oxidative annulation process, in which Rh(III) reduces to Rh(I) in a reductive elimination step and Rh(I) is re-oxidized by an oxidant to Rh(III). There is no oxidative addition step in these annulations.

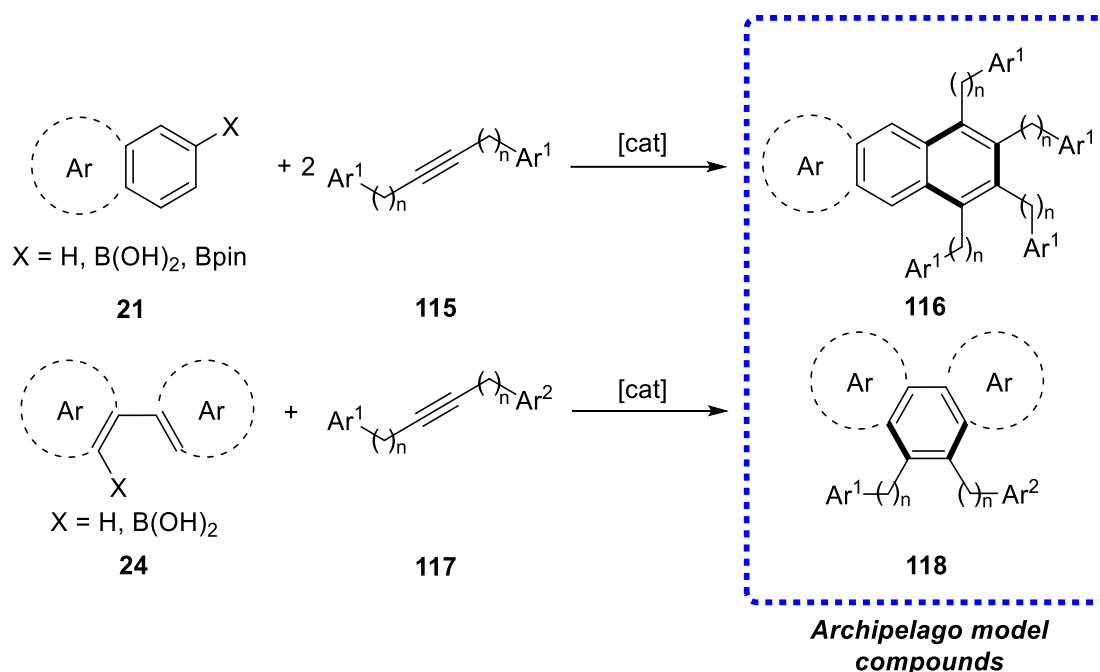
For the first-row transition metals, the cobalt-catalyzed annulations are the most widely studied. However, to make the annulations proceed, greater catalyst loading is required ( $\geq 10$  mol%) than for rhodium catalysis.

**Oxidant.** In oxidative annulations, a stoichiometric oxidant is required to regenerate the active species after the reductive elimination step. Copper or silver salts (e.g.,  $\text{Cu}(\text{OAc})_2 \cdot \text{H}_2\text{O}$  and  $\text{AgOAc}$ ) are the most common oxidants used in this process. Acetates are weak ligands so they dissociate easily in the transmetallation step. In particular, copper(II) acetate can be re-oxidized by molecular oxygen. Thus, if the reaction is run under air, a substoichiometric amount of copper(II) acetate ( $\sim 10$  mol%) can be used.

**Solvent.** Polar aprotic solvents (e.g., DMF and MeCN) are commonly used. These solvents are necessary since they can dissolve the reactants, catalyst(s), and oxidant to produce a homogeneous solution. Some other solvents also can be adopted but high temperature may be required to dissolve all components and proceed the reaction.

#### 1.4.4 Applications of alkyne annulations to archipelago compound synthesis

From the information above, I recognized that the alkyne annulation reaction could be employed to synthesize archipelago compounds, once island-tethered alkynes **115** and **117** are prepared (Scheme 1-14).



**Scheme 1-14.** Synthesis of archipelago compounds by alkyne annulations.

Alkyne annulations are superior to the earlier synthetic approaches to archipelago compounds, for the following aspects:

1. *Efficient.* Rather than stepwise synthesis, the archipelago compounds are synthesized in one-step after preparation of the aromatic substrates and alkynes. The annulation products usually do not require further modifications, which avoids the loss of these valuable compounds.
2. *High molecular weight compounds.* Most current synthetic strategies are limited to three-island synthesis. The [2+2+2] annulations shown in section 1.4.1 can afford five-island archipelago products **116**, which have higher molecular weights (>1000 g/mol). Thus, these compounds extend the scope of synthetic archipelago model compounds. They are likely to show different physical properties to simpler archipelago models.

3. *Heteroatom tolerance.* Most of the known synthetic archipelago compounds do not contain sulfur, even though sulfur is the most abundant heteroatom in asphaltenes.<sup>6</sup> From the reaction scope studies,<sup>103,117,121,135</sup> some annulation methodologies can easily incorporate sulfur, enabling the synthesis of high sulfur content archipelago compounds.

**Research Objectives.** The objective of my dissertation research was to develop new synthetic approaches to advanced archipelago compounds that have high molecular weights, high structural complexity, and variable heteroatom inclusion. To achieve this goal, island-tethered alkynes were first prepared, as will be described in chapter 2. A broad range of alkyne annulations were then optimized to provide archipelago compounds in good yields and high purities. These compounds are valuable materials for further asphaltene studies; many have already been shared with collaborators in chemistry and chemical engineering.

## *Results and Discussions*

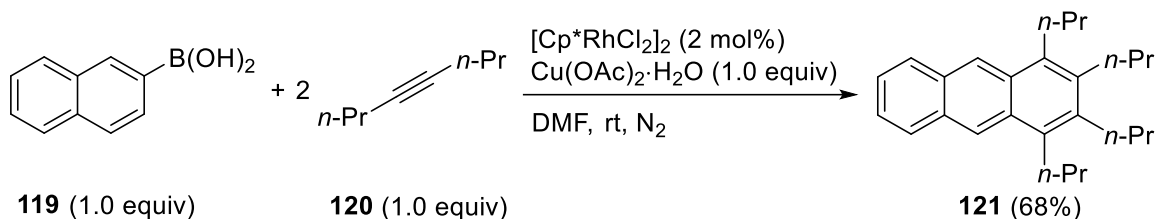
### **1.5 Probing the preliminary scope studies of alkyne annulations**

The numerous alkyne annulation reactions shown in section 1.4 provide polycyclic arenes with various structures and diverse functional groups, but the substrate scope needed to be further expanded for our needs. Miura's<sup>101</sup> and Komeyama's<sup>102</sup> [2+2+2] annulations were selected to explore the possibilities of preparing phenanthrene-type adducts, which were not reported in their papers.

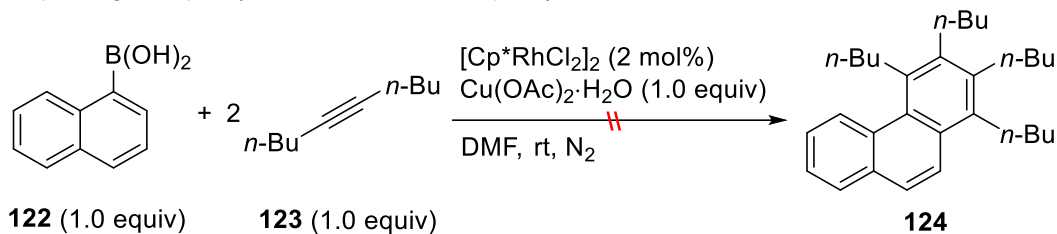
### 1.5.1 Rhodium-catalyzed annulations of 1-naphthylboronic acid with alkynes

Miura and co-workers described the annulation reaction of 2-naphthylboronic acid **119** with simple alkyne (Scheme 1-15a).<sup>101</sup> Based on their results, I attempted to replace 2-naphthylboronic acid **119** with 1-naphthylboronic acid **122** and expected to obtain a phenanthrene-type product **124**. Unfortunately, compound **124** was not observed after the reaction (Scheme 1-15b).

(a) Miura's work:



(b) Replacing 2-naphthylboronic acid to 1-naphthylboronic acid:



**Scheme 1-15.** Rhodium-catalyzed annulation of 1-naphthylboronic acid with 5-decyne.

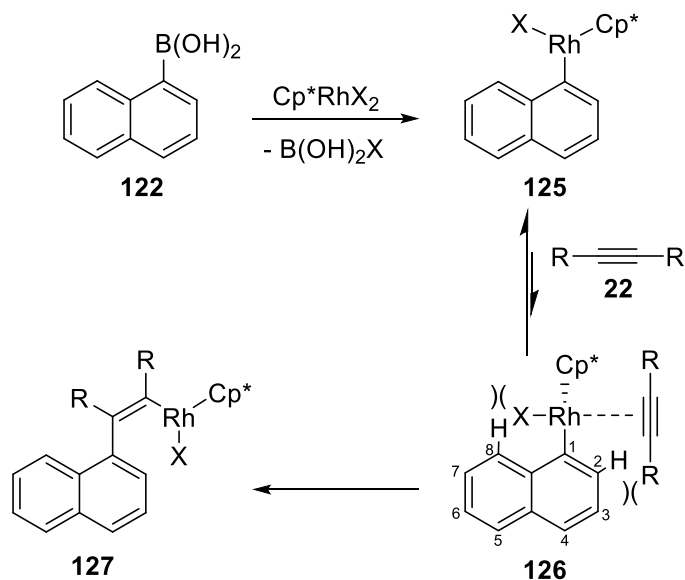
Naphthalene was the only observed product obtained from this reaction, meaning only protodeboronation occurs in this case. Several optimization experiments were carried out subsequently (e.g., replacing the boronic acid **122** with the corresponding pinacol boronate, changing the oxidant to AgOAc or anhydrous  $\text{Cu}(\text{OAc})_2$ , heating the reaction mixture), but none of these experiments generated the expected phenanthrene product **124**.

I ascribe this unsuccessful annulation to the steric inhibition of the alkyne insertion step (Scheme

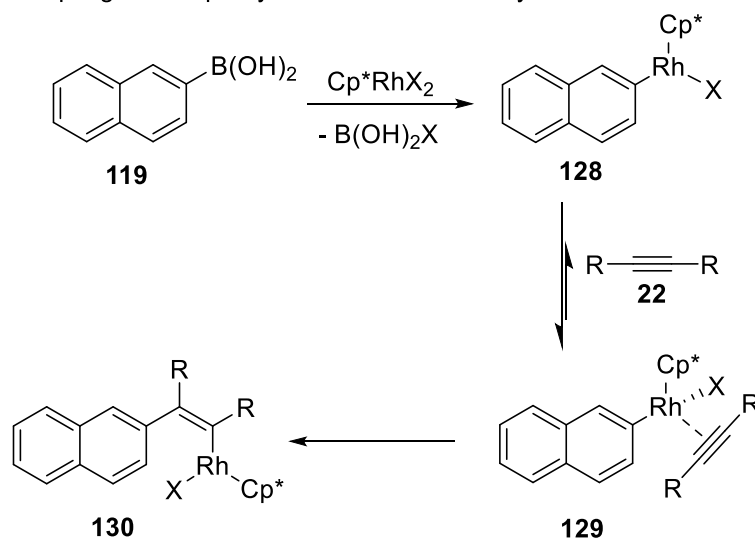
1-16). The transmetallation of 1-naphthylboronic acid **122** generates an aryl-rhodium species **125**. The alkyne coordinates to **125** to form **126**, but the 2-hydrogen in **126** may prohibit the square coplanar geometry, which is required for the insertion of the alkyne to Rh-C bond to give **127**. The X group (X = Cl or OAc) or Cp\* ligand may also interact with the 8-hydrogen and affect the insertion step. In contrast, for 2-naphthylboronic acid intermediate **129**, there is less hinderance and the square coplanar transition state can be easily achieved.



(a) Coupling of 1-naphthylboronic acid with alkyne:



(b) Coupling of 2-naphthylboronic acid with alkyne:

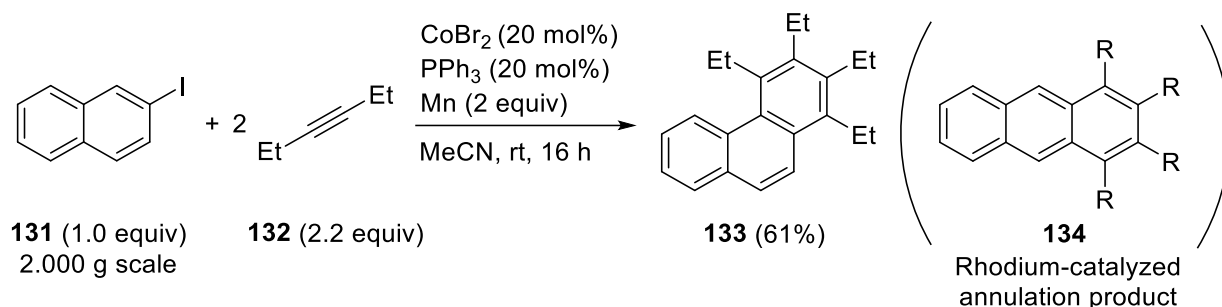


**Scheme 1-16.** Transmetalation and alkyne insertion steps for rhodium-catalyzed annulation of alkynes with (a) 1-naphthylboronic acid and (b) 2-naphthylboronic acid.

### 1.5.2 Cobalt-catalyzed annulations of 2-iodonaphthalene with alkynes

The scope of Komeyama's cobalt-catalyzed annulation reaction is mostly limited to 4-octyne and substituted iodobenzene (Scheme 1-7).<sup>102</sup> Because cobalt is an “earth-abundant” first-row transition metal, I sought to expand this annulation to 2-iodonaphthalene and to see if it can be

employed for archipelago compound synthesis. Interestingly, 2-iodonaphthalene **131** couples with 3-hexyne **132** to yield the phenanthrene adduct **133** rather than the anthracene derivatives **134** obtained from Miura's rhodium-catalyzed annulation (Equation 1-5).

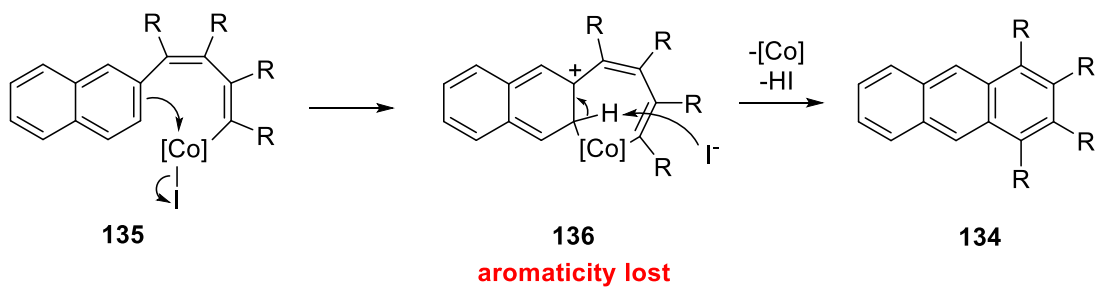


**Equation 1-5.** Cobalt-catalyzed annulation of 2-iodonaphthalene with 3-hexyne.

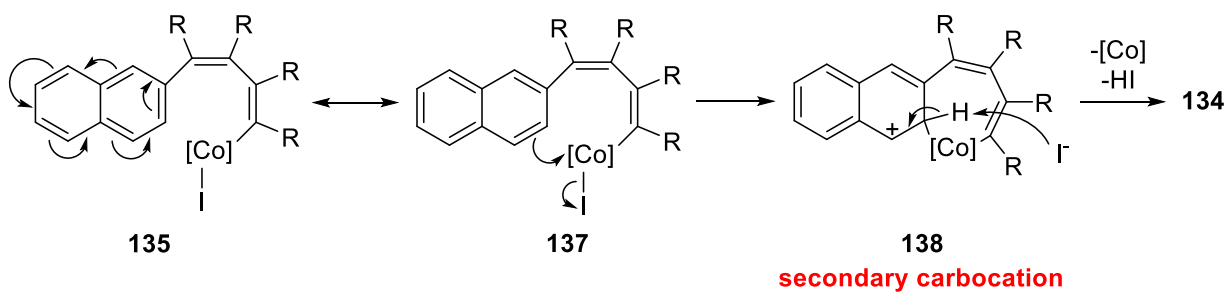
Scheme 1-17 shows a proposed explanation for the formation of the phenanthrene-type product. Komeyama and co-workers' experimental results suggest that the reaction may proceed by an electrophilic aromatic substitution (Scheme 1-7).<sup>102</sup> Based on their proposed mechanism, **135** is the intermediate formed after the alkyne insertion step. The formation of anthracene-type product **134** has two possible approaches (Scheme 1-17a), but are not favored because of breaking the entire aromaticity of the naphthalene ring (**136**) or forming a less stable secondary carbocation intermediate (**138**). The formation of phenanthrene-type product **140** can also come from two possible approaches (Scheme 1-17b). Although one intermediate still breaks the aromaticity (**139**), the other one maintains the aromaticity of the intact benzene moiety and forms a more stable tertiary carbocation (**142**). Thus, the formation of **142** is favored and the phenanthrene-type product **140** is obtained in this annulation.

(a) Formation of the anthracene product:

Possibility A:

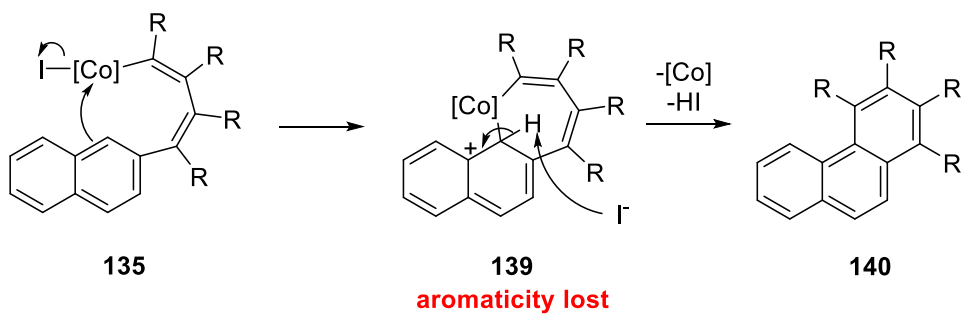


Possibility B:

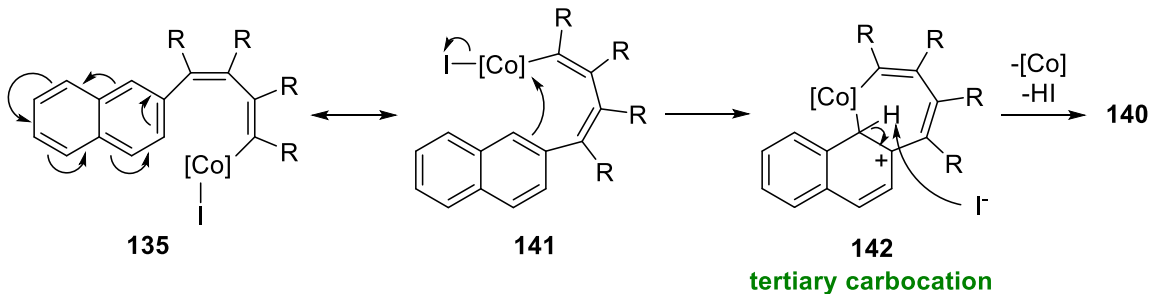


(b) Formation of the phenanthrene product:

Possibility A:

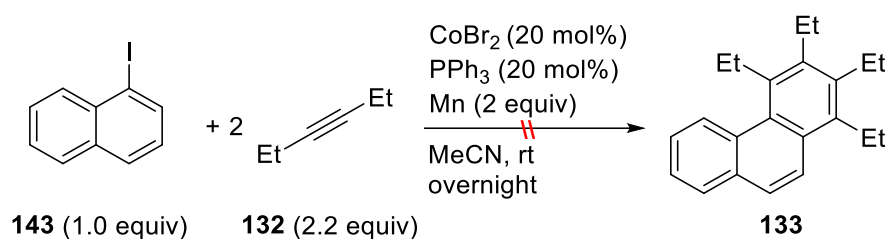


Possibility B:



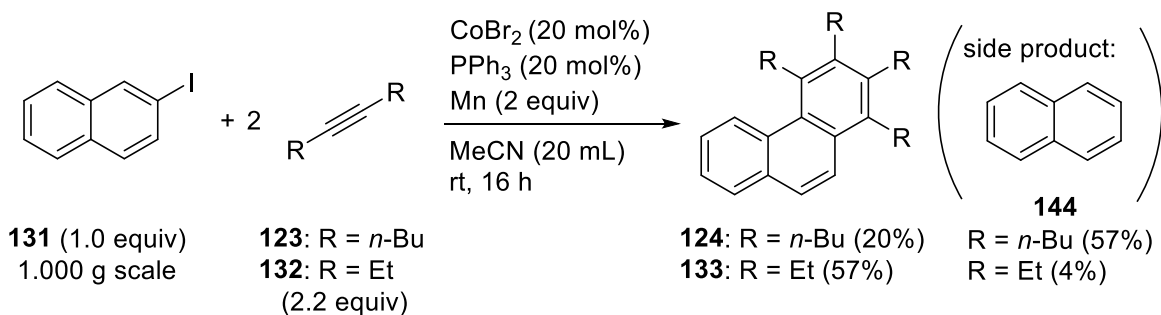
**Scheme 1-17.** Electrophilic aromatic substitution process for the formation of (a) anthracene product and (b) phenanthrene product.

Similar to Miura's rhodium-catalyzed annulation, my experiment confirms that 1-iodonaphthalene **143** also fails to couple with 3-hexyne **132** to produce phenanthrene product **133** (Equation 1-6). The steric congestion in alkyne insertion step also rationalizes this unsuccessful annulation.



**Equation 1-6.** Cobalt-catalyzed annulation of 1-iodonaphthalene with 3-hexyne.

To further test the reaction scope for 2-iodonaphthalene, 5-decyne **123** replaced 3-hexyne **132** and the annulation was repeated under the same reaction conditions. The phenanthrene product **124** was indeed obtained, but in a much lower yield. The main side product was naphthalene (Equation 1-7).



**Equation 1-7.** Cobalt-catalyzed annulations of 2-iodonaphthalene with 3-hexyne or 5-decyne.

Based on these results, I deduce that the first alkyne coordination-insertion process is less favored for 5-decyne in this coupling, for the following reasons:

1. Cobalt is a first-row transition metal so the radius of the cobalt atom is smaller than that of second-row transition metals, rendering limited coordination space around the cobalt atom. In this catalytic process,  $\text{PPh}_3$ , which is a bulky ligand, coordinates with cobalt and takes up much of the coordination sphere around cobalt. In this case, 3-hexyne, which has a smaller molecular size and less rotational interference, is more favored than 5-decyne to coordinate with cobalt.

2. After the coordination process, the longer alkyl chains in 5-decyne interact more strongly with the naphthalene structure than 3-hexyne, which makes the square coplanar geometry more difficult to achieve in the alkyne insertion step.

These results indicate that the substituent groups on alkynes have a great effect on the cobalt-catalyzed annulation. Therefore, this is not an efficient method to prepare archipelago compounds. Compared with cobalt, rhodium has a bigger atomic radius, so it is able to catalyze substituted alkyne annulations more effectively, especially for alkynes with long alkyl chains attached.

Nevertheless, the tetra-substituted phenanthrene product **133** was used as a starting material to prepare an island-tethered alkyne, which will be described in detail in section 2.5.

## Experimental Section

### General Information

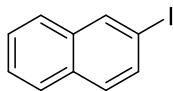
Unless otherwise noted, all compounds were used as received without any further purification. MeCN and 1,4-dioxane were dried over 3 Å molecular sieves for at least 48 h before use. Copper(I) iodide was purified according to the literature procedure.<sup>136</sup>  $^1\text{H}$  and  $^{13}\text{C}\{^1\text{H}\}$  NMR spectra were recorded on Agilent/Varian instruments (700 MHz for  $^1\text{H}$  NMR spectroscopy and

176 MHz for  $^{13}\text{C}\{^1\text{H}\}$  NMR spectroscopy) at 27 °C. Chemical shifts of  $^1\text{H}$  and  $^{13}\text{C}\{^1\text{H}\}$  NMR spectra were reported in parts per million (ppm). Chemical shifts were referenced to residual solvent peaks ( $\text{CDCl}_3$ :  $\delta_{\text{H}} = 7.26$  ppm,  $\delta_{\text{C}} = 77.06$  ppm;  $\text{CD}_2\text{Cl}_2$ :  $\delta_{\text{H}} = 5.32$  ppm,  $\delta_{\text{C}} = 53.8$  ppm). All coupling constants ( $J$  values) were reported in Hertz (Hz). Manipulations under nitrogen atmosphere were performed in a Braun dry box with an oxygen level below 1 ppm. Column chromatography was performed on silica gel 60 M (230–400 mesh). Thin-layer chromatography (TLC) was performed on pre-coated, aluminum-backed silica gel plates. Visualization of the developed TLC plate was performed by a UV lamp (254 nm). High-resolution mass spectrometric (HRMS) results were obtained from Mass Spectrometry Facility using Kratos Analytical MS-50G (EI). Elemental analyses (C, H) were obtained from Analytical and Instrumentation Laboratory using a Thermo Flash 2000 Elemental Analyzer.

#### **General procedure A – Cobalt-catalyzed annulations of 2-iodonaphthalene with alkynes<sup>102</sup>**

In a dry box,  $\text{CoBr}_2$  and Mn powder were placed in a dry 100 mL Schlenk flask with a magnetic stir bar. The flask was sealed and then moved out of the dry box. The flask was heated with a heat-gun under vacuum for 20 min. After cooling to room temperature, the flask was filled with  $\text{N}_2$ . 2-Iodonaphthalene,  $\text{PPh}_3$ , dry MeCN, and alkyne (**123**, **132**) were sequentially added to the flask through Schlenk line techniques. The reaction mixture was stirred at room temperature for 16 h and was quenched with saturated  $\text{NH}_4\text{Cl}$  solution (50 mL). The aqueous solution was extracted with  $\text{CH}_2\text{Cl}_2$  (3 times, 30 mL each) and dried over  $\text{Na}_2\text{SO}_4$ . The mixture was filtered, and the solvent was removed under reduced pressure. The residual was purified by silica column chromatography using hexane as eluent to afford the product.

## 2-Iodonaphthalene (131)

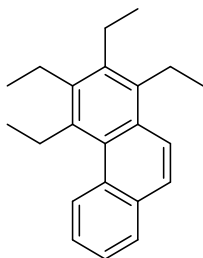


The preparation procedure is according to published work.<sup>137</sup> In a dry box, 2-bromonaphthalene (2.000 g, 9.659 mmol), NaI (2.895 g, 19.32 mmol), and CuI (92 mg, 5 mol%) were placed in a dry 100 mL Schlenk flask with a magnetic stir bar. The reaction flask was sealed and then moved out of the dry box. Dry 1,4-dioxane (20 mL) and DMEDA (104  $\mu$ L, 85 mg, 10 mol%) were added through Schlenk line techniques. The reaction mixture was stirred at 110 °C for 2 d. After cooling to room temperature, the mixture was diluted with CH<sub>2</sub>Cl<sub>2</sub> (50 mL), washed with 30% ammonium hydroxide solution (50 mL) and water (2 times, 50 mL each). The organic solution was dried over Na<sub>2</sub>SO<sub>4</sub>. The mixture was filtered, and the solvent was removed under reduced pressure to afford compound **131** as a yellow solid (2.256 g, 92%). The <sup>1</sup>H and <sup>13</sup>C{<sup>1</sup>H} NMR spectra of the product are in accordance with the literature.<sup>138</sup>

**<sup>1</sup>H NMR** (CD<sub>2</sub>Cl<sub>2</sub>, 700 MHz):  $\delta$  8.27 (s, 1H), 7.84–7.81 (m, 1H), 7.76–7.72 (m, 2H), 7.61 (d,  $J$  = 8.7 Hz, 1H), 7.53–7.49 (second order m, 2H).

**<sup>13</sup>C{<sup>1</sup>H} NMR** (CD<sub>2</sub>Cl<sub>2</sub>, 176 MHz):  $\delta$  137.0, 135.4, 134.7, 132.5, 129.8, 128.2, 127.1, 126.9, 91.7.

## 1,2,3,4-Tetraethylphenanthrene (133)



The general procedure A was used with CoBr<sub>2</sub> (344 mg, 20 mol%), Mn powder (865 mg, 15.7 mmol), 2-iodonaphthalene (2.000 g, 7.872 mmol), PPh<sub>3</sub> (413 mg, 20 mol%), 3-hexyne (1.423 g, 1968  $\mu$ L, 17.32 mmol), and MeCN (20 mL). The crude material was purified by silica column chromatography using hexane as eluent to afford compound **133** as a yellow oil (1.401 g, 61%).  $R_f$  = 0.31 (SiO<sub>2</sub>; hexane).

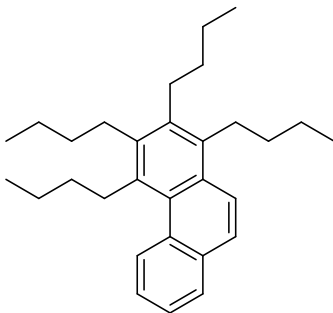
**<sup>1</sup>H NMR** (CDCl<sub>3</sub>, 700 MHz):  $\delta$  8.73–8.70 (m, 1H), 8.00 (dd,  $J$  = 9.2 Hz, 1.6 Hz, 1H), 7.91–7.88 (m, 1H), 7.69 (d,  $J$  = 9.1 Hz, 1H), 7.60–7.56 (m, 2H), 3.58–3.32 (br, 2H), 3.23–3.18 (second order m, 2H), 3.11–3.05 (second order m, 2H), 3.02–2.97 (second order m, 2H), 1.73–1.69 (second order m, 3H), 1.44–1.40 (second order m, 3H), 1.35–1.29 (m, 6H).

**<sup>13</sup>C{<sup>1</sup>H} NMR** (CDCl<sub>3</sub>, 176 MHz):  $\delta$  140.8, 138.8, 136.7, 136.1, 132.9, 131.2, 130.2, 129.9, 128.1, 127.8, 126.0, 125.4, 124.7, 123.4, 25.3, 22.8, 22.6, 22.3, 16.4, 16.2, 15.9, 15.9.

**EI HRMS**  $m/z$  calcd for C<sub>22</sub>H<sub>26</sub> (M<sup>+</sup>) 290.2035, found 290.2037.

**EA** anal. calcd for C<sub>22</sub>H<sub>26</sub>: C, 90.98; H, 9.02. Found: C, 88.77; H, 8.98. Repeat found: C, 88.86; H, 9.05.

#### 1,2,3,4-Tetrabutylphenanthrene (124)



The general procedure A was used with CoBr<sub>2</sub> (172 mg, 20 mol%), Mn powder (433 mg, 7.88



mmol), 2-iodonaphthalene (1.000 g, 3.936 mmol), PPh<sub>3</sub> (207 mg, 20 mol%), 5-decyne (1.197 g, 1563  $\mu$ L, 8.660 mmol), and MeCN (10 mL). The crude material was purified by silica column chromatography using hexane as eluent to afford compound **124** as a yellow oil (310 mg, 20%).  $R_f$  = 0.32 (SiO<sub>2</sub>; hexane).

**<sup>1</sup>H NMR** (CDCl<sub>3</sub>, 700 MHz):  $\delta$  8.65–8.61 (m, 1H), 7.98 (dd,  $J$  = 9.1 Hz, 2.7 Hz, 1H), 7.91–7.88 (m, 1H), 7.68 (dd,  $J$  = 9.1 Hz, 1.7 Hz, 1H), 7.60–7.56 (m, 2H), 3.50–3.24 (br, 2H), 3.17–3.11 (m, 2H), 3.03–2.97 (m, 2H), 2.95–2.90 (m, 2H), 2.09–2.03 (m, 2H), 1.81–1.75 (m, 2H), 1.72–1.58 (m, 12H), 1.18–1.08 (m, 12H).

**<sup>13</sup>C{<sup>1</sup>H} NMR** (CDCl<sub>3</sub>, 176 MHz):  $\delta$  139.7, 137.8, 135.6, 134.9, 132.9, 131.2, 130.3, 129.9, 128.0, 127.9, 125.8, 125.3, 124.5, 123.5, 34.1, 33.9, 33.9, 33.6, 32.6, 29.9, 29.9, 29.4, 23.7, 23.7, 23.6, 23.3, 14.1, 14.0, 14.0.

**EI HRMS**  $m/z$  calcd for C<sub>30</sub>H<sub>42</sub> (M<sup>+</sup>) 402.3287, found 402.3284.

**EA** anal. calcd for C<sub>30</sub>H<sub>42</sub>: C, 89.49; H, 10.51. Found: C, 88.92; H, 10.62. Repeat found: C, 89.11; H, 10.44.

## 2. Synthetic Approaches to Island-tethered Dialkyl Alkynes

Alkynes are hydrocarbons containing carbon-carbon triple bonds. Acetylene (ethyne) is the simplest alkyne with a formula of  $C_2H_2$ . Terminal alkynes are alkynes in which one triple-bond carbon is bonded to a hydrogen atom. Internal alkynes, in contrast to terminal alkynes, are alkynes in which both triple-bond carbons bond to substituents other than hydrogen.

Internal alkynes can also be divided into different categories based on the substituents on triple-bond carbon atoms. If the two alkyne carbons bond to aromatic substituents, the alkyne is termed a “diaryl alkyne” (e.g., diphenylacetylene). Similarly, if the two alkyne carbon atoms connect to alkyl substituents, it is a “dialkyl alkyne” (e.g., 5-decyne) (Figure 2-1). In accordance with my research objectives, preparations and characterizations of dialkyl alkynes will be the focus of this chapter.

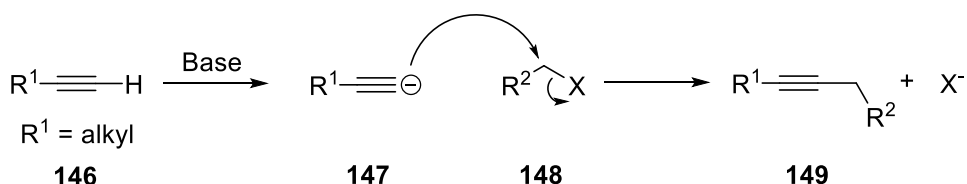


**Figure 2-1.** Representative examples of diaryl alkyne and dialkyl alkyne.

As a common functional group in nearly all areas of chemistry, including biochemistry and materials science,<sup>139</sup> alkyne synthesis suffers from a lack of widely applicable synthetic methodologies. Some factors restrict the use of traditional alkyne preparation methods. A variety of recently reported methodologies, including transition metal catalyzed cross-couplings and alkyne metathesis, now allow efficient synthesis of alkynes with diverse structures and multiple functional groups.

## 2.1 Traditional methodologies for preparing dialkyl alkynes

To prepare dialkyl alkynes, the most common strategy is deprotonation with strong base, followed by nucleophilic substitution. Protons on terminal alkynes are mildly acidic, with a  $pK_a$  of about 25.<sup>140</sup> These protons are easily removed by strong bases, such as sodium hydride, sodium amide and *n*-butyllithium (*n*-BuLi). The resulting alkynyl anion **147** can be alkylated by an electrophile **148** via a nucleophilic substitution ( $S_N2$ ) mechanism (Scheme 2-1).



**Scheme 2-1.** Dialkyl alkyne preparation by deprotonation/ $S_N2$  substitution pathway.

$S_N2$  alkylation is limited in reaction scope, for many reasons:

1. *Alkyl halides are generally limited to primary substrates.*

Tertiary alkyl halides do not react by  $S_N2$  reactions due to competitive  $E_2$ -elimination in strongly basic environments. Some secondary alkyl halides can undergo  $S_N2$  reactions, but not as easy as primary alkyl halides.

2. *Strong bases limit functional group compatibility.*

Generally, strong bases show limited chemoselectivity. Many functional groups are sensitive to strong bases (e.g., carboxylic acid, alcohol, ester). If a terminal alkyne contains a halide substituent, it may also undergo elimination reactions.

### 3. *The required additives are high boiling.*

*n*-BuLi is one of the most frequently used bases to deprotonate terminal alkynes. When *n*-BuLi is used, polar aprotic additives (e.g., DMPU, DMI) are required to break the aggregates of lithium anions in solution.<sup>141,142</sup> These additives have boiling points over 200 °C. Although some can be partially removed by subsequent aqueous work-up, these co-solvents remain in crude products and can cause purification problems.

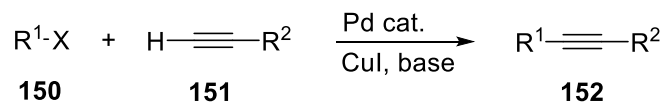
Thus, novel synthetic methodologies have been developed to solve these issues and to synthesize alkynes in a wide reaction scope.

## 2.2 Modern methodologies for preparing dialkyl alkynes

### 2.2.1 Limiting issues in cross-coupling reactions

The Sonogashira reaction is a classic catalytic cross-coupling between terminal alkynes and aryl or vinyl halides. The coupling was discovered in 1975 and developed over the decades since.<sup>143</sup> It has become an effective strategy for the preparation of internal alkynes. Palladium catalysts are commonly used for the Sonogashira reaction. Scheme 2-2 shows the mechanism of a typical palladium-catalyzed Sonogashira coupling reaction.<sup>144</sup>

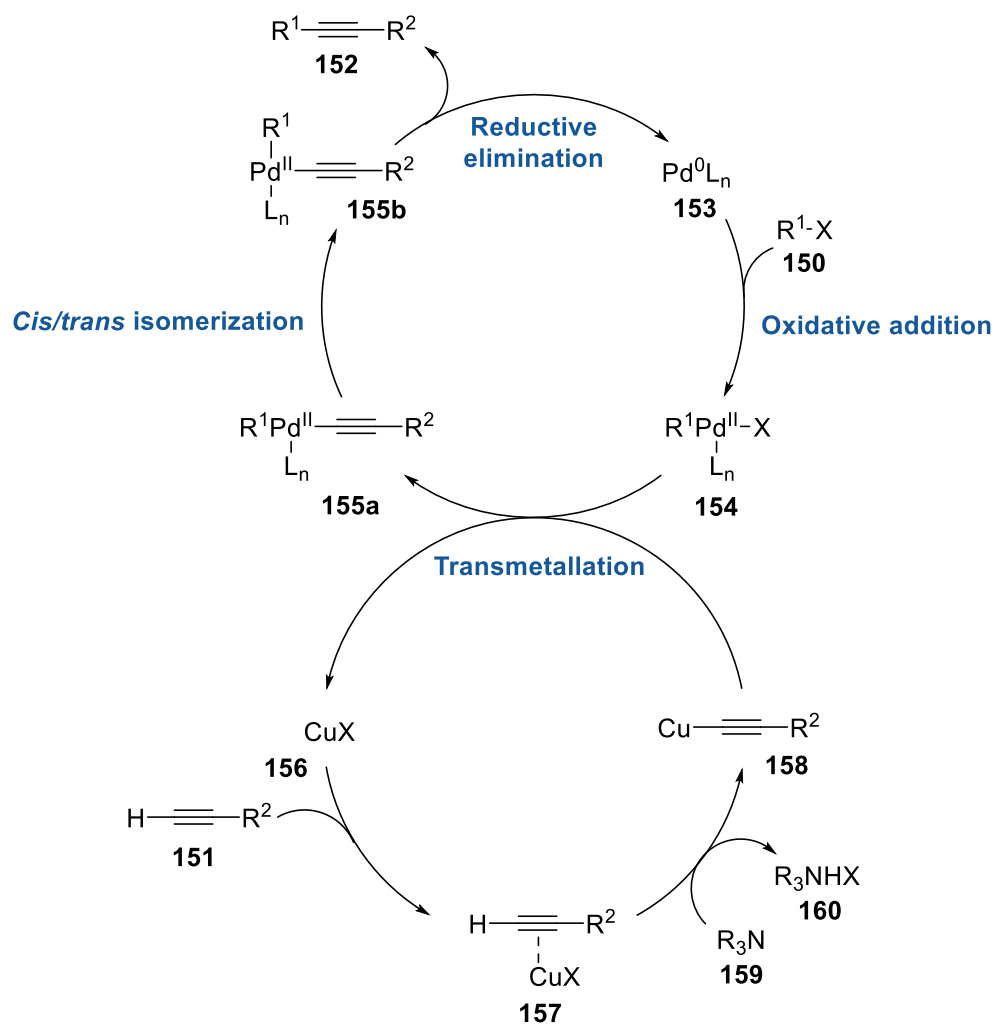
The general mechanism consists of four main steps: oxidative addition, transmetalation, *cis/trans* isomerization, and reductive elimination. Copper(I) iodide and a weak base are used to assist the transmetalation step. The tertiary amine **159** acts as the representative base in Scheme 2-2, although some inorganic bases (e.g., K<sub>2</sub>CO<sub>3</sub>, K<sub>3</sub>PO<sub>4</sub>) perform similarly.<sup>145,146</sup>



$\text{R}^1$  = aryl, vinyl

$\text{R}^2$  = aryl, vinyl, alkenyl, alkyl,  $\text{SiR}_3$

$\text{X}$  = Cl, Br, I, OTf



**Scheme 2-2.** Mechanism of typical Sonogashira couplings.<sup>144</sup>

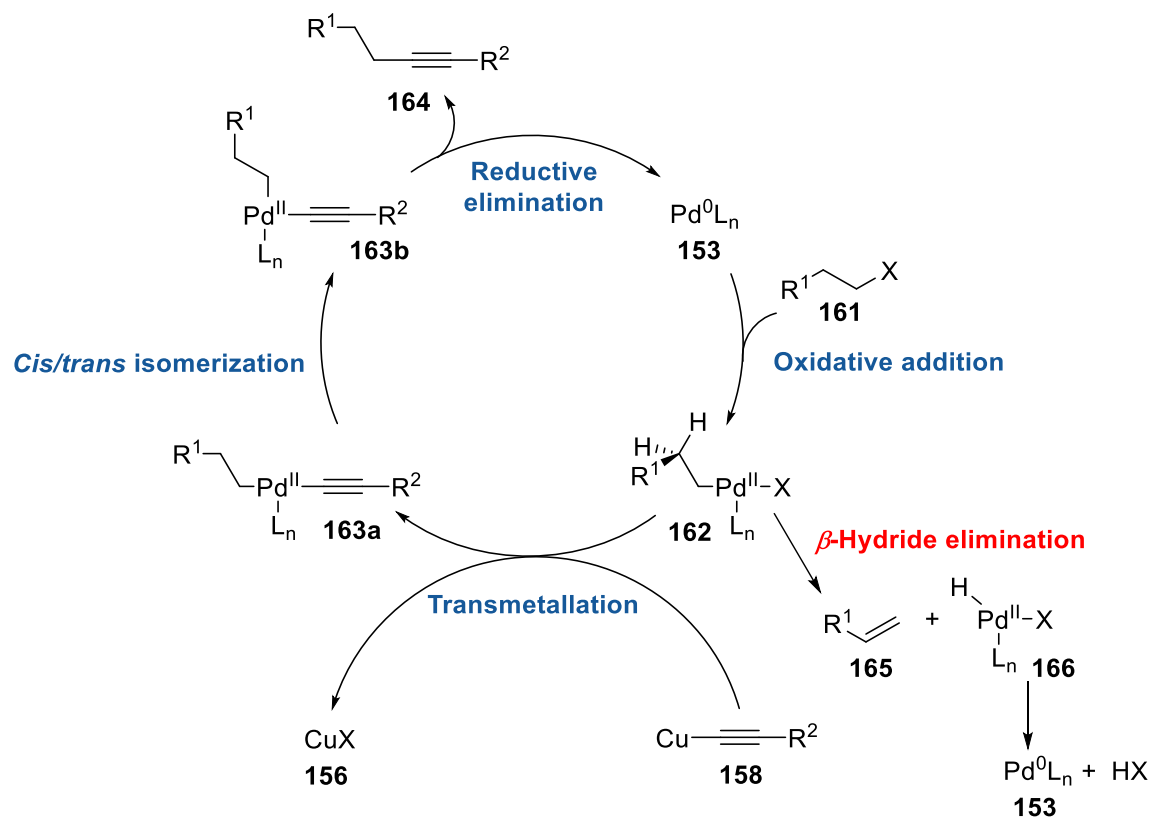
The use of alkyl halides to prepare dialkyl alkynes is rare in Sonogashira-type coupling reactions, for the following reasons:

### 1. *Slow oxidative addition.*

Due to the absence of a  $\pi$ -system, alkyl halides cannot pre-coordinate to the palladium center like aryl halides.<sup>147</sup> Moreover, Green and co-workers' computational work demonstrated that the oxidative addition of an alkyl chloride to Pd(0) has a transition state of higher energy than that of an aryl chloride.<sup>147</sup> These factors make the oxidative addition of alkyl halides to palladium center less favorable and slow.

### 2. *Uncontrolled $\beta$ -hydride elimination.*

Competitive  $\beta$ -hydride elimination is a deleterious pathway, making the cross-coupling of alkyl halides challenging. Scheme 2-3 shows the outline of this process.<sup>148</sup> The Pd(II) species **162** is obtained after the oxidative addition step. In **162**, if one  $\beta$ -hydrogen is in the *cis*-coplanar position to a vacant *d*-orbital on palladium, the  $\beta$ -hydride elimination is likely to occur competitively to deliver the undesired alkene **165**, L<sub>n</sub>Pd(0) **153**, and HX.

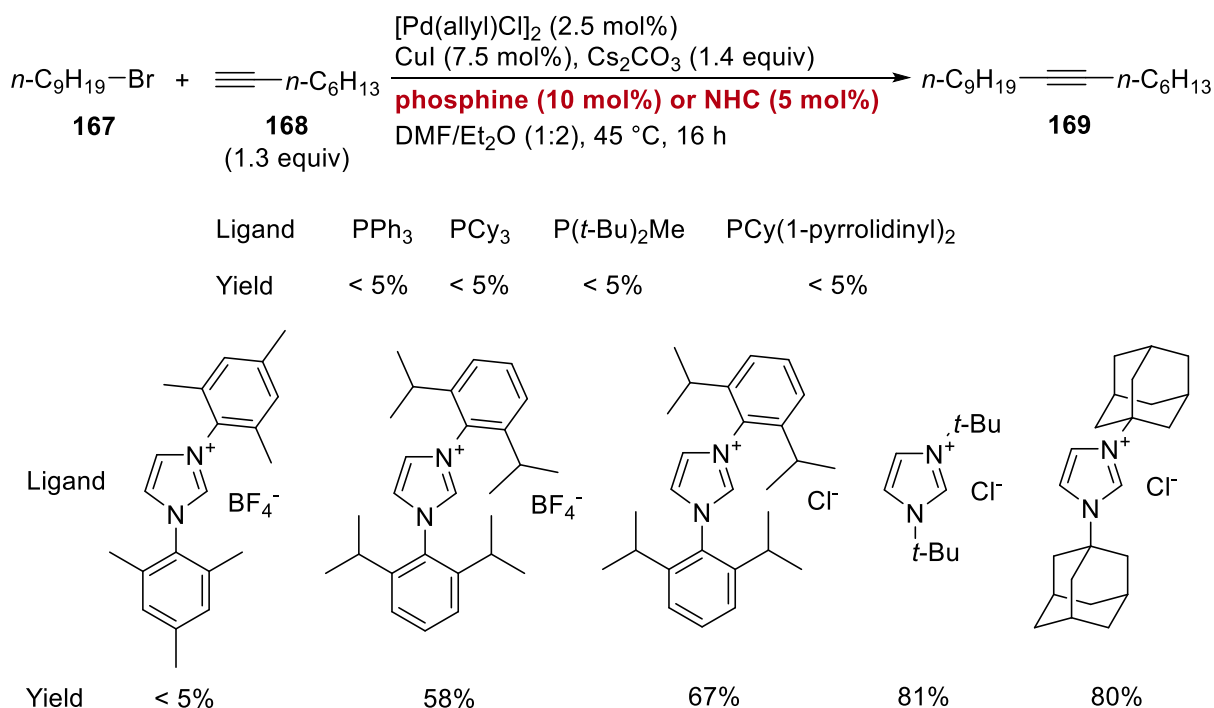


**Scheme 2-3.**  $\beta$ -Hydride elimination pathway for Sonogashira couplings.<sup>148</sup>

After oxidative addition, transmetallation of **162** with copper acetylide **158** occurs. The copper(I) iodide is added in substoichiometric amounts (<100 mol%).<sup>148</sup> This means that **158** is in low concentration and only generated gradually. Because of the low concentration, the rate of transmetallation is slow and **162** is more likely to undergo  $\beta$ -hydride elimination than transmetallation. This makes  $\beta$ -hydride elimination more difficult to control. However, by using *N*-heterocyclic carbene (NHC) ligands, Sonogashira couplings of alkyl halides with terminal alkynes were achieved. The details are discussed below.

## 2.2.2 Palladium-catalyzed Sonogashira coupling of terminal alkynes and alkyl halides using *N*-heterocyclic carbene ligands

To address the challenges stated above, Fu and co-workers reported the first example of alkyl halide Sonogashira coupling by using catalysts incorporating bulky NHC ligands in 2003 (Equation 2-1).<sup>148</sup>



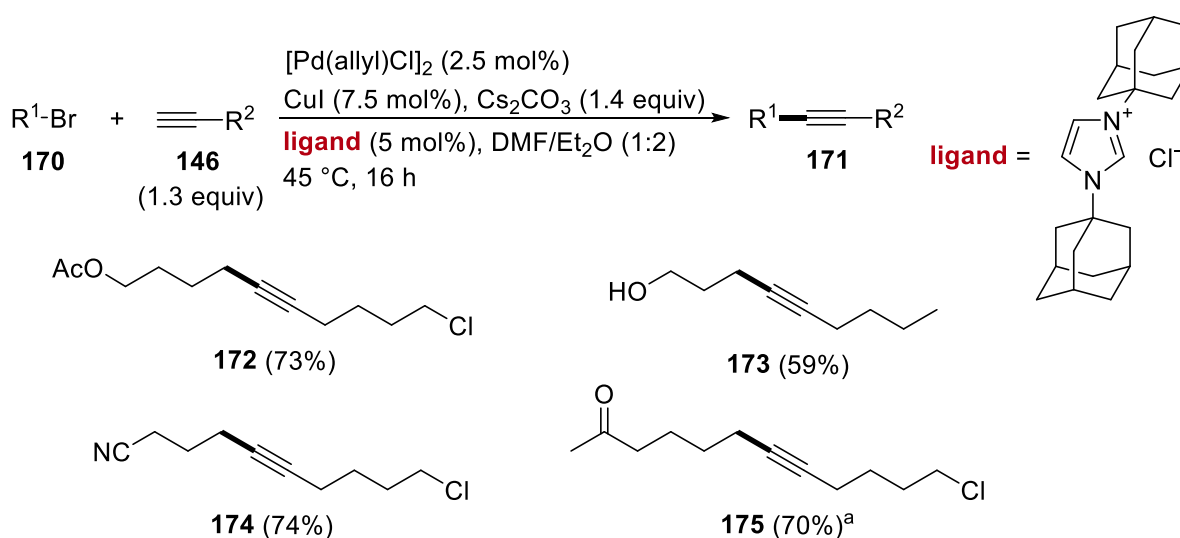
**Equation 2-1.** Effect of ligands on a Sonogashira coupling of an alkyl bromide with a terminal alkyne.<sup>148</sup>

From Fu and co-workers' experimental results, typical phosphine ligands are ineffective in the alkyl bromide coupling, but the reaction proceeds when using a very large NHC ligand. It is not difficult to understand the reason for using these bulky NHC ligands: NHC ligands are strong electron donors, which accelerate the oxidative addition step, a relative slow process for alkyl halides. The bulky substituents on the ligands inhibit the  $\beta$ -hydride elimination pathway by not



allowing the required *cis*-coplanar geometry or by making the palladium hydride species too sterically unfavorable.<sup>149,150</sup>

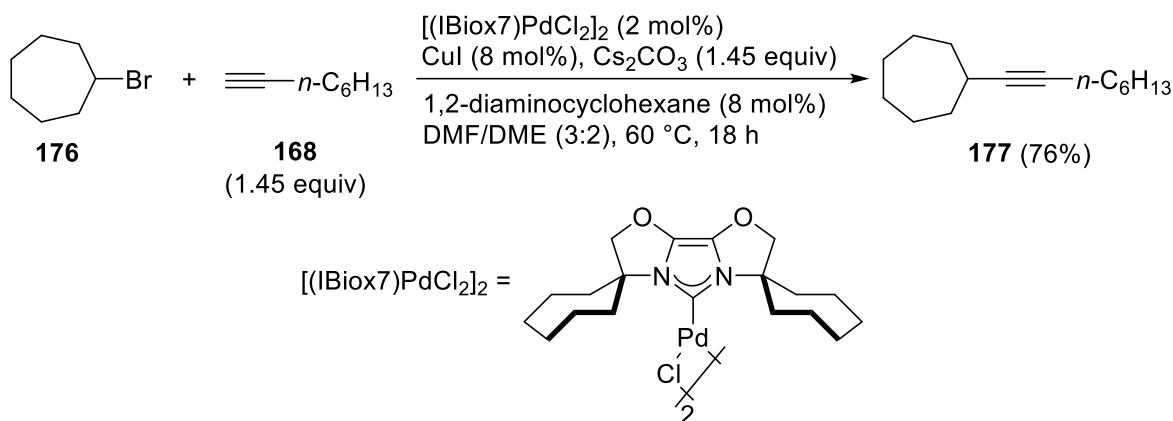
Based on these findings, Fu and co-workers investigated the reaction scope using the 1-adamantyl NHC ligand. Equation 2-2 shows some representative examples. This cross-coupling accepts a wide range of functional groups, including esters, alcohols and alkyl chlorides. These groups may not be tolerated in a strongly basic environment.



<sup>a</sup> Alkyl iodide was used and the reaction proceeded at 40 °C.

**Equation 2-2.** Representative examples of Sonogashira coupling using alkyl halides.<sup>148</sup>

Based on Fu and co-workers' pioneering work, Glorius and co-workers reported the first example of Sonogashira coupling using secondary alkyl halides in 2006 (Equation 2-3).<sup>151</sup> The coupling of bromocycloheptane **176** with 1-octyne **168** yields the internal alkyne **177** under [(IBiox7)PdCl<sub>2</sub>]<sub>2</sub> catalysis. The catalyst is made from Pd(OAc)<sub>2</sub>, LiCl and IBiox7·HOTf. The ligand serves the same purpose as the NHC ligand in Fu and co-workers' work.

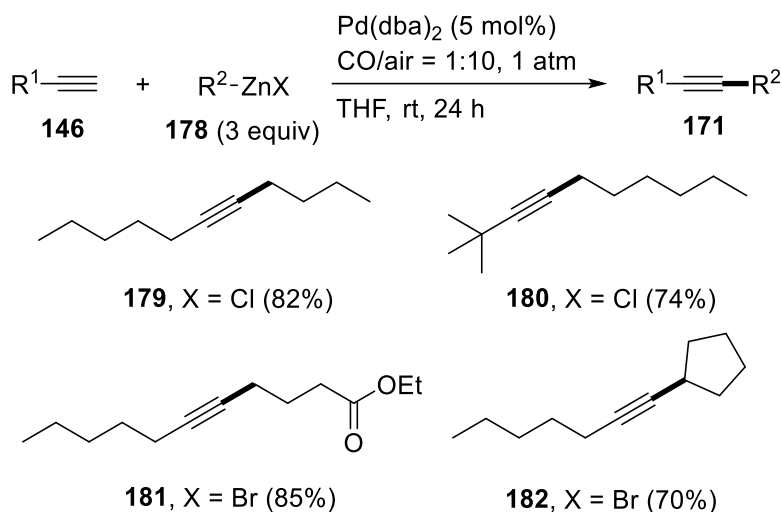


**Equation 2-3.** Sonogashira coupling of bromocycloheptane with 1-octyne.<sup>151</sup>

Besides Sonogashira coupling, other types of cross-coupling reactions were also reported for preparing dialkyl alkynes. Some of them allow the use of first-row transition metal catalysts, which are much less expensive than palladium. Selected examples are presented below.

### 2.2.3 Palladium-catalyzed oxidative cross-coupling of alkynes and alkylzinc reagents

In 2010, Lei and co-workers described a palladium-catalyzed oxidative cross-coupling of alkynes with alkylzinc reagents, a modified Negishi coupling (Equation 2-4).<sup>152</sup> In this reaction, carbon monoxide acts as a  $\pi$ -acidic ligand (a class of ligands that is able to accept electrons from metal atom to their empty  $\pi^*$  orbital), while molecular oxygen is the oxidant. The reaction scope studies have proved that this method allows the coupling of both primary and secondary alkylzinc reagents.



**Equation 2-4.** Palladium-catalyzed oxidative cross-coupling of terminal alkynes with alkylzinc reagents.<sup>152</sup>

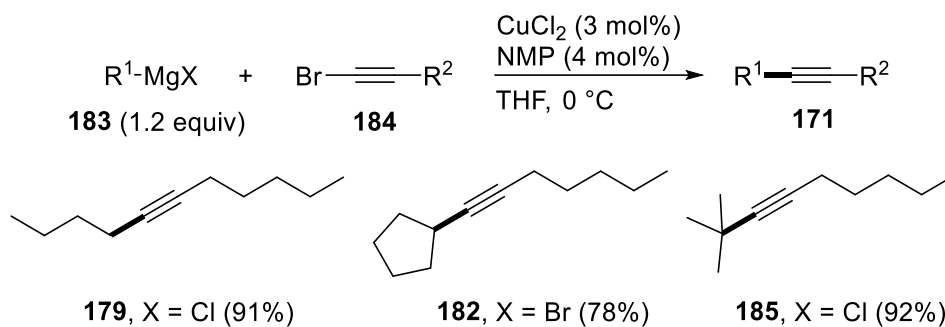
This type of cross-coupling reaction differs from the Sonogashira coupling in the following aspects.

1. The reaction requires molecular oxygen, which means this coupling does not involve an oxidative addition step. The palladium peroxo complex  $(\eta^2\text{-O}_2)\text{Pd}^{\text{II}}(\text{dba})_2$ , which is generated from  $\text{Pd}(\text{dba})_2$  and molecular oxygen, is likely to play a critical role in this coupling.<sup>153</sup>
2. Unlike using an electrophile as in Sonogashira coupling, two nucleophiles are coupled in this case. The FT-IR analyses of the reaction mixture suggested that an alkynyl zinc intermediate is formed during the reaction through the exchange of terminal alkyne with excess alkyl zinc reagent.<sup>152</sup>
3. The coupling does not require a bulky or donor ligand. Instead, carbon monoxide and dba, two  $\pi$ -acidic ligands, lead to a more electron deficient metal center.

Although Lei and co-workers did not propose a full mechanism, a reasonable rationale can be provided. The alkynyl zinc intermediate undergoes transmetallation with palladium and the Pd-C(sp) bond forms first, assisted by molecular oxygen. Subsequently, the Pd-C(sp<sup>3</sup>) bond forms in another transmetallation process. At this point, the reductive elimination occurs immediately, which suppresses the  $\beta$ -hydride elimination pathway due to the electron-deficient palladium center.

## 2.2.4 Copper-catalyzed cross-coupling of alkyl Grignard reagents and alkynyl halides

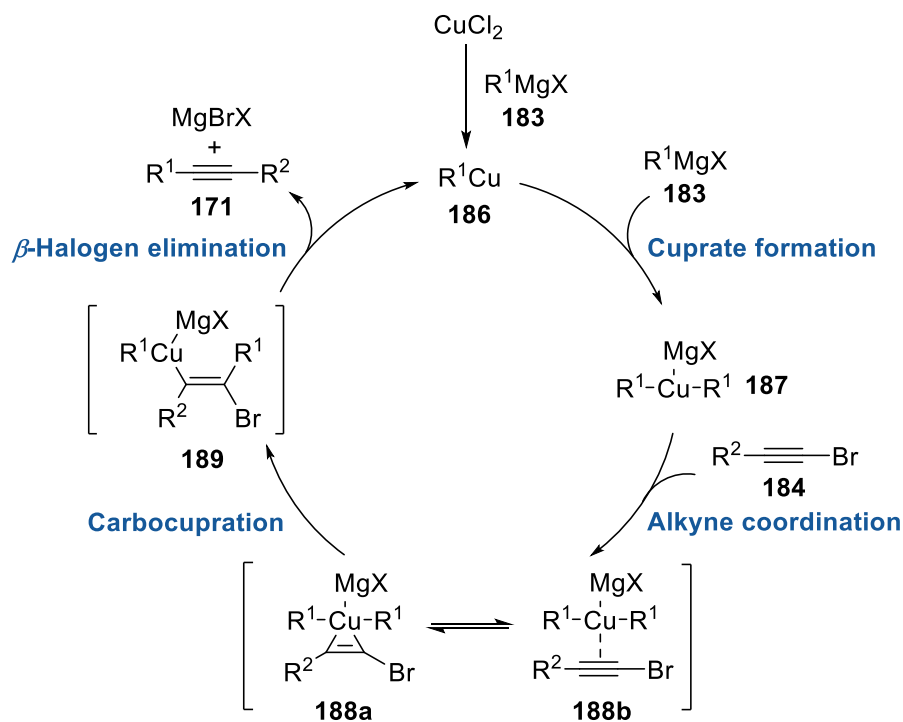
In 2010, Cahiez and co-workers reported a much different alkyne cross-coupling reaction, this time using copper(II) chloride, an alkyl Grignard reagent, and an alkynyl bromide (Equation 2-5).<sup>154</sup>



**Equation 2-5.** Copper-catalyzed cross-coupling of alkyl Grignard reagents with alkynyl bromides.<sup>154</sup>

The reaction scope includes primary, secondary, and tertiary Grignard reagents. Scheme 2-4 shows the mechanism proposed by Cahiez and co-workers based on the literature and their observations.<sup>154</sup> Cahiez suggests that a carbocupration/ $\beta$ -halogen elimination process leads to the formation of the dialkyl alkyne. In this catalytic cycle, the Cu(I) complex **186** is proposed to be

the active catalyst, which might be generated from the reduction of the pre-catalyst  $\text{CuCl}_2$  by the Grignard reagent.



**Scheme 2-4.** Proposed mechanism of copper-catalyzed cross-coupling of alkyl Grignard reagents with alkynyl bromides.<sup>154</sup>

This reaction is successful for a number of reasons:

1. *Coordinationally saturated intermediates.*

Considering the coordination of copper and the NMP ligand, species **187**, **188**, **189** are all coordinationally saturated intermediates ( $\text{Cu(I)}$ ,  $d^{10}$ , tetrahedral). In these intermediates, copper does not have a vacant site for  $\beta$ -hydride elimination to take place.

### 2. *Reversible hydride insertion.*

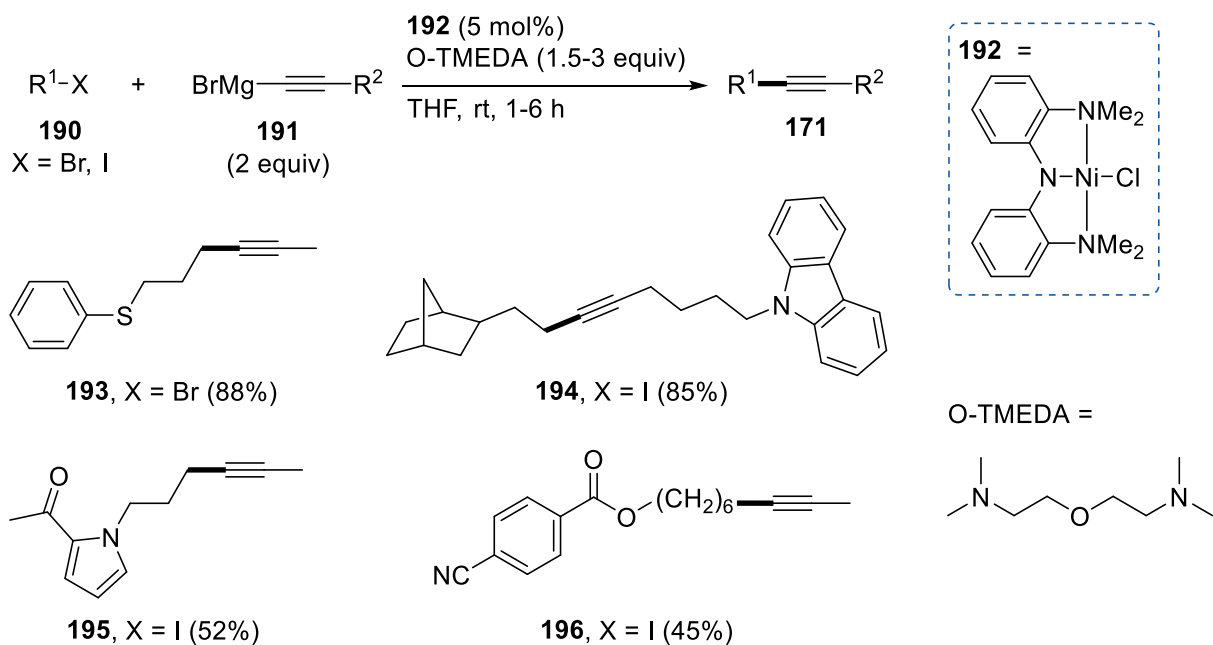
Although **186** is coordinatively unsaturated, the Cu(I) species is in a low oxidation state, unlikely to undergo reductive elimination. The hydride can insert back to give **186**, a process that does not affect the catalytic cycle.

### 3. *Electron-donating ligand and alkyl group.*

From the observations, NMP is a good  $\sigma$ -donor ligand and benefits the reaction by accelerating the carbocupration, which is a relatively slow process.<sup>154</sup> In addition, it was proposed that alkyl-Cu(I) species are more electron rich than vinyl-Cu(I) and alkynyl-Cu(I) species.<sup>155</sup> Thus, the dialkyl alkyne is formed rapidly.

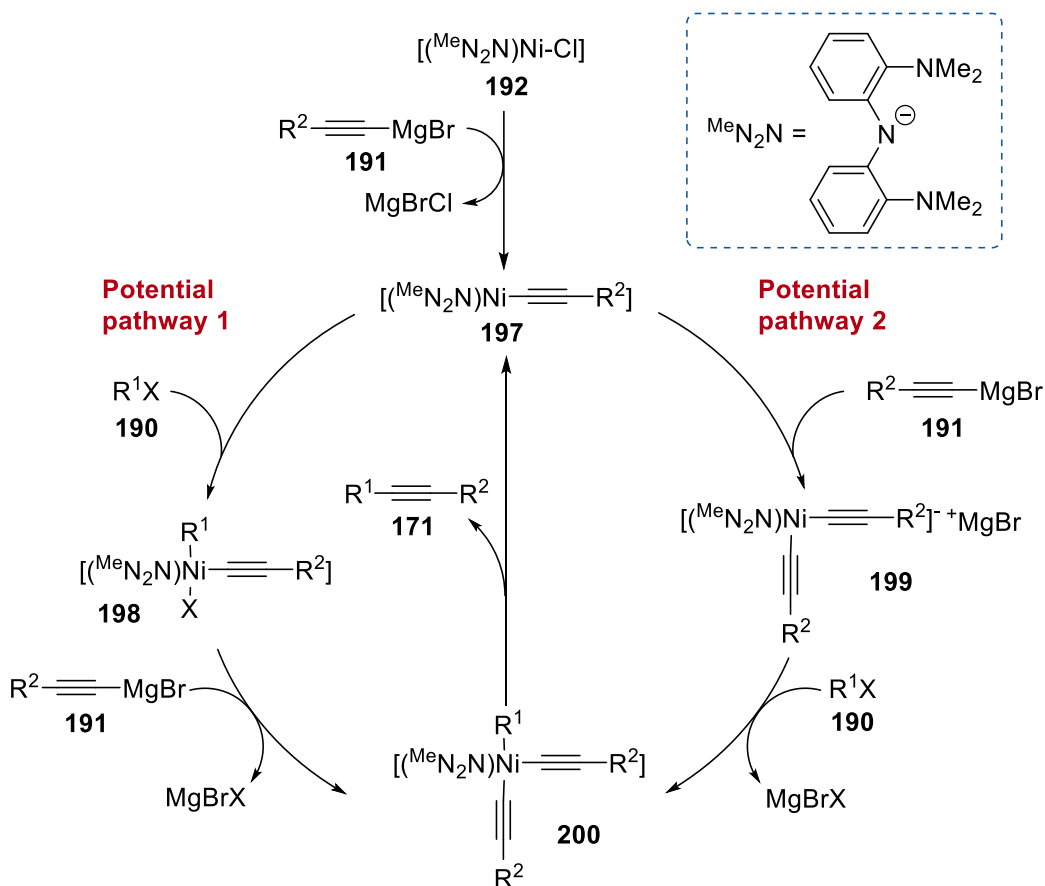
## 2.2.5 First-row transition metal-catalyzed cross-couplings of alkyl halides and alkynyl Grignard reagents

Although Cahiez's copper-catalyzed cross-coupling reaction tolerates various functional groups, some drawbacks restrict its use in synthesis. For example, sulfur-containing groups can poison copper catalysts.<sup>156</sup> In addition, the preparation of Grignard reagents from alkyl halides can be a problem. The formation of Grignard reagents is highly dependent on the activity of the substrate. Side reactions such as Wurtz coupling may also occur, leading to lower yields of alkyne products. Because the terminal proton is more acidic, alkynyl Grignard reagents can be easily obtained by stirring the corresponding terminal alkyne with a commercially available Grignard reagent (e.g., ethylmagnesium bromide). In 2011, Hu and co-workers reported a similar cross-coupling using a nickel pincer ligand catalyst **192** (Equation 2-6).<sup>156</sup>



**Equation 2-6.** Nickel-catalyzed cross-coupling of alkyl halides with alkynyl Grignard reagents.<sup>156</sup>

In this reaction, O-TMEDA is added to promote the exchange between the terminal alkyne and ethyl Grignard, and to suppress homo-coupling.<sup>156</sup> Study of the reaction scope showed that this coupling tolerates many functional groups, including sulfide, ketone, nitrile and ester. Hu and co-workers proposed a mechanism based on their experimental results (Scheme 2-5). The catalyst **192** reacts with the alkynyl Grignard reagent **191** to provide intermediate **197**, which reacts with the alkyl halide **190** and more alkynyl Grignard **191** to give the key intermediate **200**, via two possible pathways. Lastly, reductive elimination of **200** produces the dialkyl alkyne product.

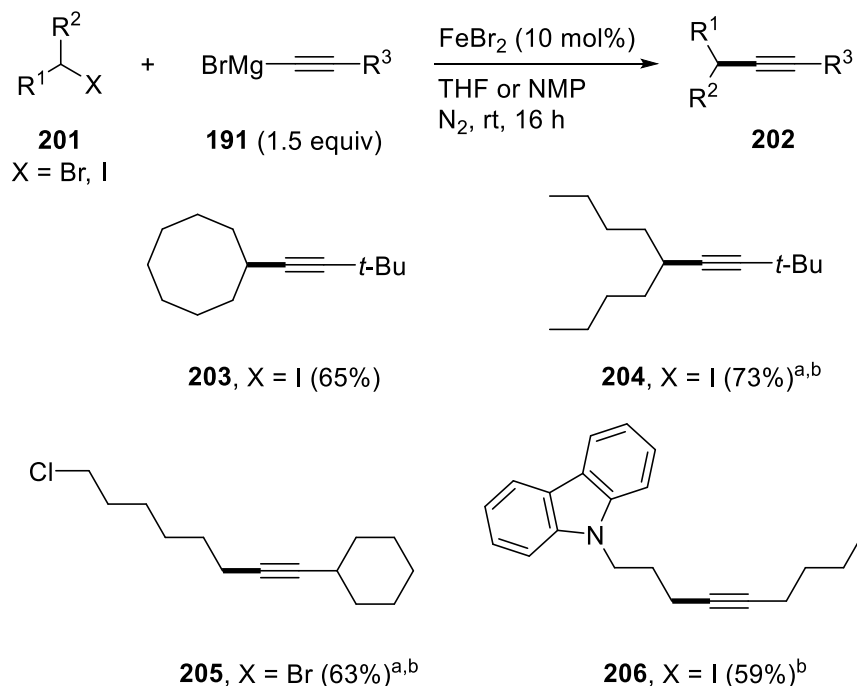


**Scheme 2-5.** Proposed mechanism for nickel-catalyzed alkyl-alkynyl cross-coupling.<sup>156</sup>

In this catalytic cycle, it can be seen that only intermediates **198** and **200** have nickel-C(sp<sup>3</sup>) bonds but both are coordinatively saturated (Ni(IV), d<sup>6</sup>, octahedral). Therefore,  $\beta$ -hydride elimination cannot occur during the reaction.

Although nickel catalyst **192** makes the synthesis of dialkyl alkynes more convenient, it is cumbersome to prepare the triamine pincer ligand required by this catalyst.<sup>157,158</sup> In 2014, Hu and co-workers reported a major improvement: catalytic cross-coupling of alkyl halide and alkynyl Grignard reagent, using iron(II) bromide as the catalyst (Equation 2-7).<sup>159</sup> This cross-coupling reaction does not require any complicated ligands, only a donor co-solvent.



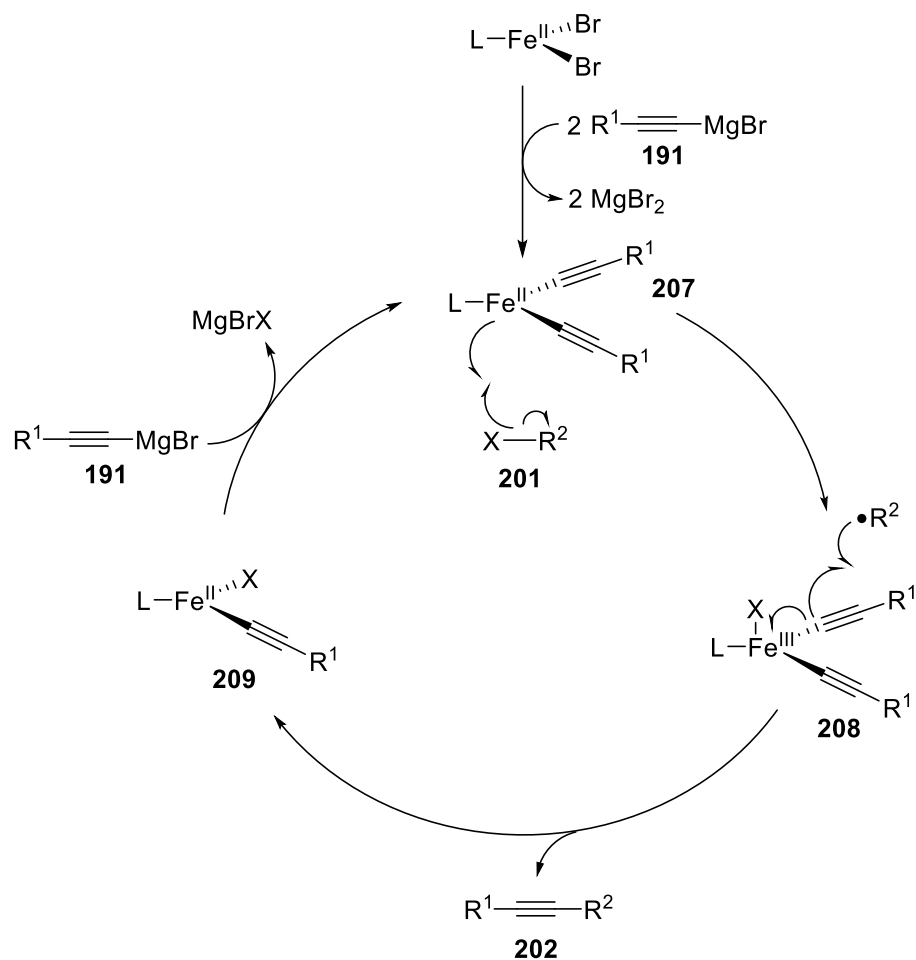


<sup>a</sup> FeBr<sub>2</sub> (20 mol%). <sup>b</sup> O-TMEDA (2 equiv).

**Equation 2-7.** Iron-catalyzed cross-coupling of alkyl halides with alkynyl Grignard reagents.<sup>159</sup>

From the reaction scope, it can be seen that coupling of cyclic and acyclic secondary alkyl halides is possible. This is the first iron-catalyzed cross-coupling of acyclic secondary alkyl halides with alkynyl Grignard reagents.<sup>159</sup> However, for primary alkyl halides, in some cases, only moderate yields are obtained.

From the experimental results, Hu and co-workers believe that the reaction involves a single electron transfer from the iron center to the alkyl halide. The proposed mechanism is shown in Scheme 2-6.<sup>159,160</sup> None of the intermediates has an Fe-C(sp<sup>3</sup>) bond during the catalytic cycle, making it impossible for  $\beta$ -hydride elimination to occur.



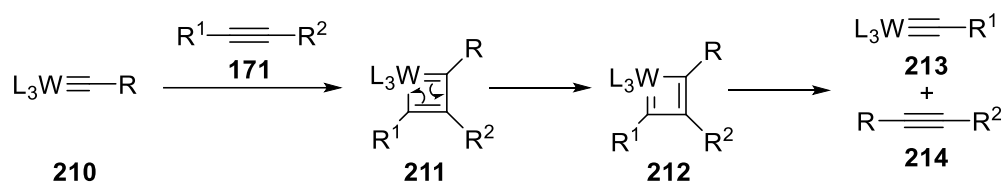
**Scheme 2-6.** Proposed mechanism for iron-catalyzed alkyl-alkynyl cross-coupling.<sup>159,160</sup>

It is well-known that the stabilities of alkyl free radicals descend in the order of tertiary > secondary > primary. The single electron transfer mechanism explains the lower yields obtained when using a primary alkyl halide. There were no examples of using tertiary alkyl halides in Hu's work, which are likely to be disfavored by steric effects.

### 2.2.6 Molybdenum- or tungsten-catalyzed alkyne metathesis

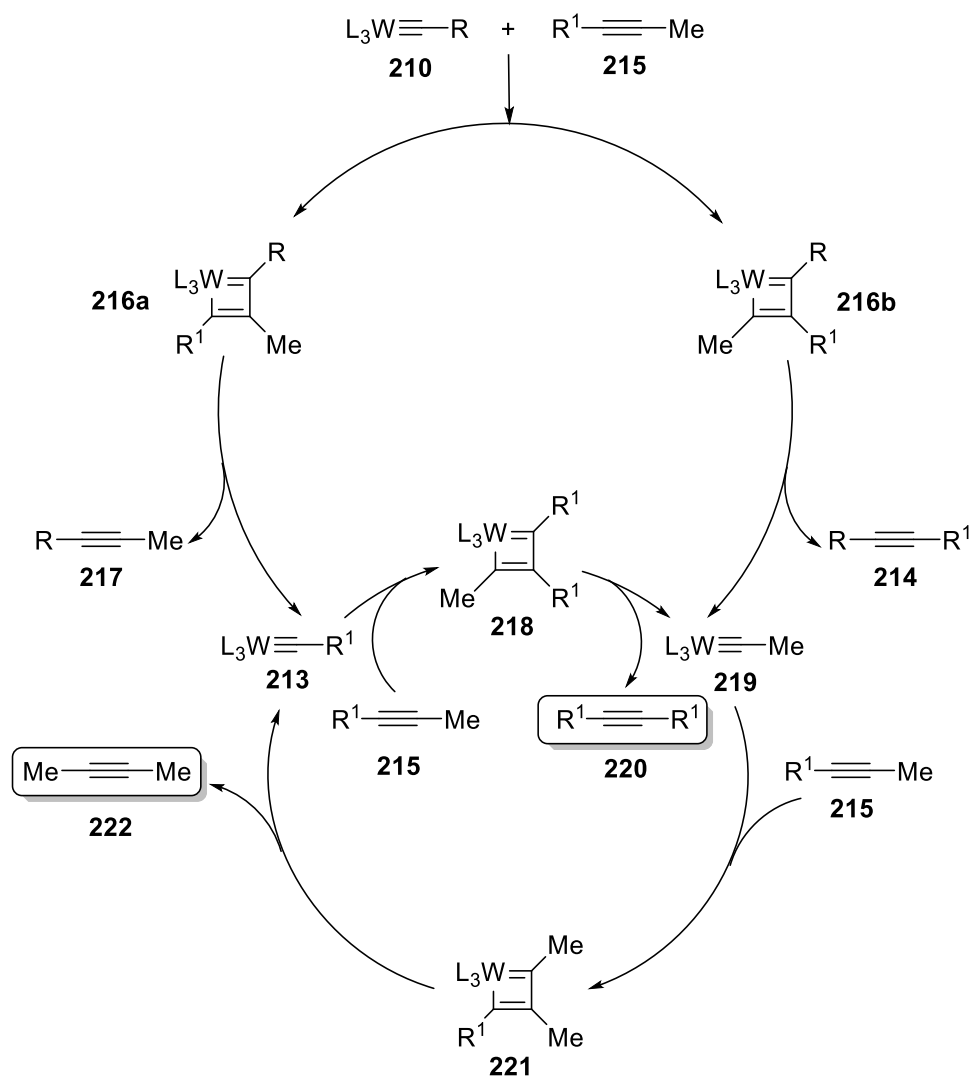
Besides cross-coupling, alkyne metathesis is also an effective way to prepare dialkyl alkynes. Transition metal-catalyzed alkyne metathesis was reported as early as 1974.<sup>161</sup> Then, Schrock-

type W(IV) alkylidyne complexes **210** were employed as catalysts<sup>162</sup> and the alkyne substrates were limited to internal alkynes.<sup>163</sup> To explain the metathesis mechanism, Schrock and co-workers proposed that metallacyclobutadiene intermediates **211** are generated from W(IV) alkylidyne catalyst **210** (Scheme 2-7).<sup>162</sup>



**Scheme 2-7.** Alkyne metathesis by Schrock-type alkylidyne catalyst via metallacyclobutadiene intermediates.<sup>162</sup>

Thus, terminal methylated alkynes **215** are commonly employed in the metathesis as the release of volatile 2-butyne **222** can drive the reaction to completion.<sup>164</sup> Scheme 2-8 shows a complete metathesis mechanism using a Schrock-type catalyst.<sup>162,165,166</sup>



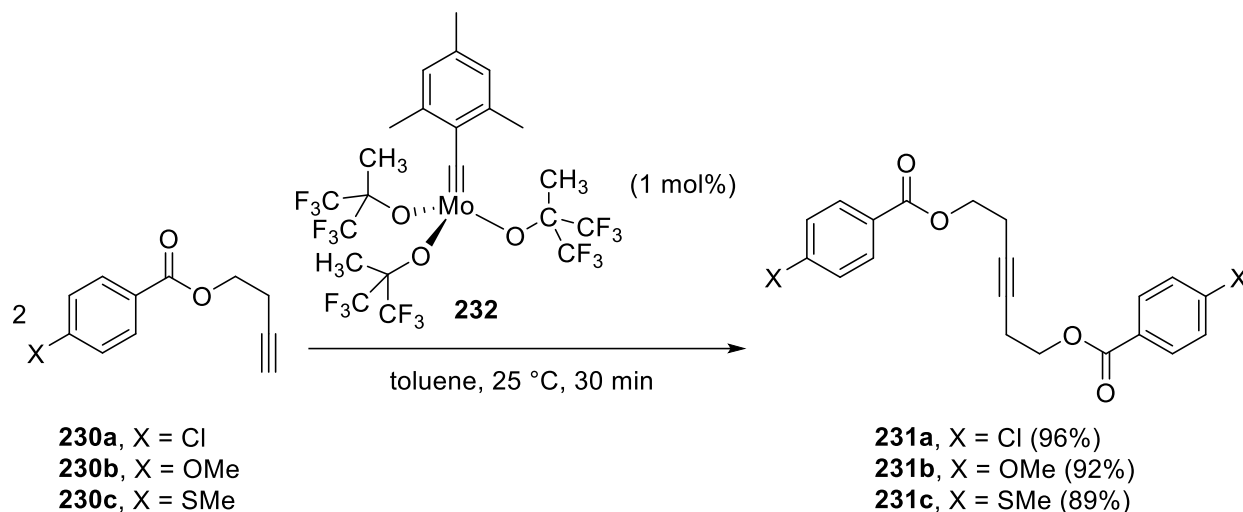
**Scheme 2-8.** Metathesis mechanism of a terminal methylated alkyne involving a Schrock-type catalyst.<sup>162,165,166</sup>

Terminal alkynes cannot be used as substrates because deprotonometallacycles (DMCs) **224** are formed and they undergo polymerization instead of metathesis (Scheme 2-9).<sup>163-166</sup>



Mortreux and co-workers proposed that quinuclidine stabilizes the methylidyne intermediate, suppressing DMC formation. However, the use of other types of alkynes, such as phenylacetylene or *t*-butyl acetylene, leads again to polymerization.

In 2012, Tamm and co-workers reported a terminal alkyne metathesis using the mesitylalkylidyne complex  $[\text{MesC}\equiv\text{Mo}\{\text{OC}(\text{CF}_3)_2\text{Me}\}_3]$  **232** (Equation 2-9).<sup>164</sup> This catalyst can also be employed for ring-closing alkyne metathesis. However, the attempts to use terminal arylalkynes still failed.



**Equation 2-9.** Molybdenum-catalyzed terminal alkyne metathesis.<sup>164</sup>

Tamm and co-workers ascribed the successful terminal alkyne metathesis to the following reasons:<sup>164</sup>

1. The introduction of the mesityl group helps to isolate the solvent-free pre-catalyst **232**, which shows high activity for alkyne metathesis. The rate of DMC formation is much slower than the rate of terminal alkyne metathesis.

2. The  $-\text{OC}(\text{CF}_3)_2\text{Me}$  ligand also suppresses DMC formation because of its low basicity.
3. The metathesis is performed at very low concentration (21 mM). High concentration of the alkyne can reverse the selectivity and lead to polymers.

In 2017, Tamm and co-workers optimized their metathesis catalysts. The two best alkyne metathesis catalysts are shown in Figure 2-2.<sup>168</sup> Both catalysts give excellent yields for homo-metathesis of terminal and internal alkynes. It should be pointed out that **233** is the first tungsten complex that catalyzes terminal alkyne metathesis efficiently.<sup>168</sup>

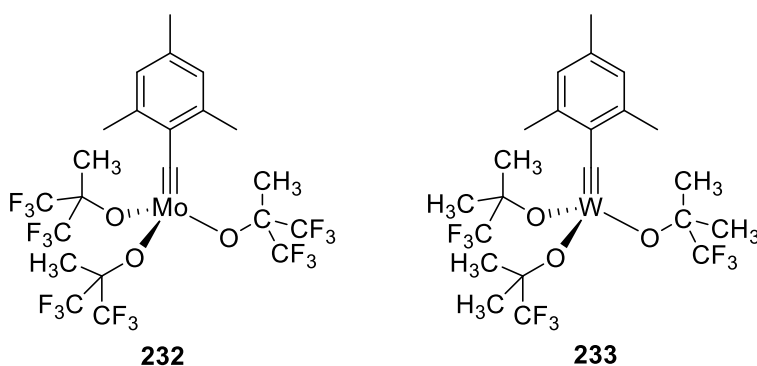


**Figure 2-2.** Two best alkyne metathesis catalysts from Tamm and co-workers' optimization studies.<sup>168</sup>

In addition to Tamm's group, Fürstner and co-workers also conducted studies on alkyne metathesis. Their molybdenum silanolate complex **234** catalyzes some terminal alkyne metathesis successfully (Figure 2-3), but its ability is highly substrate dependent. This catalyst was demonstrated to be effective for ring-closing alkyne metathesis between a terminal alkyne and an internal alkyne.<sup>169</sup>

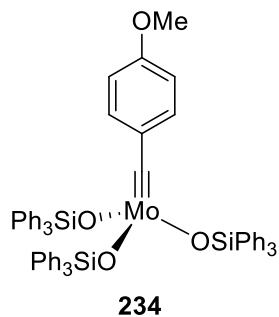
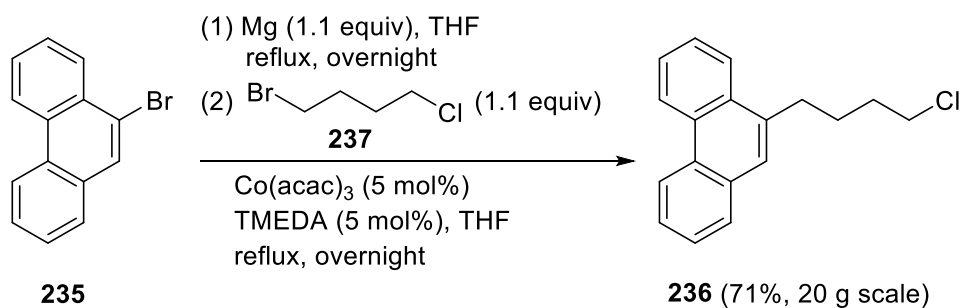


**Figure 2-3.** An alkyne metathesis catalyst prepared by Fürstner and co-workers.<sup>169</sup>

## Results and Discussions

### 2.3 Synthesis of phenanthrene-tethered dialkyl alkyne

Consistent with my research objectives, the preparation of island-tethered dialkyl alkynes is integral to the subsequent annulation process. On the basis of former group members' work, 9-(4-chlorobutyl)phenanthrene **236** was prepared on a 20 g scale by cobalt-catalyzed Kumada coupling (Equation 2-10).<sup>82,150</sup> This chloroalkylated compound is a good starting material for alkyne synthesis.

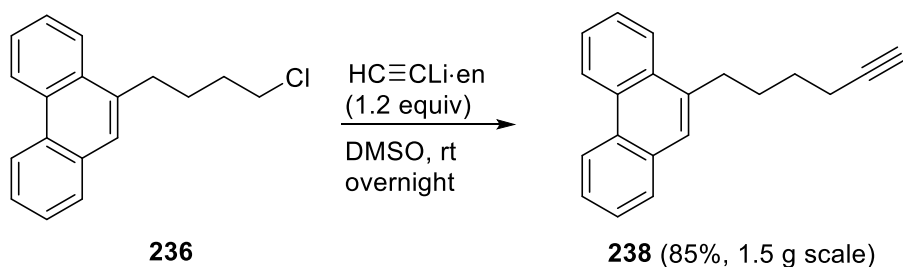


**Equation 2-10.** Synthesis of 9-(4-chlorobutyl)phenanthrene by cobalt-catalyzed Kumada coupling.<sup>82</sup>

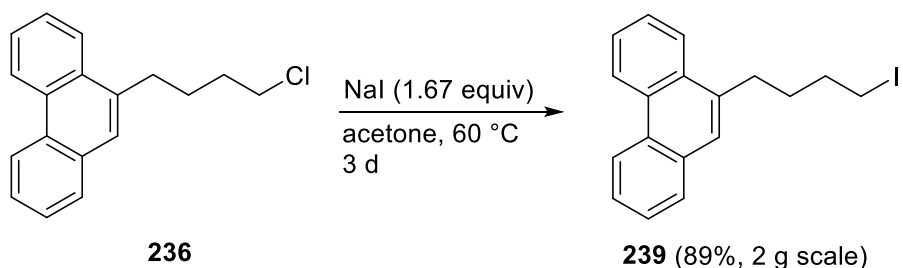


The traditional deprotonation route was selected initially, to test the feasibility of preparing phenanthrene-tethered alkyne **240**. The synthesis proceeded in three steps. An S<sub>N</sub>2 substitution of **236** by lithium acetylide produced the terminal alkyne **238** in 85% yield (Scheme 2-10a).<sup>170</sup> To make further substitution easier, a chloride/iodide exchange was carried out to obtain the iodide product **239** in 89% yield (Scheme 2-10b).<sup>171</sup> The last step involves the deprotonation/S<sub>N</sub>2 reaction of **238**.<sup>142</sup> DMI was used as the solvent to break the *n*-BuLi cluster in this process. It was found that the yield of **240** was moderate on a small-scale synthesis (77% on a 100 mg scale). However, on a 1 g scale synthesis, the yield dropped dramatically to 38% (Scheme 2-10c).

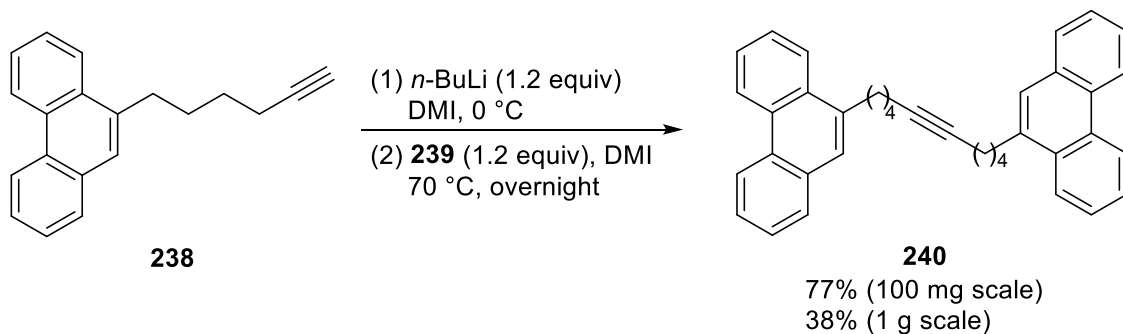
(a) Preparation of the terminal alkyne by lithium acetylide substitution:



(b) Preparation of the alkyl iodide by chloride/iodide exchange:

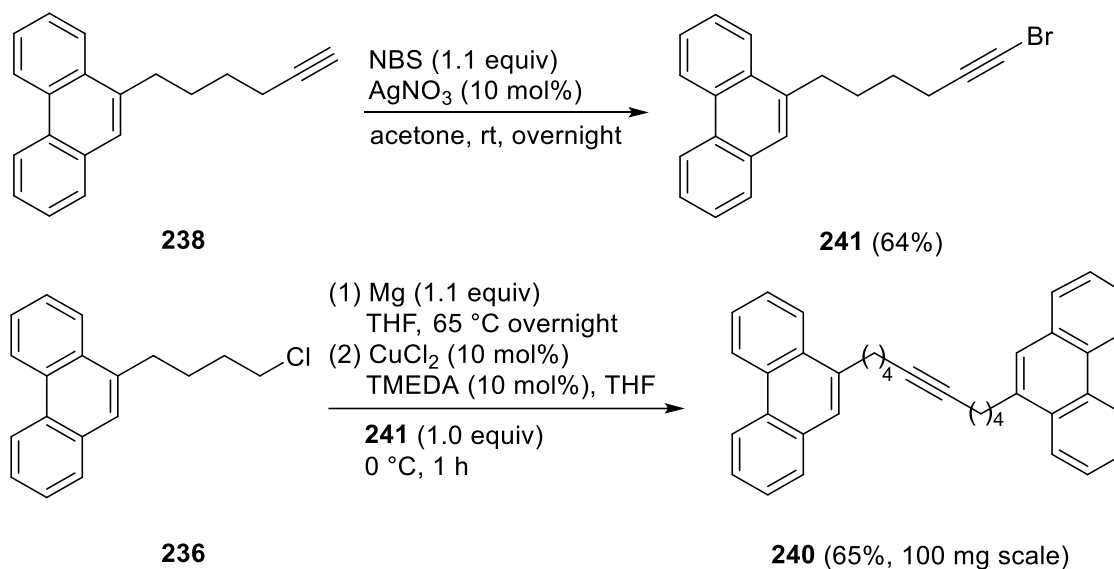


(c) Preparation of the phenanthrene-tethered dialkyl alkyne by *n*-BuLi deprotonation:



**Scheme 2-10.** Synthesis of the phenanthrene-tethered dialkyl alkyne.

To investigate other synthetic approaches, Cahiez's copper-catalyzed cross-coupling (Equation 2-5) was also tested.<sup>154</sup> Alkynyl bromide **241**, prepared from terminal alkyne **238** and *N*-bromosuccinimide (NBS), was coupled with the alkyl magnesium chloride to give **240** in 65% yield (Scheme 2-11). This methodology has two main limitations: (1) The preparation of the alkynyl bromide **241** requires an extra step, so the overall yields decrease. (2) The preparation of the Grignard reagent from alkyl chloride **236** sometimes requires repetitive activation, long

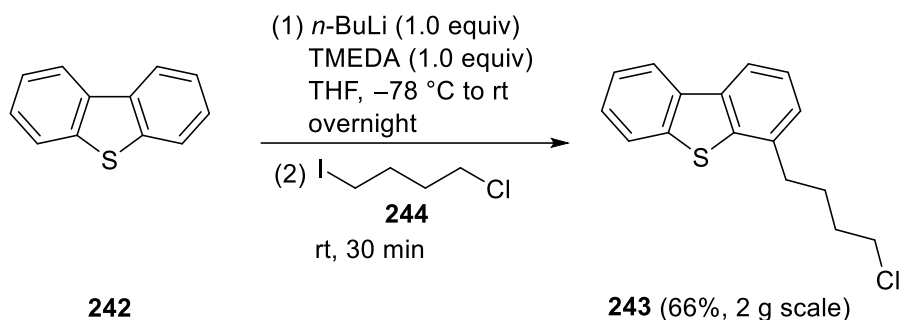


**Scheme 2-11.** Synthesis of phenanthrene-tethered dialkyl alkyne by copper-catalyzed cross-coupling.

## 2.4 Synthesis of dibenzothiophene-tethered dialkyl alkyne

As described in section 1.1.2, sulfur is the most abundant heteroatom in asphaltene samples. Most of the sulfur in asphaltenes is present as thiophenic compounds, such as benzothiophene or dibenzothiophene (DBT).<sup>30</sup> Sulfur can deactivate the catalysts during the oil refining and other catalytic processes.<sup>1, 172</sup> At the same time, due to the relatively strong aryl C-S bonds, hydrodesulfurization of dibenzothiophene is difficult.<sup>173</sup> However, sulfur-containing asphaltene model compounds are seldom studied and reported in previous work. To investigate sulfur-containing asphaltenes more thoroughly, my interest in synthetic model compounds has motivated me to prepare and characterize sulfur-containing archipelago compounds.

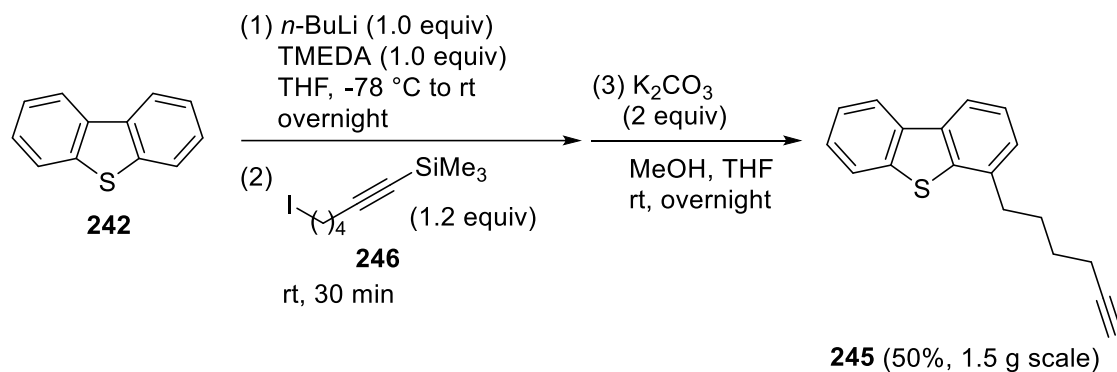
The preparation starts by deprotonation of DBT by *n*-BuLi.<sup>174</sup> Subsequent S<sub>N</sub>2 substitution by 1-chloro-4-iodobutane **244** provides 4-(4-chlorobutyl)dibenzothiophene **243**, which is used as a starting material for alkyne synthesis (Equation 2-11).



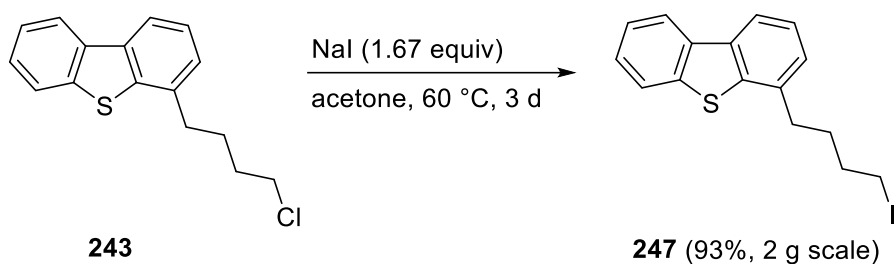
**Equation 2-11.** Synthesis of 4-(4-chlorobutyl)dibenzothiophene by deprotonation/S<sub>N</sub>2 substitution.

The synthetic process of DBT-tethered alkyne **248** is similar to the preparation of phenanthrene-tethered alkyne **240**. The only difference is the first terminal alkyne preparation step. Because the DBT-tethered terminal alkyne **245** has a similar *R<sub>f</sub>* value as the starting chloride **243**, it is difficult to isolate pure **245** when prepared by the lithium acetylide pathway. Therefore, compound **245** was prepared directly by deprotonation of DBT (Scheme 2-12a).<sup>175</sup> The iodination and subsequent alkyne deprotonation provide alkyne **248** (Schemes 2-12b and 2-12c). The observed yields were also lower on a large scale.

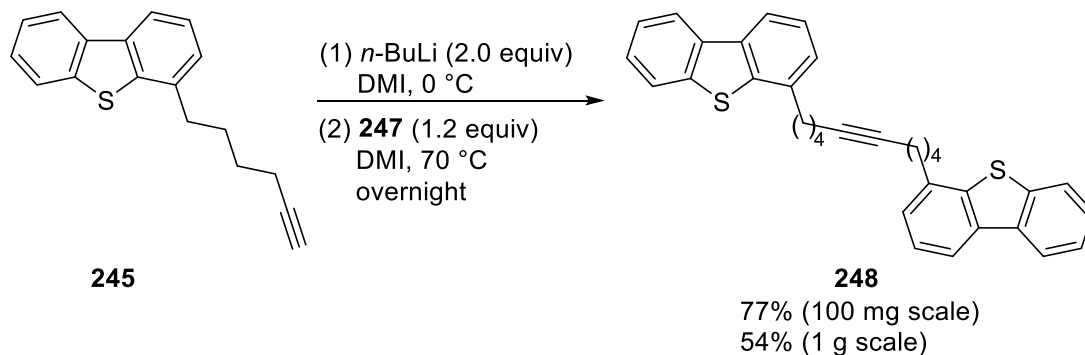
(a) Preparation of the terminal alkyne by deprotonation/substitution:



(b) Preparation of the iodide by chloride/iodide exchange:



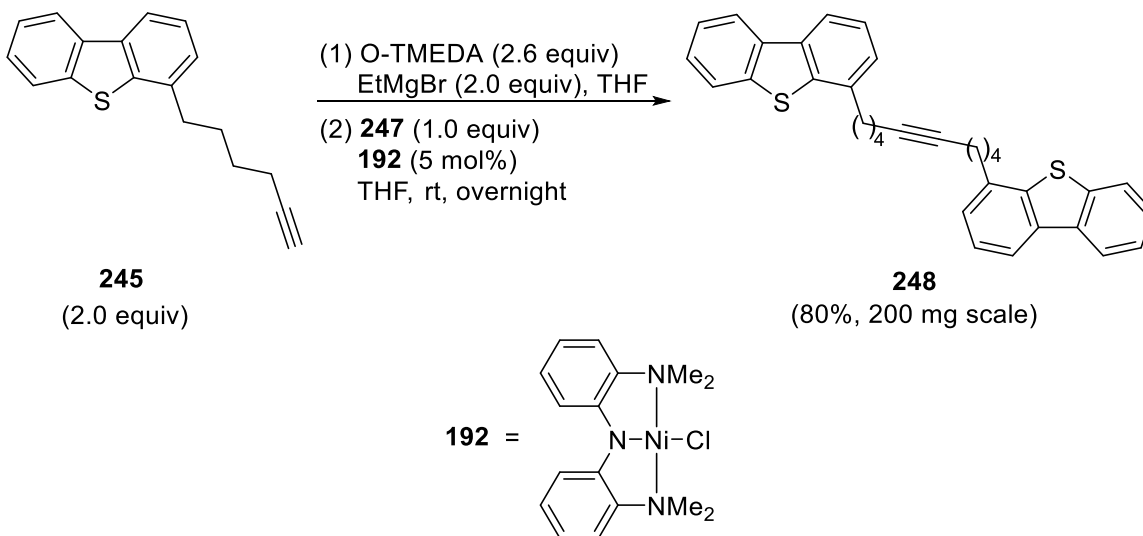
(c) Synthesis of the DBT-tethered dialkyl alkyne by *n*-BuLi deprotonation:



**Scheme 2-12.** Synthesis of DBT-tethered dialkyl alkyne.

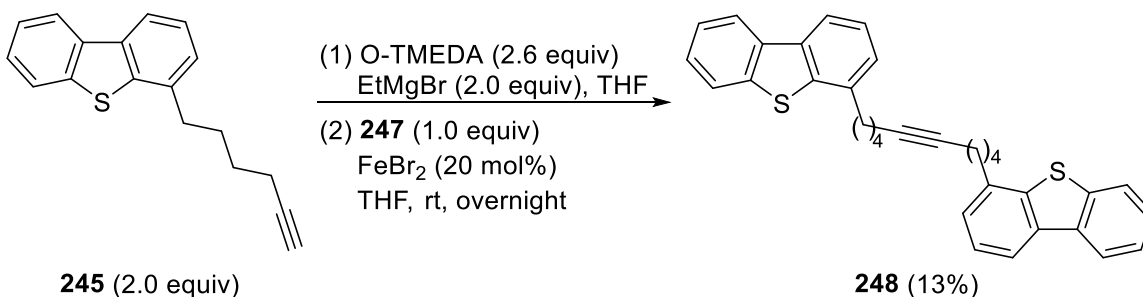
Other synthetic routes were also investigated. Because sulfur has a high affinity for copper,<sup>156</sup> Cahiez's copper-catalyzed cross-coupling<sup>154</sup> did not yield the alkyne. In this case, I tested a cross-coupling of alkynyl Grignard with alkyl iodide, using the nickel pincer catalyst **192** reported by Hu and co-workers (Equation 2-6).<sup>156</sup> 80% yield of alkyne **248** was obtained on a

200 mg scale reaction (Equation 2-12). However, the commercial sources of **192** are limited and the preparation of this pincer ligand is cumbersome.



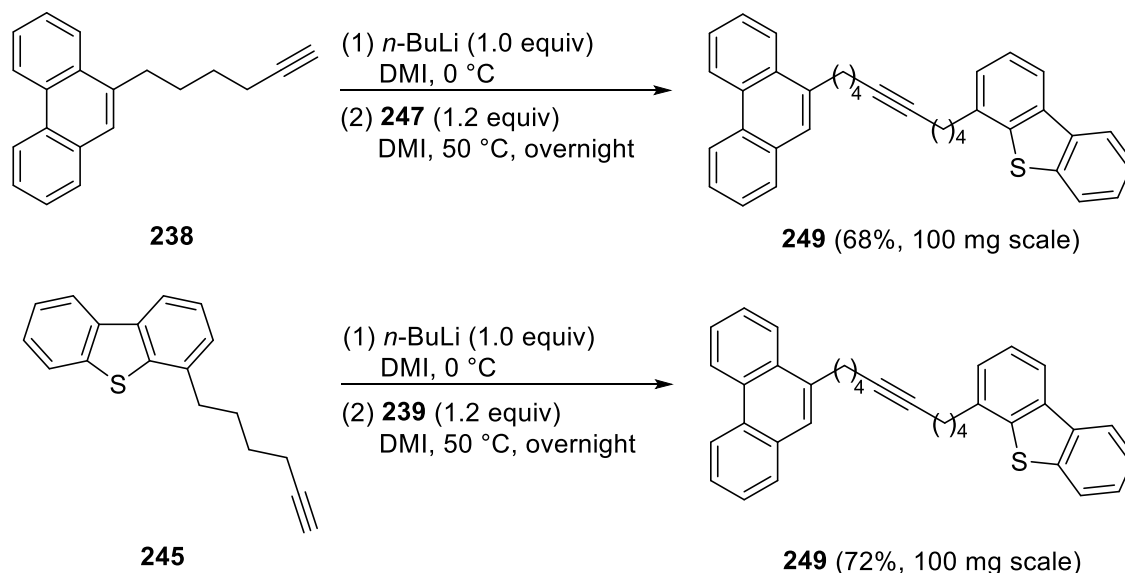
**Equation 2-12.** Synthesis of DBT-tethered dialkyl alkyne by nickel-catalyzed cross-coupling.

An iron-catalyzed coupling reported by Hu and co-workers<sup>159</sup> was also tested but the yield was very low (Equation 2-13). A free radical mechanism accounts for the low yield when using a primary alkyl halide (Scheme 2-6). After consideration of yields and costs, the previous *n*-BuLi deprotonation pathway was selected to prepare **248** on a large scale.



**Equation 2-13.** Synthesis of DBT-tethered dialkyl alkyne by iron-catalyzed cross-coupling.

An unsymmetrical alkyne **249** bearing phenanthrene and DBT islands was also synthesized for further [4+2] annulation. Similar yields were obtained when using phenanthryl alkyne **238** or DBT alkyne **245** as starting material (Scheme 2-13).



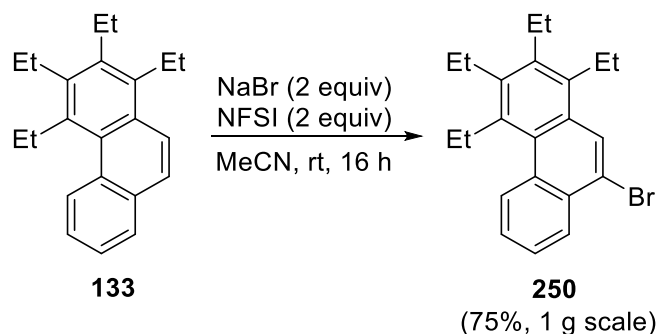
**Scheme 2-13.** Synthesis of the unsymmetrical alkyne by *n*-BuLi deprotonation/ $S_N2$  substitution.

## 2.5 Synthesis of the tetraethylphenanthrene-tethered dialkyl alkyne

Phenanthrene-tethered alkyne **240** has poor solubility in typical solvents used for coupling and characterization, such as DMF and DCM. The tetrasubstituted phenanthrene previously synthesized by cobalt-catalyzed annulation (Equation 1-5) provides the opportunity to prepare an alkyne in which the phenanthrene islands are replaced by alkyl-substituted phenanthrenes. The alkyl groups enhance the solubility of the alkyne and change the elemental composition of the final archipelago products, resulting a new library of model compounds.

To prepare this alkyne, 1,2,3,4-tetraethylphenanthrene (TEP) **133** was selected as the starting material because cobalt-catalyzed annulation provides **133** on a reasonable yield. The

bromination of **133** proceeds by using NFSI and NaBr, according to methodology reported by Li and co-workers (Equation 2-14).<sup>176</sup>

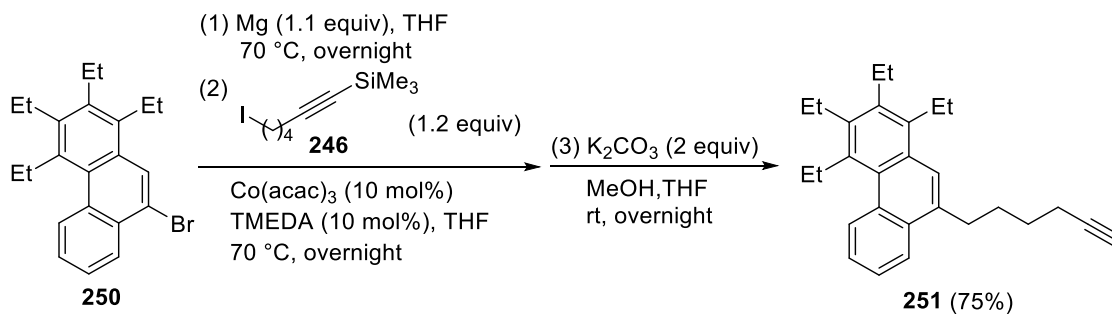


**Equation 2-14.** Synthesis of the brominated TEP.

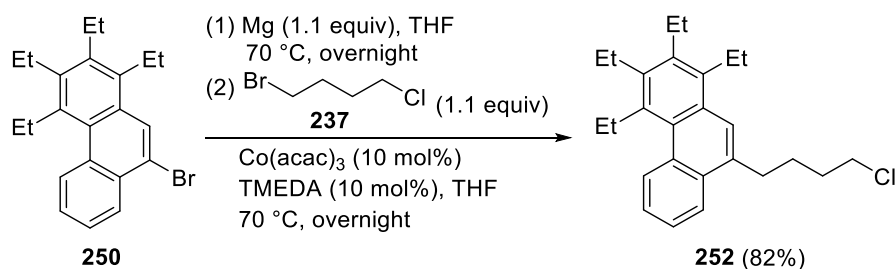
Subsequent alkylation of **250** provides terminal alkyne **251** and chloroalkylated compound **252** in 75% and 82% yields, respectively (Schemes 2-14a and 2-14b). Iodide **253** was obtained by a chloride/iodide exchange in 88% yield (Scheme 2-14c). However, none of the desired TEP-tethered alkyne **254** was detected after *n*-BuLi deprotonation and attempted S<sub>N</sub>2 substitution (Scheme 2-14d). <sup>1</sup>H and <sup>13</sup>C{<sup>1</sup>H} NMR data of the reaction mixture suggest that **253** undergoes an elimination process to give the alkene **255** in strongly basic environment. Comparing with the results from phenanthrene-tethered alkyne **240** (Scheme 2-10c), this is evidence that the ethyl groups dramatically increase the steric hinderance around the triple bond and the back-side nucleophilic addition cannot proceed.



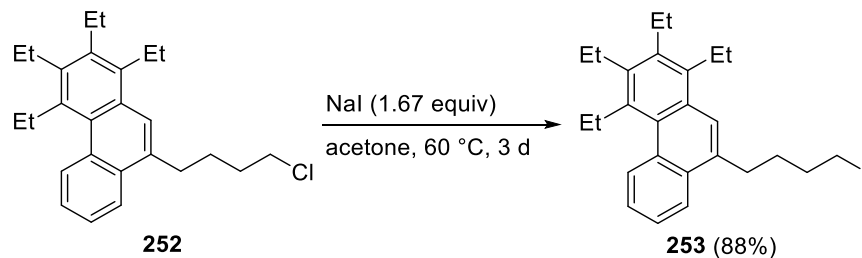
(a) Preparation of the terminal alkyne by Kumada coupling:



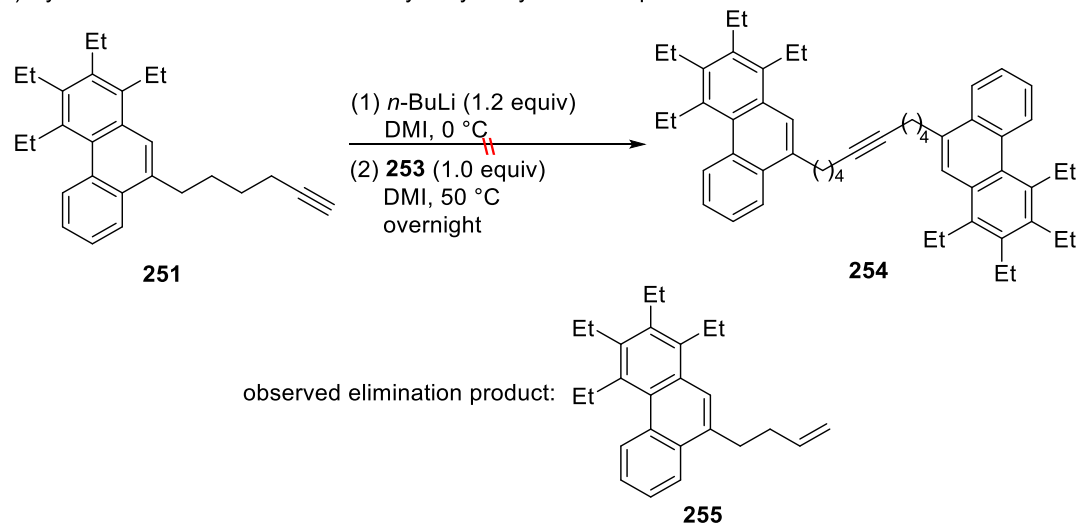
(b) Preparation of the chloroalkylated compound by Kumada coupling:



(c) Preparation of the iodoalkylated compound by chloride/iodide exchange:

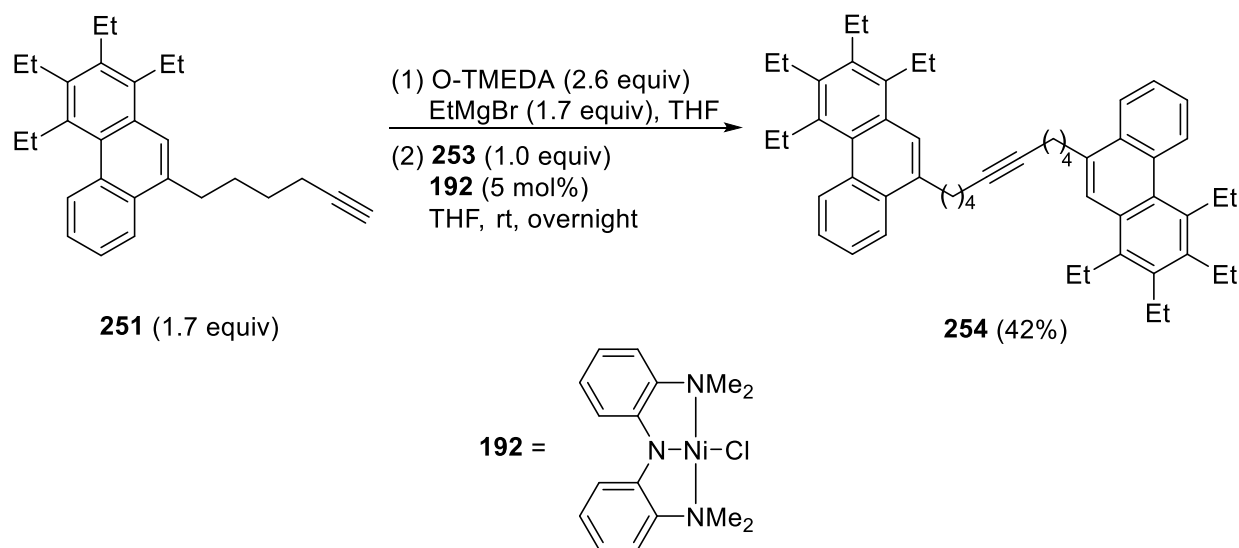


(d) Synthesis of the TEP-tethered dialkyl alkyne by *n*-BuLi deprotonation:



**Scheme 2-14.** Attempts to synthesize the TEP-tethered alkyne by *n*-BuLi deprotonation/ $\text{S}_{\text{N}}2$  substitution.

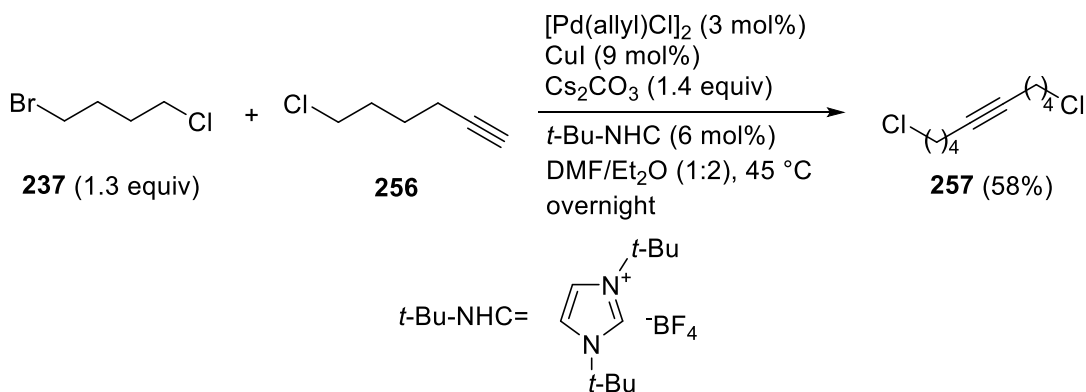
Some cross-coupling methodologies were also tested at this time, aiming to synthesize alkyne **254**. The nickel pincer catalyst **192**, which was reported by Hu and co-workers,<sup>156</sup> affords **254** in 42% yield (Equation 2-15). However, pure **254** was difficult to isolate by chromatography due to unknown impurities with similar  $R_f$  values. Other cross-couplings, including Cahiez's reaction (Equation 2-5) and Fu's reaction (Equation 2-1), provided alkyne **254** in very low or zero yields.



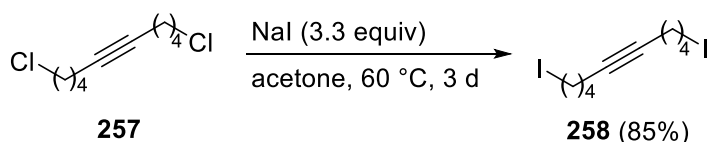
**Equation 2-15.** Synthesis of TEP-tethered dialkyl alkyne by nickel-catalyzed cross-coupling.

Therefore, an alternative synthesis pathway was explored to prepare alkyne **254**. The Kumada cross-coupling of 9-TEP magnesium bromide with 1,10-diiodo-5-decyne **258**, which was prepared by Fu's Sonogashira cross-coupling<sup>148</sup> followed by chloride/iodide exchange,<sup>171</sup> delivered the desired alkyne **254** in 32% yield (Scheme 2-15).<sup>82</sup>  $^1\text{H}$  NMR analysis showed that the pure alkyne **254** could be successfully isolated from column chromatography. Therefore, this synthetic route was selected for the preparation of **254**.

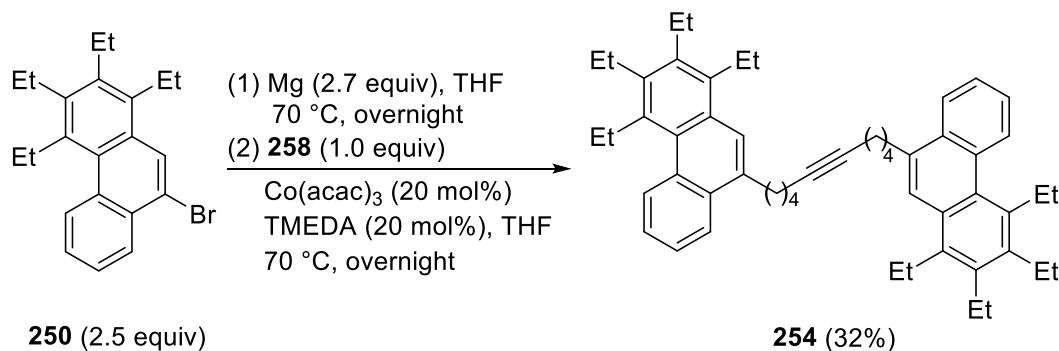
(a) Preparation of 1,10-dichloro-5-decyne by palladium-catalyzed Sonogashira cross-coupling:



(b) Preparation of 1,10-diiodo-5-decyne by chloride/iodide exchange:



(c) Synthesis of the TEP-tethered dialkyl alkyne by cobalt-catalyzed Kumada coupling:



**Scheme 2-15.** Synthesis of the TEP-tethered dialkyl alkyne by Kumada coupling.

Solubility tests reveal that **254** is easily soluble in moderately polar solvents such as dichloromethane, comparing with the less soluble phenanthrene-tethered alkyne **240**. The archipelago compounds prepared from **254** exhibit very different characteristics than phenanthrene-tethered analogs, which will be discussed in the next chapter.

## Conclusion

Phenanthrene-tethered dialkyl alkyne **240** and DBT-tethered dialkyl alkyne **248** were successfully prepared by a direct *n*-BuLi deprotonation/S<sub>N</sub>2 substitution pathway. The TEP-tethered dialkyl alkyne **254** cannot be prepared in this way, but could be obtained instead using Fu's modified Sonogashira cross-coupling<sup>148</sup> with subsequent Kumada cross-coupling.<sup>82</sup> These island-tethered alkynes have been used to synthesize archipelago model compounds, as discussed in the following chapters.

## Experimental Section

### General Information

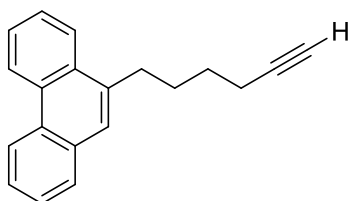
Unless otherwise noted, all compounds were used as received without any further purification. THF was distilled from sodium/benzophenone ketyl and stored under nitrogen. MeCN, DMSO, DMF, DMI, MeOH, Et<sub>2</sub>O, and acetone were dried over 3 Å molecular sieves for at least 48 h before use. Copper(I) iodide was purified according to the literature procedure.<sup>136</sup> 9-(4-Chlorobutyl)phenanthrene (**236**)<sup>82</sup> and (6-iodo-1-hexynyl)trimethylsilane (**246**)<sup>177</sup> were prepared according to literature procedures. <sup>1</sup>H and <sup>13</sup>C{<sup>1</sup>H} NMR spectra were recorded on Agilent/Varian instruments (400 or 500 or 700 MHz for <sup>1</sup>H NMR spectroscopy and 101 or 126 or 176 MHz for <sup>13</sup>C{<sup>1</sup>H} NMR spectroscopy) at 27 °C. Chemical shifts of <sup>1</sup>H and <sup>13</sup>C{<sup>1</sup>H} NMR spectra were reported in parts per million (ppm). Chemical shifts were referenced to residual solvent peaks (CDCl<sub>3</sub>: δ<sub>H</sub> = 7.26 ppm, δ<sub>C</sub> = 77.06 ppm; CD<sub>2</sub>Cl<sub>2</sub>: δ<sub>H</sub> = 5.32 ppm, δ<sub>C</sub> = 53.8 ppm). All coupling constants (*J* values) were reported in Hertz (Hz). Manipulations under nitrogen atmosphere were performed in a Braun dry box with an oxygen level below 1 ppm. Column chromatography was performed on silica gel 60 M (230–400 mesh). Thin-layer chromatography

(TLC) was performed on pre-coated, aluminum-backed silica gel plates. Visualization of the developed TLC plate was performed by a UV lamp (254 nm). High-resolution mass spectrometric (HRMS) results were obtained from Mass Spectrometry Facility using the following instruments: Kratos Analytical MS-50G (EI), Bruker 9.4T Apex-Qe FTICR (MALDI). Elemental analyses (C, H, S) were obtained from Analytical and Instrumentation Laboratory using a Thermo Flash 2000 Elemental Analyzer.

### General procedure B – Finkelstein chloride/iodide exchange reactions<sup>171</sup>

Alkyl chloride (**236**, **243**, **257**) and sodium iodide were placed in a dry 50 mL Schlenk flask with a magnetic stir bar and dry acetone was added. The reaction mixture was heated at 60 °C for 3 d. The reaction flask was cooled to room temperature and the solvent was removed under reduced pressure. The residual was dissolved in CH<sub>2</sub>Cl<sub>2</sub> and filtered. The solvent was removed under reduced pressure to afford corresponding alkyl iodide. The product can be used without further purification.

#### 1-(9-Phenanthrene)-5-hexyne (**238**)



In a dry box, 9-(4-chlorobutyl)phenanthrene **236** (1.500 g, 5.581 mmol) and lithium acetylide ethylene diamine complex (0.628 g, 6.82 mmol) were placed in a dry 50 mL Schlenk flask with a magnetic stir bar. The reaction flask was sealed and then moved out of the dry box. Dry DMSO (12 mL) was added through Schlenk line techniques. The reaction mixture was stirred at room

temperature overnight and was quenched with water (50 mL). The aqueous solution was extracted with CH<sub>2</sub>Cl<sub>2</sub> (3 times, 30 mL each) and dried over Na<sub>2</sub>SO<sub>4</sub>. The mixture was filtered, and the solvent was removed under reduced pressure. The residual was purified by silica column chromatography (hexane followed by hexane/CH<sub>2</sub>Cl<sub>2</sub> 9:1) to afford compound **238** as a white solid (1.228 g, 85%). *R*<sub>f</sub> = 0.42 (SiO<sub>2</sub>; hexane/CH<sub>2</sub>Cl<sub>2</sub> 4:1). (*Note*: the purified product may contain 10-20% starting chloride that cannot be fully removed by chromatography, but it can be used without further purification.)

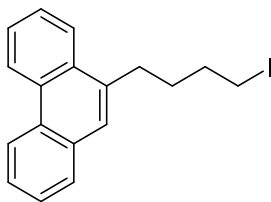
**<sup>1</sup>H NMR** (CDCl<sub>3</sub>, 700 MHz): δ 8.74 (dd, *J* = 8.1 Hz, 1.4 Hz, 1H), 8.66 (d, *J* = 8.1 Hz, 1H), 8.11 (dd, *J* = 7.7 Hz, 1.7 Hz, 1H), 7.83 (dd, *J* = 7.6 Hz, 1.5 Hz, 1H), 7.68–7.56 (m, 5H), 3.15 (t, *J* = 7.7 Hz, 2H), 2.29 (td, *J* = 7.1 Hz, 2.7 Hz, 2H), 1.99–1.93 (m, 3H), 1.73 (quint, *J* = 7.4 Hz, 2H).

**<sup>13</sup>C{<sup>1</sup>H} NMR** (CDCl<sub>3</sub>, 176 MHz): δ 136.4, 131.9, 131.3, 130.8, 129.7, 128.1, 126.6, 126.5, 126.2, 126.1, 126.0, 124.5, 123.3, 122.5, 84.4, 68.5, 32.9, 29.2, 28.5, 18.4.

**EI HRMS** *m/z* calcd for C<sub>20</sub>H<sub>18</sub> (M<sup>+</sup>) 258.1409, found 258.1408.

**EA** anal. calcd for C<sub>20</sub>H<sub>18</sub>: C, 92.98; H, 7.02. Found: C, 92.73; H, 6.96. Repeat found: C, 92.86; H, 7.02.

### 9-(4-Iodobutyl)phenanthrene (**239**)



The general procedure B was used with 9-(4-chlorobutyl)phenanthrene **236** (2.000 g, 7.441 mmol), NaI (1.862 g, 12.42 mmol), and acetone (20 mL). The crude product was dissolved in

CH<sub>2</sub>Cl<sub>2</sub> (50 mL), filtered and solvent was removed under reduced pressure to afford compound **239** as a yellow solid (2.396 g, 89%). *R*<sub>f</sub> = 0.46 (SiO<sub>2</sub>; hexane/CH<sub>2</sub>Cl<sub>2</sub> 4:1).

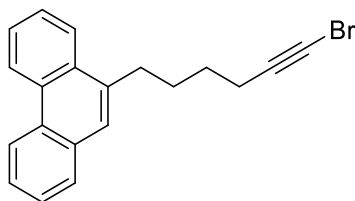
<sup>1</sup>H NMR (CDCl<sub>3</sub>, 700 MHz): δ 8.78–8.75 (m, 1H), 8.68 (d, *J* = 8.1 Hz, 1H), 8.13–8.10 (m, 1H), 7.86 (dd, *J* = 7.6 Hz, 1.5 Hz, 1H), 7.71–7.60 (m, 4H), 7.59 (s, 1H), 3.26 (t, *J* = 6.9 Hz, 2H), 3.13 (t, *J* = 7.6 Hz, 2H), 2.03–1.92 (m, 4H).

<sup>13</sup>C{<sup>1</sup>H} NMR (CDCl<sub>3</sub>, 176 MHz): δ 135.9, 131.8, 131.1, 130.7, 129.7, 128.1, 126.6, 126.6, 126.2, 126.1, 126.0, 124.3, 123.3, 122.4, 33.4, 32.3, 30.9, 6.7.

EI HRMS *m/z* calcd for C<sub>18</sub>H<sub>17</sub>I (M<sup>+</sup>) 360.0375, found 360.0374.

EA anal. calcd for C<sub>18</sub>H<sub>17</sub>I: C, 60.02; H, 4.76. Found: C, 60.38; H, 4.80. Repeat found: C, 60.24; H, 4.76.

#### 6-(9-Phenanthrene)-1-bromohex-1-yne (241)



1-(9-Phenanthrene)-5-hexyne **238** (300 mg, 1.16 mmol), *N*-bromosuccinimide (227 mg, 1.28 mmol), and AgNO<sub>3</sub> (20 mg, 10 mol%) were placed in a dry 25 mL round bottom flask with a magnetic stir bar. Dry acetone (5 mL) was added to the flask. The reaction mixture was stirred at room temperature overnight and quenched by ice cold water (20 mL). The aqueous solution was extracted with CH<sub>2</sub>Cl<sub>2</sub> (3 times, 20 mL each) and dried over Na<sub>2</sub>SO<sub>4</sub>. The mixture was filtered, and the solvent was removed under reduced pressure. The residual was purified by silica column

chromatography (hexane/CH<sub>2</sub>Cl<sub>2</sub> 9:1) to afford compound **241** as a white solid (251 mg, 64%).  
 $R_f$  = 0.33 (SiO<sub>2</sub>; hexane/CH<sub>2</sub>Cl<sub>2</sub> 9:1).

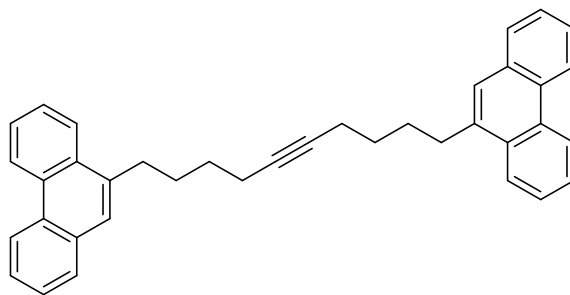
**<sup>1</sup>H NMR** (CDCl<sub>3</sub>, 700 MHz):  $\delta$  8.77–8.74 (m, 1H), 8.67 (d,  $J$  = 8.1 Hz, 1H), 8.13–8.11 (m, 1H), 7.85 (d,  $J$  = 7.6 Hz, 1H), 7.70–7.65 (m, 2H), 7.64–7.58 (m, 3H), 3.14 (t,  $J$  = 7.8 Hz, 2H), 2.32 (t,  $J$  = 7.1 Hz, 2H), 1.98–1.92 (m, 2H), 1.72 (quint,  $J$  = 7.4 Hz, 2H).

**<sup>13</sup>C{<sup>1</sup>H} NMR** (CDCl<sub>3</sub>, 176 MHz):  $\delta$  136.3, 131.9, 131.2, 130.8, 129.7, 128.1, 126.6, 126.6, 126.2, 126.1, 126.0, 124.4, 123.3, 122.5, 80.2, 38.1, 32.8, 29.2, 28.3, 19.6.

**EI HRMS**  $m/z$  calcd for C<sub>20</sub>H<sub>17</sub><sup>79</sup>Br (M<sup>+</sup>) 336.0514, found 336.0512.

**EA** anal. calcd for C<sub>20</sub>H<sub>17</sub>Br: C, 71.23; H, 5.08. Found: C, 70.96; H, 5.09. Repeat found: C, 71.14; H, 5.12.

### 1,10-Di(9-phenanthrene)-5-decyne (**240**)



1-(9-Phenanthrene)-5-hexyne **238** (1.000 g, 3.871 mmol) was placed in a dry 50 mL Schlenk flask with a magnetic stir bar. The reaction flask was charged with nitrogen and dry DMI (8 mL) was added through Schlenk line techniques. The flask was cooled to 0 °C and 1.6 M *n*-BuLi solution (2.9 mL, 4.6 mmol) was added dropwise. After complete addition, the reaction mixture was stirred at 0 °C for 30 min and the 9-(4-iodobutyl)phenanthrene (**239**) solution (8 mL DMI solution containing 1.673 g of **239**, 4.645 mmol) was added dropwise. The reaction mixture was



heated to 70 °C overnight and quenched by ice cold water (50 mL). The aqueous solution was extracted with CH<sub>2</sub>Cl<sub>2</sub> (3 times, 30 mL each) and dried over Na<sub>2</sub>SO<sub>4</sub>. The mixture was filtered, and the solvent was removed under reduced pressure. The remaining DMI was evaporated in an opening container at 90 °C for 8 h. The residual was purified by silica column chromatography (hexane/CH<sub>2</sub>Cl<sub>2</sub> 4:1 followed by hexane/CH<sub>2</sub>Cl<sub>2</sub> 2:1) to afford compound **240** as a white solid (0.721 g, 38%). *R*<sub>f</sub> = 0.25 (SiO<sub>2</sub>; hexane/CH<sub>2</sub>Cl<sub>2</sub> 4:1).

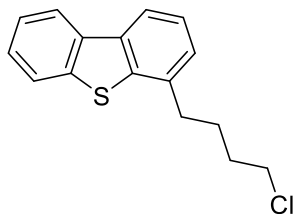
**<sup>1</sup>H NMR** (CD<sub>2</sub>Cl<sub>2</sub>, 700 MHz): δ 8.72 (dd, *J* = 8.1 Hz, 1.2 Hz, 2H), 8.64 (d, *J* = 8.1 Hz, 2H), 8.11 (dd, *J* = 7.8 Hz, 1.3 Hz, 2H), 7.78 (d, *J* = 8.2 Hz, 2H), 7.65–7.53 (m, 10H), 3.11 (t, *J* = 7.8 Hz, 4H), 2.27–2.23 (second order m, 4H), 1.94–1.89 (m, 4H), 1.66 (quint, *J* = 7.3 Hz, 4H).

**<sup>13</sup>C{<sup>1</sup>H} NMR** (CD<sub>2</sub>Cl<sub>2</sub>, 176 MHz): δ 137.1, 132.3, 131.6, 131.0, 129.9, 128.3, 127.0, 126.9, 126.5, 126.3, 126.3, 124.9, 123.5, 122.7, 80.5, 33.2, 29.6, 29.5, 18.9.

**EI HRMS** *m/z* calcd for C<sub>38</sub>H<sub>34</sub> (M<sup>+</sup>) 490.2661, found 490.2653.

**EA** anal. calcd for C<sub>38</sub>H<sub>34</sub>: C, 93.02; H, 6.98. Found: C, 91.44; H, 6.92. Repeat found: C, 91.01; H, 6.99.

#### 4-(4-Chlorobutyl)dibenzothiophene (**243**)



In a dry box, dibenzothiophene (2.000 g, 10.85 mmol) was placed in a dry 100 mL Schlenk flask with a magnetic stir bar. Dry THF (20 mL) was added. The flask was sealed and then moved out of dry box. Under Schlenk line techniques, TMEDA (1.63 mL, 1.26 g, 10.9 mmol) was added to

the flask. The flask was cooled to  $-78\text{ }^{\circ}\text{C}$  and 2.5 M *n*-BuLi solution (4.4 mL, 11 mmol) was added dropwise to the flask. The reaction mixture was warmed to room temperature and was stirred overnight. The flask was cooled to  $0\text{ }^{\circ}\text{C}$  and 1-chloro-4-iodobutane (1.34 mL, 2.39 g, 10.9 mmol) was added dropwise to the flask. The flask was warmed to room temperature and stirred for an additional 30 min. The reaction mixture was diluted with water (50 mL). The aqueous solution was extracted with  $\text{CH}_2\text{Cl}_2$  (3 times, 30 mL each) and dried over  $\text{Na}_2\text{SO}_4$ . The mixture was filtered, and the solvent was removed under reduced pressure. The residual was purified by silica column chromatography using hexane followed by hexane/ $\text{CH}_2\text{Cl}_2$  9:1 as eluent to afford compound **243** as a colorless oil (1.956 g, 66%).  $R_f = 0.41$  ( $\text{SiO}_2$ , hexane/ $\text{CH}_2\text{Cl}_2$  9:1).

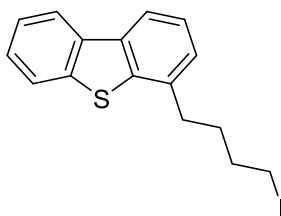
**$^1\text{H}$  NMR** ( $\text{CDCl}_3$ , 700 MHz):  $\delta$  8.18–8.15 (m, 1H), 8.04 (d,  $J = 7.9$  Hz, 1H), 7.92–7.89 (m, 1H), 7.50–7.47 (m, 2H), 7.45 (t,  $J = 7.6$  Hz, 1H), 7.30 (d,  $J = 7.4$  Hz, 1H), 3.60 (t,  $J = 6.7$  Hz, 2H), 2.95 (t,  $J = 7.7$  Hz, 2H), 2.03–1.98 (m, 2H), 1.91 (quint,  $J = 7.1$  Hz, 2H).

**$^{13}\text{C}\{^1\text{H}\}$  NMR** ( $\text{CDCl}_3$ , 176 MHz):  $\delta$  139.1, 139.0, 136.1, 136.0, 135.7, 126.7, 126.1, 124.8, 124.4, 122.8, 121.7, 119.5, 44.8, 34.3, 32.2, 26.4.

**EI HRMS**  $m/z$  calcd for  $\text{C}_{16}\text{H}_{15}^{35}\text{ClS}$  ( $\text{M}^+$ ) 274.0583, found 274.0583.

**EA** anal. calcd for  $\text{C}_{16}\text{H}_{15}\text{ClS}$ : C, 69.93; H, 5.50; S, 11.67. Found: C, 69.87; H, 5.62; S, 11.51. Repeat found: C, 69.98; H, 5.20; S, 11.84.

#### 4-(4-Iodobutyl)dibenzothiophene (**247**)



The general procedure B was used with 4-(4-chlorobutyl)dibenzothiophene **243** (2.100 g, 7.642 mmol), NaI (1.912 g, 12.76 mmol), and acetone (15 mL). The crude product was dissolved in CH<sub>2</sub>Cl<sub>2</sub> (50 mL), filtered and solvent was removed under reduced pressure to afford compound **247** as a yellow oil (2.596 g, 93%). *R*<sub>f</sub> = 0.49 (SiO<sub>2</sub>; hexane/CH<sub>2</sub>Cl<sub>2</sub> 4:1).

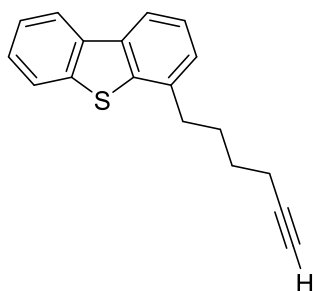
**<sup>1</sup>H NMR** (CDCl<sub>3</sub>, 700 MHz): δ 8.17–8.14 (m, 1H), 8.03 (d, *J* = 7.9 Hz, 1H), 7.90–7.87 (m, 1H), 7.49–7.45 (m, 2H), 7.44 (t, *J* = 7.6 Hz, 1H), 7.29 (d, *J* = 7.2 Hz, 1H), 3.26–3.22 (second order m, 2H), 2.95–2.91 (second order m, 2H), 1.97–1.93 (second order m, 4H).

**<sup>13</sup>C{<sup>1</sup>H} NMR** (CDCl<sub>3</sub>, 176 MHz): δ 139.1, 139.0, 136.1, 136.0, 135.8, 126.7, 126.1, 124.9, 124.4, 122.8, 121.7, 119.5, 34.0, 33.1, 30.0, 6.5.

**EI HRMS** *m/z* calcd for C<sub>16</sub>H<sub>15</sub>IS (M<sup>+</sup>) 365.9939, found 365.9937.

**EA** anal. calcd for C<sub>16</sub>H<sub>15</sub>IS: C, 52.47; H, 4.13; S, 8.75. Found: C, 52.91; H, 4.10; S, 8.38. Repeat found: C, 52.96; H, 4.09; S, 8.66.

### 1-(4-Dibenzothiophene)-5-hexyne (245)



In a dry box, dibenzothiophene (1.500 g, 8.141 mmol) was placed in a dry 100 mL Schlenk flask with a magnetic stir bar. Dry THF (20 mL) was added. The flask was sealed and then moved out of dry box. Under Schlenk line techniques, TMEDA (1.22 mL, 0.946 g, 8.14 mmol) was added to the flask. The flask was cooled to –78 °C and 1.6 M *n*-BuLi solution (5.1 mL, 8.2 mmol) was

added dropwise to the flask. The reaction mixture was warmed to room temperature and was stirred overnight. The flask was cooled to 0 °C and (6-iodo-1-hexynyl)trimethylsilane **246** (2.737 g, 9.767 mmol) was added dropwise to the flask. The reaction was warmed to room temperature and stirred for an additional 30 min. The reaction mixture was diluted with water (50 mL). The aqueous solution was extracted with CH<sub>2</sub>Cl<sub>2</sub> (3 times, 30 mL each) and dried over Na<sub>2</sub>SO<sub>4</sub>. The mixture was filtered, and the solvent was removed under reduced pressure. The residual was transferred to a 100 mL round bottom flask with a magnetic stir bar, THF/MeOH 1:1 solution (30 mL) and K<sub>2</sub>CO<sub>3</sub> (2.250g, 16.28 mmol) were added. The reaction mixture was stirred overnight. The solvent was removed under reduced pressure and the residual was purified by silica column chromatography using hexane followed by hexane/CH<sub>2</sub>Cl<sub>2</sub> 9:1 as eluent to afford compound **245** as a colorless oil (1.066 g, 50%). *R*<sub>f</sub> = 0.44 (SiO<sub>2</sub>; hexane/CH<sub>2</sub>Cl<sub>2</sub> 4:1).

**<sup>1</sup>H NMR** (CDCl<sub>3</sub>, 700 MHz): δ 8.17–8.14 (m, 1H), 8.03 (d, *J* = 7.8 Hz, 1H), 7.90–7.87 (m, 1H), 7.48–7.45 (m, 2H), 7.44 (t, *J* = 7.6 Hz, 1H), 7.30 (d, *J* = 7.3 Hz, 1H), 2.94 (t, *J* = 7.8 Hz, 2H), 2.28 (td, *J* = 7.2 Hz, 2.7 Hz, 2H), 2.00–1.94 (m, 3H), 1.68 (quint, *J* = 7.4 Hz, 2H).

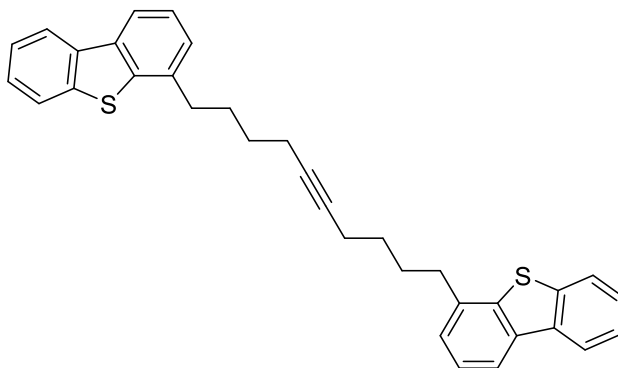
**<sup>13</sup>C{<sup>1</sup>H} NMR** (CDCl<sub>3</sub>, 176 MHz): δ 139.2, 139.1, 136.4, 136.2, 135.7, 126.6, 126.1, 124.8, 124.4, 122.8, 121.7, 119.4, 84.3, 68.5, 34.6, 28.2, 28.2, 18.3.

**EI HRMS** *m/z* calcd for C<sub>18</sub>H<sub>16</sub>S (M<sup>+</sup>) 264.0973, found 264.0972.

**EA** anal. calcd for C<sub>18</sub>H<sub>16</sub>S: C, 81.77; H, 6.10; S, 12.13. Found: C, 81.63; H, 5.95; S, 12.00.

Repeat found: C, 81.51; H, 6.02; S, 12.38.

### 1,10-Di(4-dibenzothiophene)-5-decyne (**248**)



1-(4-Dibenzothiophene)-5-hexyne **245** (1.000 g, 3.782 mmol) was placed in a dry 50 mL Schlenk flask with a magnetic stir bar. The reaction flask was charged with nitrogen and dry DMI (8 mL) was added through Schlenk line techniques. The flask was cooled to 0 °C and 1.6 M *n*-BuLi solution (4.7 mL, 7.5 mmol) was added dropwise. After complete addition, the reaction mixture was stirred at 0 °C for 30 min and the 4-(4-iodobutyl)dibenzothiophene (**247**) solution (6 mL DMI solution containing 1.731 g of **247**, 4.726 mmol) was added dropwise. The reaction mixture was heated to 70 °C overnight and quenched by ice cold water (50 mL). The aqueous solution was extracted with CH<sub>2</sub>Cl<sub>2</sub> (3 times, 30 mL each) and dried over Na<sub>2</sub>SO<sub>4</sub>. The mixture was filtered, and the solvent was removed under reduced pressure. The remaining DMI was evaporated in an opening container at 90 °C for 8 h. The residual was purified by silica column chromatography (hexane/CH<sub>2</sub>Cl<sub>2</sub> 85:15 followed by hexane/CH<sub>2</sub>Cl<sub>2</sub> 7:3) to afford compound **248** as a white solid (1.022 g, 54%). *R*<sub>f</sub> = 0.43 (SiO<sub>2</sub>; hexane/CH<sub>2</sub>Cl<sub>2</sub> 2:1).

**<sup>1</sup>H NMR** (CD<sub>2</sub>Cl<sub>2</sub>, 700 MHz): δ 8.16–8.14 (m, 2H), 8.01 (d, *J* = 7.8 Hz, 2H), 7.88–7.85 (m, 2H), 7.47–7.44 (m, 4H), 7.40 (t, *J* = 7.6 Hz, 2H), 7.28 (d, *J* = 7.2 Hz, 2H), 2.89 (t, *J* = 7.7 Hz, 4H), 2.23–2.20 (second order m, 4H), 1.93–1.88 (m, 4H), 1.59 (quint, *J* = 7.3 Hz, 4H).

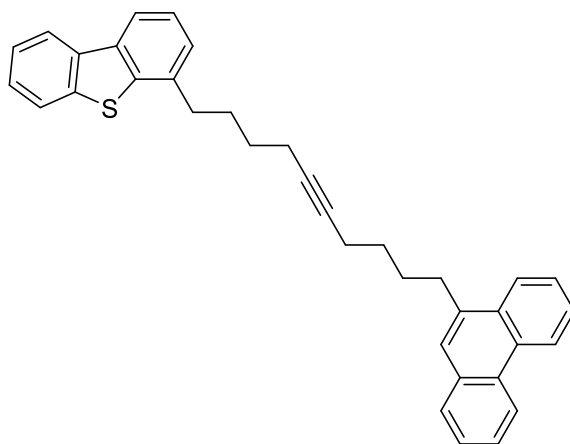
$^{13}\text{C}\{^1\text{H}\}$  NMR ( $\text{CD}_2\text{Cl}_2$ , 176 MHz):  $\delta$  139.5, 139.5, 137.2, 136.5, 135.9, 127.0, 126.5, 125.2, 124.7, 123.1, 122.1, 119.6, 80.4, 34.9, 29.2, 28.6, 18.9.

EI HRMS  $m/z$  calcd for  $\text{C}_{34}\text{H}_{30}\text{S}_2$  ( $\text{M}^+$ ) 502.1789, found 502.1786.

EA anal. calcd for  $\text{C}_{34}\text{H}_{30}\text{S}_2$ : C, 81.23; H, 6.02; S, 12.75. Found: C, 81.03; H, 6.03; S, 12.72.

Repeat found: C, 80.98; H, 6.10; S, 12.69.

### 1-(4-Dibenzothiophene)-10-(9-phenanthrene)-5-decyne (249)



1-(4-Dibenzothiophene)-5-hexyne **245** (100 mg, 0.378 mmol) was placed in a dry 10 mL Schlenk flask with a magnetic stir bar. The reaction flask was charged with nitrogen and dry DMI (2 mL) was added through Schlenk line techniques. The flask was cooled to 0 °C and 2.5 M *n*-BuLi solution (0.15 mL, 0.38 mmol) was added dropwise. After complete addition, the reaction mixture was stirred at 0 °C for 30 min and the 9-(4-iodobutyl)phenanthrene (**239**) solution (2 mL DMI solution containing 164 mg of **239**, 0.455 mmol) was added dropwise. The reaction mixture was heated to 50 °C overnight and quenched by ice cold water (20 mL). The aqueous solution was extracted with  $\text{CH}_2\text{Cl}_2$  (3 times, 20 mL each) and dried over  $\text{Na}_2\text{SO}_4$ . The mixture was filtered, and the solvent was removed under reduced pressure. The remaining DMI

was evaporated in an opening container at 90 °C for 4 h. The residual was purified by silica column chromatography (hexane/CH<sub>2</sub>Cl<sub>2</sub> 9:1 followed by hexane/CH<sub>2</sub>Cl<sub>2</sub> 4:1) to afford compound **249** as a white solid (135 mg, 72%). *R*<sub>f</sub> = 0.31 (SiO<sub>2</sub>; hexane/CH<sub>2</sub>Cl<sub>2</sub> 4:1).

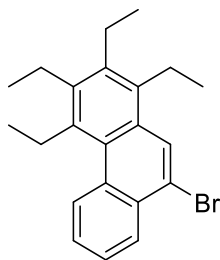
**<sup>1</sup>H NMR** (CD<sub>2</sub>Cl<sub>2</sub>, 700 MHz): δ 8.74 (d, *J* = 7.9 Hz, 1H), 8.65 (d, *J* = 8.2 Hz, 1H), 8.16–8.12 (m, 2H), 8.00 (d, *J* = 7.8 Hz, 1H), 7.88–7.86 (m, 1H), 7.82 (d, *J* = 7.7 Hz, 1H), 7.68–7.56 (m, 5H), 7.47–7.45 (m, 2H), 7.38 (t, *J* = 7.6 Hz, 1H), 7.28 (d, *J* = 7.2 Hz, 1H), 3.12 (t, *J* = 7.8 Hz, 2H), 2.90 (t, *J* = 7.8 Hz, 2H), 2.29–2.23 (m, 4H), 1.96–1.90 (m, 4H), 1.68 (quint, *J* = 7.3 Hz, 2H), 1.60 (quint, *J* = 7.3 Hz, 2H).

**<sup>13</sup>C{<sup>1</sup>H} NMR** (CD<sub>2</sub>Cl<sub>2</sub>, 176 MHz): δ 139.5, 139.4, 137.2, 137.1, 136.5, 135.9, 132.3, 131.7, 131.0, 129.9, 128.4, 127.0, 127.0, 126.9, 126.5, 126.5, 126.3, 126.3, 125.2, 124.9, 124.7, 123.5, 123.1, 122.7, 122.1, 119.6, 80.5, 80.4, 34.9, 33.2, 29.6, 29.5, 29.3, 28.6, 18.9, 18.9.

**MALDI HRMS** (DCTB) *m/z* calcd for C<sub>36</sub>H<sub>32</sub>S (M<sup>+</sup>) 496.2225, found 496.2218.

**EA** anal. calcd for C<sub>36</sub>H<sub>32</sub>S: C, 87.05; H, 6.49; S, 6.45. Found: C, 86.24; H, 6.48; S, 6.20. Repeat found: C, 86.30; H, 6.52; S, 6.27.

### 9-Bromo-1,2,3,4-tetraethylphenanthrene (**250**)



1,2,3,4-Tetraethylphenanthrene **133** (1.100 g, 3.787 mmol) and NaBr (0.779 g, 7.57 mmol) were placed in a dry 50 mL round bottom flask with a magnetic stir bar. Dry MeCN (10 mL) was

added to the flask. NFSI (2.388 g, 7.573 mmol) was added to the solution in 15 min. The reaction mixture was stirred at room temperature for 16 h. The solvent was removed under reduced pressure and the residual was purified by silica column chromatography using hexane as eluent to afford compound **250** as a colorless oil (1.048 g, 75%).  $R_f = 0.43$  (SiO<sub>2</sub>; hexane).

**<sup>1</sup>H NMR** (CDCl<sub>3</sub>, 700 MHz):  $\delta$  8.65 (d,  $J = 8.4$  Hz, 1H), 8.41 (dd,  $J = 8.2$  Hz, 1.4 Hz, 1H), 8.33 (s, 1H), 7.67 (td,  $J = 7.5$  Hz, 1.0 Hz, 1H), 7.62 (td,  $J = 7.7$  Hz, 1.5 Hz, 1H), 3.46–3.28 (br, 2H), 3.15 (q,  $J = 7.6$  Hz, 2H), 3.06 (q,  $J = 7.5$  Hz, 2H), 2.98 (q,  $J = 7.6$  Hz, 2H), 1.67 (t,  $J = 7.4$  Hz, 3H), 1.42 (t,  $J = 7.6$  Hz, 3H), 1.34–1.28 (m, 6H).

**<sup>13</sup>C{<sup>1</sup>H} NMR** (CDCl<sub>3</sub>, 176 MHz):  $\delta$  141.6, 139.5, 136.7, 135.4, 132.3, 130.8, 130.4, 129.7, 127.9, 127.4, 127.3, 126.3, 125.3, 120.7, 25.4, 22.8, 22.7, 22.2, 16.4, 16.0, 16.0, 15.9.

**EI HRMS**  $m/z$  calcd for C<sub>22</sub>H<sub>25</sub><sup>79</sup>Br (M<sup>+</sup>) 368.1140, found 368.1141.

**EA** anal. calcd for C<sub>22</sub>H<sub>25</sub>Br: C, 71.54; H, 6.82. Found: C, 71.14; H, 6.74. Repeat found: C, 70.93; H, 6.65.

### 1,10-Dichloro-5-decyne (257)



In a dry box, allylpalladium(II) chloride dimer (94 mg, 3 mol%), 1,3-di-*tert*-butylimidazolium tetrafluoroborate (138 mg, 6 mol%), CuI (147 mg, 9 mol%), and Cs<sub>2</sub>CO<sub>3</sub> (2.934 g, 9.005 mmol) were placed in a dry 50 mL Schlenk flask with a magnetic stir bar. The reaction flask was sealed and then moved out of the dry box. Dry DMF (5 mL), dry Et<sub>2</sub>O (10 mL), 6-chloro-1-hexyne (1040  $\mu$ L, 1.000 g, 8.581 mmol), and 1-bromo-4-chlorobutane (1283  $\mu$ L, 1.909 g, 11.13 mmol)



were sequentially added to the flask through Schlenk line techniques. The reaction mixture was stirred at 45 °C for 16 h. The solvent was removed under reduced pressure and the residual was purified by silica column chromatography (pentane/CH<sub>2</sub>Cl<sub>2</sub> 85:15) to afford compound **257** as a colorless liquid (1.036 g, 58%). *R*<sub>f</sub> = 0.32 (SiO<sub>2</sub>; hexane/CH<sub>2</sub>Cl<sub>2</sub> 4:1; KMnO<sub>4</sub> stain). The <sup>1</sup>H and <sup>13</sup>C{<sup>1</sup>H} NMR spectra of the product are in accordance with the literature.<sup>178</sup>

**<sup>1</sup>H NMR** (CDCl<sub>3</sub>, 700 MHz): δ 3.56 (t, *J* = 6.7 Hz, 4H), 2.21–2.18 (second order m, 4H), 1.88 (quint, *J* = 7.1 Hz, 4H), 1.65–1.60 (m, 4H).

**<sup>13</sup>C{<sup>1</sup>H} NMR** (CDCl<sub>3</sub>, 176 MHz): δ 80.0, 44.6, 31.6, 26.2, 18.1.

#### 1,10-Diiodo-5-decyne (258)



The general procedure B was used with 1,10-dichloro-5-decyne **257** (1.036 g, 5.001 mmol), NaI (2.504 g, 16.71 mmol), and acetone (10 mL). The crude product was dissolved in CH<sub>2</sub>Cl<sub>2</sub> (50 mL), filtered and solvent was removed under reduced pressure to afford compound **258** as a yellow liquid (1.649 g, 85%). *R*<sub>f</sub> = 0.44 (SiO<sub>2</sub>; hexane/CH<sub>2</sub>Cl<sub>2</sub> 4:1; KMnO<sub>4</sub> stain).

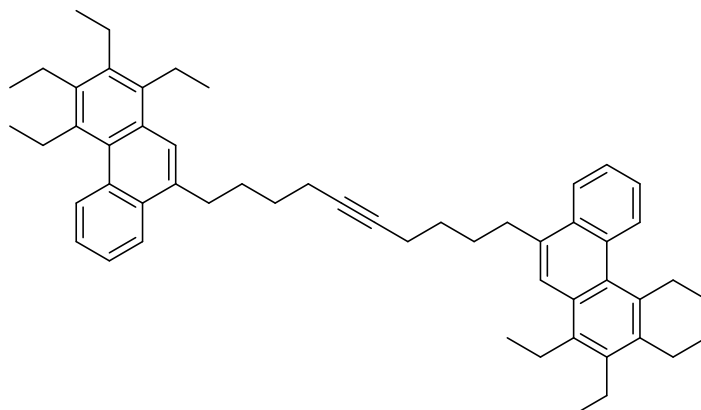
**<sup>1</sup>H NMR** (CDCl<sub>3</sub>, 700 MHz): δ 3.20 (t, *J* = 7.0 Hz, 4H), 2.20–2.16 (second order m, 4H), 1.92 (quint, *J* = 7.2 Hz, 4H), 1.61–1.56 (m, 4H).

**<sup>13</sup>C{<sup>1</sup>H} NMR** (CDCl<sub>3</sub>, 176 MHz): δ 80.0, 32.5, 29.7, 17.7, 6.4.

**EI HRMS** *m/z* calcd for C<sub>10</sub>H<sub>16</sub>I ([M – I]<sup>+</sup>) 263.0297, found 263.0295.

**EA** anal. calcd for C<sub>10</sub>H<sub>16</sub>I<sub>2</sub>: C, 30.79; H, 4.13. Found: C, 31.43; H, 4.19. Repeat found: C, 31.14; H, 4.14.

### 1,10-Di[9-(1,2,3,4-tetraethylphenanthrene)]-5-decyne (254)



In a dry box, magnesium turnings (71 mg, 2.9 mmol) were placed in a dry 50 mL Schlenk flask with a magnetic stir bar. Dry THF (5 mL) was added. The flask was sealed and then moved out of the dry box. 1,2-Dibromoethane (33 mg, 15  $\mu$ L, 0.17 mmol) was added to the flask through Schlenk line techniques. The mixture was heated and stirred at 70  $^{\circ}$ C for 2 h. After cooling to room temperature, 9-bromo-1,2,3,4-tetraethylphenanthrene (**250**) solution (5 mL THF solution containing 1.000 g of **250**, 2.707 mmol) was added dropwise by a syringe through Schlenk line techniques. The mixture was heated at 70  $^{\circ}$ C overnight and then cooled to room temperature. In a dry box, Co(acac)<sub>3</sub> (77 mg, 20 mol%) was placed in a separate 100 mL Schlenk flask and dry THF (8 mL) was added. The flask was sealed and then moved out of the dry box. TMEDA (33  $\mu$ L, 26 mg, 20 mol%) and 1,10-diiodo-5-decyne **258** (422 mg, 1.08 mmol) were added to the flask through Schlenk line techniques. The solution was cooled to 0  $^{\circ}$ C and the 9-(1,2,3,4-tetraethylphenanthrene) magnesium bromide solution was added dropwise by a syringe through Schlenk line techniques. After 4 h at 0  $^{\circ}$ C, the reaction mixture was heated to 70  $^{\circ}$ C for 2 d and then cooled to 0  $^{\circ}$ C. The mixture was quenched by 0.2 M HCl (50 mL). The aqueous solution was extracted with CH<sub>2</sub>Cl<sub>2</sub> (3 times, 30 mL each) and dried over Na<sub>2</sub>SO<sub>4</sub>. The mixture was filtered, and the solvent was removed under reduced pressure. The residual was purified by silica

column chromatography (hexane/CH<sub>2</sub>Cl<sub>2</sub> 9:1 followed by hexane/CH<sub>2</sub>Cl<sub>2</sub> 4:1) to afford compound **254** as a yellow grease (248 mg, 32%). *R*<sub>f</sub> = 0.49 (SiO<sub>2</sub>; hexane/CH<sub>2</sub>Cl<sub>2</sub> 2:1).

**<sup>1</sup>H NMR** (CDCl<sub>3</sub>, 700 MHz): δ 8.64 (d, *J* = 8.3 Hz, 2H), 8.07 (d, *J* = 7.9 Hz, 2H), 7.76 (s, 2H), 7.55 (t, *J* = 7.2 Hz, 2H), 7.51 (t, *J* = 7.2 Hz, 2H) 3.41–3.26 (br, 4H), 3.17–3.10 (m, 8H), 3.05–2.99 (second order m, 4H), 2.96–2.91 (second order m, 4H), 2.29–2.25 (m, 4H), 1.96–1.90 (m, 4H), 1.70–1.63 (m, 10H), 1.37 (t, *J* = 7.5 Hz, 6H), 1.30–1.24 (m, 12H).

**<sup>13</sup>C{<sup>1</sup>H} NMR** (CDCl<sub>3</sub>, 176 MHz): δ 140.2, 138.7, 136.3, 135.4, 134.7, 131.8, 131.7, 129.8, 129.5, 128.3, 125.3, 123.9, 123.7, 122.8, 80.3, 33.2, 29.4, 29.1, 25.4, 22.7, 22.6, 22.2, 18.7, 16.5, 16.2, 16.0, 15.9.

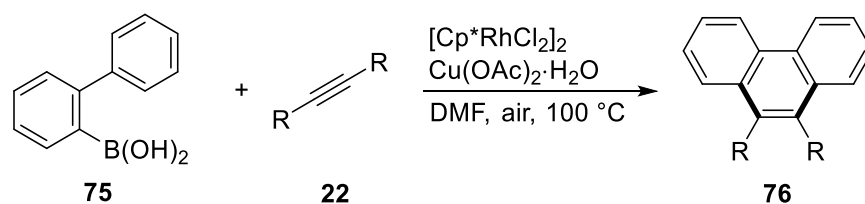
**MALDI HRMS** (DCTB) *m/z* calcd for C<sub>54</sub>H<sub>66</sub> (M<sup>+</sup>) 714.5165, found 714.5158.

**EA** anal. calcd for C<sub>54</sub>H<sub>66</sub>: C, 90.70; H, 9.30. Found: C, 88.50; H, 9.19. Repeat found: C, 88.49; H, 8.97.

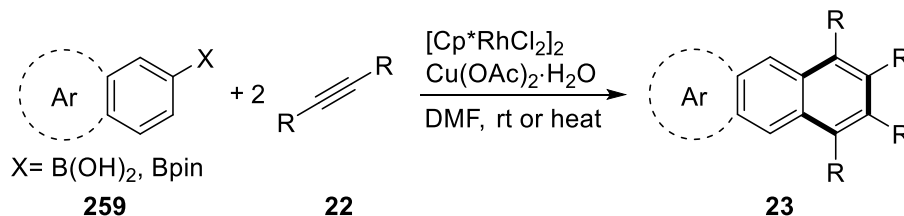
### 3. Archipelago Compounds Synthesis by Rhodium-catalyzed Aryl-boron/Alkyne Annulation

In chapter 2, the successful synthesis of island-tethered dialkyl alkynes was reported. In this chapter, these alkynes are used as starting materials to prepare archipelago model compounds, adopting Miura's cross-coupling methods (Scheme 3-1).<sup>101,110</sup>

(a) [4+2] annulations of 2-biphenylboronic acid with alkynes:



(b) [2+2+2] annulations of aryl-boron derivatives with alkynes:



**Scheme 3-1.** Miura's [4+2] and [2+2+2] annulations of aryl-boron derivatives with alkynes.<sup>101,110</sup>

All of the archipelago products were characterized by  $^1\text{H}$  and  $^{13}\text{C}\{^1\text{H}\}$  NMR spectroscopy, high-resolution mass spectrometry and elemental analysis to confirm their molecular structures. Elemental analyses were again sometimes complicated by persistent impurities or incomplete combustion.<sup>22,179</sup> In addition to standard characterization methods,  $^1\text{H}$ -Diffusion Ordered NMR Spectroscopy ( $^1\text{H}$ -DOSY) was applied to one synthetic model compound, providing solution

molecular and supramolecular structural information (e.g., hydrodynamic radius and aggregation state).

### 3.1 The synthesis of archipelago compounds by rhodium-catalyzed [4+2] annulations of 2-biphenylboronic acid with alkynes

Using alkynes **240**, **248**, **249** and **254**, [4+2] annulations with the 2-biphenylboronic acid **75** were conducted.<sup>110</sup> To improve conversions, the use of 1.5 equivalents of 2-biphenylboronic acid was necessary. The reactions afforded three-island archipelago compounds **260-263** in 64-92% yields. Results are summarized in Table 3-1.

**Table 3-1.** Synthesis of archipelago compounds by [4+2] annulations of 2-biphenylboronic acid with alkynes.

$\text{75 (1.5 equiv)} + \text{Ar}^1-(\text{CH}_2)_4\text{C}\equiv\text{C}-(\text{CH}_2)_4\text{Ar}^2 \xrightarrow[\text{DMF, air, 100 } ^\circ\text{C, 3 h}]{[\text{Cp}^*\text{RhCl}_2]_2 \text{ (5 mol\%)} \text{ Cu(OAc)}_2\cdot\text{H}_2\text{O (10 mol\%)}}$

**240, 248, 249, 254**

| Entry          | Alkyne     | Ar <sup>1</sup> | Ar <sup>2</sup> | Product    | Yield (%) |
|----------------|------------|-----------------|-----------------|------------|-----------|
| 1              | <b>240</b> | 9-phenanthrene  | 9-phenanthrene  | <b>260</b> | 64        |
| 2              | <b>248</b> | 4-DBT           | 4-DBT           | <b>261</b> | 92        |
| 3              | <b>249</b> | 9-phenanthrene  | 4-DBT           | <b>262</b> | 81        |
| 4 <sup>a</sup> | <b>254</b> | 9-TEP           | 9-TEP           | <b>263</b> | 83        |

<sup>a</sup> The reaction time was 6 h.

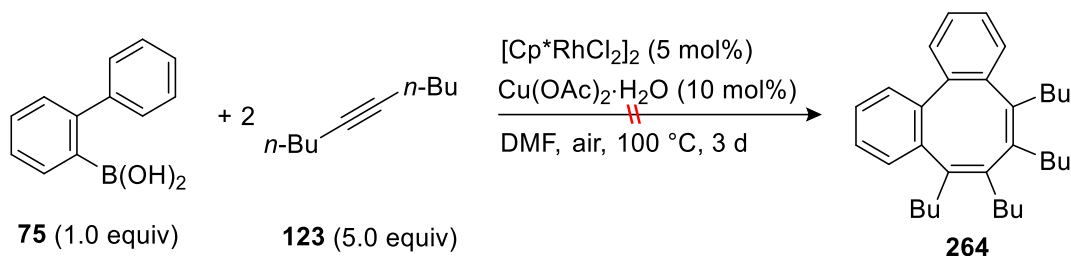
For the products with phenanthrene or DBT islands (**260**, **261**, and **262**), their solubilities in dichloromethane decreased in the order: **261** > **262** > **260**. This means that the greater number of phenanthrene islands the product contains, the lower the solubility in dichloromethane. The all-phenanthrene archipelago **260** is almost insoluble in dichloromethane as well as other common solvents. No chromatography is required to isolate this adduct. However, the poor solubility of **260** limits its use in aggregation and other studies.

The TEP-tethered compound **263** shows different characteristics compared with phenanthrene-tethered analogue **260**. Compound **263** is a light-yellow grease, while compound **260** is a white solid. Compound **263** also shows a much higher solubility than **260** in common solvents.  $^1\text{H}$  and  $^{13}\text{C}\{^1\text{H}\}$  NMR and high-resolution mass spectrometric (MALDI) data confirm the successful synthesis of **263**. However, the elemental analysis shows a large deviation from theoretical values. The measured carbon and hydrogen content is ~20% less than theoretical, but the measured H/C ratio is consistent with the structure (Table 3-2). The extra ethyl groups on phenanthrene create more adjacent quaternary carbons, which are likely to render incomplete combustion of the sample.<sup>179</sup>

**Table 3-2.** Theoretical and experimental elemental composition of compound **263**.

| Composition | Theoretical values | Measured results 1 | Measured results 2 |
|-------------|--------------------|--------------------|--------------------|
| C (%)       | 91.40              | 72.79              | 73.27              |
| H (%)       | 8.60               | 6.83               | 6.93               |
| H/C ratio   | 1.12               | 1.12               | 1.13               |

Using a large excess of 5-decyne, I confirmed that this annulation does not give any of the [2+2+2] product **264** (Equation 3-1).

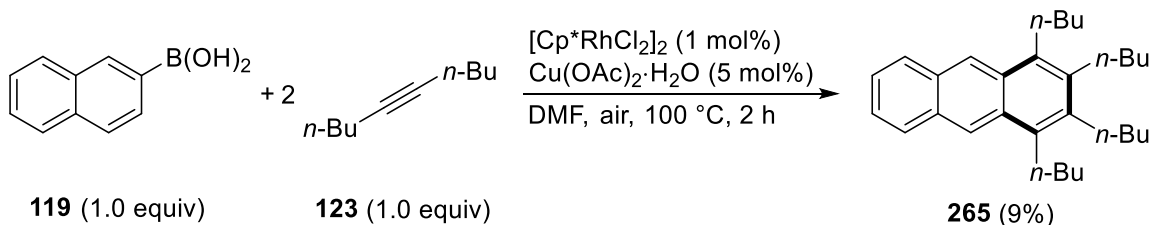


**Equation 3-1.** Attempt to synthesize [2+2+2] annulation product by 2-biphenylboronic acid and 5-decyne.

### 3.2 Optimization of the rhodium-catalyzed [2+2+2] annulations of aryl-boron derivatives with alkynes

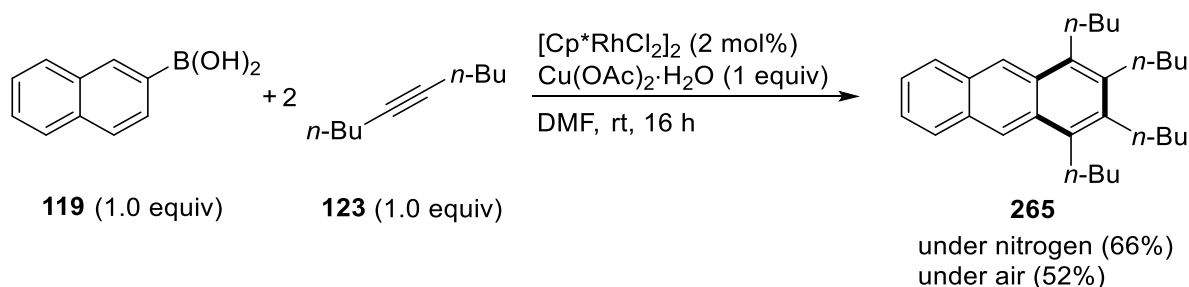
#### 3.2.1 Annulations of 2-naphthylboronic acid with dialkyl alkynes

In Miura's [2+2+2] annulation study, diphenylacetylene was the most frequently used alkyne.<sup>101</sup> For my research objectives, reactions with dialkyl alkynes were required. In an initial attempt, the reaction of 2-naphthylboronic acid **119** with 5-decyne was explored to test the feasibility of the [2+2+2] annulation, using the rhodium catalyst (1 mol%), Cu(OAc)<sub>2</sub>·H<sub>2</sub>O (5 mol%) and air as the terminal oxidant. However, the yield was disappointingly low (Equation 3-2).



**Equation 3-2.** Aerobic annulation of 2-naphthylboronic acid with 5-decyne.

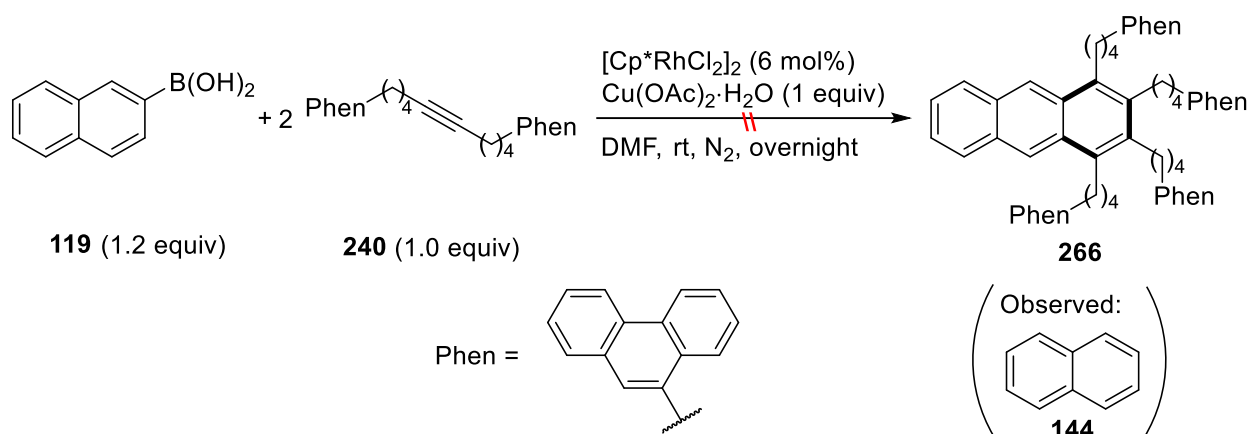
Consequently, optimization experiments were carried out to find the best reaction conditions. In all cases,  $[\text{Cp}^*\text{RhCl}_2]_2$  (2 mol%) was used to improve the yield. The yields were determined by  $^1\text{H}$  NMR spectroscopy using mesitylene as the internal standard. I found that anaerobic conditions are better for the annulation of 5-decyne with 2-naphthylboronic acid **119**, for which  $\text{Cu}(\text{OAc})_2 \cdot \text{H}_2\text{O}$  (1 equiv) is necessary (Equation 3-3). Anthracene **265** is obtained in 66% yield when the reaction is conducted under nitrogen. When the reaction is run under air, the yield drops to 52%.



**Equation 3-3.** Anaerobic annulation of 2-naphthylboronic acid with 5-decyne.

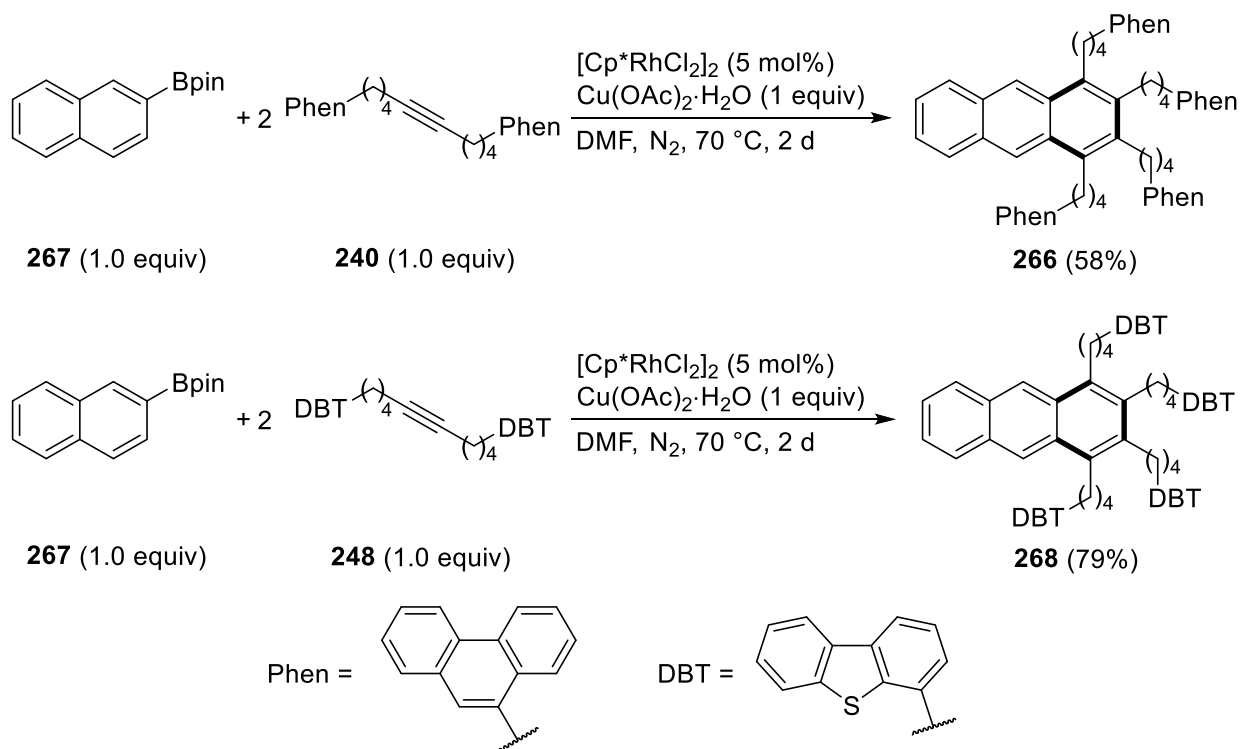
Anaerobic reaction conditions were subsequently applied to the annulation of 2-naphthylboronic acid **119** with phenanthrene-tethered alkyne **240**. However, none of the expected archipelago product **266** was obtained, even using excess boronic acid (1.2 equiv) and higher catalyst loading (6 mol%) (Equation 3-4). Only naphthalene was observed; the annulation of alkyne **240** is much slower than the reaction with 5-decyne, making protodeboronation the main reaction pathway.





**Equation 3-4.** Annulation of 2-naphthylboronic acid with phenanthrene-tethered alkyne.

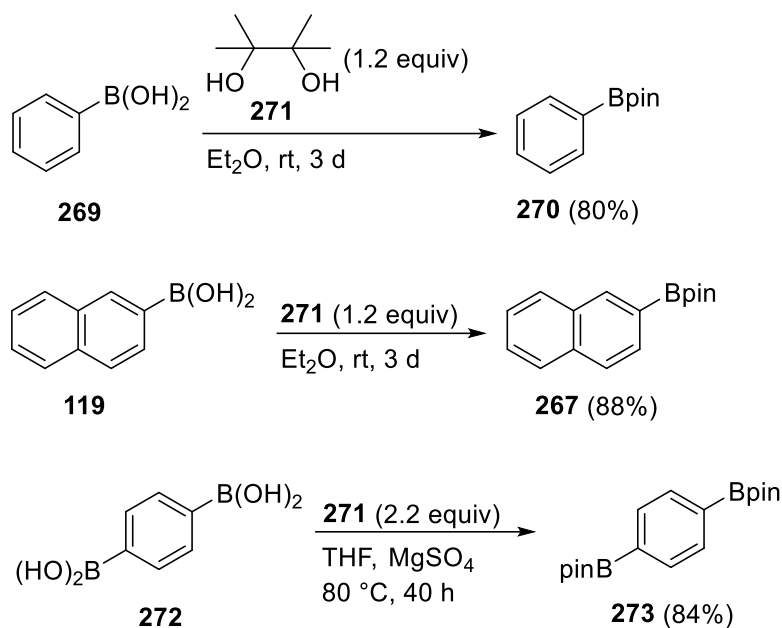
To avoid the protodeboronation, the corresponding pinacol boronate (Bpin) **267** was used to replace boronic acid **119** for optimization experiments. In addition, the reaction was conducted at 70 °C to accelerate the annulation rate. Test reactions using alkynes **240** and **248** demonstrated that these conditions produce the archipelago products in reasonable yields (Scheme 3-2). By using chromatography, the archipelago compounds **266** and **268** were isolated in 58% and 79% yields, respectively.



**Scheme 3-2.** Annulations of pinacol boronate with island-tethered alkynes.

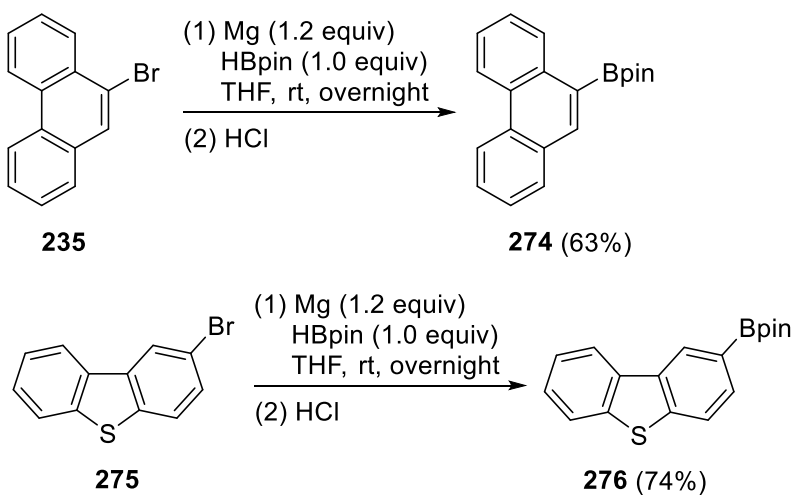
### 3.2.2 Preparation of aryl pinacol boronates

From the above optimization, aryl pinacol boronates (aryl-Bpins) are necessary for annulations of island-tethered dialkyl alkynes. Fortunately, aryl pinacol boronates can be easily prepared using boronic acids and pinacol, at least if the corresponding boronic acids are commercially available. (Scheme 3-3).<sup>180,181</sup>



**Scheme 3-3.** Preparation of aryl pinacol boronates from aryl boronic acids.

Aryl pinacol boronates can also be prepared from aryl Grignard reagents using a methodology reported by Singaram and co-workers (Scheme 3-4).<sup>182</sup>

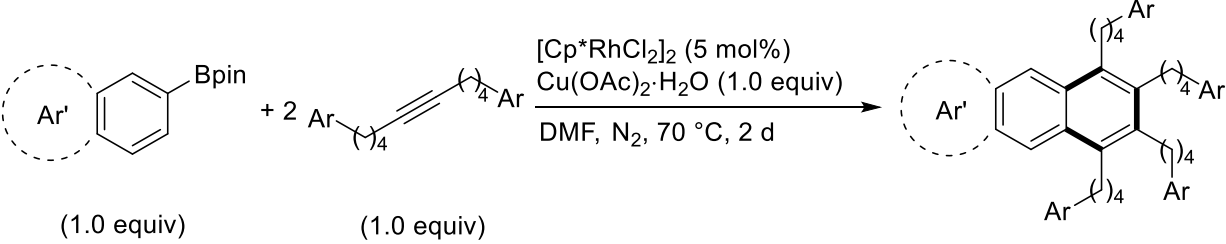
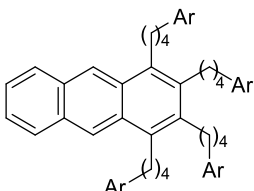
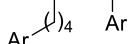
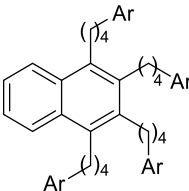


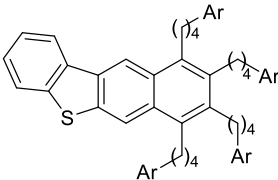
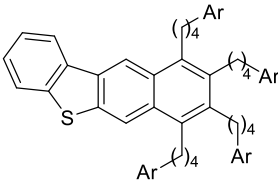
**Scheme 3-4.** Preparation of aryl pinacol boronates from aryl Grignard reagents.

### 3.3 The synthesis of archipelago compounds by rhodium-catalyzed [2+2+2] annulations of aryl pinacol boronates with alkynes

By applying optimized conditions in section 3.2.1, a number of five-island archipelago compounds were synthesized (Table 3-3). To improve the conversion of the alkyne, excess aryl pinacol boronates were used in these annulation reactions.

**Table 3-3.** Synthesis of five-island archipelago compounds by rhodium-catalyzed [2+2+2] annulations of aryl pinacol boronates with alkynes.

|  |            |                |            |   |            |    |
|---|------------|----------------|------------|---|------------|----|
| Entry   | Alkyne     | Ar             | Aryl-Bpin  | Product   | Yield (%)  |    |
| 1   | <b>240</b> | 9-phenanthrene | <b>267</b> |   | <b>266</b> | 58 |
| 2   | <b>248</b> | 4-DBT          | <b>267</b> |  | <b>268</b> | 79 |
| 3   | <b>240</b> | 9-phenanthrene | <b>270</b> |   | <b>277</b> | 80 |
| 4   | <b>248</b> | 4-DBT          | <b>270</b> |   | <b>278</b> | 90 |
| 5   | <b>254</b> | 9-TEP          | <b>270</b> |   | <b>279</b> | 70 |

| Entry | Alkyne     | Ar             | Aryl-Bpin  | Product  | Yield (%)  |    |
|-------|------------|----------------|------------|--|------------|----|
| 6     | <b>240</b> | 9-phenanthrene | <b>276</b> |  | <b>280</b> | 52 |
| 7     | <b>248</b> | 4-DBT          | <b>276</b> |  | <b>281</b> | 65 |

Three different pinacol boronates (**267**, **270**, and **276**) were coupled with three symmetrical island-bearing alkynes (**240**, **248**, and **254**) to provide archipelago adducts in good to excellent yields. Products were isolated by column chromatography using flash silica gel and hexane/CH<sub>2</sub>Cl<sub>2</sub> as eluent.

For a given pinacol boronate, the DBT-tethered alkyne always provides higher yields than the phenanthrene-tethered alkyne. A similar trend was observed for [4+2] annulations (Table 3-1, **261** > **260**). These results can also be attributed to the solubility discrepancy between the two alkynes.

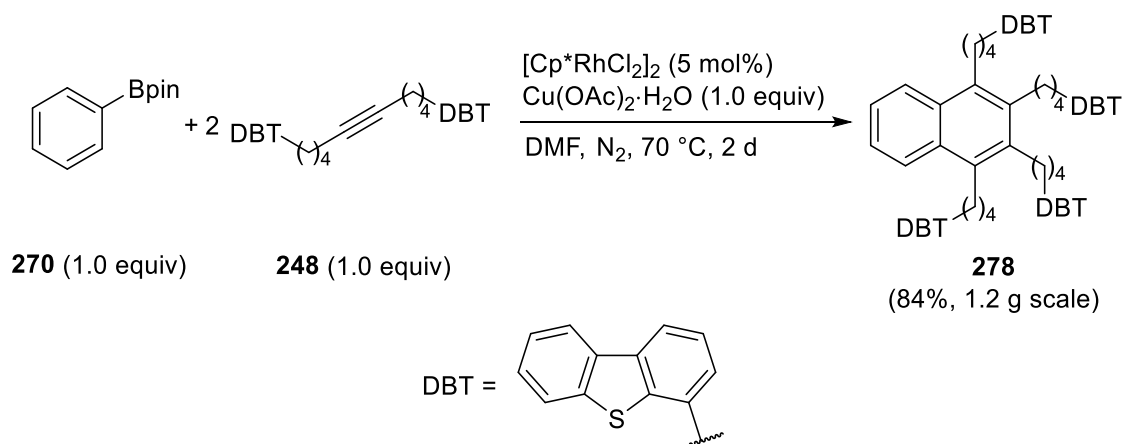
The solubilities of the products are similar to those of the alkynes. Compounds from phenanthrene-tethered alkyne (**266**, **277**, and **280**) exhibit poor solubilities in moderately polar solvents such as dichloromethane, compared with other archipelago compounds. The poor solubility of these phenanthrene adducts also makes them more difficult to separate by chromatography. Attempts to perform non-chromatographic purification by washing the crude product with hexane and extracting with toluene failed to completely remove the alkyne from these adducts.

Archipelago model compound **279** was prepared from TEP-tethered alkyne in 70% yield. The relatively low yield is presumably due to the large number of ethyl groups, which may exert

stronger steric hinderance in both alkyne coordination and insertion steps. Compound **279** is, as expected, also more soluble in dichloromethane than adducts bearing phenanthrene islands. The elemental analysis of **279** again shows a low content of carbon and hydrogen but the measured H/C ratio is consistent with the structure (anal. calcd for C<sub>114</sub>H<sub>136</sub>: C, 90.90; H, 9.10. Found: C, 83.10; H, 8.49. Repeat found: C, 83.54; H, 8.50.), a phenomenon similar to that of adduct **263** in section 3.1.

Compared with other archipelago model compounds, the structures of **280** and **281** are more complex because they do not possess an axis of symmetry. Thus, more signals are observed in the <sup>1</sup>H and <sup>13</sup>C{<sup>1</sup>H} NMR spectra for these two compounds.

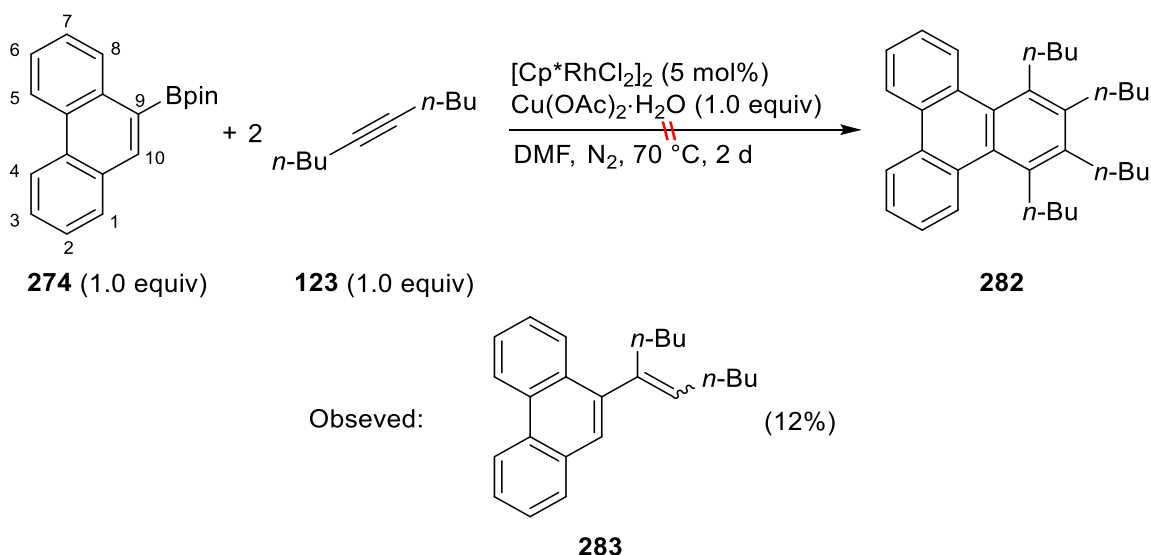
A one-gram scale synthesis was subsequently conducted, which delivered adduct **278** in 84% yield (Equation 3-5). This indicates that rhodium-catalyzed [2+2+2] annulations can be replicated on a larger scale with similar yields.



**Equation 3-5.** A large-scale synthesis of a DBT-tethered archipelago model compound.

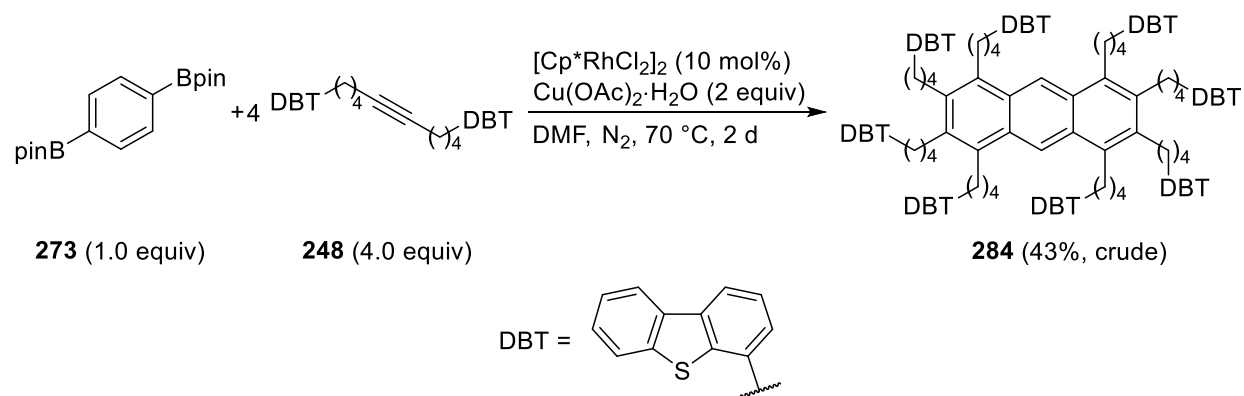
The annulation of 4,4,5,5-tetramethyl-2-(phenanthren-9-yl)-1,3,2-dioxaborolane (**274**) was also attempted using 5-decyne under the same reaction conditions. However, the desired triphenylene

product **282** was not obtained (Equation 3-6). A characteristic multiplet at 5.34 ppm was observed in  $^1\text{H}$  NMR spectrum for the reaction mixture after aqueous work-up. Therefore, the 1:1 coupling alkene product **283** was tentatively assigned and the yield of **283** was calculated to be 12% by  $^1\text{H}$  NMR spectroscopy with an internal standard. The rationalization of unsuccessful annulation of 1-naphthylboronic acid may also be relevant (Scheme 1-16) – steric congestion caused by H10 and H8 on the phenanthrene ring inhibits the alkyne insertion.



**Equation 3-6.** Attempt to synthesize a triphenylene-type adduct by annulation of 4,4,5,5-tetramethyl-2-(phenanthren-9-yl)-1,3,2-dioxaborolane with 5-decyne.

The annulation of 1,4-benzenediboronic acid bis(pinacol) ester **273** with alkyne was explored to test the possibility of making nine-island archipelago compounds (Equation 3-7). Tentatively-assigned adduct **284** was obtained in 43% yield after chromatography. High-resolution mass spectrometry (MALDI) confirmed the successful synthesis of **284**, but chromatography could not remove unknown impurities. As a result, the  $^1\text{H}$  NMR spectrum of pure **284** could not be obtained.



**Equation 3-7.** Attempt to synthesize a nine-island archipelago compound by annulation of 1,4-benzenediboronic acid bis(pinacol) ester with alkyne.

### 3.4 Chemical compositions of synthetic archipelago model compounds

To determine if my synthetic model compounds represent asphaltenes well, chemical composition is an important indicator. The chemical compositions (theoretical value) of all of the archipelago compounds synthesized in this chapter are summarized in Table 3-4.

**Table 3-4.** Compositional analyses of synthetic archipelago compounds.

| Compound   | Structure | Formula  | MW<br>(g/mol) | H/C<br>ratio | Elemental<br>compositions        |
|------------|-----------|--|---------------|--------------|----------------------------------|
| <b>260</b> |           | C <sub>50</sub> H <sub>42</sub>                | 642.89        | 0.84         | C, 93.41;<br>H, 6.59             |
| <b>261</b> |           | C <sub>46</sub> H <sub>38</sub> S <sub>2</sub> | 654.93        | 0.83         | C, 84.36;<br>H, 5.85;<br>S, 9.79 |



| Compound | Structure | Formula  | MW<br>(g/mol) | H/C<br>ratio | Elemental<br>compositions         |
|----------|-----------|--|---------------|--------------|-----------------------------------|
| 262      |           | C <sub>48</sub> H <sub>40</sub> S              | 648.91        | 0.83         | C, 88.85;<br>H, 6.21;<br>S, 4.94  |
| 263      |           | C <sub>66</sub> H <sub>74</sub>                | 867.32        | 1.12         | C, 91.40;<br>H, 8.60              |
| 266      |           | C <sub>86</sub> H <sub>74</sub>                | 1107.54       | 0.86         | C, 93.27;<br>H, 6.73              |
| 268      |           | C <sub>78</sub> H <sub>66</sub> S <sub>4</sub> | 1131.63       | 0.85         | C, 82.79;<br>H, 5.88;<br>S, 11.33 |
| 277      |           | C <sub>82</sub> H <sub>72</sub>                | 1057.48       | 0.88         | C, 93.14;<br>H, 6.86              |

| Compound | Structure | Formula  | MW<br>(g/mol) | H/C<br>ratio | Elemental<br>compositions         |
|----------|-----------|--|---------------|--------------|-----------------------------------|
| 278      |           | C <sub>74</sub> H <sub>64</sub> S <sub>4</sub> | 1081.57       | 0.86         | C, 82.18;<br>H, 5.96;<br>S, 11.86 |
| 279      |           | C <sub>114</sub> H <sub>136</sub>              | 1506.34       | 1.19         | C, 90.90;<br>H, 9.10              |
| 280      |           | C <sub>88</sub> H <sub>74</sub> S              | 1163.62       | 0.84         | C, 90.83;<br>H, 6.41;<br>S, 2.76  |
| 281      |           | C <sub>80</sub> H <sub>66</sub> S <sub>5</sub> | 1187.71       | 0.83         | C, 80.90;<br>H, 5.60;<br>S, 13.50 |

The chemical compositions of these model compounds are analyzed in following aspects:

1. *Molecular weights.*

Six model compounds from phenanthrene- or DBT-tethered alkyne via [2+2+2] annulation (**266**, **268**, **277**, **278**, **280**, and **281**) have similar molecular weights, ranging from 1050 g/mol to 1200 g/mol. Compound **279** has the highest molecular weight (1506 g/mol) because of the added ethyl groups. The molecular weights of all [2+2+2] annulation adducts are higher than most of the previous archipelago compounds shown in section 1.3, but still in the range of asphaltenes (200-1500 Da).<sup>27</sup>

The molecular weights of four adducts from [4+2] annulations (**260**, **261**, **262**, and **263**) are lower, ranging from 640 g/mol to 870 g/mol, due to the three-island structures.

2. *H/C ratio.*

For all model compounds other than the two from TEP-tethered alkyne (**263** and **279**), the H/C ratios range from 0.8 to 0.9, which are lower than the H/C ratios of most authentic asphaltene samples (1.0 to 1.2).<sup>6</sup> Considering that authentic asphaltenes always contain maltene materials,<sup>6</sup> it is acceptable that the synthetic archipelago products have a slightly lower H/C ratio.

Because of added ethyl groups, compounds **263** and **279** show a much higher H/C ratio (1.12 and 1.19) than other model compounds. Their H/C ratios are in the range of typical asphaltenes. Since many properties of bitumen are related to the H/C ratio (e.g., gravity, viscosity, distillation curve, pour point and coke formation),<sup>6</sup> these two model compounds are expected to show different characteristics from their phenanthrene analogues in asphaltene studies (e.g., mass spectrometric and pyrolysis studies). (*Note: The pour point is the temperature at which a liquid loses its flow properties and becomes a semi solid.*)<sup>183</sup>

### 3. *Elemental analysis.*

Sulfur-containing archipelago compounds have rarely been reported in previous syntheses even though sulfur is the most abundant heteroatom in asphaltenes.<sup>6</sup> As for my model compounds, six out of eleven compounds incorporate sulfur in the structure. For the four adducts from DBT-tethered alkyne (**261**, **268**, **278**, and **281**), the sulfur contents range from 9.79% to 13.50%, which are higher than most of the asphaltene samples (6% to 9%).<sup>6</sup> So, these compounds can be used to represent asphaltenes with extremely high sulfur content. Compounds **262** and **280** also contain sulfur but with lower content (4.94% and 2.76%, respectively).

Based on the analysis above, it can be seen that these archipelago compounds have very different compositions in terms of molecular weight, H/C ratio and sulfur content – they are therefore reasonable asphaltene models. Meanwhile, they create a new library of model compounds, especially those with the higher molecular weight and sulfur content.

### 3.5 Studies on the second order <sup>1</sup>H NMR signals of archipelago model compounds

All five-island archipelago compounds in section 3.3 exhibit characteristic peaks at ~3 ppm in the <sup>1</sup>H NMR spectra, some of them second order. As an example, detailed <sup>1</sup>H NMR spectrum of compound **277** is shown in Figure 3-1 (700 MHz, CDCl<sub>3</sub>).

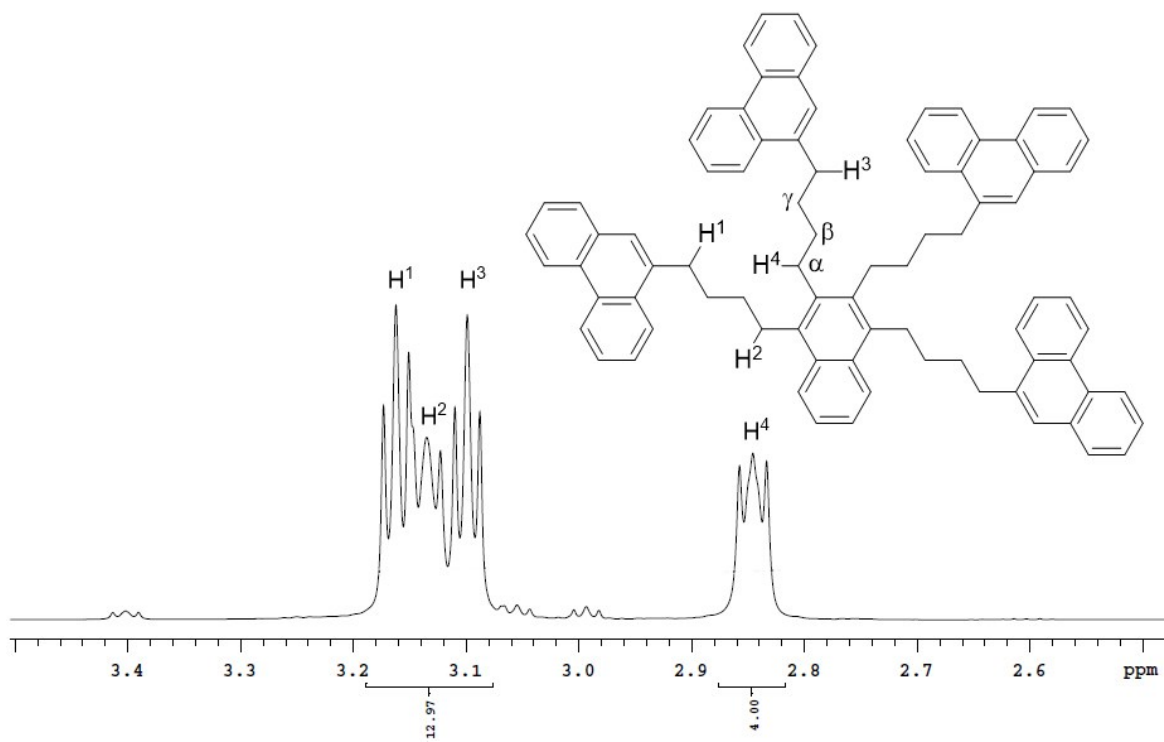
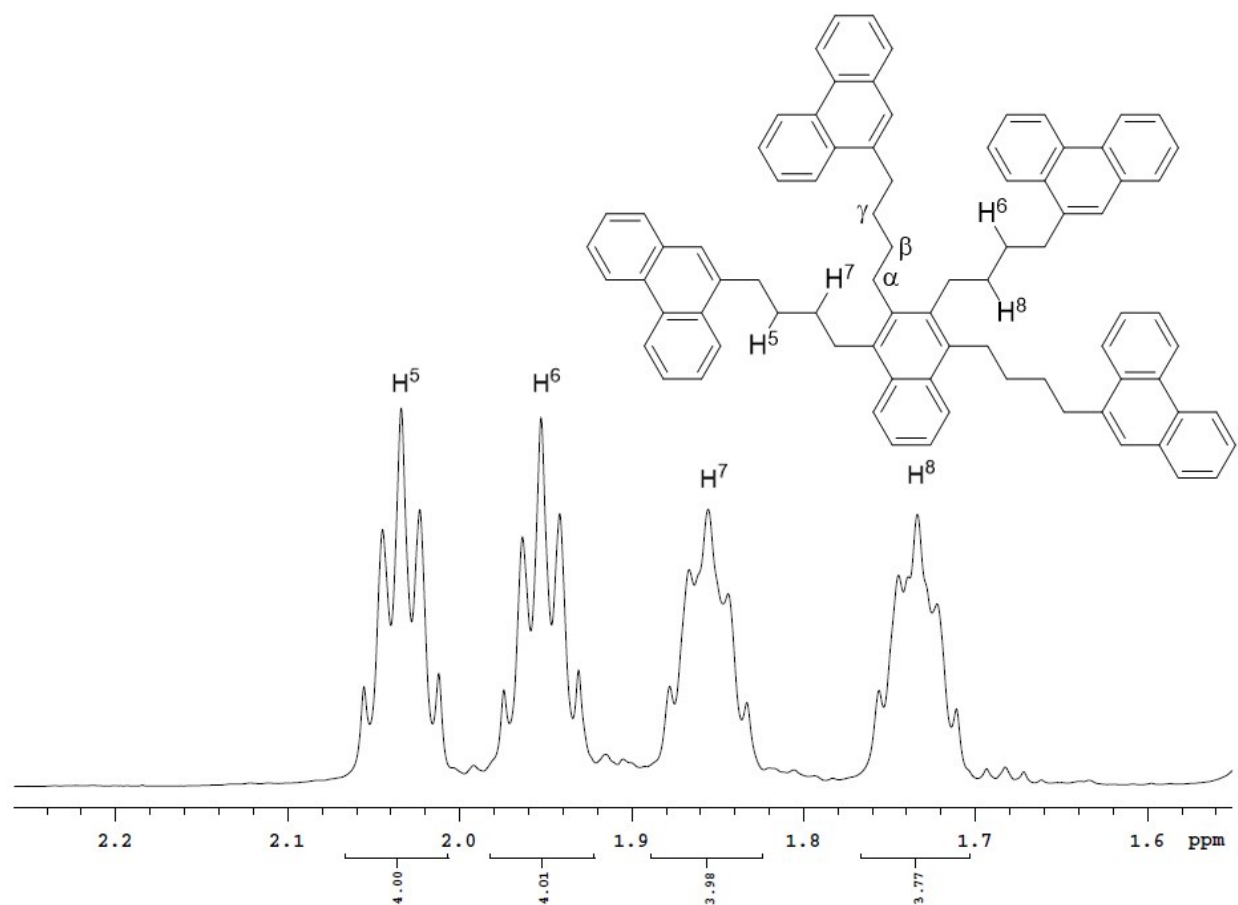


**Figure 3-1.** Detailed  $^1\text{H}$  NMR spectrum of archipelago compound **277** and signal assignments in 3.5–2.5 ppm region.

By looking at the chemical shifts, these peaks arise from the benzylic methylene groups. The 3.18–3.08 ppm signals are three overlapping resonances. To be more convenient, these four signals are labelled as “H<sup>1</sup>” to “H<sup>4</sup>” from downfield to upfield. Combined with  $^1\text{H}$ - $^1\text{H}$  COSY, HSQC and HMBC spectra (see Appendix 2), these signals are assigned as shown in Figure 3-1. The signals from the benzylic methylene groups adjacent to phenanthrene are relatively sharp and first order (H<sup>1</sup> and H<sup>3</sup>), while signals from methylene groups bonding to central naphthalene island are clearly second order, showing an irregular shape (H<sup>2</sup> and H<sup>4</sup>). This second order signal is characteristic for all tetra-methylene-substituted [2+2+2] annulation products. It is also an important feature to determine the success of annulation.

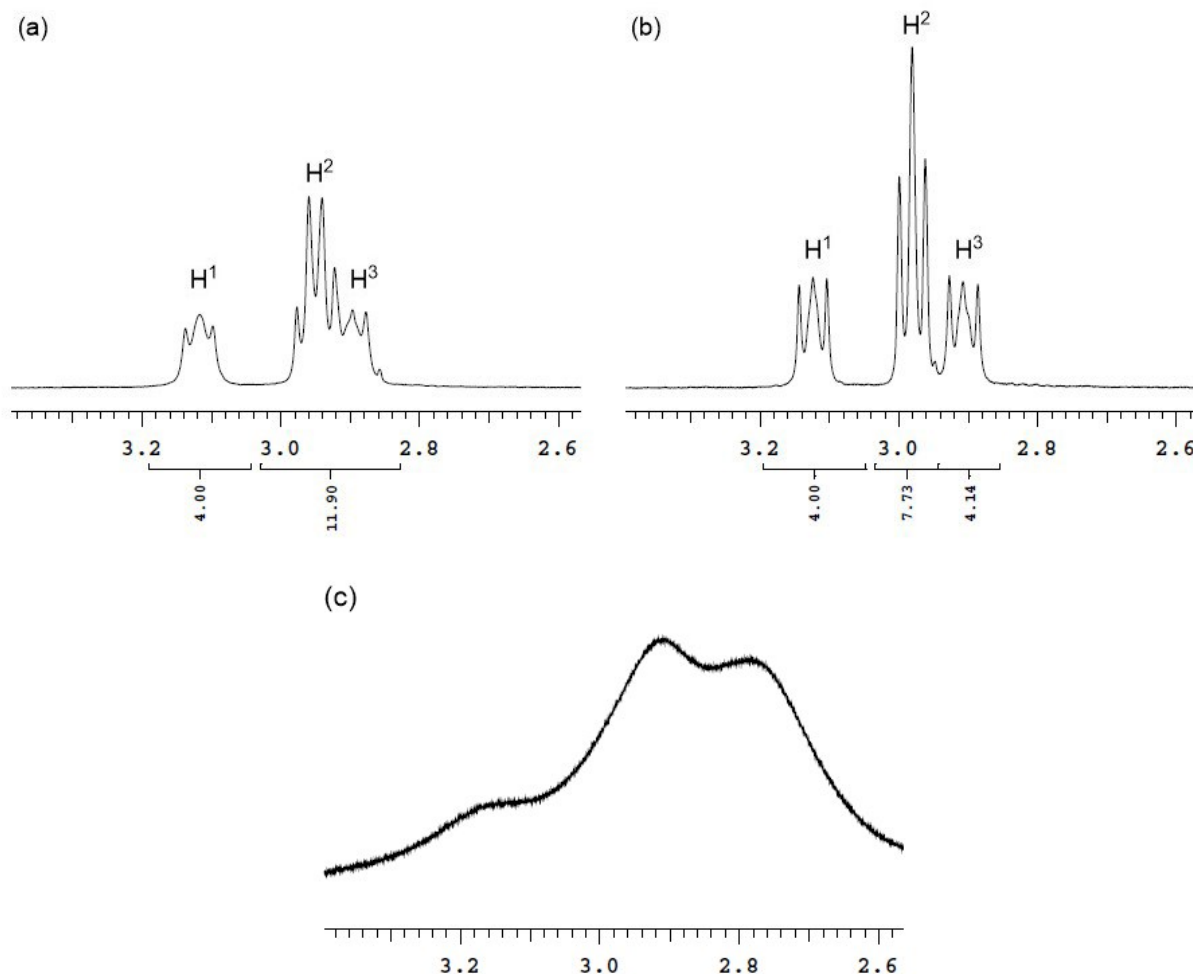
I speculate that this irregular shape is caused by the hindered rotation of the  $C^{Ar}-C^{\alpha}$  and  $C^{\alpha}-C^{\beta}$  bonds due to repulsions among the four alkyl chains. The two hydrogens on  $C^{\alpha}$  are therefore magnetically inequivalent, and they couple with the hydrogens on  $C^{\beta}$  in slightly different coupling constants. The two hydrogens on  $C^{\alpha}$  may also couple to each other (geminal coupling). These factors lead to the formation of this irregular signal. The AA'BB' second order pattern best describes this situation.<sup>184</sup>

Figure 3-2 shows that this hindered rotation also affects resonance signals of hydrogens on  $C^{\beta}$ . The signals from hydrogens on  $C^{\gamma}$  ( $H^5$  and  $H^6$ ) are close to first order quintet, while signals from hydrogens on  $C^{\beta}$  ( $H^7$  and  $H^8$ ) are second order, appearing as irregular shapes. These second order signals are triggered by the hindered rotation as well, resulting in different coupling constants between  $H^{\alpha}-H^{\beta}$  and  $H^{\beta}-H^{\gamma}$ .



**Figure 3-2.** Detailed  $^1\text{H}$  NMR spectrum of archipelago compound **277** and signal assignments in 2.2–1.6 ppm region.

To confirm the origin of these irregular signals, variable-temperature  $^1\text{H}$  NMR experiments were performed. Figure 3-3 shows detailed  $^1\text{H}$  NMR spectra of compound **277** at (a) room temperature, (b) 100 °C, and (c) –80 °C (400 MHz, toluene- $d^8$ ).



**Figure 3-3.** Detailed  $^1\text{H}$  NMR spectra of archipelago compound **277** at (a) room temperature, (b) 100 °C, and (c) -80 °C.

From Figure 3-3(a), the signals  $\text{H}^1$  and  $\text{H}^3$  are assigned to methylene groups bonded to the central naphthalene.  $\text{H}^2$  is from the benzylic methylene bonded to phenanthrene; it appears as an overlapping set of two signals. When the sample is heated to 100 °C, as shown in Figure 3-3(b), all signals become sharper.  $\text{H}^2$  and  $\text{H}^3$  completely separate. The signals from  $\text{H}^1$  and  $\text{H}^3$  are still second order, but look more like a first-order triplet, presumably because the carbon-carbon bonds rotate faster at higher temperature. If the sample is cooled to -80 °C, as shown in Figure



3-3(c), all three signals combine to a broad peak. The signals in aromatic region are also observed to broaden and the splitting patterns that can be observed at room temperature are invisible at  $-80\text{ }^{\circ}\text{C}$ . These broad peaks are caused by the much slower rotation of the carbon-carbon bonds. However, the temperature is still not low enough to separate all rotamers.<sup>185</sup> The variable-temperature experiments further suggest that the irregular signals are caused by hindered C-C bond rotation, due to the repulsion of the four substituents, and that those interactions persist even at high temperature.

### 3.6 Characterization of an archipelago model compound by $^1\text{H}$ -Diffusion-Ordered NMR Spectroscopy ( $^1\text{H}$ -DOSY)

#### 3.6.1 Introduction to the $^1\text{H}$ -DOSY technique

$^1\text{H}$ -Diffusion-Ordered NMR Spectroscopy ( $^1\text{H}$ -DOSY) is a technique developed by Morris and Johnson in 1992<sup>186</sup> and widely used in petroleum,<sup>187-190</sup> polymer,<sup>191</sup> and biomacromolecular research.<sup>192</sup> The technique allows measuring the diffusion coefficient ( $D$ ) of a solute, which is highly dependent on the size of the molecule. The relationship between the diffusion coefficient  $D$  and hydrodynamic radius  $R_H$  is given by the Stokes-Einstein equation (1).<sup>187</sup>

$$D = \frac{k_B T}{6\pi\eta R_H} \quad (1)$$

where  $k_B$  is the Boltzmann constant,  $T$  is the absolute temperature,  $\eta$  is the solution viscosity. From the Stokes-Einstein equation, large molecules, which usually have larger hydrodynamic radii, should give smaller diffusion coefficients than small molecules in a solution.

An example  $^1\text{H}$ -DOSY NMR spectrum of archipelago compound **278** in  $\text{CD}_2\text{Cl}_2$  is shown in Figure 3-4. In this two-dimensional spectrum, the horizontal axis is the chemical shift from  $^1\text{H}$  NMR spectroscopy and the vertical axis is the diffusion coefficient  $D$ .

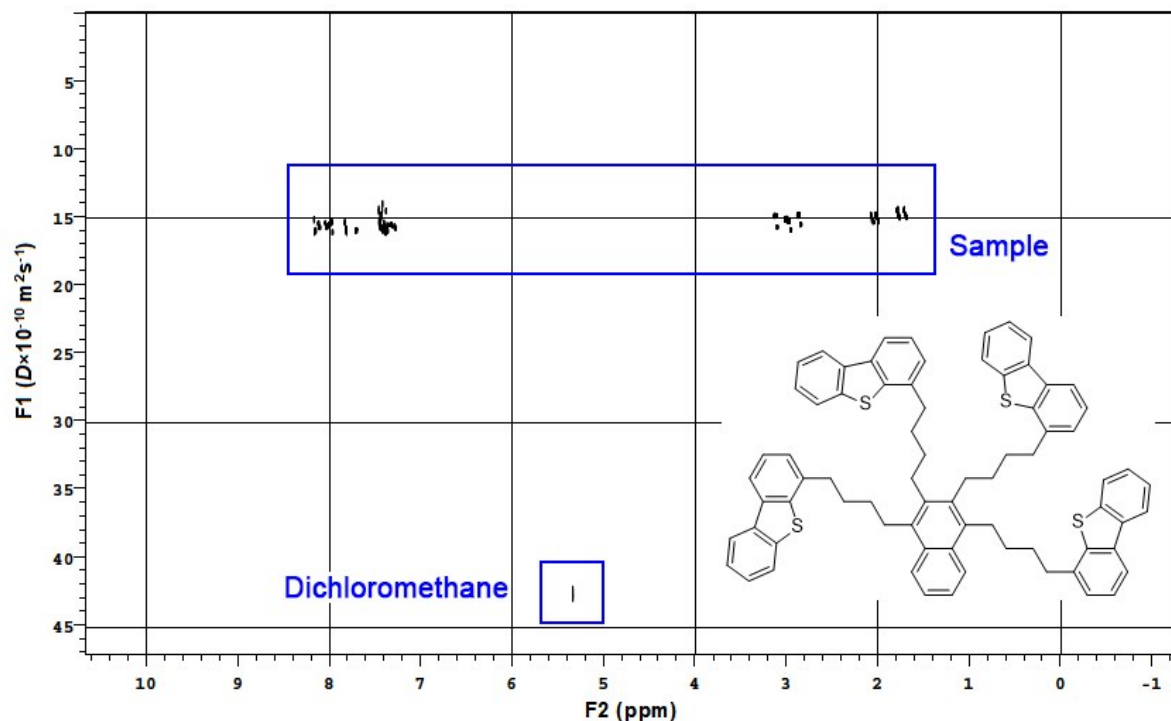


**Figure 3-4.**  $^1\text{H}$ -DOSY NMR spectrum of archipelago model compound **278** in  $\text{CD}_2\text{Cl}_2$ .

From the spectrum, it can be seen that the archipelago compound **278** has a smaller diffusion coefficient at  $\sim 16 \times 10^{-10} \text{ m}^2 \text{ s}^{-1}$ , while dichloromethane has a larger diffusion coefficient at  $\sim 43 \times 10^{-10} \text{ m}^2 \text{ s}^{-1}$ , which is in alignment with the Stokes-Einstein equation. Therefore, the  $^1\text{H}$ -DOSY is capable of separating signals in a mixture if all components have very different molecular sizes.<sup>190</sup>

$^1\text{H}$ -DOSY has been used in several studies to investigate asphaltene and its aggregation. Quoineaud and co-workers described the first asphaltene  $^1\text{H}$ -DOSY NMR spectrum in 2008.<sup>187</sup>

They employed  $^1\text{H}$ -DOSY to measure the diffusion coefficient and subsequently used it to calculate the molecular weight and hydrodynamic radii of asphaltenes. In 2014, Neto and co-workers reported asphaltene aggregation tests using  $^1\text{H}$ -DOSY.<sup>188</sup> They observed aggregation behavior from  $^1\text{H}$ -DOSY NMR spectrum and ascribed the aggregation to  $\pi$ - $\pi$  stacking in continental structures. Subsequently in 2017, Subramanian and co-workers studied the characteristics and properties of asphaltene fractions adsorbed onto calcium carbonate using  $^1\text{H}$ -DOSY.<sup>189</sup> In 2020, Romão and co-workers demonstrated that the presence of resin can influence the asphaltene aggregates by using  $^1\text{H}$ -DOSY.<sup>190</sup>

$^1\text{H}$ -DOSY NMR studies of synthetic asphaltene model compounds have not been reported. Herein, a synthetic archipelago compound is characterized by  $^1\text{H}$ -DOSY to obtain information about molecular shape and aggregation in solution.

### 3.6.2 Characterization of an archipelago model compound by $^1\text{H}$ -DOSY

To investigate my synthetic archipelago compounds, **278** was selected as the sample because it has been obtained on a large-scale synthesis, and it is more soluble than phenanthrene-bearing compounds. Samples with different concentrations from 10 mM to 120 mM (saturated) in  $\text{CD}_2\text{Cl}_2$  were prepared. Diffusion coefficients of the compound **278** ( $D_{Arc}$ ) and dichloromethane ( $D_{DCM}$ ) were measured in each sample. The relative diffusion coefficient ( $D_{rel}$ ) is defined as:

$$D_{rel} = \frac{D_{Arc}}{D_{DCM}} \quad (2)$$

The diffusion coefficient results from  $^1\text{H}$ -DOSY NMR spectra are summarized in Table 3-5. Figures 3-5, 3-6, and 3-7 present the variation trends of  $D_{Arc}$ ,  $D_{DCM}$  and  $D_{rel}$  as a function of compound **278** concentration, respectively.

**Table 3-5.** Diffusion coefficients and relative diffusion coefficients as a function of compound **278** concentration in CD<sub>2</sub>Cl<sub>2</sub>.

| [ <b>278</b> ] (mM) | $D_{Arc}$ ( $10^{-10}\text{m}^2\text{s}^{-1}$ ) <sup>a</sup> | $D_{DCM}$ ( $10^{-10}\text{m}^2\text{s}^{-1}$ ) | $D_{rel}$ |
|---------------------|--|---|-----------|
| 10                  | 17.3   | 46.4  | 0.37      |
| 20                  | 16.9   | 44.0  | 0.38      |
| 30                  | 17.6   | 43.2  | 0.41      |
| 40                  | 16.5   | 42.6  | 0.39      |
| 50                  | 16.9   | 44.2  | 0.38      |
| 60                  | 16.5   | 43.0  | 0.38      |
| 70                  | 16.9   | 42.1  | 0.40      |
| 80                  | 17.0   | 42.1  | 0.40      |
| 90                  | 16.8   | 42.0  | 0.40      |
| 100                 | 15.5   | 41.5  | 0.37      |
| 110                 | 11.5   | 36.6  | 0.31      |
| 120 (saturated)     | 7.6  | 33.4  | 0.23      |

<sup>a</sup> The diffusion coefficients were obtained at 3.0 ppm.

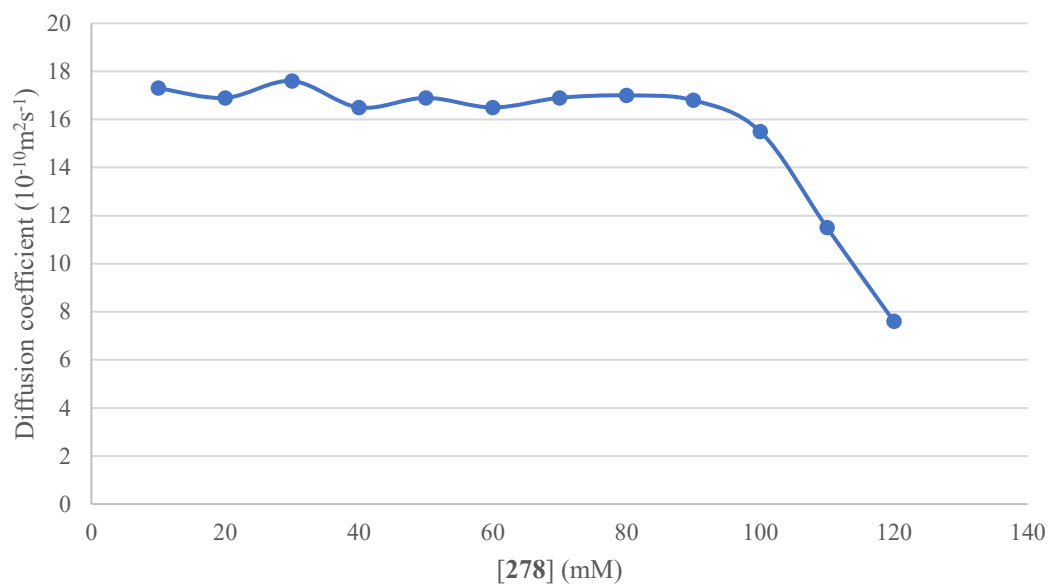


**Figure 3-5.** Diffusion coefficients of compound **278** as a function of **278** concentration.

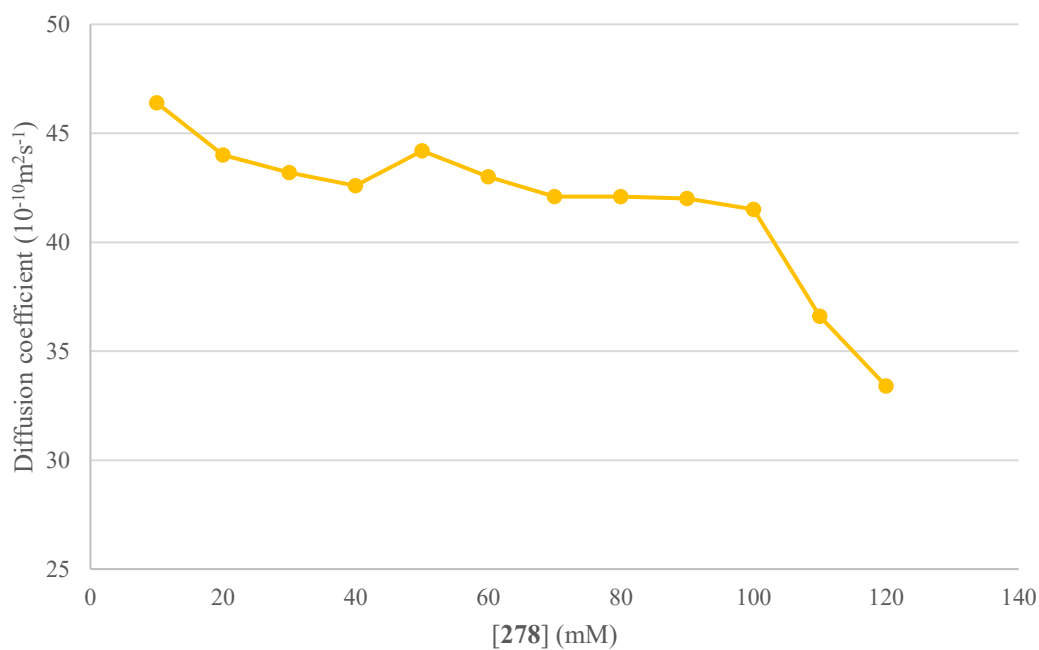


**Figure 3-6.** Diffusion coefficients of dichloromethane as a function of **278** concentration.

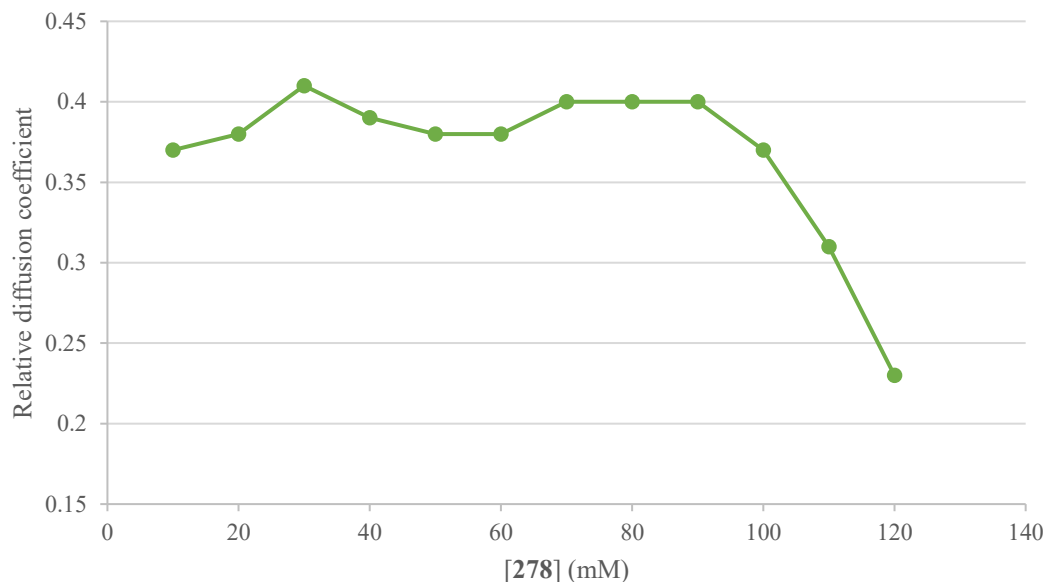


**Figure 3-7.** Relative diffusion coefficients as a function of **278** concentration.

The  $^1\text{H}$ -DOSY results are summarized and discussed below.

1. *Variation tendencies of diffusion coefficients ( $D_{Arc}$ ,  $D_{DCM}$ ) and relative diffusion coefficients ( $D_{rel}$ ).*

From Figures 3-5 and 3-6, we can see that the  $D_{Arc}$  and  $D_{DCM}$  values are approximately constant at concentrations below 100 mM. In this range, the solvent-solvent interaction and solute-solvent interaction are the predominant interactions.<sup>187</sup> As the concentration continues to increase, the solute-solute interaction become more significant.<sup>187</sup> The diffusions of the solute as well as the solvent are influenced, rendering decreased  $D_{Arc}$  and  $D_{DCM}$  values. Beyond 120 mM, the compound starts to precipitate from the solution to give white floccules on the bottom of the NMR tube, suggesting that intermolecular aggregation of the solute leads to precipitation.

As shown in Figure 3-7, the variation tendency of  $D_{rel}$  is similar to  $D_{Arc}$  and  $D_{DCM}$ , which is nearly constant at concentrations below 100 mM and drops dramatically starting at 100 mM. This suggests that the diffusion of the compound **278** is more affected at high concentrations than diffusion of DCM.

## 2. Shape of the archipelago compound.

According to Quoineaud and co-workers,<sup>187</sup> the shape of the solute molecule can be determined by using diffusion coefficients  $D$ , as described by:

$$\frac{D_1}{D_2} = \left(\frac{M_2}{M_1}\right)^\alpha \quad (3)$$

where  $D_1$  and  $D_2$  are the diffusion coefficients of the solute and solvent at infinite dilution,  $M_1$  and  $M_2$  are the molecular weights of the solute and solvent.  $\alpha$  is a factor based on the shape of the particle. Using the  $D_{Arc}$  and  $D_{DCM}$  values at 10 mM concentration, the  $\alpha$  is calculated:

$$\alpha = 0.39 \quad (4)$$

As described by Quoineaud and co-workers,<sup>187</sup> for a spherical particle, the  $\alpha$  is supposed to be 0.33. A value of 0.50 for  $\alpha$  may indicate the flat disk shape of the solute. The 0.39 value of the  $\alpha$  for this compound suggests that the shape is between spherical and flat disk. This result hints that archipelago compounds are not planar in solution. The alkyl chains in archipelago compound will twist and intramolecular  $\pi$ - $\pi$  stacking (parallel type and/or perpendicular type) between islands may exist, which may explain why these archipelago compounds precipitate as an amorphous powder and not as crystals.

### 3. Hydrodynamic radius.

According to the Stokes-Einstein equation (1), taking the average value of  $D_{Arc}$  from 10 mM to 90 mM ( $16.9 \times 10^{-10} \text{ m}^2\text{s}^{-1}$ ) and approximately setting the solution viscosity to  $0.41 \text{ MPa}\cdot\text{s}$ ,<sup>193</sup> the hydrodynamic radius of compound **278** is calculated:

$$R_{Arc} = 3.13 \text{ \AA} \quad (5)$$

However, the Stokes-Einstein equation is only applicable to spherical particles for which the hydrodynamic radius is at least five times bigger than the hydrodynamic radius of the solvent. For particles which do not match this requirement, a modified Stokes-Einstein equation (6) was introduced by Macchioni and co-workers.<sup>194</sup>

$$D = \frac{k_B T}{c(R_{solv}, R_H) f_s \pi \eta R_H} \quad (6)$$

where  $c(R_{solv}, R_H)$  is a correction factor related to the size of the molecule. The  $c(R_{solv}, R_H)$  value is provided by Chen and co-workers:<sup>195</sup>

$$c(R_{solv}, R_H) = \frac{6}{1 + 0.695 \left( \frac{R_{solv}}{R_H} \right)^{2.234}} \quad (7)$$

where  $R_{solv}$  and  $R_H$  are the hydrodynamic radii of the solvent and the sample compound, respectively.

In the modified Stokes-Einstein equation (6),  $f_s$  is another correction factor for non-spherical particles.  $f_s$  is determined by the ratio of the major semiaxis ( $a$ ) to the minor semiaxis ( $b$ ) in molecule.  $f_s$  equals to 1 for spherical particles while  $f_s$  is bigger than 1 for non-spherical particles. According to the calculation by Macchioni and co-workers,  $f_s$  is no greater than 1.1 if the  $a/b$



value is smaller than 3.<sup>194</sup> Combining with the shape information from the  $\alpha$  result (4),  $f_s$  is set approximately to 1 in further calculations.

By employing the modified Stokes-Einstein equation (6) and correction factor (7), using the  $R_{DCM} = 2.49 \text{ \AA}$ ,<sup>194</sup> the corrected hydrodynamic radius of the archipelago compound **278** is calculated:

$$R_{Arc} (\text{corrected}) = 3.92 \text{ \AA} \quad (8)$$

This value is the hydrodynamic radius of compound **278** in dilute solution. It is used to calculate the hydrodynamic radius of **278** in concentrated solution and then to compare with that of asphaltenes, which are discussed below.

#### 4. Aggregation estimation from $D_{rel}$ .

The diffusion coefficient  $D$  provides potential information pertinent to asphaltene aggregation. For example, Kawashima and co-workers calculated hydrodynamic radii of several asphaltene samples at different concentrations using diffusion coefficients  $D$  with the Stokes-Einstein equation (1).<sup>196</sup> They found that the hydrodynamic radii of asphaltenes in concentrated solutions were larger than that in dilute solutions, which probably indicates that asphaltene constituents form aggregates in concentrated solutions.

Inspired by Kawashima and co-workers' work, a rough estimate of the aggregation was made from my <sup>1</sup>H-DOSY results, by measuring the difference in the hydrodynamic radius of **278** in dilute and saturated solutions. However, compared with dilute solution, the viscosity  $\eta$  in saturated solution changed significantly and the value is unknown, which prevents us from directly calculating the hydrodynamic radius by using the modified Stoke-Einstein equation (6).

Therefore, another method was attempted from the relative diffusion coefficient  $D_{rel}$ .<sup>194</sup> Using the modified Stokes-Einstein equation (6) with  $f_s = 1$  for both compound **278** and dichloromethane, for a given concentration, the  $D_{rel}$  can be represented as:

$$D_{rel} = \frac{D_{Arc}}{D_{DCM}} = \frac{\frac{k_B T}{c_{Arc} \pi \eta R_{Arc}}}{\frac{k_B T}{c_{DCM} \pi \eta R_{DCM}}} = \frac{c_{DCM} R_{DCM}}{c_{Arc} R_{Arc}} \quad (9)$$

where  $c_{Arc}$  and  $c_{DCM}$  are the correction factors for **278** and dichloromethane, respectively. These factors are not affected by the concentration of the solution, as shown in (7).<sup>195</sup> Thus, for dilute and saturated samples, the ratio of the  $D_{rel}$  can be represented as:

$$\frac{D_{rel}(dil.)}{D_{rel}(sat.)} = \frac{\frac{c_{DCM} R_{DCM}}{c_{Arc} R_{Arc}(dil.)}}{\frac{c_{DCM} R_{DCM}}{c_{Arc} R_{Arc}(sat.)}} = \frac{R_{Arc}(sat.)}{R_{Arc}(dil.)} \quad (10)$$

Using the average  $D_{rel}$  value from 10 mM to 90 mM [ $D_{rel}(dil.) = 0.39$ ] and  $D_{rel}$  value at 120 mM [ $D_{rel}(sat.) = 0.23$ ], the ratio of hydrodynamic radii is calculated:

$$\frac{R_{Arc}(sat.)}{R_{Arc}(dil.)} = \frac{D_{rel}(dil.)}{D_{rel}(sat.)} = 1.7 \quad (11)$$

By applying the corrected hydrodynamic radius in dilute solution (8), the hydrodynamic radius of compound **278** in saturated solution is:

$$R_{Arc}(\text{saturated}) = 6.6 \text{ \AA} \quad (12)$$

This result gives a hint that some of the archipelago model compound **278** forms aggregates at higher concentrations.

### 5. Discrepancies of diffusion results between asphaltenes and archipelago compound **278**.

After obtaining the relevant data for archipelago compound **278** from <sup>1</sup>H-DOSY, I compared it with the data obtained from asphaltenes in the literature. However, some discrepancies are

observed, which may provide directions for further preparation and study of asphaltene model compounds.

(1) *Diffusion coefficients and hydrodynamic radii.* According to published work, asphaltenes usually have diffusion coefficients similar to or smaller than  $10 \times 10^{-10} \text{ m}^2\text{s}^{-1}$  and hydrodynamic radii larger than 5 Å (and in most cases, larger than 10 Å) regardless of concentration.<sup>187,188,190,196</sup> This indicates that the molecular sizes of authentic asphaltenes are much larger than that of archipelago compound **278**. Considering that the molecular weight of **278** is in the range of the molecular weight of asphaltenes (as described in section 1.1.2), the discrepancies of diffusion coefficients and hydrodynamic radii are probably due to stronger intermolecular interactions in real asphaltenes. Acid-base pairs, hydrogen bonding assemblies and metal Lewis base coordination, as suggested by Gray and co-workers,<sup>66</sup> may lead to larger hydrodynamic radii and smaller diffusion coefficients in real asphaltene aggregates than archipelago model compound **278**.

(2) *Minimum concentration for asphaltenes to aggregate.* Studies of asphaltenes illustrated that aggregates are formed even at very low concentrations (e.g., 0.1 g/L).<sup>196-198</sup> In dilute solutions, monomers and aggregates usually exhibit signature diffusion coefficients.<sup>196</sup> These phenomena were not observed in compound **278**, which alone is not a representative model for asphaltene aggregates.

Based on our findings in <sup>1</sup>H-DOSY NMR study, I would like to tentatively provide some recommendations for further studies on asphaltene model compounds:

(1) *Heteroatom model compounds.* The oxygen- or nitrogen-containing functional groups, such as alcohol, carboxyl and amine, are key groups for the formation of hydrogen bonding and acid-

base interactions. Further designs of asphaltene model compounds should consider compounds with these functional groups. However, this also poses greater challenges for synthesis and purification.

(2) *Mixed model compounds.* Asphaltene is an extremely complex mixture, so it is unlikely that the use of a single model compound can imitate asphaltene aggregation. A mixture of several continental and archipelago models with elemental compositions comparable to asphaltenes may give similar diffusion coefficients and hydrodynamic radii as asphaltenes and hence need to be studied in the future.

## Conclusion

Archipelago model compounds have been successfully synthesized by applying Miura's rhodium-catalyzed [2+2+2] and [4+2] annulation reactions,<sup>101,110</sup> using aryl-boron derivatives and island-tethered alkynes. These model compounds are quite different from previously synthesized model compounds, based on molecular weight and chemical compositions. Variable-temperature <sup>1</sup>H NMR spectroscopy provides evidence of the limited rotational freedom of the four adjacent alkyl chains in these compounds. <sup>1</sup>H-DOSY provides the diffusion coefficients of an archipelago model compound in solution at different concentrations. Calculations using diffusion coefficients demonstrate the aggregation of this model compound in saturated solution, but also find discrepancies between the model compound and asphaltenes.

## Experimental Section

### General Information

Unless otherwise noted, all compounds were used as received without any further purification. THF was distilled from sodium/benzophenone ketyl and stored under nitrogen. DMF and Et<sub>2</sub>O were dried over 3 Å molecular sieves for at least 48 h before use. [Cp\*RhCl<sub>2</sub>]<sub>2</sub>,<sup>199</sup> 2-bromodibenzothiophene (**275**),<sup>200</sup> phenyl boronic acid pinacol ester (**270**),<sup>180</sup> naphthalene-2-boronic acid pinacol ester (**267**),<sup>180</sup> 1,4-benzenediboronic acid bis(pinacol) ester (**273**),<sup>181</sup> and 4,4,5,5-tetramethyl-2-(phenanthren-9-yl)-1,3,2-dioxaborolane (**274**)<sup>182</sup> were prepared according to literature procedures. <sup>1</sup>H, <sup>13</sup>C{<sup>1</sup>H}, and <sup>11</sup>B{<sup>1</sup>H} NMR spectra were recorded on Agilent/Varian instruments (400 or 500 or 700 MHz for <sup>1</sup>H NMR spectroscopy, 101 or 126 or 176 MHz for <sup>13</sup>C{<sup>1</sup>H} NMR spectroscopy, and 128 MHz for <sup>11</sup>B{<sup>1</sup>H} NMR spectroscopy) at 27 °C. Chemical shifts of <sup>1</sup>H, <sup>13</sup>C{<sup>1</sup>H}, and <sup>11</sup>B{<sup>1</sup>H} NMR spectra were reported in parts per million (ppm). Chemical shifts were referenced to residual solvent peaks (CDCl<sub>3</sub>: δ<sub>H</sub> = 7.26 ppm, δ<sub>C</sub> = 77.06 ppm; CD<sub>2</sub>Cl<sub>2</sub>: δ<sub>H</sub> = 5.32 ppm, δ<sub>C</sub> = 53.8 ppm). All coupling constants (*J* values) were reported in Hertz (Hz). Column chromatography was performed on silica gel 60 M (230–400 mesh). Thin-layer chromatography (TLC) was performed on pre-coated, aluminum-backed silica gel plates. Visualization of the developed TLC plate was performed by a UV lamp (254 nm). High-resolution mass spectrometric (HRMS) results were obtained from Mass Spectrometry Facility using the following instruments: Kratos Analytical MS-50G (EI), Bruker 9.4T Apex-Qe FTICR (MALDI). Elemental analyses (C, H, S) were obtained from Analytical and Instrumentation Laboratory using a Thermo Flash 2000 Elemental Analyzer.

## **<sup>1</sup>H-Diffusion Ordered NMR Spectroscopy Information**

<sup>1</sup>H-Diffusion Ordered NMR Spectroscopic (<sup>1</sup>H-DOSY) measurements were performed on a 600 MHz four-channel Varian VNMRJ spectrometer equipped with a HCN Z-gradient probe using OpenVNMRJ 2.1A as the acquisition and processing software. The Oneshot45 DOSY pulse sequence (1,2) was used for all diffusion measurements. All experiments were carried out at 27 °C. The gradient time is 2 ms. The diffusion delay was optimized for each sample using the Oneshot45 pulse sequence using 7 different pulsed field gradient strengths from 2.0 G/cm to 59.5 G/cm. The gradient strengths are given as DAC (digital to analogue converter) units, as gzlv11. The final DOSY experiment was acquired using 15 different pulsed field gradient strengths from 2.0 G/cm to 59.5 G/cm with 4 scans for each experiment. Data were processed with a base line correction (spline fit), a discrete two component fit using peak heights and corrected for non-uniform pulsed field gradients and plotted using the DOSY module in OpenVNMRJ 2.1A.

Samples with different concentrations were prepared using compound **278** from 6.5 mg to 77.9 mg in 0.6 mL CD<sub>2</sub>Cl<sub>2</sub> (99.9% D). Each sample was added to 5 mm NMR tubes and stored at room temperature before measurement.

### **General procedure C – [4+2] annulations of 2-biphenylboronic acid with alkynes<sup>110</sup>**

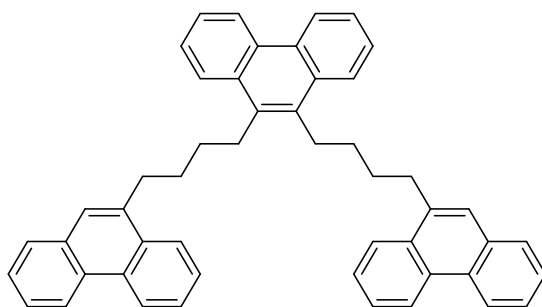
2-Biphenylboronic acid **75**, alkyne (**248**, **249**, **254**), [Cp\*RhCl<sub>2</sub>]<sub>2</sub>, and Cu(OAc)<sub>2</sub>·H<sub>2</sub>O were placed in a dry 10 mL round bottom flask with a magnetic stir bar. Dry DMF was added and the flask was equipped with a condenser. The reaction mixture was heated to 100 °C for 3 h or 6 h under air. After cooling to room temperature, the mixture was quenched with water (30 mL). The aqueous solution was extracted with CH<sub>2</sub>Cl<sub>2</sub> (3 times, 20 mL each) and dried over Na<sub>2</sub>SO<sub>4</sub>. The

mixture was filtered, and the solvent was removed under reduced pressure. The residual was purified by silica column chromatography using hexane/CH<sub>2</sub>Cl<sub>2</sub> eluent to afford the product.

#### General procedure D – [2+2+2] annulations of pinacol boronates with alkynes<sup>101</sup>

Pinacol boronate (**267**, **270**, **276**), alkyne (**240**, **248**, **254**), [Cp\*RhCl<sub>2</sub>]<sub>2</sub>, and Cu(OAc)<sub>2</sub>·H<sub>2</sub>O were placed in a dry 10 mL Schlenk flask with a magnetic stir bar. The reaction flask was charged with nitrogen and dry DMF was added through Schlenk line techniques. The reaction mixture was heated to 70 °C for 2 d. After cooling to room temperature, the mixture was quenched with water (30 mL). The aqueous solution was extracted with CH<sub>2</sub>Cl<sub>2</sub> (3 times, 20 mL each) and dried over Na<sub>2</sub>SO<sub>4</sub>. The mixture was filtered, and the solvent was removed under reduced pressure. The residual was purified by silica column chromatography using hexane/CH<sub>2</sub>Cl<sub>2</sub> eluent to afford the product.

#### 9,10-Bis[4-(9-phenanthrene)butyl]phenanthrene (**260**)



2-Biphenylboronic acid **75** (41 mg, 0.21 mmol), 1,10-di(9-phenanthrene)-5-decyne **240** (68 mg, 0.14 mmol), [Cp\*RhCl<sub>2</sub>]<sub>2</sub> (4.3 mg, 5 mol%), and Cu(OAc)<sub>2</sub>·H<sub>2</sub>O (2.8 mg, 10 mol%) were placed in a dry 10 mL round bottom flask with a magnetic stir bar. Dry DMF (3 mL) was added and the flask was equipped with a condenser. The reaction mixture was heated to 100 °C for 3 h under air. After cooling to room temperature, the mixture was quenched with water (30 mL). The

aqueous solution was extracted with CH<sub>2</sub>Cl<sub>2</sub> (3 times, 30 mL each) and dried over Na<sub>2</sub>SO<sub>4</sub>. The upper suspension was transferred to another round bottom flask and the solvent was removed under reduced pressure. The crude material was carefully washed with ice cold hexane/CH<sub>2</sub>Cl<sub>2</sub> 2:1 solution (3 times, 10 mL each) to afford compound **260** as a white solid (58 mg, 64%). *R*<sub>f</sub> = 0.43 (SiO<sub>2</sub>; hexane/CH<sub>2</sub>Cl<sub>2</sub> 2:1).

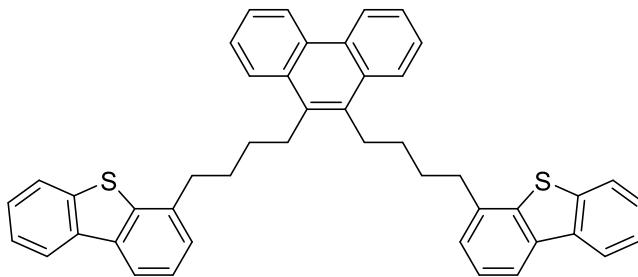
**<sup>1</sup>H NMR** (CDCl<sub>3</sub>, 500 MHz): δ 8.72 (t, *J* = 7.8 Hz, 4H), 8.62 (d, *J* = 8.0 Hz, 2H), 8.10 (t, *J* = 7.3 Hz, 4H), 7.78 (d, *J* = 7.2 Hz, 2H), 7.64–7.52 (m, 14H), 3.26–3.21 (second order m, 4H), 3.17 (t, *J* = 7.7 Hz, 4H), 2.10–2.03 (m, 4H), 1.93–1.85 (m, 4H).

**<sup>13</sup>C{<sup>1</sup>H} NMR** (CDCl<sub>3</sub>, 126 MHz): δ 136.5, 133.8, 131.9, 131.3, 131.3, 130.8, 129.9, 129.7, 128.1, 126.7, 126.6, 126.6, 126.1, 126.0, 125.5, 124.7, 124.4, 123.3, 123.0, 122.5, 33.3, 30.9, 30.8, 29.4.

**MALDI HRMS** (DCTB) *m/z* calcd for C<sub>50</sub>H<sub>42</sub> (M<sup>+</sup>) 642.3287, found 642.3278.

**EA** anal. calcd for C<sub>50</sub>H<sub>42</sub>: C, 93.41; H, 6.59. Found: C, 92.09; H, 6.62. Repeat found: C, 91.89; H, 6.60.

#### 9,10-Bis[4-(4-dibenzothiophene)butyl]phenanthrene (**261**)



The general procedure C was used with 2-biphenylboronic acid **75** (41 mg, 0.21 mmol), 1,10-di(4-dibenzothiophene)-5-decyne **248** (70 mg, 0.14 mmol), [Cp\*RhCl<sub>2</sub>]<sub>2</sub> (4.3 mg, 5 mol%),



Cu(OAc)<sub>2</sub>·H<sub>2</sub>O (2.8 mg, 10 mol%), and DMF (3 mL). The reaction mixture was heated to 100 °C for 3 h. The crude material was purified by silica column chromatography (hexane/CH<sub>2</sub>Cl<sub>2</sub> 4:1) to afford compound **261** as a white solid (84 mg, 92%). *R*<sub>f</sub> = 0.50 (SiO<sub>2</sub>; hexane/CH<sub>2</sub>Cl<sub>2</sub> 2:1).

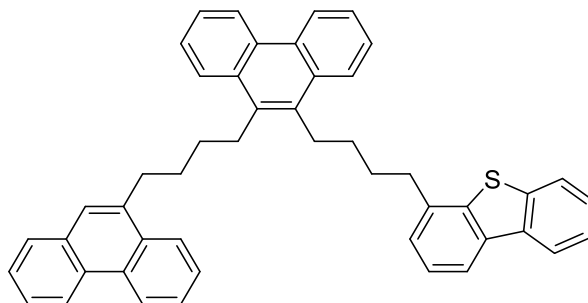
<sup>1</sup>H NMR (CDCl<sub>3</sub>, 700 MHz): δ 8.73–8.70 (m, 2H), 8.14–8.11 (m, 2H), 8.09–8.06 (m, 2H), 8.01 (d, *J* = 7.6 Hz, 2H), 7.82–7.79 (m, 2H), 7.61–7.57 (m, 4H), 7.45–7.38 (m, 6H), 7.29 (d, *J* = 7.0 Hz, 2H), 3.24–3.20 (second order m, 4H), 3.00 (t, *J* = 7.8 Hz, 4H), 2.09 (quint, *J* = 7.6 Hz, 4H), 1.88–1.82 (m, 4H).

<sup>13</sup>C{<sup>1</sup>H} NMR (CDCl<sub>3</sub>, 176 MHz): δ 139.2, 139.1, 136.6, 136.2, 135.7, 133.7, 131.3, 129.9, 126.7, 126.6, 126.1, 125.5, 124.8, 124.7, 124.3, 123.0, 122.8, 121.7, 119.4, 35.0, 30.6, 29.6, 29.3.

**MALDI HRMS** (DCTB) *m/z* calcd for C<sub>46</sub>H<sub>38</sub>S<sub>2</sub> (M<sup>+</sup>) 654.2415, found 654.2410.

**EA** anal. calcd for C<sub>46</sub>H<sub>38</sub>S<sub>2</sub>: C, 84.36; H, 5.85; S, 9.79. Found: C, 82.68; H, 5.85; S, 8.42. Repeat found: C, 82.28; H, 5.77; S, 8.62.

**9-[4-(4-Dibenzothiophene)butyl]-10-[4-(9-phenanthrene)butyl]phenanthrene (262)**



The general procedure C was used with 2-biphenylboronic acid **75** (44 mg, 0.22 mmol), 1-(4-dibenzothiophene)-10-(9-phenanthrene)-5-decyne **249** (74 mg, 0.15 mmol), [Cp\*RhCl<sub>2</sub>]<sub>2</sub> (4.6 mg, 5 mol%), Cu(OAc)<sub>2</sub>·H<sub>2</sub>O (3.0 mg, 10 mol%), and DMF (3 mL). The reaction mixture was heated

to 100 °C for 3 h. The crude material was purified by silica column chromatography (SiO<sub>2</sub>; hexane/CH<sub>2</sub>Cl<sub>2</sub> 4:1) to afford compound **262** as a white solid (79 mg, 81%). *R*<sub>f</sub> = 0.46 (SiO<sub>2</sub>; hexane/CH<sub>2</sub>Cl<sub>2</sub> 2:1).

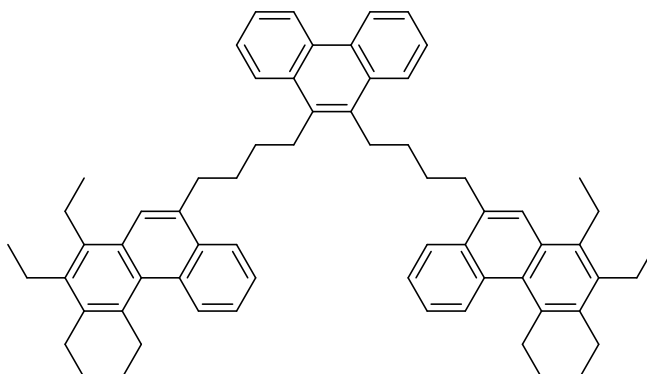
**<sup>1</sup>H NMR** (CD<sub>2</sub>Cl<sub>2</sub>, 700 MHz): δ 8.75–8.70 (m, 3H), 8.66 (d, *J* = 8.2 Hz, 1H), 8.16 (dd, *J* = 8.2 Hz, 1.4 Hz, 1H), 8.13–8.11 (m, 2H), 8.10–8.07 (m, 1H), 8.01 (dd, *J* = 7.8 Hz, 0.8 Hz, 1H), 7.81–7.76 (m, 2H), 7.66–7.54 (m, 9H), 7.44–7.38 (m, 3H), 7.31 (d, *J* = 6.5 Hz, 1H), 3.27–3.20 (m, 6H), 3.00 (t, *J* = 7.8 Hz, 2H), 2.12–2.06 (m, 4H), 1.92–1.81 (m, 4H).

**<sup>13</sup>C{<sup>1</sup>H} NMR** (CD<sub>2</sub>Cl<sub>2</sub>, 126 MHz): 139.5, 139.4, 137.1, 137.1, 136.5, 136.0, 134.2, 134.1, 132.3, 131.7, 131.6, 131.0, 130.1, 130.0, 128.4, 127.0, 127.0, 126.9, 126.5, 126.5, 126.3, 126.3, 125.8, 125.2, 125.1, 124.8, 124.7, 123.5, 123.2, 123.1, 122.8, 122.0, 119.7, 35.3, 33.6, 31.2, 31.1, 30.9, 30.0, 29.7, 29.6.

**MALDI HRMS** (DCTB) *m/z* calcd for C<sub>48</sub>H<sub>40</sub>S (M<sup>+</sup>) 648.2851, found 648.2842.

**EA** anal. calcd for C<sub>48</sub>H<sub>40</sub>S: C, 88.85; H, 6.21; S, 4.94. Found: C, 88.00; H, 6.07; S, 4.85. Repeat found: C, 87.93; H, 6.17; S, 5.17.

**9,10-Bis{4-[9-(1,2,3,4-tetraethylphenanthrene)]butyl}phenanthrene (263)**



The general procedure C was used with 2-biphenylboronic acid **75** (29 mg, 0.15 mmol), 1,10-di[9-(1,2,3,4-tetraethylphenanthrene)]-5-decyne **254** (70 mg, 0.098 mmol), [Cp\*RhCl<sub>2</sub>]<sub>2</sub> (3.0 mg, 5 mol%), Cu(OAc)<sub>2</sub>·H<sub>2</sub>O (2.0 mg, 10 mol%), and DMF (3 mL). The reaction mixture was heated to 100 °C for 6 h. The crude material was purified by silica column chromatography (hexane/CH<sub>2</sub>Cl<sub>2</sub> 4:1) to afford compound **263** as a yellow grease (70 mg, 83%). *R*<sub>f</sub> = 0.47 (SiO<sub>2</sub>; hexane/CH<sub>2</sub>Cl<sub>2</sub> 2:1).

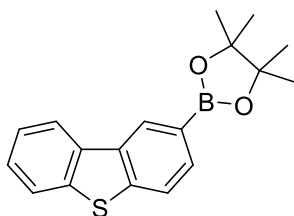
**<sup>1</sup>H NMR** (CDCl<sub>3</sub>, 700 MHz): δ 8.74 (d, *J* = 7.9 Hz, 2H), 8.65 (d, *J* = 8.3 Hz, 2H), 8.11 (d, *J* = 8.2 Hz, 4H), 7.81 (s, 2H), 7.62–7.59 (m, 2H), 7.55 (t, *J* = 7.4 Hz, 4H), 7.53–7.50 (m, 2H), 3.42–3.32 (br, 4H), 3.32–3.28 (second order m, 4H), 3.25–3.22 (m, 4H), 3.15–3.11 (m, 4H), 3.06–3.01 (m, 4H), 2.96–2.92 (m, 4H), 2.14–2.09 (m, 4H), 1.99–1.93 (m, 4H), 1.66 (t, *J* = 7.4 Hz, 6H), 1.33 (t, *J* = 7.6 Hz, 6H), 1.31–1.26 (m, 12H).

**<sup>13</sup>C{<sup>1</sup>H} NMR** (CDCl<sub>3</sub>, 176 MHz): δ 140.2, 138.7, 136.3, 135.4, 134.6, 133.8, 131.8, 131.7, 131.3, 129.9, 129.9, 129.6, 128.4, 126.6, 125.4, 125.4, 124.8, 124.0, 123.5, 123.0, 122.7, 33.6, 31.0, 30.9, 29.4, 25.4, 22.7, 22.6, 22.2, 16.5, 16.2, 16.0, 16.0.

**MALDI HRMS** (DCTB) *m/z* calcd for C<sub>66</sub>H<sub>74</sub> (M<sup>+</sup>): 866.5791, found 866.5783.

**EA** anal. calcd for C<sub>66</sub>H<sub>74</sub>: C, 91.40; H, 8.60. Found: C, 72.79; H, 6.83. Repeat found: C, 73.27; H, 6.93.

**2-(Dibenzo[*b,d*]thiophen-2-yl)-4,4,5,5-tetramethyl-1,3,2-dioxaborolane (276)**



The preparation procedure is according to published work.<sup>182</sup> Magnesium turnings (44 mg, 1.8 mmol) were placed in a dry 25 mL Schlenk flask. The magnesium turnings were activated by addition of a small amount of iodine crystals and warming until iodine sublimed. The Schlenk flask was cooled to room temperature and was charged with nitrogen. THF (2 mL) and pinacolborane (220  $\mu$ L, 195 mg, 1.52 mmol) was added to the flask through Schlenk line techniques and the 2-bromo-dibenzothiophene (**275**) solution (3 mL THF solution containing 400 mg of **275**, 1.52 mmol) was added dropwise in 15 min by a syringe with constant stirring. The reaction mixture was stirred overnight at room temperature. The mixture was cooled to 0 °C and was quenched by 3 M HCl (3 mL). After the addition of HCl solution, the mixture was stirred for an additional 30 min. The reaction mixture was then diluted with water (50 mL), extracted with CH<sub>2</sub>Cl<sub>2</sub> (3 times, 30 mL each) and dried over Na<sub>2</sub>SO<sub>4</sub>. The mixture was filtered, and the solvent was removed under reduced pressure. The residual was purified by silica column chromatography (hexane/CH<sub>2</sub>Cl<sub>2</sub> 4:1 followed by hexane/CH<sub>2</sub>Cl<sub>2</sub> 2:1) to afford compound **276** as a yellow grease (347 mg, 74%). *R*<sub>f</sub> = 0.28 (SiO<sub>2</sub>; hexane/CH<sub>2</sub>Cl<sub>2</sub> 2:1).

**<sup>1</sup>H NMR** (CDCl<sub>3</sub>, 700 MHz):  $\delta$  8.67 (s, 1H), 8.29–8.26 (m, 1H), 7.94–7.91 (second order m, 1H), 7.90–7.88 (second order m, 1H), 7.87–7.85 (m, 1H), 7.48–7.46 (m, 2H), 1.43 (s, 12H).

**<sup>13</sup>C{<sup>1</sup>H} NMR** (CDCl<sub>3</sub>, 176 MHz):  $\delta$  142.8, 139.2, 135.6, 135.1, 132.6, 128.3, 126.7, 124.5, 122.7, 122.1, 121.8, 84.0, 24.9.

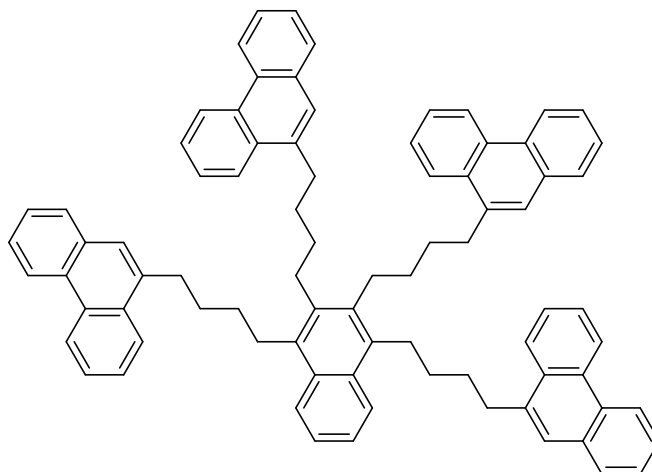
**<sup>11</sup>B{<sup>1</sup>H} NMR** (CDCl<sub>3</sub>, 128 MHz):  $\delta$  31.9 (br s).

**EI HRMS** *m/z* calcd for C<sub>18</sub>H<sub>19</sub><sup>11</sup>BO<sub>2</sub>S (M<sup>+</sup>) 310.1199, found 310.1203.

**EA** anal. calcd for C<sub>18</sub>H<sub>19</sub>BO<sub>2</sub>S: C, 69.69; H, 6.17, S, 10.33. Found: C, 70.00; H, 6.28; S, 9.93.

Repeat found: C, 70.13; H, 6.32; S, 9.94.

**1,2,3,4-Tetra[4-(9-phenanthrene)butyl]naphthalene (277)**



The general procedure D was used with phenyl boronic acid pinacol ester **270** (29 mg, 0.14 mmol), 1,10-di(9-phenanthrene)-5-decyne **240** (70 mg, 0.14 mmol), [Cp\*RhCl<sub>2</sub>]<sub>2</sub> (4.4 mg, 5 mol%), Cu(OAc)<sub>2</sub>·H<sub>2</sub>O (29 mg, 0.14 mmol), and DMF (3 mL). The crude material was purified by silica column chromatography (hexane/CH<sub>2</sub>Cl<sub>2</sub> 4:1) to afford compound **277** as a white solid (60 mg, 80%). *R*<sub>f</sub> = 0.26 (SiO<sub>2</sub>; hexane/CH<sub>2</sub>Cl<sub>2</sub> 2:1).

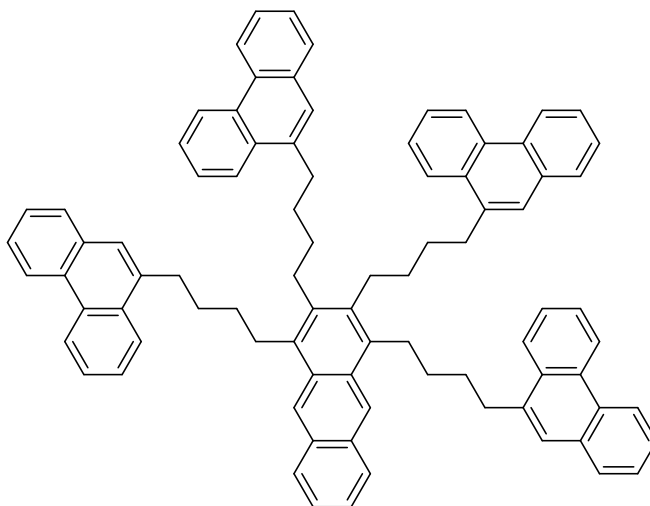
<sup>1</sup>H NMR (CDCl<sub>3</sub>, 700 MHz): δ 8.73 (d, *J* = 7.9 Hz, 2H), 8.65 (d, *J* = 8.1 Hz, 4H), 8.58 (d, *J* = 8.1 Hz, 2H), 8.12 (dd, *J* = 7.7 Hz, 1.4 Hz, 2H), 8.06–8.02 (m, 4H), 7.80 (dd, *J* = 7.6 Hz, 1.3 Hz, 2H), 7.74 (dd, *J* = 7.6 Hz, 1.3 Hz, 2H), 7.65–7.47 (m, 20H), 7.43–7.41 (second order m, 2H), 3.18–3.08 (m, 12H), 2.86–2.81 (second order m, 4H), 2.06–2.01 (m, 4H), 1.98–1.93 (m, 4H), 1.89–1.83 (m, 4H), 1.76–1.70 (m, 4H).

<sup>13</sup>C{<sup>1</sup>H} NMR (CDCl<sub>3</sub>, 176 MHz): δ 136.7, 136.5, 136.4, 134.3, 132.0, 131.9, 131.3, 131.2, 130.8, 130.7, 129.7, 129.7, 128.1, 128.1, 126.6, 126.6, 126.5, 126.1, 126.1, 126.0, 125.9, 125.9, 124.8, 124.6, 124.4, 124.3, 123.3, 123.2, 122.5, 122.4, 33.3, 33.2, 31.8, 31.4, 30.9, 30.9, 30.5, 29.2.

**MALDI HRMS** (DCTB)  $m/z$  calcd for  $C_{82}H_{72}$  ( $M^+$ ) 1056.5634, found 1056.5631.

**EA** anal. calcd for  $C_{82}H_{72}$ : C, 93.14; H, 6.86. Found: C, 91.01; H, 6.87. Repeat found: C, 91.08; H, 6.89.

**1,2,3,4-Tetra[4-(9-phenanthrene)butyl]anthracene (266)**



The general procedure D was used with naphthalene-2-boronic acid pinacol ester **267** (36 mg, 0.14 mmol), 1,10-di(9-phenanthrene)-5-decyne **240** (70 mg, 0.14 mmol),  $[Cp^*RhCl_2]_2$  (4.4 mg, 5 mol%),  $Cu(OAc)_2 \cdot H_2O$  (29 mg, 0.14 mmol), and DMF (3 mL). The crude material was purified by silica column chromatography (hexane/ $CH_2Cl_2$  4:1) to afford compound **266** as a yellow solid (46 mg, 58%).  $R_f$  = 0.26 ( $SiO_2$ ; hexane/ $CH_2Cl_2$  2:1).

**$^1H$  NMR** ( $CDCl_3$ , 700 MHz):  $\delta$  8.74 (dd,  $J$  = 7.8 Hz, 1.5 Hz, 2H), 8.65 (d,  $J$  = 8.3 Hz, 4H), 8.58 (d,  $J$  = 8.1 Hz, 2H), 8.54 (s, 2H), 8.14 (dd,  $J$  = 7.7 Hz, 1.7 Hz, 2H), 8.06 (d,  $J$  = 8.2 Hz, 2H), 7.93–7.91 (second order m, 2H), 7.79 (d,  $J$  = 7.8 Hz, 2H), 7.74 (d,  $J$  = 7.9 Hz, 2H), 7.66–7.48 (m, 20H), 7.44–7.41 (second order m, 2H), 3.30–3.25 (second order m, 4H), 3.21–3.18 (m, 4H),

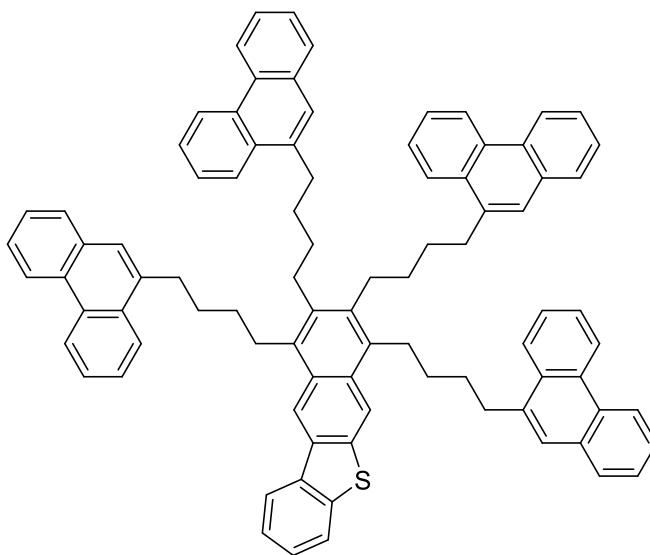
3.13–3.10 (m, 4H), 2.91–2.86 (second order m, 4H), 2.13–2.08 (m, 4H), 2.00–1.92 (m, 8H), 1.80–1.74 (m, 4H).

$^{13}\text{C}\{^1\text{H}\}$  NMR ( $\text{CDCl}_3$ , 176 MHz): 136.6, 136.4, 136.3, 133.7, 132.0, 131.9, 131.3, 131.2, 130.9, 130.8, 130.7, 130.2, 129.7, 129.7, 128.3, 128.1, 128.1, 126.6, 126.6, 126.5, 126.2, 126.1, 126.1, 126.0, 125.9, 125.9, 124.9, 124.4, 124.3, 123.3, 123.2, 122.9, 122.5, 122.4, 33.3, 33.2, 31.7, 31.3, 30.9, 30.7, 29.4.

**MALDI HRMS** (DCTB)  $m/z$  calcd for  $\text{C}_{86}\text{H}_{74}$  ( $\text{M}^+$ ) 1106.5791, found 1106.5781.

**EA** anal. calcd for  $\text{C}_{86}\text{H}_{74}$ : C, 93.27; H, 6.73. Found: C, 91.00; H, 6.89. Repeat found: C, 90.66; H, 6.93.

**7,8,9,10-Tetra[4-(9-phenanthrene)butyl]benzo[*b*]naphtho[2,3-*d*]thiophene (280)**



The general procedure D was used with 2-(dibenzo[*b,d*]thiophen-2-yl)-4,4,5,5-tetramethyl-1,3,2-dioxaborolane **276** (44 mg, 0.14 mmol), 1,10-di(9-phenanthrene)-5-decyne **240** (70 mg, 0.14 mmol),  $[\text{Cp}^*\text{RhCl}_2]_2$  (4.4 mg, 5 mol%),  $\text{Cu}(\text{OAc})_2 \cdot \text{H}_2\text{O}$  (29 mg, 0.14 mmol), and DMF (3 mL).

The crude material was purified by silica column chromatography (hexane/CH<sub>2</sub>Cl<sub>2</sub> 4:1) to afford compound **280** as a white solid (44 mg, 52%). *R*<sub>f</sub> = 0.32 (SiO<sub>2</sub>, hexane/CH<sub>2</sub>Cl<sub>2</sub> 2:1).

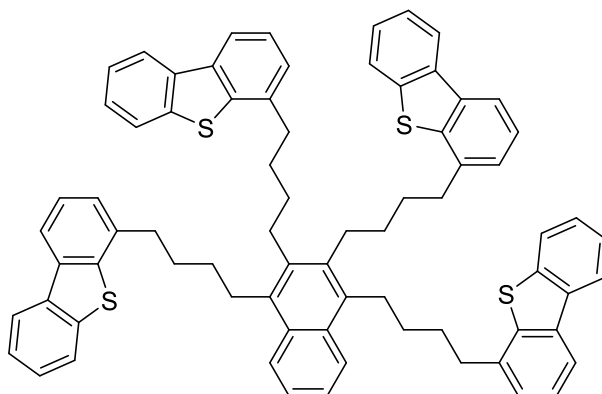
**<sup>1</sup>H NMR** (CDCl<sub>3</sub>, 700 MHz): δ 8.77 (s, 1H), 8.75–8.71 (m, 2H), 8.66–8.63 (m, 4H), 8.59–8.56 (m, 2H), 8.45 (s, 1H), 8.16–8.11 (m, 3H), 8.05 (t, *J* = 8.3 Hz, 2H), 7.84 (d, *J* = 7.7 Hz, 1H), 7.80 (d, *J* = 7.0 Hz, 1H), 7.77 (d, *J* = 7.2 Hz, 1H), 7.75–7.72 (m, 2H), 7.66–7.42 (m, 22H), 3.30–3.26 (second order m, 2H), 3.22–3.16 (m, 6H), 3.13–3.08 (m, 4H), 2.90–2.85 (m, 4H), 2.14–2.04 (m, 4H), 2.00–1.89 (m, 8H), 1.79–1.72 (m, 4H).

**<sup>13</sup>C{<sup>1</sup>H} NMR** (CDCl<sub>3</sub>, 176 MHz): δ 140.3, 137.1, 136.8, 136.5, 136.5, 136.3, 136.1, 135.7, 134.4, 133.9, 133.2, 132.0, 131.9, 131.9, 131.3, 131.2, 131.0, 130.8, 130.8, 130.7, 129.7, 129.7, 128.9, 128.1, 128.1, 127.4, 126.6, 126.6, 126.5, 126.2, 126.2, 126.1, 126.1, 126.0, 125.9, 124.5, 124.4, 124.4, 124.3, 123.3, 123.3, 123.2, 122.9, 122.5, 122.5, 121.6, 117.4, 116.7, 33.3, 33.3, 33.2, 31.8, 31.7, 31.6, 31.4, 30.9, 30.9, 30.7, 30.7, 29.5, 29.4.

**MALDI HRMS** (DCTB) *m/z* calcd for C<sub>88</sub>H<sub>74</sub>S (M<sup>+</sup>) 1162.5511, found 1162.5500.

**EA** anal. calcd for C<sub>88</sub>H<sub>74</sub>S: C, 90.83; H, 6.41; S, 2.76. Found: C, 89.67; H, 6.43; S, 2.73. Repeat found: C, 89.74; H, 6.45; S, 2.76.

### 1,2,3,4-Tetra[4-(4-dibenzothiophene)butyl]naphthalene (**278**)





Phenyl boronic acid pinacol ester **270** (507 mg, 2.48 mmol), 1,10-di(4-dibenzothiophene)-5-decyne **248** (1.250 g, 2.486 mmol), [Cp\*RhCl<sub>2</sub>]<sub>2</sub> (77 mg, 5 mol%), and Cu(OAc)<sub>2</sub>·H<sub>2</sub>O (496 mg, 2.48 mmol) were placed in a dry 50 mL Schlenk flask with a magnetic stir bar. The reaction flask was charged with nitrogen and dry DMF (20 mL) was added through Schlenk line techniques. The reaction mixture was heated to 70 °C for 2 d and was quenched with water (50 mL). The aqueous solution was extracted with CH<sub>2</sub>Cl<sub>2</sub> (3 times, 50 mL each) and dried over Na<sub>2</sub>SO<sub>4</sub>. The mixture was filtered, and the solvent was removed under reduced pressure. The residual was purified by silica column chromatography (hexane/CH<sub>2</sub>Cl<sub>2</sub> 4:1) to afford compound **278** as a white solid (1.125 g, 84%). *R*<sub>f</sub> = 0.43 (SiO<sub>2</sub>; hexane/CH<sub>2</sub>Cl<sub>2</sub> 2:1).

**<sup>1</sup>H NMR** (CD<sub>2</sub>Cl<sub>2</sub>, 700 MHz): δ 8.16–8.13 (m, 2H), 8.10 (d, *J* = 7.8 Hz, 2H), 8.03 (d, *J* = 7.8 Hz, 2H), 8.00–7.96 (m, 4H), 7.81 (dd, *J* = 6.9 Hz, 1.5 Hz, 2H), 7.70 (d, *J* = 7.8 Hz, 2H), 7.46–7.35 (m, 14H), 7.31 (d, *J* = 6.9 Hz, 2H), 7.28 (d, *J* = 7.2 Hz, 2H), 3.14–3.09 (second order m, 4H), 3.01–2.95 (m, 8H), 2.88–2.83 (second order m, 4H), 2.10–1.99 (m, 8H), 1.80–1.74 (m, 4H), 1.72–1.66 (m, 4H).

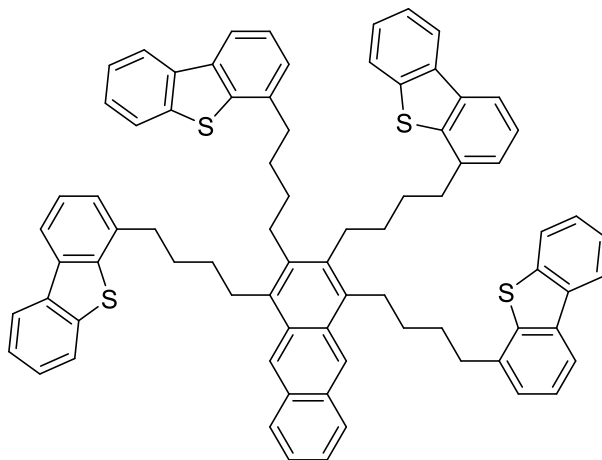
**<sup>13</sup>C{<sup>1</sup>H} NMR** (CD<sub>2</sub>Cl<sub>2</sub>, 176 MHz): δ 139.5, 139.4, 139.4, 137.2, 137.1, 137.1, 136.5, 136.5, 136.0, 136.0, 134.6, 131.6, 127.0, 126.9, 126.5, 126.4, 125.2, 125.2, 124.9, 124.8, 124.7, 124.6, 123.1, 123.1, 122.0, 122.0, 119.6, 119.6, 35.3, 35.2, 31.8, 31.5, 30.6, 30.1, 30.0, 29.3.

**MALDI HRMS** (DCTB) *m/z* calcd for C<sub>74</sub>H<sub>64</sub>S<sub>4</sub> (M<sup>+</sup>) 1080.3891, found 1080.3880.

**EA** anal. calcd for C<sub>74</sub>H<sub>64</sub>S<sub>4</sub>: C, 82.18; H, 5.96; S, 11.86. Found: C, 82.17; H, 6.24; S, 11.93.

Repeat found: C, 82.27; H, 6.30; S, 12.11.

### 1,2,3,4-Tetra[4-(4-dibenzothiophene)butyl]anthracene (**268**)



The general procedure D was used with naphthalene-2-boronic acid pinacol ester **267** (35 mg, 0.14 mmol), 1,10-di(4-dibenzothiophene)-5-decyne **248** (70 mg, 0.14 mmol), [Cp\*RhCl<sub>2</sub>]<sub>2</sub> (4.3 mg, 5 mol%), Cu(OAc)<sub>2</sub>·H<sub>2</sub>O (28 mg, 0.14 mmol), and DMF (3 mL). The crude material was purified by silica column chromatography (hexane/CH<sub>2</sub>Cl<sub>2</sub> 4:1) to afford compound **268** as a yellow solid (62 mg, 79%). *R*<sub>f</sub> = 0.37 (SiO<sub>2</sub>; hexane/CH<sub>2</sub>Cl<sub>2</sub> 2:1).

**<sup>1</sup>H NMR** (CD<sub>2</sub>Cl<sub>2</sub>, 700 MHz): δ 8.49 (s, 2H), 8.16–8.13 (m, 2H), 8.10 (d, *J* = 7.6 Hz, 2H), 8.02 (d, *J* = 7.8 Hz, 2H), 7.99 (d, *J* = 7.8 Hz, 2H), 7.90–7.88 (second order m, 2H), 7.84–7.81 (m, 2H), 7.70 (d, *J* = 7.8 Hz, 2H), 7.47–7.35 (m, 14H), 7.33 (d, *J* = 7.3 Hz, 2H), 7.28 (d, *J* = 7.2 Hz, 2H), 3.26–3.22 (second order m, 4H), 3.04–3.01 (m, 4H), 2.99–2.96 (m, 4H), 2.91–2.87 (second order m, 4H), 2.15–2.10 (m, 4H), 2.05–1.99 (m, 4H), 1.88–1.82 (m, 4H), 1.76–1.70 (m, 4H).

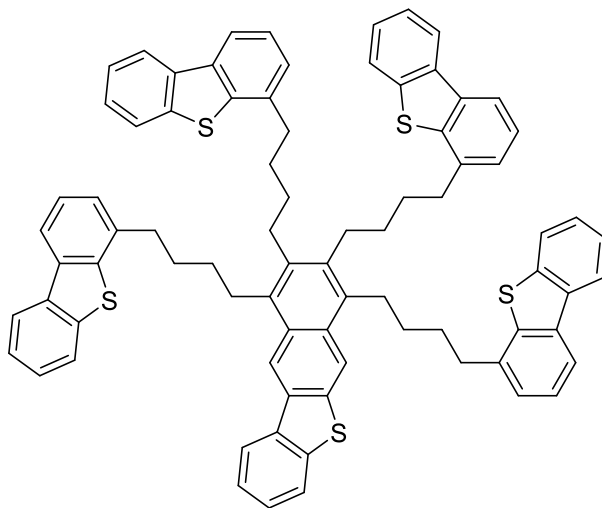
**<sup>13</sup>C{<sup>1</sup>H} NMR** (CD<sub>2</sub>Cl<sub>2</sub>, 176 MHz): δ 139.5, 139.4, 139.4, 137.2, 137.1, 136.8, 136.5, 136.5, 136.0, 136.0, 134.1, 131.1, 130.6, 128.5, 127.0, 126.9, 126.5, 126.5, 125.2, 125.2, 125.2, 124.7, 124.7, 123.1, 123.1, 123.1, 122.1, 122.0, 119.6, 119.6, 35.2, 35.2, 31.7, 31.2, 30.8, 30.1, 30.0, 29.5.

**MALDI HRMS** (DCTB)  $m/z$  calcd for  $C_{78}H_{66}S_4$  ( $M^+$ ) 1130.4047, found 1130.4031.

**EA** anal. calcd for  $C_{78}H_{66}S_4$ : C, 82.79; H, 5.88; S, 11.33. Found: C, 81.97; H, 5.93; S, 11.06.

Repeat found: C, 82.14; H, 5.96; S, 11.26.

**7,8,9,10-Tetra[4-(4-dibenzothiophene)butyl]benzo[*b*]naphtho[2,3-*d*]thiophene (281)**



The general procedure D was used with 2-(dibenzo[*b,d*]thiophen-2-yl)-4,4,5,5-tetramethyl-1,3,2-dioxaborolane **276** (43 mg, 0.14 mmol), 1,10-di(4-dibenzothiophene)-5-decyne **248** (70 mg, 0.14 mmol),  $[Cp^*RhCl_2]_2$  (4.3 mg, 5 mol%),  $Cu(OAc)_2 \cdot H_2O$  (28 mg, 0.14 mmol), and DMF (3 mL). The crude material was purified by silica column chromatography (hexane/ $CH_2Cl_2$  4:1) to afford compound **281** as a white solid (54 mg, 65%).  $R_f$  = 0.35 ( $SiO_2$ ; hexane/ $CH_2Cl_2$  2:1).

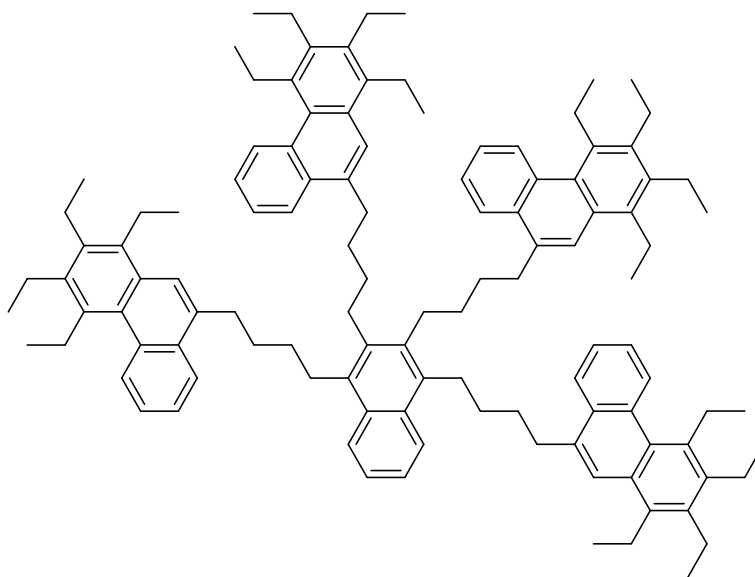
**$^1H$  NMR** ( $CD_2Cl_2$ , 700 MHz):  $\delta$  8.72 (s, 1H), 8.39 (s, 1H), 8.16–8.12 (m, 3H), 8.11–8.09 (m, 2H), 8.03–7.97 (m, 4H), 7.84–7.80 (m, 3H), 7.70 (t,  $J$  = 8.3 Hz, 2H), 7.49–7.31 (m, 16H), 7.28 (t,  $J$  = 6.9 Hz, 2H), 3.27–3.23 (second order m, 2H), 3.18–3.14 (second order m, 2H), 3.06–2.95 (m, 8H), 2.91–2.86 (m, 4H), 2.16–2.06 (m, 4H), 2.05–1.98 (m, 4H), 1.90–1.79 (m, 4H), 1.76–1.69 (m, 4H).

$^{13}\text{C}\{^1\text{H}\}$  NMR ( $\text{CD}_2\text{Cl}_2$ , 176 MHz):  $\delta$  140.5, 139.5, 139.4, 139.4, 137.6, 137.1, 137.1, 136.9, 136.6, 136.5, 136.5, 136.0, 136.0, 135.9, 134.8, 134.0, 133.5, 131.3, 129.2, 127.7, 127.0, 127.0, 126.9, 126.5, 126.5, 126.5, 125.2, 125.2, 124.8, 124.7, 124.7, 124.7, 123.1, 123.1, 123.1, 122.1, 122.0, 122.0, 119.7, 119.6, 117.7, 117.0, 35.2, 35.2, 31.8, 31.7, 31.5, 31.3, 30.8, 30.8, 30.1, 30.0, 29.9, 29.6.

**MALDI HRMS** (DCTB)  $m/z$  calcd for  $\text{C}_{80}\text{H}_{66}\text{S}_5$  ( $\text{M}^+$ ) 1186.3768, found 1186.3757.

**EA** anal. calcd for  $\text{C}_{80}\text{H}_{66}\text{S}_5$ : C, 80.90; H, 5.60; S, 13.50. Found: C, 80.88; H, 5.66; S, 13.77.  
Repeat found: C, 80.90; H, 5.70; S, 14.06.

**1,2,3,4-Tetra{4-[9-(1,2,3,4-tetraethylphenanthrene)]butyl}naphthalene (279)**



The general procedure D was used with phenyl boronic acid pinacol ester **270** (22 mg, 0.11 mmol), 1,10-di[9-(1,2,3,4-tetraethylphenanthrene)]-5-decyne **254** (76 mg, 0.11 mmol),  $[\text{Cp}^*\text{RhCl}_2]_2$  (3.3 mg, 5 mol%),  $\text{Cu}(\text{OAc})_2 \cdot \text{H}_2\text{O}$  (21 mg, 0.11 mmol), and DMF (3 mL). The

crude material was purified by silica column chromatography (hexane/CH<sub>2</sub>Cl<sub>2</sub> 3:1) to afford compound **279** as a yellow solid (56 mg, 70%). *R*<sub>f</sub> = 0.32 (hexane/CH<sub>2</sub>Cl<sub>2</sub> 2:1).

**<sup>1</sup>H NMR** (CDCl<sub>3</sub>, 700 MHz): δ 8.64 (d, *J* = 8.3 Hz, 2H), 8.60–8.57 (m, 2H), 8.09 (d, *J* = 7.8 Hz, 2H), 8.05–8.01 (m, 4H), 7.80 (s, 2H), 7.75 (s, 2H), 7.53 (t, *J* = 7.2 Hz, 2H), 7.50 (t, *J* = 7.3 Hz, 2H), 7.41–7.35 (m, 6H), 3.42–3.24 (br, 8H), 3.22–2.88 (m, 40H), 2.10–1.98 (m, 8H), 1.93–1.87 (m, 4H), 1.85–1.79 (m, 4H), 1.67–1.60 (m, 12H), 1.36–1.23 (m, 36H).

**<sup>13</sup>C{<sup>1</sup>H} NMR** (CDCl<sub>3</sub>, 176 MHz): δ 140.2, 140.1, 138.7, 138.6, 136.8, 136.3, 136.2, 135.4, 135.4, 134.8, 134.7, 134.3, 131.9, 131.8, 131.7, 131.7, 131.3, 129.9, 129.8, 129.6, 129.5, 128.3, 128.3, 125.4, 124.6, 123.9, 123.9, 123.6, 123.4, 122.6, 122.6, 33.7, 32.1, 31.6, 31.2, 31.0, 30.6, 29.2, 25.4, 22.7, 22.7, 22.6, 22.2, 22.1, 16.5, 16.5, 16.2, 16.0, 16.0.

**MALDI HRMS** (DCTB) *m/z* calcd for C<sub>113</sub>H<sub>136</sub><sup>13</sup>C (M<sup>+</sup>): 1506.0676, found 1506.0679.

**EA** anal. calcd for C<sub>114</sub>H<sub>136</sub>: C, 90.90; H, 9.10. Found: C, 83.10; H, 8.49. Repeat found: C, 83.54; H, 8.50.

## 4. Synthesis of Cationic Nitrogen-containing Archipelago

### Compounds by Rhodium-catalyzed Arene/Alkyne Annulations

Nitrogen-embedded PAHs are a series of cationic derivatives of *N*-heterocyclic aromatic compounds. Representative examples of cationic nitrogen-embedded PAHs are quinolinium, isoquinolinium, quinolizinium and benzoquinolizinium salts (Figure 4-1). These structures and their analogues are important motifs found in natural alkaloids,<sup>201,202</sup> and are widely utilized in many areas such as ionic liquids,<sup>203-206</sup> fluorescent dyes,<sup>207-209</sup> and DNA intercalators.<sup>210-212</sup>

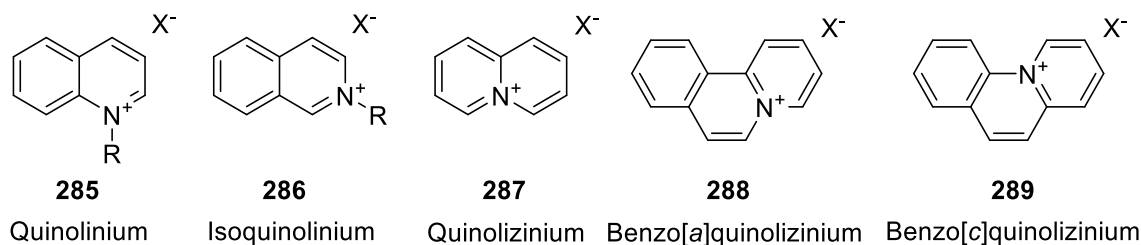


**Figure 4-1.** Examples for cationic nitrogen-embedded PAHs.

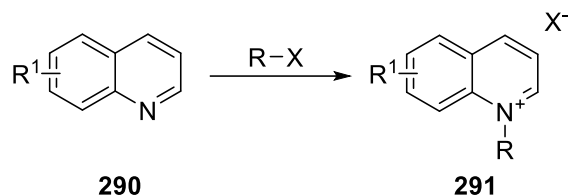
In this chapter, asphaltene archipelago compounds with cationic nitrogen are prepared by [4+2] annulations of nitrogen-containing substrates and alkynes. I expected that these products could not only be utilized as a new category of asphaltene models, but also have potential application prospects in other fields.

#### 4.1 Synthetic approaches to cationic nitrogen-embedded PAHs

In addition to the annulation reactions introduced in section 1.4.2, many unrelated synthetic approaches have also been developed to obtain nitrogen-embedded PAHs. Some examples are illustrated and discussed below.

#### 4.1.1 Synthetic approaches to quinolinium and isoquinolinium motifs

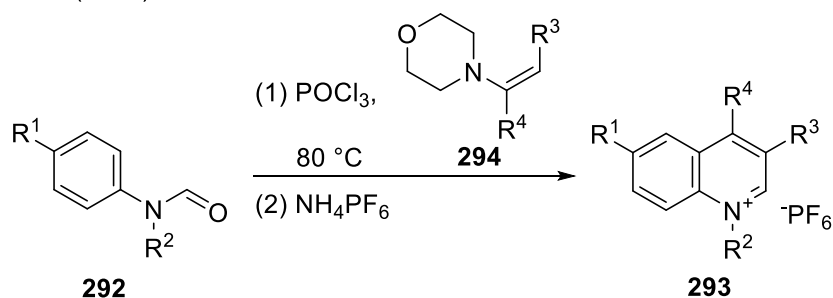
To prepare quinolinium salts **291**, one of the traditional methods is to alkylate the quinoline using simple alkyl halides (Equation 4-1).<sup>213,214</sup>



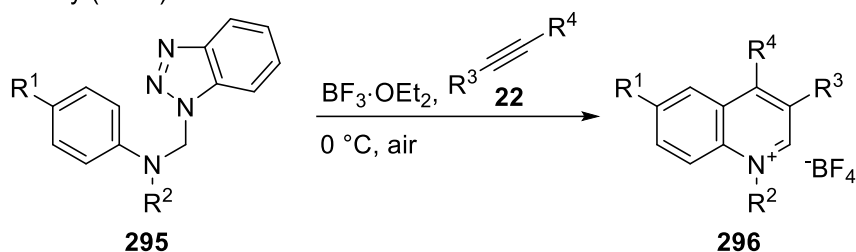
**Equation 4-1.** Quinolinium salt preparation by reaction of quinoline with alkyl halide.<sup>213,214</sup>

Although this method is simple, it requires a synthetic quinoline, which adds an extra step and limits the scope of quinolinium synthesis. Several direct approaches have been reported to make the synthesis of quinolinium salts more convenient and efficient. Examples are described by Meth-Cohn,<sup>215</sup> Katritzky,<sup>216</sup> Wang,<sup>217</sup> and Cheng,<sup>218</sup> using *N*-substituted aniline (**292**, **295**, **300**) or aryl azide substrates **297** (Scheme 4-1).

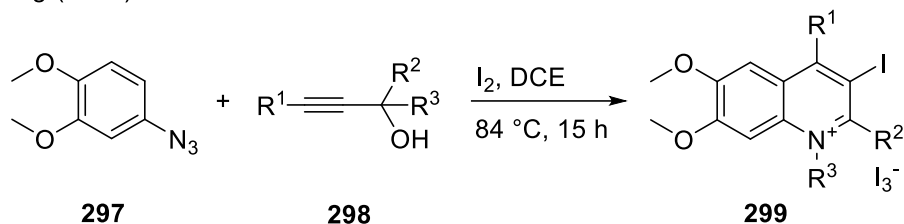
Meth-Cohn (1995):



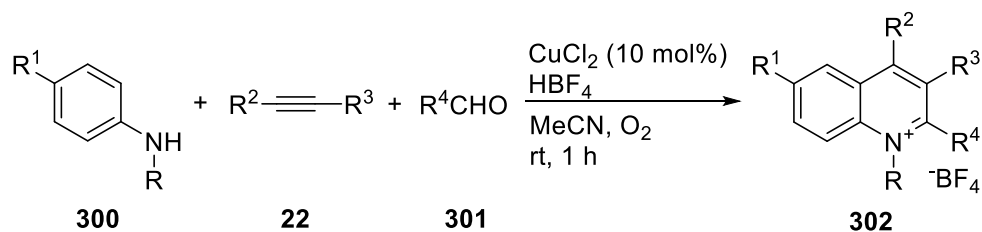
Katritzky (1998):



Wang (2017):



Cheng (2020):



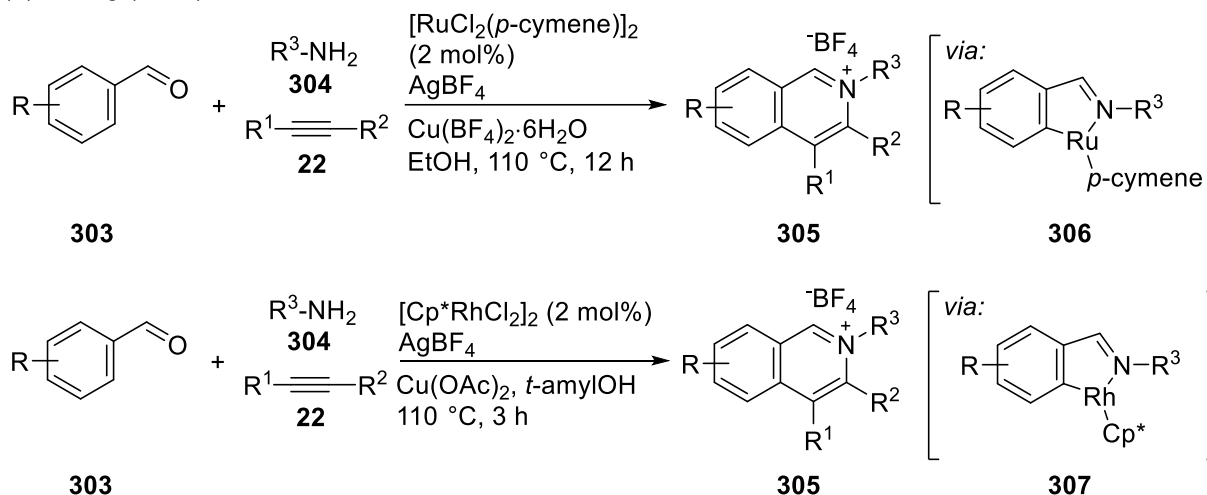
**Scheme 4-1.** Direct syntheses of quinolinium motifs.<sup>215-218</sup>

Similar to quinolinium salts, isoquinolinium cations can also be obtained by alkylation using a corresponding isoquinoline.<sup>214,219</sup> One-pot syntheses were achieved by ruthenium- or rhodium-catalyzed [4+2] alkyne annulations, as reported by Cheng and co-workers (Scheme 4-2a).<sup>220,221</sup>

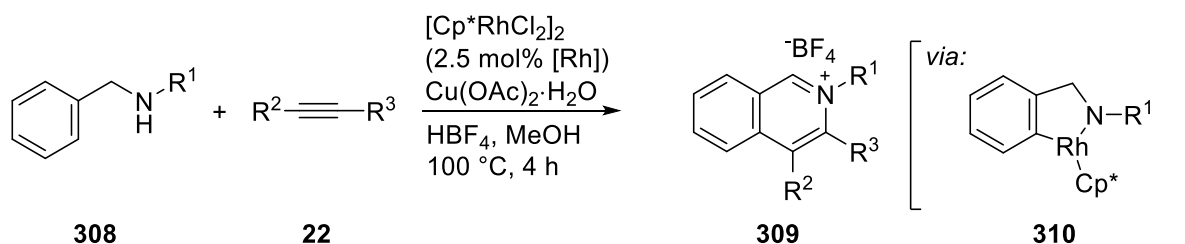


Another rhodium-catalyzed annulation example was provided by Jun *et al.*, using secondary benzylamines **308** as substrates (Scheme 4-2b).<sup>222</sup> The authors proposed that the catalytic cycle generates an intermediate 1,2-dihydroisoquinoline, which is oxidized by Cu(OAc)<sub>2</sub> and HBF<sub>4</sub> to form the isoquinolinium salt **309**.<sup>222</sup>

(a) Cheng (2012):



(b) Jun (2013):



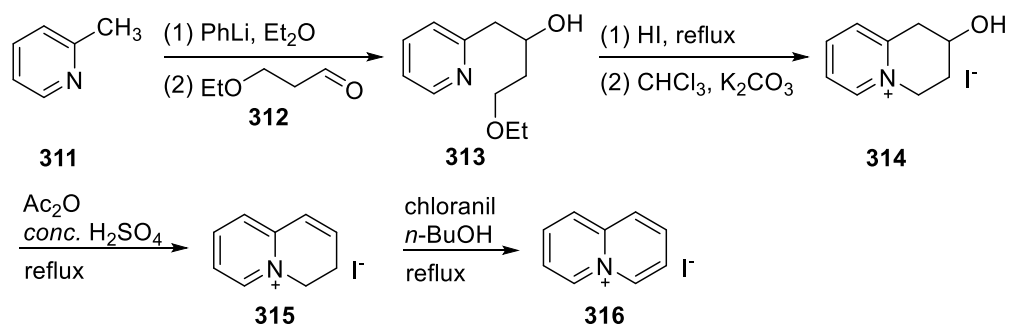
**Scheme 4-2.** Synthesis of isoquinolinium salts by [4+2] alkyne annulation reactions.<sup>220-222</sup>

#### 4.1.2 Synthetic approaches to quinolizinium and benzoquinolizinium motifs

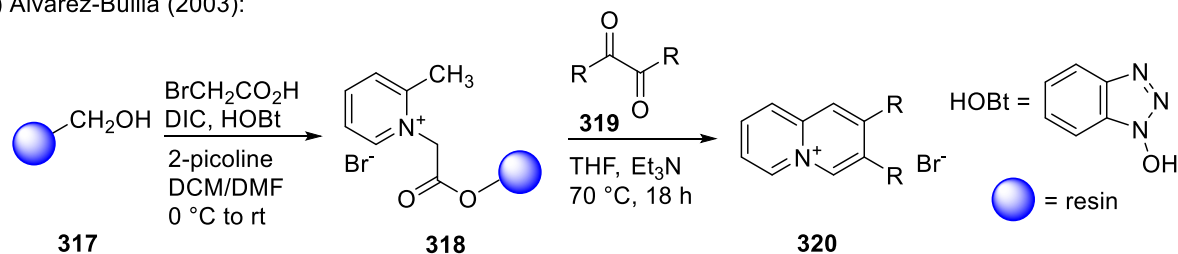
Unlike quinolinium or isoquinolinium salts, quinolizinium or benzoquinolizinium salts cannot be generated by simple alkylation. The first synthesis of quinolizinium ring system was achieved by Boekelheide in 1954 (Scheme 4-3a).<sup>223</sup> Other synthetic approaches have also been developed,

including [4+2] cyclizations by Alvarez-Builla, Cuadro (Schemes 4-3b and 4-3c),<sup>224,225</sup> ring-closing metathesis (RCM) by Cuadro (Scheme 4-3d)<sup>226</sup> and [4+2] alkyne annulation by Cheng (Scheme 4-3e).<sup>127</sup>

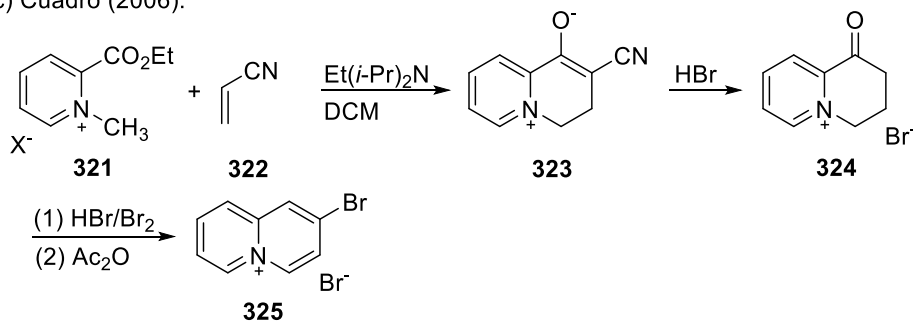
(a) Boekelheide (1954):



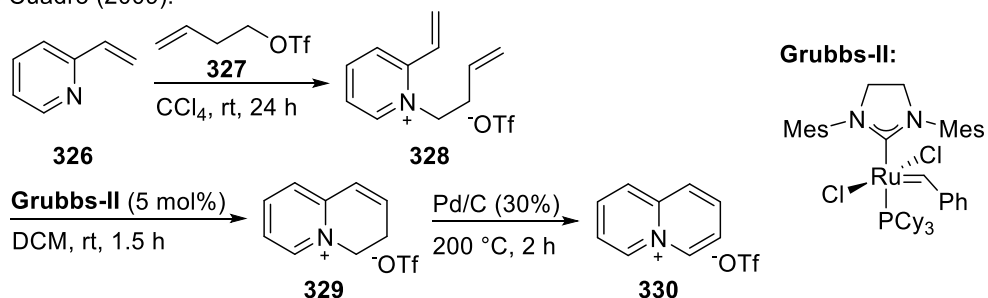
(b) Alvarez-Builla (2003):



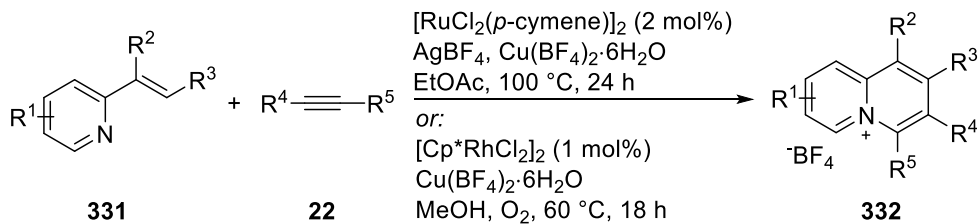
(c) Cuadro (2006):



(d) Cuadro (2009):



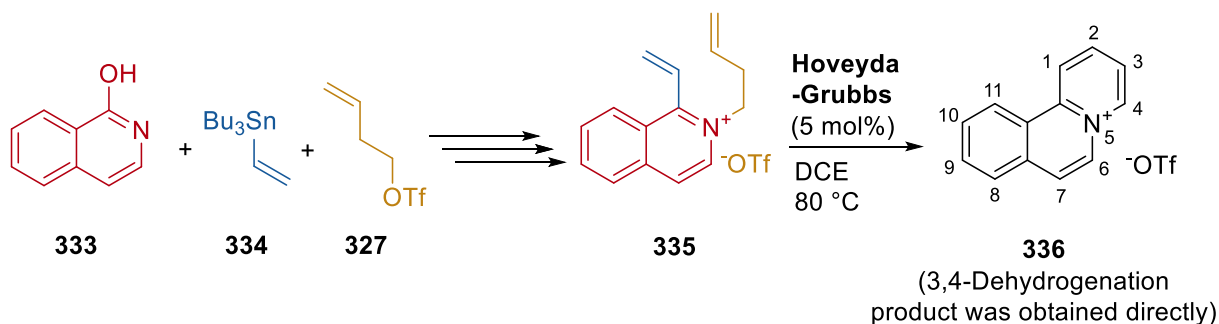
(e) Cheng (2013):



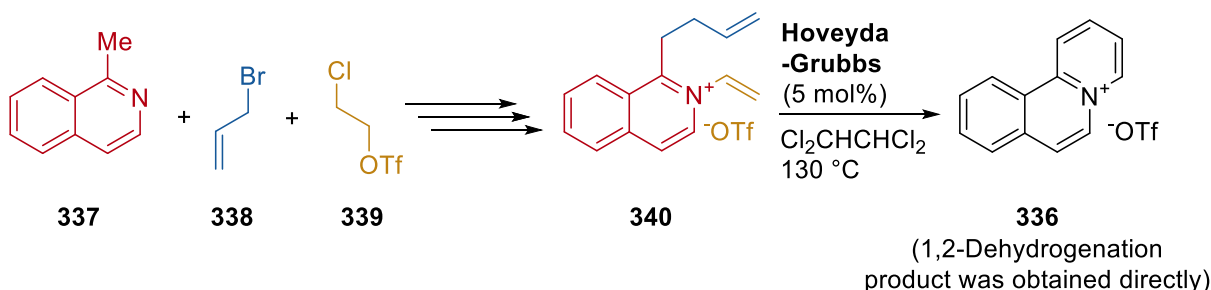
**Scheme 4-3.** Syntheses of quinolinizinium motifs.<sup>127, 223-226</sup>

Traditional syntheses of benzo[*a*]quinolizinium salts were achieved by dozens of cyclization routes, but almost all require multiple steps and harsh conditions.<sup>227-230</sup> To be more efficient, Cuadro and co-workers explored three RCM routes to prepare benzo[*a*]quinolizinium motifs and found that C6-C7 metathesis gives the highest overall yield (Scheme 4-4).<sup>231,232</sup>

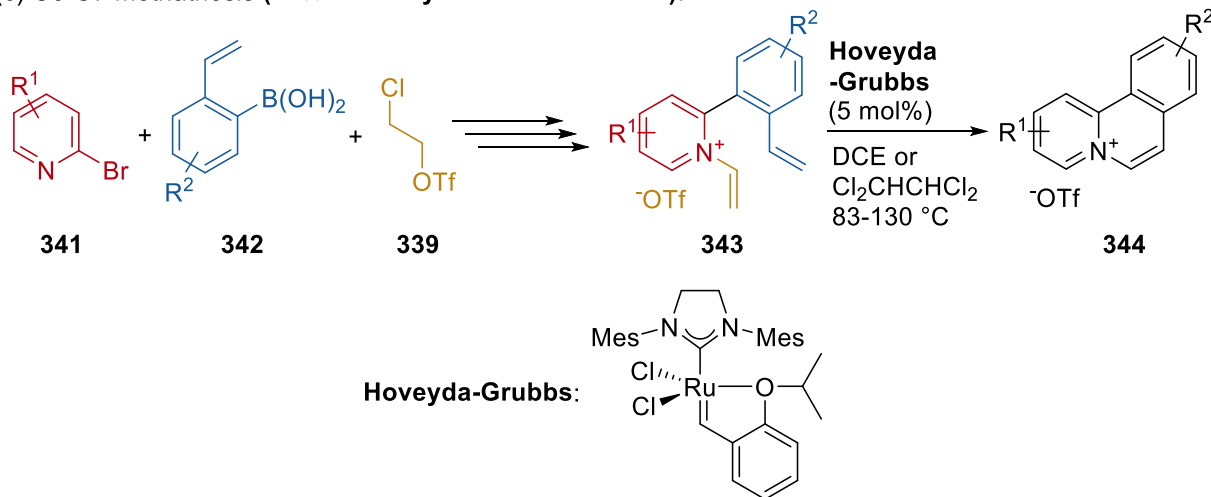
(a) C1-C2 metathesis (**25% overall yield**)



(b) C3-C4 metathesis (**11% overall yield**):

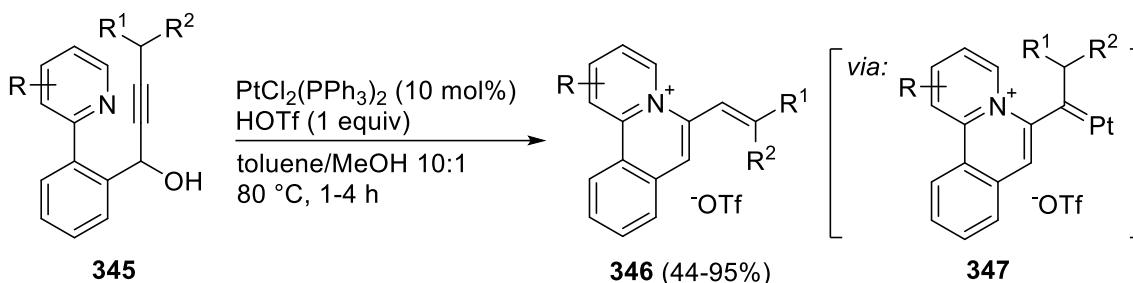


(c) C6-C7 methathesis (**39% overall yield for R<sup>1</sup> = R<sup>2</sup> = H**):



**Scheme 4-4.** Synthesis of benzo[*a*]quinolizinium motifs via three RCM routes by Cuadro and co-workers.<sup>232</sup>

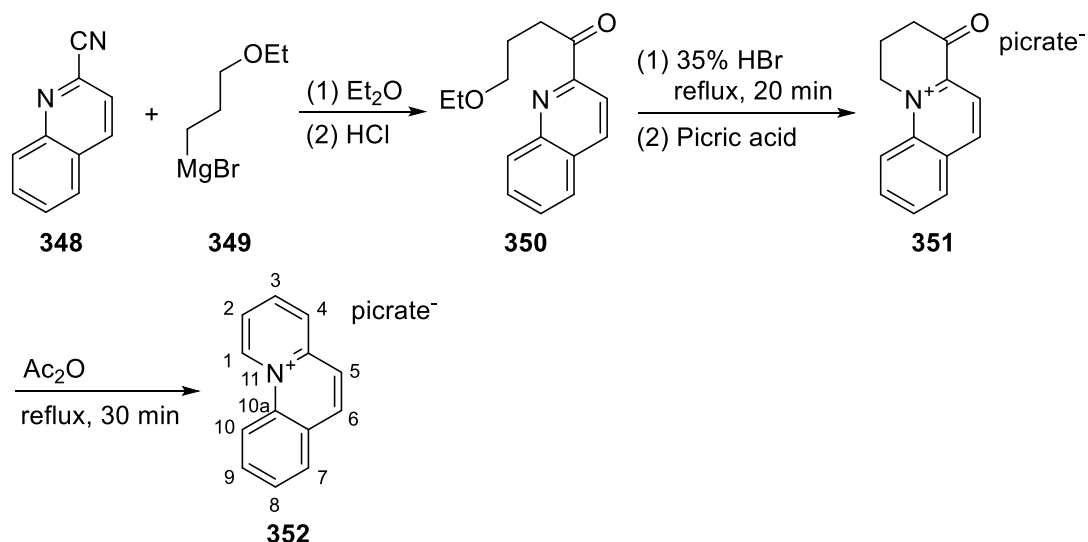
In 2018, Kim and co-workers reported a platinum-catalyzed intramolecular cyclization for preparing benzo[*a*]quinolizinium salts (Equation 4-2).<sup>233</sup> The authors proposed that the reaction proceeds through a platinum-carbene intermediate **347**.<sup>233</sup> In contrast to 2-phenylpyridine/alkyne annulations (Schemes 1-10 and 1-11), this methodology produces benzo[*a*]quinolizinium structures with only one substituent, which is on the 6-position.



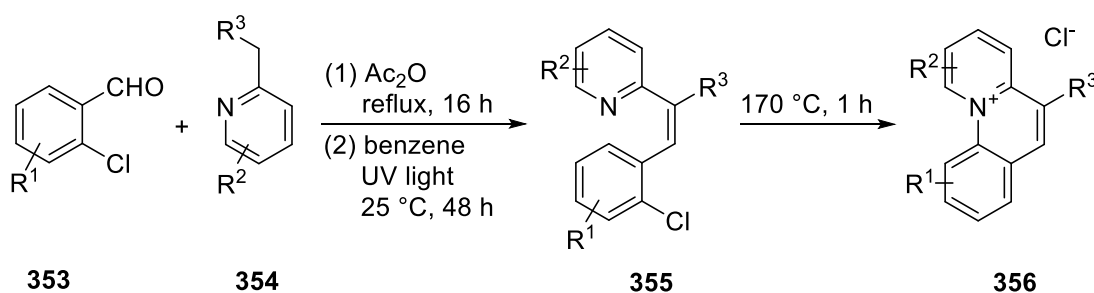
**Equation 4-2.** Synthesis of benzo[*a*]quinolizinium motif by platinum-catalyzed intramolecular cyclization.<sup>233</sup>

Compared with benzo[*a*]quinolizinium motifs, there are fewer reports on the synthesis of the benzo[*c*]quinolizinium ring systems (Scheme 4-5). Early syntheses of benzo[*c*]quinolizinium structures were completed by formation of the C1-N11 (Scheme 4-5a)<sup>234</sup> or C10a-N11 bonds (Scheme 4-5b).<sup>235</sup> In 2013, Cheng and co-workers prepared a 1,2-diphenyl substituted benzo[*c*]quinolizinium salt **358** by [4+2] annulation of 2-vinylquinoline **357** with diphenylacetylene (Scheme 4-5c),<sup>127</sup> but they did not provide additional examples using other alkynes or substituted 2-vinylquinolines.

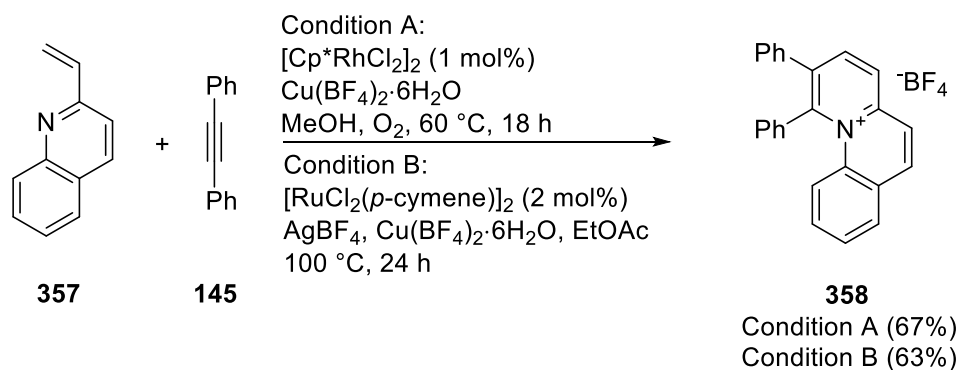
(a) Jones (1958):



(b) Bradsher (1966):



(c) Cheng (2013):



**Scheme 4-5.** Synthetic approaches to benzo[*c*]quinolizinium motifs.<sup>127,234,235</sup>

From the literature reviewed above, it can be seen that alkyne annulations are superior to most of the other approaches to prepare nitrogen-embedded PAHs, especially for benzoquinolizinium

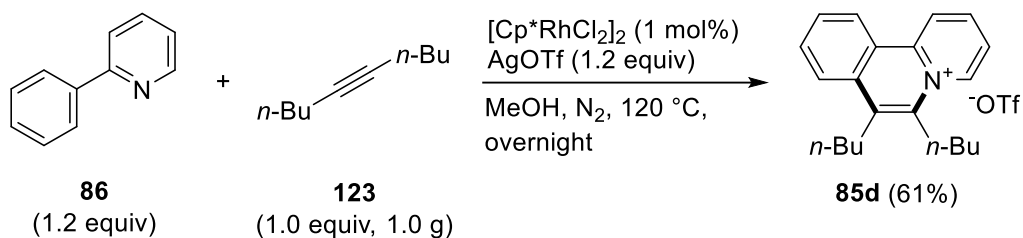
salts, because alkyne annulations use readily available starting substrates and complete the synthesis in one step under relatively mild reaction conditions.

## *Results and Discussions*

### **4.2 The synthesis of archipelago compounds by [4+2] annulations of 2-phenylpyridine with alkynes**

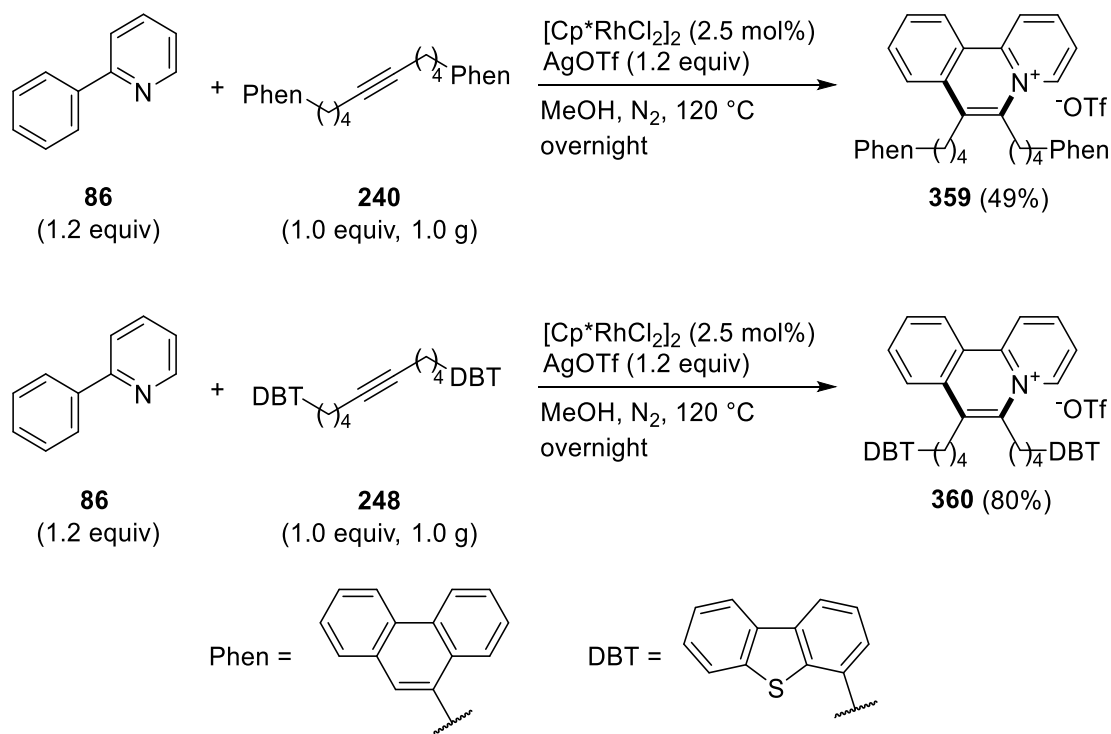
As described in section 1.4.2, [4+2] annulations of 2-phenylpyridine and alkyne afford adducts containing benzo[*a*]quinolizinium backbones (Schemes 1-10, 1-11).<sup>116,117</sup> If island-tethered alkynes are used, I anticipated obtaining archipelago model compounds incorporating cationic nitrogen. These compounds should have obviously increased polarities than the neutral archipelago compounds reported in chapter 3. Therefore, they could represent asphaltenes with strong acid-base interactions and create a new library of model compounds.

In an initial attempt, 2-phenylpyridine **86** and 5-decyne were chosen as substrates, leading to a benzo[*a*]quinolizinium adduct, using Huang's annulation.<sup>116</sup> Considering that triflic acid (HOTf) is strongly acidic and corrosive, silver triflate was added instead as the source of triflate anion. Adduct **85d** was obtained in 61% yield on a 1 g scale (Equation 4-3), which is a much larger scale than reported in Huang and co-workers' original report.



**Equation 4-3.** Rhodium-catalyzed [4+2] annulation of 2-phenylpyridine with 5-decyne.

Subsequently, couplings of 2-phenylpyridine **86** with two island-tethered alkynes (**240**, **248**) were conducted, using the same reaction conditions, except that 2.5 mol% of  $[\text{Cp}^*\text{RhCl}_2]_2$  was used to improve the yields. The reactions afford three-island archipelago compounds **359** and **360** in 49% and 80% yields, respectively (Scheme 4-6).

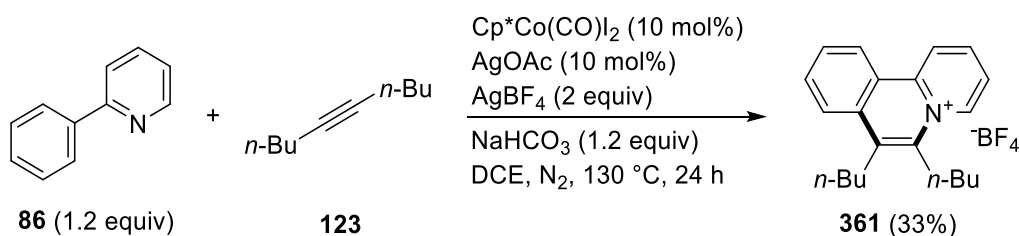


**Scheme 4-6.** Rhodium-catalyzed [4+2] annulations of 2-phenylpyridine with island-tethered alkynes.



All three benzo[*a*]quinolizinium adducts (**85d**, **359**, **360**) were purified by column chromatography on flash silica gel using CH<sub>2</sub>Cl<sub>2</sub>/MeOH as eluent. They are more polar than the archipelago compounds in chapter 3, which were purified using hexane/CH<sub>2</sub>Cl<sub>2</sub> as eluent. Non-chromatographic purification by washing the crude product with a hexane/Et<sub>2</sub>O/MeOH mixture, which was introduced in Huang's paper, does not fully separate the adduct from the residual alkyne.

The cobalt-catalyzed [4+2] annulation reported by Cheng and co-workers<sup>117</sup> was also tested using 5-decyne (Equation 4-4). The benzo[*a*]quinolizinium compound **361** was obtained in a modest 33% yield using Cp\*Co(CO)I<sub>2</sub> as the pre-catalyst. So, this strategy is not an efficient way to prepare benzo[*a*]quinolizinium archipelago compounds. A similarly low yield was observed in the cobalt-catalyzed annulation of 5-decyne with 2-iodonaphthalene, as discussed in section 1.5.2.



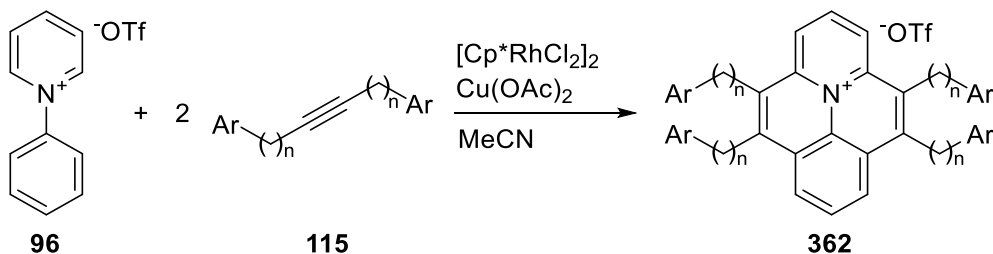
**Equation 4-4.** Cobalt-catalyzed [4+2] annulation of 2-phenylpyridine with 5-decyne.

### 4.3 The synthesis of archipelago compounds by [4+2] annulations of *N*-phenylpyridinium triflate with alkynes

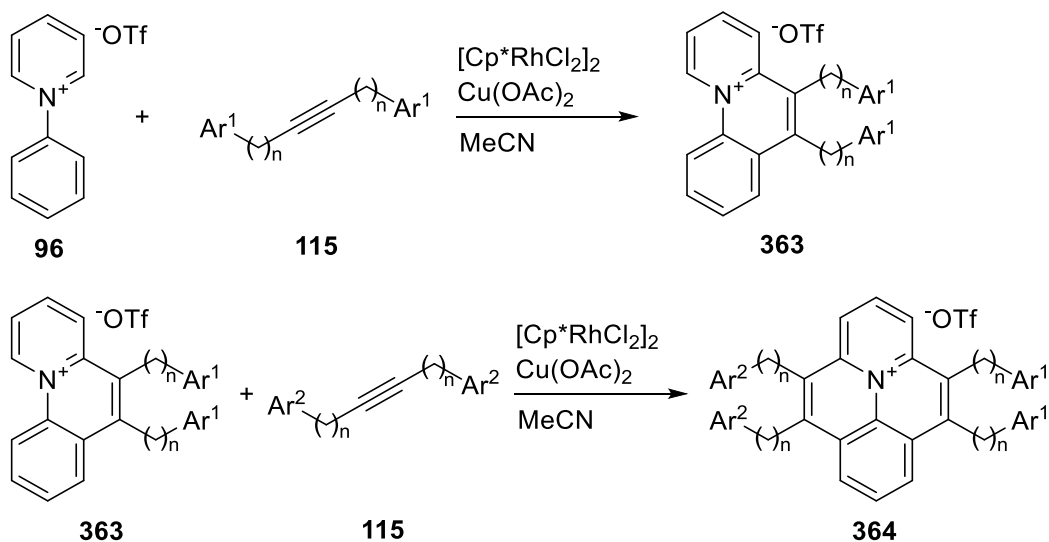
The [4+2] annulation of *N*-phenylpyridinium triflate **96** with alkynes, as described by Wang and co-workers,<sup>121</sup> is also a promising strategy for the preparation of cationic aza-arene archipelago compounds (Scheme 4-7). Benzo[*c*]quinolizinium structures are obtained by this strategy, rather

than benzo[*a*]quinolizinium motifs in Huang's and Cheng's annulations.<sup>116,117</sup> In particular, the double [4+2] annulation is expected to provide five-island archipelago compounds **362** (Scheme 4-7a). If a double annulation proceeds in a stepwise fashion with two different alkynes, an unsymmetrical archipelago compound **364** will be produced (Scheme 4-7b).

(a) Synthesis of symmetrical five-island archipelago compounds by double [4+2] annulation:



(b) Synthesis of unsymmetrical archipelago compounds by two-step [4+2] annulation:

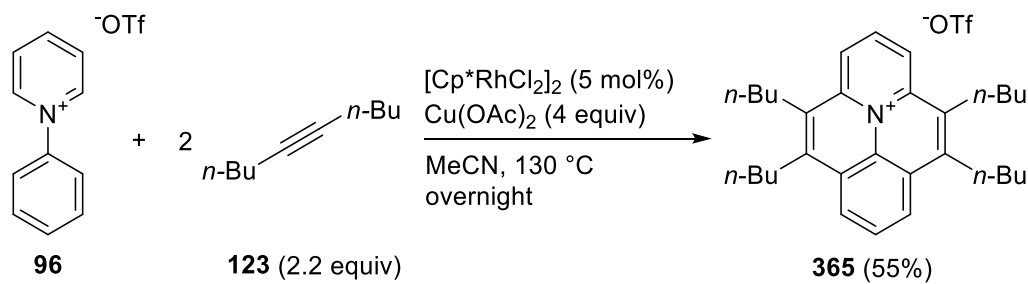


**Scheme 4-7.** Proposed syntheses of (a) symmetrical five-island archipelago compounds and (b) unsymmetrical archipelago compounds by rhodium-catalyzed [4+2] annulations of *N*-phenylpyridinium triflate with island-tethered alkynes.

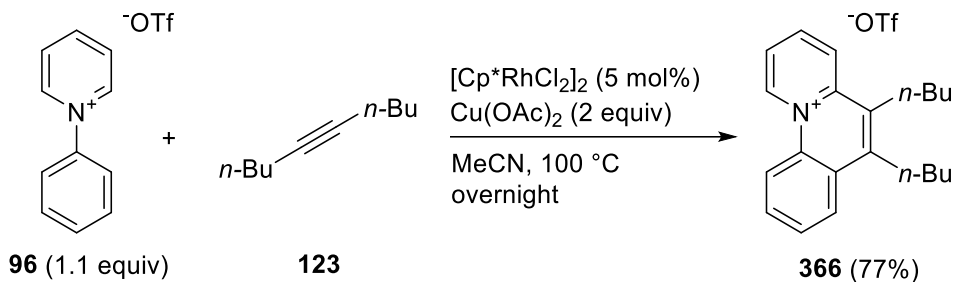
### 4.3.1 Annulations of *N*-phenylpyridinium triflate with 5-decyne

Reactions of 5-decyne with **96** were conducted initially to test the feasibility of making archipelago compounds (Scheme 4-8).

(a) Rh-catalyzed double [4+2] annulation of *N*-phenylpyridinium triflate with 5-decyne:



(b) Rh-catalyzed single [4+2] annulation of *N*-phenylpyridinium triflate with 5-decyne:



**Scheme 4-8.** Rhodium-catalyzed (a) double and (b) single [4+2] annulation of *N*-phenylpyridinium triflate with 5-decyne.

These results are discussed below:

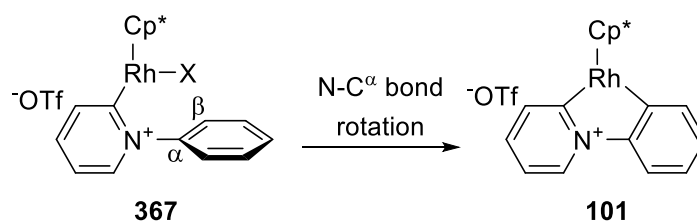
#### 1. *Reactions yields and adduct separations.*

The double [4+2] annulation generates tetrabutyl-substituted adduct **365** in 55% yield (Scheme 4-8a). The dibutyl-substituted adduct **366** obtained by single [4+2] annulation was isolated in 77% yield (Scheme 4-8b).

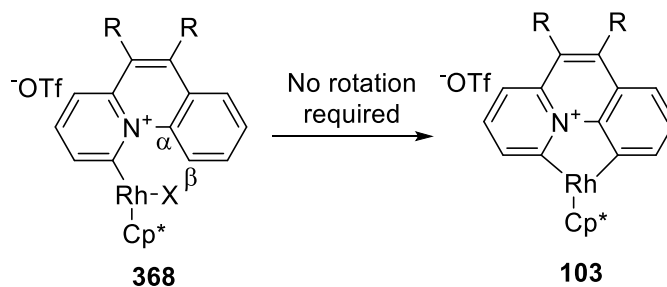
Cations **365** and **366** were purified by column chromatography on flash silica gel and  $\text{CH}_2\text{Cl}_2/\text{MeOH}$  eluent. In the reaction depicted in Scheme 4-8(a), none of the single alkyne adduct **366** was observed. However, in the reaction depicted Scheme 4-8(b), the formation of the double adduct **365** was competitive. These findings indicate that the second annulation is likely to have a faster rate than the first.

A possible explanation for these results is shown in Scheme 4-9. During the first [4+2] annulation, N- $\text{C}^\alpha$  bond rotation in **367** is required for  $\text{C}^\beta$ -H activation and the formation of the five-membered rhodacycle **101** (Scheme 4-9a). However, in the second [4+2] annulation, the N- $\text{C}^\alpha$  bond in **368** cannot rotate. The  $\text{C}^\beta$ -H bond is permanently situated in the same plane with the Rh-C bond, which makes the formation of rhodacycle **103** faster (Scheme 4-9b).

(a) Formation of the rhodacycle in the first [4+2] annulation:



(b) Formation of the rhodacycle in the second [4+2] annulation:



**Scheme 4-9.** Formation of the five-membered rhodacycle in (a) the first [4+2] annulation and (b) the second [4+2] annulation.

As expected, the single annulation adduct **366** was found to be more polar than the double annulation adduct **365**. During chromatographic purification of **366**, side product **365** eluted from the column first. The elution of **366** requires a higher ratio of MeOH in CH<sub>2</sub>Cl<sub>2</sub>/MeOH eluent. The polarity difference between these two adducts can be explained as follows: (1) The double adduct **365** is symmetrical and the dipoles from two sides cancel each other. The single adduct **366** has a stronger molecular dipole moment. (2) The greater number of alkyl groups in **365** also make this adduct less polar.

## *2. Luminescence.*

Single and double adducts **366** and **365** exhibit different fluorescence characteristic under long-wave ultraviolet light (365 nm). When dissolved in solution or spotted on TLC plate, the single annulation adduct **366** fluoresces dark purple while double annulation adduct **365** emits cyan light under ultraviolet irradiation, which helps us to distinguish the two compounds easily.

To further investigate the luminescence properties, UV-Vis and fluorescence spectra of these two compounds were obtained (see Appendix 3). In the UV-Vis analysis, double adduct **365** exhibits absorptions at 249, 287, 339, 356, 421, and 446 nm, which is consistent with its yellow powder appearance. Single adduct **366** shows absorptions at 262, 286, 309, 364, and 382 nm. The compound should appear as a white powder from UV-Vis result, but actually, the compound is a dark brown powder. One possible explanation for **366**'s dark appearance is that the visible light reflects between the stack layers of the compound in solid state and finally the light is absorbed, which prevents the light from coming out.

The Lambert-Beer's Law (13) provides the relationship between the extinction coefficient and the absorbance from UV-Vis spectra.<sup>236</sup>

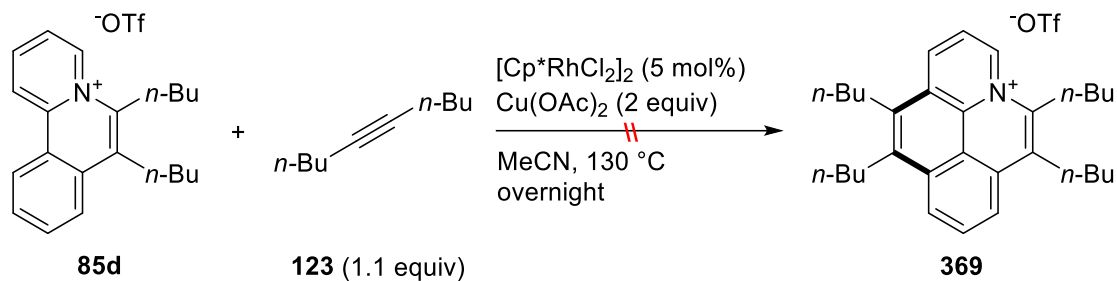
$$A = \varepsilon cL \quad (13)$$

where  $A$  is the absorbance of the peak,  $c$  is the concentration (mol/L),  $L$  is the path length (cm), and  $\varepsilon$  is the molar extinction coefficient ( $\text{L}\cdot\text{mol}^{-1}\cdot\text{cm}^{-1}$ ). By applying Lambert-Beer's Law (13), the molar extinction coefficients  $\varepsilon$  of **365** and **366** are calculated to be  $2.00\times 10^5 \text{ L}\cdot\text{mol}^{-1}\cdot\text{cm}^{-1}$  and  $1.37\times 10^5 \text{ L}\cdot\text{mol}^{-1}\cdot\text{cm}^{-1}$  at the highest absorbances (287 nm for **365** and 262 nm for **366**), respectively.

The fluorescence spectrum results reveal that the double adduct **365** emits at 470 nm, while the single adduct **366** emits at 416 nm (see Appendix 3). The emission wavelengths of these two adducts are consistent with the observations under long-wave UV irradiation (365 nm), in which **365** emits cyan light while **366** shows purple light.

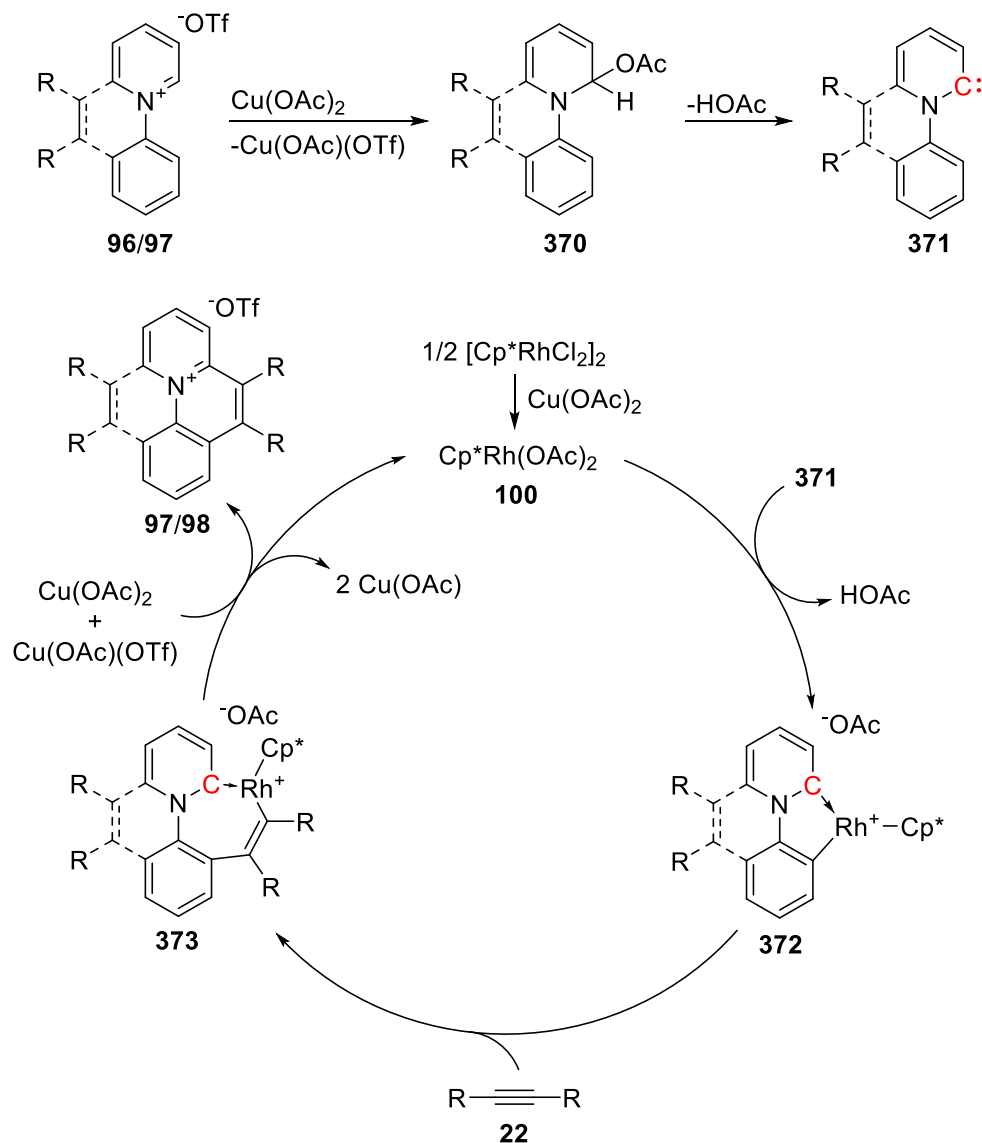
### 3. *Further investigations of the reaction mechanism.*

The reaction of benzo[*a*]quinolizinium compound **85d** with 5-decyne was carried out, following the same reaction conditions for annulations of *N*-phenylpyridinium triflate, to test the possibility of making tetra-substituted adduct **369** (Equation 4-5). Surprisingly, the expected product was not observed, which supports Wang and co-workers' postulate that the formation of an undetermined pyridine-based carbene intermediate plays a key role during the C-H activation step in this annulation process.<sup>121</sup>



**Equation 4-5.** Attempt of [4+2] annulation using benzo[*a*]quinolizinium compound **85d** and 5-decyne.

Based on some previous reports on carbene-metal complexes with similar structures,<sup>122-124</sup> I propose a plausible mechanism for this annulation involving the carbene intermediate (Scheme 4-10). The nucleophilic addition of acetate to the C=N bond in **96** or **97** provides intermediate **370**, in which the acetate is added to the carbon adjacent to the nitrogen. The carbene intermediate **371** is generated by an  $\alpha$ -elimination of **370**. Subsequent coordination, alkyne insertion and reductive elimination steps are similar to the original mechanism proposed by Wang.<sup>121</sup>

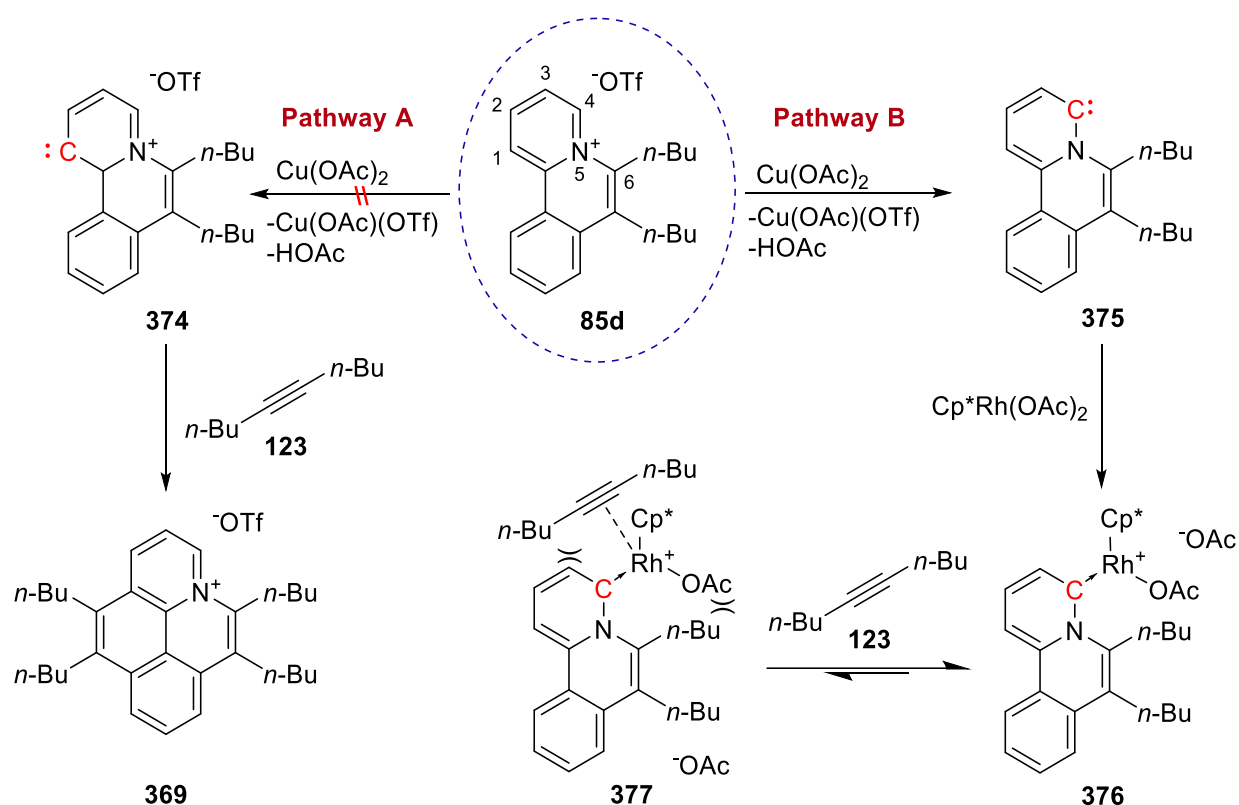


**Scheme 4-10.** A plausible Wang's annulation mechanism including the carbene intermediate.

The unsuccessful annulation using benzo[*a*]quinolizinium salt **85d** in Equation 4-5 can be rationalized by adopting the carbene mechanism above, which is shown in Scheme 4-11 in detail. It is obvious that adduct **369** cannot be obtained from this annulation because it is impossible to generate a carbene on the C1 position to give intermediate **374** via the nucleophilic addition/ $\alpha$ -elimination process (Pathway A). Instead, the carbene ligand must be generated on the C4



position to produce **375** (Pathway B). Subsequent coordination provides aryl-rhodium intermediate **376**, but the alkyne coordination and insertion is not favored due to the repulsions induced by the butyl group on C6 or the hydrogen on C3, which is similar to the unsuccessful annulation using 1-naphthylboronic acid in Scheme 1-16. Thus, **85d** does not give any annulation products under this reaction condition.



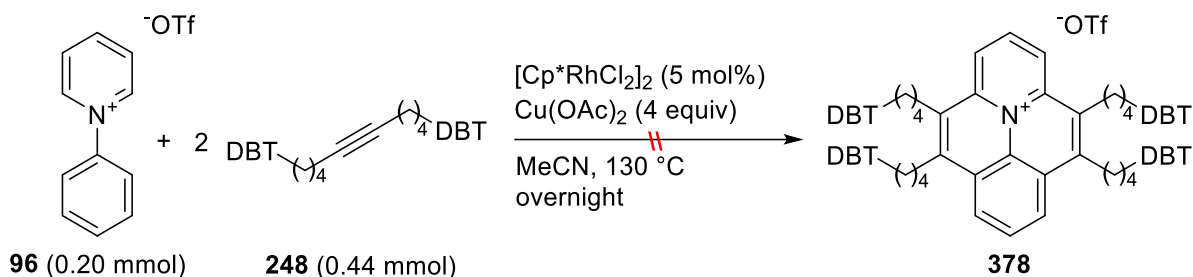
**Scheme 4-11.** Carbene generation and alkyne insertion steps for annulation using benzo[*a*]quinolizinium salt **85d**.

#### 4.3.2 Annulations of *N*-phenylpyridinium triflate with island-tethered alkynes

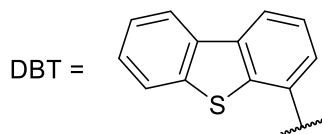
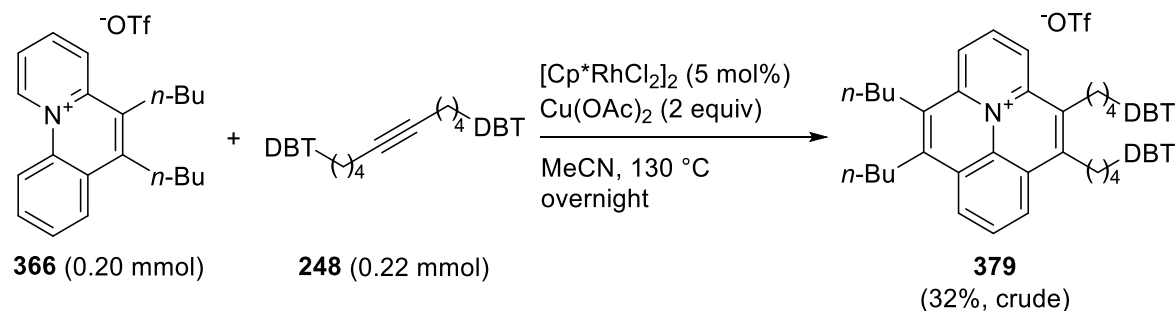
The successful annulations in section 4.3.1 suggest the feasibility of accessing benzo[*c*]quinolizinium archipelago compounds. DBT-tethered alkyne **248** was selected initially,

since **248** always produces archipelago compounds in higher yields than phenanthrene-tethered alkyne in previous synthesis. However, the results were not as expected (Scheme 4-12).

(a) Rh-catalyzed double [4+2] annulation of *N*-phenylpyridinium triflate with DBT-tethered alkyne:



(b) Rh-catalyzed single [4+2] annulation of benzo[*c*]quinolizinium compound **366** with DBT-tethered alkyne:

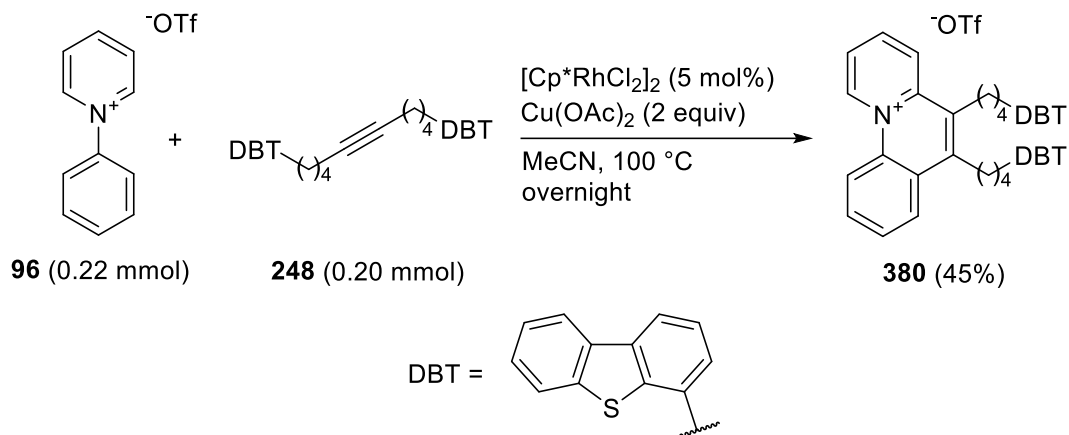


**Scheme 4-12.** Synthesis of archipelago compounds by rhodium-catalyzed [4+2] annulations of DBT-tethered alkyne with (a) *N*-phenylpyridinium triflate and (b) benzo[*c*]quinolizinium compound **366**.

The double [4+2] annulation of alkyne with **96** afforded only a low yield of a product that shows cyan fluorescence under long-wave ultraviolet light (365 nm). The mass of this adduct was insufficient to acquire a  $^1\text{H}$  NMR spectrum to confirm the structure (**378**, Scheme 4-12a).

The unsymmetrical archipelago compound could be prepared by single [4+2] annulation, using the DBT-tethered alkyne and benzo[*c*]quinolizinium product **366** (Scheme 4-12b). The adduct **379** was isolated, but in only 32% yield after chromatography. High-resolution mass spectrometry (ESI) confirms the formation of **379**. However, the  $^1\text{H}$  and  $^{13}\text{C}\{^1\text{H}\}$  NMR spectra show the presence of many impurities in the nominally purified compound (multiple peaks at 0.8-2.2 ppm in  $^1\text{H}$  NMR spectrum and 10-38 ppm in  $^{13}\text{C}\{^1\text{H}\}$  NMR spectrum from impurities). Thus, this annulation does not provide either tetra-DBT or di-DBT substituted product in acceptable yield and purity. Wang and co-workers also observed reduced yields when using a thiophene-containing alkyne.<sup>121</sup> Based on these results, I believe that some undetermined interactions of electron-rich sulfur with the pyridine-based carbene intermediate might lead to the reduced yields or even failure of these annulations.

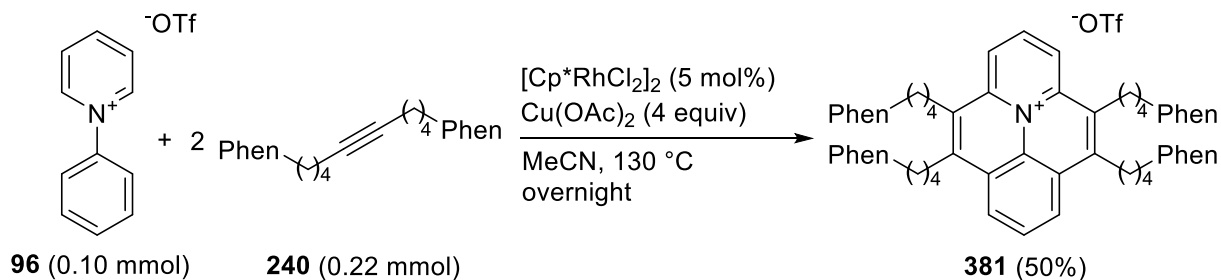
The single [4+2] annulation reaction between **96** with DBT-tethered alkyne was then attempted. The desired benzo[*c*]quinolizinium compound **380** was obtained in 45% yield in relatively high purity (Equation 4-6), albeit the yield was much lower than the testing reaction using 5-decyne in Scheme 4-8b. Therefore, **380** is the only DBT-tethered archipelago product I was able to obtain using this methodology.



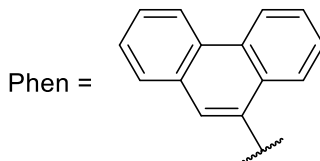
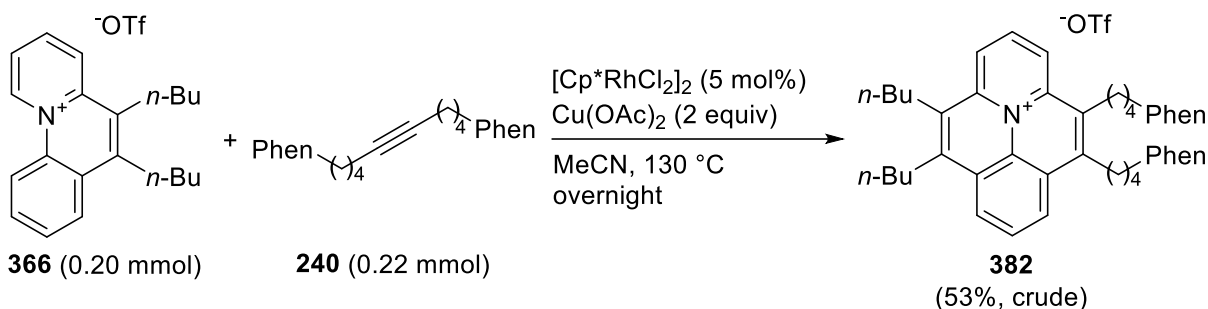
**Equation 4-6.** Synthesis of an archipelago compound by rhodium-catalyzed single [4+2] annulation of DBT-tethered alkyne with *N*-phenylpyridinium triflate.

The phenanthrene-tethered alkyne **240** was subsequently adopted, maintaining the same reaction conditions used for the DBT-tethered alkyne. Adducts **381** and **382** were obtained in reasonable 50 and 53% yields, respectively (Scheme 4-13).

(a) Rh-catalyzed double [4+2] annulation of *N*-phenylpyridinium triflate with phenanthrene-tethered alkyne:



(b) Rh-catalyzed single [4+2] annulation of benzo[*c*]quinolizinium compound **366** with phenanthrene-tethered alkyne:

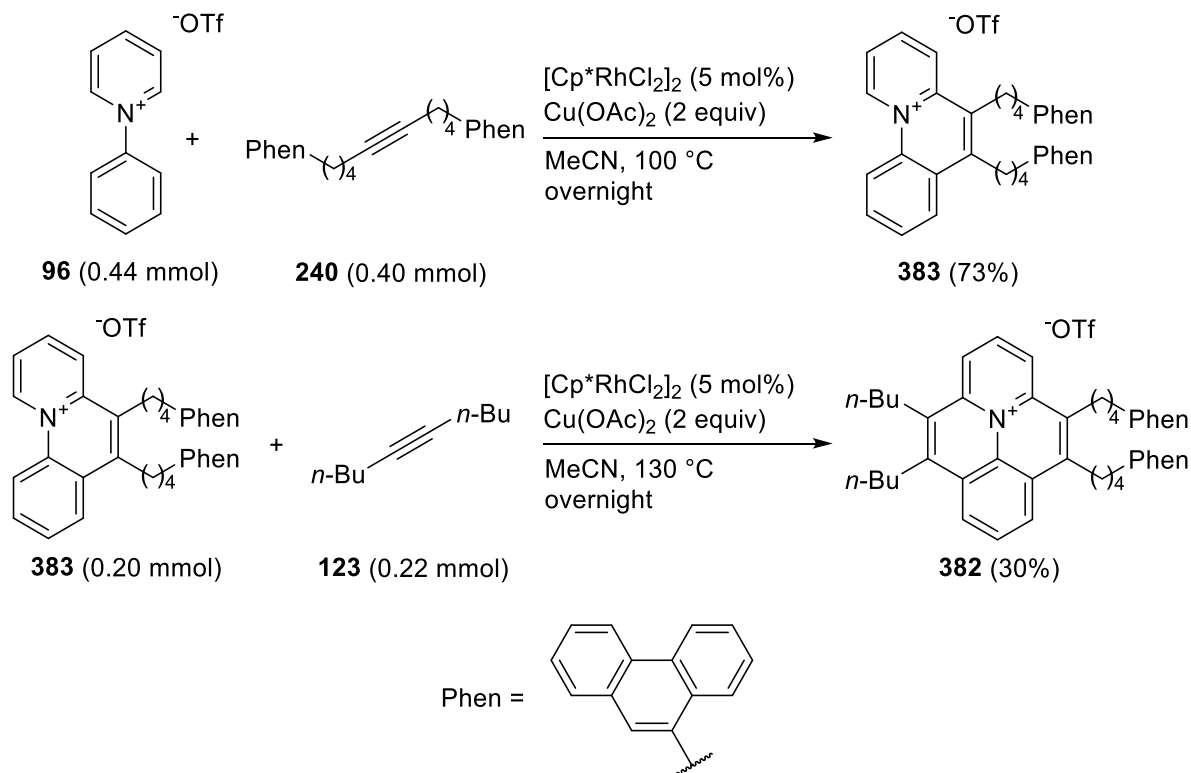


**Scheme 4-13.** Synthesis of archipelago compounds by rhodium-catalyzed [4+2] annulations of phenanthrene-tethered alkyne with (a) *N*-phenylpyridinium triflate and (b) benzo[*c*]quinolizinium compound **366**.

The five-island product **381** was isolated from chromatography as a yellow powder (Scheme 4-13a). This compound shows the same cyan fluorescence as its analogue **365** under long-wave ultraviolet light (365 nm). The solubility of **381** remains poor in dichloromethane and chloroform, similar to other archipelago compounds bearing multiple phenanthrene islands. The purity of **381** was confirmed by  $^1\text{H}$  and  $^{13}\text{C}\{^1\text{H}\}$  NMR spectroscopy and elemental analysis.

The unsymmetrical adduct **382** was also isolated in a similar yield (Scheme 4-13b).  $^1\text{H}$  NMR spectrum of **382** shows the presence of minor impurities (broad peaks at 1.1-1.3 ppm and 0.7-0.9 ppm, probably due to the presence of grease), but the overall quality of the product is higher than that of DBT-tethered analogue **379**. High-resolution mass spectrometry (ESI) confirms the successful synthesis of **382**, but combustion analysis of **382** deviates from theoretical, with much lower carbon content and higher sulfur content (anal. calcd for  $\text{C}_{60}\text{H}_{58}\text{F}_3\text{NO}_3\text{S}$ : C, 77.48; H, 6.29; N, 1.51; S, 3.45. Found: C, 70.88; H, 6.44; N, 1.40; S, 5.64. Repeat found: C, 70.98; H, 6.38; N, 1.40; S, 5.22).

Therefore, an alternative synthetic route was attempted (Scheme 4-14). Benzo[*c*]quinolizinium adduct **383** was prepared first and isolated in 73% yield from **96** and the phenanthrene-tethered alkyne. Subsequent annulation of **383** with 5-decyne produced **382** in 30% yield. Purified compound **382** from this route shows 30% less impurities in  $^1\text{H}$  NMR spectrum than **382** prepared in Scheme 4-13b, and the elemental analysis result was closer to the theoretical content (anal. calcd for  $\text{C}_{60}\text{H}_{58}\text{F}_3\text{NO}_3\text{S}$ : C, 77.48; H, 6.29; N, 1.51; S, 3.45. Found: C, 76.56; H, 6.52; N, 1.58; S, 2.95. Repeat found: C, 76.35; H, 6.46; N, 1.58; S, 3.21). Thus, the purity of **382** was improved over the previous preparation shown in Scheme 4-13b.



**Scheme 4-14.** An alternative route for synthesizing the unsymmetrical compound **382**.

## Conclusion

Cationic nitrogen-embedded archipelago compounds have been successfully synthesized by minor modification of known rhodium-catalyzed [4+2] annulations. 2-Phenylpyridine couples with alkynes to provide cations benzo[*a*]quinolizinium archipelago compounds with either phenanthrene or DBT islands. Single [4+2] annulations of *N*-phenylpyridinium triflate **96** with disubstituted alkynes produce benzo[*c*]quinolizinium archipelago compounds. Double [4+2] annulations of **96** with DBT-tethered alkyne do not generate the desired product, but five-island and unsymmetrical archipelago compounds are obtained from the phenanthrene-tethered alkyne. All successfully isolated compounds in this chapter are shown in Figure 4-2.

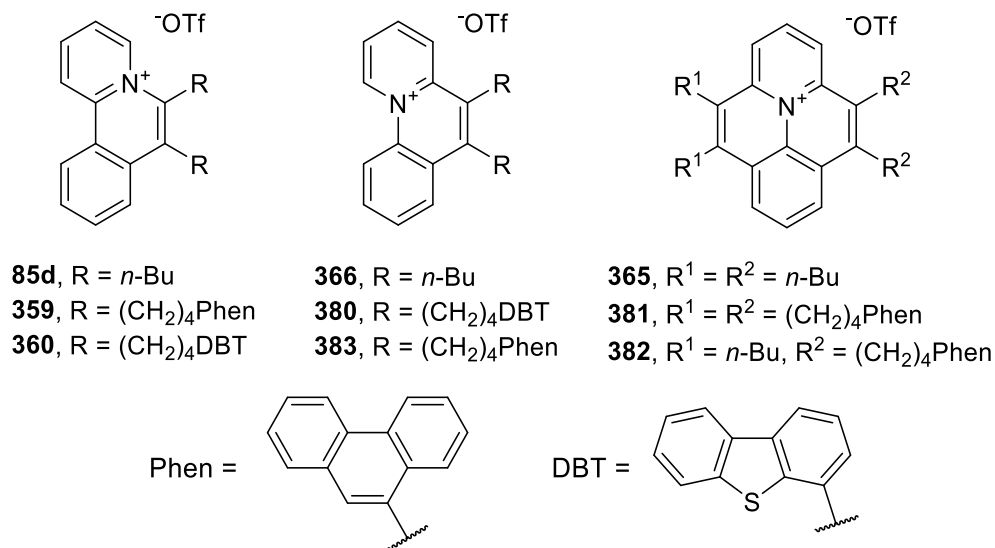


**Figure 4-2.** List of all cationic nitrogen-containing compounds prepared in chapter 4.

## Experimental Section

### General Information

Unless otherwise noted, all compounds were used as received without any further purification. DCM, MeOH, MeCN, and PhCl were dried over 3 Å molecular sieves for at least 48 h before use. [Cp\*RhCl<sub>2</sub>]<sub>2</sub>,<sup>199</sup> *N*-phenylpyridinium triflate (**96**),<sup>121</sup> diphenyliodonium triflate (for the preparation of **96**),<sup>237</sup> and cupric stearate (for the preparation of **96**)<sup>238</sup> were prepared according to literature procedures. <sup>1</sup>H, <sup>13</sup>C{<sup>1</sup>H}, and <sup>19</sup>F NMR spectra were recorded on Agilent/Varian instruments (500 or 700 MHz for <sup>1</sup>H NMR spectroscopy, 126 or 176 MHz for <sup>13</sup>C{<sup>1</sup>H} NMR spectroscopy, and 376 MHz for <sup>19</sup>F NMR spectroscopy) at 27 °C. Chemical shifts of <sup>1</sup>H, <sup>13</sup>C{<sup>1</sup>H}, and <sup>19</sup>F NMR spectra were reported in parts per million (ppm). Chemical shifts were referenced to residual solvent peaks (DMSO-*d*<sub>6</sub>: δ<sub>H</sub> = 2.49 ppm, δ<sub>C</sub> = 39.5 ppm). All coupling constants (*J* values) were reported in Hertz (Hz). Column chromatography was performed on silica gel 60 M



(230–400 mesh). Thin-layer chromatography (TLC) was performed on pre-coated, aluminum-backed silica gel plates. Visualization of the developed TLC plate was performed by a UV lamp (254 nm and 365 nm). High-resolution mass spectrometric (HRMS) results were obtained from Mass Spectrometry Facility using Agilent Technologies 6220 oaTOF (ESI). Elemental analyses (C, H, N, S) were obtained from Analytical and Instrumentation Laboratory using a Thermo Flash 2000 Elemental Analyzer. UV-Vis and Fluorescence spectra were obtained from Analytical and Instrumentation Laboratory using a Hewlett Packard 8453 UV-VIS Spectrophotometer and a Horiba-PTI QM-8075-11 Fluorescence System.

For some adducts, signals in  $^1\text{H}$  NMR spectra always appear as broad peaks after several attempts, hence the second order coupling cannot be determined.

#### **General procedure E – [4+2] annulations of 2-phenylpyridine with alkynes<sup>116</sup>**

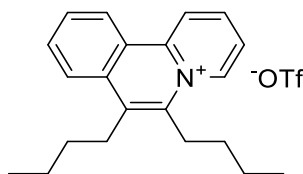
2-Phenylpyridine **86**, alkyne (**123**, **240**, **248**),  $[\text{Cp}^*\text{RhCl}_2]_2$ , and AgOTf were placed in a dry 100 mL Schlenk flask with a magnetic stir bar. The reaction flask was charged with nitrogen and dry MeOH was added through Schlenk line techniques. The reaction mixture was heated to 120 °C overnight and was quenched with water (50 mL). The aqueous solution was extracted with  $\text{CH}_2\text{Cl}_2$  (3 times, 30 mL each) and dried over  $\text{Na}_2\text{SO}_4$ . The mixture was filtered, and the solvent was removed under reduced pressure. The residual was purified by silica column chromatography using  $\text{CH}_2\text{Cl}_2/\text{MeOH}$  eluent to afford the product.

#### **General procedure F – Single/double [4+2] annulations of *N*-phenylpyridinium triflate with alkynes<sup>121</sup>**

*N*-phenylpyridinium triflate **96**, alkyne (**123**, **240**, **248**),  $[\text{Cp}^*\text{RhCl}_2]_2$ , and  $\text{Cu}(\text{OAc})_2$  were placed in a dry 25 mL Schlenk flask with a magnetic stir bar. The reaction flask was charged with

nitrogen and dry MeCN was added through Schlenk line techniques. The reaction mixture was heated at indicated temperature overnight. After cooling to room temperature, the solvent was removed under reduced pressure. The residual was purified by silica column chromatography using CH<sub>2</sub>Cl<sub>2</sub>/MeOH eluent to afford the product.

**6,7-Dibutylbenzo[*a*]quinolizinium trifluoromethanesulfonate (85d)**



The general procedure E was used with 2-phenylpyridine **86** (1240  $\mu$ L, 1.347 g, 8.680 mmol), 5-decyne (1305  $\mu$ L, 1.000 g, 7.233 mmol), [Cp\*RhCl<sub>2</sub>]<sub>2</sub> (44.7 mg, 1 mol%), AgOTf (2.230 g, 8.679 mmol), and MeOH (25 mL). The crude material was purified by silica column chromatography (CH<sub>2</sub>Cl<sub>2</sub>/MeOH 98:2 followed by CH<sub>2</sub>Cl<sub>2</sub>/MeOH 95:5) to afford compound **85d** as a yellow solid (1.962 g, 61%). *R*<sub>f</sub> = 0.42 (SiO<sub>2</sub>; CH<sub>2</sub>Cl<sub>2</sub>/MeOH 95:5).

**<sup>1</sup>H NMR** (DMSO-*d*<sub>6</sub>, 700 MHz):  $\delta$  9.55–9.49 (m, 2H), 9.10 (d, *J* = 8.4 Hz, 1H), 8.61 (t, *J* = 7.9 Hz, 1H), 8.32 (d, *J* = 8.5 Hz, 1H), 8.23 (t, *J* = 7.0 Hz, 1H), 8.10 (t, *J* = 7.6 Hz, 1H), 7.97 (t, *J* = 7.7 Hz, 1H), 3.42–3.37 (second order m, 2H), 3.22–3.17 (second order m, 2H), 1.73–1.55 (m, 8H), 1.02–0.97 (m, 6H).

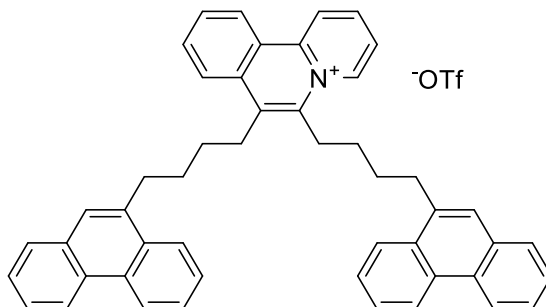
**<sup>13</sup>C{<sup>1</sup>H} NMR** (DMSO-*d*<sub>6</sub>, 176 MHz):  $\delta$  142.6, 138.7, 138.3, 135.5, 133.9, 132.8, 130.8, 129.9, 125.9, 124.7, 124.6, 123.9, 123.6, 31.7, 28.3, 28.2, 28.1, 22.3, 22.0, 13.6, 13.5.

**<sup>19</sup>F NMR** (DMSO-*d*<sub>6</sub>, 376 MHz):  $\delta$  –77.72 (s).

**ESI HRMS** exact mass *m/z* calcd for C<sub>21</sub>H<sub>26</sub>N<sup>+</sup> ([M – OTf]<sup>+</sup>) 292.2060, found 292.2054.

EA anal. calcd for C<sub>22</sub>H<sub>26</sub>F<sub>3</sub>NO<sub>3</sub>S: C, 59.85; H, 5.94; N, 3.17; S, 7.26. Found: C, 59.90; H, 5.92; N, 3.03; S, 7.26. Repeat found: C, 59.92; H, 5.98; N, 3.06; S, 7.05.

**6,7-Di[4-(9-phenanthrene)butyl]benzo[*a*]quinolizinium trifluoromethanesulfonate (359)**



The general procedure E was used with 2-phenylpyridine **86** (350  $\mu$ L, 380 mg, 2.45 mmol), 1,10-di(9-phenanthrene)-5-decyne **240** (1.000 g, 2.038 mmol), [Cp\*RhCl<sub>2</sub>]<sub>2</sub> (31.5 mg, 2.5 mol%), AgOTf (628 mg, 2.44 mmol), and MeOH (20 mL). The crude material was purified by silica column chromatography (CH<sub>2</sub>Cl<sub>2</sub>/MeOH 98:2 followed by CH<sub>2</sub>Cl<sub>2</sub>/MeOH 95:5) to afford compound **359** as a yellow solid (792 mg, 49%). *R*<sub>f</sub> = 0.22 (SiO<sub>2</sub>; CH<sub>2</sub>Cl<sub>2</sub>/MeOH 95:5).

**<sup>1</sup>H NMR** (DMSO-*d*<sub>6</sub>, 700 MHz):  $\delta$  9.51–9.47 (m, 2H), 9.10 (d, *J* = 8.5 Hz, 1H), 8.79–8.75 (m, 2H), 8.72–8.68 (m, 2H), 8.54 (t, *J* = 7.9 Hz, 1H), 8.33 (d, *J* = 8.3 Hz, 1H), 8.15–8.10 (m, 3H), 8.05 (t, *J* = 7.6 Hz, 1H), 7.98 (t, *J* = 7.6 Hz, 1H), 7.83–7.78 (m, 2H), 7.63–7.52 (m, 10H), 3.48–3.43 (second order m, 2H), 3.30–3.25 (second order m, 2H), 3.14–3.08 (m, 4H), 2.03–1.97 (m, 4H), 1.85–1.72 (m, 4H).

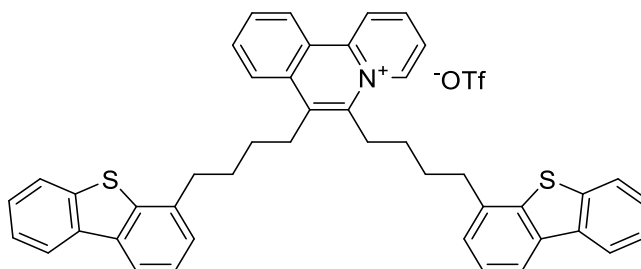
**<sup>13</sup>C{<sup>1</sup>H} NMR** (DMSO-*d*<sub>6</sub>, 126 MHz):  $\delta$  142.6, 138.5, 138.2, 136.0, 135.9, 135.6, 133.9, 132.9, 131.2, 130.8, 130.6, 130.5, 130.1, 129.9, 129.0, 127.8, 127.8, 126.7, 126.7, 126.4, 126.2, 126.1, 126.0, 125.7, 125.7, 124.9, 124.4, 124.4, 124.3, 123.9, 123.6, 123.3, 122.6, 32.1, 32.1, 29.5, 29.5, 29.1, 28.6, 28.2, 26.0.

**$^{19}\text{F}$  NMR** (DMSO- $d_6$ , 376 MHz):  $\delta$  -77.72 (s).

**ESI HRMS** exact mass  $m/z$  calcd for  $\text{C}_{49}\text{H}_{42}\text{N}^+$  ( $[\text{M} - \text{OTf}]^+$ ) 644.3317, found 644.3307.

**EA** anal. calcd for  $\text{C}_{50}\text{H}_{42}\text{F}_3\text{NO}_3\text{S}$ : C, 75.64; H, 5.33; N, 1.76; S, 4.04. Found: C, 74.55; H, 5.31; N, 1.73; S, 3.89. Repeat found: C, 74.38; H, 5.31; N, 1.72; S, 3.81.

**6,7-Di[4-(4-dibenzothiophene)butyl]benzo[*a*]quinolizinium trifluoromethanesulfonate (360)**



The general procedure E was used with 2-phenylpyridine **86** (341  $\mu\text{L}$ , 370 mg, 2.39 mmol), 1,10-di(4-dibenzothiophene)-5-decyne **248** (1.000 g, 1.990 mmol),  $[\text{Cp}^*\text{RhCl}_2]_2$  (30.7 mg, 2.5 mol%), AgOTf (613 mg, 2.39 mmol), and MeOH (20 mL). The crude material was purified by silica column chromatography ( $\text{CH}_2\text{Cl}_2/\text{MeOH}$  98:2 followed by  $\text{CH}_2\text{Cl}_2/\text{MeOH}$  95:5) to afford compound **360** as a yellow solid (1.277 g, 80%).  $R_f$  = 0.38 ( $\text{SiO}_2$ ;  $\text{CH}_2\text{Cl}_2/\text{MeOH}$  95:5).

**$^1\text{H}$  NMR** (DMSO- $d_6$ , 500 MHz):  $\delta$  9.49–9.44 (m, 2H), 9.08 (d,  $J$  = 8.4 Hz, 1H), 8.55 (t,  $J$  = 7.8 Hz, 1H), 8.30–8.23 (m, 3H), 8.16–8.11 (m, 3H), 8.04 (t,  $J$  = 7.7 Hz, 1H), 7.96 (t,  $J$  = 7.7 Hz, 1H), 7.87–7.83 (m, 2H), 7.48–7.37 (m, 6H), 7.35–7.31 (m, 2H), 3.46–3.40 (m, 2H), 3.28–3.21 (m, 2H), 2.92–2.86 (m, 4H), 2.06–1.98 (m, 4H), 1.79–1.64 (m, 4H).

**$^{13}\text{C}\{^1\text{H}\}$  NMR** (DMSO- $d_6$ , 126 MHz):  $\delta$  142.7, 138.6, 138.1, 138.0, 138.0, 137.9, 135.8, 135.7, 135.5, 135.5, 135.1, 135.1, 133.9, 132.8, 130.7, 129.9, 126.9, 126.3, 126.2, 126.0, 125.1, 125.0,

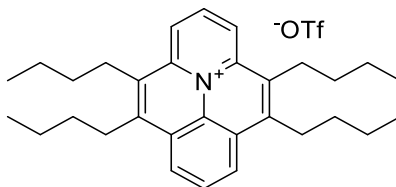
124.8, 124.7, 124.4, 123.9, 123.6, 122.8, 122.1, 122.0, 119.8, 119.8, 33.9, 33.9, 29.2, 28.5, 28.3, 28.1, 27.8, 25.8.

$^{19}\text{F}$  NMR (DMSO- $d_6$ , 376 MHz):  $\delta$  -77.76 (s).

**ESI HRMS** exact mass  $m/z$  calcd for  $\text{C}_{45}\text{H}_{38}\text{NS}_2^+$  ( $[\text{M} - \text{OTf}]^+$ ) 656.2440, found 656.2444.

**EA** anal. calcd for  $\text{C}_{46}\text{H}_{38}\text{F}_3\text{NO}_3\text{S}_3$ : C, 68.55; H, 4.75; N, 1.74; S, 11.93. Found: C, 68.04; H, 5.15; N, 1.56; S, 12.21. Repeat found: C, 68.49; H, 5.18; N, 1.57; S, 12.14.

**4,5,9,10-Tetrabutylbenzo[*ij*] pyrido[2,1,6-*de*]quinolizinium trifluoromethanesulfonate (365)**



The general procedure F was used with *N*-phenylpyridinium triflate **96** (61 mg, 0.20 mmol), 5-decyne (79  $\mu\text{L}$ , 61 mg, 0.44 mmol),  $[\text{Cp}^*\text{RhCl}_2]_2$  (6.2 mg, 5 mol%),  $\text{Cu}(\text{OAc})_2$  (145 mg, 0.80 mmol), and MeCN (2.5 mL). The reaction mixture was heated at 130  $^\circ\text{C}$  overnight. The crude material was purified by silica column chromatography ( $\text{CH}_2\text{Cl}_2/\text{MeOH}$  99:1) to afford compound **365** as a yellow solid (64 mg, 55%).  $R_f$  = 0.41 ( $\text{SiO}_2$ ;  $\text{CH}_2\text{Cl}_2/\text{MeOH}$  95:5).

$^1\text{H}$  NMR (DMSO- $d_6$ , 700 MHz):  $\delta$  8.80 (d,  $J$  = 8.2 Hz, 2H), 8.73 (t,  $J$  = 8.2 Hz, 1H), 8.60 (d,  $J$  = 7.9 Hz, 2H), 8.36 (t,  $J$  = 7.9 Hz, 1H), 3.30–3.23 (m, 8H), 1.71–1.57 (m, 16H), 1.01 (t,  $J$  = 7.3 Hz, 12H).

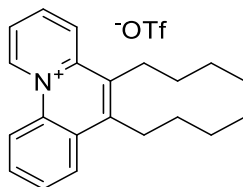
$^{13}\text{C}\{^1\text{H}\}$  NMR (DMSO- $d_6$ , 176 MHz):  $\delta$  143.4, 140.6, 136.9, 132.1, 130.4, 129.4, 126.4, 123.7, 120.9, 31.2, 30.7, 28.5, 22.5, 22.3, 13.7, 13.7.

$^{19}\text{F}$  NMR (DMSO- $d_6$ , 376 MHz):  $\delta$  -77.79 (s).

**ESI HRMS** exact mass  $m/z$  calcd for  $C_{31}H_{42}N^+$  ( $[M - OTf]^+$ ) 428.3312, found 428.3309.

**EA** anal. calcd for  $C_{32}H_{42}F_3NO_3S$ : C, 66.53; H, 7.33; N, 2.42; S, 5.55. Found: C, 67.17; H, 7.32; N, 2.44; S, 5.01. Repeat found: C, 67.41; H, 7.43; N, 2.46; S, 4.80.

**5,6-Dibutylbenzo[*c*]quinolizinium trifluoromethanesulfonate (366)**



The general procedure F was used with *N*-phenylpyridinium triflate **96** (400 mg, 1.31 mmol), 5-decyne (215  $\mu$ L, 165 mg, 1.19 mmol),  $[Cp^*RhCl_2]_2$  (36.8 mg, 5 mol%),  $Cu(OAc)_2$  (432 mg, 2.38 mmol), and MeCN (10 mL). The reaction mixture was heated at 100  $^{\circ}C$  overnight. The crude material was purified by silica column chromatography ( $CH_2Cl_2/MeOH$  99:1 followed by  $CH_2Cl_2/MeOH$  95:5) to afford compound **366** as a black solid (406 mg, 77%).  $R_f$  = 0.25 ( $SiO_2$ ;  $CH_2Cl_2/MeOH$  95:5).

**$^1H$  NMR** ( $DMSO-d_6$ , 700 MHz):  $\delta$  10.34 (d,  $J$  = 7.0 Hz, 1H), 9.08 (d,  $J$  = 9.0 Hz, 1H), 8.77 (d,  $J$  = 8.7 Hz, 1H), 8.61 (t,  $J$  = 7.9 Hz, 1H), 8.49 (d,  $J$  = 8.3 Hz, 1H), 8.19 (t,  $J$  = 7.0 Hz, 1H), 8.11 (t,  $J$  = 7.9 Hz, 1H), 8.05 (t,  $J$  = 7.6 Hz, 1H), 3.29–3.25 (second order m, 2H), 3.22–3.18 (second order m, 2H), 1.66–1.55 (m, 8H), 0.99 (t,  $J$  = 7.2 Hz, 6H).

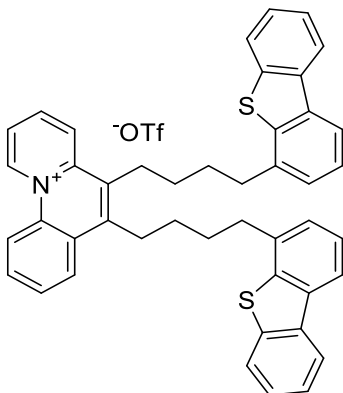
**$^{13}C\{^1H\}$  NMR** ( $DMSO-d_6$ , 176 MHz):  $\delta$  145.9, 142.6, 140.5, 135.1, 133.3, 131.7, 131.0, 130.5, 126.5, 126.0, 125.0, 123.2, 118.6, 32.2, 31.6, 28.4, 27.8, 22.5, 22.3, 13.7, 13.6.

**$^{19}F$  NMR** ( $DMSO-d_6$ , 376 MHz):  $\delta$  -77.77 (s).

**ESI HRMS** exact mass  $m/z$  calcd for  $C_{21}H_{26}N^+$  ( $[M - OTf]^+$ ) 292.2060, found 292.2058.

EA anal. calcd for C<sub>22</sub>H<sub>26</sub>F<sub>3</sub>NO<sub>3</sub>S: C, 59.85; H, 5.94; N, 3.17; S, 7.26. Found: C, 59.78; H, 5.95; N, 3.07; S, 6.90. Repeat found: C, 59.84; H, 5.98; N, 3.07; S, 7.02.

**5,6-Di[4-(4-dibenzothiophene)butyl]benzo[*c*]quinolizinium trifluoromethanesulfonate (380)**



The general procedure F was used with *N*-phenylpyridinium triflate **96** (67 mg, 0.22 mmol), 1,10-di(4-dibenzothiophene)-5-decyne **248** (101 mg, 0.201 mmol), [Cp\*RhCl<sub>2</sub>]<sub>2</sub> (6.2 mg, 5 mol%), Cu(OAc)<sub>2</sub> (73 mg, 0.40 mmol), and MeCN (4 mL). The reaction mixture was heated at 100 °C overnight. The crude material was purified by silica column chromatography (CH<sub>2</sub>Cl<sub>2</sub>/MeOH 98:2 followed by CH<sub>2</sub>Cl<sub>2</sub>/MeOH 95:5) to afford compound **380** as a black solid (72 mg, 45%). *R*<sub>f</sub> = 0.15 (SiO<sub>2</sub>; CH<sub>2</sub>Cl<sub>2</sub>/MeOH 95:5).

**<sup>1</sup>H NMR** (DMSO-*d*<sub>6</sub>, 500 MHz): δ 10.26–10.20 (m, 1H), 9.01–8.95 (d, *J* = 9.0 Hz, 1H), 8.65–8.61 (m, 1H), 8.49 (t, *J* = 7.8 Hz, 1H), 8.37–8.32 (m, 1H), 8.25–8.19 (m, 2H), 8.14–8.07 (m, 3H), 8.04 (t, *J* = 7.7 Hz, 1H), 7.92 (t, *J* = 7.5 Hz, 1H), 7.85–7.80 (m, 2H), 7.45–7.35 (m, 6H), 7.33–7.28 (m, 2H), 3.28–3.11 (m, 4H), 2.90–2.84 (m, 4H), 2.04–1.95 (m, 4H), 1.68–1.59 (m, 4H).

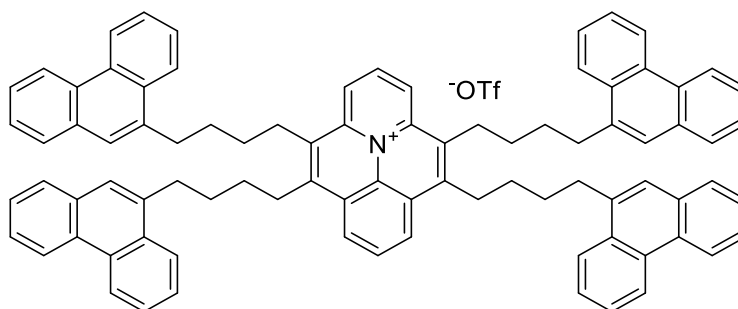
**<sup>13</sup>C{<sup>1</sup>H} NMR** (DMSO-*d*<sub>6</sub>, 126 MHz): δ 145.7, 142.3, 140.3, 138.0, 137.9, 135.8, 135.7, 135.5, 135.1, 135.0, 133.2, 131.6, 130.7, 130.3, 126.9, 126.3, 126.3, 126.2, 125.8, 125.0, 124.8, 124.6, 123.1, 122.7, 122.0, 119.7, 118.5, 33.9, 33.9, 29.6, 29.0, 28.4, 28.2, 27.9.

**<sup>19</sup>F NMR** (DMSO-*d*<sub>6</sub>, 376 MHz): δ −77.70 (s).

**ESI HRMS** exact mass *m/z* calcd for C<sub>45</sub>H<sub>38</sub>NS<sub>2</sub><sup>+</sup> ([M – OTf]<sup>+</sup>) 656.2440, found 656.2435.

**EA** anal. calcd for C<sub>46</sub>H<sub>38</sub>F<sub>3</sub>NO<sub>3</sub>S<sub>3</sub>: C, 68.55; H, 4.75; N, 1.74; S, 11.93. Found: C, 67.40; H, 5.14; N, 1.70; S, 11.09. Repeat found: C, 67.46; H, 5.11; N, 1.71; S, 11.39.

**4,5,9,10-Tetra[4-(9-phenanthrene)butyl]benzo[*ij*]pyrido[2,1,6-*de*]quinolizinium trifluoromethanesulfonate (381)**



The general procedure F was used with *N*-phenylpyridinium triflate **96** (31 mg, 0.10 mmol), 1,10-di(9-phenanthrene)-5-decyne **240** (108 mg, 0.220 mmol), [Cp<sup>\*</sup>RhCl<sub>2</sub>]<sub>2</sub> (3.1 mg, 5 mol%), Cu(OAc)<sub>2</sub> (73 mg, 0.40 mmol), and MeCN (4 mL). The reaction mixture was heated at 130 °C overnight. The crude material was purified by silica column chromatography (CH<sub>2</sub>Cl<sub>2</sub>/MeOH 99:1 followed by CH<sub>2</sub>Cl<sub>2</sub>/MeOH 97:3) to afford compound **381** as a yellow solid (64 mg, 50%). *R*<sub>f</sub> = 0.34 (SiO<sub>2</sub>; CH<sub>2</sub>Cl<sub>2</sub>/MeOH 95:5).

**<sup>1</sup>H NMR** (DMSO-*d*<sub>6</sub>, 700 MHz): δ 8.68–8.63 (m, 4H), 8.62–8.57 (m, 4H), 8.48–8.44 (m, 2H), 8.36–8.32 (m, 1H), 8.30–8.26 (m, 2H), 8.08–8.03 (m, 4H), 7.99–7.95 (m, 1H), 7.75 (d, *J* = 7.6 Hz, 2H), 7.71 (d, *J* = 7.6 Hz, 2H), 7.57–7.46 (m, 20H), 3.19–3.05 (m, 16H), 2.00–1.94 (m, 8H), 1.74–1.66 (m, 8H).



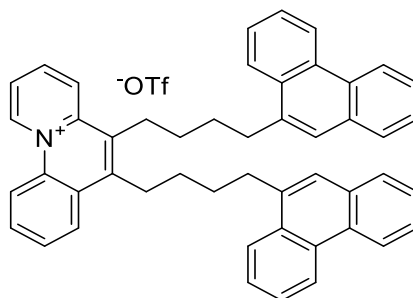
$^{13}\text{C}\{^1\text{H}\}$  NMR (DMSO- $d_6$ , 126 MHz):  $\delta$  143.2, 140.0, 135.8, 135.7, 131.6, 131.1, 131.1, 130.4, 130.4, 129.9, 129.7, 128.9, 128.9, 127.7, 126.7, 126.6, 126.2, 126.1, 125.8, 125.8, 125.7, 124.2, 123.5, 123.2, 122.5, 120.6, 32.1, 32.1, 29.4, 29.2, 28.7, 28.6, 28.1.

$^{19}\text{F}$  NMR (DMSO- $d_6$ , 376 MHz):  $\delta$  -77.71 (s).

ESI HRMS exact mass  $m/z$  calcd for  $\text{C}_{87}\text{H}_{74}\text{N}^+$  ( $[\text{M} - \text{OTf}]^+$ ) 1132.5816, found 1132.5806.

EA anal. calcd for  $\text{C}_{88}\text{H}_{74}\text{F}_3\text{NO}_3\text{S}$ : C, 82.41; H, 5.82; N, 1.09; S, 2.50. Found: C, 80.07; H, 5.89; N, 1.12; S, 2.46. Repeat found: C, 79.96; H, 5.82; N, 1.08; S, 2.37.

**5,6-Di[4-(9-phenanthrene)butyl]benzo[*c*]quinolizinium trifluoromethanesulfonate (383)**



The general procedure F was used with *N*-phenylpyridinium triflate **96** (134 mg, 0.439 mmol), 1,10-di(9-phenanthrene)-5-decyne **240** (196 mg, 0.399 mmol),  $[\text{Cp}^*\text{RhCl}_2]_2$  (12.4 mg, 5 mol%),  $\text{Cu}(\text{OAc})_2$  (145 mg, 0.798 mmol), and MeCN (8 mL). The reaction mixture was heated at 100 °C overnight. The crude material was purified by silica column chromatography ( $\text{CH}_2\text{Cl}_2/\text{MeOH}$  98:2 followed by  $\text{CH}_2\text{Cl}_2/\text{MeOH}$  95:5) to afford compound **383** as a grey solid (232 mg, 73%).  $R_f$  = 0.31 ( $\text{SiO}_2$ ;  $\text{CH}_2\text{Cl}_2/\text{MeOH}$  95:5).

$^1\text{H}$  NMR (DMSO- $d_6$ , 700 MHz):  $\delta$  10.25 (d,  $J$  = 6.9 Hz, 1H), 9.01 (d,  $J$  = 9.0 Hz, 1H), 8.76 (d,  $J$  = 7.0 Hz, 2H), 8.71–8.67 (m, 3H), 8.50 (t,  $J$  = 7.8 Hz, 1H), 8.42 (d,  $J$  = 8.1 Hz, 1H), 8.13–8.09 (m, 3H), 8.06 (t,  $J$  = 7.8 Hz, 1H), 7.94 (t,  $J$  = 7.6 Hz, 1H), 7.80 (t,  $J$  = 8.8 Hz, 2H), 7.62–7.52 (m,

10H), 3.33–3.28 (m, 2H), 3.24–3.19 (m, 2H), 3.13–3.08 (m, 4H), 2.02–1.94 (m, 4H), 1.75–1.68 (m, 4H).

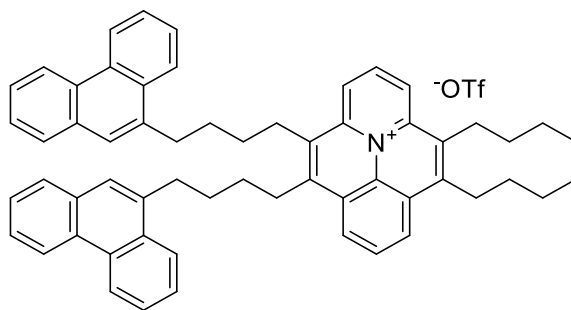
**$^{13}\text{C}\{^1\text{H}\}$  NMR** (DMSO- $d_6$ , 126 MHz):  $\delta$  145.9, 142.4, 140.3, 136.0, 135.9, 135.0, 133.2, 131.6, 131.2, 130.9, 130.5, 130.3, 130.0, 129.0, 127.8, 126.7, 126.7, 126.5, 126.3, 126.1, 125.9, 125.8, 125.7, 124.9, 124.3, 123.3, 123.1, 122.6, 118.6, 32.2, 32.1, 29.8, 29.6, 29.4, 29.2, 28.5, 28.0.

**$^{19}\text{F}$  NMR** (DMSO- $d_6$ , 376 MHz):  $\delta$  -77.72 (s).

**ESI HRMS** exact mass  $m/z$  calcd for  $\text{C}_{49}\text{H}_{42}\text{N}^+$  ( $[\text{M} - \text{OTf}]^+$ ) 644.3317, found 644.3310.

**EA** anal. calcd for  $\text{C}_{50}\text{H}_{42}\text{F}_3\text{NO}_3\text{S}$ : C, 75.64; H, 5.33; N, 1.76; S, 4.04. Found: C, 74.55; H, 5.36; N, 1.74; S, 3.65. Repeat found: C, 74.51; H, 5.37; N, 1.75; S, 3.77.

**4,5-Di[4-(9-phenanthrene)butyl]-9,10-dibutylbenzo[*ij*]pyrido[2,1,6-*de*]quinolizinium trifluoromethanesulfonate (382)**



5,6-Di[4-(9-phenanthrene)butyl]benzo[*c*]quinolizinium trifluoromethanesulfonate **383** (159 mg, 0.20 mmol), 5-decyne (40  $\mu\text{L}$ , 30 mg, 0.22 mmol),  $[\text{Cp}^*\text{RhCl}_2]_2$  (6.2 mg, 5 mol%), and  $\text{Cu}(\text{OAc})_2$  (73 mg, 0.40 mmol) were placed in a dry 25 mL Schlenk flask with a magnetic stir bar. The reaction flask was charged with nitrogen and dry MeCN (4 mL) was added through Schlenk line techniques. The reaction mixture was heated at 130  $^\circ\text{C}$  overnight. After cooling to room temperature, the solvent was removed under reduced pressure. The residual was purified by

silica column chromatography (CH<sub>2</sub>Cl<sub>2</sub>/MeOH 99:1 followed by CH<sub>2</sub>Cl<sub>2</sub>/MeOH 97:3) to afford compound **382** as a brown solid (56 mg, 30%). *R*<sub>f</sub> = 0.34 (SiO<sub>2</sub>; CH<sub>2</sub>Cl<sub>2</sub>/MeOH 95:5).

**<sup>1</sup>H NMR** (DMSO-*d*<sub>6</sub>, 700 MHz): δ 8.67–8.51 (m, 7H), 8.44–8.40 (m, 2H), 8.19–8.15 (m, 1H), 8.07–8.01 (m, 2H), 7.75–7.69 (m, 2H), 7.56–7.46 (m, 10H), 3.26–3.11 (m, 8H), 3.08–3.02 (m, 4H), 2.00–1.93 (m, 4H), 1.77–1.69 (m, 4H), 1.65–1.56 (m, 8H), 1.01 (t, *J* = 7.0 Hz, 6H).

**<sup>13</sup>C{<sup>1</sup>H} NMR** (DMSO-*d*<sub>6</sub>, 126 MHz): δ 143.3, 143.2, 140.2, 140.2, 136.5, 135.8, 135.7, 131.8, 131.8, 131.1, 131.0, 130.4, 130.3, 129.9, 129.9, 129.1, 128.8, 127.6, 126.6, 126.5, 126.1, 126.1, 126.0, 125.7, 125.6, 124.1, 123.6, 123.5, 123.1, 122.4, 120.7, 32.1, 32.1, 31.0, 30.6, 29.4, 29.3, 28.7, 28.5, 28.2, 22.5, 22.3, 13.7.

**<sup>19</sup>F NMR** (DMSO-*d*<sub>6</sub>, 376 MHz): δ –77.71 (s).

**ESI HRMS** exact mass *m/z* calcd for C<sub>59</sub>H<sub>58</sub>N<sup>+</sup> ([M – OTf]<sup>+</sup>) 780.4564, found 780.4549.

**EA** anal. calcd for C<sub>60</sub>H<sub>58</sub>F<sub>3</sub>NO<sub>3</sub>S: C, 77.48; H, 6.29; N, 1.51; S, 3.45. Found: C, 76.56; H, 6.52; N, 1.58; S, 2.95. Repeat found: C, 76.35; H, 6.46; N, 1.58; S, 3.21.

## 5. Conclusions and Future Perspectives

### 5.1 Project summary

The objective of my dissertation research was to develop efficient methodologies for constructing archipelago structures that represent asphaltenes obtained from various natural resources. This goal was achieved by using rhodium-catalyzed alkyne annulation reactions, and these structures better mimic the structure of asphaltenes than those previously reported.

As a starting point for this project, dialkyl alkynes with phenanthrene, DBT or TEP islands were prepared via deprotonation/alkylation or transition metal-catalyzed cross-coupling reactions. Annulations of these island-tethered alkynes with aryl-boron derivatives were optimized to produce archipelago model compounds in good yields. In particular, several sulfur-containing archipelago compounds were obtained for the first time, which makes up the deficiencies of previous synthetic approaches and provides more choices for further asphaltene studies. The archipelago compounds bearing multiple phenanthrene islands exhibit poor solubilities, this problem was addressed by the synthesis of TEP-tethered archipelago compounds. In addition, <sup>1</sup>H-DOSY NMR spectra provided solution information for a DBT-tethered model compound, which was used to calculate the hydrodynamic radii and to estimate the aggregation behavior of that compound.

Subsequently, annulations of alkynes with nitrogen-containing substrates were adopted to generate cationic nitrogen-embedded archipelago compounds. Compared with neutral archipelago adducts, these compounds show obviously increased polarities. The cation-anion interactions in these compounds make them good models for Gray's supramolecular asphaltene assemblies.<sup>66</sup> However, some compounds could not be obtained in acceptable yields or purities,

leaving room for future optimization and generalization.

## 5.2 Unresolved issues and future objectives

### 5.2.1 Archipelago compounds from triethylpyrene islands

Although archipelago model compounds with TEP islands were successfully prepared, the low yield from Kumada coupling for preparing TEP-tethered alkyne **254** (Scheme 2-15) restrains the large-scale synthesis and applications of these compounds to supramolecular analysis and petroleum science. From my results, none of the catalytic reactions tested so far could provide **254** in a reasonable yield. So, I consider a possibility of replacing the TEP island with other polyalkyl-substituted aromatics. Triethyl-substituted bromopyrene **15e** (Figure 5-1), which has been previously prepared in our group on a 1 g scale by Diner *et al.*,<sup>82</sup> could be a good replacement for the TEP island. The distant ethyl groups in **15e** are less likely to inhibit the preparation, thus enabling large-scale synthesis of triethylpyrene-tethered archipelago compounds.

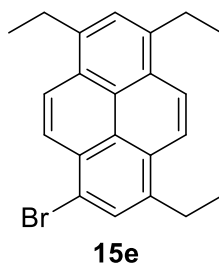


**Figure 5-1.** Triethyl-substituted bromopyrene prepared by Diner *et al.*<sup>82</sup>

The expected [2+2+2] and [4+2] annulation products from **15e** are shown in Figure 5-2. The molecular weights and H/C ratios of these two model compounds are similar to the TEP-tethered analogs and are still in the range of nature asphaltene.

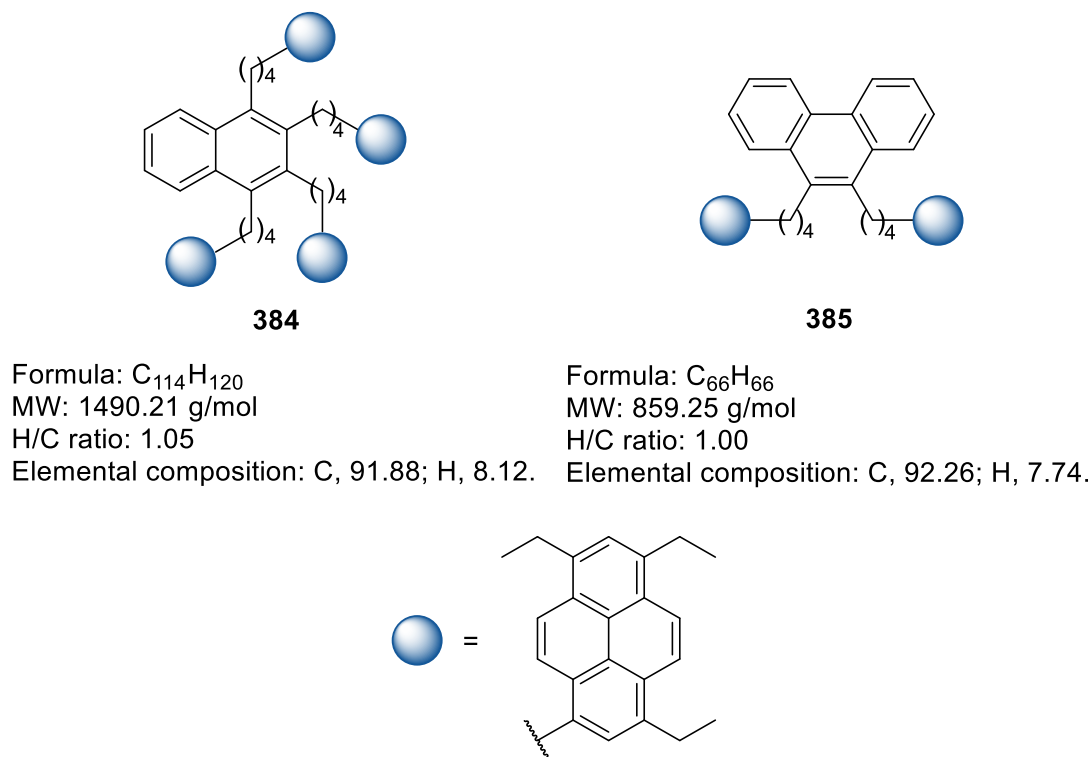


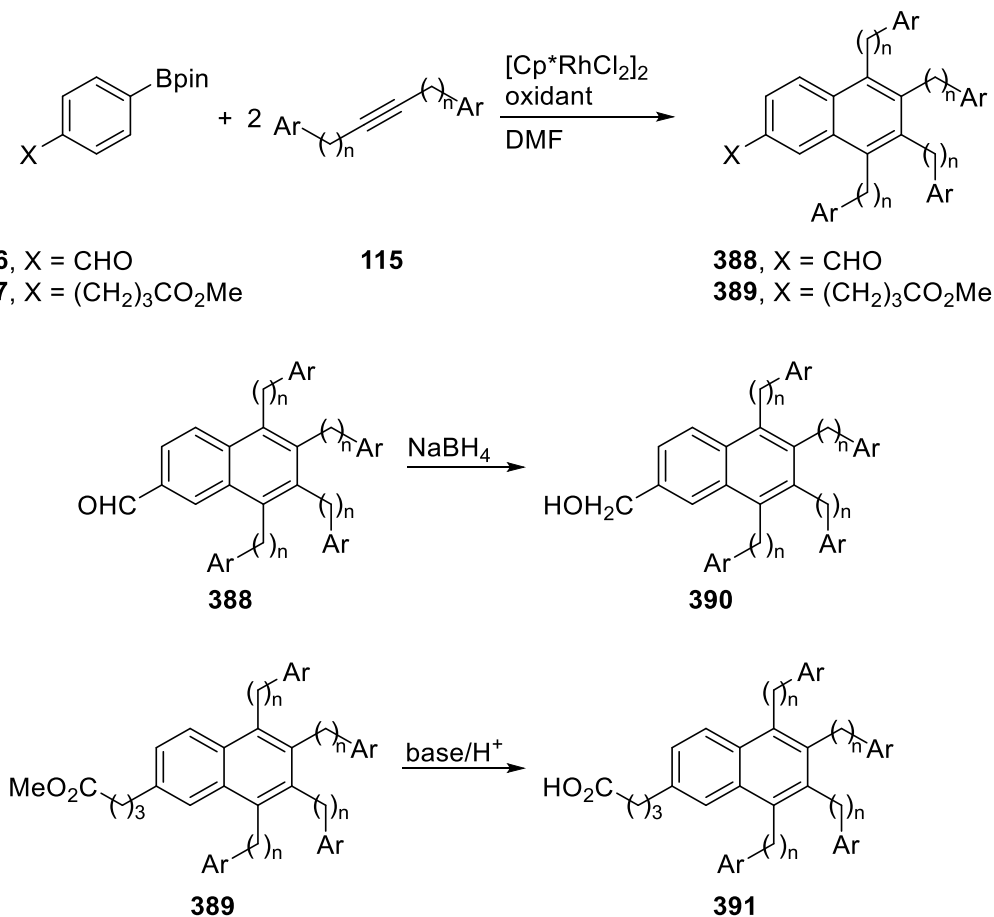
**Figure 5-2.** Expected archipelago model compounds from triethylpyrene island.

### 5.2.2 Archipelago compounds containing oxygen functional groups

As described in section 1.1.2, oxygen is the second most abundant heteroatom in asphaltenes<sup>6</sup> and it is mostly found in functional groups such as carboxylic acids, alcohols and ketones.<sup>30,31,34</sup> According to Gray's supramolecular asphaltene model, acid-base interactions and hydrogen bonding, which partially arise from oxygen-containing functional groups, are two of main interactions leading to asphaltene aggregation.<sup>66</sup> However, almost none of the current

archipelago model compounds contain these functional groups, which restrict the utility of related aggregation studies.

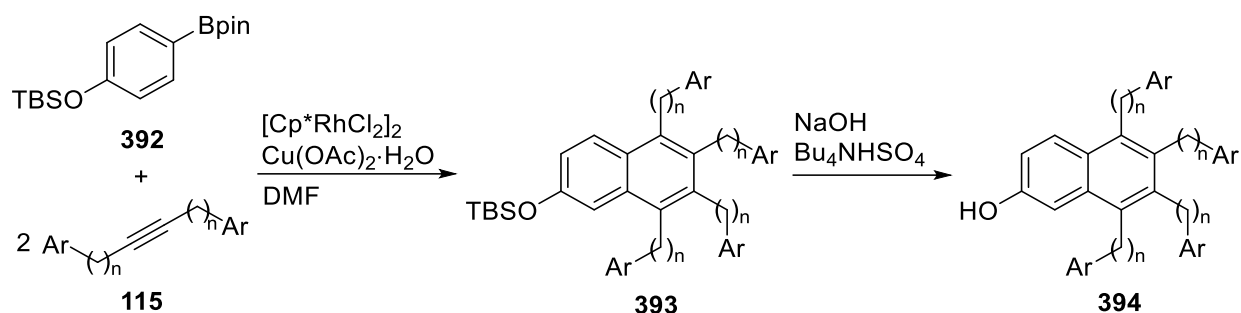
Probable synthetic routes for archipelago compounds containing alcohol (**390**) or carboxyl (**391**) groups are elaborated in Scheme 5-1. The starting pinacol boronates **386** and **387** could be prepared by literature procedures.<sup>239-241</sup> The annulations of island-tethered alkynes with **386** or **387**, which were proved to be feasible by Miura and co-workers (**43** and **44** in Scheme 1-6),<sup>101</sup> will produce aldehyde- or ester-containing archipelago product **388** or **389**. The reduction of **388** by NaBH<sub>4</sub> will provide alcohol-containing archipelago compound **390**. Treating **389** with base and subsequent acidification will afford carboxyl-containing archipelago compound **391**.



**Scheme 5-1.** Possible synthetic routes for archipelago compounds with alcohol or carboxyl groups.

The phenol-containing archipelago compound **394** can be prepared by annulation of TBS-protected pinacol boronate **392** and subsequent deprotection (Scheme 5-2).<sup>242</sup> **390**, **391**, and **394** are expected to have intermolecular hydrogen bonding, and hence show stronger aggregation behavior.





**Scheme 5-2.** Possible synthetic route for archipelago compounds with phenol groups.

### 5.2.3 Biomarker anion-containing archipelago compounds

The synthesis of cationic nitrogen-embedded archipelago compounds in chapter 4 provides support for studying asphaltene models involving acid-base interactions, but these models can be further optimized to better imitate asphaltenes if the triflate anions are replaced by alkyl carboxylates. I attempted to exchange the anions in these compounds (e.g., mixing the solution of archipelago compounds with sodium bicarbonate or sodium benzoate solution), but did not observe any reactions to occur. The recovered product was still the starting triflate salt. These results indicate that a general procedure must still be established for this process.

In addition, many porphyrin-containing model compounds have been reported<sup>88-90</sup> but examples of porphyrin structure with alkyl carboxylic acid or carboxylate groups are rare. At present, Munashe Chizema in our research group is conducting relevant synthesis of carboxyl-containing porphyrin structures **395** (Figure 5-3) starting from *spirulina* algae.

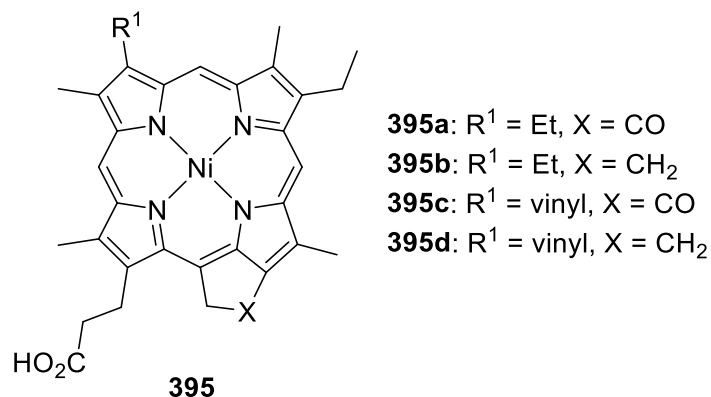
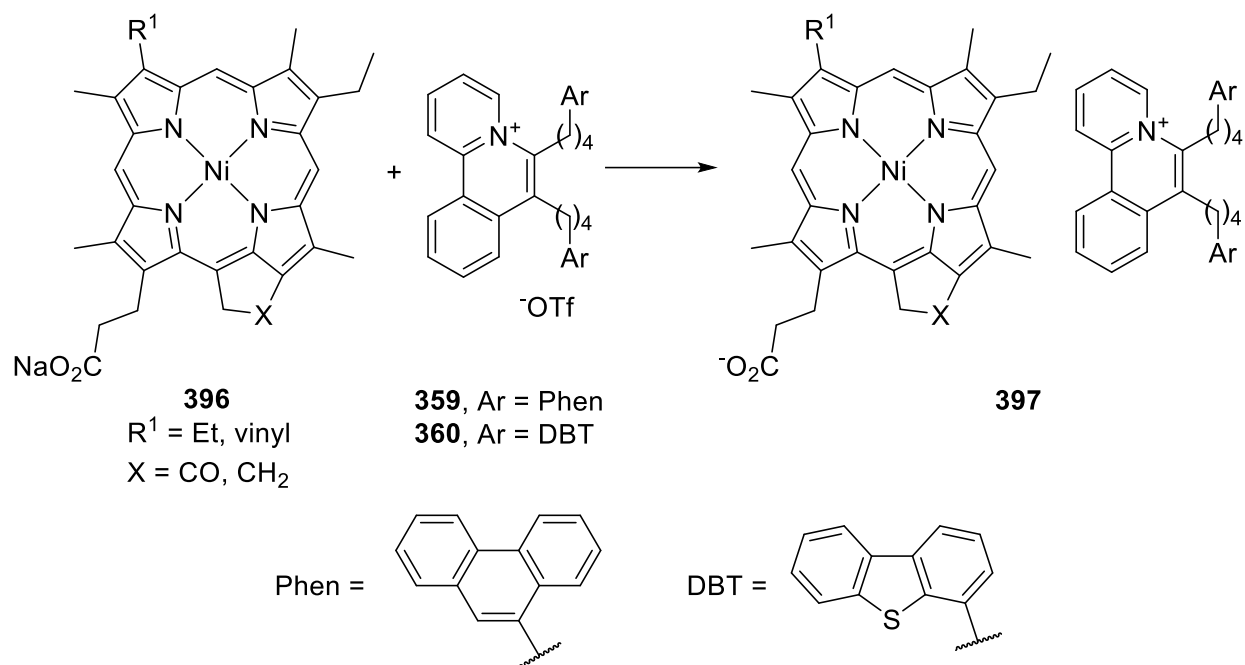


**Figure 5-3.** Target structures of carboxyl-containing porphyrin synthesis.

After the preparation of **395**, the ion exchange of the cationic archipelago compounds with sodium salts of **395** (i.e., **396**) is expected to proceed, to explore the benzoquinolizinium cation-porphyrin anion heterodimers **397** (Equation 5-1). The supramolecular characterization of **397** will be conducted once it is prepared (e.g.,  $^1\text{H}$ -DOSY studies). I hypothesize that these heterodimers should be valuable materials for studying the effects of intermolecular interactions on asphaltene aggregation.



**Equation 5-1.** Ion exchanges of cationic nitrogen-embedded archipelago compounds with carboxyl-containing porphyrin structures (exemplified by a benzo[*a*]quinolizinium structure).

## Bibliography

- (1) Leòn, V.; Kumar, M. *Biotechnol. Bioprocess Eng.* **2005**, *10*, 471–481.
- (2) Haji-Akbari, N.; Masirisuk, P.; Hoepfner, M. P.; Fogler, H. S. *Energy Fuels* **2013**, *27*, 2497–2505.
- (3) Gray, M. R. *Upgrading Oilsands Bitumen and Heavy Oil*; The University of Alberta Press: Edmonton, 2015.
- (4) Santos, R. G.; Loh, W.; Bannwart, A. C.; Trevisan, O. V. *Brazilian J. Chem. Eng.* **2014**, *31*, 571–590.
- (5) Strausz, O. P.; Morales-Izquierdo, A.; Kazmi, N.; Montgomery, D. S.; Payzant, J. D.; Safarik, I.; Murgich, J. *Energy Fuels* **2010**, *24*, 5053–5072.
- (6) Strausz, O. P.; Lown, E. M. *The Chemistry of Alberta Oil Sands, Bitumens and Heavy Oils*; Alberta Energy Research Institute: Calgary, 2003.
- (7) Yaghi, B. M.; Al-Bemani, A. *Energy Sources* **2002**, *24*, 93–102.
- (8) Li, X.; Chi, P.; Guo, X.; Sun, Q. *Fuels* **2019**, *255*, 115825.
- (9) Groenzin, H.; Mullins, O. C. *J. Phys. Chem. A* **1999**, *103*, 11237–11245.
- (10) Fan, T.; Buckley, J. S. *Energy Fuels* **2002**, *16*, 1571–1575.
- (11) Maqbool, T.; Balgoa, A. T.; Fogler, H. S. *Energy Fuels* **2009**, *23*, 3681–3686.
- (12) Mullins, O. C.; Sheu, E. Y.; Hammami, A.; Marshall, A. G. *Asphaltenes, Heavy Oils, and Petroleomics*; Springer: New York, 2007; Vol. 1.
- (13) Maqbool, T.; Srikiratiwong, P.; Fogler, H. S. *Energy Fuels* **2011**, *25*, 694–700.
- (14) Peramanu, S.; Singh, C.; Agrawala, M.; Yarranton, H. W. *Energy Fuels* **2001**, *15*, 910–917.
- (15) Molina V., D.; Ariza, E.; Poveda, J. C. *Energy Fuels* **2017**, *31*, 133–139.
- (16) Molina V., D.; León, E. A.; Chaves-Guerrero, A. *Energy Fuels* **2017**, *31*, 8997–9005.
- (17) Buckley, J. S. *Energy Fuels* **2012**, *26*, 4086–4090.
- (18) Zhao, B.; Shaw, J. M. *Energy Fuels* **2008**, *22*, 1080–1092.
- (19) Eskin, D.; Mohammadzadeh, O.; Akbarzadeh, K.; Taylor, S. D.; Ratulowski, J. *Can. J. Chem. Eng.* **2016**, *94*, 1202–1217.
- (20) Stark, J. L.; Asomaning, S. *Pet. Sci. Technol.* **2003**, *21*, 569–579.
- (21) Strausz, O. P.; Torres, M.; Lown, E. M.; Safarik, I.; Murgich, J. *Energy Fuels* **2006**, *20*, 2013–2021.

- (22) Scott, D. E. Mechanism of iodine-catalyzed multicomponent cyclocondensation reactions: Synthesis of polysubstituted quinoline "archipelago" asphaltene mimics, Ph. D. Dissertation, University of Alberta, Edmonton, AB, **2019**.
- (23) Yen, T. F. *Chemistry of Asphaltenes*; Bunger, J. W., Li, N. C., Eds.; American Chemical Society: Washington, D.C, 1982; Chapter 4.
- (24) Schuler, B.; Meyer, G.; Peña, D.; Mullins, O. C.; Gross, L. *J. Am. Chem. Soc.* **2015**, *137*, 9870–9876.
- (25) Groenzin, H.; Mullins, O. C. *Energy Fuels* **2000**, *14*, 677–684.
- (26) Pomerantz, A. E.; Hammond, M. R.; Morrow, A. L.; Mullins, O. C.; Zare, R. N. *J. Am. Chem. Soc.* **2008**, *130*, 7216–7217.
- (27) Hurt, M. R.; Borton, D. J.; Choi, H. J.; Kenttämaa, H. I. *Energy Fuels* **2013**, *27*, 3653–3658.
- (28) Pinkston, D. S.; Duan, P.; Gallardo, V. A.; Habicht, S. C.; Tan, X.; Qian, K.; Gray, M.; Mullen, K.; Kenttämaa, H. I. *Energy Fuels* **2009**, *23*, 5564–5570.
- (29) Neumann, A.; Chacón-Patiño, M. L.; Rodgers, R. P.; Rüger, C. P.; Zimmermann, R. *Energy Fuels* **2021**, *35*, 3808–3824.
- (30) Speight, J. G. *Oil Gas Sci. Technol.* **2004**, *59*, 467–477.
- (31) Sheu, E. Y.; Mullins, O. C. *Asphaltenes Fundamentals and Applications*, Plenum Press, New York, **1995**.
- (32) Strausz, O. P.; Mojelsky, T. W.; Faraji, F.; Lown, E. M.; Peng, P. *Energy Fuels* **1999**, *13*, 207–227.
- (33) Schmitter, J.M.; Garrigues, P.; Ignatiadis, I.; De Vazelhes, R.; Perin, F.; Ewald, M.; Arpino, P. *Org. Geochem.* **1984**, *6*, 579–586.
- (34) Rose, K. D.; Francisco, M. A. *Energy Fuels* **1987**, *1*, 233–239.
- (35) Stoyanov, S. R.; Yin, C. -X.; Gray, M. R.; Stryker, J. M.; Gusarov, S.; Kovalenko, A. J. *Phys. Chem. B* **2010**, *114*, 2180–2188.
- (36) Verne-Mismer, J.; Ocampo, R.; Bauder, C.; Callot, H. J.; Albrecht, P. *Energy Fuels* **1990**, *4*, 639–643.
- (37) Liu, H.; Mu, J.; Wang, Z.; Ji, S.; Shi, Q.; Guo, A.; Chen, K.; Lu, J. *Energy Fuels* **2015**, *29*, 4803–4813.
- (38) Yarranton, H. W.; Masliyah, J. H. *AIChE J.* **1996**, *42*, 3533–3543.
- (39) Spiecker, P. M.; Gawrys, K. L.; Kilpatrick, P. K. *J. Colloid Interface Sci.* **2003**, *267*, 178–193.
- (40) Mullins, O. C.; Martínez-Haya, B.; Marshall, A. G. *Energy Fuels* **2008**, *22*, 1765–1773.

- (41) Yarranton, H. W.; Alboudwarej, H.; Jakher, R. *Ind. Eng. Chem. Res.* **2000**, *39*, 2916–2924.
- (42) Acevedo, S.; Guzman, K.; Ocanto, O. *Energy Fuels* **2010**, *24*, 1809–1812.
- (43) Smith, D. F.; McKenna, A. M.; Corilo, Y. E.; Rodgers, R. P.; Marshall, A. G.; Heeren, R. M. *Energy Fuels* **2014**, *28*, 6284–6288.
- (44) Sabbah, H.; Morrow, A. L.; Pomerantz, A. E.; Mullins, O. C.; Tan, X.; Gray, M. R.; Azyat, K.; Tykwinski, R. R.; Zare, R. N. *Energy Fuels* **2010**, *24*, 3589–3594.
- (45) Borton, D.; Pinkston, D. S.; Hurt, M. R.; Tan, X.; Azyat, K.; Scherer, A.; Tykwinski, R.; Gray, M.; Qian, K.; Kenttämä, H. I. *Energy Fuels* **2010**, *24*, 5548–5559.
- (46) Hoepfner, M. P.; Vilas Bôas Fávero, C.; Haji-Akbari, N.; Fogler, H. S. *Langmuir* **2013**, *29*, 8799–8808.
- (47) Merino-Garcia, D.; Andersen, S. I. *Pet. Sci. Technol.* **2003**, *21*, 507–525.
- (48) Merino-Garcia, D.; Murgich, J.; Andersen, S. I. *Pet. Sci. Technol.* **2004**, *22*, 735–738.
- (49) Wei, D.; Orlandi, E.; Simon, S.; Sjöblom, J.; Suurkuusk, M.; *J. Therm. Anal. Calorim.* **2015**, *120*, 1835–1846.
- (50) Groenzin, H.; Mullins, O. C.; Eser, S.; Mathews, J.; Yang, M. G.; Jones, D. *Energy Fuels* **2003**, *17*, 498–503.
- (51) Aske, N.; Kallevik, H.; Johnsen, E. E.; Sjöblom, J. *Energy Fuels* **2002**, *16*, 1287–1295.
- (52) Auflem, I. H.; Havre, T. E.; Sjöblom, J. *Colloid Polym. Sci.* **2002**, *280*, 695–700.
- (53) Barbour, R. V.; Petersen, J. C. *Anal. Chem.* **1974**, *46*, 273–277.
- (54) Moschopedis, S. E.; Speight, J. G. *Fuel* **1976**, *55*, 187–192.
- (55) Ruiz-Morales, Y.; Mullins, O. C. *Energy Fuels* **2007**, *21*, 256–265.
- (56) Östlund, J. -A.; Wattana, P.; Nydén, M.; Fogler, H. S. *J. Colloid Interface Sci.* **2004**, *271*, 372–380.
- (57) Kawashima, H.; Takanohashi, T.; Iino, M.; Matsukawa, S. *Energy Fuels* **2008**, *22*, 3989–3993.
- (58) Yen, T. F.; Erdman, J. G.; Pollack, S. S. *Anal. Chem.* **1961**, *33*, 1587–1594.
- (59) Mullins, O. C. *Energy Fuels* **2010**, *24*, 2179–2207.
- (60) Mullins, O. C. *Annu. Rev. Anal. Chem.* **2011**, *4*, 393–418.
- (61) Mullins, O. C.; Sabbah, H.; Eyssautier, J.; Pomerantz, A. E.; Barré, L.; Andrews, A. B.; Ruiz-Morales, Y.; Mostowfi, F.; McFarlane, R.; Goual, L.; Lepkowicz, R.; Copper, T.; Orbulescu, J.; Leblanc, R. M.; Edwards, J.; Zare, R. N. *Energy Fuels* **2012**, *26*, 3986–4003.

- (62) Gross, L.; Mohn, F.; Moll, N.; Liljeroth, P.; Meyer, G. *Science* **2009**, *325*, 1110–1114.
- (63) Schuler, B.; Fatayer, S.; Meyer, G.; Rogel, E.; Moir, M.; Zhang, Y.; Harper, M. R.; Pomerantz, A. E.; Bake, K. D.; Witt, M.; Peña, D.; Kushnerick, J. D.; Mullins, O. C.; Ovalles, C.; van den Berg, F. G. A.; Gross, L. *Energy Fuels* **2017**, *31*, 6856–6861.
- (64) Tanaka, R.; Sato, E.; Hunt, J. E.; Winans, R. E.; Sato, S.; Takanohashi, T. *Energy Fuels* **2004**, *18*, 1118–1125.
- (65) Rakotonradany, F.; Fenniri, H.; Rahimi, P.; Gawrys, K. L.; Kilpatrick, P. K.; Gray, M. R. *Energy Fuels* **2006**, *20*, 2439–2447.
- (66) Gray, M. R.; Tykwinski, R. R.; Stryker, J. M.; Tan, X. *Energy Fuels* **2011**, *25*, 3125–3134.
- (67) Gawrys, K. L.; Blankenship, G. A.; Kilpatrick, P. K. *Langmuir* **2006**, *22*, 4487–4497.
- (68) Rueda-Velázquez, R. I.; Freund, H.; Qian, K.; Olmstead, W. N.; Gray, M. R. *Energy Fuels* **2013**, *27*, 1817–1829.
- (69) Chacón-Patiño, M. L.; Blanco-Tirado, C.; Orrego-Ruiz, J. A.; Gómez-Escudero, A.; Combariza, M. Y. *Energy Fuels* **2015**, *29*, 6330–6341.
- (70) Murgich, J.; Abanero, J. A.; Strausz, O. P. *Energy Fuels* **1999**, *13*, 278–286.
- (71) Sheremata, J. M.; Gray, M. R.; Dettman, H. D.; McCaffrey, W. C. *Energy Fuels* **2004**, *18*, 1377–1384.
- (72) Chacón-Patiño, M. L.; Rowland, S. M.; Rodgers, R. P. *Energy Fuels* **2017**, *31*, 13509–13518.
- (73) Chacón-Patiño, M. L.; Rowland, S. M.; Rodgers, R. P. *Energy Fuels* **2018**, *32*, 314–328.
- (74) Chacón-Patiño, M. L.; Rowland, S. M.; Rodgers, R. P. *Energy Fuels* **2018**, *32*, 9106–9120.
- (75) Schuler, B.; Zhang, Y.; Collazos, S.; Fatayer, S.; Meyer, G.; Pérez, D.; Guitián, E.; Harper, M. R.; Kushnerick, J. D.; Peña, D.; Gross, L. *Chem. Sci.* **2017**, *8*, 2315–2320.
- (76) Chen, P.; Joshi, Y. V.; Metz, J. N.; Yao, N.; Zhang, Y. *Energy Fuels* **2020**, *34*, 12135–12141.
- (77) Sabbah, H.; Morrow, A. L.; Pomerantz, A. E.; Zare, R. N. *Energy Fuels* **2011**, *25*, 1597–1604.
- (78) Alshareef, A. H.; Scherer, A.; Tan, X.; Azyat, K.; Stryker, J. M.; Tykwinski, R. R.; Gray, M. R. *Energy Fuels* **2011**, *25*, 2130–2136.
- (79) Alshareef, A. H.; Tan, X.; Diner, C.; Zhao, J.; Scherer, A.; Azyat, K.; Stryker, J. M.; Tykwinski, R. R.; Gray, M. R. *Energy Fuels* **2014**, *28*, 1692–1700.
- (80) Akbarzadeh, K.; Bressler, D. C.; Wang, J.; Gawrys, K. L.; Gray, M. R.; Kilpatrick, P. K.; Yarranton, H. W. *Energy Fuels* **2005**, *19*, 1268–1271.

- (81) Tan, X.; Fenniri, H.; Gray, M. R. *Energy Fuels* **2008**, *22*, 715–720.
- (82) Diner, C.; Scott, D. E.; Tykwinski, R. R.; Gray, M. R.; Stryker, J. M. *J. Org. Chem.* **2015**, *80*, 1719–1726.
- (83) Nyadong, L.; Lai, J.; Thompsen, C.; LaFrancois, C. J.; Cai, X.; Song, C.; Wang, J.; Wang, W. *Energy Fuels* **2018**, *32*, 294–305.
- (84) Globek, T. W.; Faase, R. A.; Rasmussen, M. H.; Tykwinski, R. R.; Stryker, J. M.; Andersen, S. I.; Baio, J. E.; Weidner, T. *Langmuir* **2021**, *37*, 9785–9792.
- (85) Scott, D. E.; Aloisio, M. D.; Rodriguez, J. F.; Morimoto, M.; Hamilton, R. J.; Brown, O.; Tykwinski, R. R.; Stryker, J. M. *Adv. Synth. Catal.* **2021**, *363*, 4720–4727.
- (86) Scherer, A.; Hampel, F.; Gray, M. R.; Stryker, J. M.; Tykwinski, R. R. *J. Phys. Org. Chem.* **2012**, *25*, 597–606.
- (87) Schulze, M.; Scott, D. E.; Scherer, A.; Hampel, F.; Hamilton, R. J.; Gray, M. R.; Tykwinski, R. R.; Stryker, J. M. *Org. Lett.* **2015**, *17*, 5930–5933.
- (88) Morimoto, M.; Fukatsu, N.; Tanaka, R.; Takanohashi, T.; Kumagai, H.; Morita, T.; Tykwinski, R. R.; Scott, D. E.; Stryker, J. M.; Gray, M. R.; Sato, T.; Yamamoto, H. *Energy Fuels* **2018**, *32*, 11296–11303.
- (89) Schulze, M.; Scherer, A.; Hampel, F.; Stryker, J. M.; Tykwinski, R. R. *Chem. Eur. J.* **2016**, *22*, 3378–3386.
- (90) Cardozo, S. D.; Schulze, M.; Tykwinski, R. R.; Gray, M. R. *Energy Fuels* **2015**, *29*, 1494–1502.
- (91) Scott, D. E.; Schulze, M.; Stryker, J. M.; Tykwinski, R. R. *Chem. Soc. Rev.* **2021**, *50*, 9202–9239.
- (92) Watanabe, M.; Chen, K. -Y.; Chang, Y. J.; Chow, T. J. *Acc. Chem. Res.* **2013**, *46*, 1606–1615.
- (93) Anthony, J. E. *Angew. Chem. Int. Ed.* **2008**, *47*, 452–483.
- (94) Sundar, V. C.; Zaumseil, J.; Podzorov, V.; Menard, E.; Willett, R. L.; Someya, T.; Gershenson, M. E.; Rogers, J. A. *Science* **2004**, *303*, 1644–1646.
- (95) Schwarze, M.; Tress, W.; Beyer, B.; Gao, F.; Scholz, R.; Poelking, C.; Ortstein, K.; Günther, A. A.; Kasemann, D.; Andrienko, D.; Leo, K. *Science* **2016**, *352*, 1446–1449.
- (96) Brummond, K. M.; Kocsis, L. S. *Acc. Chem. Res.* **2015**, *48*, 2320–2329.
- (97) Xu, F.; Hershey, K. W.; Holmes, R. J.; Hoyer, T. R. *J. Am. Chem. Soc.* **2016**, *138*, 12739–12742.



- (98) Prusty, N.; Banjare, S. K.; Mohanty, S. R.; Nanda, T.; Yadav, K.; Ravikumar, P. C. *Org. Lett.* **2021**, *23*, 9041–9046.
- (99) Takahashi, T.; Li, Y.; Stepnicka, P.; Kitamura, M.; Liu, Y.; Nakajima, K.; Kotori, M. *J. Am. Chem. Soc.* **2002**, *124*, 576–582.
- (100) Huang, W.; Zhou, X.; Kanno, K.; Takahashi, T. *Org. Lett.* **2004**, *6*, 2429–2431.
- (101) Fukutani, T.; Hirano, K.; Satoh, T.; Miura, M. *J. Org. Chem.* **2011**, *76*, 2867–2874.
- (102) Komeyama, K.; Kashiwara, T.; Takaki, K. *Tetrahedron Lett.* **2013**, *42*, 5659–5662.
- (103) Pham, M. V.; Cramer, N. *Angew. Chem. Int. Ed.* **2014**, *53*, 3484–3487.
- (104) Wu, G.; Rheingold, A. L.; Geib, S. J.; Heck, R. F. *Organometallics* **1987**, *6*, 1941–1946.
- (105) Larock, R. C.; Doty, M. J.; Tian, Q.; Zenner, J. M. *J. Org. Chem.* **1997**, *62*, 7536–7537.
- (106) Ueura, K.; Satoh, T.; Miura, M. *J. Org. Chem.* **2007**, *72*, 5362–5367.
- (107) Honjo, Y.; Shibata, Y.; Kudo, E.; Namba, T.; Masutomi, K.; Tanaka, K. *Chem. Eur. J.* **2018**, *24*, 317–321.
- (108) Chen, H.; Ouyang, L.; Liu, J.; Shi, W. -J.; Chen, G.; Zheng, L. *J. Org. Chem.* **2019**, *84*, 12755–12763.
- (109) Ilies, L.; Matsumoto, A.; Kobayashi, M.; Yoshikai, N.; Nakamura, E. *Synlett* **2012**, *23*, 2381–2384.
- (110) Nagata, T.; Satoh, T.; Nishii, Y.; Miura, M. *Synlett* **2016**, *27*, 1707–1710.
- (111) Wang, C.; Rakshit, S.; Glorius, F. *J. Am. Chem. Soc.* **2010**, *132*, 14006–14008.
- (112) Matsumoto, A.; Ilies, L.; Nakamura, E. *J. Am. Chem. Soc.* **2011**, *133*, 6557–6559.
- (113) Nagata, T.; Hirano, K.; Satoh, T.; Miura, M. *J. Org. Chem.* **2014**, *79*, 8960–8967.
- (114) Yan, J.; Yoshikai, N. *Org. Lett.* **2017**, *19*, 6630–6633.
- (115) Wei, B.; Zhang, D.; Chen, Y. -H.; Lei, A.; Knochel, P. *Angew. Chem. Int. Ed.* **2019**, *58*, 15631–15635.
- (116) Zhang, G.; Yang, L.; Wang, Y.; Xie, Y.; Huang, H. *J. Am. Chem. Soc.* **2013**, *135*, 8850–8853.
- (117) Prakash, S.; Muralirajan, K.; Cheng, C.-H. *Angew. Chem. Int. Ed.* **2016**, *128*, 1876–1880.
- (118) Li, L.; Brennessel, W. W.; Jones, W. D. *J. Am. Chem. Soc.* **2008**, *130*, 12414–12419.
- (119) Luo, C.-Z.; Gandeepan, P.; Jayakumar, J.; Parthasarathy, K.; Chang, Y.-W.; Cheng, C.-H. *Chem. Eur. J.* **2013**, *19*, 14181–14846.

- (120) Lao, Y.-X.; Zhang, S.-S.; Liu, X.-G.; Jiang, C.-Y.; Wu, J.-Q.; Li, Q.; Huang, Z.-S.; Wang, H. *Adv. Synth. Catal.* **2016**, *358*, 2186–2191.
- (121) Ge, Q.; Hu, Y.; Li, B.; Wang, B. *Org. Lett.* **2016**, *18*, 2483–2486.
- (122) Gómez-Bujedo, S.; Alcarazo, M.; Pichon, C.; Álvarez, E.; Fernández, R.; Lassaletta, J. M. *Chem. Commun.* **2007**, 1180–1182.
- (123) Segarra, C.; Mas-Marzá, E.; Benítez, M.; Mata, J. A.; Peris, E. *Angew. Chem., Int. Ed.* **2012**, *51*, 10841–10845.
- (124) Hata, K.; Segawa, Y.; Itami, K. *Chem. Commun.* **2012**, *48*, 6642–6644.
- (125) Umeda, N.; Tsurugi, H.; Satoh, T.; Miura, M. *Angew. Chem. Int. Ed.* **2008**, *47*, 4019–4022.
- (126) Tan, X.; Liu, B.; Li, X.; Li, B.; Xu, S.; Song, H.; Wang, B. *J. Am. Chem. Soc.* **2012**, *134*, 16163–16166.
- (127) Luo, C. -Z.; Gandeepan, P.; Cheng, C. -H. *Chem. Commun.* **2013**, *49*, 8528–8530.
- (128) Li, S. -S.; Wang, C. -Q.; Lin, H.; Zhang, X. -M. Dong, L. *Org. Lett.* **2015**, *17*, 3018–3021.
- (129) Wang, H.; Moselage, M.; González, M. J.; Ackermann, L. *ACS Catal.* **2016**, *6*, 2705–2709.
- (130) Liang, Y.; Jiao, N. *Angew. Chem. Int. Ed.* **2016**, *55*, 4035–4039.
- (131) Ghorai, D.; Dutta, C. Choudhury, J. *ACS Catal.* **2016**, *6*, 709–713.
- (132) Villar, J. M.; Suárez, J.; Varela, J. A.; Saá, C. *Org. Lett.* **2017**, *19*, 1702–1705.
- (133) Martínez-Yáñez, N.; Suárez, J.; Cajaraville, A.; Varela, J. A.; Saá, C. *Org. Lett.* **2019**, *21*, 1779–1783.
- (134) Streit, A. D.; Zoll, A. J.; Hoang, G. L.; Ellman, J. A. *Org. Lett.* **2020**, *22*, 1217–1221.
- (135) Satoh, T.; Miura, M. *Chem. Eur. J.* **2010**, *16*, 11212–11222.
- (136) Kauffman, G. B.; Fang, L. Y. *Inorg. Syn.* **1983**, *22*, 101–103.
- (137) Klapars, A.; Buchwald, S. L. *J. Am. Chem. Soc.* **2002**, *124*, 14844–14845.
- (138) Cannon, K. A.; Geuther, M. E.; Kelly, C. K.; Lin, S.; MacArthur, A. H. R. *Organometallics* **2011**, *30*, 4067–4073.
- (139) Diederich, F.; Stang, P. J.; Tykwinski, R. R. *Acetylene Chemistry: Chemistry, Biology and Material Science*, Wiley-VCH Verlag GmbH & Co. KGaA, Weinheim, **2005**.
- (140) Smith, M. B. *March's Advanced Organic Chemistry: Reactions, Mechanisms, and Structure*, 7th Ed.; John Wiley & Sons, Inc., New Jersey, **2013**.
- (141) Topolovčan, N.; Panov, I.; Kotora, M. *Synlett* **2016**, *27*, 432–436.

- (142) Wolf, J.; Babics, M.; Wang, K.; Saleem, Q.; Liang, R.; Hansen, M. R.; Beaujuge, P. M. *Chem. Mater.* **2016**, *28*, 2058–2066.
- (143) Sonogashira, K.; Tohda, Y.; Hagihara, N. *Tetrahedron Lett.* **1975**, *16*, 4467–4470.
- (144) Chinchilla, R.; Nájera, C. *Chem. Rev.* **2007**, *107*, 874–922.
- (145) Gallop, C. W. D.; Chen, M.-T.; Navarro, O. *Org. Lett.* **2014**, *16*, 3724–3727.
- (146) Mino, T.; Suzuki, S.; Hirai, K.; Sakamoto, M.; Fujita, T. *Synlett* **2011**, *9*, 1277–1280.
- (147) Green, J. C.; Herbert, B. J.; Lonsdale, R. *J. Organomet. Chem.* **2005**, *690*, 6054–6067.
- (148) Eckhardt, M.; Fu, G. C. *J. Am. Chem. Soc.* **2003**, *125*, 13642–13643.
- (149) Pompeo, M.; Froese, R. D. J.; Hadei, N.; Organ, M. G. *Angew. Chem., Int. Ed.* **2012**, *51*, 11354–11357.
- (150) Diner, C. Scalable and concise approaches for the synthesis of “archipelago model” asphaltene compounds. Ph. D. Dissertation, University of Alberta, Edmonton, AB, **2015**.
- (151) Altenhoff, G.; Würtz, S.; Glorius, F. *Tetrahedron Lett.* **2006**, *47*, 2925–2928.
- (152) Chen, M.; Zheng, X.; Li, W.; He, J.; Lei, A. *J. Am. Chem. Soc.* **2010**, *132*, 4101–4103.
- (153) Adamo, C.; Amatore, C.; Ciofini, I.; Jutand, A.; Lakmini, H. *J. Am. Chem. Soc.* **2006**, *128*, 6829–6836.
- (154) Cahiez, G.; Gager, O.; Buendia, J. *Angew. Chem. Int. Ed.* **2010**, *49*, 1278–1281.
- (155) Thapa, S.; Kafle, A.; Gurung, S. K.; Montoya, A.; Riedel, P.; Giri, R. *Angew. Chem. Int. Ed.* **2015**, *54*, 8236–8240.
- (156) Vechorkin, O.; Godinat, A.; Scopelliti, R.; Hu, X. *Angew. Chem. Int. Ed.* **2011**, *50*, 11777–11781.
- (157) Csok, Z.; Vechorkin, O.; Harkins, S. B.; Scopelliti, R.; Hu, X. *J. Am. Chem. Soc.* **2008**, *130*, 8156–8157.
- (158) Ren, P.; Vechorkin, O.; Csok, Z.; Salihu, I.; Scopelliti, R.; Hu, X. *Dalton Trans.* **2011**, *40*, 8906–8911.
- (159) Cheung, C. W.; Ren, P.; Hu, X. *Org. Lett.* **2014**, *16*, 2566–2569.
- (160) Hatakeyama, T.; Okada, Y.; Yoshimoto, Y.; Nakamura, M. *Angew. Chem. Int. Ed.* **2011**, *50*, 10973–10976.
- (161) Mortreux, A.; Blanchard, M. *J. Chem. Soc., Chem. Commun.* **1974**, *19*, 786–787.
- (162) Wengrovius, J. H.; Sancho, J.; Schrock, R. R. *J. Am. Chem. Soc.* **1981**, *103*, 3932–3934.

- (163) McCullough, L. G.; Listemann, M. L.; Schrock, R. R.; Churchill, M. R.; Ziller, J. W. *J. Am. Chem. Soc.* **1983**, *105*, 6729–6730.
- (164) Haberlag, B.; Freytag, M.; Daniliuc, C. G.; Jones, P. G.; Tamm, M. *Angew. Chem. Int. Ed.* **2012**, *51*, 13019–13022.
- (165) Bray, A.; Mortreux, A.; Petit, F.; Petit, M.; Szymanska-Buzar, T. *J. Chem. Soc., Chem. Commun.* **1993**, *2*, 197–199.
- (166) Mortreux, A.; Petit, F.; Petit, M.; Szymanska-Buzar, T. *J. Mol. Catal.* **1995**, *96*, 95–105.
- (167) Coutelier, O.; Mortreux, A. *Adv. Synth. Catal.* **2006**, *348*, 2038–2042.
- (168) Bittner, C.; Ehrhorn, H.; Bockfeld, D.; Brandhorst, K.; Tamm, M. *Organometallics* **2017**, *36*, 3398–3406.
- (169) Fürstner, A. *J. Am. Chem. Soc.* **2021**, *143*, 15538–15555.
- (170) Smith, W. N.; Beumel, O. F. *Synthesis* **1974**, *6*, 441–443.
- (171) Baughman, T. W.; Sworen, J. C.; Wagener, K. B. *Tetrahedron* **2004**, *60*, 10943–10948.
- (172) Beale, A. M.; Gibson, E. K.; O'Brien, M. G.; Jacques, S. D. M.; Cernik, R. J.; Di Michiel, M.; Cobden, P. D.; Pirgon-Galin, Ö.; van de Water, L.; Watson, M. J.; Weckhuysen, B. M. *J. Catal.* **2014**, *314*, 94–100.
- (173) Shafi, R.; Hutchings, G. J. *Catal. Today* **2000**, *59*, 423–442.
- (174) Kuehm-Caubère, C.; Adach-Becker, S.; Fort, Y.; Caubère, P. *Tetrahedron* **1996**, *52*, 9087–9092.
- (175) Tian, P. -P.; Cai, S. -H.; Liang, Q. -J.; Zhou, X. -Y.; Xu, Y. -H.; Loh, T. -P. *Org. Lett.* **2015**, *17*, 1636–1639.
- (176) Shi, C.; Miao, Q.; Ma, L.; Lu, T.; Yang, D.; Chen, J.; Li, Z. *ChemistrySelect* **2019**, *4*, 6043–6047.
- (177) Zhong, Z.; Wang, Z.-Y.; Ni, S.-F.; Dang, L.; Lee, H. K.; Peng, X.-S.; Wong, H. N. C. *Org. Lett.* **2019**, *21*, 700–704.
- (178) Lee, Y. H.; Denton, E. H.; Morandi, B. *Nat. Chem.* **2021**, *13*, 123–130.
- (179) Marcó, A.; Compañó, R.; Rubio, R.; Casals, I. *Mikrochim. Acta* **2003**, *142*, 13–19.
- (180) Tan, P. W.; Haughey, M.; Dixon, D. J. *Chem. Commun.* **2015**, *51*, 4406–4409.
- (181) Mueller, C. J.; Klein, T.; Gann, E.; McNeill, C. R.; Thelakkat, M. *Macromolecules* **2016**, *49*, 3749–3760.
- (182) Clary, J. W.; Rettenmaier, T. J.; Snelling, R.; Bryks, W.; Banwell, J.; Wipke, W. T.; Singaram, B. *J. Org. Chem.* **2011**, *76*, 9602–9610.

- (183) Akhil, A. G.; Mohammed, A. K. P. K.; Akhilesh, S.; Muhammad, A. C. A.; Khan, S.; Kanna, R. *Int. Ref. J. Eng. Sci.* **2017**, *6*, 1–4.
- (184) *Organic Chemistry Data Collection, NMR Spectroscopy*.  
<https://organicchemistrydata.org/hansreich/resources/nmr/?page=05-hmr-15-aabb%2F> (accessed 2022-03-04)
- (185) Jackman, L. M.; Sternhell, S. *Applications of Nuclear Magnetic Resonance Spectroscopy in Organic Chemistry 2nd Edition*; Pergamon Press, 1969.
- (186) Morris, K. F.; Johnson, C. S. *J. Am. Chem. Soc.* **1992**, *114*, 3139–3141.
- (187) Durand, E.; Clemancey, M.; Quoineaud, A.-A.; Verstraete, J.; Espinat, D.; Lancelin, J.-M. *Energy Fuels* **2008**, *22*, 2604–2610.
- (188) da Silva Oliveira, E. C.; Neto, A. C.; Lacerda Júnior, V.; de Castro, E. V. R.; de Menezes, S. M. C. *Fuel* **2014**, *117*, 146–151.
- (189) Subramanian, S.; Sørland, G. H.; Simon, S.; Xu, Z.; Sjöblom, J. *Colloids Surf., A* **2017**, *514*, 79–90.
- (190) Madeira, N. C. L.; Rainha, K. P.; Mendonça, J.; Lacerda, V.; Chinelatto, L. S.; De Menezes, S. M. C.; Porto, C. F. D. C.; Pinto, F. E.; Filgueiras, P. R.; Romão, W.; Neto, Á. C. *Energy Fuels* **2020**, *34*, 5679–5688.
- (191) Li, W.; Chung, H.; Daeffler, C.; Johnson, J. A.; Grubbs, R. H. *Macromolecules* **2012**, *45*, 9595–9603.
- (192) Didenko, T.; Boelens, R.; Rüdiger, S. G. D. *Protein Eng. Des. Sel.* **2011**, *24*, 99–103.
- (193) Pal, A., Bhardwaj, R.K. *J. Chem. Sci.* **2001**, *113*, 215–225.
- (194) Macchioni, A.; Ciancaleoni, G.; Zuccaccia, C.; Zuccaccia, D. *Chem. Soc. Rev.* **2008**, *37*, 479–489.
- (195) Chen, H. C.; Chen, S. H. *J. Phys. Chem.* **1984**, *88*, 5118–5121.
- (196) Kawashima, H.; Takanohashi, T.; Iino, M.; Matsukawa, S. *Energy Fuels* **2008**, *22*, 3989–3993.
- (197) Lisitza, N. V.; Freed, D. E.; Sen, P. N.; Song, Y. -Q. *Energy Fuels* **2009**, *23*, 1189–1193.
- (198) Norinaga, K.; Wargardalam, V. J.; Takasugi, S.; Iino, M.; Matsukawa, S. *Energy Fuels* **2001**, *15*, 1317–1318.
- (199) White, C.; Yates, A.; Maitlis, P. M.; Heinekey, D. M., *Inorg. Synth.* **1992**, *29*, 228–234.
- (200) Zhao, S.; Liang, J.; Guo, T.; Wang, Y.; Chen, X.; Fu, D.; Xiong, J.; Ying, L.; Yang, W.; Peng, J.; Cao, Y. *Organic Electronics* **2016**, *38*, 130–138.
- (201) Krane, B. D.; Fagbule, M. O.; Shamma, M.; Gozler, B. *J. Nat. Prod.* **1984**, *47*, 1–43.

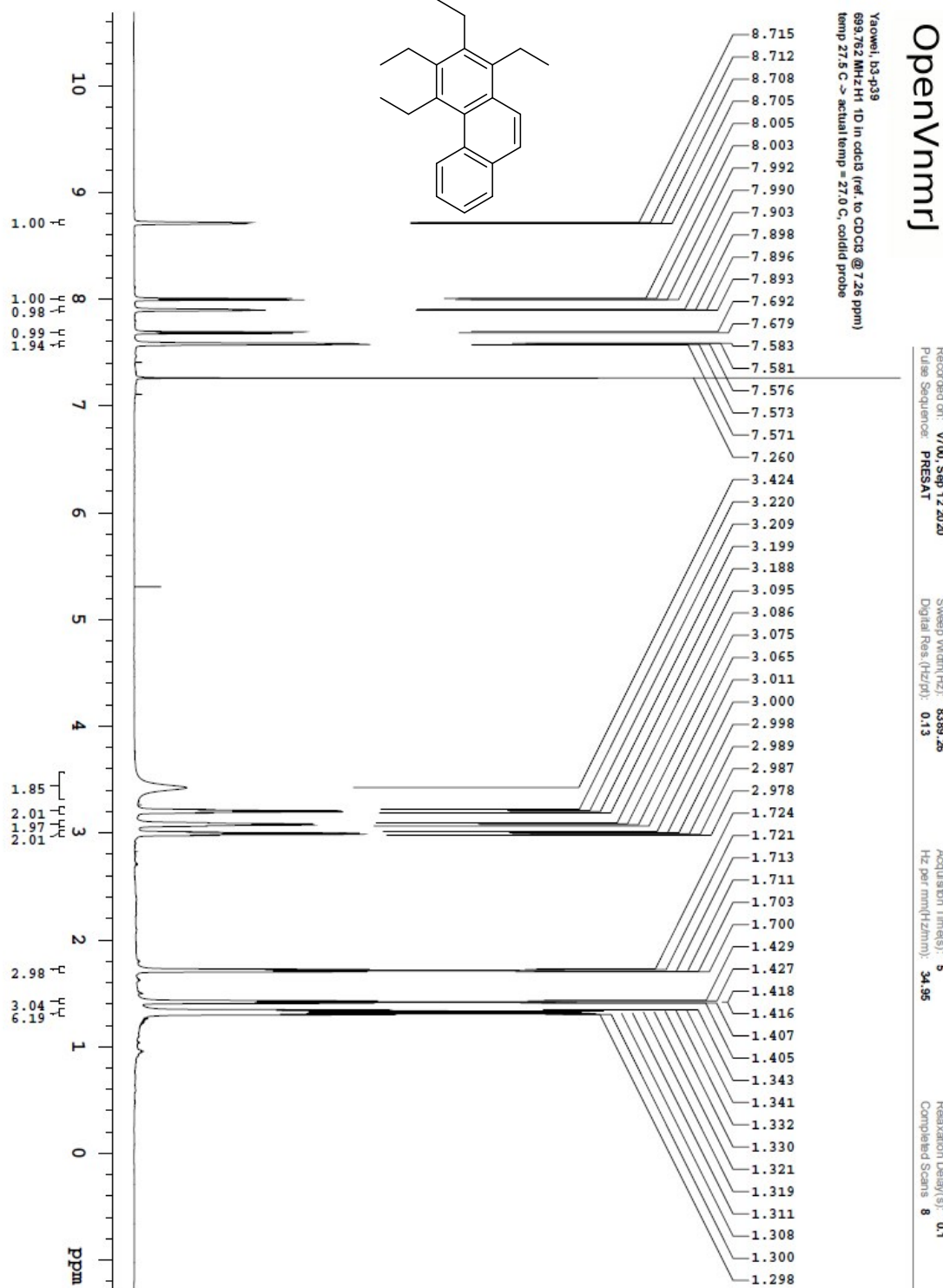
- (202) Mori-Quiroz, L. M.; Hedrick, S. L.; De Los Santos, A. R.; Clift, M. D. *Org. Lett.* **2018**, *20*, 4281–4284.
- (203) Petkovic, M.; Seddon, K. R.; Rebelo, L. P. N.; Pereira, C. S. *Chem. Soc. Rev.* **2011**, *40*, 1383–1403.
- (204) Lava, K.; Evrard, Y.; Van Hecke, K.; Van Meervelt, L.; Binnemans, K. *RSC Advances* **2012**, *2*, 8061–8070.
- (205) Królikowska, M.; Karpińska, M.; Zawadzki, M. *J. Phys. Chem. B* **2012**, *116*, 4292–4299.
- (206) Królikowska, M.; Karpińska, M. *Fluid Phase Equilib.* **2015**, *400*, 1–7.
- (207) Marcelo, G.; Pinto, S.; Cañeque, T.; Mariz, I. F. A.; Cuadro, A. M.; Vaquero, J. J.; Martinho, J. M. G.; Maçôas, E. M. S. *J. Phys. Chem. A* **2015**, *119*, 2351–2362.
- (208) Geddes, C. D.; Douglas, P.; Moore, C. P.; Wear, T. J.; Egerton, P. L. *Dyes and Pigments* **1999**, *43*, 59–63.
- (209) Geddes, C. D.; Apperson, K.; Birch, D. J. S. *Dyes and Pigments* **2000**, *44*, 69–74.
- (210) Ihmels, H.; Faulhaber, K.; Vedaldi, D.; Dall’Acqua, F.; Viola, G. *Photochem. Photobiol.* **2005**, *81*, 1107–1115.
- (211) Ihmels, H.; Otto, D.; Dall’Acqua, F.; Faccio, A.; Moro, S.; Viola, G. *J. Org. Chem.* **2006**, *71*, 8401–8411.
- (212) Granzhan, A.; Ihmels, H.; *Synlett* **2016**, *27*, 1775–1793.
- (213) Murthy, A. S. N.; Bhardwaj, A. P. *Spectrochim. Acta A* **1983**, *39*, 415–418.
- (214) Tang, J.; Chen, X.; Zhao, C. -Q.; Li, W. -J.; Li, S.; Zheng, X. -L.; Yuan, M. -L.; Fu, H. -Y.; Li, R. -X.; Chen, H. *J. Org. Chem.* **2021**, *86*, 716–730.
- (215) Meth-Cohn, O.; Taylor, D. L. *Tetrahedron* **1995**, *51*, 12869–12882.
- (216) Katritzky, A. R.; Semenzin, D.; Yang, B.; Pleyne, D. P. M. *J. Heterocyclic Chem.* **1998**, *35*, 467–470.
- (217) Wu, Y.; Shao, M.; Feng, Z.; Gu, X.; Hong, Y.; Cui, Q.; Ren, L.; Wang, S. *Asian J. Org. Chem.* **2017**, *6*, 76–82.
- (218) Cheng, L. -C.; Chen, W. -C.; Santhoshkumar, R.; Chao, T. -H.; Cheng, M. -J.; Cheng, C. -H. *Eur. J. Org. Chem.* **2020**, 2116–2129.
- (219) Deady, L. W. *Aust. J. Chem.* **1981**, *34*, 163–170.
- (220) Parthasarathy, K.; Senthilkumar, N.; Jayakumar, J.; Cheng, C. -H. *Org. Lett.* **2012**, *14*, 3478–3481.
- (221) Jayakumar, J.; Parthasarathy, K.; Cheng, C.-H. *Angew. Chem. Int. Ed.* **2012**, *51*, 197–200.

- (222) Kim, D.-S.; Park, J.-W.; Jun, C.-H. *Adv. Synth. Catal.* **2013**, *355*, 2667–2679.
- (223) Boekelheide, V.; Gall, W. G. *J. Am. Chem. Soc.* **1954**, *76*, 1832–1836.
- (224) Delgado, F.; Linares, M. L.; Alajarán, R.; Vaquero, J. J.; Alvarez-Builla, J. *Org. Lett.* **2003**, *5*, 4057–4060.
- (225) García-Cuadrado, D.; Cuadro, A. M.; Barchín, B. M.; Nuñez, A.; Cañeque, T.; Alvarez-Builla, J.; Vaquero, J. J. *J. Org. Chem.* **2006**, *71*, 7989–7995.
- (226) Nuñez, A.; Abarca, B.; Cuadro, A. M.; Alvarez-Builla, J.; Vaquero, J. J. *J. Org. Chem.* **2009**, *74*, 4166–4176.
- (227) Glover, E. E.; Jones, G. *J. Chem. Soc.* **1958**, 3021–3028.
- (228) Kimber, R. W. L.; Parham, J. C. *J. Org. Chem.* **1963**, *28*, 3205–3206.
- (229) Mariano, P. S.; Krochmal, E. Jr.; Leone, A. *J. Org. Chem.* **1977**, *42*, 1122–1125.
- (230) Arai, S.; Takeuchi, T.; Ishikawa, M.; Takeuchi, T.; Yamazaki, M.; Hida, M. *J. Chem. Soc., Perkin Trans. I* **1987**, *3*, 481–487.
- (231) Núñez, A.; Cuadro, A. M.; Alvarez-Builla, J.; Vaquero, J. J. *Org. Lett.* **2007**, *9*, 2977–2980.
- (232) Nuñez, A.; Abarca, B.; Cuadro, A. M.; Alvarez-Builla, J.; Vaquero, J. J. *Eur. J. Org. Chem.* **2011**, 1280–1290.
- (233) Li, F.; Cho, J.; Tan, S.; Kim, S. *Org. Lett.* **2018**, *20*, 824–827.
- (234) Glover, E. E.; Jones, G. *J. Chem. Soc.* **1958**, 3021–3028.
- (235) Fozard, A.; Bradsher, C. K. *J. Org. Chem.* **1966**, *31*, 2346–2349.
- (236) Yu, W. W.; Qu, L.; Guo, W.; Peng, X. *Chem. Mater.* **2003**, *15*, 2854–2860.
- (237) Osuský, P.; Nociarová, J.; Smolíček, M.; Gyepes, R.; Georgiou, D.; Polyzos, I.; Fakis, M.; Hrobárik, P. *Org. Lett.* **2021**, *23*, 5512–5517.
- (238) Ganguly, M.; Panigrahi, S.; Chandrakumar, K. R. S.; Sasmal, A. K.; Pal, A.; Pal, T. *Dalton Trans.* **2014**, *43*, 11624–11636.
- (239) Razi, S. S.; Koo, Y. H.; Kim, W.; Yang, W.; Wang, Z.; Gobeze, H.; D’Souza, F.; Zhao, J.; Kim, D. *Inorg. Chem.* **2018**, *57*, 4877–4890.
- (240) Zhang, L.; Si, X.; Yang, Y.; Witzel, S.; Sekine, K.; Rudolph, M.; Rominger, F.; Hashmi, A. S. K. *ACS Catal.* **2019**, *9*, 6118–6123.
- (241) Zaidlewicz, M.; Wolan, A. *J. Organomet. Chem.* **2002**, *657*, 129–135.
- (242) Crouch, R. D.; Stieff, M.; Frie, J. L.; Cadwallader, A. B.; Bevis, D. C. *Tetrahedron Lett.* **1999**, *40*, 3133–3136.

# Appendix 1: $^1\text{H}$ and $^{13}\text{C}\{^1\text{H}\}$ NMR Spectra

## 1,2,3,4-Tetraethylphenanthrene (133)

File: /mnt/ds00/home/44/msnm/rrnt/data/1D\_FROM\_NMRSERVICE/awew/2020.09/2020.09.12/v7\_b3-p38\_joc38\_20.03\_H1\_1D



OpenVnmrj

Department of Chemistry, University of Alberta

Recorded on: 07/09/2020  
Pulse Sequence: PRESAT

Sweep Width(Hz): 8389.26  
Digital Res (Hz/pt): 0.13

Acquisition Time(s): 5  
Hz per ppm(Hz/ppm): 34.95

Relaxation Delay(s): 0.1  
Completed Scans: 8

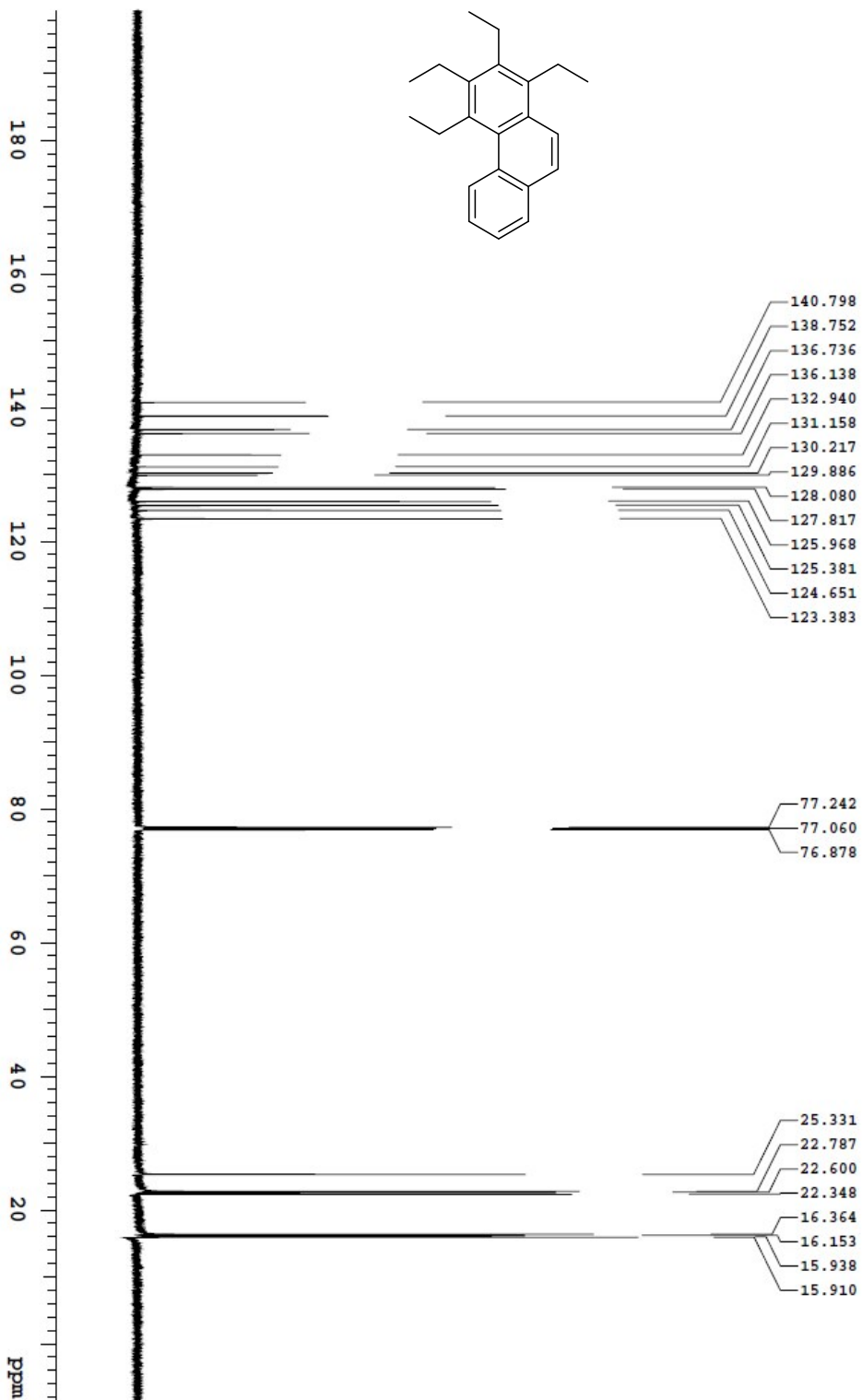
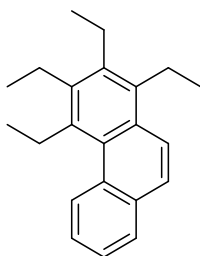


# OpenVnmrj

Department of Chemistry, University of Alberta

|                                       |                                  |                                 |                               |
|---------------------------------------|----------------------------------|---------------------------------|-------------------------------|
| Recorded on: <b>v700, Sep 12 2020</b> | Sweep Width(Hz): <b>36764.7</b>  | Acquisition Time(s): <b>1</b>   | Relaxation Delay(s): <b>1</b> |
| Pulse Sequence: <b>s2pul</b>          | Digital Res. (Hz/p): <b>0.28</b> | Fz per mm(hz/mm): <b>153.19</b> | Completed Scans: <b>112</b>   |

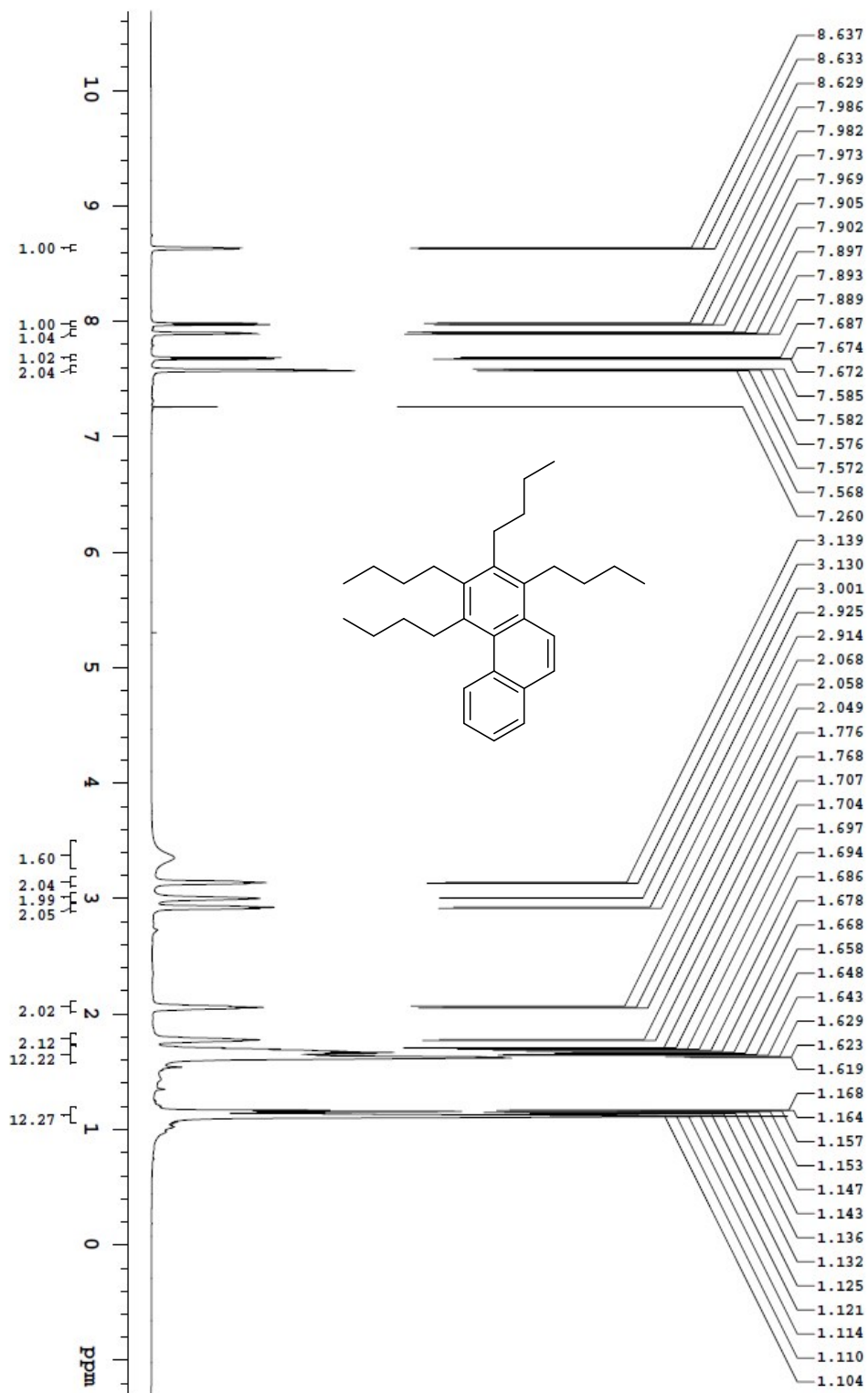
Yaowei\_b3-p39  
175.871 MHz C13{H1} 1D in cdcl3 (ref. to CDCl3 @ 77.06 ppm)  
temp 27.5 C -> actual temp = 27.0 C, coldid probe



File: /mnt/d600/home/14j/mrnmr/mrdata/14j\_DATA\_FROM\_NMRSERVICE/yaowei/2020.09/2020.09.12.v7\_b3-p39\_loc38\_20.04\_C13\_1D

# 1,2,3,4-Tetrabutylphenanthrene (124)

File: /mnt/d60/home/v4/mrnm/rnmdata/ATA\_FROM\_NMRSERVICE/2020.07.01/v7\_d2-p185-pure\_joc43\_01.33\_H1\_1D



Yaowei\_b2-p186  
699.762 MHz <sup>1</sup>H 1D in cdcl3 (ref. to CDCl3 @ 7.26 ppm)  
temp 27.5 C -> actual temp = 27.0 C, coldid probe

OpenVnmrj

Department of Chemistry, University of Alberta

Recorded on: **1700, Jul 1 2020**  
Pulse Sequence: **PRESAT**

Sweep Width(Hz): **8389.26**  
Digital Res.(Hz/D): **0.13**

Acquisition Time(s): **5**  
Hz per mm(Hz/mm): **34.95**

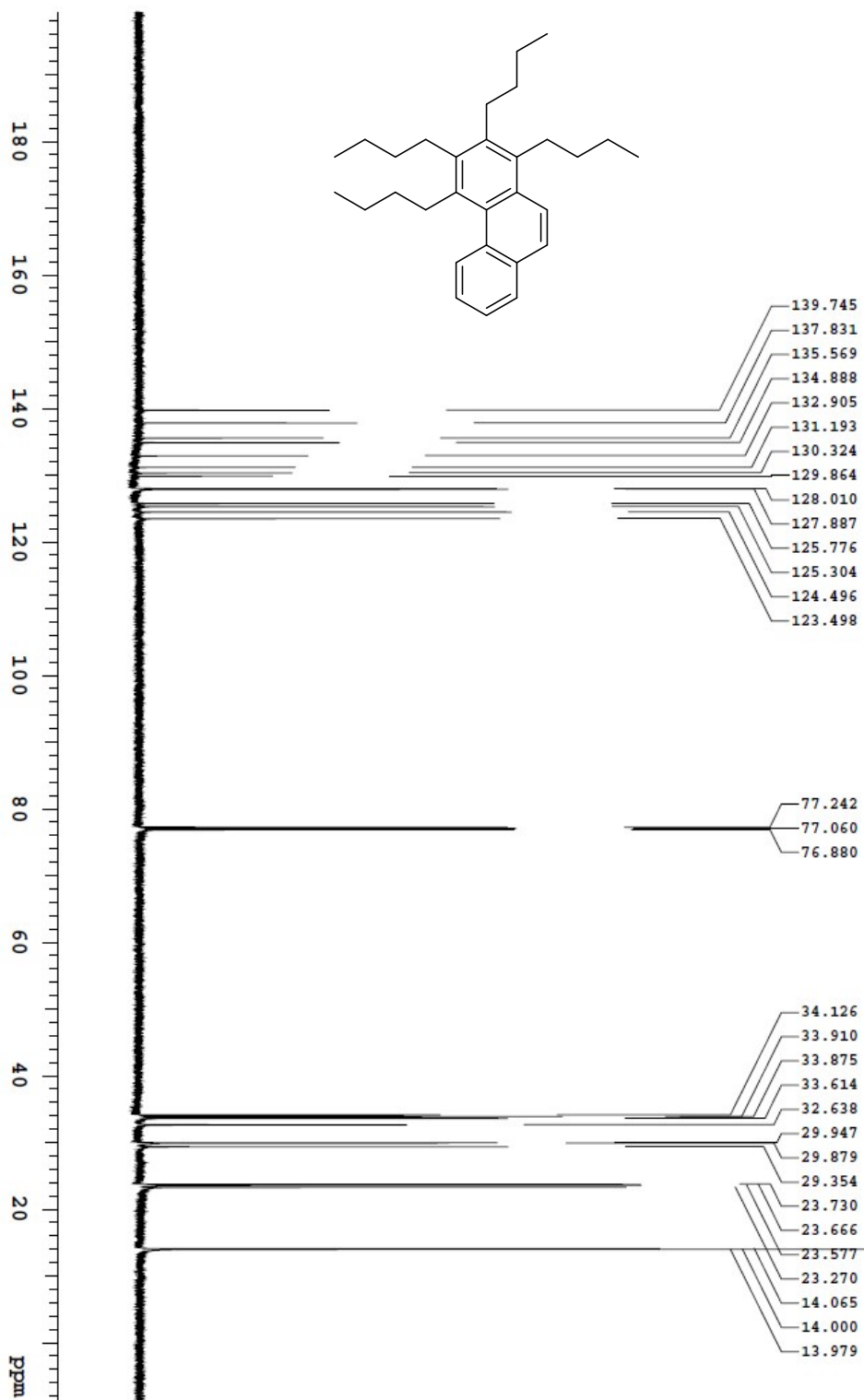
Relaxation Delay(s): **0.1**  
Completed Scans: **8**

# OpenVnmrj

Department of Chemistry, University of Alberta

|                 |                   |                     |         |                      |        |                      |    |
|-----------------|-------------------|---------------------|---------|----------------------|--------|----------------------|----|
| Recorded on:    | v7.00, Jul 1 2020 | Sweep Width(Hz):    | 36764.7 | Acquisition Time(s): | 1      | Relaxation Delay(s): | 1  |
| Pulse Sequence: | szpul             | Digital Res.(Hz/M): | 0.28    | Fz per mm(Hz/mm):    | 153.19 | Completed Scans:     | 88 |

Yaowei, h2-p185  
175.971 MHz C13(1H) 1D in cdcbs (ref. to CDCl3 @ 77.06 ppm)  
temp 27.5 C -> actual temp = 27.0 C, coldid probe



File: /mnt/d60/home14/mnmr/mnmrdata/DATA\_FROM\_NMRSE/RVIC/Yaowei/2020.07.20/20.07.01.v7\_h2-p185-pure\_lock43\_0134\_C13\_1D

# OpenVnmrj

Department of Chemistry, University of Alberta

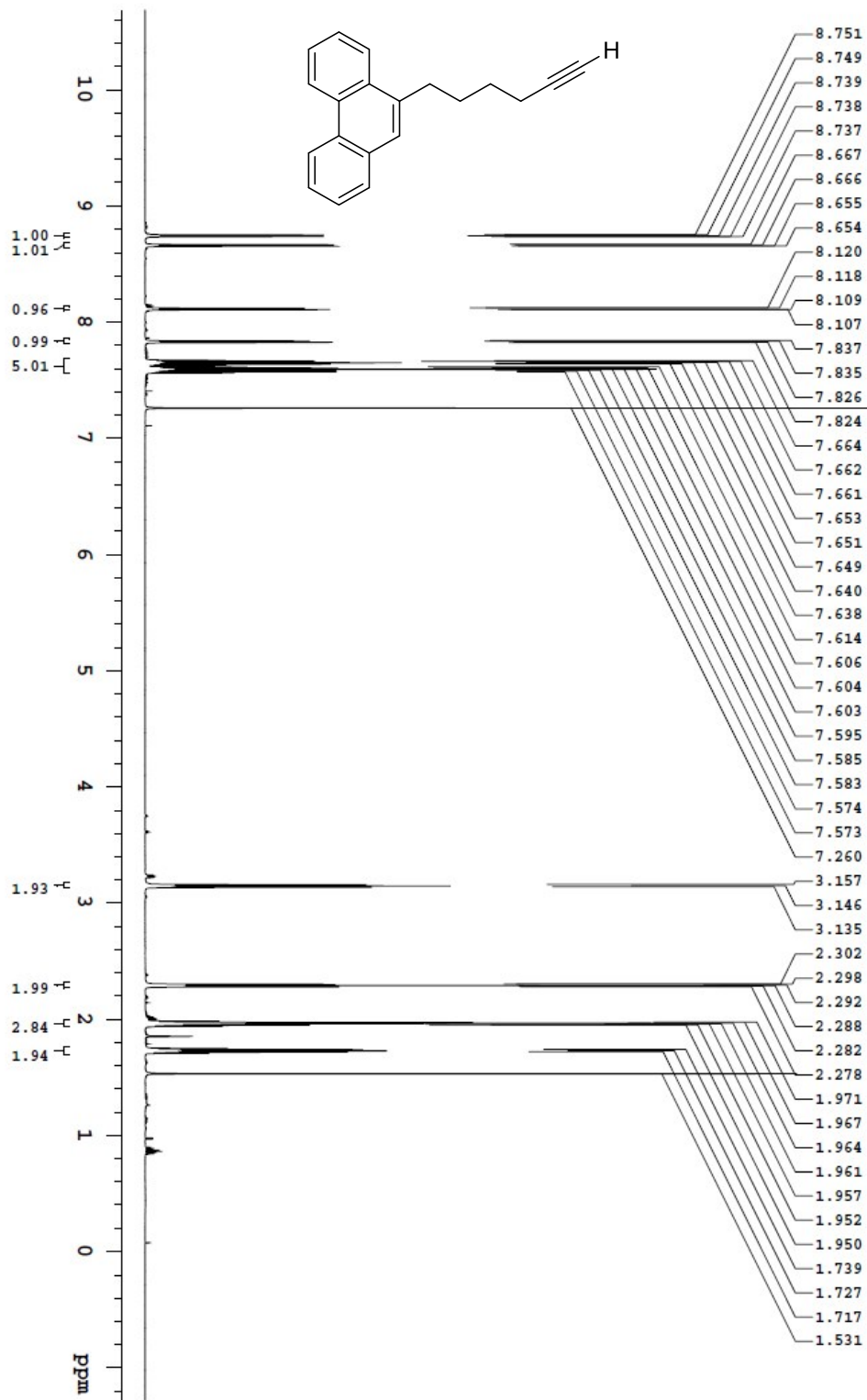
Recorded on: **07/01/2018**  
Pulse Sequence: **PRESAT**

Sweep Width(Hz): **6389.26**  
Digital Res.(Hz/p1): **0.13**

Acquisition Time(s): **5**  
Hz per nmh(hz/nm): **34.95**

Relaxation Delay(s): **0.1**  
Completed Scans: **8**

Yaowei\_b2-p27  
698.762 MHz H1 1D in cdcl3 (ref. to CDCl3 @ 7.26 ppm)  
temp 27.5 C -> actual temp = 27.0 C, coldid probe



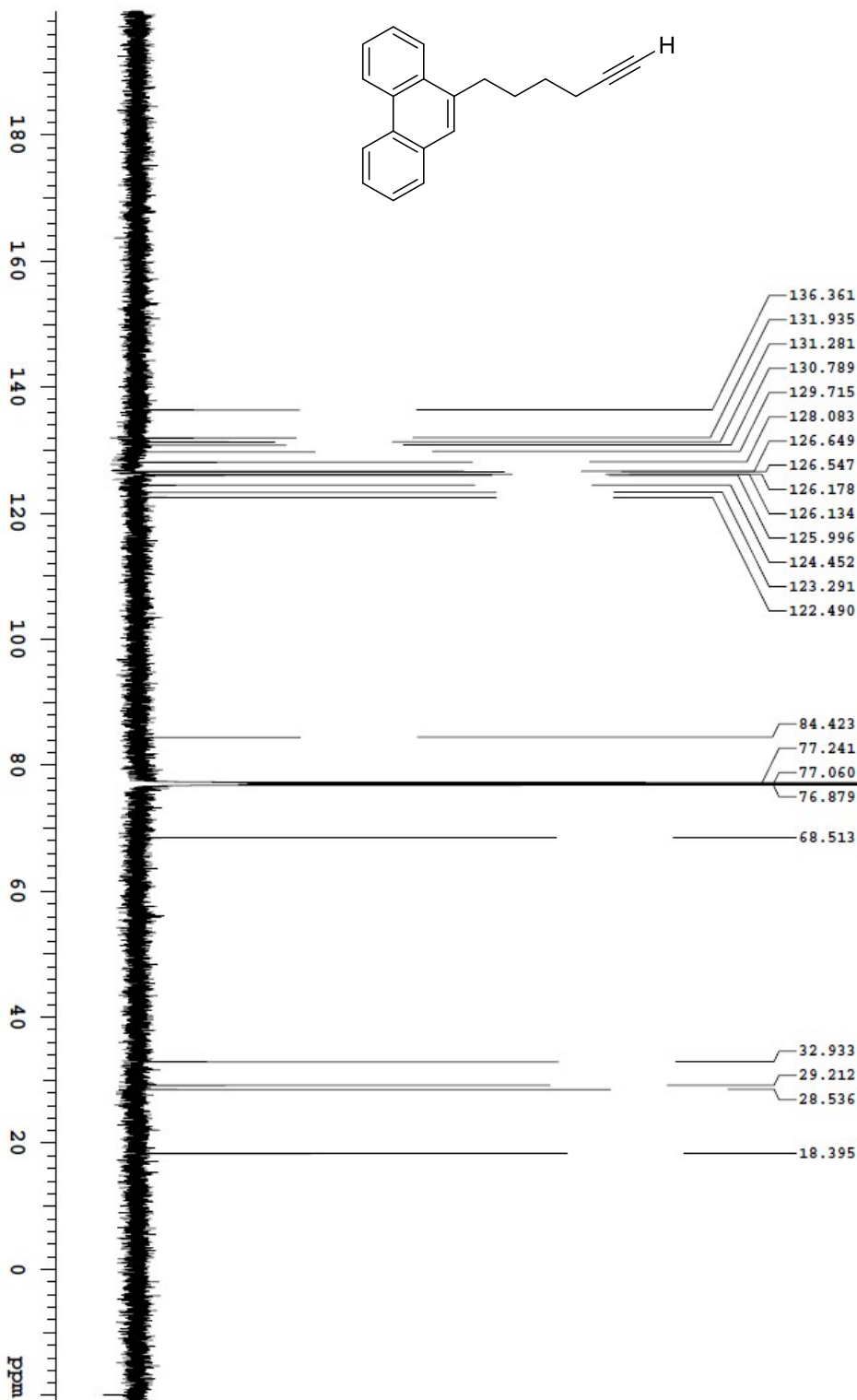
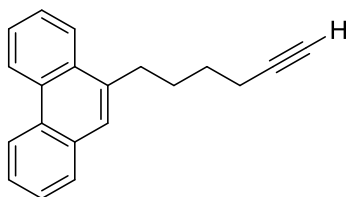
File: /mnt/d600/home/144/jnmr/mrnmrdata/DATA\_FROM\_NMRSEVIC/CEV/yaowei/2018.06/2018.06.11.v7\_b2-p13\_frecy\_loc42\_13.06\_H1\_1D

# OpenVnmrj

Department of Chemistry, University of Alberta

|                 |                          |                       |                |                      |              |                      |            |
|-----------------|--------------------------|-----------------------|----------------|----------------------|--------------|----------------------|------------|
| Recorded on:    | <b>v700, Jun 11 2018</b> | Sweep Width(Hz):      | <b>48076.9</b> | Acquisition Time(s): | <b>1</b>     | Relaxation Delay(s): | <b>1</b>   |
| Pulse Sequence: | <b>sgpu</b>              | Digital Res. (Hz/pt): | <b>0.37</b>    | Fz. per (mm/Hz/mm):  | <b>16232</b> | Completed Scans:     | <b>256</b> |

Yaowei, h2-p27  
175.975 MHz <sup>13</sup>C{<sup>1</sup>H} 1D in cdcbs (ref. to CDCl<sub>3</sub> @ 77.06 ppm)  
temp 27.5 C -> actual temp = 27.0 C, coldid probe



File: /mnt/d60/home/y4/mnmr/mnmrdata/DATA\_FROM\_NMRSE/RVIC/EY/yaowei/2018.06/2018.06.11/v7\_02-p13\_1ecoy\_1b-cd2\_13.07\_C13\_1D

# OpenVnmrj

Department of Chemistry, University of Alberta

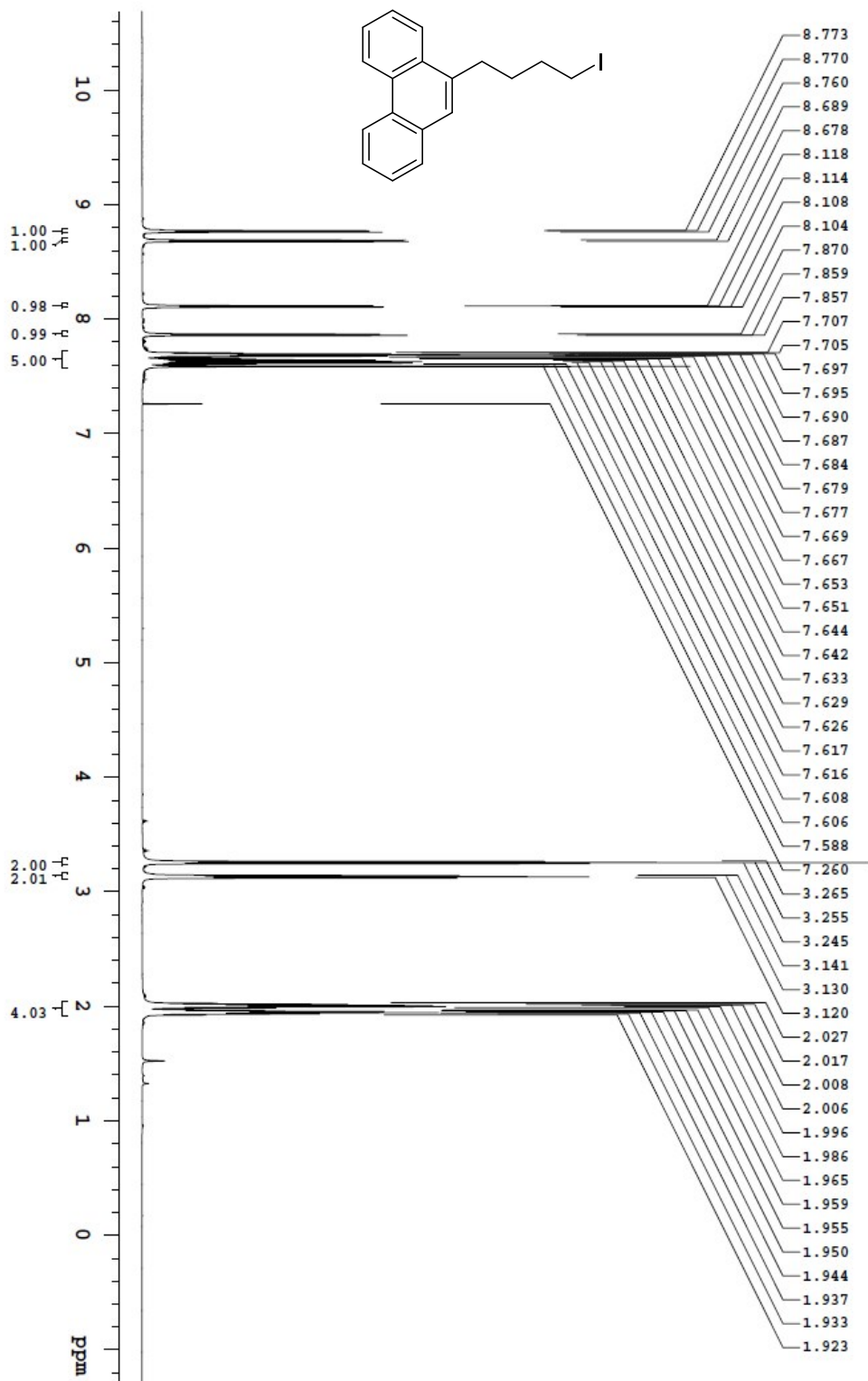
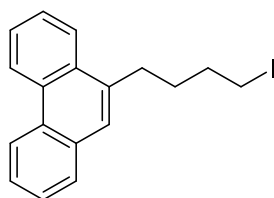
Recorded on: **v700, Aug 23 2021**  
Pulse Sequence: **FRESAT**

Sweep Width(Hz): **8389.26**  
Digital Res.(Hz/pt): **0.13**

Acquisition Time(s): **5**  
Hz per mm(Hz/mm): **34.95**

Relaxation Delay(s): **0.1**  
Completed Scans: **8**

Yaoxuei, h2-p19  
689.762 MHz <sup>1</sup>H 1D in cdcl3 (ref to CDCl3 @ 7.26 ppm)  
temp 27.5 C -> actual temp = 27.0 C; coldid probe



File: /mnt/d500/home14/msnmr/mrdata/ATA\_FROM\_NMRSEVIC/EYaoxuei2021.08/2021.08.23.v7\_d2-p19\_joc31\_22.55\_H1\_1D



# OpenVnmrj

Department of Chemistry, University of Alberta

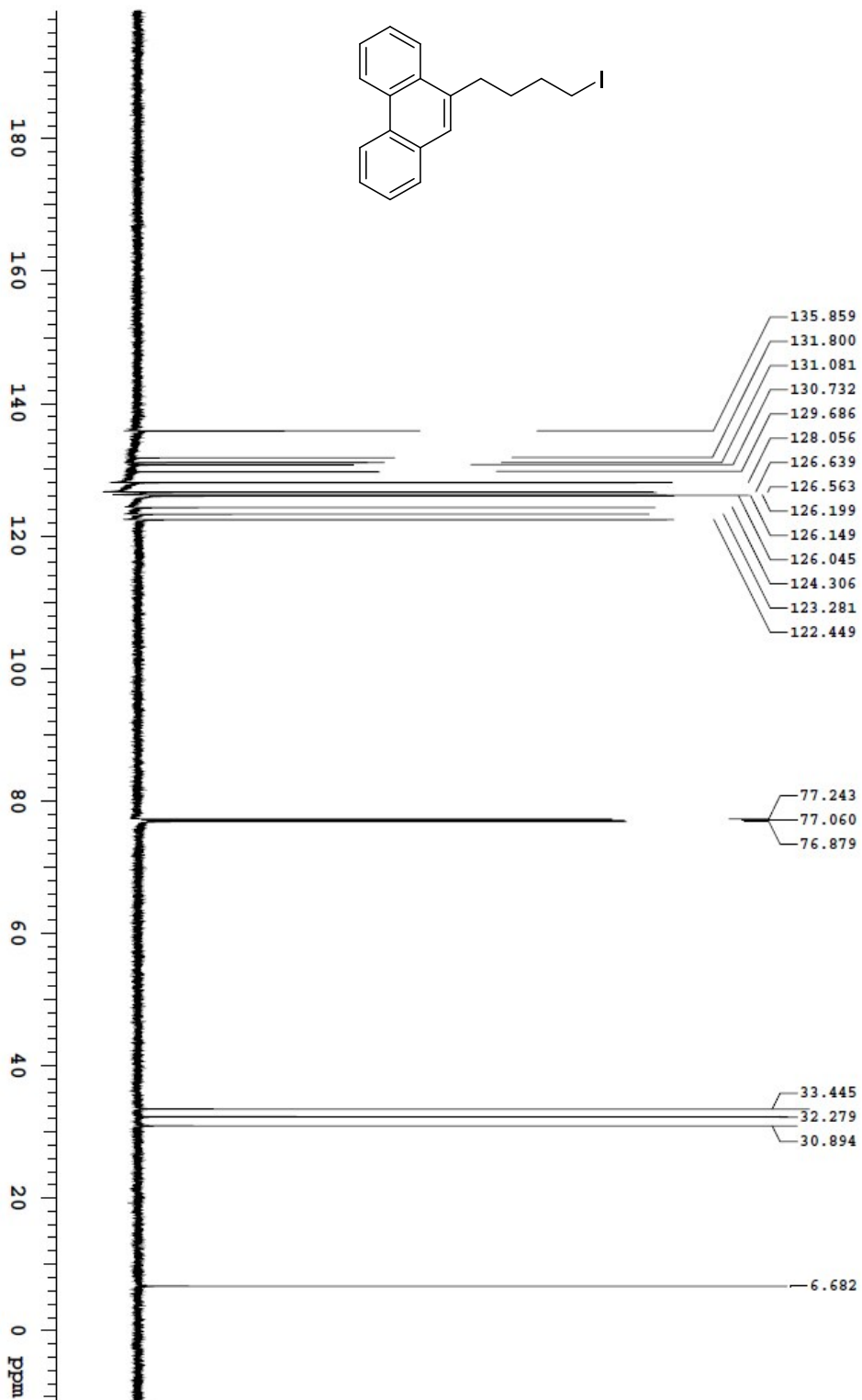
Recorded on: **v700, Aug 23 2021**  
Pulse Sequence: **s2pul**

Sweep Width(Hz): **46296.3**  
Digital Res (Hz/P): **0.35**

Acquisition Time(s): **1**  
Hz per mm(Hz/mm): **154.55**

Relaxation Delay(s): **1**  
Completed Scans: **28**

Yaowei, b2-p19  
175.976 MHz C13(H1) 1D in cdcl3 (ref. to CDCl3 @ 77.06 ppm)  
temp 27.5 C -> actual temp = 27.0 C, coldid probe



File: /mnt/d600/home/y4/mrnmr/data/1D/1D\_NMRSE/RVIC/1D/20210823/v7\_b2-p19\_boc31\_22.56\_C13\_1D

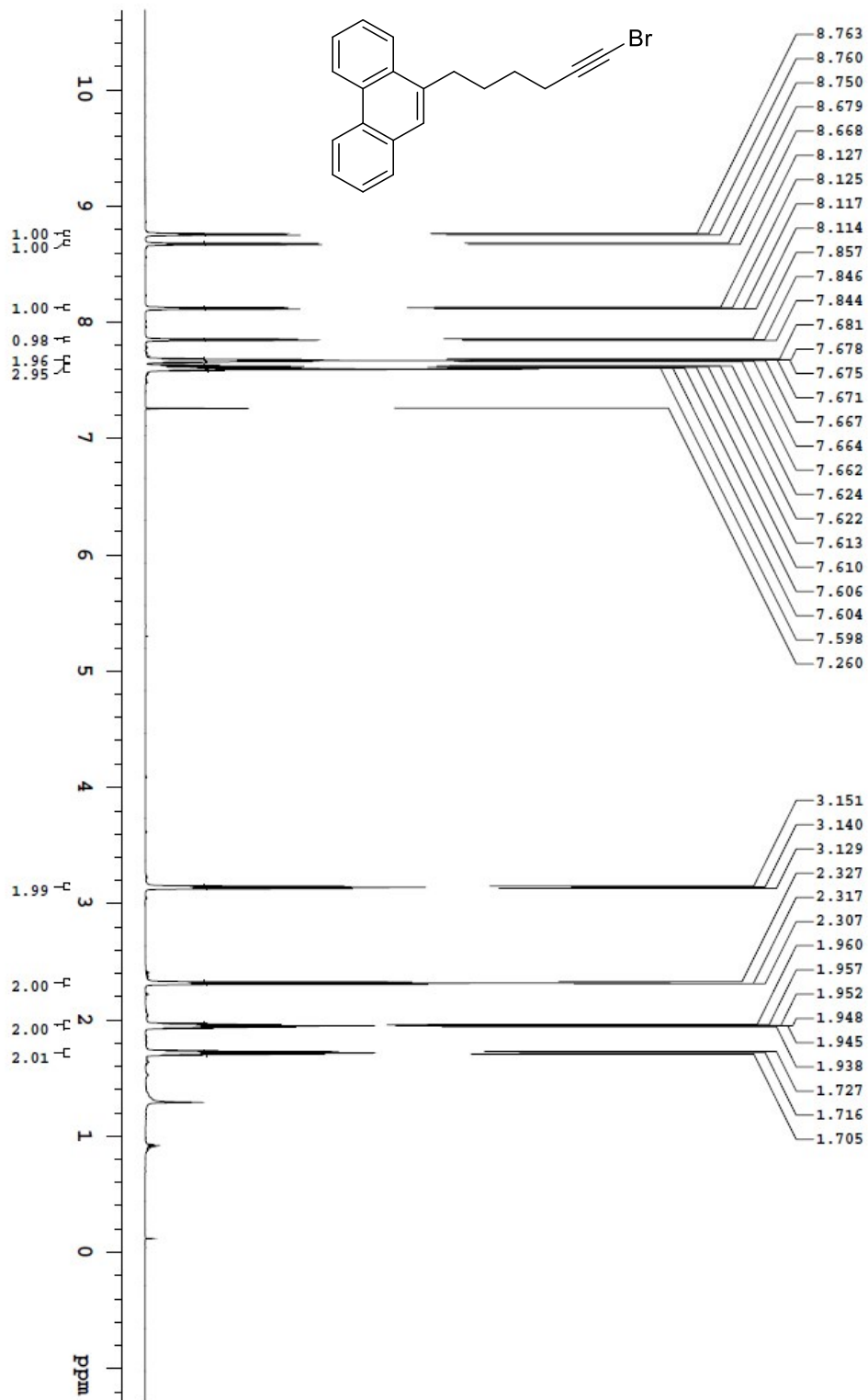
Yaowei\_b2-p145  
698.762 MHz H1 1D in cdcl3 (ref. to CDCl3 @ 7.26 ppm)  
temp 27.5 C -> actual temp = 27.0 C, coldid probe

Recorded on: V700, Sep 30 2019  
Pulse Sequence: PRESAT

Sweep Width(Hz): 6389.26  
Digital Res.(Hz/p1): 0.13

Acquisition Time(s): 5  
Hz per mem(Hz/mem): 34.95

Relaxation Delay(s): 0.1  
Completed Scans: 8



File: /mnt/d600/home/14jmsnmr/mrdata/DATA\_FROM\_NMRSERVICE/yaowei/2019.09/2019.09.30.V7\_b2-p145\_locd2\_19.00\_H1\_1D



# OpenVnmrj

Department of Chemistry, University of Alberta

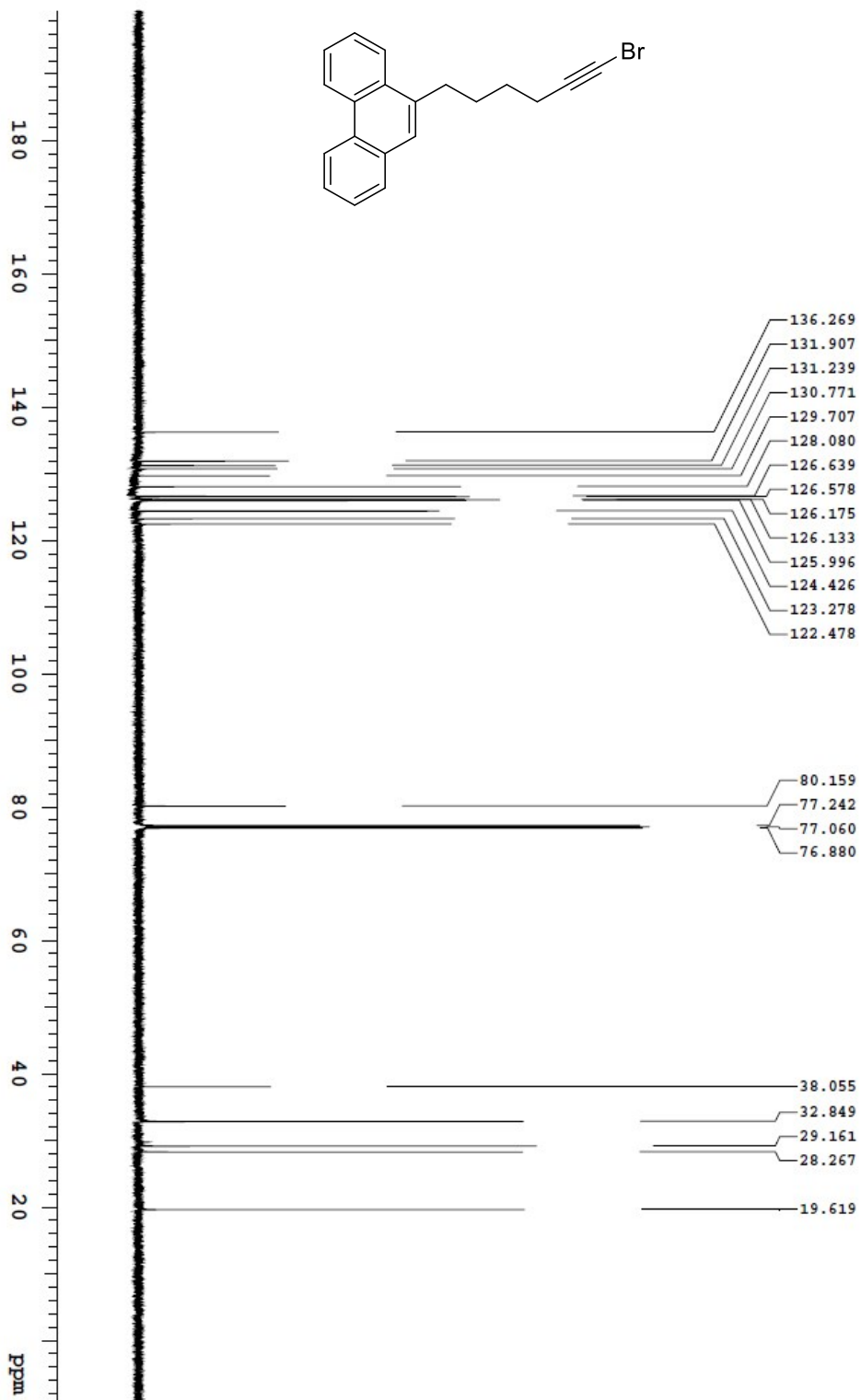
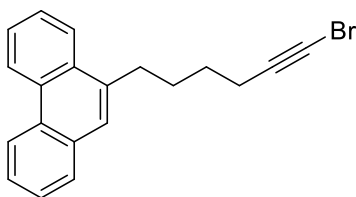
Recorded on: **VT00, Sep 30 2019**  
Pulse Sequence: **s2pul**

Sweep Width(Hz): **3676.47**  
Digital Res.(Hz/p): **0.28**

Acquisition Time(s): **1**  
Hz per mm(Hz/mm): **153.19**

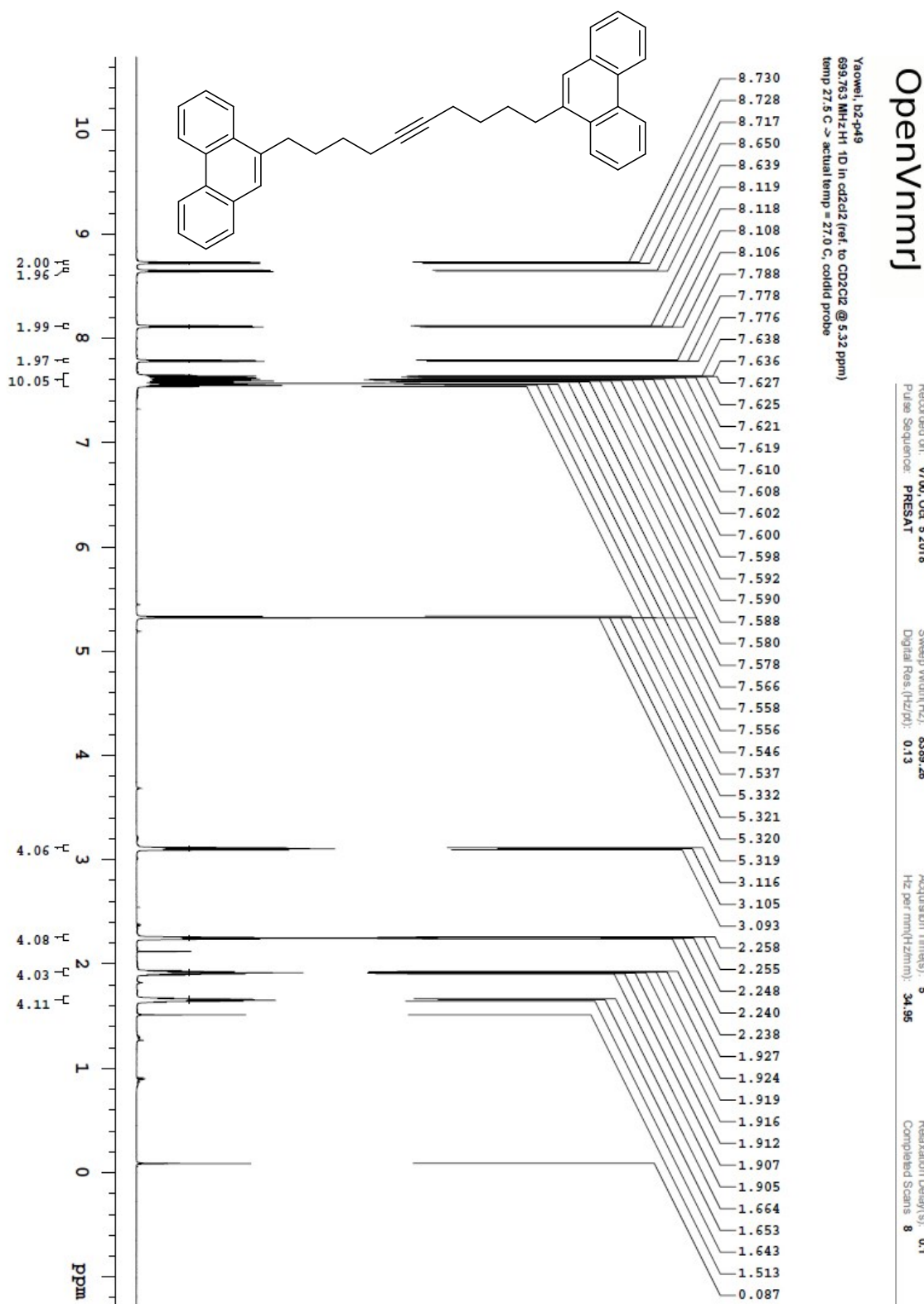
Relaxation Delay(s): **1**  
Completed Scans: **80**

Yaowei\_b2-p145  
175.971 MHz C13(H1) 1D in cdcl3 (ref. to CDCl3 @ 77.06 ppm)  
temp 27.5 C -> actual temp = 27.0 C, coldid probe



File: /mnt/600/home/14/jmsnmr/mrdata/1D\_FROM\_NMRSERVICE/yaowei/2019.09/2019.09.30.VT\_b2-p145\_b042\_13.01\_C13\_1D

# 1,10-Di(9-phenanthrene)-5-decyne (240)



OpenVnmrj

Department of Chemistry, University of Alberta

Recorded on: **VT00, Oct 5 2018**  
Pulse Sequence: **PRESAT**

Sweep Width(Hz): **8389.26**  
Digital Res.(Hz/pp): **0.13**

Acquisition Time(s): **5**  
Hz per mm(Hz/mm): **34.95**

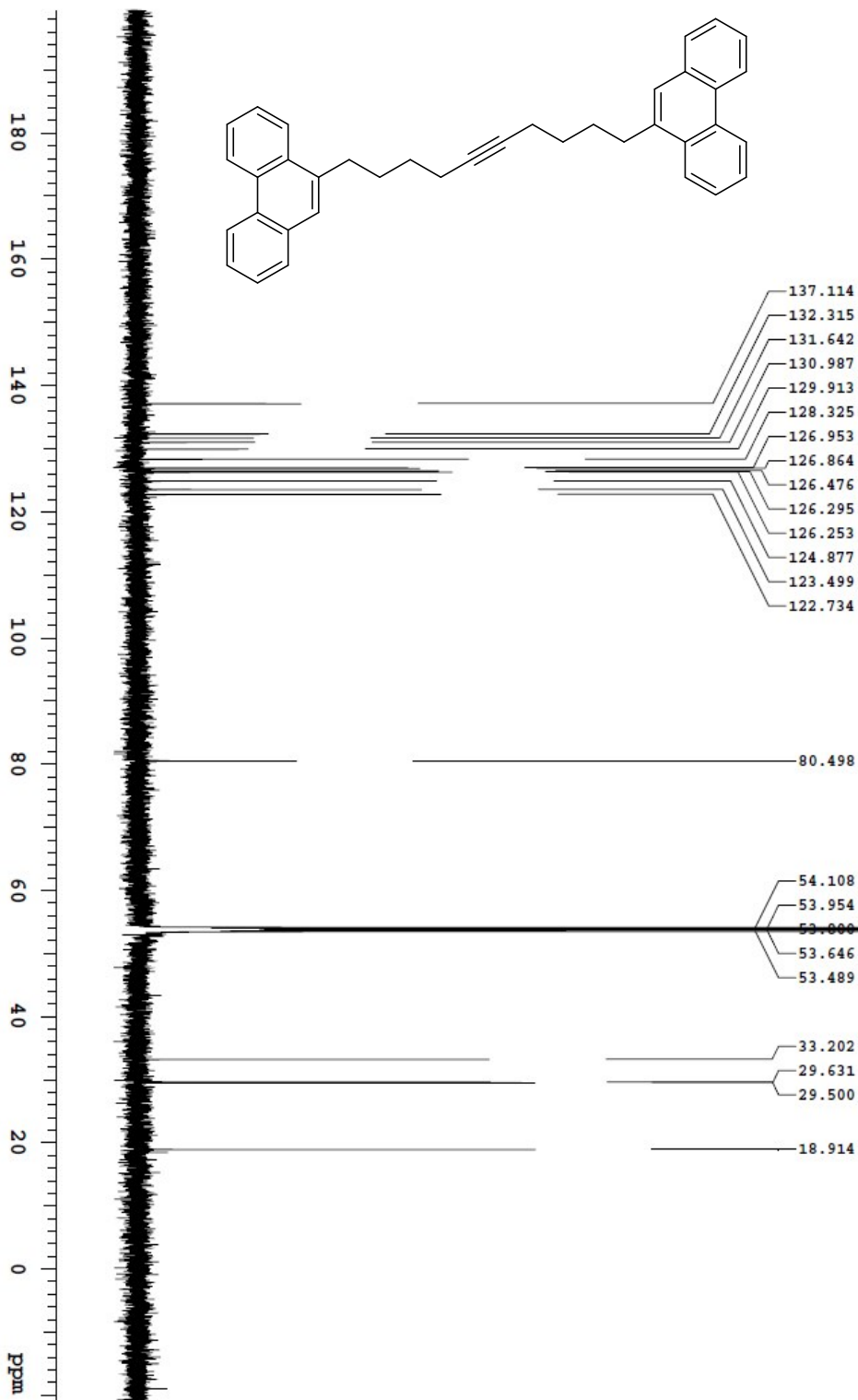
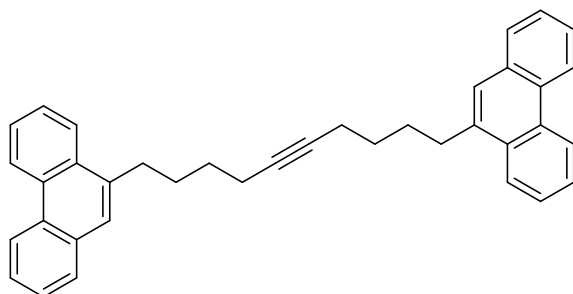
Relaxation Delay(s): **0.1**  
Completed Scans: **8**

# OpenVnmrj

Department of Chemistry, University of Alberta

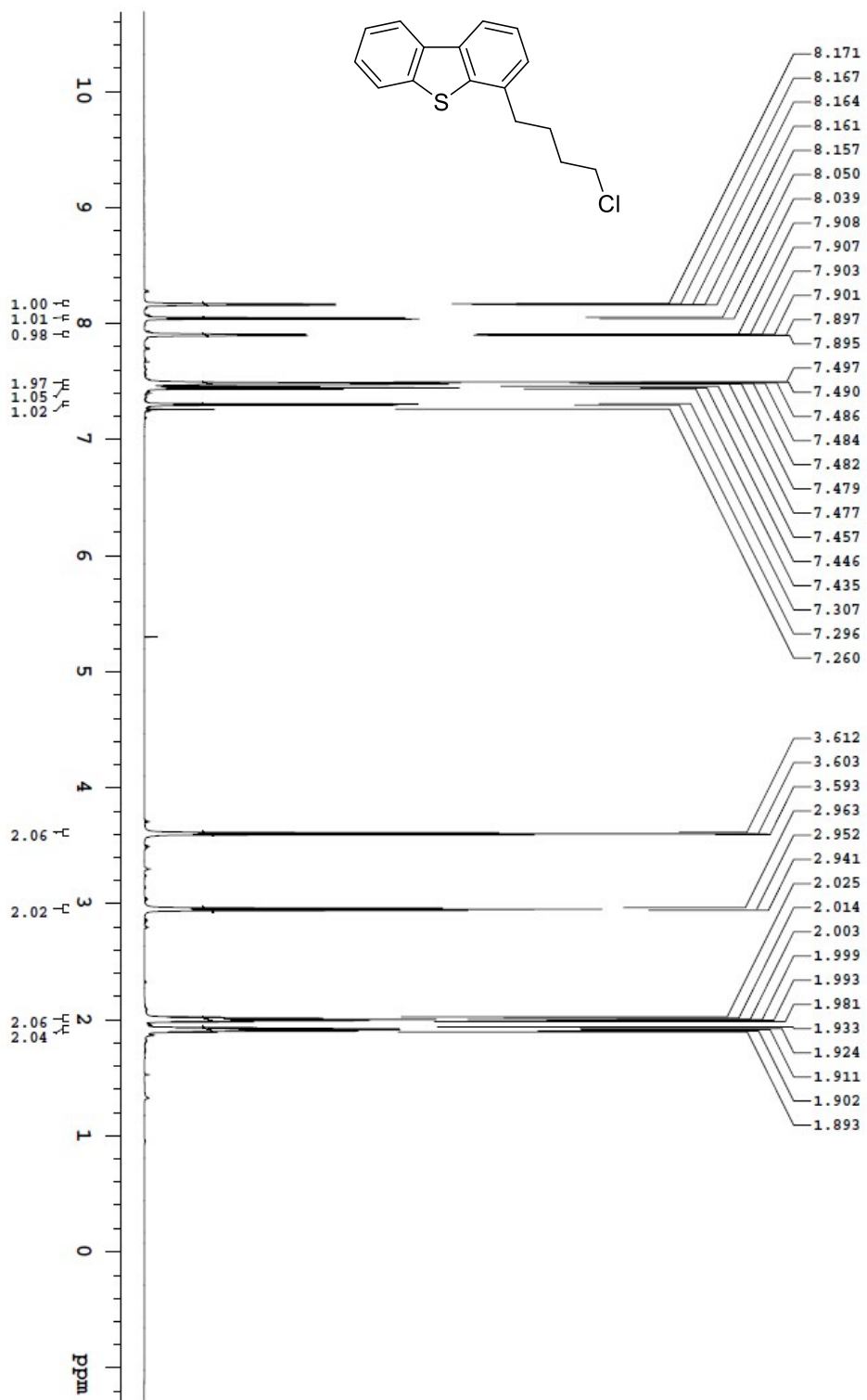
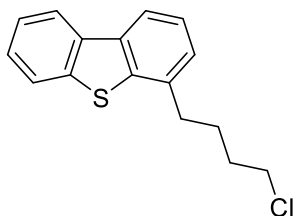
|                                      |                                  |                                 |                               |
|--------------------------------------|----------------------------------|---------------------------------|-------------------------------|
| Recorded on: <b>V700, Oct 5 2018</b> | Sweep Width(Hz): <b>48076.9</b>  | Acquisition Time(s): <b>1</b>   | Relaxation Delay(s): <b>1</b> |
| Pulse Sequence: <b>s2pul</b>         | Digital Res.(Hz/pt): <b>0.37</b> | Hz per mm(Hz/mm): <b>161.78</b> | Completed Scans: <b>256</b>   |

Yaowei, b2-p43  
175.975 MHz C13(H1) 1D in cd2cl2 (ref. to CD2Cl2 @ 53.8 ppm)  
temp 27.5 C -> actual temp = 27.0 C, coldid probe



File: /mnt/d60/home/14j/nmr/nmrdata/DATA\_FROM\_NMRSERV/CEY/yaowei/2018\_10/2018\_10.05\_V7\_b2-p41\_lock3\_16.48\_C13\_1D

# 4-(4-Chlorobutyl)dibenzothiophene (243)



File: /mnt/d60/home/14jmsm/rmcdab/DA/TA\_FROM\_NMRSERVICE/aoew/2019.10/2019.10.08.v7\_b2-p147\_boc42\_02.23\_H1\_1D

OpenVnmrj

Yaowei, b2-p147  
699.762 MHz H1 1D in cdcl3 (ref. to CDCl3 @ 7.26 ppm)  
temp 27.5 C -> actual temp = 27.0 C, coldid probe

Department of Chemistry, University of Alberta

Recorded on: **V700, Oct 8 2019**  
Pulse Sequence: **PRESAT**

Sweep Width(Hz): **8389.26**  
Digital Res. (Hz/D): **0.13**

Acquisition Time(s): **5**  
Hz per mm(Hz/mm): **34.95**

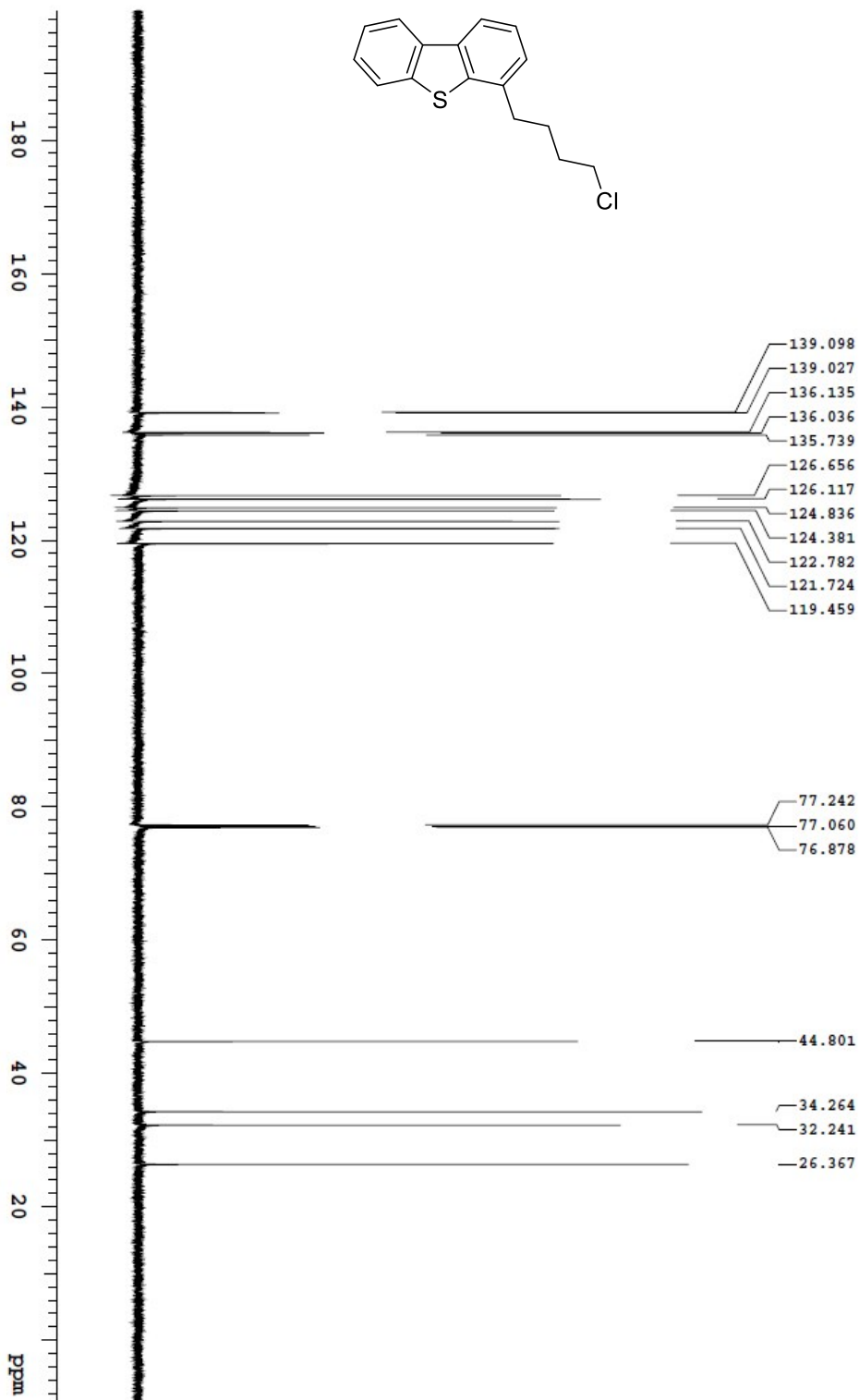
Relaxation Delay(s): **0.1**  
Completed Scans: **8**

# OpenVnmrj

Department of Chemistry, University of Alberta

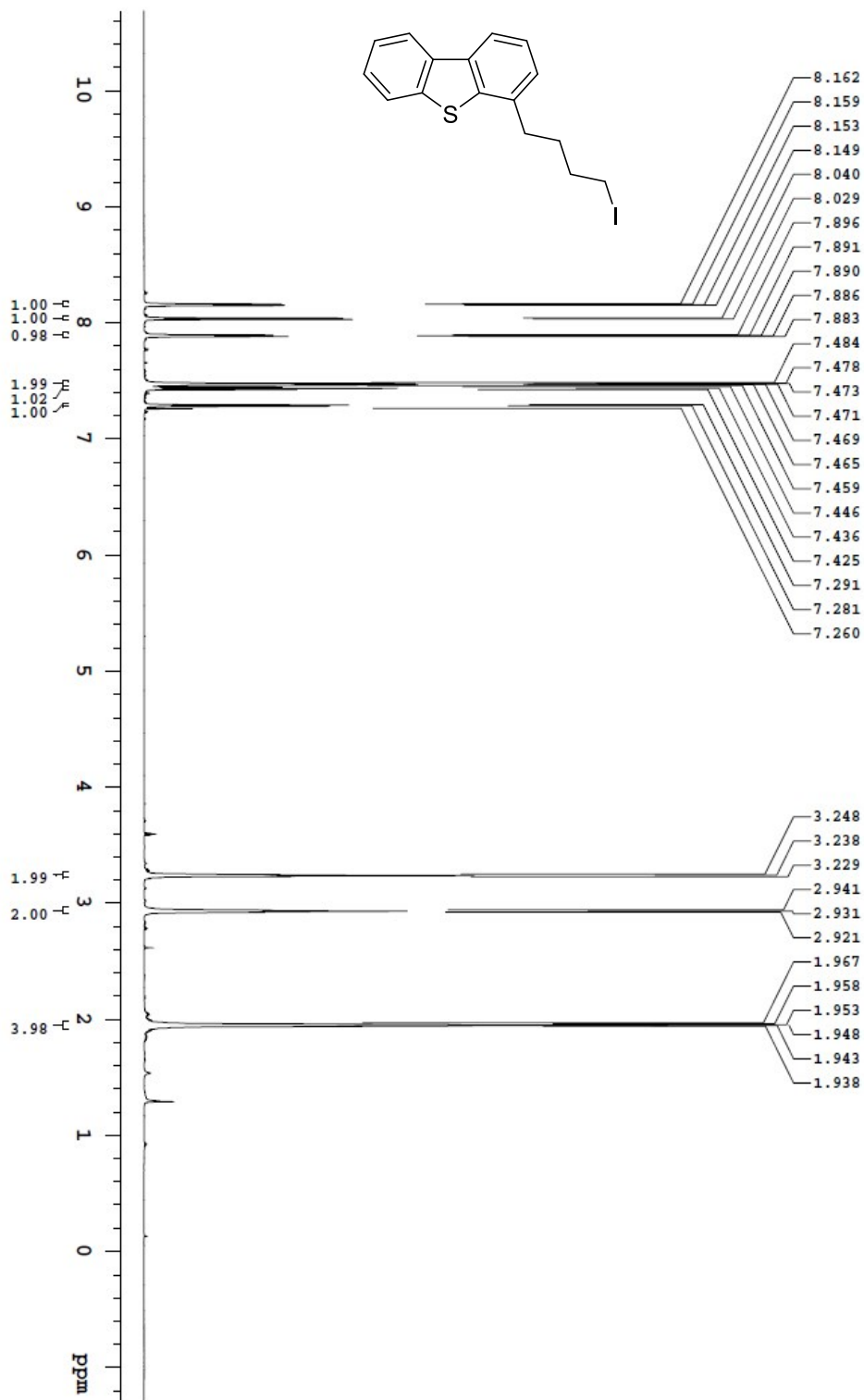
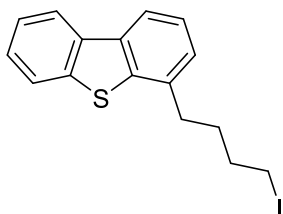
|                                      |                                 |                                 |                               |
|--------------------------------------|---------------------------------|---------------------------------|-------------------------------|
| Recorded on: <b>7:00, Oct 8 2019</b> | Sweep Width(Hz): <b>3676.47</b> | Acquisition Time(s): <b>1</b>   | Relaxation Delay(s): <b>1</b> |
| Pulse Sequence: <b>s2pul</b>         | Digital Res.(Hz/p): <b>0.28</b> | Hz per mm(Hz/mm): <b>153.19</b> | Completed Scans: <b>16</b>    |

Yaowei, h2-p147  
175.971 MHz C13{H1} 1D in cdcl3 (ref. to CDCl3 @ 77.06 ppm)  
temp 27.5 C -> actual temp = 27.0 C, coldid probe



File: /mnt/d600/home/14/msnmr/mrncdab/1D/1D\_FROM\_NMRSERVICE/yaowei/2019\_10/20/19\_10/08/v7\_h2-p147\_kod42\_02\_24\_C13\_1D

# 4-(4-Iodobutyl)dibenzothiophene (247)



File: /mnt/d0/home/14/jmsm/rmr/data/DATE\_FROM\_NMRSERVICE/2019/09/20/19.09.10.v7\_b2-p135-pure\_boc43\_12.48\_H1\_1D

OpenVmrj

Department of Chemistry, University of Alberta

Recorded on: **v700, Sep 10 2019**  
Sweep Width(Hz): **8389.26**  
Pulse Sequence: **PRESAT**  
Digital Res. (Hz/pd): **0.13**

Acquisition Time(s): **5**  
Hz per mm(Hz/mm): **34.96**

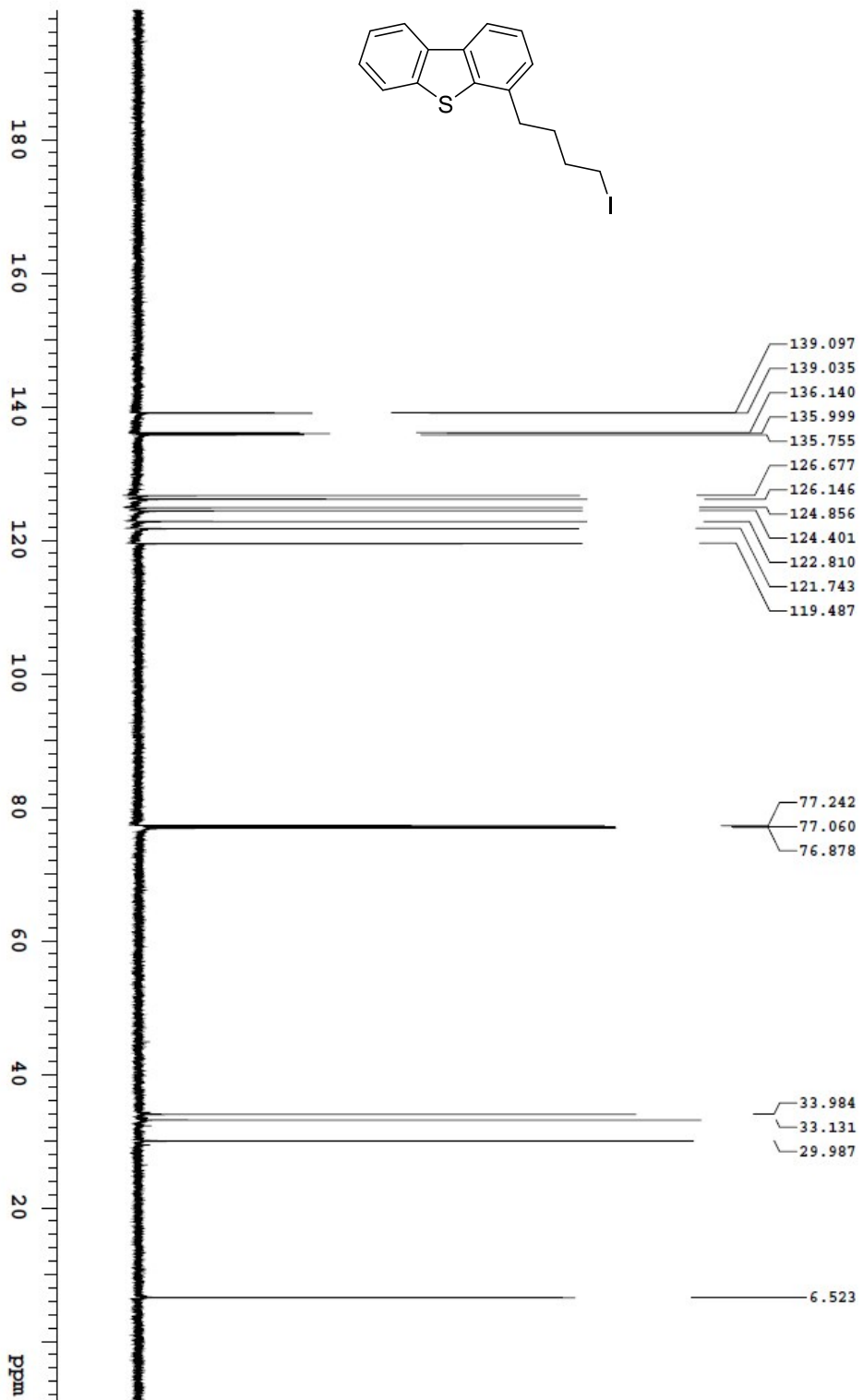
Relaxation Delay(s): **0.1**  
Completed Scans: **8**

Yaowei, b2-p135  
693.762 MHz H1 1D in cdcl3 (ref. to CDCl3 @ 7.26 ppm)  
temp 27.5 C -> actual temp = 27.0 C, coldid probe

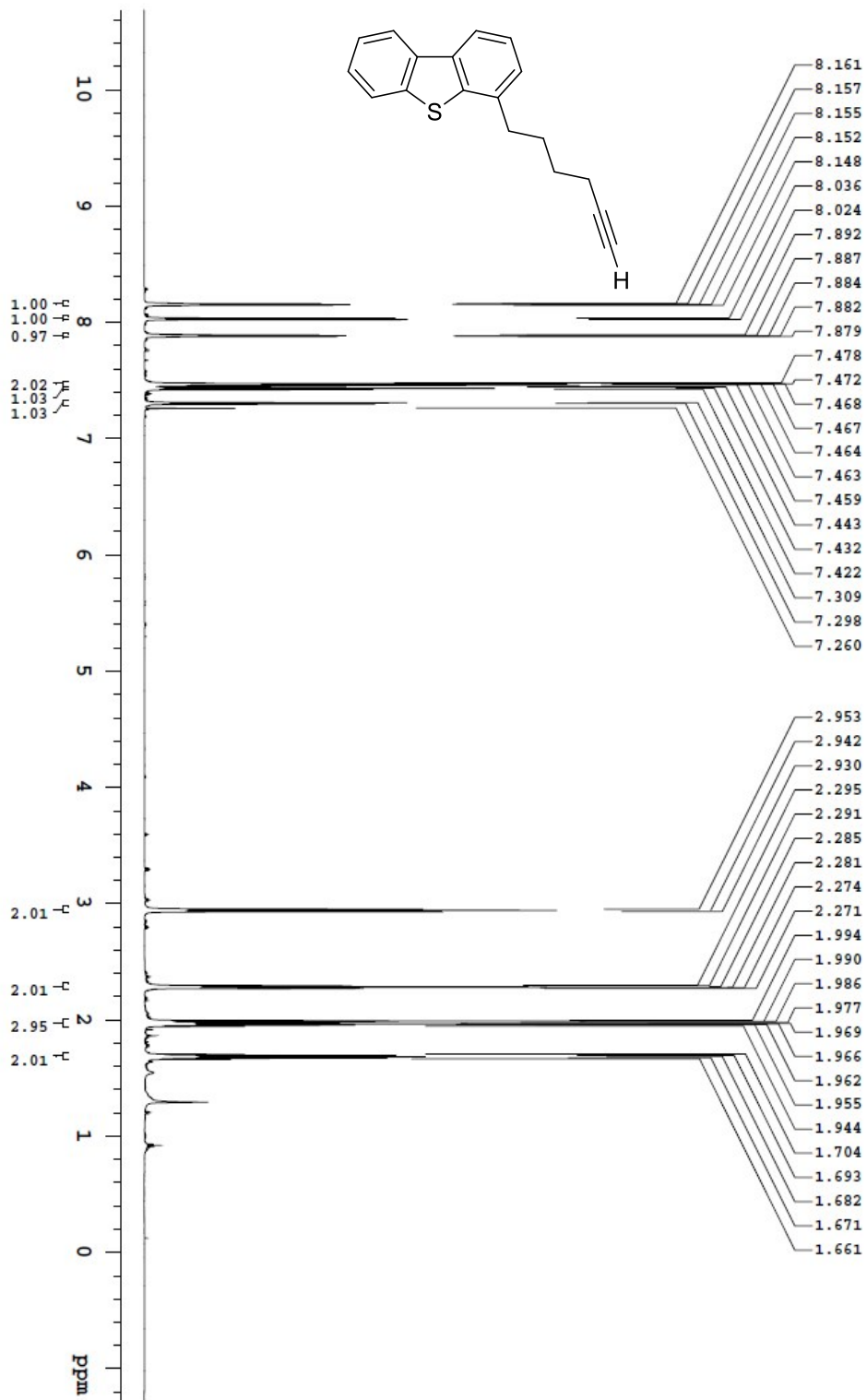
## OpenVnmrj

|                 |                          |                     |                |                      |               |                      |           |
|-----------------|--------------------------|---------------------|----------------|----------------------|---------------|----------------------|-----------|
| Recorded on:    | <b>v700, Sep 10 2019</b> | Sweep Width(Hz):    | <b>36764.7</b> | Acquisition Time(s): | <b>1</b>      | Relaxation Delay(s): | <b>1</b>  |
| Pulse Sequence: | <b>s2pul</b>             | Digital Res.(Hz/D): | <b>0.28</b>    | Fz per mm(Hz/mm):    | <b>153.19</b> | Completed Scans:     | <b>36</b> |

Yaowei, h2-p135  
175,971 MHz C13(41) 1D in cdcl3 ref. to CDC13 @ 77.06 ppm)  
temp 27.5 C -> actual temp = 27.0 C, coldid probe





Recorded on: **VT00\_Sep\_9\_2019**  
Pulse Sequence: **PRESAT**Sweep Width(Hz): **6389.26**  
Digital Res.(Hz/pt): **0.13**Acquisition Time(s): **5**  
Hz per mm(Hz/mm): **34.95**Relaxation Delay(s): **0.1**  
Completed Scans: **8**Yaowei\_b2-p137  
699.762 MHz <sup>1</sup>H 1D in cdcl<sub>3</sub> (ref. to CDCl<sub>3</sub> @ 7.26 ppm)  
temp 27.5 C -> actual temp = 27.0 C, coldid probe

File: /mnt/d80/home/14jnsnm/mnt/data/DA1A\_FROM\_NMRSERVICE/yaowei/2019.09/2019.09.09.VT\_b2-p137-pure\_lcdc3\_18.09\_H1\_1D



# OpenVnmrj

Department of Chemistry, University of Alberta

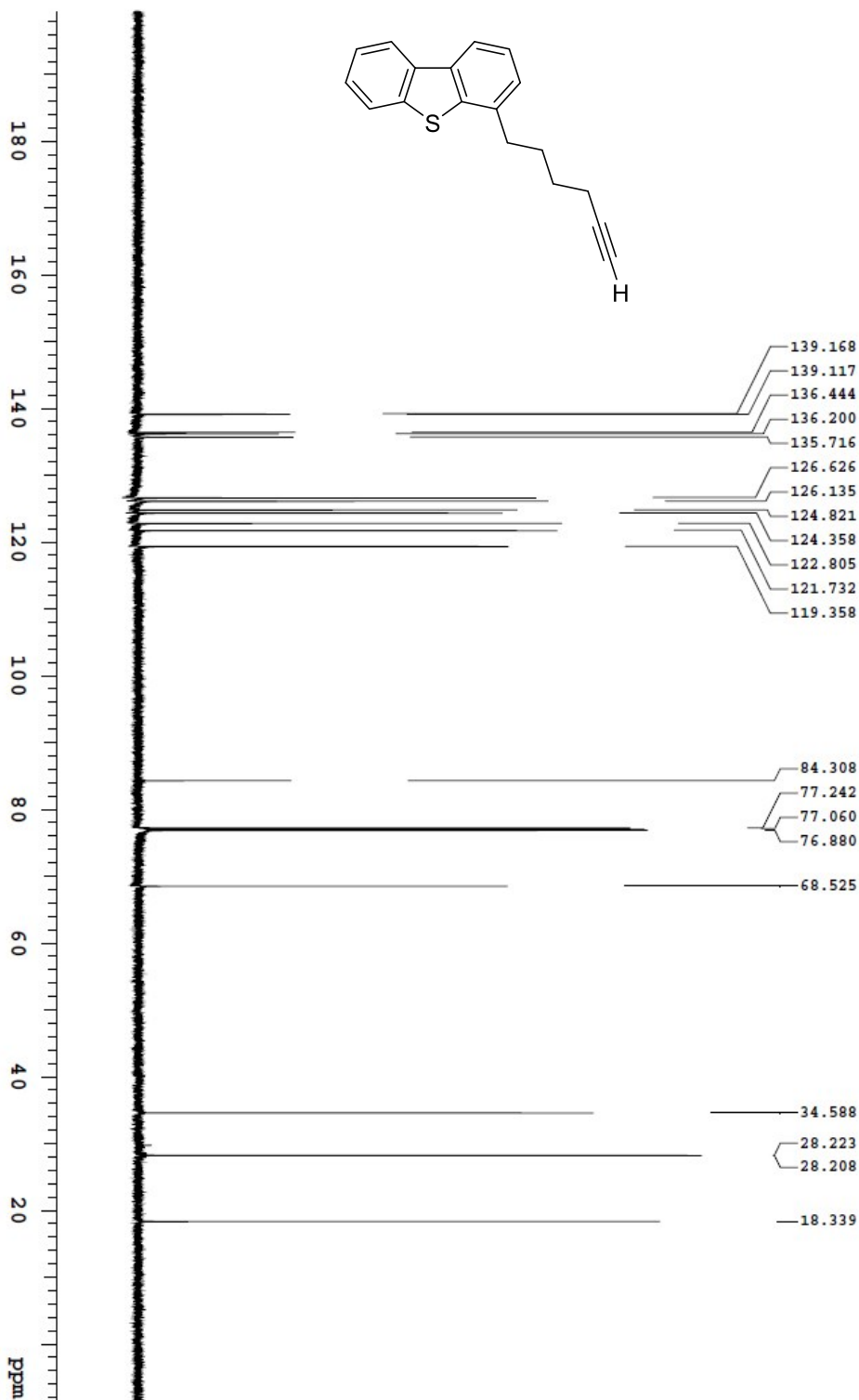
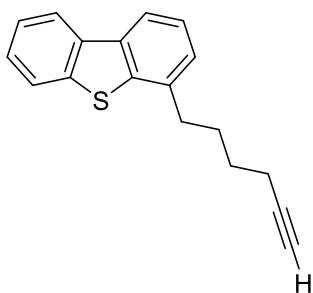
Recorded on: **0700, Sep 9 2019**  
Pulse Sequence: **s2pul**

Sweep Width(Hz): **36764.7**  
Digital Res.(Hz/pd): **0.28**

Acquisition Time(s): **1**  
Hz per mm(Hz/mm): **153.19**

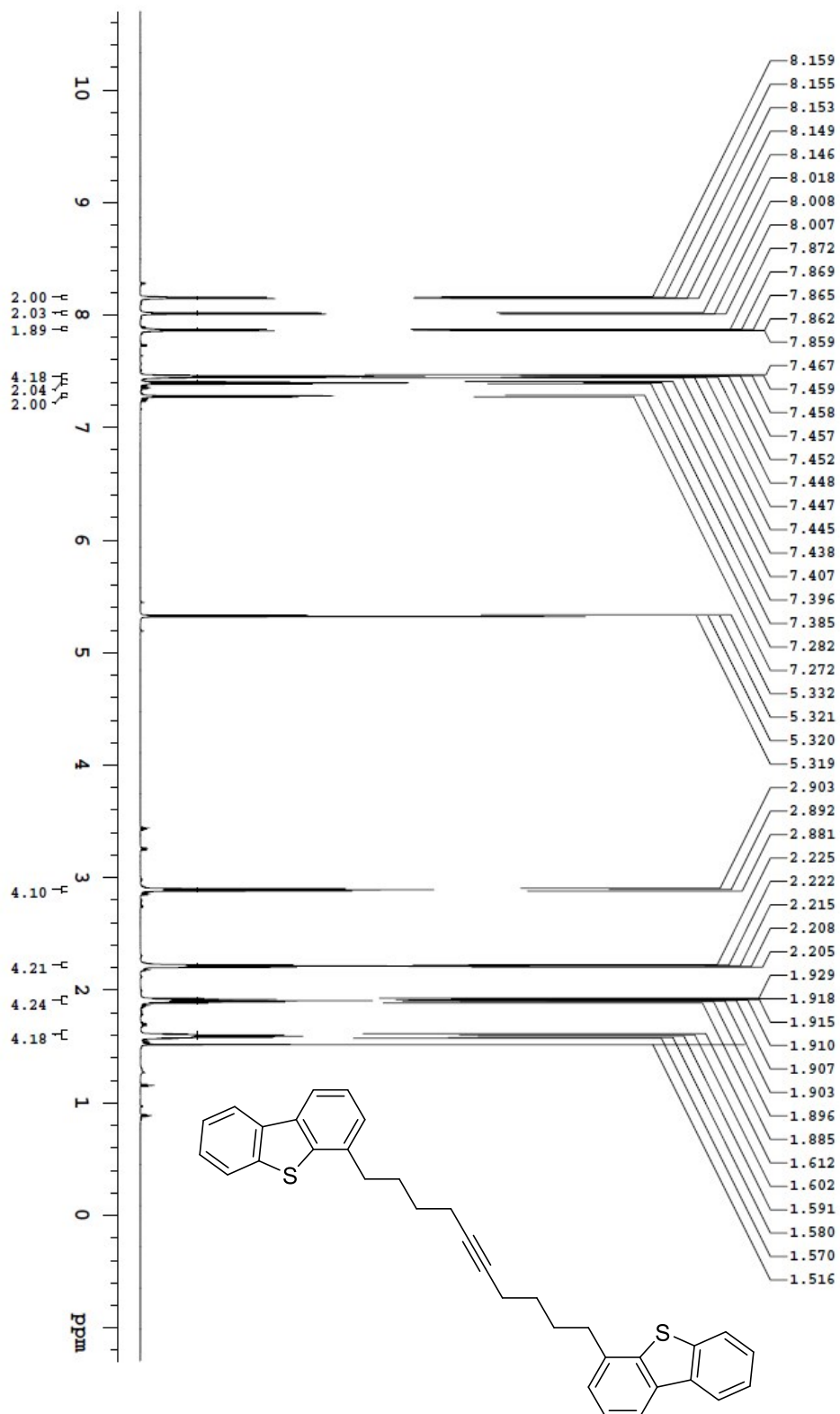
Relaxation Delay(s): **1**  
Completed Scans: **40**

Yaowei, b2-p137  
175.871 MHz C13{H1} 1D in cdcl3 (ref. to CDCl3 @ 77.06 ppm)  
temp 27.5 C -> actual temp = 27.0 C, coldid probe



File: /mnt650/home/14/jmsm/ntm/da/DA\_FROM\_NMRSERVICE/yaowei/2019.09.20/19.09.09.v7\_b2-p137-pure\_bocS\_18\_10\_C13\_1D

# 1,10-Di(4-dibenzothiophene)-5-decyne (248)



File: /mnt/d60/home/14/jnsen/mrdata/DATA\_FROM\_NMRSERVICE/30wsl/2021\_02/2021\_02\_22/v7\_b3-p35\_joc37\_20.02\_H1\_1D

OpenVnmrj

Department of Chemistry, University of Alberta

Recorded on: v700, Feb 22 2021  
Pulse Sequence: PRESAT

Sweep Width(Hz): 8389.26  
Digital Res.(Hz/p): 0.13

Acquisition Time(s): 5  
Hz per mHz(m): 34.96

Relaxation Delay(s): 0.1  
Completed Scans: 8

Yaowei, b3-p35  
698.763 MHz H1 1D in cd2cl2 (ref. to CD2Cl2 @ 5.32 ppm)  
temp 27.5 C -> actual temp = 27.0 C, coldid probe

# OpenVnmrj

Department of Chemistry, University of Alberta

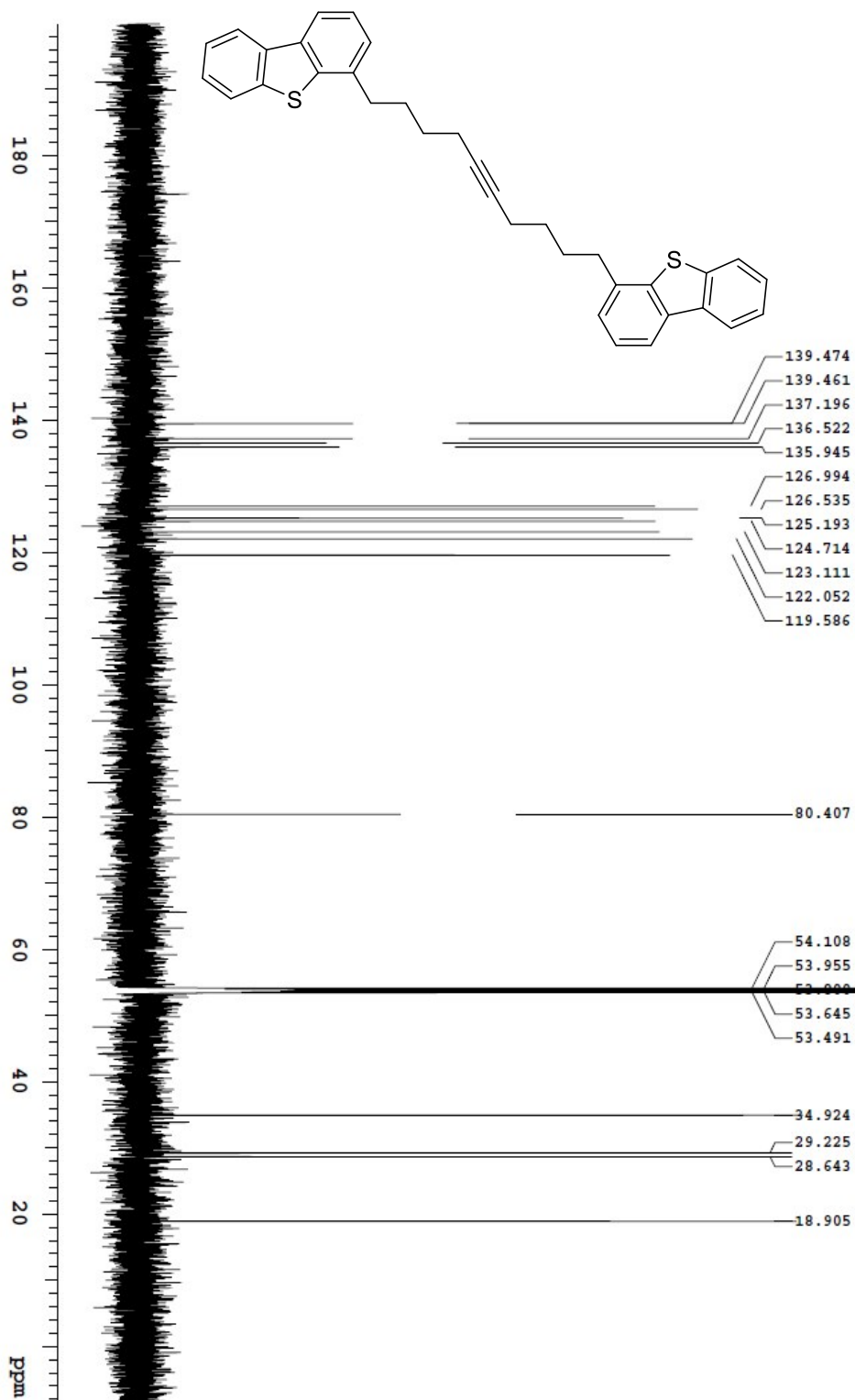
Recorded on: **v700, Feb 22 2021**  
Pulse Sequence: **s2pul**

Sweep Width(Hz): **36764.7**  
Digital Res.(Hz/pp): **0.28**

Acquisition Time(s): **1**  
Hz per mm(Hz/mm): **153.19**

Relaxation Delay(s): **1**  
Completed Scans: **128**

Yaowe, b3-p35  
175.872 MHz C13(H1) 1D in cd2cl2 (ref. to CD2Cl2 @ 53.8 ppm)  
temp 27.5 C -> actual temp = 27.0 C, coldid probe



File: /mnt/d600/home/14j/mnmr/nmrdata/DA7A\_FROM\_NMRSERVICE/yaowe/2021.02/2021.02.22.v7\_b3-p35\_joc57\_20.03\_C13\_1D

# OpenVnmrj

Department of Chemistry, University of Alberta

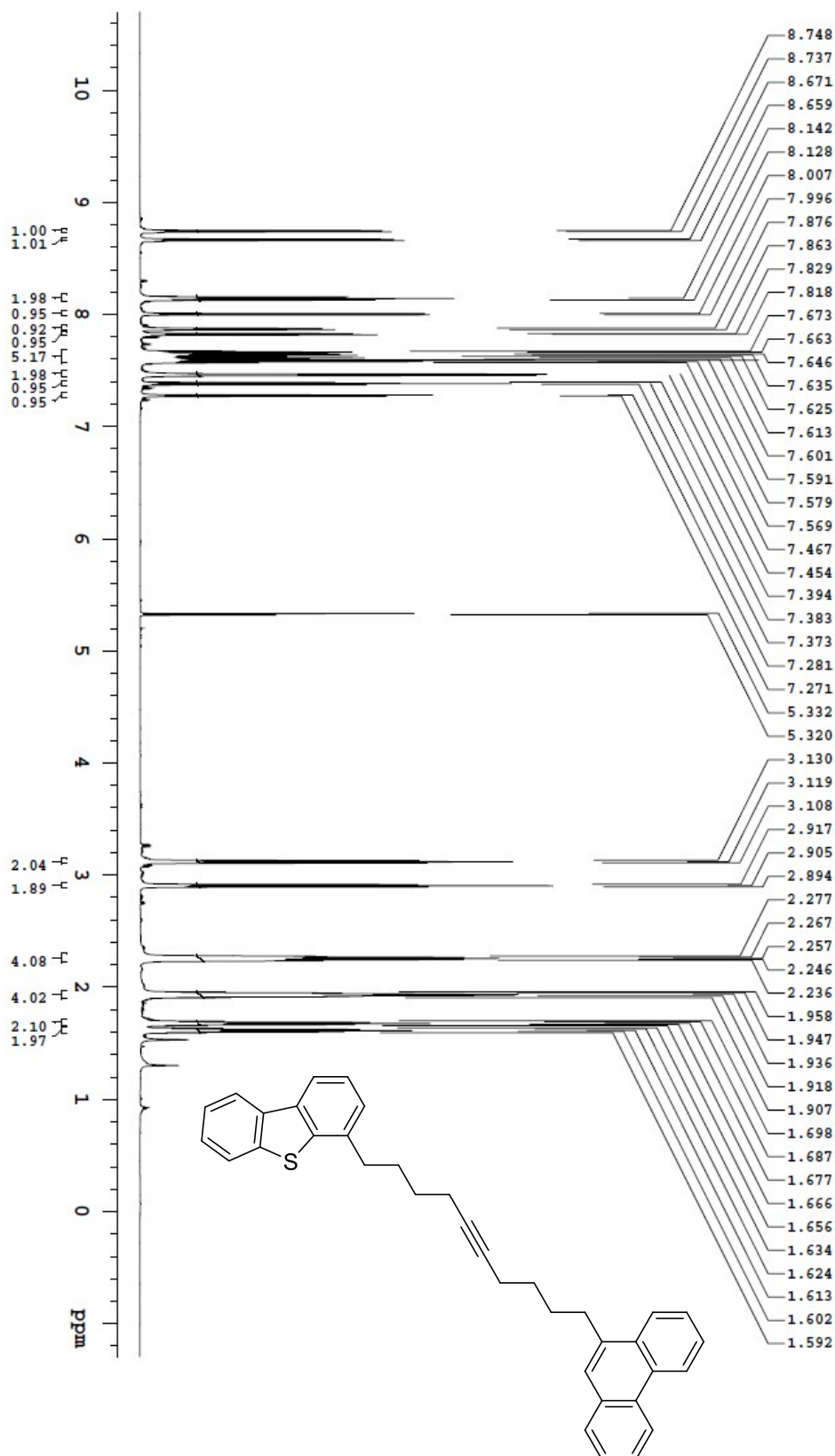
Recorded on: **v700, Sep 1 2020**  
Pulse Sequence: **PRESAT**

Sweep Width(Hz): **8389.26**  
Digital Res.(Hz/pt): **0.13**

Acquisition Time(s): **5**  
Hz per mm(Hz/mm): **34.95**

Relaxation Delay(s): **0.1**  
Completed Scans: **8**

Yaowei, b3-p29  
699.763 MHz H1 1D in cd2cl2 (ref. to CD2Cl2 @ 5.32 ppm)  
temp 27.5 C -> actual temp = 27.0 C, coldid probe



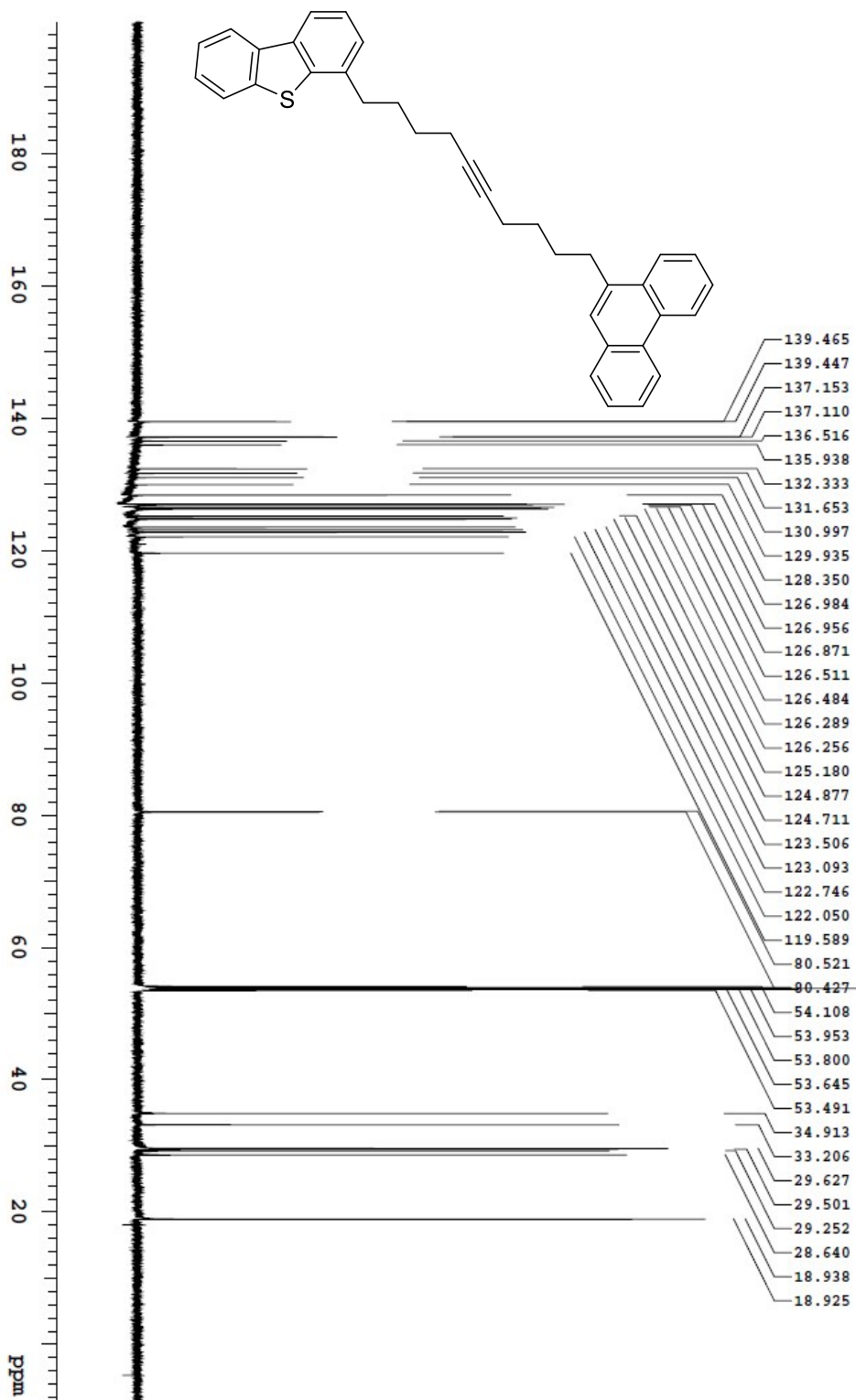
File: /mnt/d600/home/14/jmsm/nmr/data/DATA\_FROM\_NMRSERVICE/yaowei/2020.09/2020.09.01.v7\_b3-p29\_lock3\_20.03\_H1\_1D

# OpenVnmrj

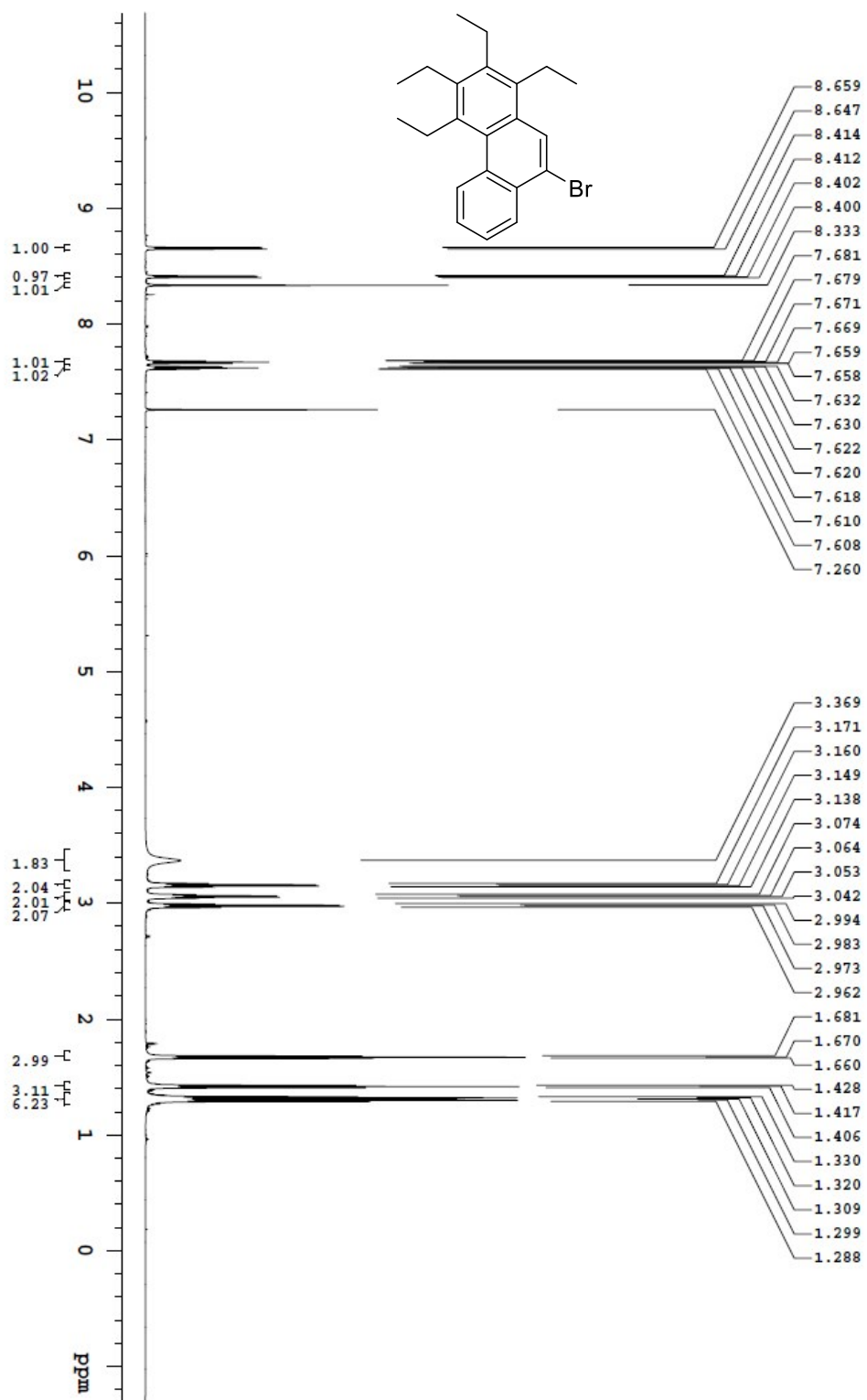
Department of Chemistry, University of Alberta

|                 |                  |                       |         |                      |        |                      |     |
|-----------------|------------------|-----------------------|---------|----------------------|--------|----------------------|-----|
| Recorded on:    | V700, Sep 1 2020 | Sweep Width(Hz):      | 36764.7 | Acquisition Time(s): | 1      | Relaxation Delay(s): | 1   |
| Pulse Sequence: | szpul            | Digital Res. (Hz/pt): | 0.28    | Fz. per mm(Hz/mm):   | 153.19 | Completed Scans:     | 256 |

Yaowei, b3-p29  
173.972 MHz <sup>13</sup>C{<sup>1</sup>H} 1D in cd<sub>2</sub>d<sub>2</sub> (ref. to CD<sub>2</sub>C<sub>2</sub> @ 53.8 ppm)  
temp 27.5 C -> actual temp = 27.0 C, coldid probe



File: /mnt/d60/home/14/mrnmr/mrdata/DATA\_FROM\_NMRSERVICE/yaowei/2020/09/20/2009.01.v7\_b3-p29\_boc43\_20.04\_C13\_1D

Recorded on: **v700, Sep 15 2020**  
Pulse Sequence: **PRESAT**Sweep Width(Hz): **8389.26**  
Digital Res.(Hz/ppt): **0.13**Acquisition Time(s): **5**  
Hz per mm(Hz/mm): **34.95**Relaxation Delay(s): **0.1**  
Completed Scans: **8**Yaowei, b3-p41  
699.762 MHz <sup>1</sup>H 1D in cdcl<sub>3</sub> (ref. to CDCl<sub>3</sub> @ 7.26 ppm)  
temp 27.5 C > actual temp = 27.0 C, coldid probe

File: /mnt/ds00/home/14/jmsm/jmldata/DATE\_FROM\_NMRSERVICE/yaowei/2020.09/2020.09.15.v7\_b3-p41\_j0043\_2207\_H1\_1D

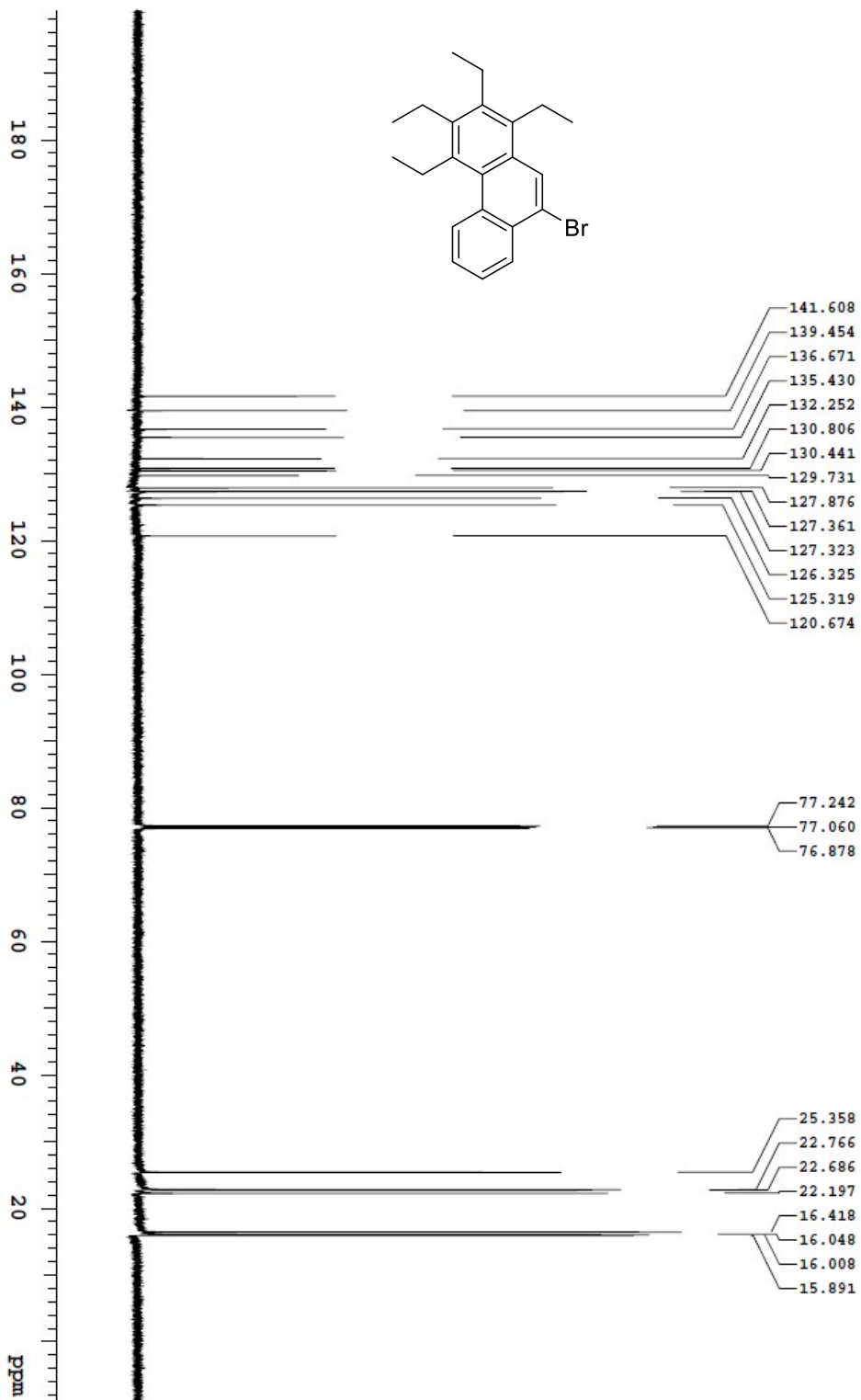
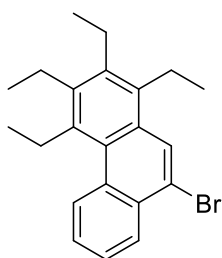


# OpenVnmrj

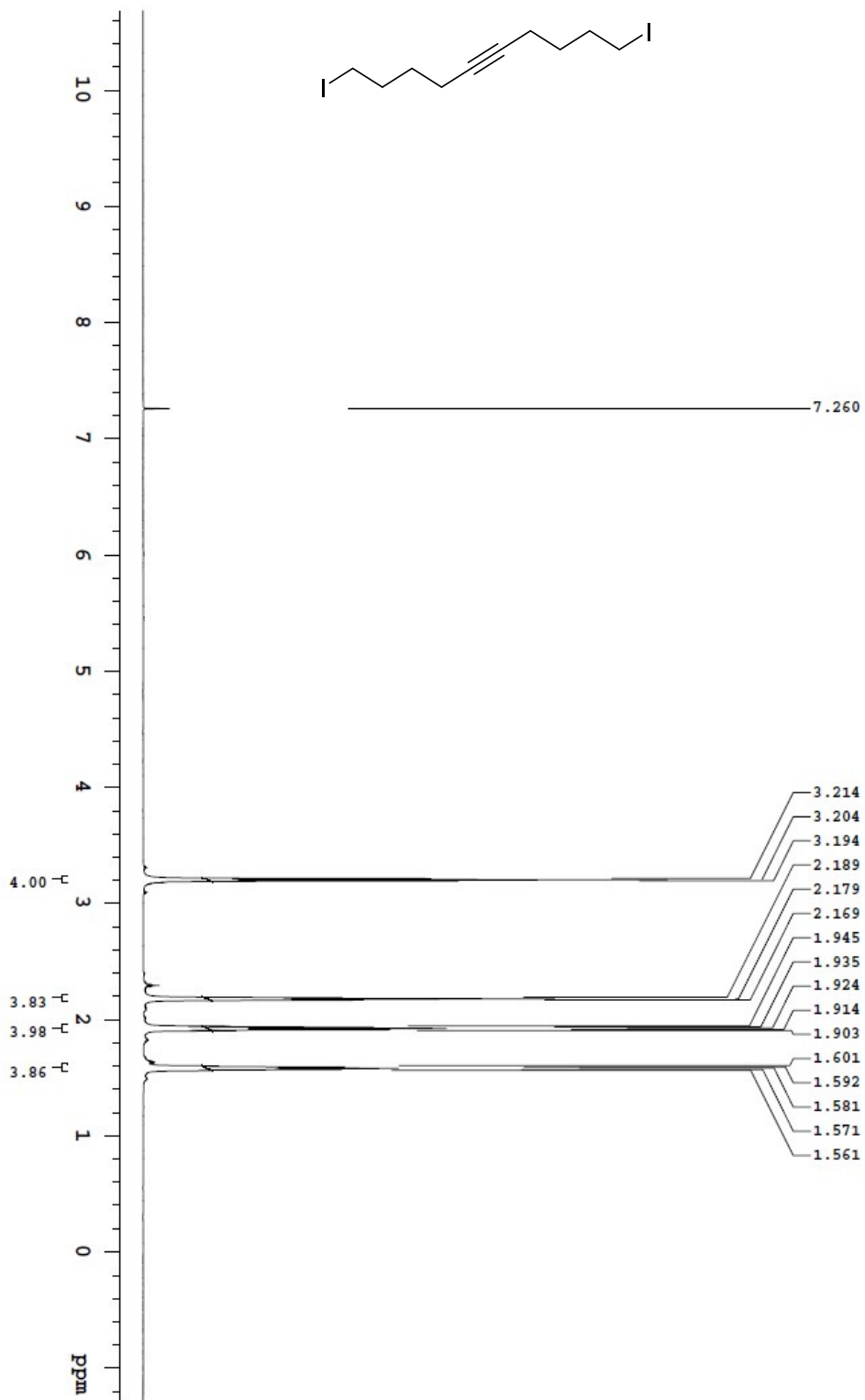
Department of Chemistry, University of Alberta

|                 |                   |                      |         |                      |        |                      |    |
|-----------------|-------------------|----------------------|---------|----------------------|--------|----------------------|----|
| Recorded on:    | V700, Sep 15 2020 | Sweep Width(Hz):     | 36764.7 | Acquisition Time(s): | 1      | Relaxation Delay(s): | 1  |
| Pulse Sequence: | s2pul             | Digital Res. (Hz/p): | 0.28    | Fz per mm(Hz/mm):    | 153.19 | Completed Scans:     | 36 |

Yaowei\_b3-p41  
175.971 MHz C13(H1) 1D in cdc13 (ref. to CDCl3 @ 77.06 ppm)  
temp 27.5 C -> actual temp = 27.0 C, coldid probe



File: /mnt/d60/home/14j/nmr/nmrdata/DATA\_FROM\_NMRSERVICE/yaowei/2020.09.15/v7\_b3-p41\_loc43\_22.08\_C13\_1D

Recorded on: **V700, Feb 9 2021**  
Pulse Sequence: **PRESAT**Sweep Width(Hz): **8388.26**  
Digital Res.(Hz/pp): **0.13**Acquisition Time(s): **5**  
Hz per ppm(Hz/pp): **34.96**Relaxation Delay(s): **0.1**  
Completed Scans: **8**Yaowei, b3-p87  
699.762 MHz <sup>1</sup>H 1D in cdcl3 (ref. to CDCl3 @ 7.26 ppm)  
temp 27.5 C -> actual temp = 27.0 C, coldid probe

## 1,10-Diiodo-5-decyne (258)

File: /mnt/600/home/14jmsnmr/mrdata/DAIA\_FROM\_NMRSERVICE/yaowei/2021.02.09.V7\_b3-p87-pure\_1oc43\_1046\_H1\_1D



# OpenVnmrj

Department of Chemistry, University of Alberta

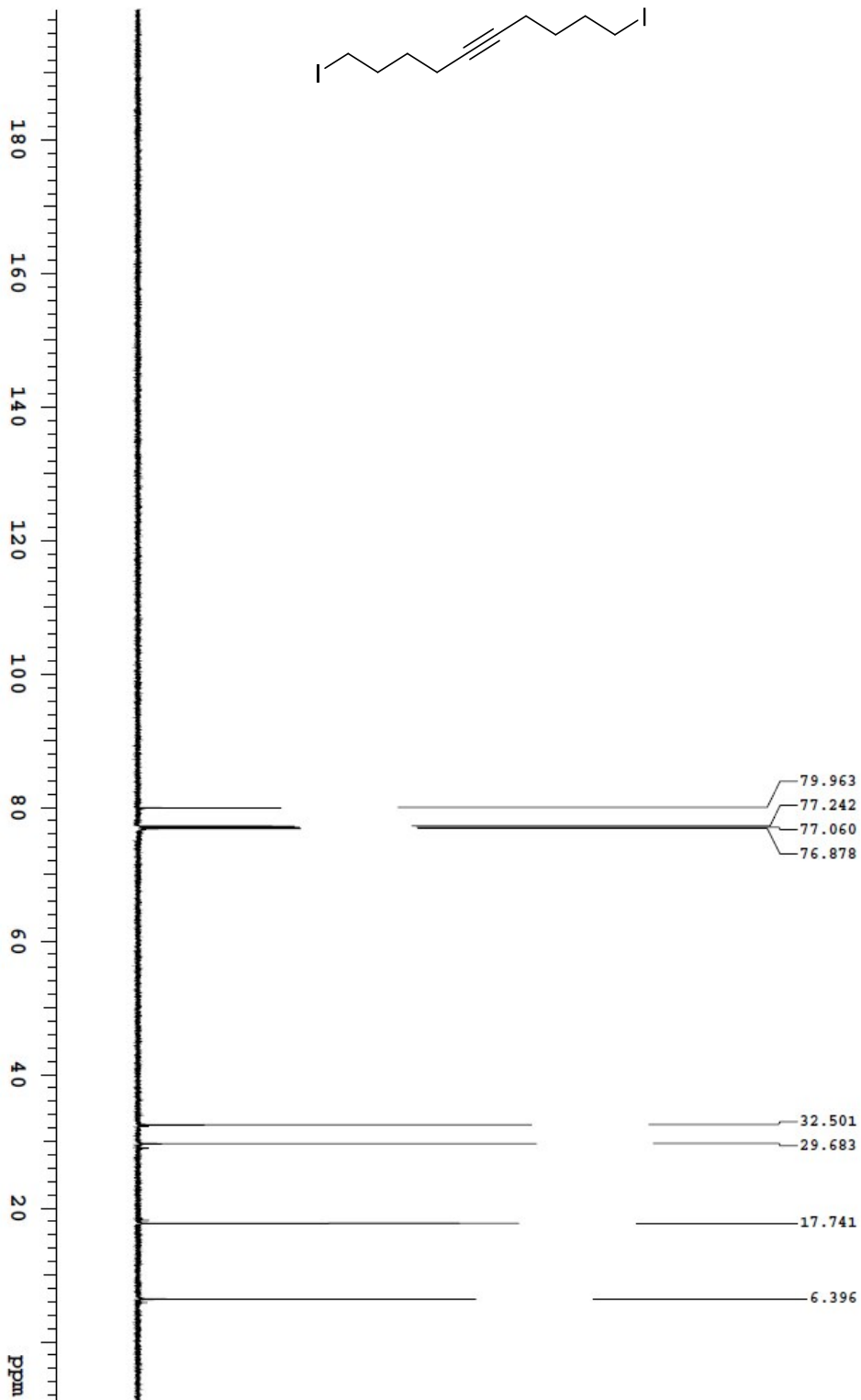
Recorded on: **v700, Feb 9 2021**  
Pulse Sequence: **s2pul**

Sweep Width(Hz): **36764.7**  
Digital Res.(Hz/p): **0.28**

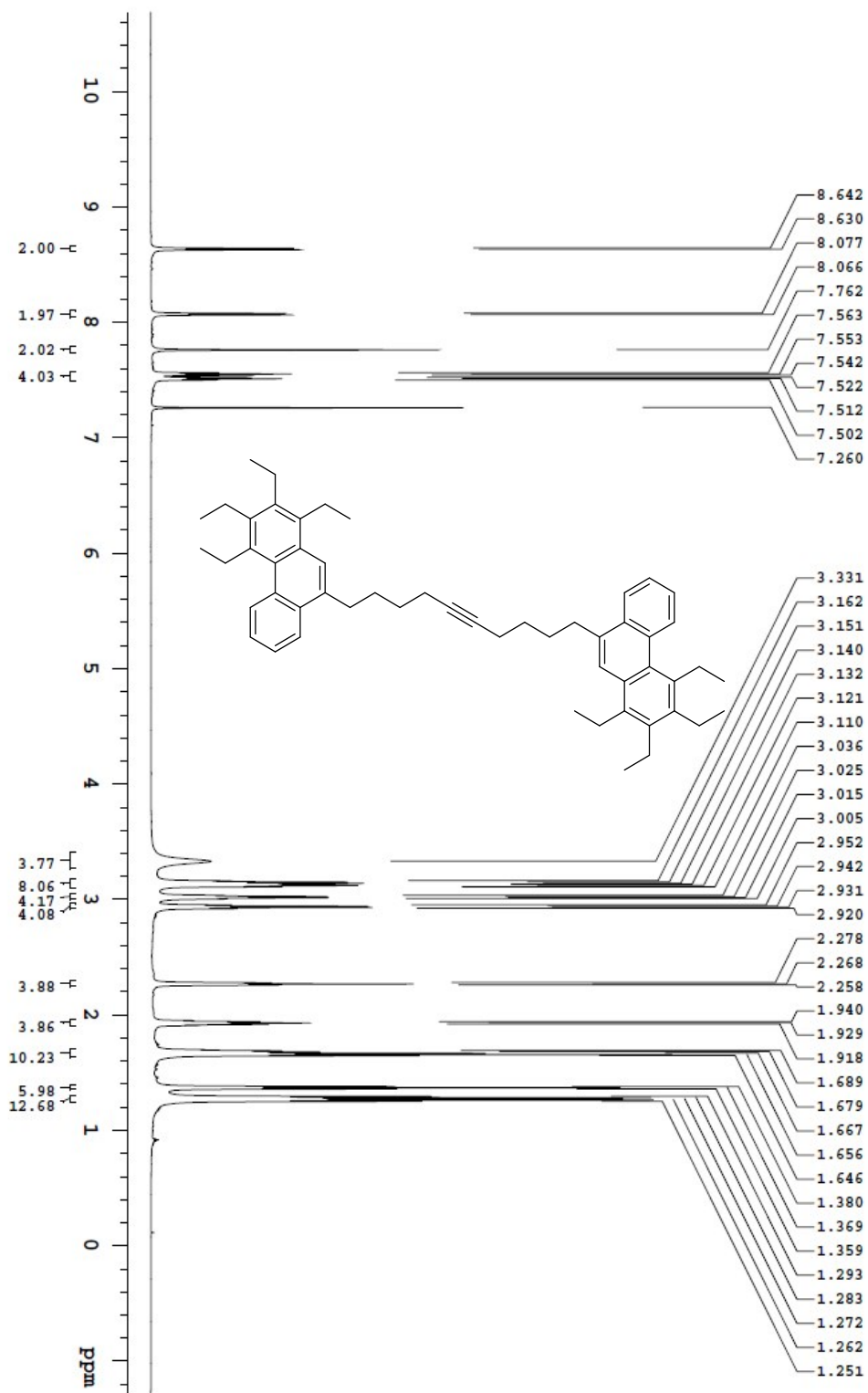
Acquisition Time(s): **1**  
Hz per mm(Hz/mm): **153.19**

Relaxation Delay(s): **1**  
Completed Scans: **116**

Yaowei, b3-p87  
175.571 MHz C13(H1) 1D in cdcl3 (ref. to CDCl3 @ 77.06 ppm)  
temp 27.5 C -> actual temp = 27.0 C, coldid probe



File: /mnt/d600/home/14/mnmr/mrdata/DAVA\_FROM\_NMRSERVICE/yaowei/2021.02/2021.02.09/v7\_03-p87-pure\_lock43\_10.47\_C13\_1D

Recorded on: **VT00, Feb 8 2021**  
Pulse Sequence: **PRESAT**Sweep Width(Hz): **8389.26**  
Digital Res.(Hz/gf): **0.13**Acquisition Time(s): **5**  
Hz per mm(Hz/mm): **34.96**Relaxation Delay(s): **0.1**  
Completed Scans: **8**Yaowei, b3-p89  
699.762 MHz H1 1D in cdcl3 (ref. to CDCl3 @ 7.26 ppm)  
temp 27.5 C -> actual temp = 27.0 C, coldid probe

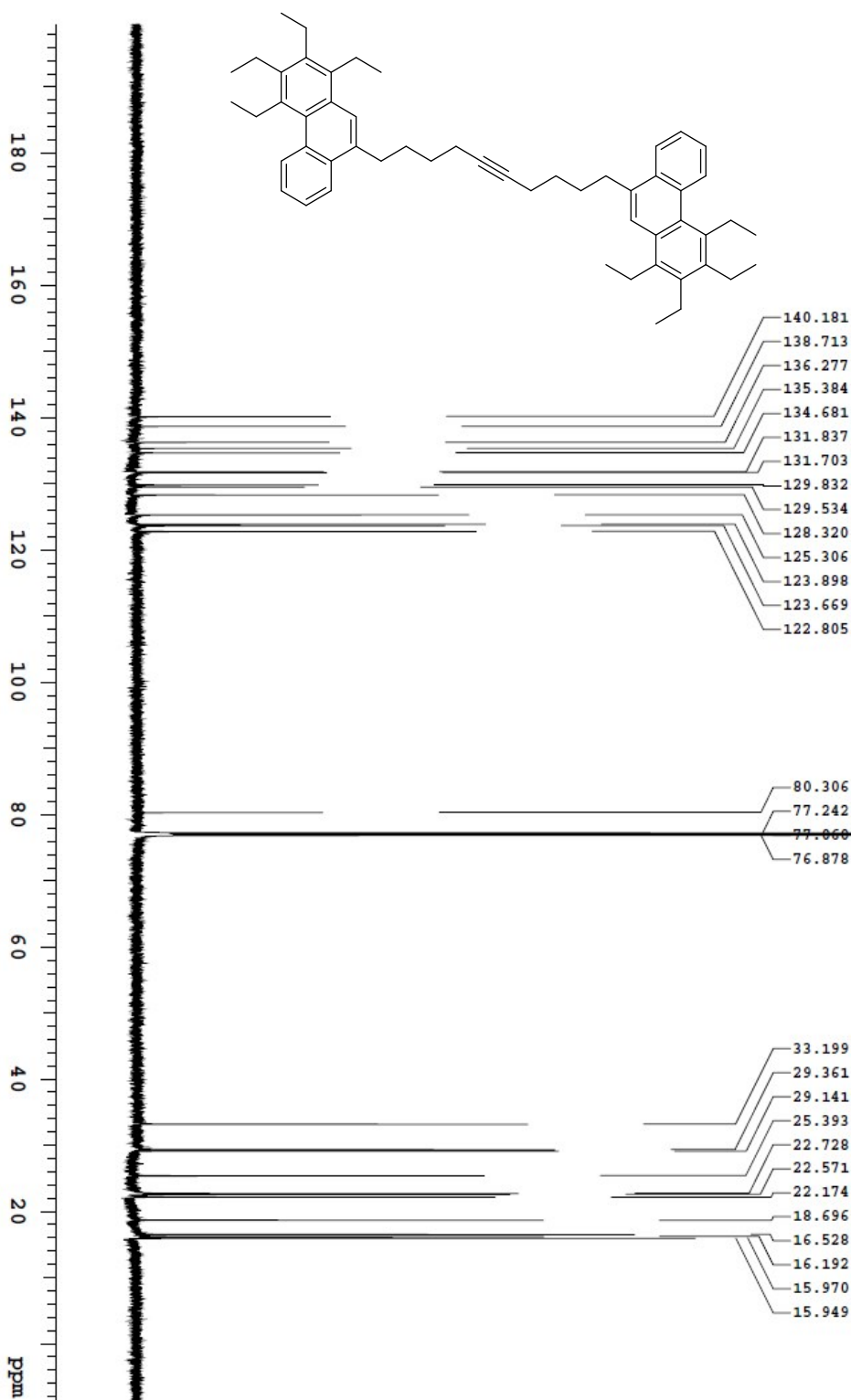
File: /mnt/d60/home/14/jnsnmr/mrdata/VT00\_NMRSERVICE/yaowei/2021.02/08.VT\_b3-p89-pure\_joc41\_11.31.H1\_1D

# OpenVnmrj

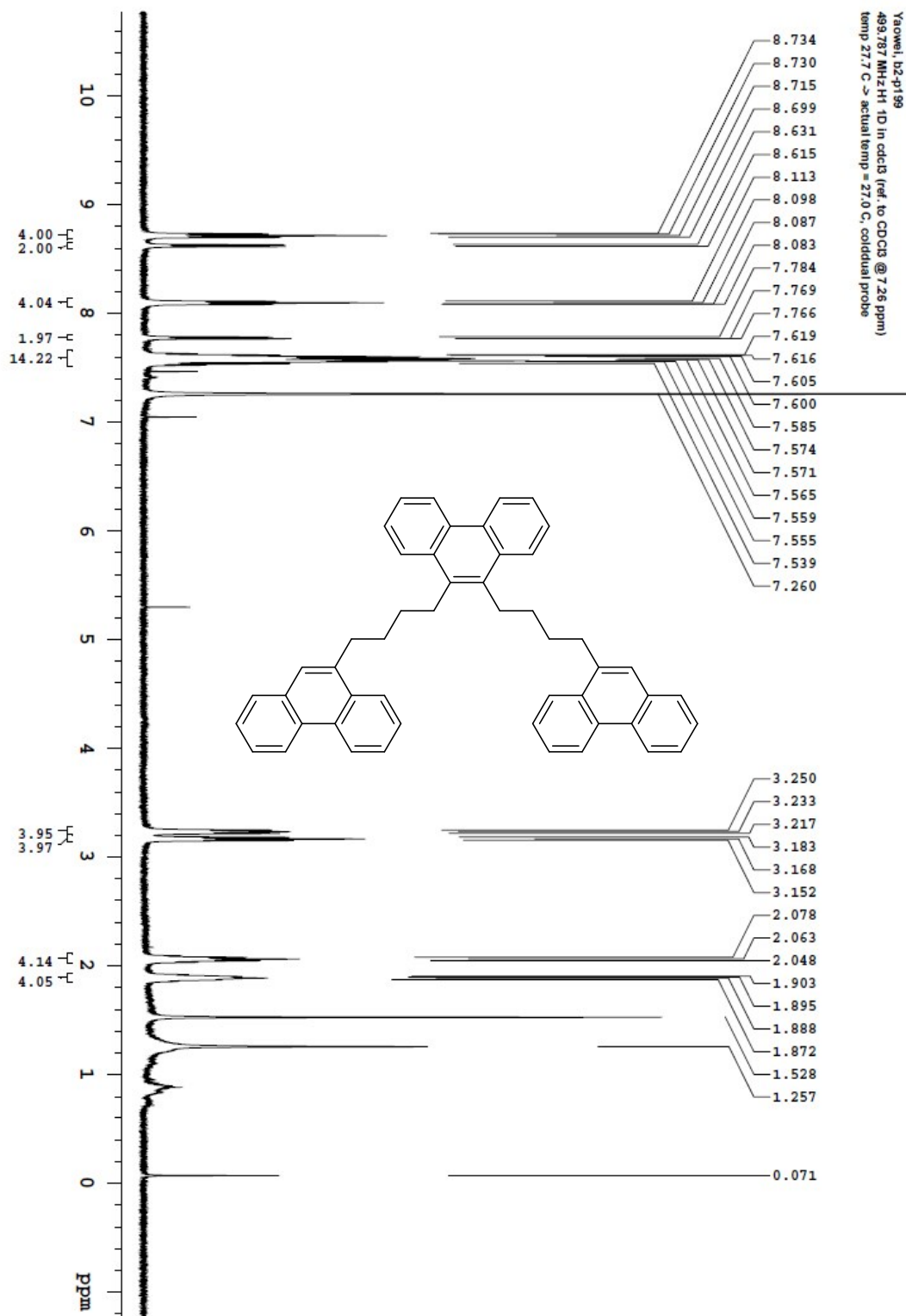
Department of Chemistry, University of Alberta

|                 |                         |                      |                |                      |               |                      |            |
|-----------------|-------------------------|----------------------|----------------|----------------------|---------------|----------------------|------------|
| Recorded on:    | <b>v700, Feb 8 2021</b> | Sweep Width(Hz):     | <b>36764.7</b> | Acquisition Time(s): | <b>1</b>      | Relaxation Delay(s): | <b>1</b>   |
| Pulse Sequence: | <b>s2pu1</b>            | Digital Res.(Hz/pp): | <b>0.28</b>    | Hz per mm(Hz/mm):    | <b>153.19</b> | Completed Scans:     | <b>128</b> |

Yaowei, b3-p89  
175.971 MHz C13{H1} 1D in cdcl3 (ref. to CDCl3 @ 77.06 ppm)  
temp 27.5 C -> actual temp = 27.0 C, coldid probe



# 9,10-Bis[4-(9-phenanthrene)butyl]phenanthrene (260)



File: /mnt/d600/home/14/jmsnmr/mrdata/DAI\_FROM\_NMRSERVICE/aoew/2020.09/2020.09.10.u5\_b2-p199\_loc11\_20.37\_H1\_1D

OpenVnmrj

Department of Chemistry, University of Alberta

Recorded on: u500, Sep 10 2020  
Pulse Sequence: PRESAT

Sweep Width(Hz): 6009.62  
Digital Res.(Hz/pp): 0.09

Acquisition Time(s): 5  
Hz per mm(Hz/mm): 25.04

Relaxation Delay(s): 0.1  
Completed Scans: 8

# OpenVnmrj

Department of Chemistry, University of Alberta

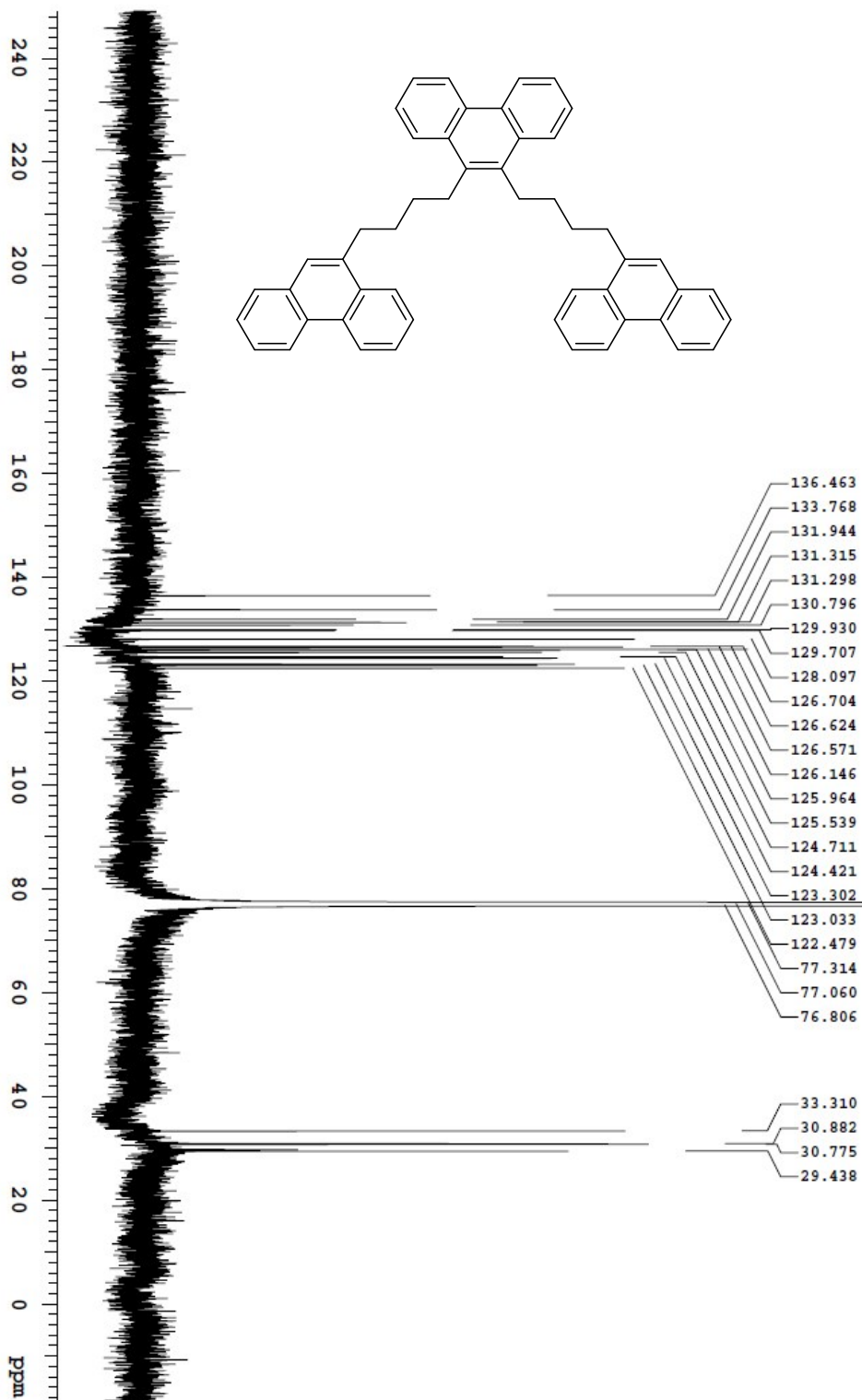
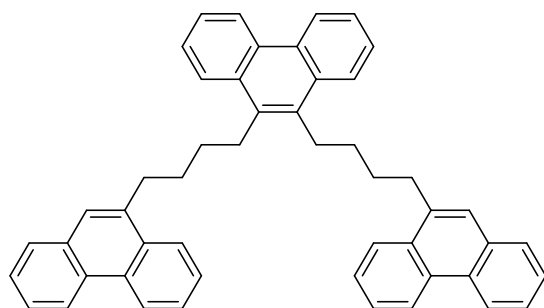
Recorded on: **u500, Sep 10 2020**  
Pulse Sequence: **s2pul**

Sweep Width(Hz): **33783.8**  
Digital Res.(Hz/pt): **0.26**

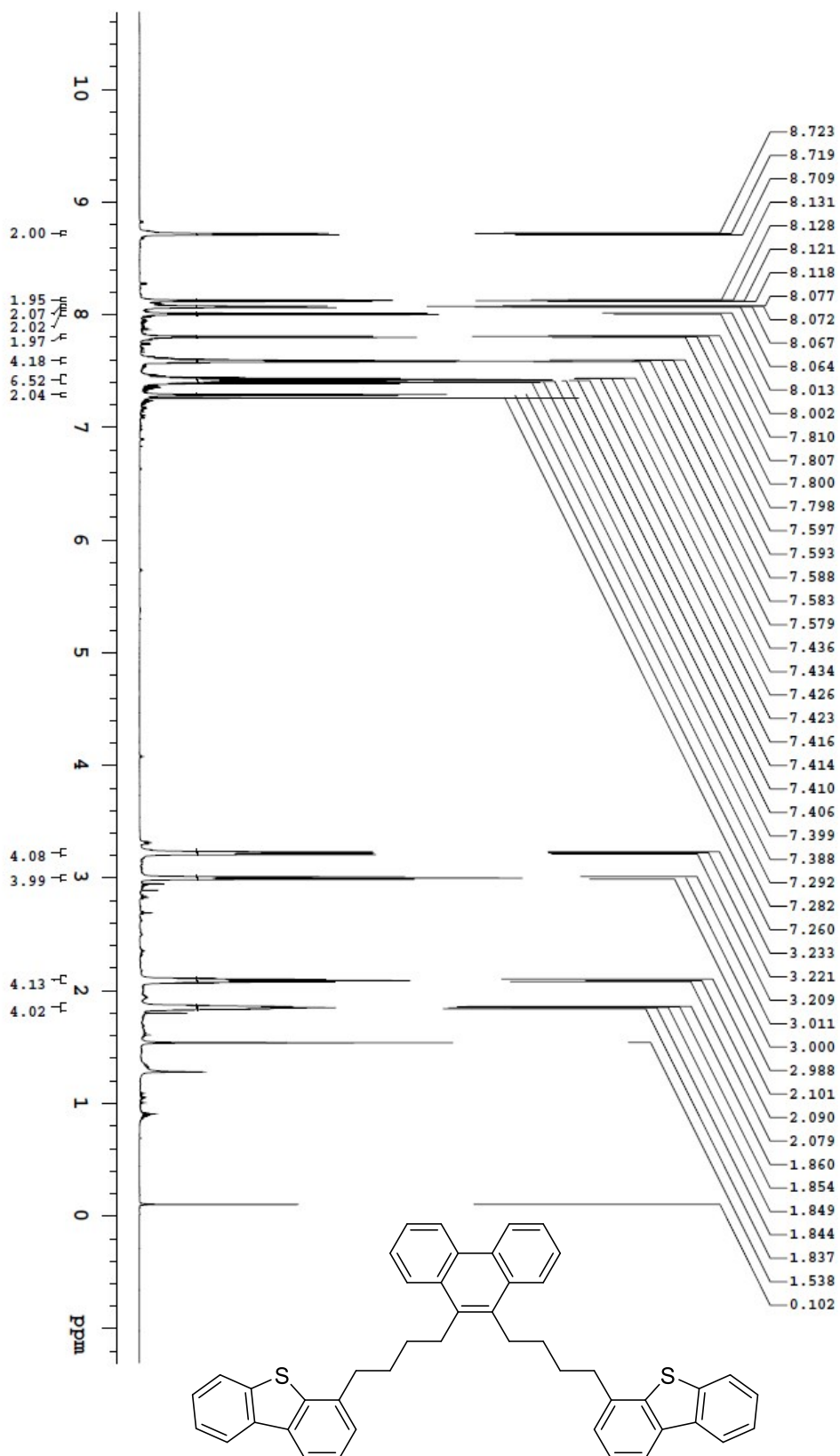
Acquisition Time(s): **1**  
Hz per mhz(hz/mhz): **140.76**

Relaxation Delay(s): **1**  
Completed Scans: **5000**

Yaowei, b2-p199  
125.685 MHz C13{H1} 1D in cdc1b (ref. to CDCl3 @ 77.06 ppm)  
temp 27.7 C -> actual temp = 27.0 C, coldlual probe



File: /mnt/d500/home/14/mrsmr/mrsmr/da/b1/DATA\_FROM\_NMRSERVICE/yaowei/2020/09/20/20.09.10.u5\_02-p199\_loc11\_20.38\_C13\_1D

Recorded on: **v700, Jul 15 2020**  
Pulse Sequence: **PRESAT**Sweep Width(Hz): **6389.26**  
Digital Res.(Hz/pf): **0.13**Acquisition Time(s): **5**  
Hz per mem(Hz/mm): **34.96**Relaxation Delay(s): **0.1**  
Completed Scans: **8**Yaowei, b2-p197  
699.762 MHz H1 1D in cdc3 (ref. to CDCl3 @ 7.26 ppm)  
temp 27.5 C -> actual temp = 27.0 C, coldid probe

## 9,10-Bis[4-(4-dibenzothiophene)butyl]phenanthrene (261)

File: /mnt/d60/home/14/jmsm/mrdata/DAIA\_FROM\_NMRSERVICE/yaowei/2020.07/2020.07.15.v7\_b2-p197\_bx87\_17.43\_H1\_1D

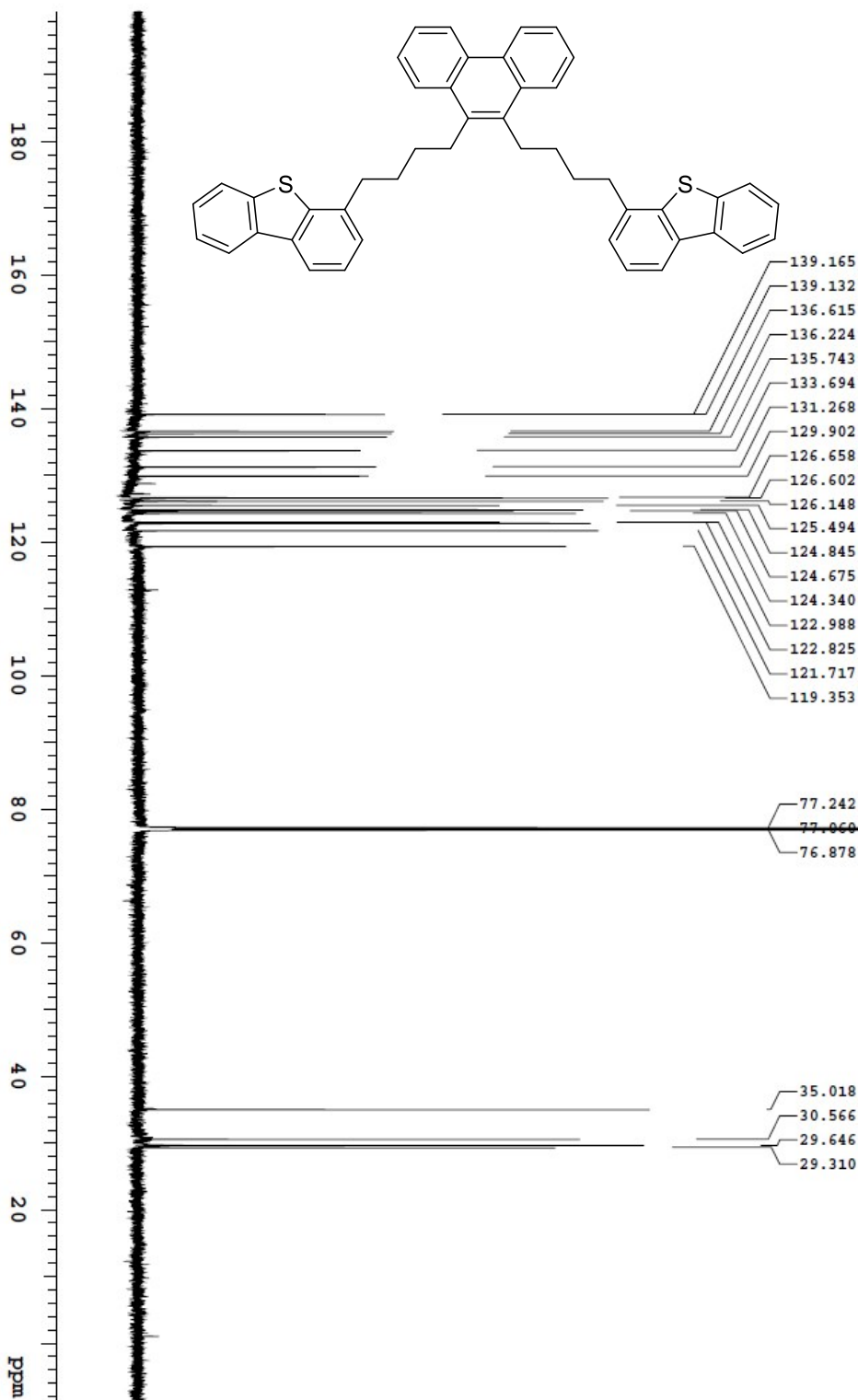


# OpenVnmrj

Department of Chemistry, University of Alberta

|                                       |                                  |                                 |                               |
|---------------------------------------|----------------------------------|---------------------------------|-------------------------------|
| Recorded on: <b>v700, Jul 15 2020</b> | Sweep Width(Hz): <b>36764.7</b>  | Acquisition Time(s): <b>1</b>   | Relaxation Delay(s): <b>1</b> |
| Pulse Sequence: <b>s2pul</b>          | Digital Res. (Hz/p): <b>0.28</b> | Hz per mm(Hz/mm): <b>153.19</b> | Completed Scans: <b>256</b>   |

Yaoxuei, h2-p1 97  
175.971 MHz C13(41) 1D in cdc13 ref. to CDC13 @ 77.06 ppm)  
temp 27.5 C -> actual temp = 27.0 C, coldid probe



File: /mnt/d60/home/14/mnmr/rnmr/data/DATA\_FROM\_NMRSEVICE/yaoxuei/2020.07/2020.07.15.v7\_d2-p197\_loc87\_22.55\_C13\_1D

# OpenVnmrj

Department of Chemistry, University of Alberta

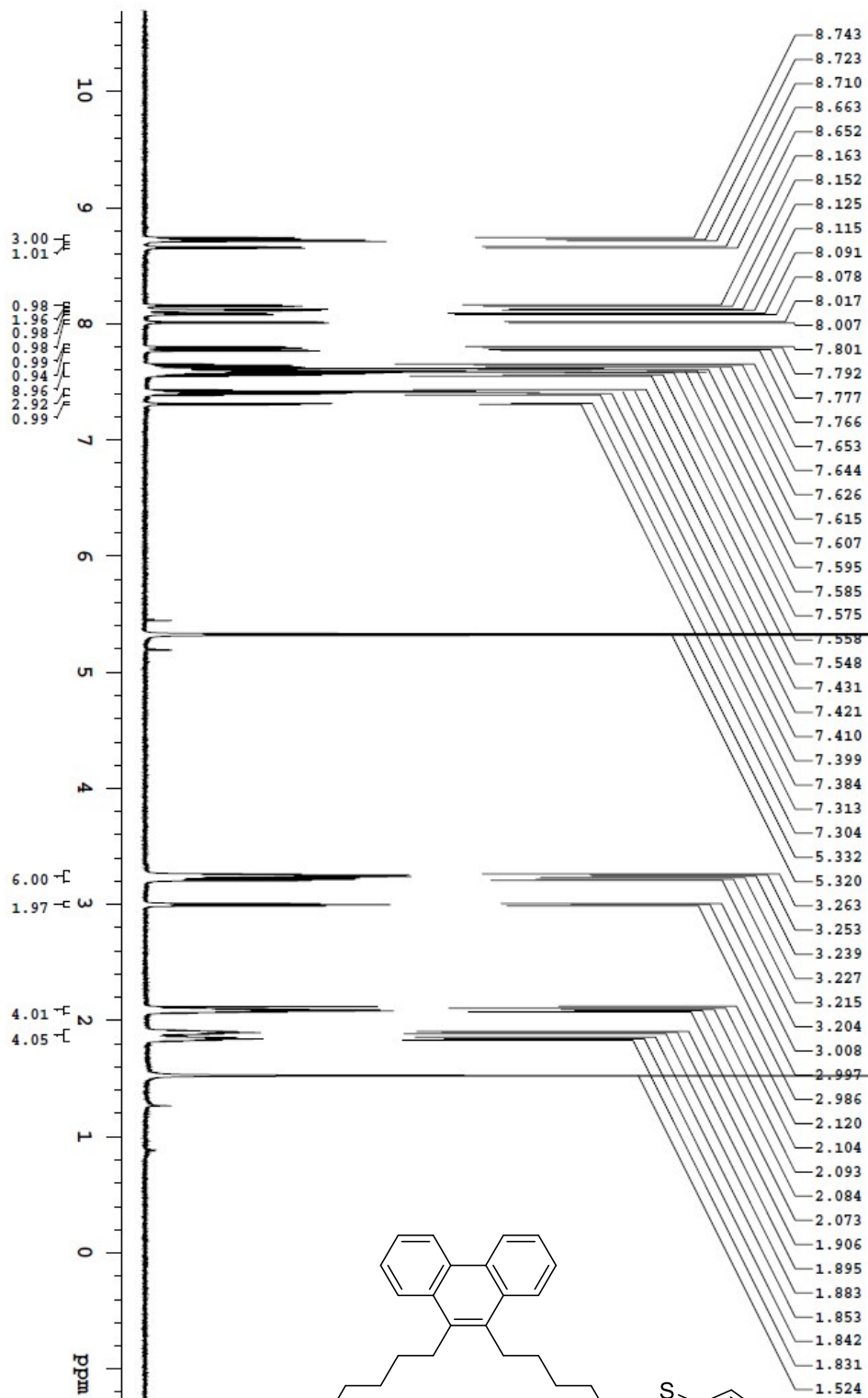
Recorded on: v700, Sep 9 2020  
Pulse Sequence: PRESAT

Sweep Width(Hz): 8389.26  
Digital Res.(Hz/p): 0.13

Acquisition Time(s): 5  
Hz per mmf(hz/mm): 34.95

Relaxation Delay(s): 0.1  
Completed Scans: 8

Yaowei, b3-p33  
693.753 MHz <sup>1</sup>H 1D in cd2cl2 (ref. to CD2Cl2 @ 5.32 ppm)  
temp 27.5 C -> actual temp = 27.0 C, coldid probe



File: /mnt/d60/home/14/mnmr/mnmrdata/DATA\_FROM\_NMRSERVICE/yaowei/2020.09/2020.09.09.v7\_b3-p33\_Joc43\_20.03\_H1\_1D

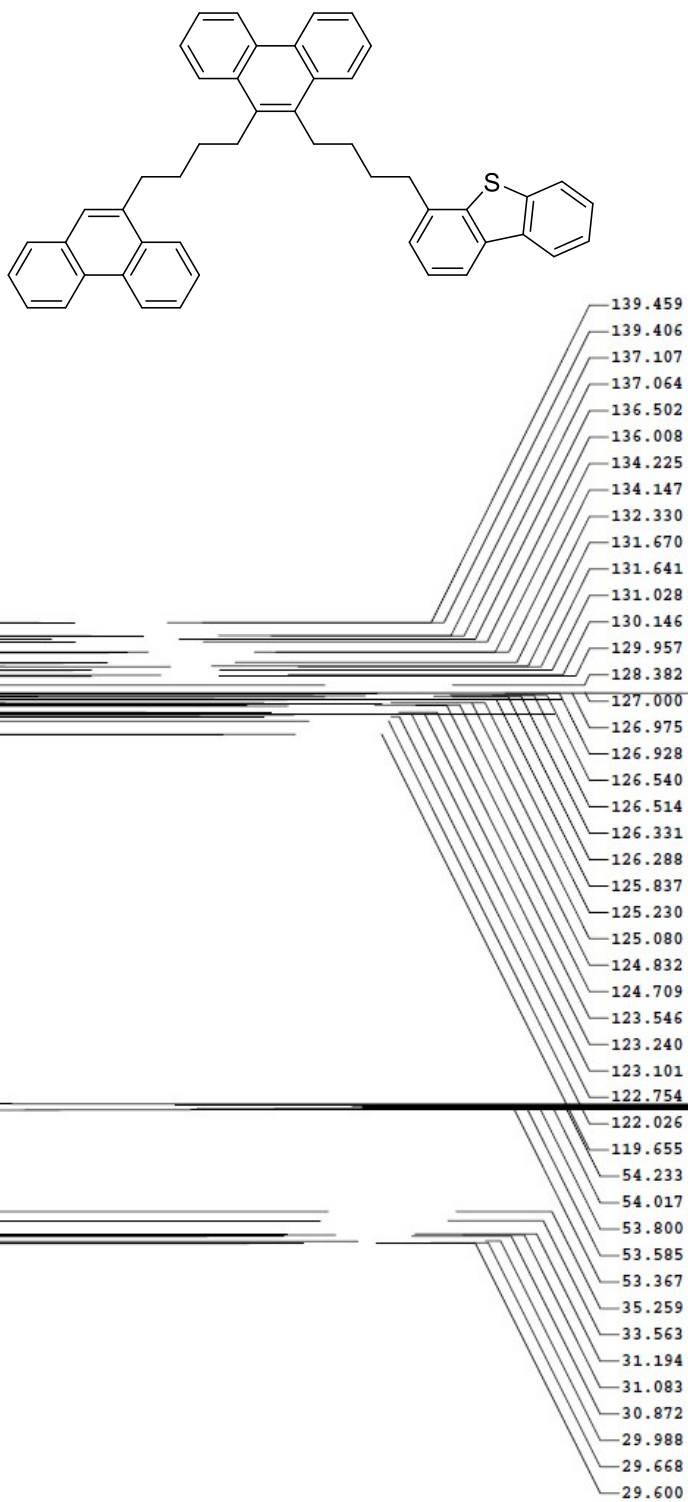


# OpenVnmrj

Department of Chemistry, University of Alberta

|                                       |                                  |                                 |
|---------------------------------------|----------------------------------|---------------------------------|
| Recorded on: <b>u500, Sep 10 2020</b> | Sweep Width(Hz): <b>33783.8</b>  | Acquisition Time(s): <b>1</b>   |
| Pulse Sequence: <b>s2pul</b>          | Digital Res.(Hz/pp): <b>0.26</b> | Hz per mm(Hz/mm): <b>140.76</b> |
|                                       |                                  | Relaxation Delay(s): <b>1</b>   |
|                                       |                                  | Completed Scans: <b>512</b>     |

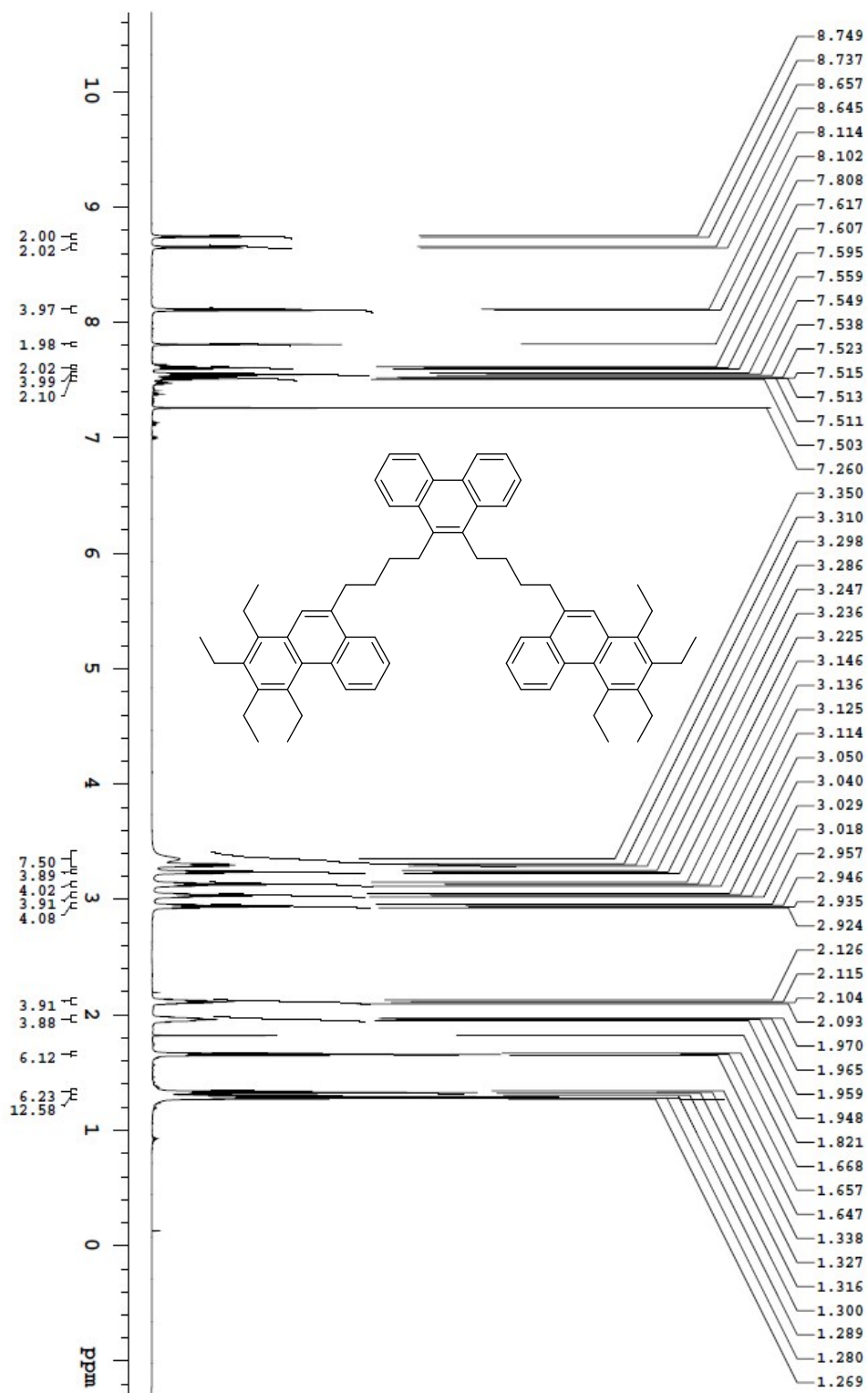
Yaowei\_b3-p33  
125.686 MHz C13(H1) 1D in cd2cl2 (ref. to CDCl2 @ 53.8 ppm)  
temp 27.7 C -> actual temp = 27.0 C, cold dual probe



File: /mnt/d00/home/14/jnmr/nmr/data/DAI\_A\_FROM\_NMR/CEV/yaowei/2020.09/2020.09.10.u5\_b3-p33\_loc10\_12.15\_C13\_1D

Recorded on: **V700, Feb 12 2021**  
Pulse Sequence: **PRESAT**Sweep Width(Hz): **8389.26**  
Digital Res.(Hz/ppt): **0.13**Acquisition Time(s): **5**  
Hz per mm(Hz/mm): **34.96**Relaxation Delay(s): **0.1**  
Completed Scans: **8**

Yaowei, b3-p77

699.762 MHz <sup>1</sup>H 1D in cdcl<sub>3</sub> (ref. to CDCl<sub>3</sub> @ 7.26 ppm)  
temp 27.5 C -> actual temp = 27.0 C; coldid probe

## 9,10-Bis{4-[9-(1,2,3,4-tetraethylphenanthrene)]butyl}phenanthrene (263)

File: /mnt/d600/home/14/jmsm/mrdata/DATA\_FROM\_NMRSERVICE/yaowei/2021.02/2021.02.12/V700\_b3-p77-pure\_loc43\_0146\_H1\_1D

Relaxation Delay(s): 1  
Completed Scans 128

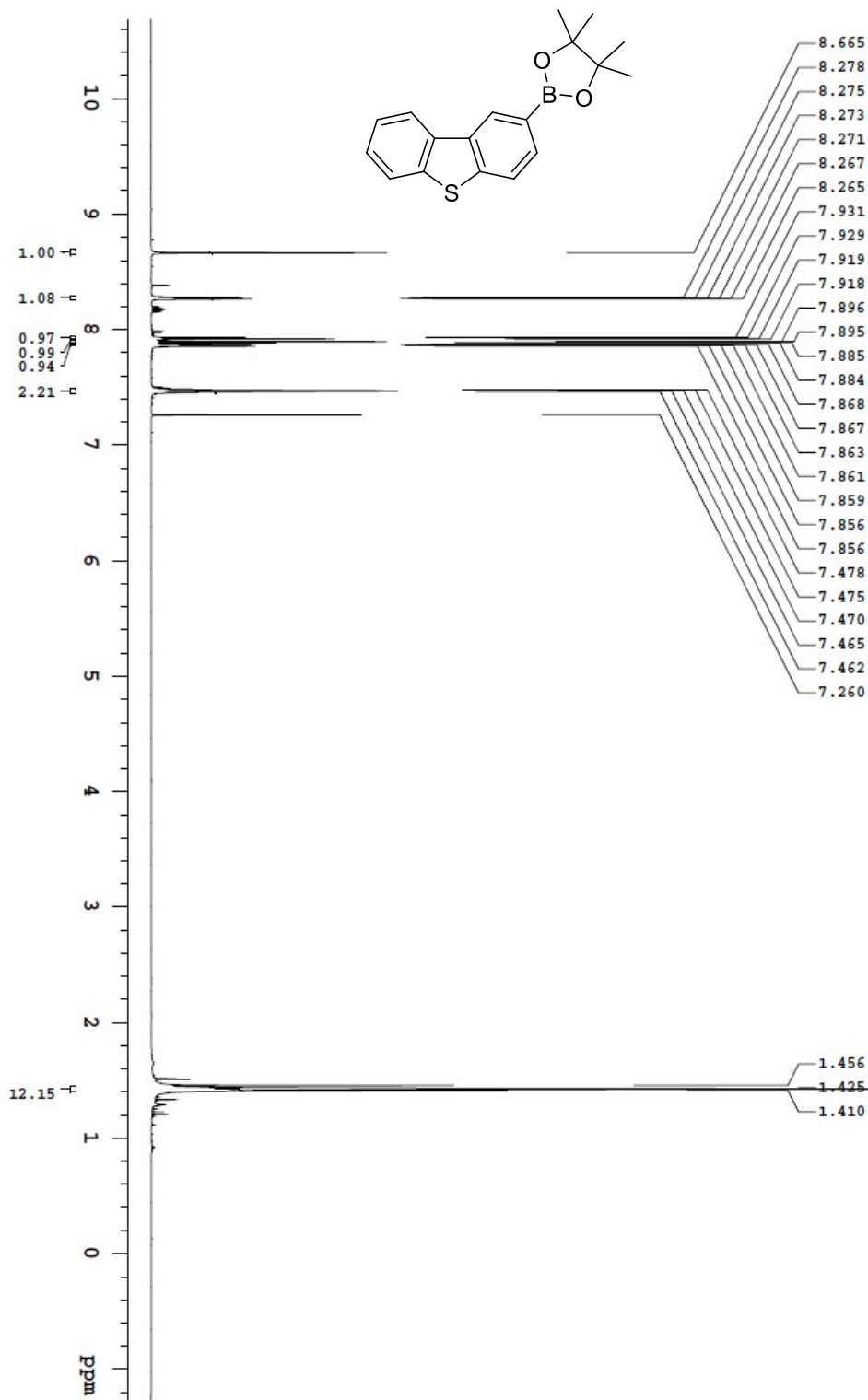
Chemical structure of compound 10 is shown above the spectrum. The structure is a symmetrical molecule with a central biphenyl core. Each phenyl ring of the biphenyl is connected via a propyl chain to a 1,2,3,4-tetrahydronaphthalene system. The 1,2,3,4-tetrahydronaphthalene system has an ethyl group at the 1-position and a propyl group at the 2-position.

<sup>13</sup>C NMR spectrum (CDCl<sub>3</sub>) of compound 10. The x-axis represents chemical shift in ppm, ranging from 0 to 180. The spectrum shows several peaks in the aromatic region (122-140 ppm), a triplet for the CDCl<sub>3</sub> solvent at 77.242, 77.060, and 76.878 ppm, and several peaks in the aliphatic region (15.969-33.619 ppm).

| Chemical Shift (ppm) |
|----------------------|
| 140.216              |
| 138.717              |
| 136.277              |
| 135.432              |
| 134.646              |
| 133.819              |
| 131.834              |
| 131.737              |
| 131.325              |
| 129.911              |
| 129.864              |
| 129.569              |
| 128.364              |
| 126.642              |
| 125.448              |
| 125.392              |
| 124.762              |
| 123.951              |
| 123.546              |
| 122.966              |
| 122.725              |
| 77.242               |
| 77.060               |
| 76.878               |
| 33.619               |
| 30.990               |
| 30.886               |
| 29.421               |
| 25.395               |
| 22.723               |
| 22.579               |
| 22.168               |
| 16.542               |
| 16.217               |
| 15.981               |
| 15.969               |

## OpenVnmrj

Department of Chemistry, University of Alberta

Recorded on: **v700, Oct 20 2021**  
Pulse Sequence: **PRESAT**Sweep Width(Hz): **8389.25**  
Digital Res.(Hz/pp): **0.13**Acquisition Time(s): **5**  
Hz per mm(Hz/mm): **34.95**Relaxation Delay(s): **0.1**  
Completed Scans: **8**Yaowei, b2-p93  
699.762 MHz H<sup>1</sup> 1D in cdcl3 (ref. to CDCl<sub>3</sub> @ 7.26 ppm)  
temp 27.5 C -> actual temp = 27.0 C, coldid probe

File: /mnt/ds00/home14/mnmr/mnmrdata/DATA\_FROM\_NMRSEVICE/yaowei/2021.10.20/21.10.20.v7\_02-p93\_0c37\_20.34\_H1\_1D

# OpenVnmrj

Department of Chemistry, University of Alberta

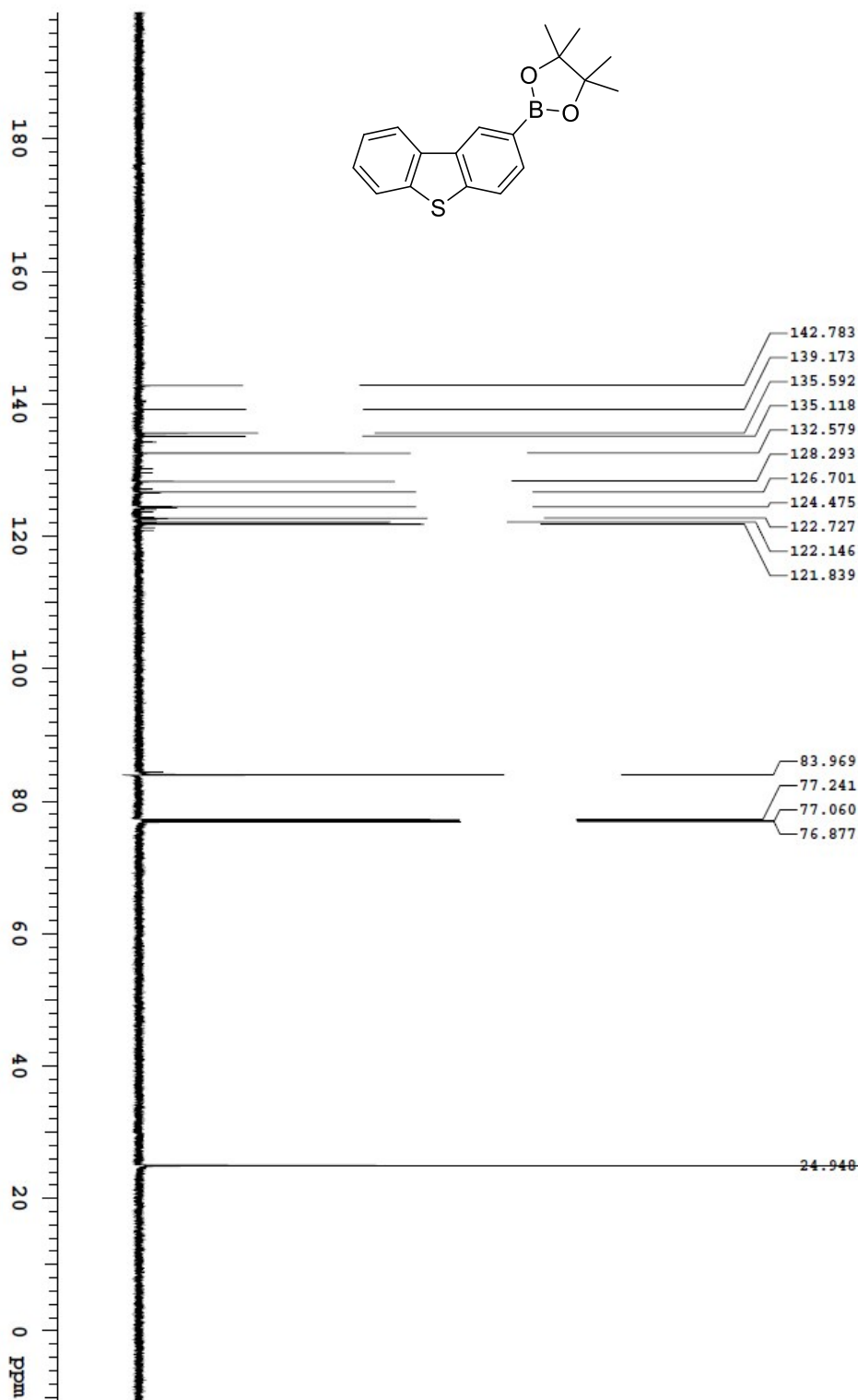
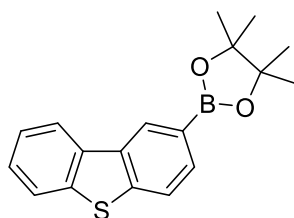
Recorded on: **v700, Oct 20 2021**  
Pulse Sequence: **s2pul**

Sweep Width(Hz): **46296.3**  
Digital Res.(Hz/p): **0.35**

Acquisition Time(s): **1**  
Hz per mm(Hz/mm): **154.37**

Relaxation Delay(s): **1**  
Completed Scans: **48**

Yaowei, h2-p93  
175.976 MHz C13{H1} 1D in cdcl3 (ref. to CDCl3 @ 77.06 ppm)  
temp 27.5 C -> actual temp = 27.0 C, coldid probe



File: /mnt/d50/home/y4/mrnmr/mrdata/DA1A\_FROM\_NMRSEVIC/EYaowei/2021\_10/20/21\_10\_20\_V7\_h2-p93\_16x37\_20.35\_C13\_1D



# OpenVnmrj

Department of Chemistry, University of Alberta

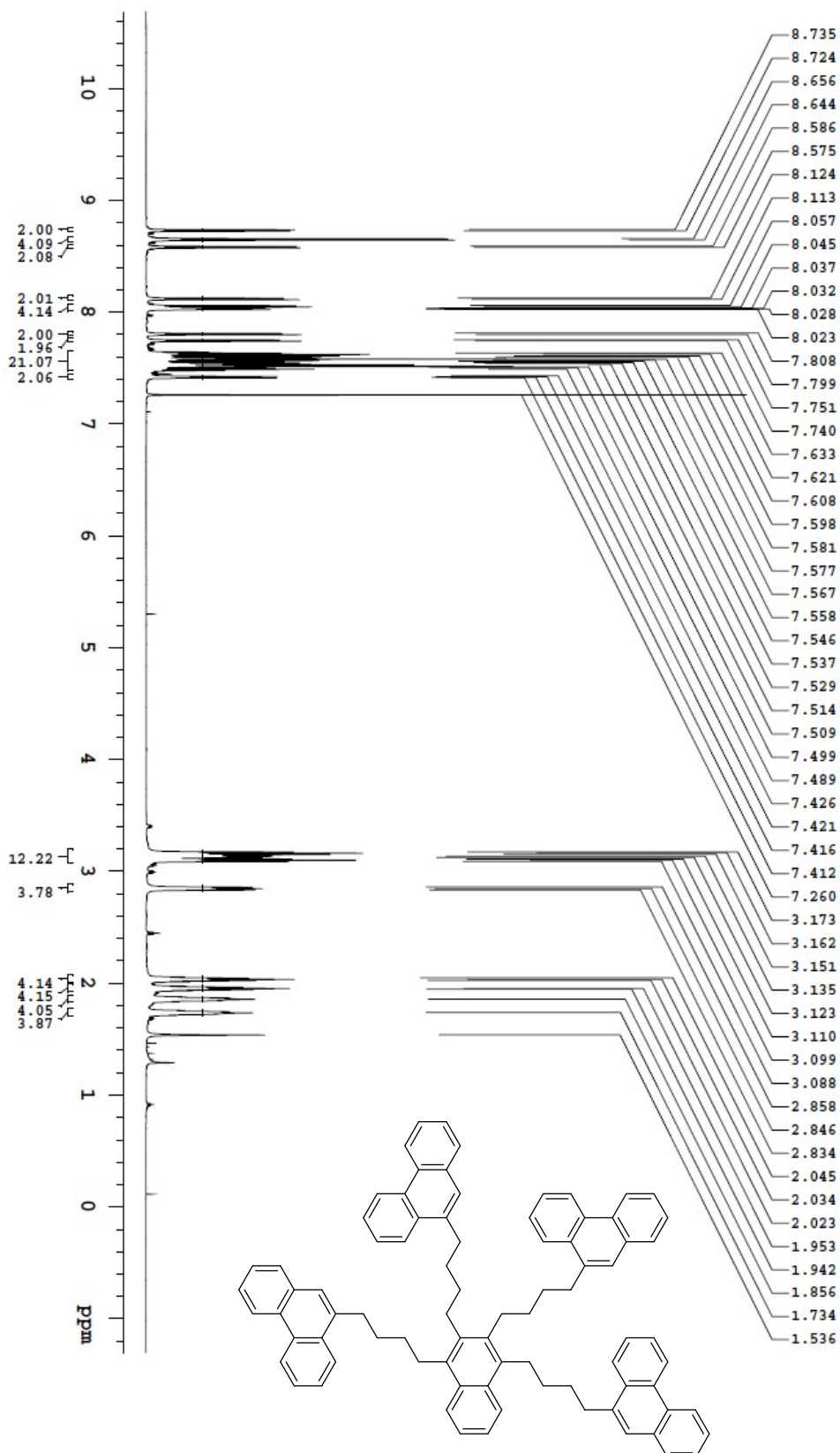
Recorded on: **0700\_JUL 28 2021**  
 Pulse Sequence: **PRB3AT**

Sweep Width(Hz): **8389.26**  
 Digital Res.(Hz/pt): **0.13**

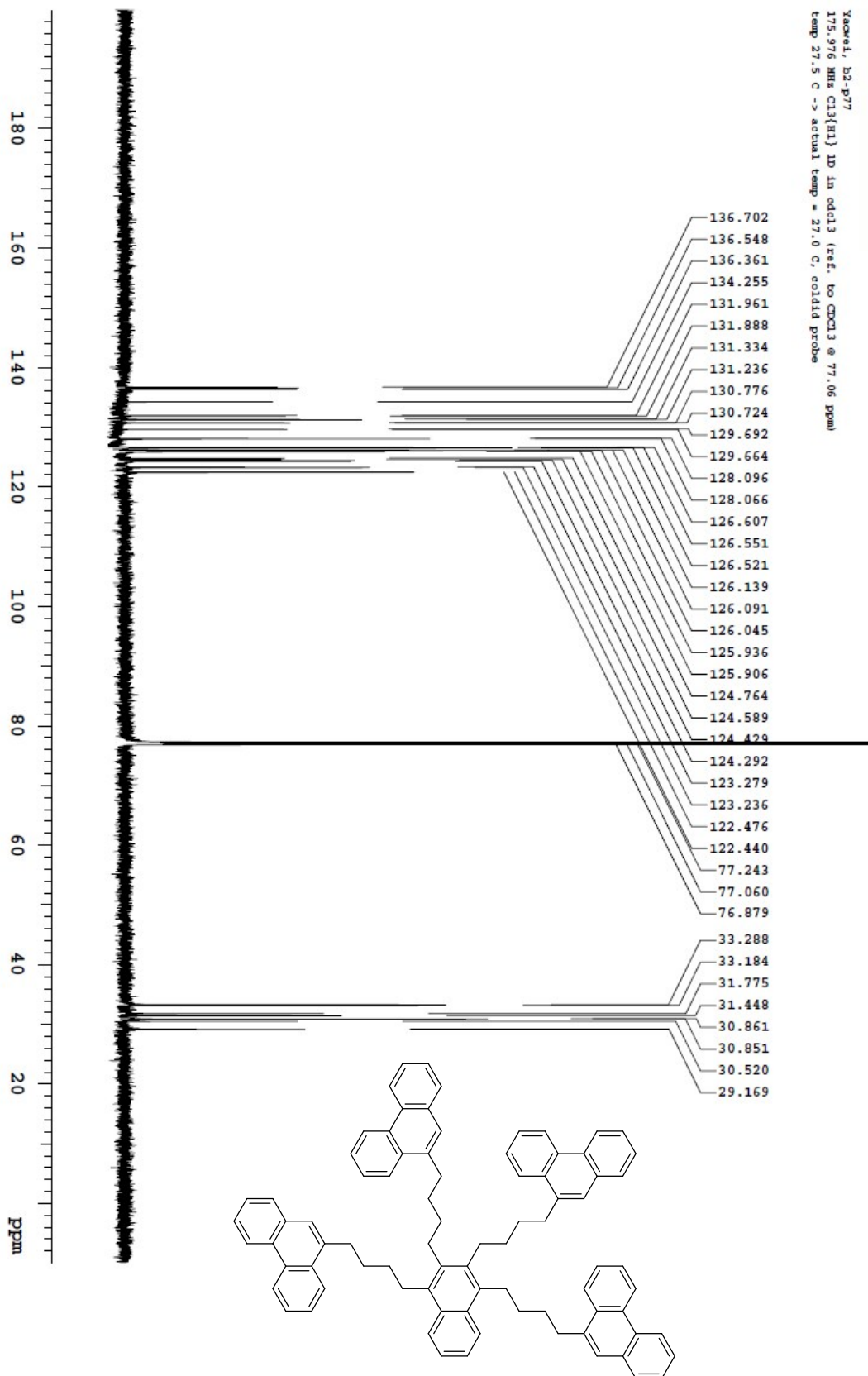
Acquisition Time(s): **5**  
 Hz per mm(Hz/mm): **34.95**

Relaxation Delay(s): **0.1**  
 Completed Scans: **8**

Yacwe1, b2-p77  
 699.762 MHz H1 JD In edcl3 (ref. to CXC13 @ 7.26 ppm)  
 Temp 27.5 C -> actual temp = 27.0 C, coldid probe



Yacovet, b2-p77  
175.976 MHz  $\text{CHCl}_3\{\text{H}\}$  ID in cdc13 (ref. to  $\text{CHCl}_3$  @ 77.06 ppm)  
temp 27.5 C -> actual temp = 27.0 C, coldid probe



File: /mnt/d600/home14/jmsnmr/nmrdata/DATA\_FROM\_NMRSERVICE/Yaowei/2021.07/2021.07.26\_v7\_b2-p77\_loc37\_03.26\_C13\_1D

# OpenVmrj

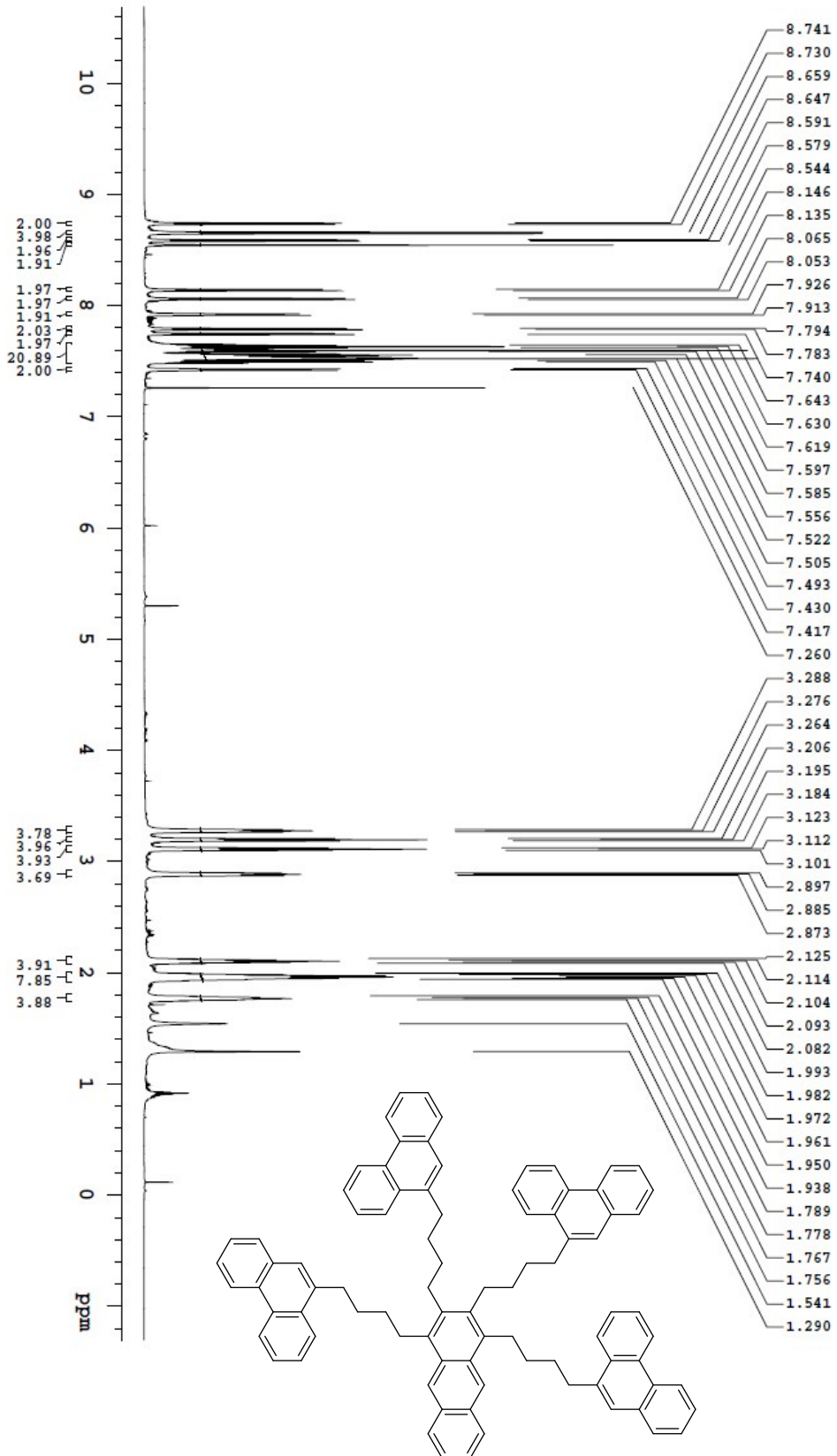
Recorded on: **V700, Jun 24 2020**  
Pulse Sequence: **PRESAT**

Sweep Width(Hz): **8389.26**  
Digital Res.(Hz/pt): **0.13**

Acquisition Time(s): **5**  
Hz per mm(Hz/mm): **34.95**

Relaxation Delay(s): **0.1**  
Completed Scans **8**

Yaowei, b2-p189  
699.762 MHz <sup>1</sup>H 1D in cdcl<sub>3</sub> (ref. to CDCl<sub>3</sub> @ 7.26 ppm)  
temp 27.5 C -> actual temp = 27.0 C, coldid probe



File: /mnt/d60/home14/jmsnm/rnmrdata/DATA\_FROM\_NMRSERVICE/awwei/2020.06/2020.06.24.v7\_b2-p189\_loc91\_10.31\_H1\_1D



# OpenVnmrj

Department of Chemistry, University of Alberta

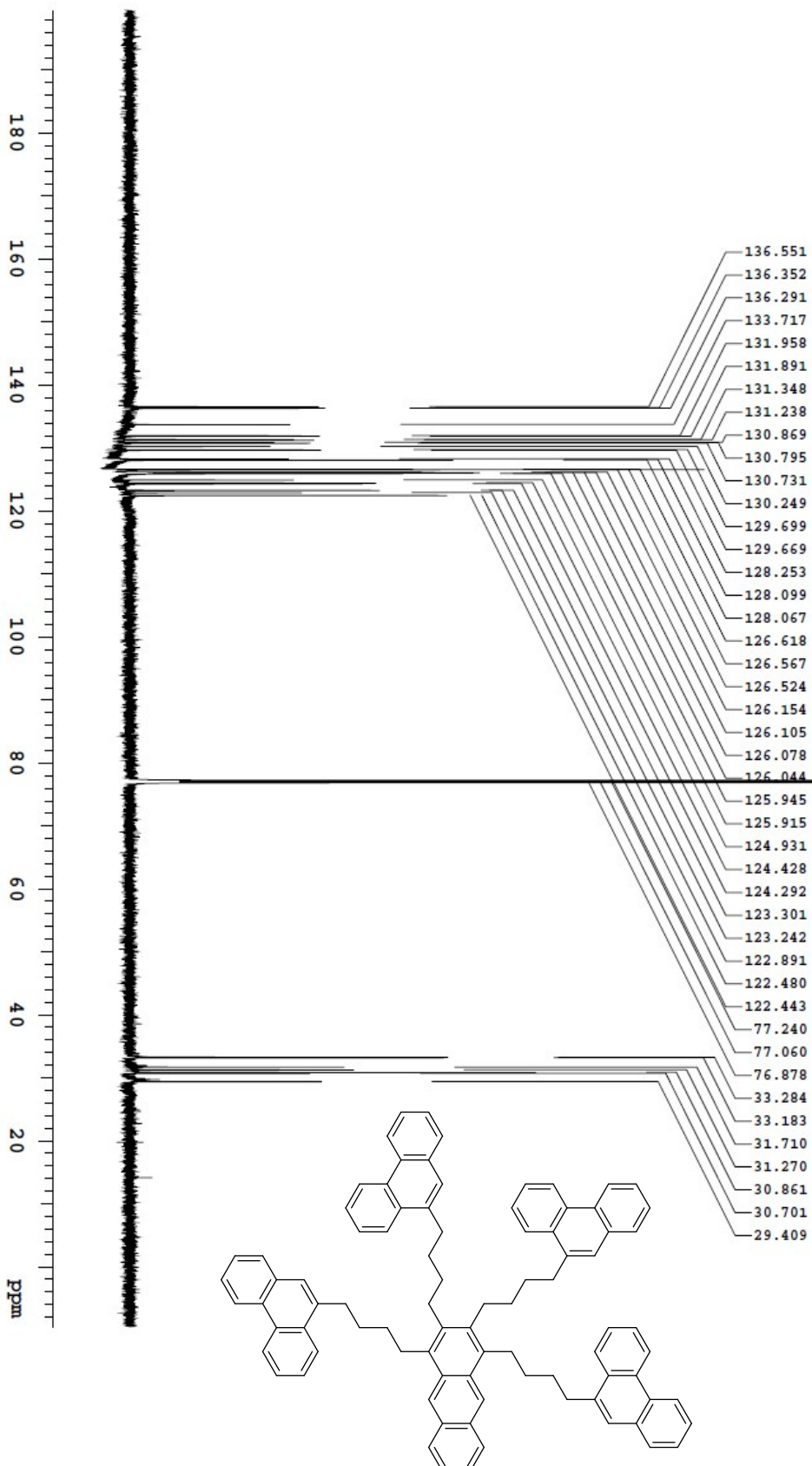
Recorded on: **V700, Jun 24 2020**  
Pulse Sequence: **s2pul**

Sweep Width(Hz): **36764.7**  
Digital Res.(Hz/p): **0.28**

Acquisition Time(s): **1**  
Hz per mm(Hz/mm): **153.19**

Relaxation Delay(s): **1**  
Completed Scans: **256**

Yaoxuei, h2-p189  
175.971 MHz C13(H1) 1D in cdcl3 (ref. to CDCB @ 77.06 ppm)  
temp 27.5 C -> actual temp = 27.0 C; coldid probe



File: /mnt/d60/home/14/mnmr/mnmr/data/DA1A\_FROM\_NMRSEVICE/Yaoxuei/2020.06/2020.06.24.V7\_h2-p189\_loc9\_1\_10.32\_C13\_1D

# OpenVnmrj

Department of Chemistry, University of Alberta

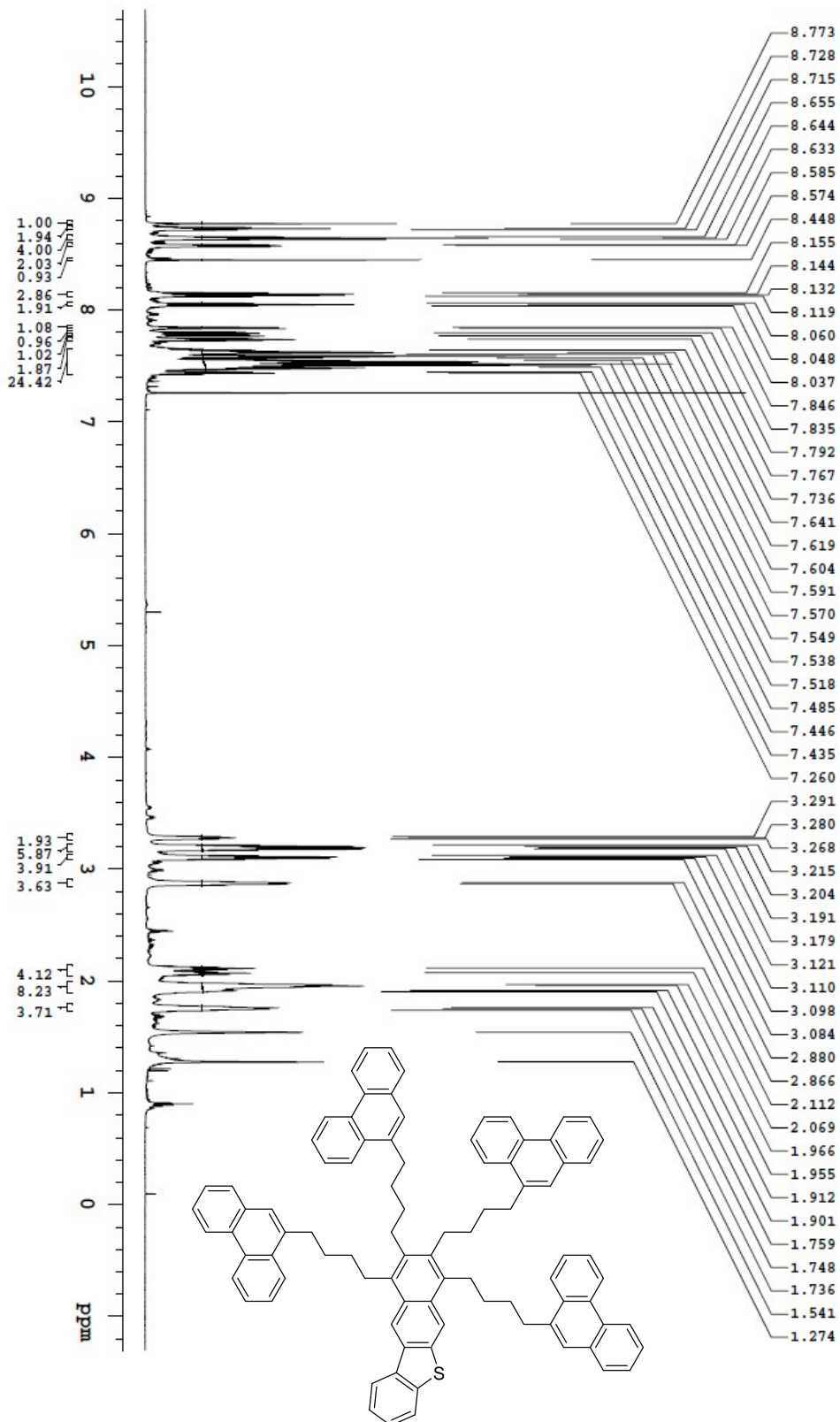
Recorded on: **0700\_Jul 28 2021**  
Pulse Sequence: **PRESAT**

Sweep Width(Hz): **6389.26**  
Digital Res. (Hz/p): **0.13**

Acquisition Time(s): **5**  
Hz per mm(Hz/mm): **34.96**

Relaxation Delay(s): **0.1**  
Completed Scans: **8**

Yaowei\_b2-p87  
698.762 MHz H1 1D in cdcl3 (ref. to CDCl3 @ 7.26 ppm)  
temp 27.5 C -> actual temp = 27.0 C, coldid probe



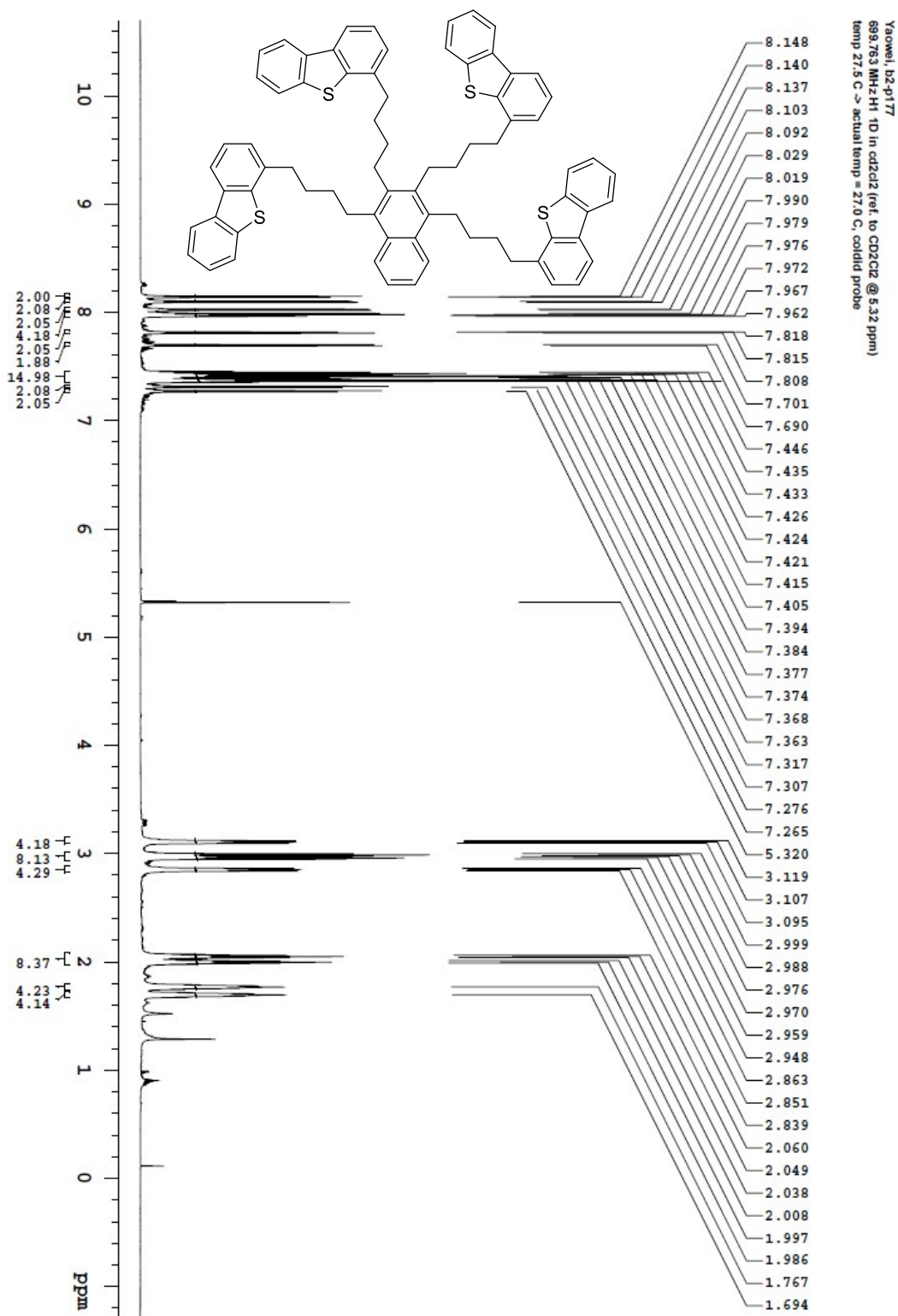
File: /mnt/600/home/14/jnsnmr/mvdata/DATA\_FROM\_NMRSERVICE/yaowei/2021.07/2021.07.28.VI\_b2-p87\_joc37\_20.02.H1\_1D

Relaxation Delay(s): **1**  
Completed Scans **128**

Chemical structure of compound 10 is shown below the spectrum. The structure is a complex polycyclic aromatic hydrocarbon (PAH) derivative, featuring a central benzene ring substituted with a thiophene group, a naphthalen-1-ylmethyl group, and a 2-(naphthalen-1-yl)ethyl group.

254

# 1,2,3,4-Tetra[4-(4-dibenzothiophene)butyl]naphthalene (278)



File: /mnt/d60/home/14/mrsmr/mrdata/14\_FROM\_NMRSEVIC/ET/2021.09/2021.09.07/V7\_D2-p177\_10c37\_20.03\_H1\_1D

OpenVnmrj

Department of Chemistry, University of Alberta

Recorded on: **v700, Sep 7 2021**  
Pulse Sequence: **PRESAT**

Sweep Width(Hz): **8389.26**  
Digital Res. (Hz/Pt): **0.13**

Acquisition Time(s): **5**  
Hz per mm(Hz/mm): **34.95**

Relaxation Delay(s): **0.1**  
Completed Scans: **8**



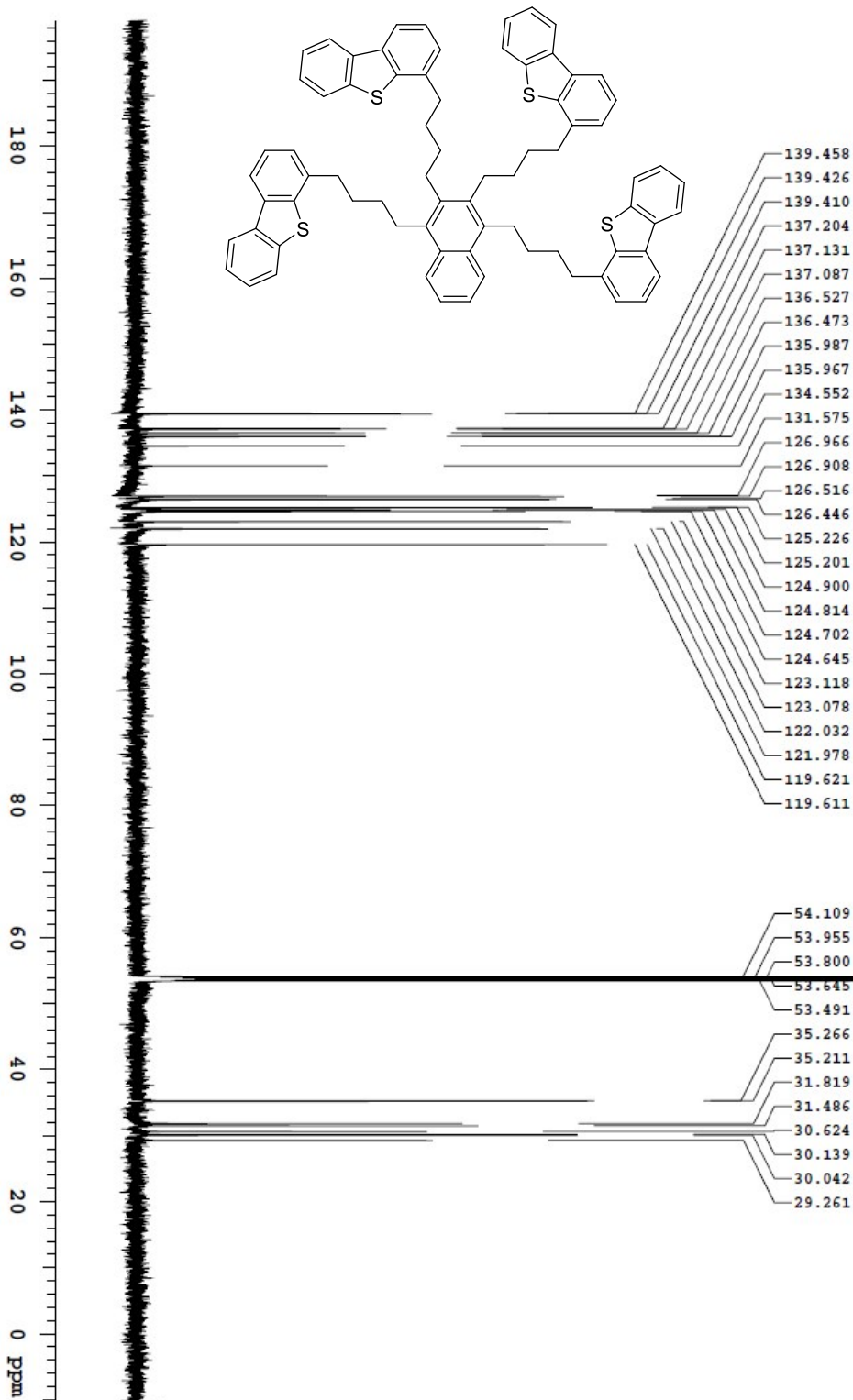
## OpenVnmrj

Recorded on: **V700, Sep 7 2021**  
Pulse Sequence: **szpul**  
Sweep Width(Hz): **46296.3**  
Digital Res.(Hz/p): **0.35**

Acquisition Time(s): **1**  
Hz per mm(Hz/mm): **153.99**

Relaxation Delay(s): **1**  
Completed Scans: **128**

Yaowei, h2-p177  
175.976 MHz C13{H1} 1D in cdd2d2 (ref. to CD2Cl2 @ 53.8 ppm)  
temp 27.5 C -> actual temp = 27.0 C, coldid probe



File: /mnt/d50/home14/jmsnmr/nmrdata/DATA\_FROM\_NMRSEVICE/yaowei2021.09/2021.09.07.v7\_h2-p177\_10037\_20.04\_C13\_1D

# OpenVnmrj

Department of Chemistry, University of Alberta

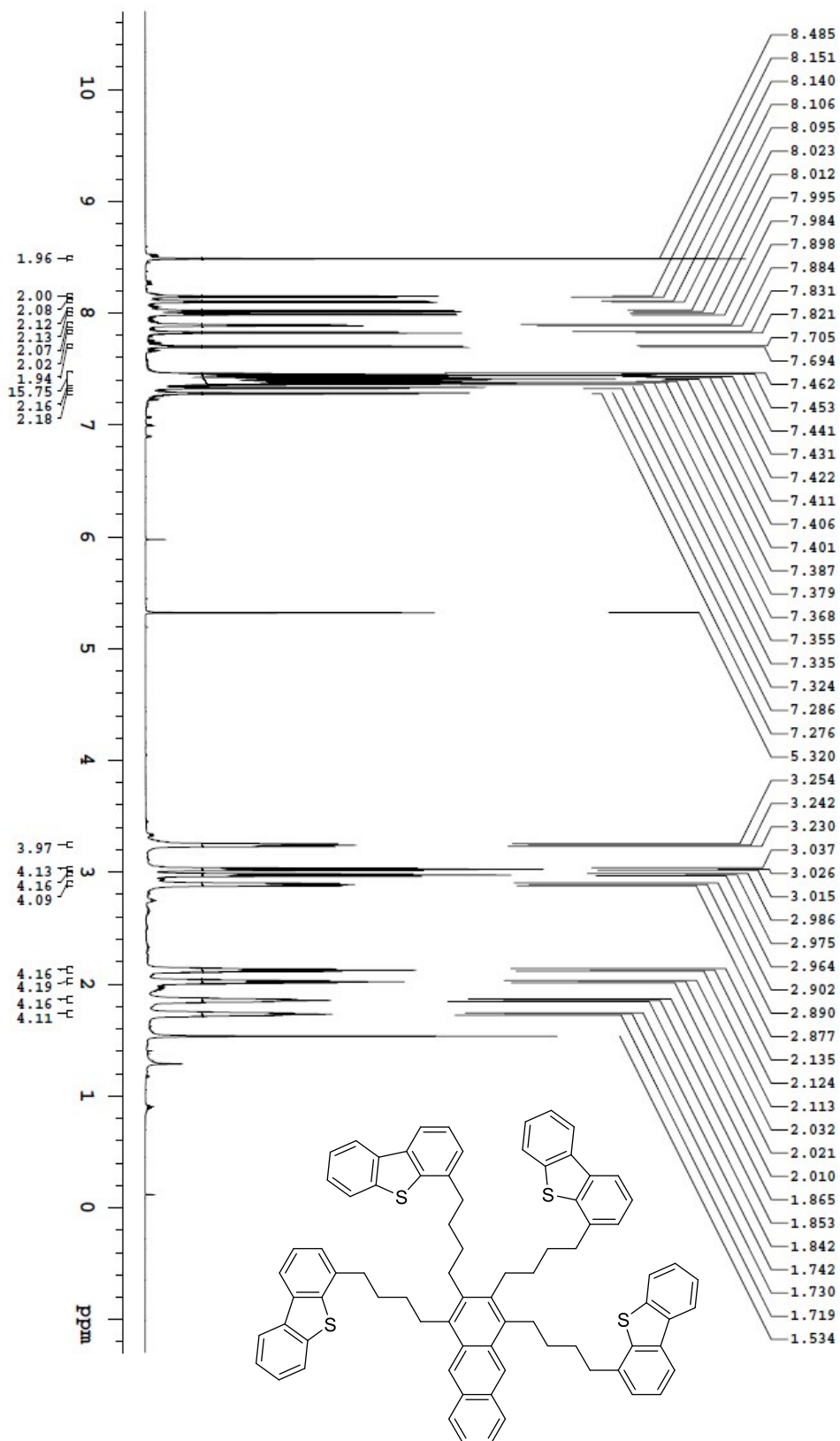
Recorded on: 07/00, Jul 28 2021  
Pulse Sequence: PRESAT

Sweep Width(Hz): 6389.26  
Digital Res. (Hz/pp): 0.13

Acquisition Time(s): 5  
Hz per nmh(Hz/nm): 34.96

Relaxation Delay(s): 0.1  
Completed Scans: 8

Yaowei\_b2-p183  
698.763 MHz H1 1D in cd2cl2 (ref. to CD2Cl2 @ 5.32 ppm)  
temp 27.5 C -> actual temp = 27.0 C, coldid probe

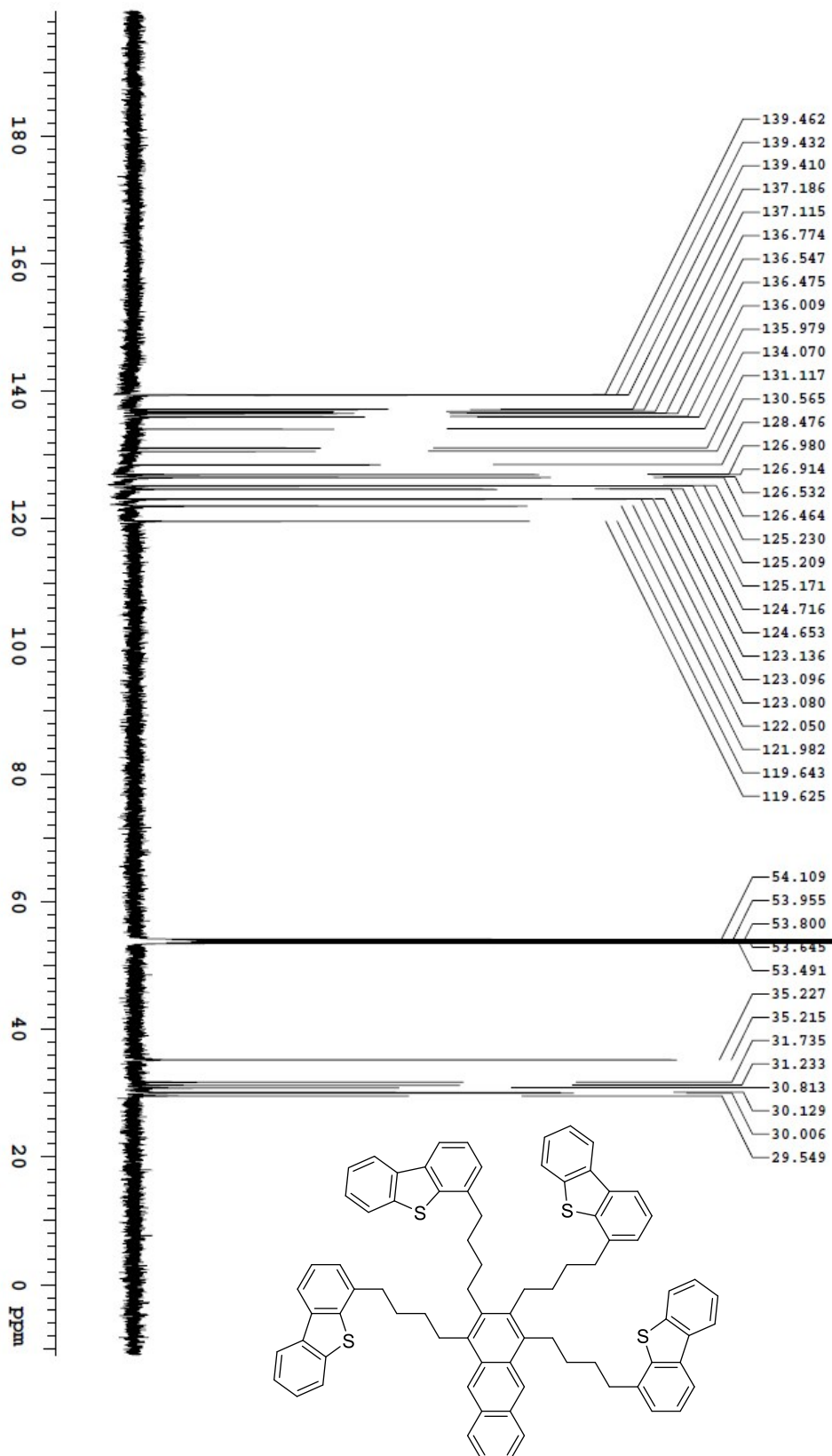


# OpenVnmrj

Department of Chemistry, University of Alberta

Recorded on: **v700, Jul 28 2021** Sweep Width(Hz): **46296.3** Acquisition Time(s): **1** Relaxation Delay(s): **1**  
 Pulse Sequence: **s2pul** Digital Res. (Hz/pt): **0.35** Hz per mm(Hz/mm): **154.42** Completed Scans: **128**

Yaowei, b2-p183  
 175.976 MHz C13{H} 1D in cd2cl2 (ref. to CDCl3 @ 53.8 ppm)  
 temp 27.5 C -> actual temp = 27.0 C, coldid probe



File: /mnt/d60/home/14/jmsm/rmr/delta/DA\_1\_FROM\_NMRSERVICE/yaowei/2021\_07/2021\_07\_28/v7\_b2-p183\_boc38\_20.55\_C13\_1D

# OpenVnmrj

Department of Chemistry, University of Alberta

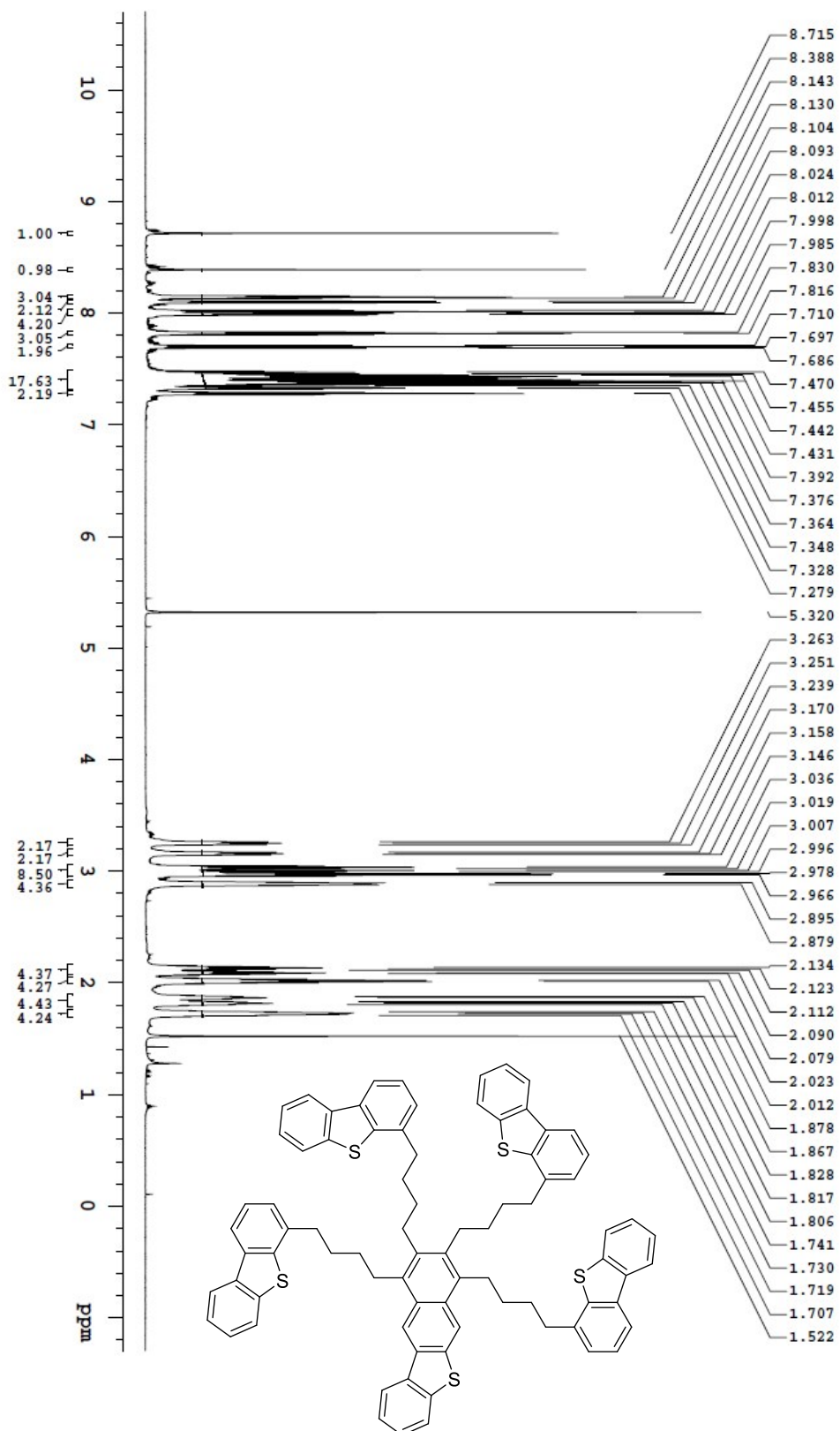
Recorded on: **V700, Aug 10 2024**  
Pulse Sequence: **PRESAT**

Sweep Width(Hz): 8389.26  
Digital Res.(Hz/pl): 0.13

Acquisition Time(s): **5**  
Hz per mm(Hz/mm): **34.95**

Relaxation Delay(s): **0.1**  
Completed Scans **8**

Yaowei, b2-p179  
699.763 MHz  $^1\text{H}$  1D in cd2cl2 (ref. to CD2Cl2 @ 5.32 ppm)  
temp 27.5 C  $\rightarrow$  actual temp = 27.0 C, coldid probe



File: /mnt/d600/home14/jmsnm/rmmdata/DATA\_FROM\_NIMRSERVICE/powell/2021.08/2021.08.10.v7\_b2-p179\_loc37\_20.02\_H1\_1D



# OpenVnmrj

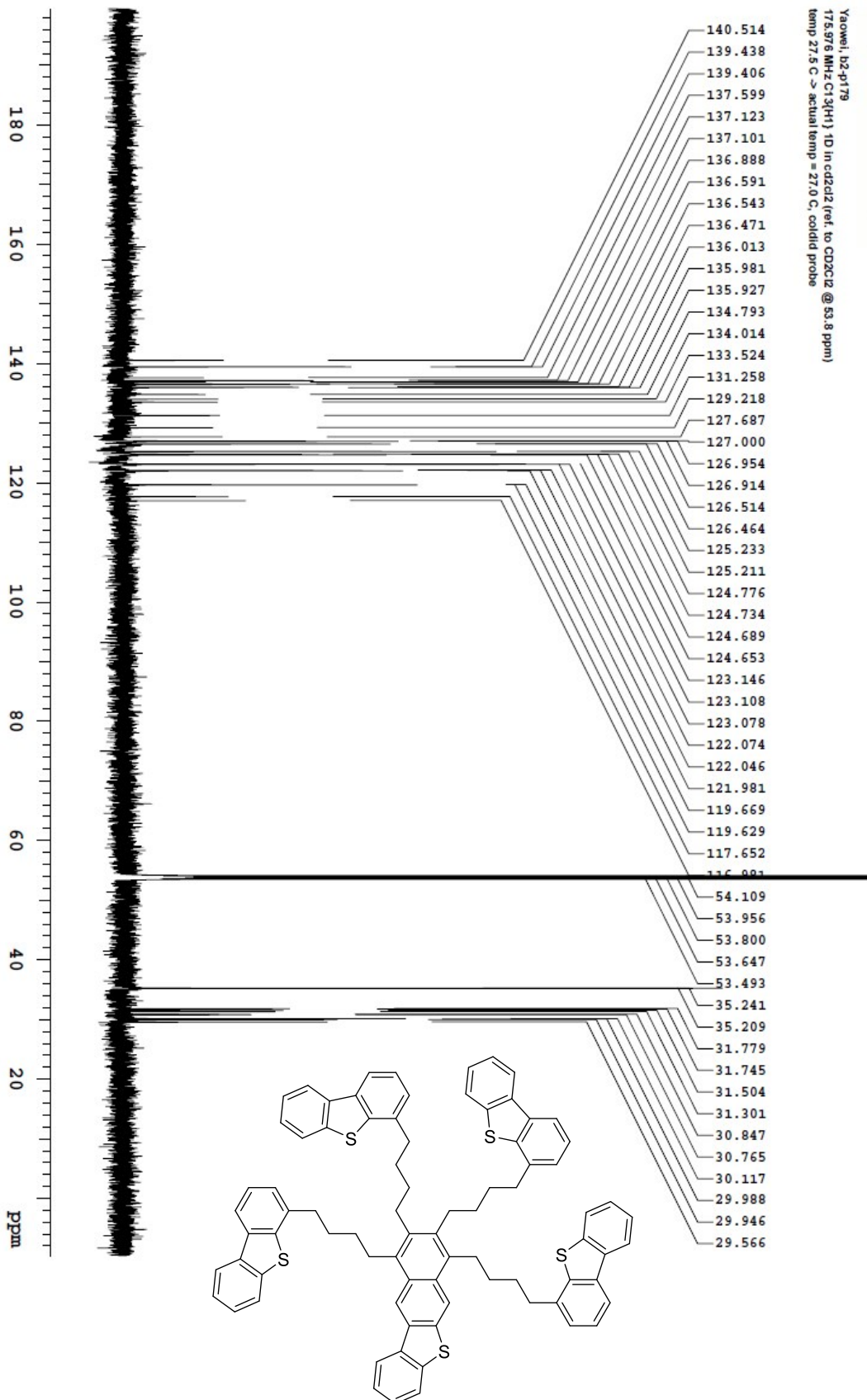
Department of Chemistry, University of Alberta

Recorded on: **V700, Aug 10 2021** Sweep Width(Hz): **46296.3**  
Pulse Sequence: **s2pul** Digital Res. (Hz/pp): **0.35**

Acquisition Time(s): **1**  
Hz per nm(Hz/mm): **153.29**

Relaxation Delay(s): **1**  
Completed Scans: **128**

Yaowei, b2-p179  
175.576 MHz C13(H1) 1D in cd2cl2 (ref. to CDCl3 @ 53.8 ppm)  
temp 27.5 C -> actual temp = 27.0 C, coldid probe



File: /mnt/d600/home/14j/mnmr/mnmrdata/DATA\_FROM\_NMRSERVICE/yaowe/2021.08/2021.08.10.v7\_b2-p179\_loc37\_20.03\_C13\_1D

# OpenVmrj

Yaowei, D3-p91  
699.762 MHz H1 1D in cdCl<sub>3</sub> (ref. to CDCl<sub>3</sub> @ 7.26 ppm)  
temp 27.5 C -> actual temp = 27.0 C, coldid probe

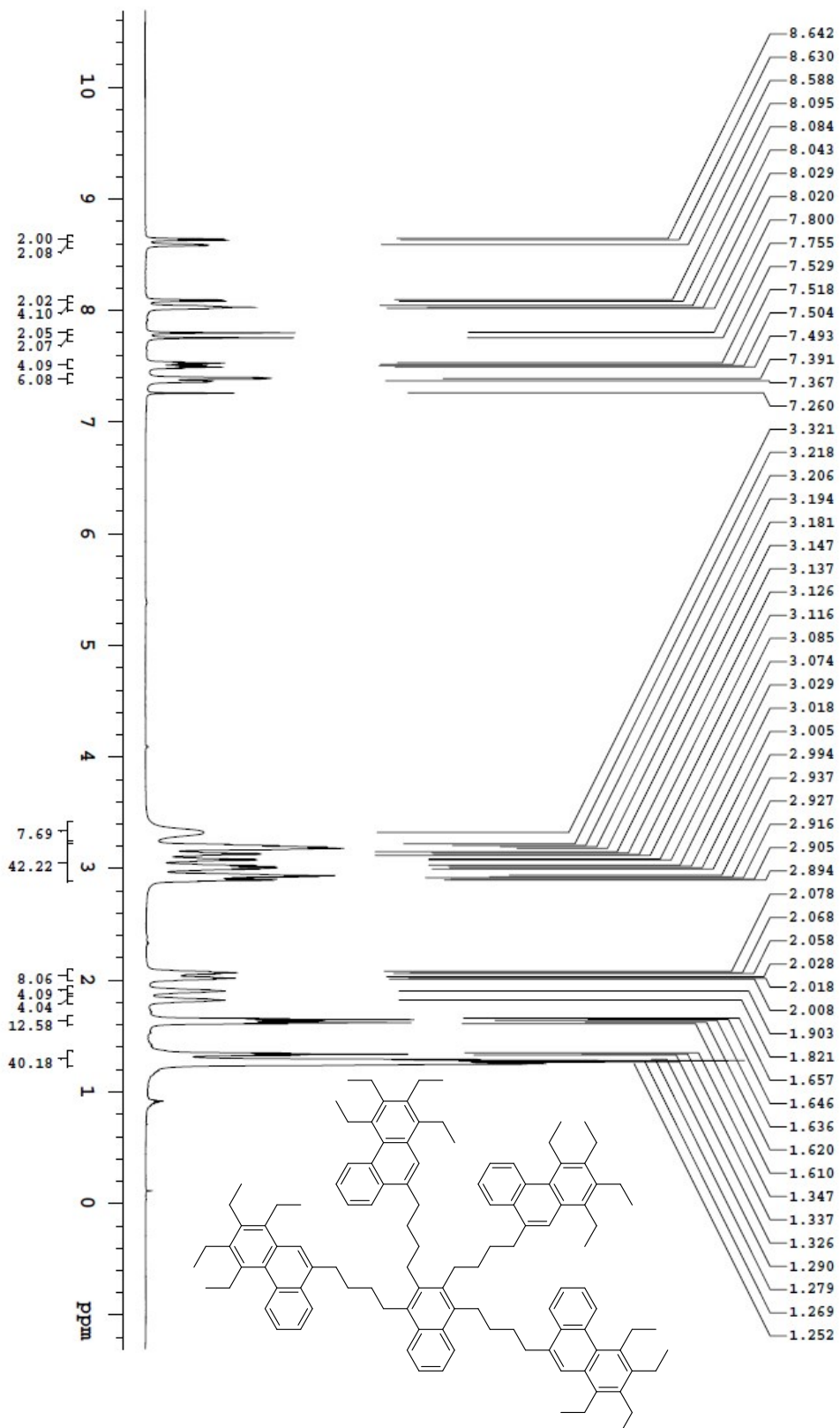
Department of Chemistry, University of Alberta

Recorded on: **V700, Feb 27 2021**  
Pulse Sequence: **PRESAT**

Sweep Width(Hz): 8389.26  
Digital Res.(Hz/pl): 0.13

Acquisition Time(s): **5**  
Hz per mm(Hz/mm): **34.95**

Relaxation Delay(s): **0.1**  
Completed Scans **8**



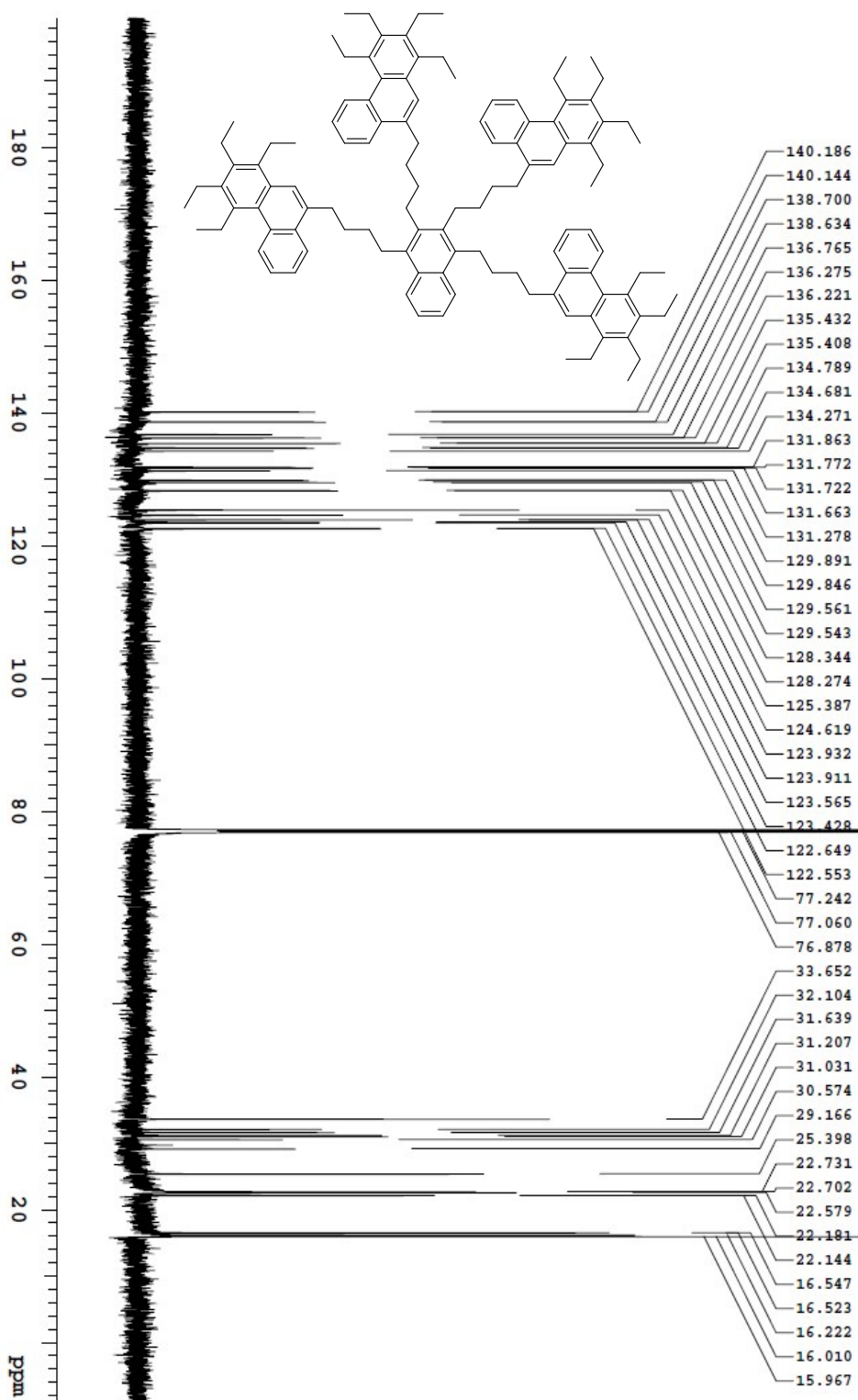
File: /mnt/d600/home14/jfmsnm/rmrdata/DATA\_FROM\_NIMRSERVICE/aowei2021.02/2021.02.27.v7\_b3-p91\_loc37\_12.55\_H1\_1D

# OpenVnmrj

Department of Chemistry, University of Alberta

|                                       |                                   |                                 |                               |
|---------------------------------------|-----------------------------------|---------------------------------|-------------------------------|
| Recorded on: <b>V700, Feb 27 2021</b> | Sweep Width(Hz): <b>36764.7</b>   | Acquisition Time(s): <b>1</b>   | Relaxation Delay(s): <b>1</b> |
| Pulse Sequence: <b>s2pul</b>          | Digital Res. (Hz/pt): <b>0.28</b> | Hz per mm(Hz/mm): <b>153.19</b> | Completed Scans: <b>128</b>   |

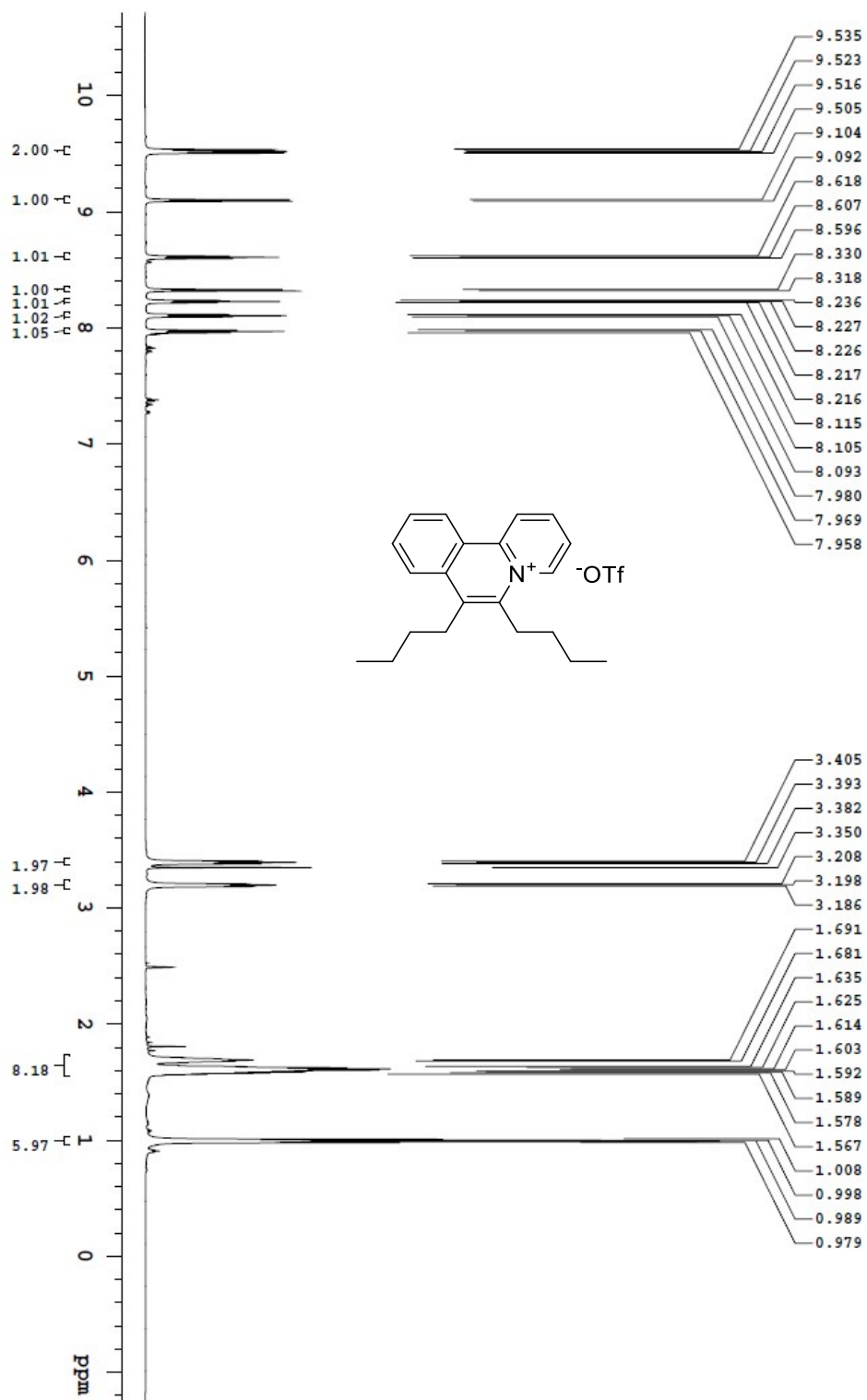
Yaowei, b3-p91  
 175.971 MHz C13(H1) 1D in cdcl3 (ref. to CDCl3 @ 77.06 ppm)  
 temp 27.5 C -> actual temp = 27.0 C, coldid probe



File: /mnt/d00/home/44/mnmr/mnt/data/TA\_FROM\_NMRSERVICE/yaowei/2021.02/2021.02.27.V7\_b3-p91\_joc57\_1256\_C13\_1D

Recorded on: **V700, Sep 3 2021**  
Pulse Sequence: **PRESAT**Sweep Width(Hz): **8389.28**  
Digital Res. (Hz/p): **0.13**Acquisition Time(s): **5**  
Hz per mm(Hz/mm): **34.95**Relaxation Delay(s): **0.1**  
Completed Scans: **8**

Yaoxuei, b2-p165

699.765 MHz <sup>1</sup>H 1D in dmsol (ref. to DMSO @ 2.49 ppm)  
temp 27.5 C -> actual temp = 27.0 C, coldid probe

## OpenVnmrj

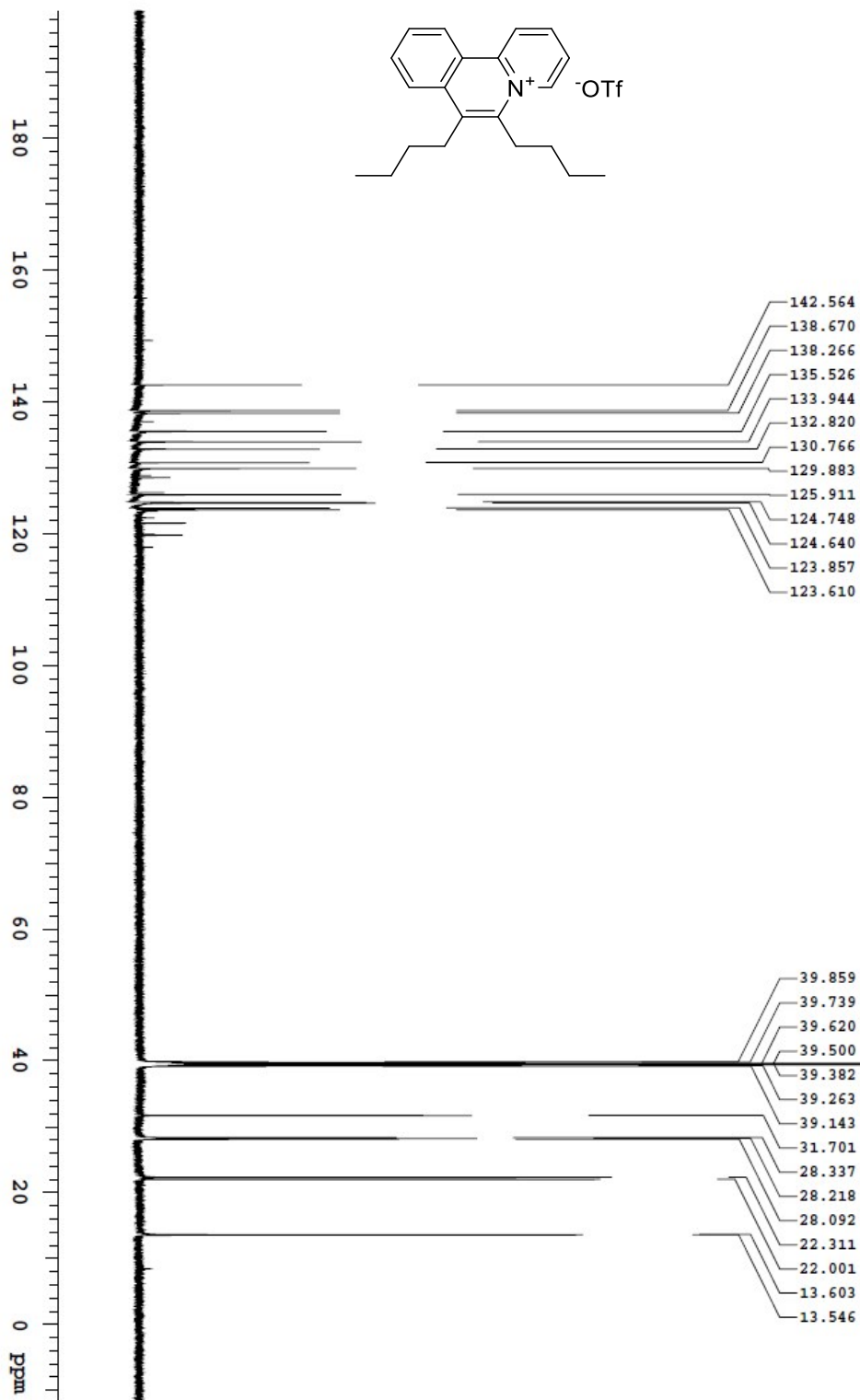
Recorded on: **VT00\_Sep 3 2021**  
Pulse Sequence: **s2pul**

Sweep Width(Hz): **46296.3**  
Digital Res (Hz/pt): **0.35**

Acquisition Time(s): **1**  
Hz per mm(Hz/mm): **154.87**

Relaxation Delay(s): **1**  
Completed Scans: **128**

Yaoweil\_b2-p165  
175.876 MHz C13(H1) 1D in dmsol (ref. to DMSO @ 39.5 ppm)  
temp 27.5 C -> actual temp = 27.0 C, coldid probe

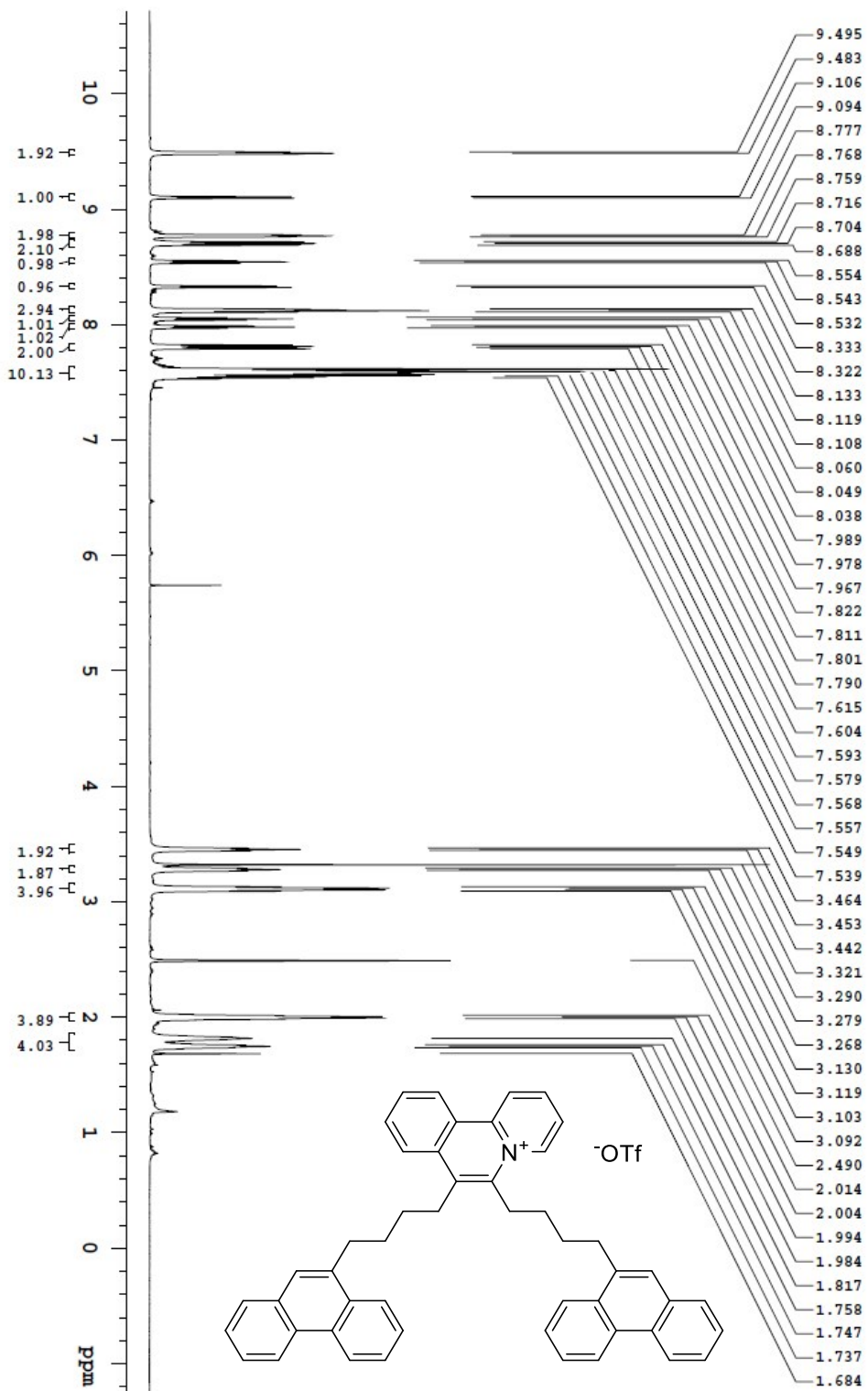


File: /mnt/d600/home/14j/mnmr/mnrdata/DA7A\_FROM\_NMRSERVICE/yaoweil/2021\_09/2021\_09\_03\_v7\_b2-p165\_lox37\_20\_13\_C13\_1D



6,7-Di[4-(9-phenanthrene)butyl]benzo[*a*]quinolizinium trifluoromethanesulfonate (359)

File: /mnt/d60/home/14/jmsm/mrdata/DAI\_FROM\_NMRSERVICE/aoew/2021.11/2021.11.22/V7\_b2-p169\_boc31\_16\_17\_H1\_1D



Yaoewi, b2-p169  
693.765 MHz H1 1D in dmsd (ref. to DMSO @ 2.49 ppm)  
temp 27.5 C -> actual temp = 27.0 C, coldid probe

OpenVnmrj

Department of Chemistry, University of Alberta

Recorded on: V700, Nov 22 2021  
Pulse Sequence: PRESAT

Sweep Width(Hz): 8389.26  
Digital Res. (Hz/pt): 0.13

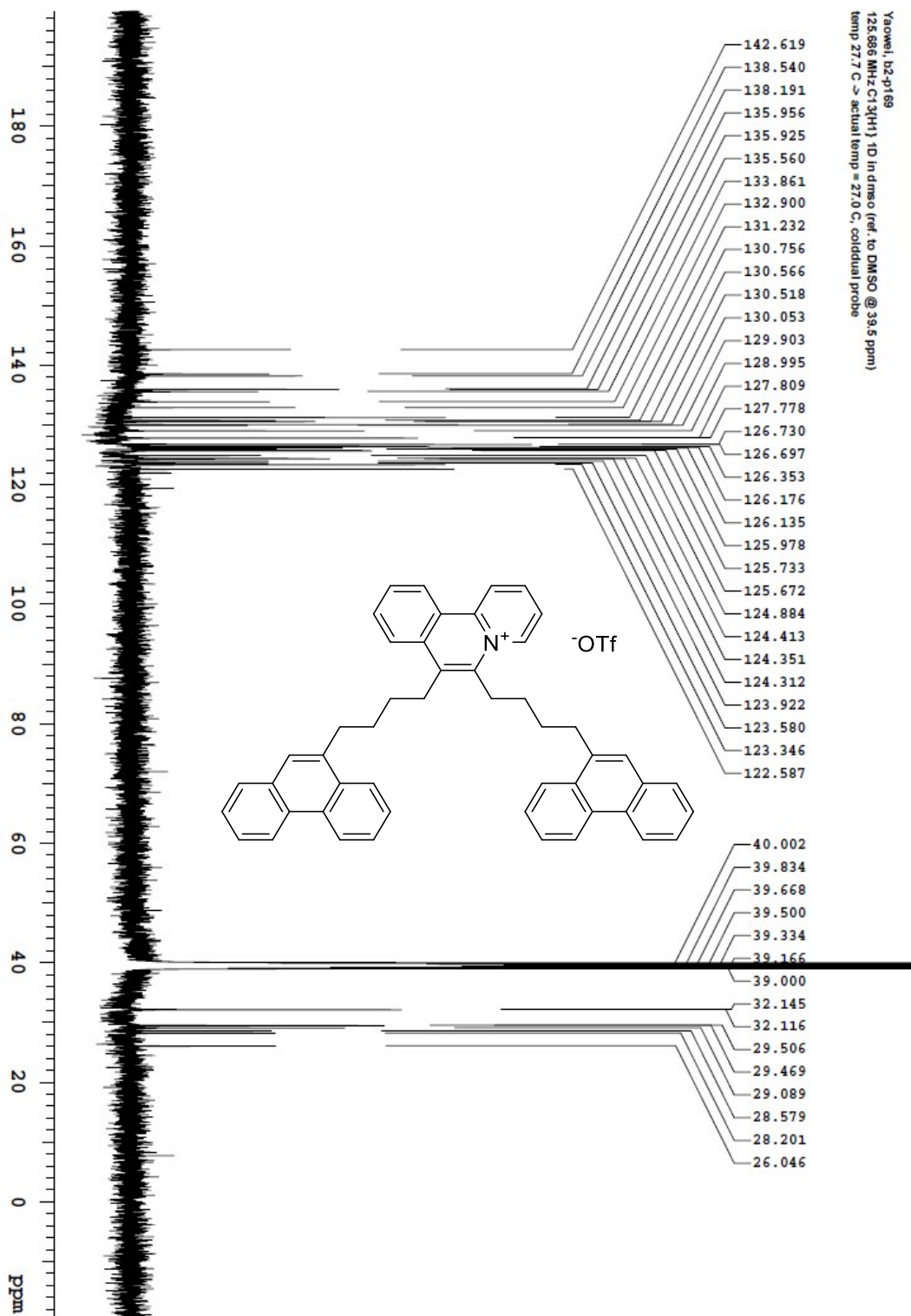
Acquisition Time(s): 5  
Hz per mHz(mHz): 34.95

Relaxation Delay(s): 0.1  
Completed Scans: 8

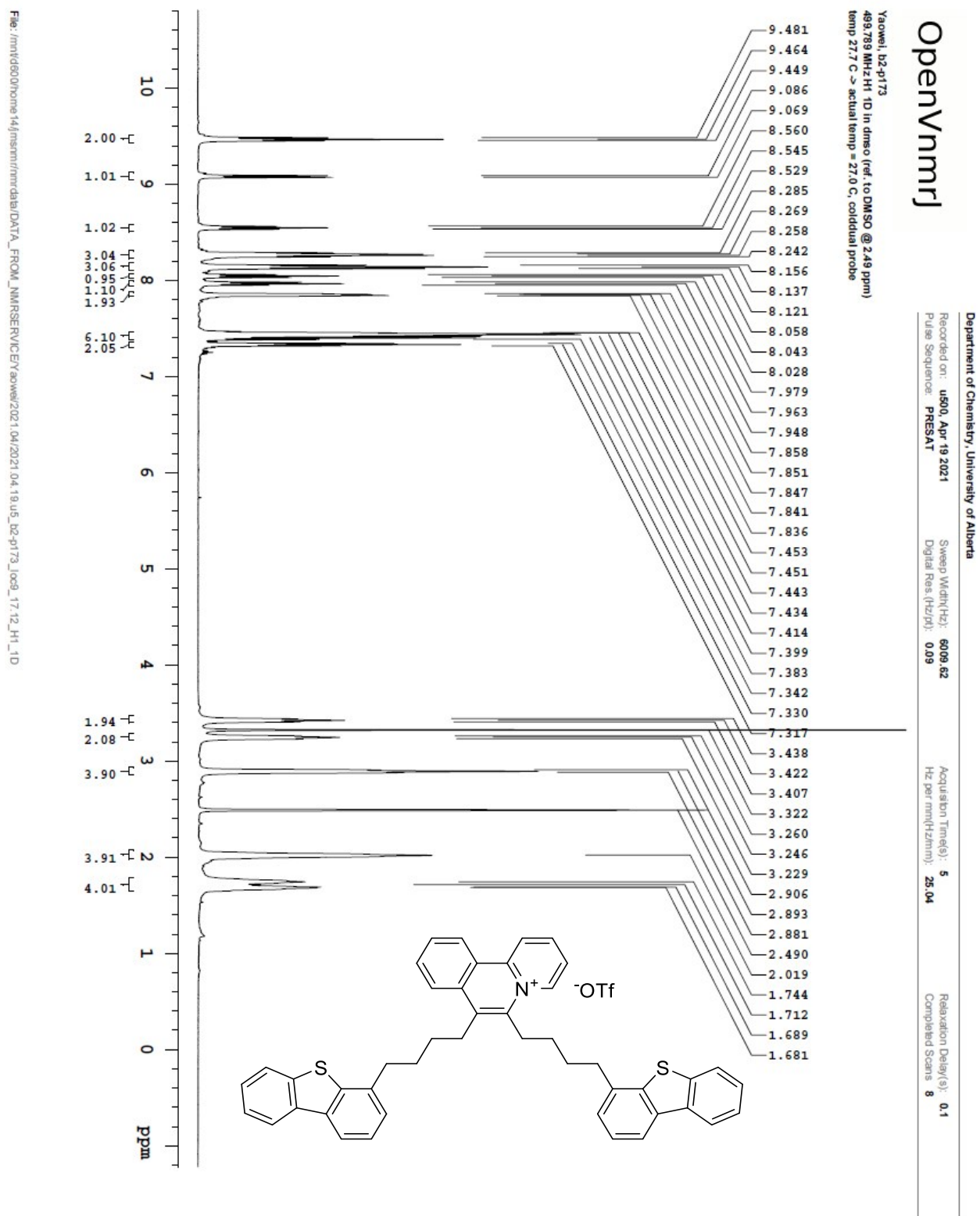
Recorded on: **u500, Nov 22 2021**  
Pulse Sequence: **s2pul**

Sweep Width(Hz): 33783.8  
Digital Res.(Hz/pt): 0.26

Acquisition Time(s): 1  
Hz per mm(Hz/mm): 114.85

Relaxation Delay(s): 1  
Completed Scans 84

6,7-Di[4-(4-dibenzothiophene)butyl]benzo[*a*]quinolizinium trifluoromethanesulfonate (360)



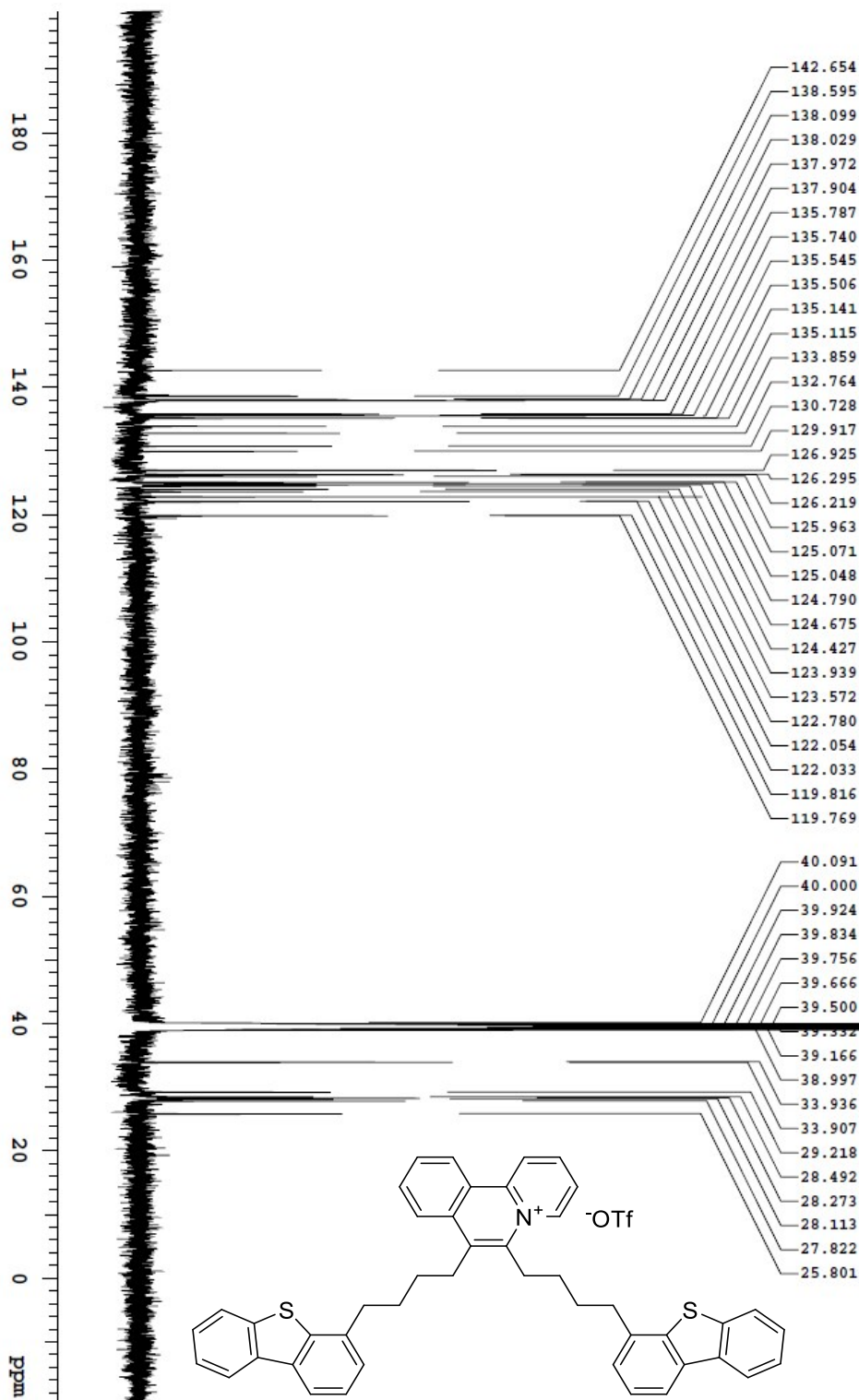


# OpenVnmrj

Department of Chemistry, University of Alberta

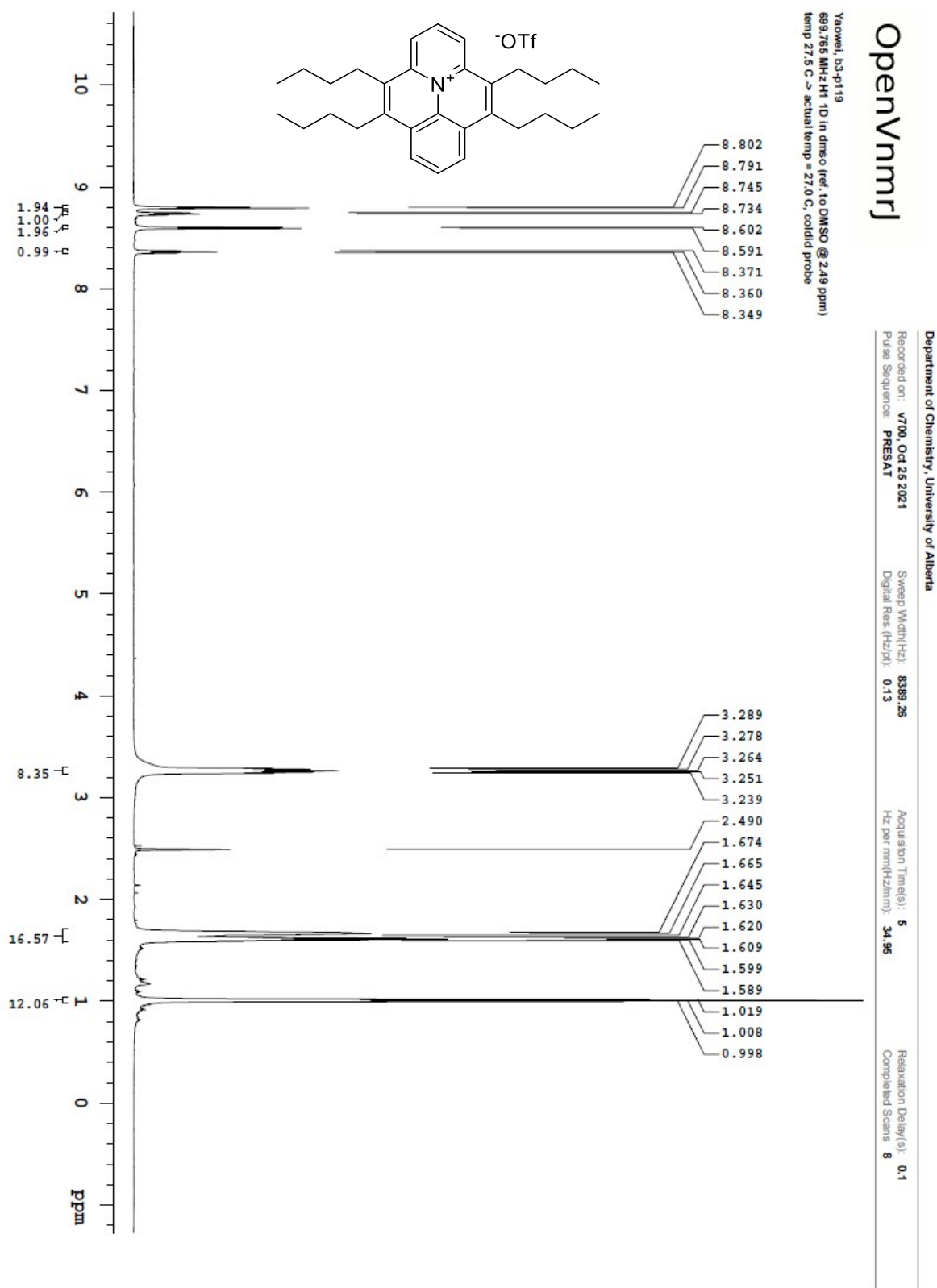
|                                       |                                   |                                 |                               |
|---------------------------------------|-----------------------------------|---------------------------------|-------------------------------|
| Recorded on: <b>us00, Apr 19 2021</b> | Sweep Width(Hz): <b>33783.8</b>   | Acquisition Time(s): <b>1</b>   | Relaxation Delay(s): <b>1</b> |
| Pulse Sequence: <b>s2pul</b>          | Digital Res. (Hz/pt): <b>0.26</b> | Hz per mm(Hz/mm): <b>114.76</b> | Completed Scans: <b>128</b>   |

Yaowei, b2-p173  
125.686 MHz C13{H1} 1D in dmso (ref. to DMSO @ 39.5 ppm)  
temp 27.7 C -> actual temp = 27.0 C, coldtial probe



File: /mnt/d600/home/14/jmsm/mrdata/DATA\_FROM\_NMRSERVICE/yaowei/2021.04.19.u5\_b2-p173\_loc9\_17.13\_C13\_1D

# 4,5,9,10-Tetrabutylbenzo[*ij*]pyrido[2,1,6-*de*]quinolizinium trifluoromethanesulfonate(365)

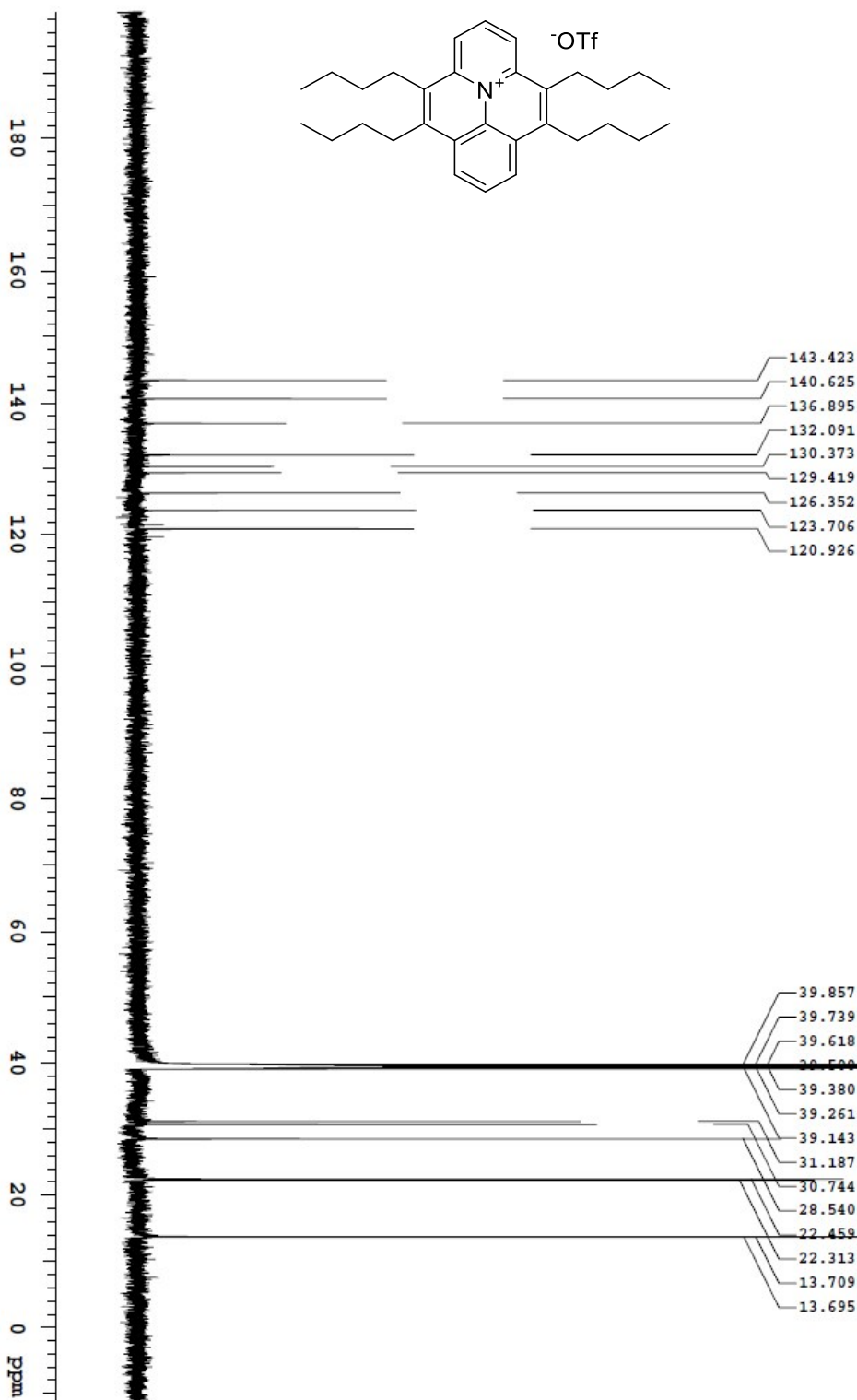
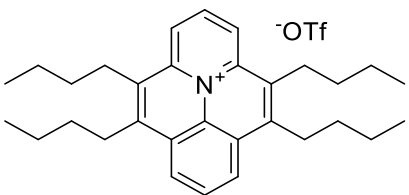


# OpenVnmrj

Department of Chemistry, University of Alberta

|                                       |                                   |                                |                               |
|---------------------------------------|-----------------------------------|--------------------------------|-------------------------------|
| Recorded on: <b>V700, Oct 25 2021</b> | Sweep Width(Hz): <b>46296.3</b>   | Acquisition Time(s): <b>1</b>  | Relaxation Delay(s): <b>1</b> |
| Pulse Sequence: <b>szpul</b>          | Digital Res. (Hz/pt): <b>0.35</b> | Fz per mm(12mm): <b>154.75</b> | Completed Scans: <b>128</b>   |

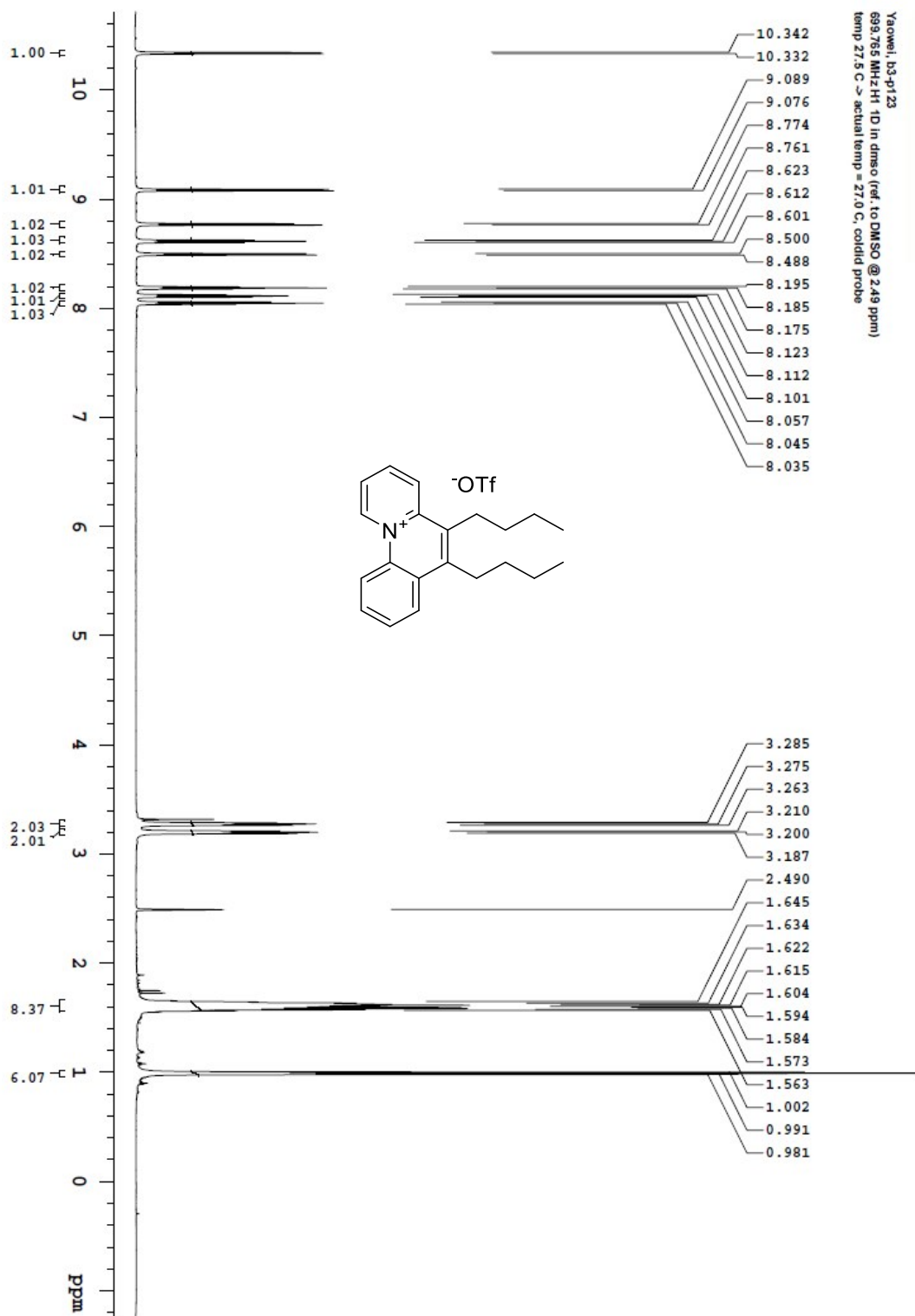
Yaowei, b3-p119  
175.976 MHz <sup>13</sup>C{<sup>1</sup>H} 1D in dmsol (ref. to DMSO @ 39.5 ppm)  
temp 27.5 C -> actual temp = 27.0 C, coldid probe



File: /mnt/d60/home14/mrnmr/data/1D/FROM\_NMRSE/RVIC/EYaowei/20211020/211025/v7\_b3-p119\_loc43\_2039\_C13\_1D

# 5,6-Dibutylbenzo[*c*]quinolizinium trifluoromethanesulfonate (366)

File: /mnt/ds00/home/14/jmsm/mr/data/TA\_FROM\_NMRSERVICE/2021.11/2021.11.02/VJ\_b3-p123\_boc43\_15.06\_H1\_1D



OpenVnmrj

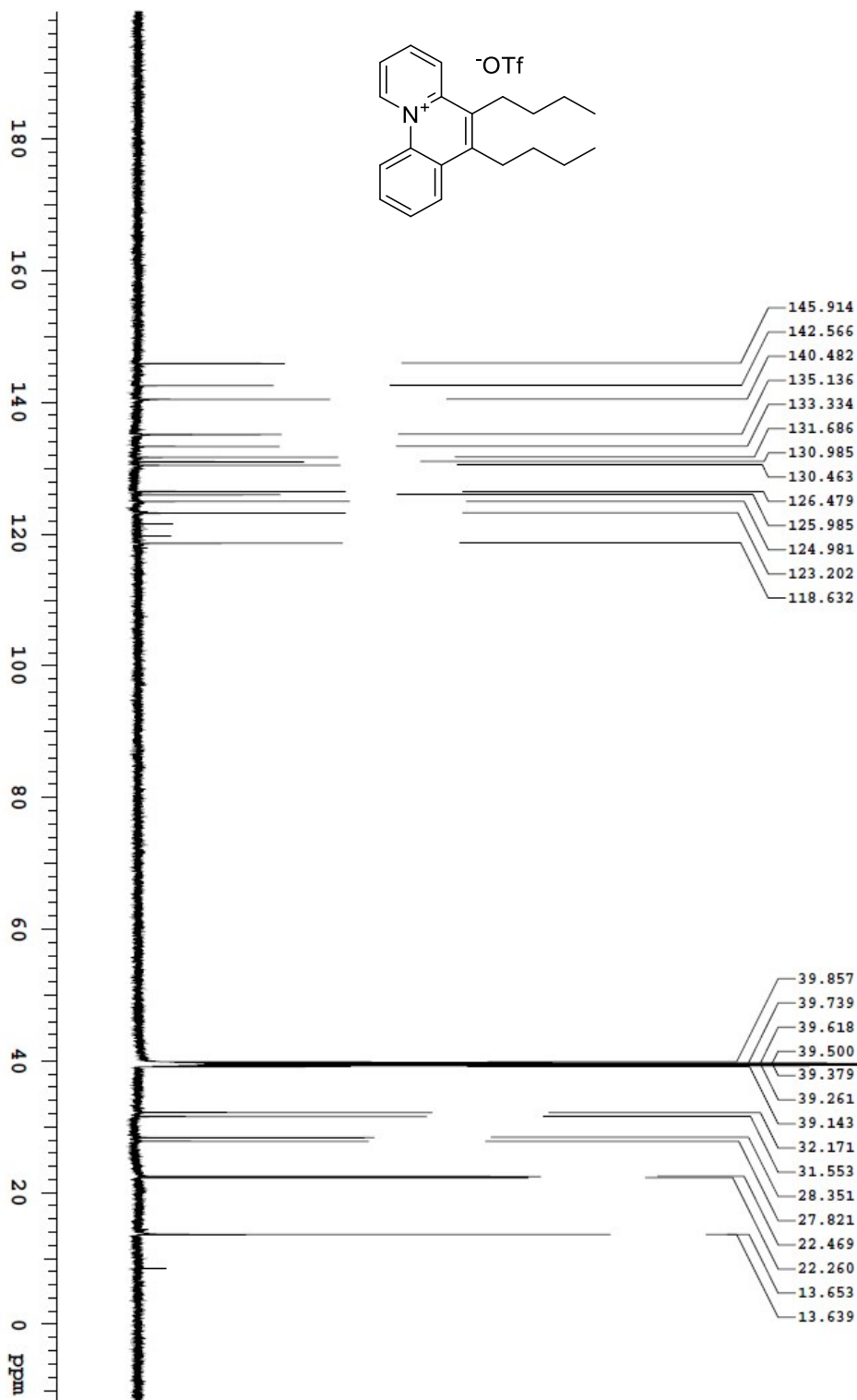
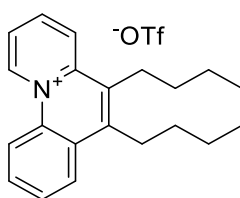
Department of Chemistry, University of Alberta  
Recorded on: **V700**, Nov 2 2021  
Pulse Sequence: **PRESAT**

Sweep Width(Hz): **8389.26**  
Digital Res.(Hz/p): **0.13**

Acquisition Time(s): **5**  
Hz per mm(Hz/mm): **34.95**

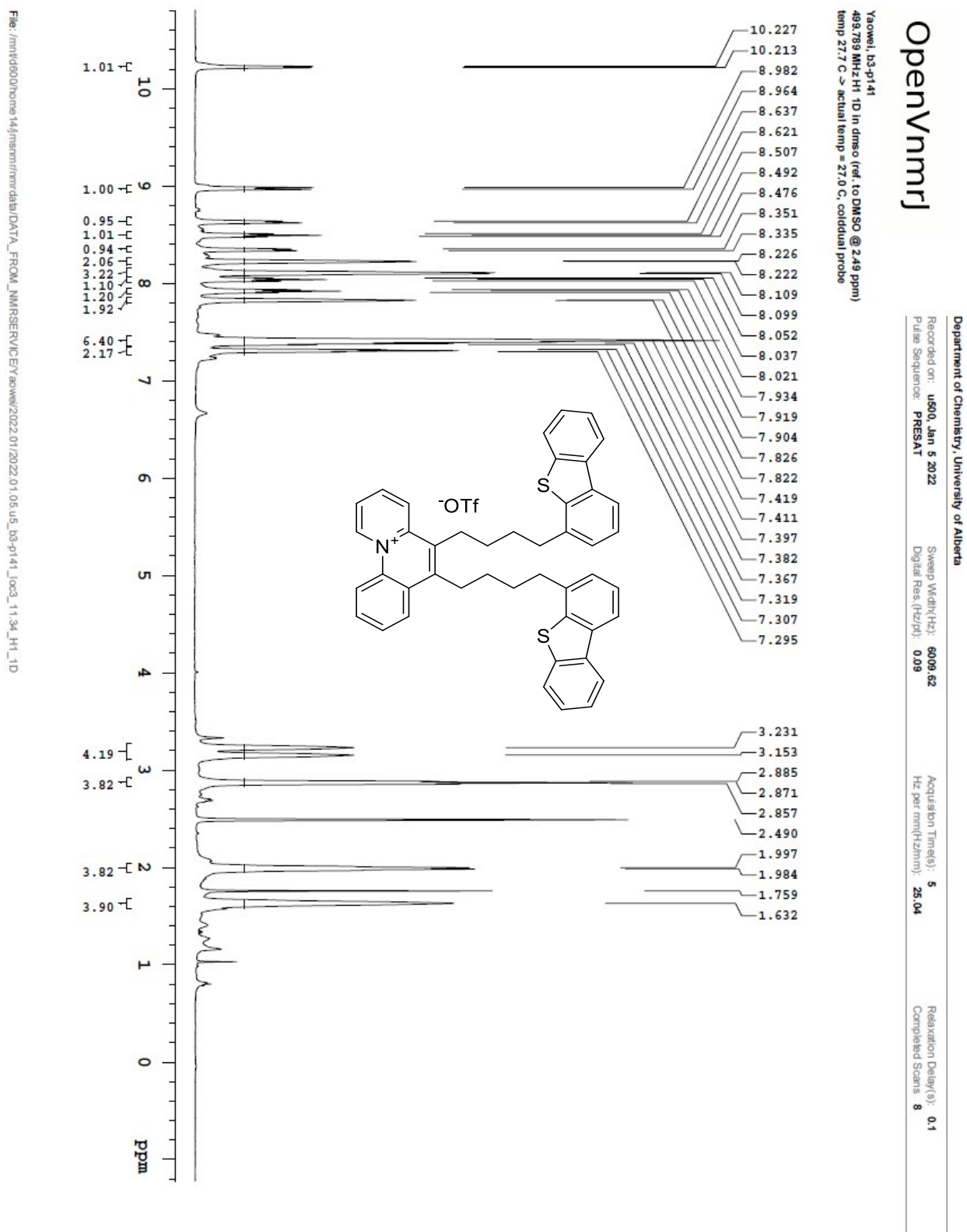
Relaxation Delay(s): **0.1**  
Completed Scans: **8**

Relaxation Delay(s): **1**  
Completed Scans **128**



File: /mnt/d600/home14/jmsnm/rmrdata/DATA\_FROM\_NMRSERVICE/apowe/2021.11/2021.11.02.v7\_b3-p123\_loc43\_15.07\_C13\_1D

# 5,6-Di[4-(4-dibenzothiophene)butyl]benzo[*c*]quinolizinium trifluoromethanesulfonate (380)





# OpenVnmrj

Department of Chemistry, University of Alberta

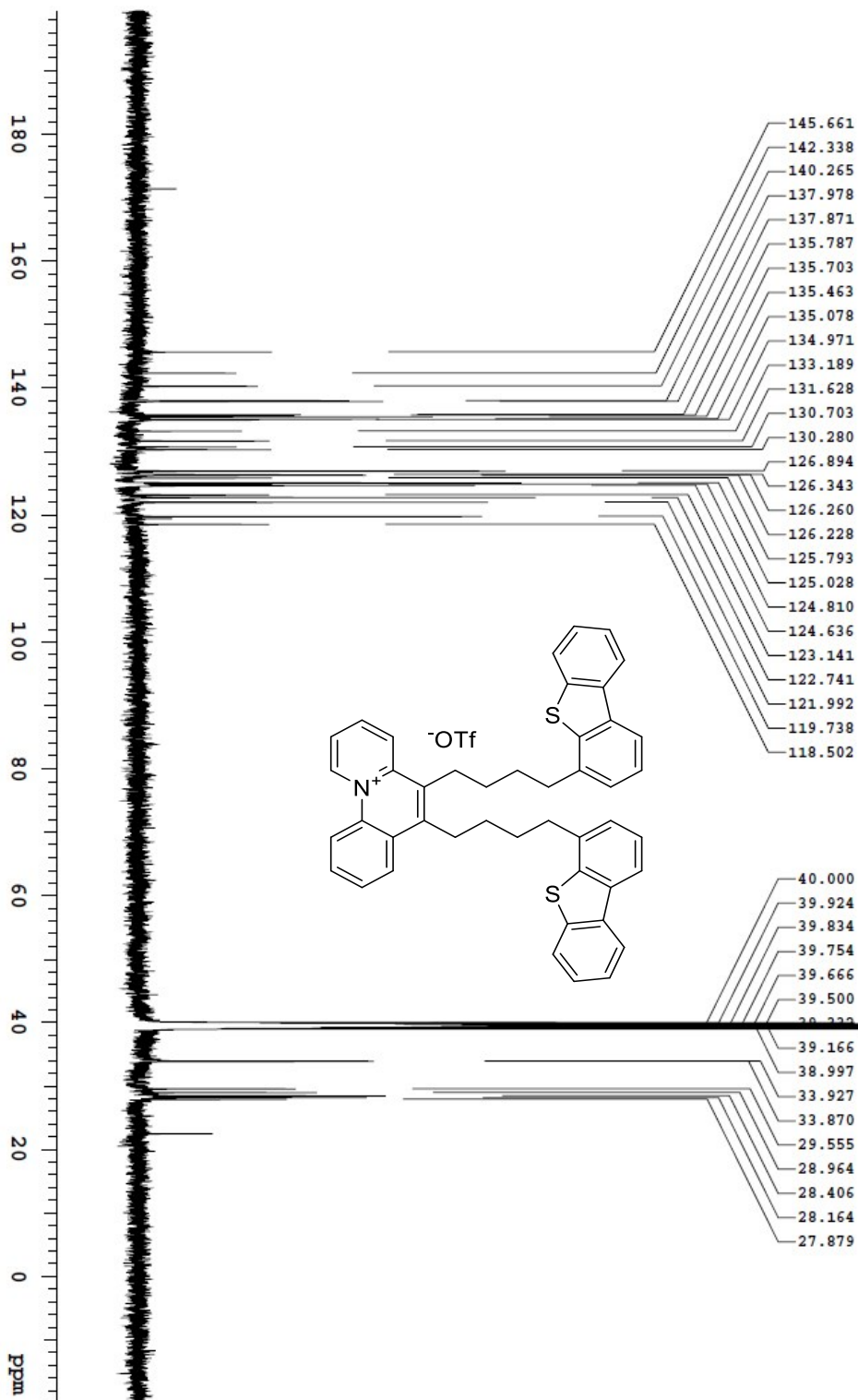
Recorded on: **u500, Jan 5 2022**  
Pulse Sequence: **s2pul**

Sweep Width(Hz): **33783.8**  
Digital Res.(Hz/D): **0.26**

Acquisition Time(s): **1**  
Hz per mm(Hz/mm): **114.94**

Relaxation Delay(s): **1**  
Completed Scans: **128**

Yaowei, b3-p14f  
125.686 MHz C13{H1} 1D in dmsd (ref. to DMSO @ 38.5 ppm)  
temp 27.7 C -> actual temp = 27.0 C, cold dual probe



File: /mnt/d500/home/44/msnmr/rrr/data/DA7A\_FROM\_JNMRSERVICE/202201/2022.01.05.u5\_b3-p14f\_joc3\_11.36\_C13\_1D

# OpenVmrj

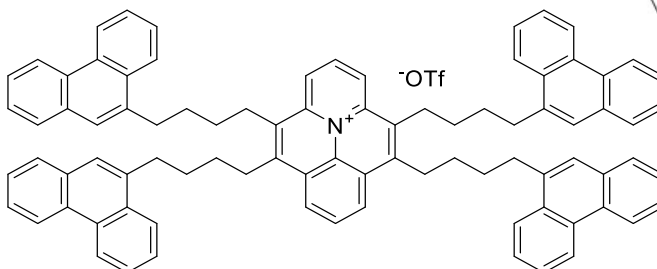
Recorded on: **V700, Nov 25 2021**  
Pulse Sequence: **PRESAT**

Sweep Width(Hz): 8389.26  
Digital Res.(Hz/pt): 0.13

Acquisition Time(s): **5**  
Hz per mm(Hz/mm): **34.95**

Relaxation Delay(s): 0.1  
Completed Scans 8

Yaowei, b3-p133  
699.765 MHz H1 1D in dmsO (ref. to DMSO @ 2.49 ppm)  
temp 27.5 C -> actual temp = 27.0 C, coldid probe

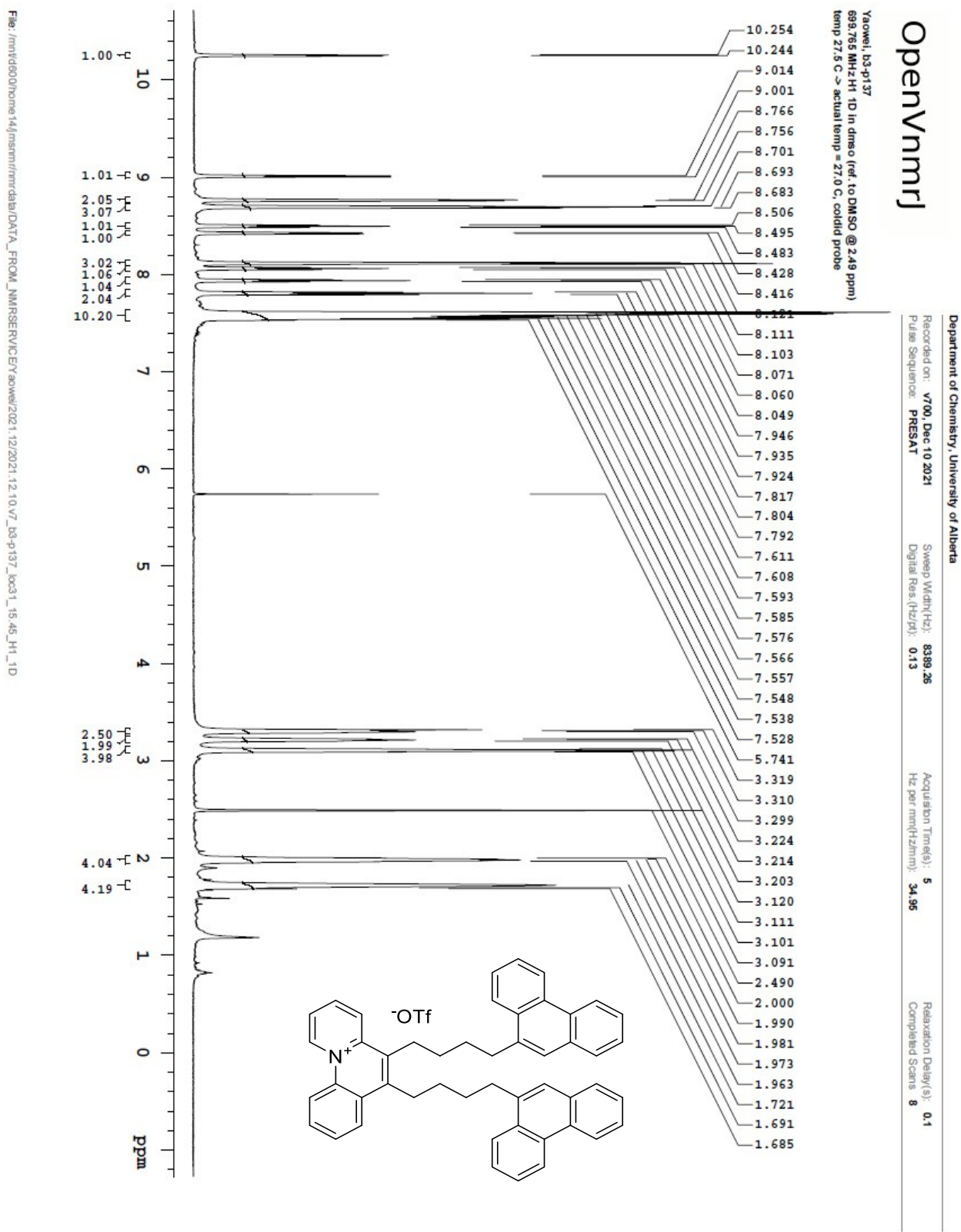




Relaxation Delay(s): **1**  
Completed Scans **128**



# 5,6-Di[4-(9-phenanthrene)butyl]benzo[c]quinolizinium trifluoromethanesulfonate (383)

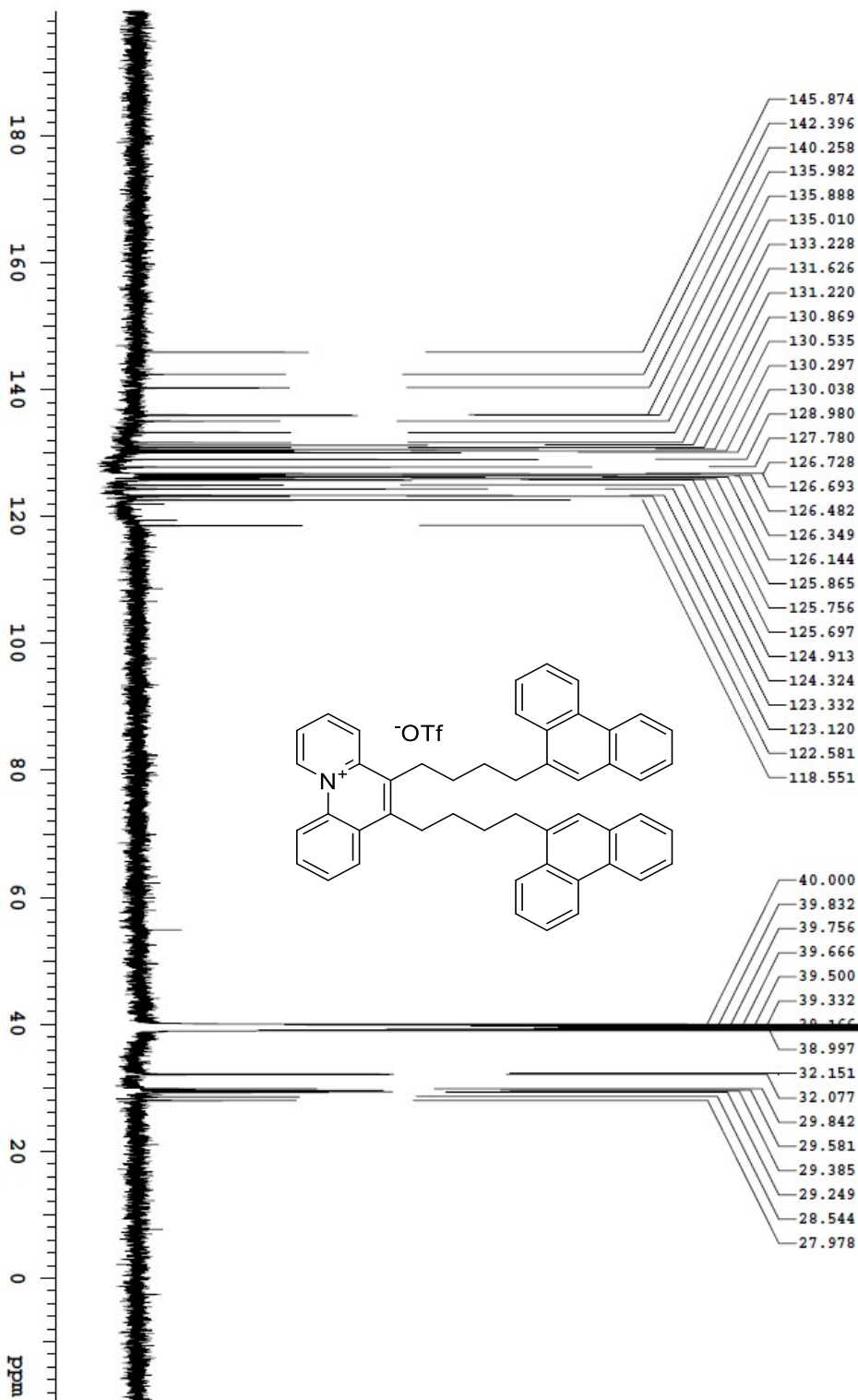


# OpenVnmrj

Department of Chemistry, University of Alberta

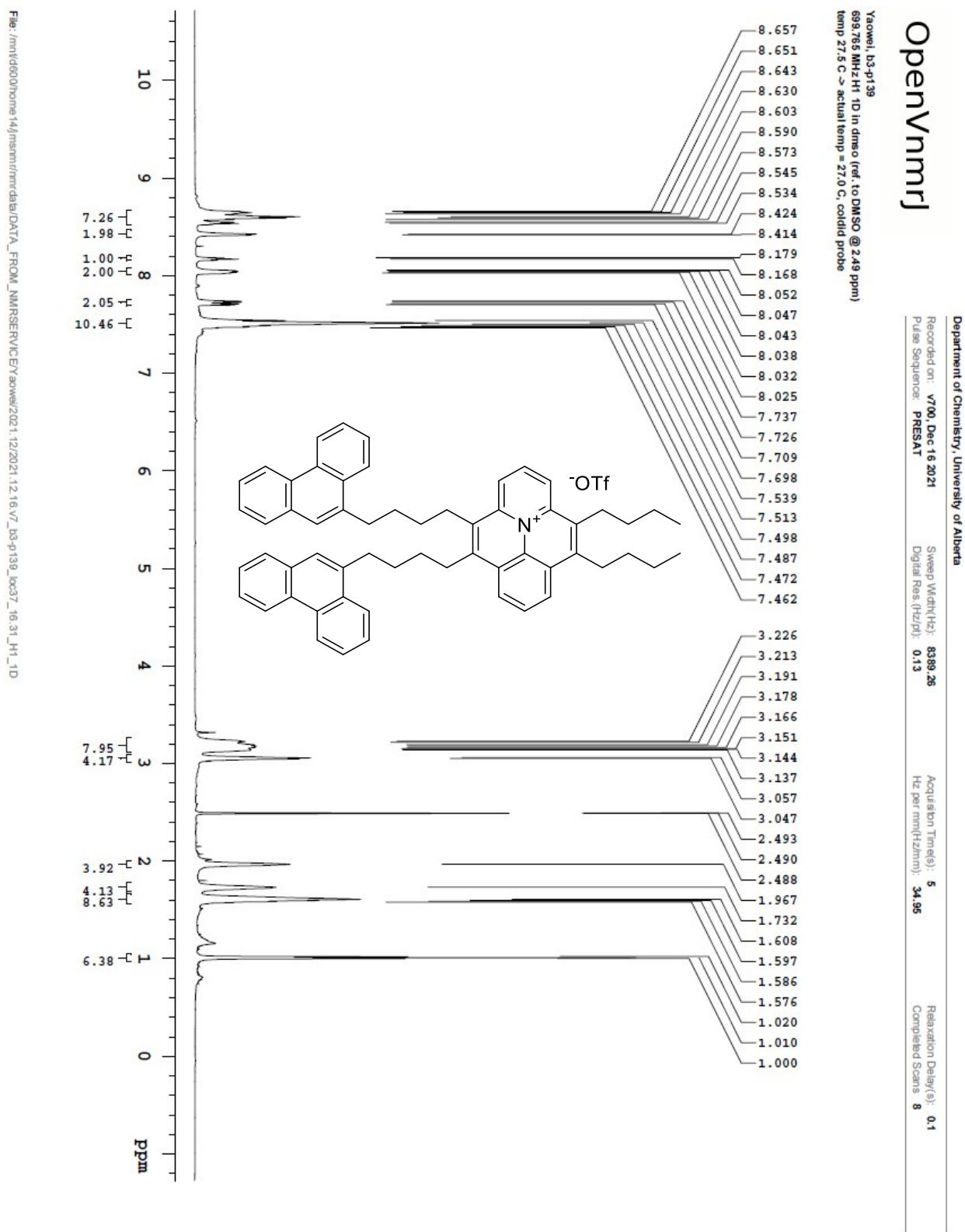
|                                       |                                  |                                 |
|---------------------------------------|----------------------------------|---------------------------------|
| Recorded on: <b>us00, Dec 10 2021</b> | Sweep Width(Hz): <b>33783.8</b>  | Acquisition Time(s): <b>1</b>   |
| Pulse Sequence: <b>s2pul</b>          | Digital Res.(Hz/p1): <b>0.26</b> | Hz per mm(Hz/mm): <b>115.04</b> |
|                                       |                                  | Relaxation Delay(s): <b>1</b>   |
|                                       |                                  | Completed Scans: <b>256</b>     |

Yaowei, b3-p137  
125.585 MHz C13{H1} 1D in dmsco (ref. to DMSO @ 39.5 ppm)  
temp 27.7 C -> actual temp = 27.0 C, coldstart probe



File: /mnt/d600/home/14/mnmr/mrdata/DATA\_FROM\_NMRSERVICE/yaowei/2021\_12/10 u5\_b3-p137\_loc3\_15.53\_C13\_1D

**4,5-Di[4-(9-phenanthrene)butyl]-9,10-dibutylbenzo[*ij*]pyrido[2,1,6-*de*]quinolizinium trifluoromethanesulfonate (382)**



# OpenVnmrj

Department of Chemistry, University of Alberta

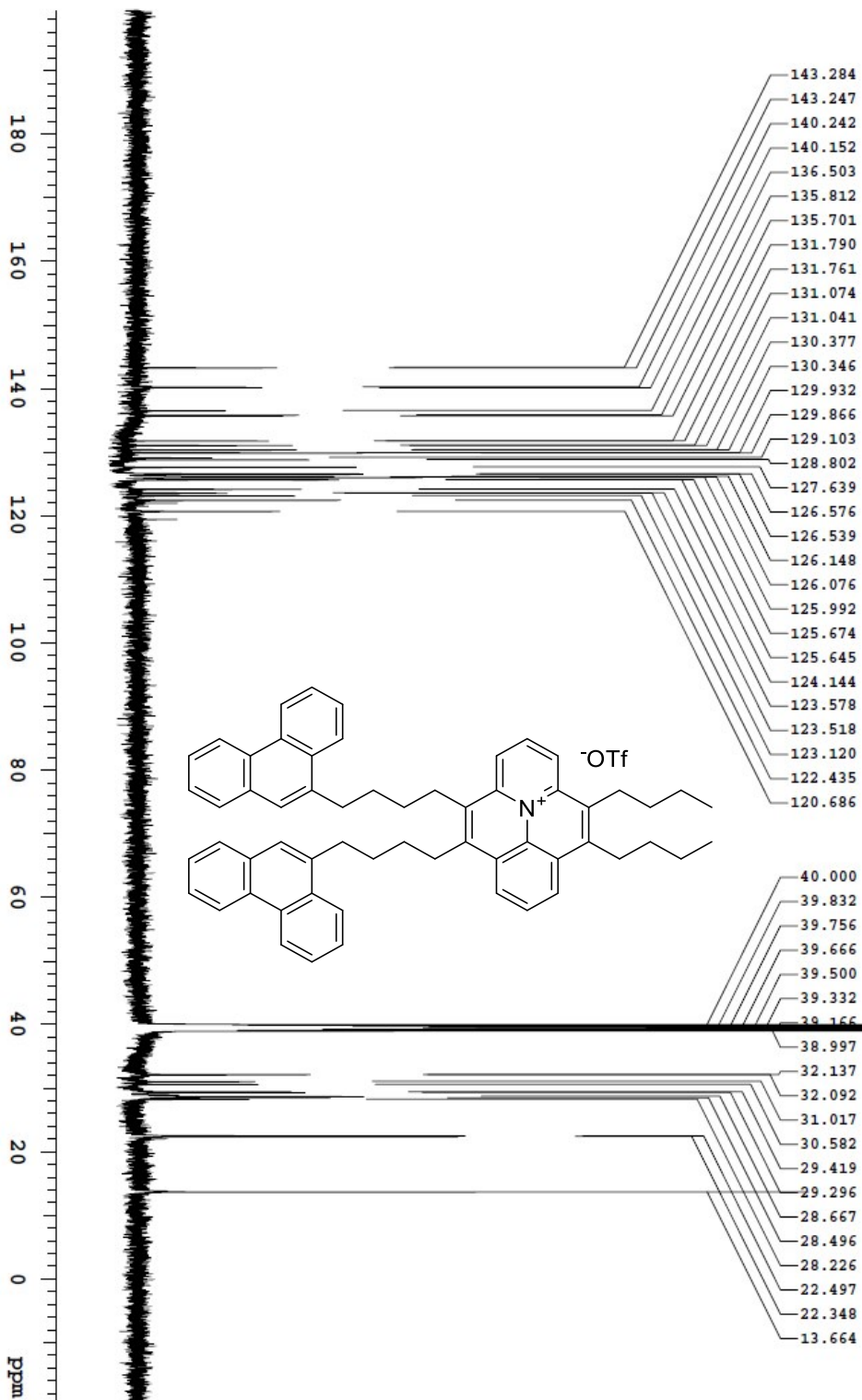
Recorded on: **us00, Nov 18 2021**  
 Pulse Sequence: **s2pul**

Sweep Width(Hz): **33783.8**  
 Digital Res.(Hz/p): **0.26**

Acquisition Time(s): **1**  
 Hz per mm(Hz/mm): **114.98**

Relaxation Delay(s): **1**  
 Completed Scans: **128**

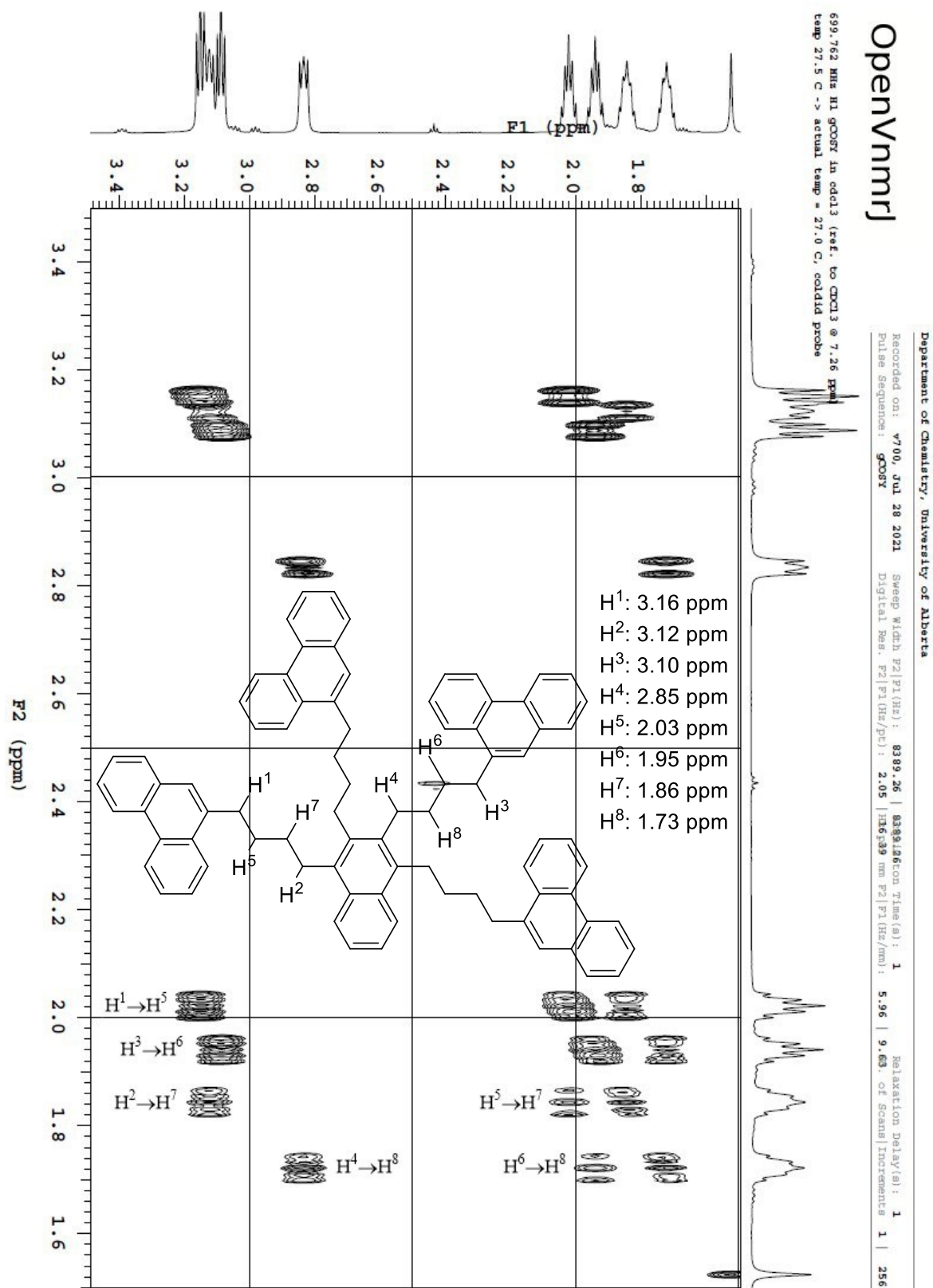
Yaoxuei\_b3-p129  
 125.686 MHz C13{H1} 1D in dmsc (ref. to DMSO @ 39.5 ppm)  
 temp 27.7 C -> actual temp = 27.0 C, cold dual probe



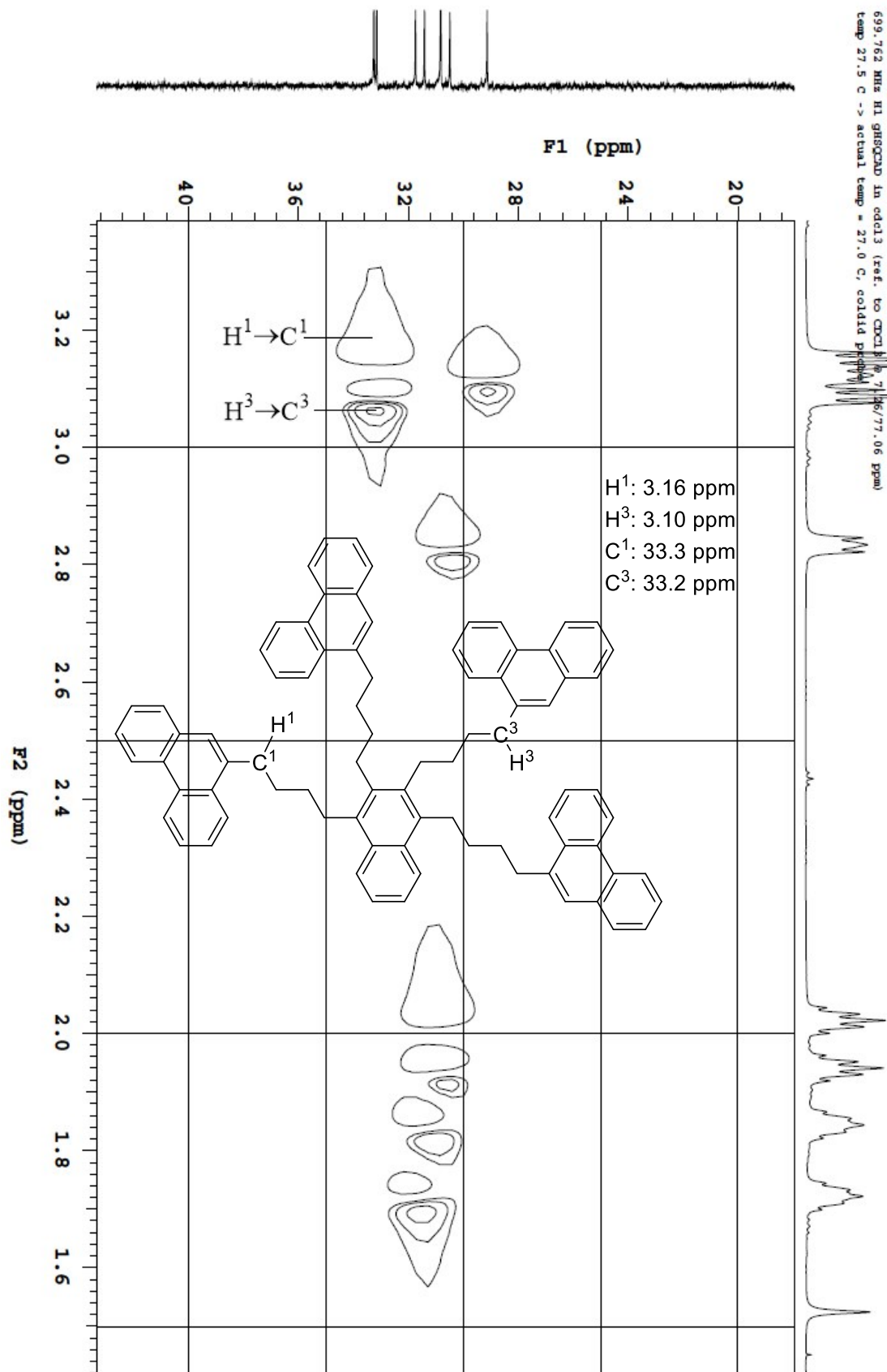
File: /mnt/d60/home/14j/nmr/nmrdata/14j/14j\_18\_u5\_03-p129\_1005\_15\_35\_C13\_1D



## Appendix 2: $^1\text{H}$ - $^1\text{H}$ COSY, HSQC, and HMBC Spectra



Yacvel, b2-p77  
699.762 MHz H1 ghsocad in cdcl3 (ref. to CCl4  $\delta$  7.26/77.06 ppm)  
temp 27.5 C -> actual temp = 27.0 C, couldd provide



# OpenVnmrj

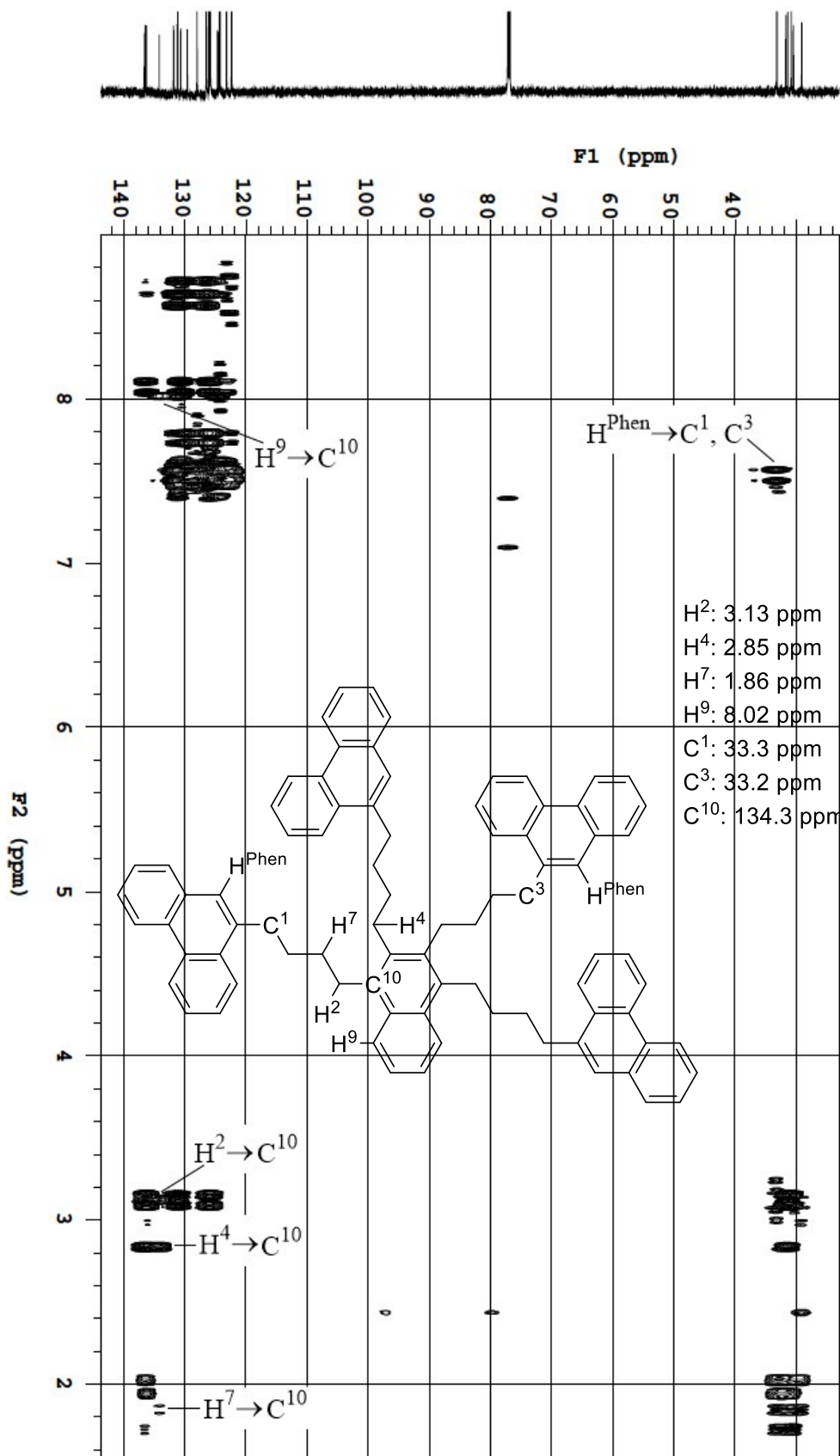
Department of Chemistry, University of Alberta

Recorded on: **7700, Jul 28 2021**  
Pulse Sequence: **gmsrcad**

Sweep Width F2(F1(Hz)): **8389.26** | 4750594000 Time(s): **0.25**  
Digital Res. F2(F1(Hz/pc)): **2.05** | 182999 mm F2(F1(Hz/mm)): **22.27**

Relaxation Delay(s): **1.50004**  
146.96f Scans/Incrments **2** | **128**

Yacvel, b2-p77  
699.762 MHz H1 gmsrcad in cdcl3 (ref. to CDCl3 @ 7.26/77.0 ppm)  
temp 27.5 C -> actual temp = 27.0 C coldid probe





## Appendix 3: UV-Vis and Fluorescence Spectra

UV-Vis Spectrum for **365** (CH<sub>2</sub>Cl<sub>2</sub>).

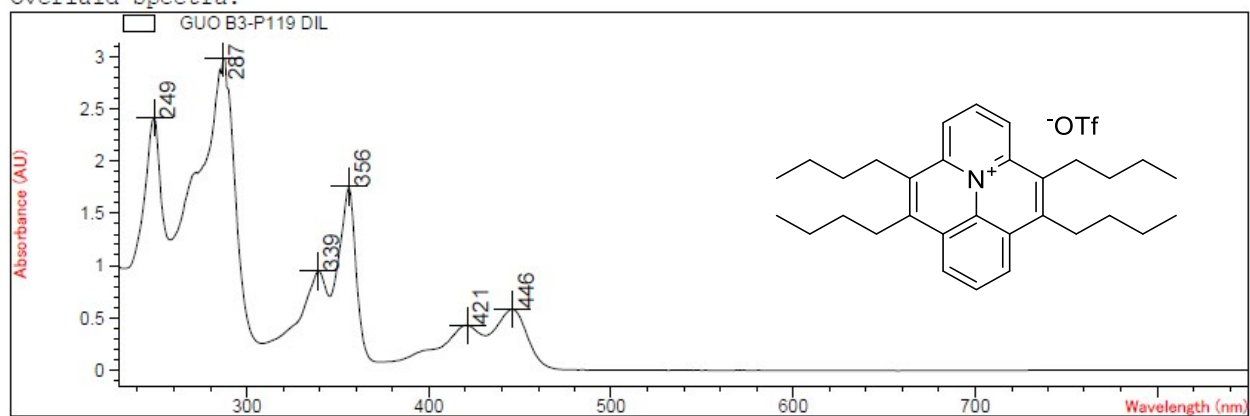
=====

|                      |                               |             |
|----------------------|-------------------------------|-------------|
| Spectrum/Peak Report | Date 2022-02-24 Time 08:30:11 | Page 1 of 1 |
|----------------------|-------------------------------|-------------|

=====

Method file : <method not saved>  
Information : Default Method  
Data File : <data not saved>

Overlaid Spectra:



| # | Name            | Peaks (nm) | Abs (AU) | # | Name | Peaks (nm) | Abs (AU) |
|---|-----------------|------------|----------|---|------|------------|----------|
| 1 | GUO B3-P119 DIL | 287.0      | 2.98140  | 1 |      | 339.0      | 0.94419  |
| 1 |                 | 249.0      | 2.41110  | 1 |      | 446.0      | 0.58291  |
| 1 |                 | 356.0      | 1.75350  | 1 |      | 421.0      | 0.43013  |

Instrument S/N : DE00000000

Report generated by : A & I LAB CHEMISTRY

Signature: .....

\*\*\* End Spectrum/Peak Report \*\*\*

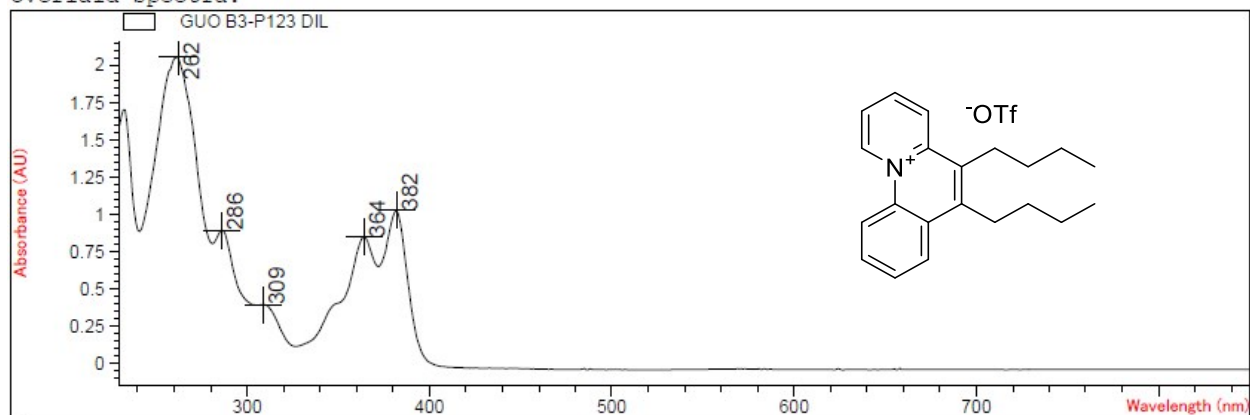
# UV-Vis Spectrum for **366** (CH<sub>2</sub>Cl<sub>2</sub>).

Spectrum/Peak Report

Date 2022-02-24 Time 08:31:58 Page 1 of 1

Method file : <method not saved>  
 Information : Default Method  
 Data File : C:\Chem32\1\DATA\DATA 2022\STRYKER\GUO\20220224\GUO B3-P123 DIL.SD  
 Created : 2/24/22 8:23:57

Overlaid Spectra:



| # | Name            | Peaks (nm) | Abs (AU) | # | Name | Peaks (nm) | Abs (AU) |
|---|-----------------|------------|----------|---|------|------------|----------|
| 1 | GUO B3-P123 DIL | 262.0      | 2.05490  | 1 |      | 364.0      | 0.85050  |
| 1 |                 | 382.0      | 1.02720  | 1 |      | 309.0      | 0.39679  |
| 1 |                 | 286.0      | 0.89546  |   |      |            |          |

Instrument S/N : DE00000000

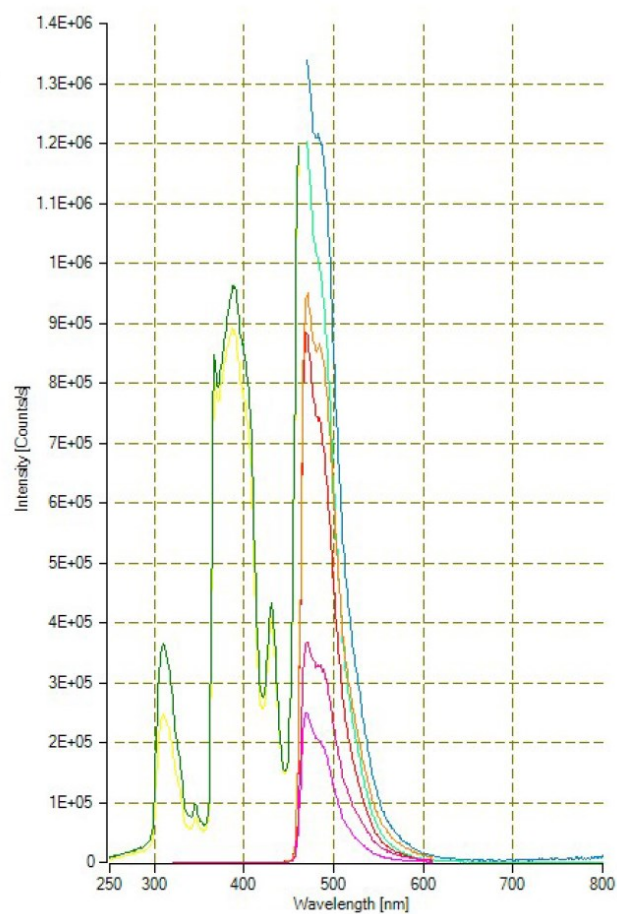
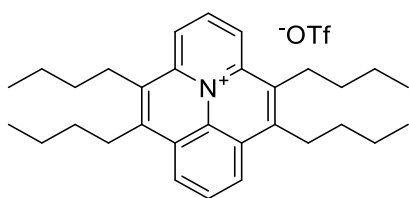
Report generated by : A & I LAB CHEMISTRY

Signature: .....

\*\*\* End Spectrum/Peak Report \*\*\*

Fluorescence Spectrum for **365** (CH<sub>2</sub>Cl<sub>2</sub>).

- Emission with excitation at 460 nm
- Emission with excitation at 460 nm (corrected)
- Emission with excitation at 385 nm
- Emission with excitation at 385 nm (corrected)
- Emission with excitation at 310 nm
- Emission with excitation at 310 nm (corrected)
- Excitation with emission at 470 nm
- Excitation with emission at 470 nm (corrected)



Fluorescence Spectrum for **366** (CH<sub>2</sub>Cl<sub>2</sub>).

- Emission with excitation at 330 nm
- Emission with excitation at 330 nm (corrected)
- Emission with excitation at 395 nm
- Emission with excitation at 395 nm (corrected)
- Excitation with emission at 415 nm
- Excitation with emission at 415 nm (corrected)

